

Contribution of inhibitory neurons to the amyotrophic lateral sclerosis and frontotemporal dementia continuum : focus on the motor and social phenotypes associated with FUS protein

Félicie Lorenc

▶ **To cite this version:**

Félicie Lorenc. Contribution of inhibitory neurons to the amyotrophic lateral sclerosis and frontotemporal dementia continuum : focus on the motor and social phenotypes associated with FUS protein. Neuroscience. Université de Strasbourg, 2024. English. ⟨NNT : 2024STRAJ072⟩. ⟨tel-05442461⟩

HAL Id: tel-05442461

https://theses.hal.science/tel-05442461v1

Submitted on 5 Jan 2026

HAL is a multi-disciplinary open access archive for the deposit and dissemination of scientific research documents, whether they are published or not. The documents may come from teaching and research institutions in France or abroad, or from public or private research centers.

L'archive ouverte pluridisciplinaire **HAL**, est destinée au dépôt et à la diffusion de documents scientifiques de niveau recherche, publiés ou non, émanant des établissements d'enseignement et de recherche français ou étrangers, des laboratoires publics ou privés.



HAL Authorization

Université de Strasbourg

UNIVERSITÉ DE STRASBOURG

École Doctorale des Sciences de la Vie et de la Santé STRASBOURG

ÉCOLE DOCTORALE DES SCIENCES DE LA VIE ET DE LA SANTÉ

INSERM U1329 – Strasbourg Translational Neuroscience and Psychiatry

THÈSE présentée par :

Félicie LORENC

soutenue le : **18 octobre 2024**

pour obtenir le grade de : **Docteure de l'Université de Strasbourg**

Discipline / Spécialité : Neurosciences

Contribution of inhibitory neurons to the amyotrophic lateral sclerosis and frontotemporal dementia continuum: Focus on the motor and social phenotypes associated with FUS protein

THÈSE dirigée par :

M. DUPUIS Luc	Directeur de recherche, Université de Strasbourg

THÈSE encadrée par :

Mme CASSEL Raphaelle	Maitresse de conférences, Université de Strasbourg

RAPPORTEURS :

Mme LÉVI Sabine	Directrice de recherche, Université Paris Sciences et Lettres
M. BLUM David	Directeur de recherche, Université de Lille

EXAMINATEURS :

Mme GODIN Juliette	Directrice de recherche, Université de Strasbourg
M. KABASHI Edor	Directeur de recherche, Université Paris-Cité

Warning to the reader

This document is the result of a long process approved by the jury and made available to members of the academic community. It is subject to the intellectual property rights of its author. This implies an obligation to quote and reference when using this document. Furthermore, any infringement, plagiarism, unlawful reproduction or representation will be prosecuted.

Intellectual Property Code

Article L122-4 : Any representation or reproduction in whole or in part without the consent of the author or his successors in title or assigns is unlawful. The same applies to translation, adaptation or transformation, arrangement or reproduction by any art or process whatsoever.

Articles L335-1 to L335-9 : Penal provisions.

Avertissement

Ce document est le fruit d'un long travail approuvé par le jury de soutenance et mis à disposition des membres de la communauté universitaire. Il est soumis à la propriété intellectuelle de l'autrice. Cela implique une obligation de citation et de référencement lors de l'utilisation de ce document. D'autre part, toute contrefaçon, plagiat, reproduction ou représentation illicite encourt une poursuite pénale.

Code de la Propriété Intellectuelle

Article L122-4 : Toute représentation ou reproduction intégrale ou partielle faite sans le consentement de l'autrice ou de ses ayants droit ou ayants cause est illicite. Il en est de même pour la traduction, l'adaptation ou la transformation, l'arrangement ou la reproduction par un art ou un procédé quelconque.

Articles L335-1 à L335-9 : Dispositions pénales.

License attributed by the author



This work © 2024 by Félicie Lorenc is licensed under Creative Commons Attribution-NonCommercial-ShareAlike 4.0 International (CC BY-NC-SA 4.0).
To view a copy of this license, visit https://creativecommons.org/licenses/by-nc-sa/4.0/

Remerciements

Quatre ans et un jour plus tard, il est maintenant le moment d'écrire les remerciements et de trier les échantillons. Je n'ai pas particulièrement hâte de ranger les étagères du 4°C ou les tiroirs du -20°C (ne le dites pas à Sylvie !). En revanche, c'est avec grand plaisir que je remercie toutes les personnes qui, de près ou d'un peu moins près, m'ont accompagnée durant ce projet de thèse.

J'adresse un immense merci à mon directeur de thèse, **Luc Dupuis**, et mon encadrante, **Raphaelle Cassel**. Merci pour votre aide, vos conseils et votre optimisme durant ces quatre années (et la demi-année de stage de Master). Je suis très reconnaissante que vous m'ayez accordé votre confiance et ce projet qui me tient tant à cœur. Vous m'avez incitée à ne pas minimiser la rigueur et l'importance des résultats que j'ai obtenus, et même s'il faut que je m'entraine encore un peu à voir le verre à moitié plein, je sais que je repars grandie grâce à vous. **Luc**, merci de m'avoir accueillie dans ton laboratoire (et de m'avoir accordé une prolongation !). Merci pour toutes les opportunités de participation à des congrès et les collaborations que nous avons pu mettre en place. Je mesure la chance que j'ai eue, et t'en suis extrêmement reconnaissante. Merci aussi pour le chauffage d'appoint au Bâtiment 3, sans ça, j'aurais fait ma thèse avec des orteils en moins. **Raphaelle**, j'ai tant de choses à dire qu'il va me falloir 355 pages supplémentaires. Heureusement, tu es toujours partante pour relire et corriger mon travail, quel que soit le nombre de pages (ou la langue) ! Je suis si contente d'avoir pu travailler à tes côtés et si fière du chemin que nous avons parcouru toutes les deux. Ce fut une réelle joie de partager nos -petites et grandes- réussites, ainsi qu'une vision de la science pleine d'humanité (surtout quand il s'agit de travailler avec des animaux, alors même que les souriceaux n'ont pas hésité à te grignoter les doigts). Merci pour ta pédagogie, ta bienveillance, ta gentillesse et ton soutien. Tu m'as fait découvrir la caractérisation comportementale de modèles murins en m'accueillant sur ton projet, et m'as ensuite donné les outils pour gérer le mien. De cela je retiens une citation (qui n'est pas de toi, mais aurait pu l'être !) « Tous les modèles sont faux, mais certains sont utiles » (G. Box). Luc, Raphaelle, je suis contente d'avoir pu développer des modèles utiles à vos côtés. Encore merci pour tout.

Je souhaite également remercier les membres de mon jury de thèse, **Sabine Lévi**, **David Blum**, **Juliette Godin** et **Edor Kabashi**. Je suis très reconnaissante que vous ayez accepté d'évaluer mon travail et attends avec impatience de pouvoir échanger avec vous. Un grand merci pour le temps que vous m'accordez.

Merci à Juliette Godin et **Chantal Mathis** qui ont pu voir ce projet évoluer lors des comités de suivi individuel, et qui ont apporté beaucoup de retours positifs et conseils bienveillants.

J'adresse aussi de chaleureux remerciements à toutes les personnes externes au laboratoire avec qui j'ai eu le plaisir de collaborer. I would like to thank **Sabine Liebscher** and **Vanessa Kan** for their invaluable contribution with the calcium imaging work on my -numerous- mouse lines. I am grateful for our fruitful discussions and for your willingness to share your expertise and support. Merci à **Delphine Roussel** pour la caractérisation de l'activité neuronale des souriceaux. J'ai été touchée par ta motivation et ta patience lors de l'écriture de la demande d'autorisation de projet. Ça n'a pas été simple, mais j'ai hâte de voir ce que les enregistrements vont donner. Enfin, j'aimerais exprimer ma gratitude à **Isadora Lenoël** et **Christian Lobsiger** pour m'avoir permis de participer à l'analyse comportementale de leurs lignées de souris. Ce fut un plaisir de mettre ma maitrise d'Ethovision au profit de collègues aussi gentils et d'un projet si élégant.

Je tiens à adresser mille mercis aux personnels des plateformes techniques dont l'aide et l'implication ont rendu possible mon travail de thèse. Merci à **Pascal Kessler** pour son aide avec la microscopie. Tu as toujours répondu à mes sollicitations avec beaucoup d'entrain, d'humour et de gentillesse, alors même que les marquages Hoechst (ou FUS, ou ChAT, …) n'étaient vraiment pas arrangeants pour les analyses d'images. Merci aussi d'avoir continué à m'accueillir à bras ouverts alors que j'étais la seule dont la session faisait crasher Zen (oups). Merci à **Célian Pitard**, **Christiane Rieger**, **Lénaïc Marczak**, **Claudia Spielmann** et **Christophe Richert** et **Bocar Kane** pour leur travail au sein de l'animalerie. Je suis extrêmement reconnaissante que vous ayez pris soin de mes petites crevettes et grosses patates. Même si j'avais sûrement

les souris les plus gentilles de Strasbourg, je sais tout ce que cela représente. Merci aussi pour nos échanges et votre aide pour améliorer, toujours plus, le bien-être de ces souris.

J'ai forcément une pensée pour ces dernières : pour les mâles têtus qui refusaient de rester agrippés à la grille ; les mâles curieux qui regardaient ce qui se passait chez les voisins plutôt que de s'intéresser à l'intrus dans leur cage ; les mamans clémentes qui me laissaient manipuler leurs petits et envahir leur cage de nourriture avec diverses consistances ; toutes ces souris avec qui j'ai travaillé et qui m'ont entendue dire beaucoup de bêtises pour occuper nos longues heures de tests comportementaux.

En parlant de soutien technique, je remercie du fond du cœur l'incroyable trio **Marion**, **Aurélie** et **Paul** dont l'aide avec le génotypage et la préparation des tissus a été aussi précieuse qu'ils ne le sont. Malgré la quantité d'échantillons, le travail répétitif et les difficultés, votre contribution a toujours été accompagnée de sourires, entrain, bonne humeur et gentillesse. Merci pour votre rigueur qui m'a permis de vous faire entièrement confiance lorsque j'étais en comportement. **Queen B**, tu as été à mes côtés du partage de bureau au Bâtiment 3 jusqu'aux dernières séances d'inclusion dans l'agar, et même lorsque tu n'étais plus là, tu as continué d'assurer la bonne ambiance et la convivialité dans l'équipe. Merci pour tous les superbes moments que nous avons passé chez toi et/ou grâce à toi. **Aurélie**, je reste émerveillée par ta maitrise du micro-onde, et bien que je me sois faite à l'idée que mon agar soit du caramel, je continue d'espérer qu'un jour je puisse t'arriver à la cheville. Merci d'avoir pris soin de nous, que ce soit grâce à la sophrologie ou à tes talents pour le karaoké. Vous êtes des femmes en or, ne changez rien, de votre douceur de Princesses Disney à votre franc-parler de Gremlins, merci pour tout ! **Pôl**, merci de n'avoir jamais baissé les bras face à mes génotypages récalcitrants. Je sais que depuis les échantillons Vgat, tu détestes le Gel Red au moins autant que les légumes, et je te comprends tout à fait (sauf pour les légumes). Tu as toujours été fier de moi quand je prenais le temps de trier et ranger les biopsies, et c'était ma source première de motivation. Merci pour ton immense gentillesse que tu ne perds que lorsque tu veux gagner à un jeu de société.

Merci également au fabuleux duo **Sylvie** et **Véronique** d'avoir gentiment pris le relais pour analyser la localisation de FUS et compter les neurones quand je suis partie en rédaction. Merci pour vos conseils, votre persévérance face aux marquages n'ayant pas fonctionnés et vos superbes PowerPoint. Votre maitrise de Fiji n'a d'égal que votre aptitude à nous régaler avec de succulents gâteaux (faits maisons) ou tablettes de chocolat. Merci **Steph** pour ton aide avec l'analyse du RI et les commandes, ainsi que pour tes réponses à mes nombreuses questions. Après toutes ces années, je peux enfin le dire : je n'ai plus peur de toi ! Je sais que tu as un cœur tendre et peut-être -3 à chaque œil à cause des vidéos du RI (pardon). Si je trouve d'autres jolies fèves, promis elles seront pour toi. Enfin, merci **Claudia** pour ton aide avec les tests moteurs des jeunes souriceaux et l'organisation des challenges Au Boulot À Vélo. De la peinture sur la tête des souris à la préparation d'affiches ABAV, nous avons partagé des moments pour le moins artistiques et sportifs.

Salim, merci pour tes conseils lors de la préparation des échantillons pour le séquençage, et merci pour l'analyse de ces données. J'ai hâte de voir ce que ça va donner pour les neurones inhibiteurs. **Matei**, merci de m'avoir incitée à découvrir le phénotypage métabolique (c'est vrai que c'est chouette l'hypothalamus). Merci aussi pour toutes ces fois où tu as pris de mes nouvelles, et merci pour nos échanges, des plus sérieux aux plus loufoques, des plus scientifiques aux plus drôles (et souvent les deux combinés). Je sais que je t'ai manqué pendant la rédaction, même si tu prétends le contraire sur le tableau du couloir.

Alors que la fin de thèse approche à grand pas, je ne peux m'empêcher de penser à vous avec un peu de nostalgie et beaucoup d'amour : merci **Marguerite**, **Olga** et **Marina** d'avoir été les meilleures co-thésardes de l'Univers (rien que ça) ! Je suis si heureuse de vous avoir rencontrées et d'avoir pu vivre cette expérience avec vous. Merci pour la relation d'écoute, de soutien et d'empouvoirement que nous avons construite. Merci pour toutes nos discussions sur la thèse, la recherche, les femmes en science, ou les bienfaits -scientifiquement prouvés- du chocolat. **Maggie**, je ne sais par où commencer, si ce n'est peut-être en citant une grande dame mystérieuse : j'ai été vraiment « contente de partager ma [thèse] avec toi » (tu sais que ta citation originale ne peut figurer ici). J'ai adoré découvrir nos traits de caractère si différents et qui m'ont permis de tant apprendre à tes côtés. Un jour peut-être je serai aussi optimiste, confiante et joviale que toi, en attendant j'espère que la longueur de ma thèse (oups) fait honneur à ta volubilité. Merci pour tes conseils

et ton soutien durant la rédaction. Ton dévouement a même permis que nous courrions une seconde fois ensemble (!), mais clairement, je n'ai pas le niveau pour te suivre. Au fait, as-tu pensé à refermer ta gourde de thé ? **Olgux**, grâce à toi j'ai pu vivre de Ferrero Rocher et d'eau fraiche. Merci pour ton immense gentillesse, toutes tes délicates attentions, et tes mots remplis d'amour qui avaient le don de me rebooster. Je suis si contente d'avoir pu t'accompagner à Baltimore et de ne pas t'avoir perdue dans notre appartement -beaucoup trop grand-. Tu es la preuve vivante que Scorpion est le meilleur signe astrologique (qui en doutait ?). J'ai adoré préparer avec toi des évènements au CRBS, c'est certainement dû à notre grande compatibilité. Surtout reste comme tu es, mais en un peu plus hydratée. **Marina**, I wanted to write my thanks to you in Spanish, and although my vocabulary is very limited, I have two words that sum it all up: ¡Muchas gracias y croquetas! Thank you for being the best tour guide in Barcelona and Vienna, and thank you for saying I was the "most Spanish" of the PhD students (which I appreciated considering I lost my tan in Strasbourg). I am glad you followed me when I wanted to create the PhD and PostDoc Organisation of CRBS (we did it!). Keep on being the best singer in the office, even when it comes to French songs.

Je remercie également l'ensemble des membres de l'équipe pour leur accueil chaleureux, leurs retours constructifs sur mon projet, ainsi que pour la bonne ambiance qui accompagnait nos grandes tablées du midi. Un merci tout particulier à celles et ceux qui ont gardé Gemma pendant les congrès, même si parfois, le bout de son nez est tout ce qu'elle a daigné vous montrer. **Caro**, merci pour tes judicieuses propositions lorsque je présentais mes résultats, et merci pour tes encouragements tout au long de la Strasbourgeoise. **Fred**, merci d'avoir répondu à mes nombreuses questions liées à l'animalerie ou aux demandes d'autorisation de projet. Tu l'as toujours fait avec beaucoup de gentillesse, alors même qu'il te fallait fouiller dans les agréments, manuels d'utilisation d'Ethovision, et j'en passe. **Marc**, merci d'avoir mis tes talents de bricoleur au profit de la construction d'un test moteur pour les souriceaux. **José**, merci pour tes conseils avisés au sujet des analyses statistiques. **Valérie** et **Chantal**, merci pour l'organisation de la Semaine du Cerveau, c'était un super moment dans la vie de l'équipe et du CRBS. **Charlotte**, grâce à toi j'ai recommencé à jouer aux Sims, et je ne sais pas vraiment si c'est une bonne situation, mais je t'en remercie grandement. **Cédric**, merci d'être un Poufsouffle apportant beaucoup de bonne humeur à l'équipe, et merci de m'avoir aidée à résoudre le meurtre odieusement commis par [spoiler]. Merci à vous deux pour votre gaieté et votre humour. **Geoffrey**, merci d'avoir projeté des films d'horreur pas trop effrayants quand j'osais braver mes peurs (ce fut rare, mais intense pour mon cœur). A l'inverse, tu es le seul qui prononçait « jaune » correctement, et mes oreilles t'en sont reconnaissantes. Enfin, je souhaite tout le meilleur à la relève, Aurélien, Chaïma, Farah, Isabelle, Lingyi et Nathan. Profitez bien de votre thèse !

Merci aussi aux anciens membres du laboratoire qui m'ont accueillie avec beaucoup de gentillesse et de conseils avisés, sur la thèse ainsi que sur les bars à jeux strasbourgeois. J'ai beaucoup apprécié que vous me laissiez gagner à notre toute première partie de Galérapagos. C'est bien la seule fois où j'ai pu monter sur le radeau. **Gina**, j'ai adoré tes histoires insolites et l'énergie que tu transmets autour de toi. Merci pour ton aide avec les anticorps anti-VGluT2 et pour avoir dit que j'étais une super cliente. Merci surtout pour tous tes conseils et retours d'expérience sur le monde du travail. **Alex** et **Cyril**, membres originaux du meilleur bureau du CRBS (dont je tairais ici le nom officiel, car je ne l'assume toujours pas). Merci d'avoir répondu à mes questions de tout début de thèse, et merci d'avoir si souvent embêté Guerite, ça a vraiment mis une super ambiance dans le bureau. **Aurore**, tu as été de loin la meilleure voisine de paillasse. Merci pour ta douceur, ta gentillesse, et tes magnifiques étiquettes de bouteilles. L'organisation de ces dernières satisfaisait amplement mon -très léger- perfectionnisme, et ta bouture de pothos a trouvé sa place sur mes bureaux, au CRBS comme à l'appartement. Merci **Margaux** pour les rires et la bonne humeur que tu as apportés, ainsi que pour ta fougue légendaire autour du babyfoot. Merci **Johan** car ton humour nous a offert certains des meilleurs moments du laboratoire (Marguerite t'a souvent facilité la tâche, mais le mérite te revient). **Laura**, j'ai été contente de te retrouver en congrès, merci pour nos discussions autour des posters ou d'un verre. Merci également à **Alizée** et **Matis**, que j'ai eu le plaisir d'encadrer pour leurs stages. J'ai été très contente de pouvoir travailler à vos côtés, et de vous partager un petit bout de mon projet.

Cette thèse n'aurait pas été la même sans les rencontres faites aux différents étages du CRBS. **Lauriane**, merci d'avoir ponctué la deuxième moitié de ma thèse de ton rire communicatif et de soirées jeux. Grâce à toi j'ai pu être la fille d'Hermione Granger le temps d'une journée, je t'en suis si reconnaissante. **Quentin**,

merci de ne pas voler les sacoches de mon vélo quand tu finiras ta thèse (j'en ai besoin, même si elles prennent beaucoup de place dans le local). Emma, Katka, Cristina, Adrien, Kirsley et Nicolas, merci de nous avoir suivis dans la création de l'organisation des doctorant·es et post-doctorant·es du CRBS. Un merci tout particulier à toi **Emma**, ainsi qu'à ton bolide, pour m'avoir aidée à déménager mon bureau pour la rédaction.

Je pense également à toutes les copines et les copains qui étaient là avant et pendant la thèse. Même si je n'ai pas pu vous voir autant que je l'aurais souhaité, passer un peu de temps avec vous est toujours une bouffée d'air frais et je chéris nos amitiés. **Tagoune**, **Candou** et **Oli**, merci d'être une source infaillible de bienveillance, soutien, sororité, encouragement et humour engagé. Avec vous mon monde est plus beau, notamment parce qu'il sent la tisane et les cinnamon rolls. Je vous adore les filles, surtout restez extraordinaires ! **Marion** et **Toitoine**, merci d'avoir été à mes côtés des fous rires en cours jusqu'aux râleries lors des manips. Jpp que vous soyez des personnes aussi formidables. Un énorme merci pour tout votre soutien et vos conseils lors de la rédaction, vous êtes incroyables.

Enfin, merci à ma famille pour l'expression de son soutien et sa fierté durant mes études. Merci de m'avoir encouragée et accompagnée, y compris pour mes nombreux déménagements.

Simon, my partner in life, science, crime and binge-watching. You are an amazing human -slash- genius. Your help during the PhD was amazing and made all the difference. Your opinions and advice shaped some of my experiments, figures and even part of this manuscript. I am thrilled I had the chance to learn so much thanks to you and your passionate scientific discussions. Thank you for always pushing me and believing in me more than I did. Even though I was not a damsel in distress, you were always there for me. So supportive. Not like statistics and R codes, always getting in my way. The numbers were scary, and some parts of the PhD were difficult, but I didn't worry. I knew if I got confused, you'd be right here in the front row. Thank you for being my harbor. Your love is a lighthouse. I can't wait to sail from the day to the wonders awaiting us out there. Adventure is calling and I'm going to win for you like I know you want me to do. **Gemma**, merci d'avoir été si contente et affectueuse quand je rentrais le soir en sentant la souris. Merci aussi de t'être toujours inquiétée que mon clavier et ma souris d'ordinateur reste au chaud durant la rédaction de ce manuscrit, y compris quand j'en avais besoin. Ton soutien tranquille -et si peu envahissant- m'a apporté beaucoup de réconfort. Merci également à **Dominique** et **Jean-Jacques** pour vos venues à Strasbourg, votre intérêt sincère pour mon projet, vos cartes postales toujours pleines d'humour et vos encouragements.

Sister, merci d'avoir été là pour moi des premières souris que j'ai manipulées jusqu'à ma soutenance. Merci pour nos appels trop longs et nos retrouvailles trop courtes. Merci pour toute ton aide et pour tes conseils, attentions et vidéos de chat (bisous Oli). Un merci tout particulier de t'occuper du pot, et ce avec toute l'organisation qui nous caractérise. J'ai tellement de chance d'avoir une petite sœur aussi merveilleuse. **Mamounette**, merci de me montrer l'exemple lorsqu'il s'agit d'apprendre à relativiser et à se faire confiance. J'ai encore du chemin à parcourir mais je sais que je le ferai en étant bien accompagnée. **Papounet**, merci de ne t'être jamais découragé et d'avoir tenté tous les créneaux de la semaine pour prendre de mes nouvelles et me conseiller lors des coups de mou. Merci aussi pour ton aide à distance quand j'avais besoin de réparer mon vélo, sans ça mes trajets auraient été bien plus compliqués. **Béa**, merci pour les confitures maisons qui m'ont sustentée durant la rédaction, et merci d'avoir dit que tu apprécies mon humour (ça m'a fait super plaisir). **Benoit**, merci pour toutes les fois où tu as proposé de mettre tes connaissances en anglais au profit de ma thèse (it was nice of you). **Mamie Christiane** et **Papy Michel**, merci de m'avoir choyée quand je venais me ressourcer chez vous, et merci de vous être autant intéressés à mon travail. Vous savoir fiers de moi compte énormément. Mes illustrations ne sont pas faites à l'encre de chine et mes photos de neurones ne valent pas les étoiles de « Voyage galactique », mais j'ai écrit 280 pages, vous vous rendez compte ?

Mamie Annie, j'aurais tout donné pour que tu puisses continuer de courir avec nous dans le jardin. Tu sais que cette thèse, et tous mes combats contre la SLA, ils sont pour toi. Merci d'être ma plus grande source de motivation, courage, force et résilience. Merci de veiller sur moi et de m'avoir laissé des souvenirs si doux de notre complicité. Je n'ai pas eu l'occasion de te parler de mon rêve de devenir Docteure en Neurosciences, mais alors qu'il se réalise, c'est forcément à toi que je pense. J'espère que tu es fière.

Durant cette thèse j'ai été financée par un contrat doctoral, ainsi que par de généreuses donations de l'Association pour la Recherche sur la Sclérose Latérale Amyotrophique et de la Fondation Anne-Marie et Roger Dreyfus, abritée à la Fondation de France.

Table of contents

List of figures **14**

List of tables **15**

List of abbreviations **16**

INTRODUCTION

Part 1: Amyotrophic lateral sclerosis (ALS) **19**

1. Definition 19
2. Clinical presentation 20
   - 2.1. Motor symptoms 20
   - 2.2. Neuropsychiatric impairments 21
3. Epidemiology 22
   - 3.1. Incidence and prevalence 22
   - 3.2. Risk factors and identified causes 22
     - A. Age and sex 23
     - B. Environment 23
     - C. Genetics 24
4. Diagnosis 25
5. Prognosis and staging 25
6. Treatments 26

Part 2: Frontotemporal dementia (FTD) **28**

1. Definition 28
2. Clinical presentation 29
   - 2.1. Behavioural variant 29
   - 2.2. Primary progressive aphasia 29
   - 2.3. Motor symptoms 30
3. Epidemiology 30
   - 3.1. Incidence and prevalence 30
   - 3.2. Risk factors and identified causes 31
     - A. Age and sex 31
     - B. Environment 31
     - C. Genetics 31
4. Diagnosis 32
5. Prognosis and staging 32
6. Treatments 33

Part 3: ALS-FTD continuum **34**

1. Genetic continuum 34
   - 1.1. Chromosome 9 open reading frame 72 (C9ORF72) 35
   - 1.2. Transactive response DNA binding protein of 43 kDa (TARDBP) 35
   - 1.3. TANK-binding kinase 1 (TBK1) 36
   - 1.4. Superoxide dismutase 1 (SOD1) 36
   - 1.5. Microtubule-associated protein tau (MAPT) 37
   - 1.6. Progranulin (GRN) 37
2. Histopathological continuum 38
3. Proposed pathogenic mechanisms 39
4. Neuronal circuit dysfunctions 40

Part 4: Inhibitory neurons **42**
1. Inhibitory neurotransmitters 42
1.1. GABAergic transmission 42
A. Organisation of the synapse 42
B. GABA receptors 43
1.2. Glycinergic transmission 44
A. Organisation of the synapse 44
B. Glycine receptors 44
1.3. Focus on the shared vesicular transporter 45
2. Inhibitory neuronal populations 46
2.1. Cerebral neocortex 46
A. Parvalbumin neurons 47
B. Somatostatin neurons 47
C. 5HT3aR neurons 48
D. Long-range projecting GABAergic neurons 48
2.2. Ventral horn of the lumbar spinal cord 49
A. $V0_D$ interneurons 49
B. V1 interneurons 50
C. V2b interneurons 50
3. Development of the inhibitory system 50
3.1. Transition from depolarisation to hyperpolarisation 51
3.2. Focus on two aspects of the neocortex postnatal development 53
A. Programmed cell death of inhibitory neurons 53
B. Transition from synchronisation to decorrelation 54
3.3. Focus on two aspects of the spinal cord embryonic development 55
A. Transition from GABAergic to glycinergic synapses 55
B. Influence of inhibitory neurons on motor neuron development 56
4. Physiological functions of inhibitory neurons 56
4.1. Balance between excitation and inhibition 56
4.2. Regulation of behavioural and cognitive processes 57
4.3. Control of movements 58
4.4. Ageing of the inhibitory system 58

Part 5: Involvement of inhibitory neurons in ALS-FTD **60**
1. Pathological evidence of inhibitory neuron impairments in the brains of ALS and FTD patients 64
1.1. Uncertainty regarding the levels of neurotransmitter 64
1.2. Decreased binding to GABA receptors 64
1.3. Loss of neurons and neurites 66
1.4. Altered composition of GABA receptors 66
2. Neurophysiological evidence of inhibitory neuron impairments in the brains of ALS and FTD patients 68
2.1. Reduced inhibitory transmission 68
2.2. Altered neuronal oscillations 70
3. Pathological evidence of inhibitory neuron impairments in the spinal cords of ALS patients 71
3.1. Loss of neurons and neurites 71
3.2. Altered composition of GABA receptors 72
4. Neurophysiological evidence of inhibitory neuron impairments in the spinal cords of ALS patients 73
5. What is the relationship between impairments in inhibitory neurons and symptoms of ALS and FTD? 73
5.1. Inhibitory neurons impairments are associated to specific motor symptoms in ALS patients 74

5.2. Inhibitory neurons impairments are correlated with behavioural phenotypes in FTD patients ... 74
5.3. Inhibitory neurons impairments are correlated with cognitive phenotypes in ALS and FTD patients ... 75
6. What are the mechanisms leading to decreased inhibition in ALS and FTD? ... 75
6.1. Presynaptic transcriptional alterations leading to inhibitory neuron dysfunction and death ... 76
6.2. Postsynaptic transcriptional alterations modifying the composition of inhibitory receptors ... 76
6.3. Abnormal elimination of inhibitory synapses by microglia ... 78
6.4. Abnormal depolarising action of GABA ... 78
6.5. Exacerbated inhibition of inhibitory neurons ... 79
7. Contribution of inhibitory neuron impairments to symptoms ... 79
7.1. Inhibitory neurons influence motor neuron activity and death in ALS mouse models ... 79
7.2. Inhibitory neurons contribute to locomotor phenotype in ALS mouse models ... 81
8. Future directions: inhibitory neurons as a possible therapeutic target ... 82
8.1. Increasing the activity of GABA receptors in ALS patients ... 83
8.2. Regulating neuronal activity in ALS and FTD patients ... 84
9. Inhibitory neuron impairments in ALS-FTD mouse models ... 86
9.1. Mutation of TARDBP to model ALS and FTD ... 86
9.2. Mutation of SOD1 to model ALS ... 87
9.3. Mutation of MAPT to model FTD ... 89
9.4. Highlights from the characterisation of ALS-FTD mouse models ... 90

Part 6: Involvement of fused in sarcoma in ALS-FTD ... 91
1. Properties ... 91
1.1. Structure ... 91
1.2. Nucleocytoplasmic shuttling ... 92
1.3. Autoregulation ... 92
1.4. Liquid-liquid phase separation ... 93
2. Physiological functions ... 94
2.1. Nuclear functions ... 94
2.2. Cytoplasmic and synaptic functions ... 95
3. Pathological conditions ... 96
3.1. Germline mutations in ALS ... 97
3.2. Delocalisation and aggregation in ALS and FTD ... 97
3.3. Typical ALS and FTD symptoms associated with FUS ... 98
3.4. Proposed pathogenic mechanisms ... 99
A. Gain of function ... 100
B. Loss of function ... 100
4. $Fus^{\Delta NLS/+}$ mouse line as a model of ALS and FTD ... 101

OBJECTIVES

Scientific question ... 107

Experimental approach ... 107

RESULTS

Publication 1: Cytoplasmic accumulation of FUS in inhibitory neurons impairs cortical activity and sociability in mice ... 113

Supplementary data **146**
1. Social phenotyping of $Fus^{Resc/+}$ and $Fus^{Trunc/+}$ mice 146
2. Metabolic phenotyping of $Fus^{Resc/+}$ and $Fus^{Trunc/+}$ mice 152

Publication 2: Cytoplasmic accumulation of FUS in inhibitory neurons results in postnatal muscle weakness and death in mice **162**

Supplementary data **181**

DISCUSSION

Manipulation of FUS localisation in inhibitory neurons **188**
1. Was our targeting of inhibitory neurons specific? 188
   A. Did we only target neurons? 188
   B. Did we only target inhibitory neurons? 189
2. Was our targeting of inhibitory neurons efficient? 190
3. Was FUS completely depleted from the nucleus in $Trunc^{-/-}$ pups? 192
4. Does FUS cytoplasmic accumulation alter neuronal density? 192

Mechanisms underlying the observed motor deficits **194**
1. Do inhibitory neurons contribute to FUS-related motor defects? 194
2. Are cortical inhibitory neurons impaired in $Fus^{\Delta NLS/+}$ mice? 196
3. Are spinal inhibitory neurons impaired in $Fus^{\Delta NLS/+}$ mice? 197
4. Could $Trunc^{-/-}$ pups model a juvenile motor neuron disease? 198

Mechanisms underlying the increased sociability **201**
1. Which mechanisms could underlie the increased sociability? 201
2. Does this highlight an increased perseverance? 204

Contribution of FUS in the regulation of neuronal activity **206**
1. Which mechanisms could underlie the increased spontaneous neuronal activity? 206
2. Is there a link between seizures and the ALS-FTD continuum? 208
3. Could $Trunc^{-/-}$ pups die from fatal seizures? 210

Validity and limitation of the study **214**
4. Relevance of the choice of mouse lines 214
   A. $Fus^{\Delta NLS/+}$ mice as a model of ALS and FTD 214
   B. $Vgat^{Cre}$ mice to target inhibitory neurons 216
5. Relevance of the follow-up of disease progression 218

Inhibitory neurons as a possible therapeutic target **219**

RÉSUMÉ EN FRANÇAIS **227**

REFERENCES **249**

ANNEXES

Publication 3: FUS-dependent gene expression links neuronal vulnerability to genetic risk in ALS/FTD **295**

Publication 4: ALS/FTD-linked TBK1 deficiency in microglia induces an aged-liked, primed microglial signature and drives social memory deficits in mice **299**

List of figures

Figure 1: ALS is primarily characterised by the degeneration of the motor system. 19

Figure 2: ALS manifests as a range of phenotypes. 21

Figure 3: FTD manifests as a range of phenotypes. 28

Figure 4: Genetic overlap of ALS and FTD. 34

Figure 5: Pathological overlap of ALS and FTD. 38

Figure 6: The ALS-FTD continuum is associated with a range of pathogenic cellular pathways. 39

Figure 7: Organisation of a GABAergic synapse. 43

Figure 8: Organisation of a glycinergic synapse. 45

Figure 9: Inhibitory neuronal populations in the neocortex. 47

Figure 10: Inhibitory neuronal populations in the ventral spinal cord. 49

Figure 11: Milestones in the postnatal development of the inhibitory system in the mouse neocortex. 51

Figure 12: Developmental switch from depolarisation to hyperpolarisation. 52

Figure 13: Circuits motifs highlighting the relationship between excitation and inhibition. 57

Figure 14: Main inhibitory neuron impairments reported in the brains of ALS and FTD patients. 65

Figure 15: Spinal inhibitory neurons involved in locomotor control, and main alterations reported in ALS patients. 72

Figure 16: Several mechanisms, likely to be complementary, could account for the decreased inhibition in ALS and FTD. 76

Figure 17: Impairments of inhibitory neurons influence the development of locomotor deficits in ALS mouse models. 81

Figure 18: Enhancing or stabilising the inhibitory activity represents a promising therapeutic approach to alleviate locomotor deficits. 83

Figure 19: Schematic representation of messenger RNA and protein sequences of FUS. *FUS* gene comprises 15 exons. 91

Figure 20: Proposed mechanisms for the autoregulation of FUS. 93

Figure 21: Summary of the main nuclear and cytoplasmic functions of FUS. 96

Figure 22: Phase separations and aggregation of FUS. 98

Figure 23: Summary of the main results previously obtained from the characterisation of *Fus*$^{\Delta NLS/+}$ adult mice. 102

Figure 24: In the *Fus* locus, LoxP sequences allow to manipulate the truncation of the NLS domain. 108

Figure 25: Schematic representation of the main mouse lines included in this project. 109

Figure 26: Summary of the main results obtained from the characterisation of *Fus*$^{\Delta NLS/+}$, *Fus*$^{Resc/+}$ and *Fus*$^{Trunc/+}$ adult mice. 113

Figure 27: Summary of the main results obtained from the characterisation of Trunc$^{-/-}$ pups. 162

Figure 28: Main results obtained from the characterisation of Trunc$^{-/-}$ pups and comparison with the postnatal development of the cortical inhibitory system. 211

Résumé en français :

Figure 29: Résumé des principaux résultats précédemment obtenus lors de la caractérisation des souris *Fus*$^{\Delta NLS/+}$ adultes. 228

Figure 30: Dans le gène *Fus*, les séquences LoxP permettent de manipuler la troncation du domaine NLS. 230

Figure 31: Représentation schématique des principales lignées de souris inclues dans ce projet. 231

Figure 32: Résumé des principaux résultats obtenus lors de la caractérisation des souris adultes *Fus*$^{\Delta NLS/+}$, *Fus*$^{Resc/+}$ et *Fus*$^{Trunc/+}$ 233

Figure 33: Résumé des principaux résultats obtenus lors de la caractérisation des souriceaux Trunc$^{-/-}$ 236

Several illustrations were created with BioRender.com.

List of tables

Table 1: ALS and FTD patients display broad alterations in the composition of $GABA_A$ receptors. 67

Table 2: ALS and FTD patients exhibit common alterations in neurophysiological parameters linked to cortical inhibition. 69

Table 3: In FTD patients classified according to their clinical diagnosis or underlying aetiology, the incidence rate of seizures is variable. 209

List of abbreviations

A	ALS	Amyotrophic lateral sclerosis
	ALSFRS-R	Revised ALS functional rating scale
C	C9ORF72	Chromosome 9 open reading frame 72
	CSP	Cortical silent period
E	E	Embryonic day
F	FTD	Frontotemporal dementia
	FUS	Fused in sarcoma
G	GABA	Gamma-aminobutyric acid
	GAD	Glutamic acid decarboxylase
	GAT	GABA transporter
	GlyT	Glycine transporter
	GRN	Progranulin
K	KCC2	Potassium-chloride cotransporter 2
L	LICI	Long-interval intracortical inhibition
M	MAPT	Microtubule associated protein tau
N	NKCC1	Sodium-potassium-chloride cotransporter 1
	NLS	Nuclear localisation signal
	non-VIP	5HT3a neurons not expressing VIP
P	P	Postnatal day
R	RGG domain	Domain enriched in arginine-glycine-glycine motifs
S	SICI	Short-interval intracortical inhibition
	SOD1	Superoxide dismutase 1
T	TARDBP	Transactive response DNA binding protein of 43 kDa (gene)
	Tau	Tubuline associated unit
	TBK1	TANK-binding kinase 1
	TDP-43	Transactive response DNA binding protein of 43 kDa (protein)
V	VGAT	Vesicular GABA transporter
	VIP	Vasoactive intestinal polypeptide
#	[11C]flumazenil	Flumazenil labelled with carbon-11
	5HT3aR	Serotonin (also called 5-hydroxytryptamine) 3a receptor

Introduction

Part 1: Amyotrophic lateral sclerosis (ALS)

Amyotrophic lateral sclerosis (ALS), also known as *maladie de Charcot* in French, is a neurodegenerative disease with a complex aetiology and a wide range of underlying pathological mechanisms. The investigation of this disease is challenging due to the rarity of patients, the high degree of heterogeneity and the short survival period. One area of interest has been the identification of disease subtypes, whereby patients would exhibit common characteristics and therapeutic targets. Here, I will provide an overview of the disease, from its definition to the current management of patients. We will see that this multisystemic and multifactorial disease is still poorly understood, diagnosed and treated.

1. Definition

ALS is a fatal neurodegenerative disease and the most frequent adult-onset motor neuron disorder. It is primarily characterised by the degeneration of two populations of motor neurons (Figure 1). Corticospinal neurons, also known as upper motor neurons, are situated within the motor cortex and project to the brainstem motor nuclei and anterior horn of the spinal cord. Bulbar and spinal motor neurons, also known as lower motor neurons, are localised in the brainstem and spinal cord, respectively, and innervate striated skeletal muscle.

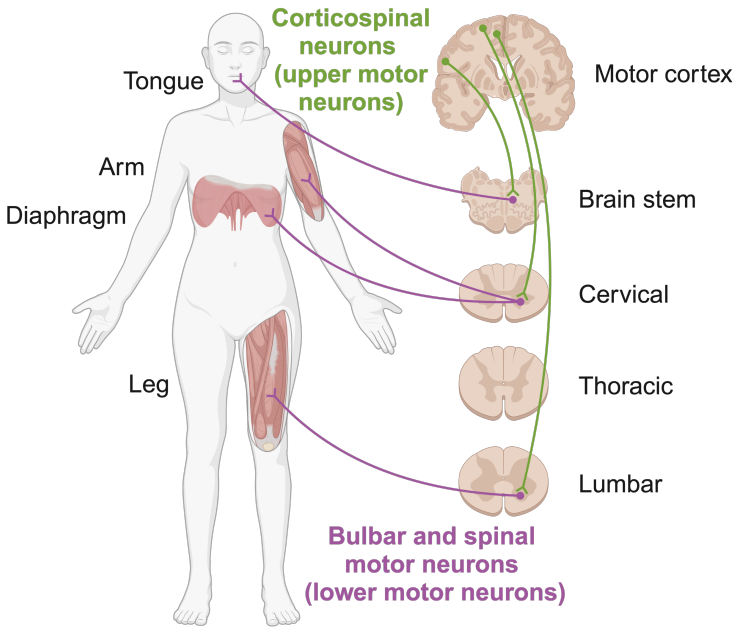


Figure 1: ALS is primarily characterised by the degeneration of the motor system. The motor system is constituted by corticospinal, bulbar, and spinal motor neurons, which undergo degeneration in ALS. Adapted from Feldman et al., 2022.

Disease onset typically occurs between 51 and 66 years, and patients usually die from respiratory failure 3 to 5 years after diagnosis. There is currently no effective treatment, underscoring the need to elucidate the underlying causes and risk factors to identify potential therapeutic targets.

2. Clinical presentation

2.1. Motor symptoms

ALS is historically considered as a motor disorder, manifesting in a range of phenotypes (Figure 2). Two main forms are classically distinguished based on the site of onset of the initial clinical manifestations. The spinal form is observed in 60 to 75% of patients and is characterised by weakness in the muscles of the upper or lower limbs. Patients can present with symptoms predominantly associated with the degeneration of cortical motor neurons, including overresponsive reflexes (hyperreflexia) and increased muscle tone resulting in muscle stiffness (hypertonia or spasticity). Conversely, patients can present with symptoms associated with the dysfunction of bulbar and spinal motor neurons, including atrophy, cramps, as well as spontaneous and involuntary muscle contractions and relaxations (fasciculations). In both cases, the involvement of the other population of motor neurons becomes apparent at later stages of the disease. The bulbar form affects 20 to 30% of patients and is typified by weakness of the bulbar muscles. This is associated with swallowing difficulties (dysphagia), speaking and articulation impairments (dysarthria), and tongue fasciculations. The remaining 5 to 10% include rare manifestations of a respiratory form, hemiplegic presentation, or flail arm and leg syndrome. All these forms are associated with different prognoses, with the spinal form being the least severe, and the respiratory form leading to the shortest survival.

Irrespective of the form, most patients initially present with focal symptoms in a single body segment, such as subtle weakness or cramping. As the disease progresses, it typically spreads in an anatomically contiguous manner, possibly involving axonal connectivity (Walhout et al., 2018). As a consequence, the contralateral side and adjacent anatomical segments begin to exhibit symptoms. However, non-contiguous development of symptoms is also possible. In both cases, as different sets of motor neurons degenerate, there is a progressive generalisation of the atrophy and paralysis of the target muscles. Ultimately, this results in overall damage to the motor system and a gradual loss of motor capacities. At this stage, patients require the use of a wheelchair and full-time care, while only supportive and palliative measures are available.

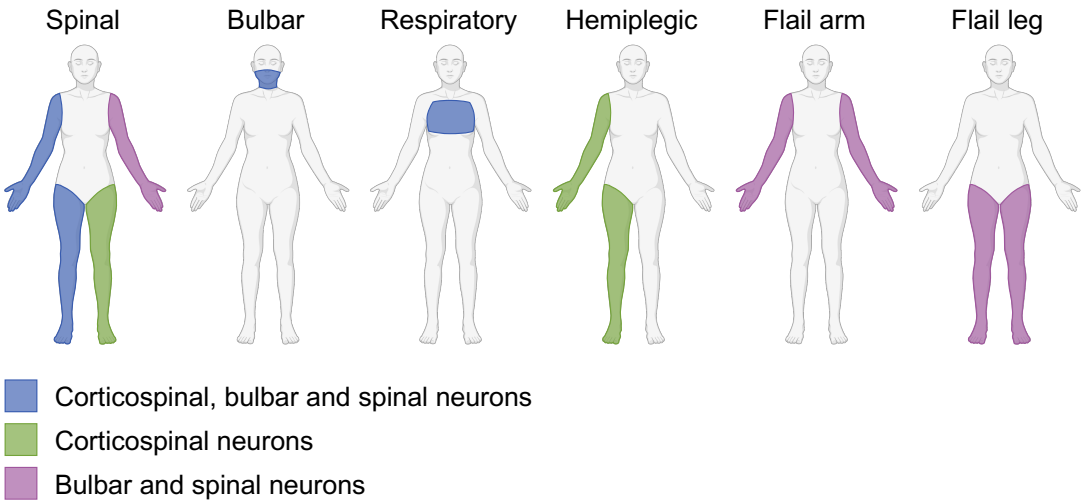


Figure 2: ALS manifests as a range of phenotypes. ALS patients exhibit symptoms associated with corticospinal motor neuron dysfunction (in green), bulbar and spinal motor neuron dysfunction (in purple), or a combination of both (in blue). The first symptoms observed depend on the neuronal population initially affected. Adapted from Feldman et al., 2022.

It is commonly accepted that the sensory and autonomic nervous systems are resilient in ALS. Sphincter and extraocular muscles continue to function even in late disease stages, prompting researchers to investigate the differences between vulnerable and resilient motor neurons, with the aim of identifying the cause of the degeneration of the former. Nevertheless, there is an emerging awareness of autonomic dysfunction in the disease (Fang et al., 2017), and a need for a more detailed examination of potential sensory deficits. The redefinition of the disease, notably with the recognition of neuropsychiatric symptoms, has constituted a significant advancement in the field, reducing the risk of misdiagnosis and enabling the provision of more effective symptomatic treatments for patients. However, sensory and autonomic deficits fall beyond the scope of this manuscript.

2.2. Neuropsychiatric impairments

It is now recognised that ALS is a multisystemic disorder, with a number of patients exhibiting non-motor symptoms, including behavioural, cognitive and psychiatric impairments. Approximately 50% of patients present with varying patterns and severities of behavioural and cognitive deficits, which can occur at an early stage of the disease (Pender et al., 2020). Behavioural deficits include disinhibition, irritability, apathy, a lack of sympathy or empathy, changes in dietary habits and stereotyped behaviours. Cognitive impairments encompass deficits in executive functions, social cognition, and verbal fluency. Working memory can be impaired, whereas long-term and spatial memories remain largely intact. These symptoms have been associated to dysfunction in both cortical and subcortical regions, extending beyond the motor system. In particular, there appears to be a correlation between abnormal structural connectivity

and motor deficits, while disrupted functional connectivity aligns with behavioural and cognitive impairments (Basaia et al., 2020). Moreover, up to 15% of patients fulfil the diagnostic criteria for frontotemporal dementia (Pender et al., 2020). The existence of a continuum between ALS and frontotemporal dementia is now widely acknowledged and will be discussed in greater detail (Part 3, page 34). Finally, depressive and anxiety disorders, fatigue, and sleep disruptions are commonly observed in patients. A sense of despair and preoccupation with the end of life are two prominent features. Not all patient subgroups exhibit the same risk of developing behavioural, cognitive and psychiatric impairments. For instance, some causal-mutations or a bulbar onset of the disease were identified as risk factors of developing cognitive impairments (Yang et al., 2021). Nevertheless, it is important to identify these symptoms and assess their impact on the patients. In particular, behavioural abnormalities and cognitive dysfunction were found to evolve as the disease progress (Beeldman et al., 2020; Crockford et al., 2018), and were associated with a poorer prognosis (Bersano et al., 2020). Patients with cognitive decline exhibit a more rapid functional decline and shorter survival than patients with steady cognitive status. Hence, targeting these symptoms would preserve the quality of life of patients and may slow the progression of motor impairments.

3. Epidemiology

3.1. Incidence and prevalence

ALS is considered as a relatively rare disease, with a lifetime risk of 1 in 350. However, the global annual incidence is estimated to be between 1 and 4 new cases per 100 000 persons (Longinetti and Fang, 2019), which makes it the most common adult-onset motor neuron disease. Given the relatively short life expectancy, the prevalence of ALS is low, with approximately 4 to 8 cases per 100 000 persons. Epidemiological studies show that the number of ALS patients is variable between continents and ethnic groups. However, data regarding the exact geographic distribution of the disease are lacking in certain geographical regions, which may bias this observation. In France, 3 to 4 new cases are diagnosed daily, while it is estimated that there are approximately 6 000 French patients every year (Couratier et al., 2016). On a global scale, some studies reported a stable incidence of ALS over the past three decades, while others suggested a potential increase (Xu et al., 2020). The latter is expected, due to the extended life expectancy and economic growth in numerous aging populations (Arthur et al., 2016). Likewise, ALS prevalence may progressively increase, as management and treatments improve.

3.2. Risk factors and identified causes

ALS is a heterogeneous and multifactorial disease that seem to arise from complex relationships between age (including age-related cellular damage), a burden of

environmental exposures and genetic susceptibility (Al-Chalabi and Hardiman, 2013). In addition, it is becoming increasingly clear that although neuronal death results from different causes, this can converge to common downstream mechanisms.

A. Age and sex

The risk of developing ALS increases with age, is highest around 60 to 79 years, and then decreases (Marin et al., 2018). It is important to note that the symptoms exhibited by elderly patients may be mistaken for the ageing process, which can complicate the diagnosis and potentially introduce biases into the previous result. In addition to acting as a risk factor, the age of patients may be correlated with their survival. Most patients present with initial symptoms between the ages of 51 and 66, with a median survival of 3 to 5 years following diagnosis. In juvenile forms of ALS, symptoms manifest before the age of 25 and progress at a slow rate for over a decade. In contrast, late forms of ALS emerge after the age of 75 and result in death within a few months.

The incidence of ALS also exhibits variation based on sex, with an overall standardised male-to-female ratio between 1 and 2 (Fontana et al., 2021). This ratio is subject to changes depending on the geographic region under consideration, the age at which symptoms first manifest, and the form of ALS. It has been observed that elderly women may be more prone to develop the bulbar form of ALS, whereas young men may be more susceptible to the spinal form of the disease (Chiò et al., 2020). It was proposed that the male-to-female ratio in ALS is gradually declining. This could be attributed to enhanced diagnostic capabilities for women, particularly the elderly, and the fact that women are more exposed to environmental risk factors for ALS than before. Nevertheless, further global and regional studies are necessary to ascertain whether male sex is no longer regarded as a risk factor for ALS.

B. Environment

An increasing body of evidence indicates that environmental factors may play a role in the development of ALS. In particular, it has been proposed that ALS is associated with a progressive accumulation of environmental exposures, including lifestyle factors, throughout the lifespan. A significant body of research has been conducted to examine the potential impact of occupational, residential and professional factors on the risk of developing ALS. There is an historical association between ALS and intense physical activity, a hypothesis that has been supported by several studies (Daneshvar et al., 2021; Julian et al., 2021). Military service is also a recurring factor in the assessment of risk for ALS (McKay et al., 2021). Exposure to plasma persistent organic pollutants (Su et al., 2016) and blood metals (Figueroa-Romero et al., 2020; Peters et al., 2021) was found to correlate with an increased risk of developing ALS, and can influence survival (Goutman

et al., 2019). Additionally, lifetime alcohol consumption, smoking and low body mass index were also reported to increase ALS risk (Ludolph et al., 2023).

C. Genetics

The genetic architecture of ALS is highly complex. To date, more than 40 genes have been identified as being associated with the disease. The frequency, penetrance and mode of inheritance of these genes vary. Overall, ALS is based on monogenic inheritance of rare variants (Cady et al., 2015), meaning that a single gene causes the disease. However, growing evidence suggests possible oligogenic inheritance (a few genes cause the disease) and polygenic inheritance (several genes cause the disease). ALS is also characterized by incomplete heritability, ranging from 37 to 66% depending on the studies (Ryan et al., 2019). Several factors, such as structural variants, epigenetic changes, and environmental factors, may influence heritability (Theunissen et al., 2020; Zhang et al., 2022). In particular, growing evidence reports that the environment impacts the risk and progression of ALS in a gene-dependent manner. Finally, ALS exhibit a genetic pleiotropy, in which a single gene can cause multiple phenotypic manifestations.

ALS is currently classified as either familial or sporadic. In 10 to 15% of cases, the disease manifests with a familial pattern of inheritance, resulting from mutations that are predominantly transmitted as a dominant trait. Known genetic mutations are identified in approximately 70% of familial cases, and both the progression and severity of familial ALS differ depending on the affected gene. Conversely, 85 to 90% of ALS cases are classified as sporadic, as they occur without a documented family history. Known genetic mutations are identified in approximately 15% of sporadic cases, while there is no known cause in the remaining 85%. It is possible that sporadic cases which harbour low penetrant mutations and belong to small families may in fact be familial cases (Al-Chalabi and Lewis, 2011). In addition, incomplete or inaccurate knowledge of family history may lead to misclassification. Consequently, familial ALS may represent 20% of cases. As genetic testing is more widely implemented, it may be beneficial to use the presence or absence of ALS mutations to propose a molecular subclassification of the disease. It has therefore been proposed to distinguish between genetically confirmed and non-genetically confirmed cases.

Increasing epidemiologic evidence associate ALS with a wide spectrum of neuropsychiatric disorders among family members, including autism, schizophrenia, psychosis, suicide, depression, and alcoholism (O'Brien et al., 2017).

4. Diagnosis

In the absence of specific symptoms or biomarkers, the diagnosis of ALS can be a long and meticulous process (Falcão de Campos et al., 2022). It consists in a clinical investigation to exclude other possible and more common diseases, which need to be thoroughly evaluated before being eliminated. This investigation comprises a combination of clinical history and neurological examination, as well as serological and electrodiagnostic testing. Ultimately, the diagnosis of ALS can be delayed for several months. The latter requires a history of progressive weakness spreading within a region or to other regions, with an involvement of corticospinal, bulbar and spinal motor neurons. The revised El Escorial criteria is used to categorise patients as either possible, probable, probable laboratory-supported, or definite ALS, depending on the clinical presentation and electromyography results (Brooks et al., 2000).

Given the rapid progression of the disease, it is particularly important to be efficient and to encourage early neurological referral in order to avoid unnecessary procedures, propose disease-modifying treatments, and facilitate patient enrolment into clinical trials. The current recommendations emphasise the importance of referring patients to a neurologist when they present with progressive limb weakness, swallowing and speaking difficulties, neuromuscular respiratory failure, unexplained weight loss, changes in cognition or executive function, and a family history of neurodegenerative or neuropsychiatric diseases.

While not part of the formal diagnostic criteria for ALS, it also appears essential to evaluate cognition and behaviour (Gosselt et al., 2020), at least to propose adapted supportive therapies. The ALS Cognitive Behavioural Screen (Woolley et al., 2010) and the Edinburgh Cognitive and Behavioural ALS Screen (Abrahams et al., 2014) are two validated, multidomain assessment tools developed for ALS patients, which cover the largest number of cognitive or behavioural impairments specific to ALS. A number of other behavioural and cognitive screening questionnaires exist and can be completed by healthcare professionals or caregivers to assess the evolution of symptoms in patients.

5. Prognosis and staging

For the moment, there is no efficient and accurate tool available for predicting the clinical course of ALS. A number of factors have been demonstrated to impact prognosis, including clinical and demographic characteristics (e.g., age at symptom onset and site of symptom onset), genetic architecture, environmental exposures, weight loss, respiratory function and non-invasive ventilation. Despite this knowledge, prognosis is difficult to predict as it appears to be specific to each patient. The existence of significant intra-familial variation in disease phenotypes and progression lends further support to this

notion. Nevertheless, clinical staging methods can be invaluable for the comparison of participants in clinical studies. In this regard, clinicians typically use the revised functional rating score (ALSFRS-R), which has been demonstrated to be a valuable tool for monitoring the progression of the disease (Bakker et al., 2017). This is achieved by assessing a range of motor capacities that are pertinent to daily life, as well as speech, swallowing and respiration. Novel staging paradigms have also been devised, including the King's system, which is based on the number of affected regions of the body (Roche et al., 2012). Finally, since behavioural and cognitive symptoms may evolve over time, it is also imperative to conduct regular assessments to adapt the supportive therapies.

Regarding biomarker, the levels of neurofilament light chain in the cerebrospinal fluid and blood appear to be an efficient predictor of disease progression (Benatar et al., 2024; Lu et al., 2015). Neurofilaments constitute a specific category of intermediate filaments, serving as indispensable constituents of the cytoskeleton within the nervous system. They play a pivotal role in maintaining the structural integrity of axons. Following damage and degeneration of axons, neurofilaments are released into the cerebrospinal fluid and subsequently into the blood, thus allowing for the measurement of increased levels in these fluids. Elevated levels correlate with a faster disease progression rate, more aggressive disease phenotypes and a shorter survival (Shahim et al., 2024). In some pre-symptomatic gene carriers, neurofilament levels were found to be elevated a few months before the appearance of the first mild motor symptoms (Benatar et al., 2022, 2018; Bjornevik et al., 2021; Weydt et al., 2016). However, this was not true for all patients, thus underscoring the complexity of using neurofilament levels as a biomarker of early disease. In contrast, neurofilament levels appear to be an efficacious pharmacodynamic marker of ALS progression during clinical trials.

6. Treatments

A restricted range of pharmaceutical agents is presently available, and their impact on disease progression is limited. Riluzole was the first pharmaceutical compound to be approved by the Food and Drug Administration in 1995, and the European Medicines Agency in 1996. It is currently suggested that this sodium channel blocker increases the median survival of patients by 6 to 19 months (Andrews et al., 2020), while exerting neuroprotective effects through several mechanisms of action, which collectively contribute to reduce neuronal activity. This encompasses a reduction in glutamate release into the synaptic cleft, coupled with an enhanced reuptake of glutamate by astrocytes, an inhibition of glutamate receptors, a potentiation of GABA receptors, and a diminished reuptake of GABA. The Food and Drug Administration (but not the European Medicines Agency) also approved the use of Edavarone in 2017. Edavarone was initially developed to reduce oxidative stress and neuroinflammatory response. This pharmacological agent has been associated with the slowing of functional decline and the preservation of

respiratory function in ALS patients in half of the studies conducted to date (Witzel et al., 2022). Nevertheless, there is currently no evidence to suggest that this treatment will result in an extension of life expectancy.

To maintain the quality of life of patients, a comprehensive range of supportive therapies are organised and adapted as the disease progresses. Following diagnosis, the primary objective is to preserve the autonomy of patients and alleviate their symptoms. This is achieved through the provision of a range of symptomatic medical treatments, in addition to physical, occupational, psychological, speech and nutritional therapies (Tzeplaeff et al., 2023). With this multidisciplinary approach, several symptoms can be targeted, including cramps, spasticity, pain, depression, anxiety, fatigue, respiratory distress and weight loss. In particular, non-invasive ventilation was found to improve survival and quality of life (Radunovic et al., 2017). Gastrostomy is an effective therapy for supporting nutrition, but is likely of greater benefit when established early in the disease course (López-Gómez et al., 2021), while high calorie nutrition might be helpful for rapidly progressing patients (Ludolph et al., 2020). The use of robotic assistance is becoming increasingly prevalent to facilitate mobility and communication. Finally, access to palliative care can improve the quality of life of patients and primary caregivers, as end-of-life discussions appear to be essential. In all, ALS patients receive a multidisciplinary care plan that has been shown to have a positive effect on disease progression, survival and quality of life (Klavžar et al., 2020; Martin et al., 2017).

A number of therapeutic approaches are currently in development or undergoing evaluation in pre-clinical and clinical studies. These include the use of antibodies targeting mutant proteins, anti-inflammatory therapies, and stem cells-based strategy to provide neurotrophic support (Tzeplaeff et al., 2023). In addition, there is a growing consensus that gene therapy is promising for the treatment of ALS. One strategy is to silence genes which have a known toxic gain-of-function by targeting the messenger RNA with antisense oligonucleotides. The first clinical trial with Tofersen, which is directed against the superoxide dismutase 1 gene, exhibited encouraging outcomes, characterised by a reduction in the protein and neurofilament levels (Miller et al., 2020; Wiesenfarth et al., 2024). Participants who commenced the treatment at an early disease stage exhibited a less pronounced functional decline than those who initiated therapy later during the open-label extension phase of the trial. In light of these observations, participants are being monitored in a long-term evaluation trial, and an additional study has been initiated to examine the effects of Tofersen in presymptomatic individuals who carry a mutation.

Part 2: Frontotemporal dementia (FTD)

Frontotemporal dementia (FTD) is also a neurodegenerative disease with a complex aetiology. The investigation of this disorder is notably challenging due to the rarity of patients and their high degree of heterogeneity. As previously, I will provide an overview of the disease, from its definition to the therapies currently available. We will see that this disease is poorly understood, diagnosed and treated, which highlights the necessity to develop new models to gain deeper insight into the mechanisms at play.

1. Definition

FTD is a fatal neurodegenerative disease that represents one of the most common causes of cognitive decline in patients under the age of 65. It is the third most common form of dementia in all age groups, after Alzheimer's disease and dementia with Lewy bodies. This term describes a clinically diverse group of disorders, characterised by a relatively selective degeneration of the frontal and temporal lobes. The disease typically manifests in individuals around the fifth decade of life, with a mean age of onset of 56 years. The average lifespan of patients diagnosed with this condition is 7 to 13 years, with the majority succumbing to complications arising from comorbidities and malnutrition. Currently, there is no effective treatment available.

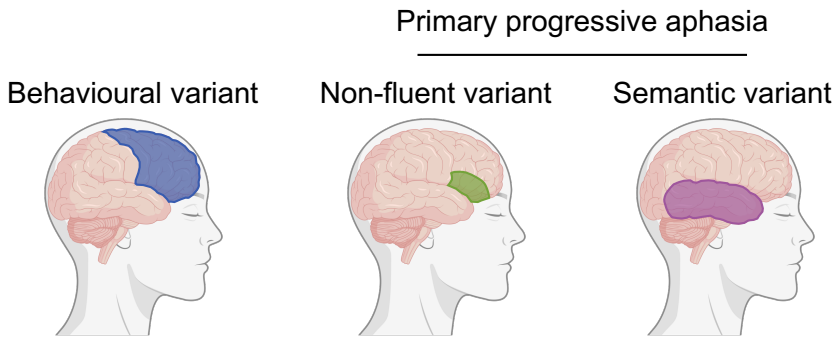


Figure 3: FTD manifests as a range of phenotypes. FTD patients exhibit symptoms associated with frontal and temporal dysfunction. The first symptoms observed depend on the brain region initially affected.

The term FTD encompasses three clinical manifestations, which are distinguished based on the initial brain region affected and the resulting symptoms (Figure 3). In the behavioural variant of FTD, the frontal lobe is initially damaged, which gives rise to a gradual progression of behavioural alterations. This variant constitutes between 50 and 70% of all cases of FTD. The mean age at onset is approximately 58 years, with an average survival period of 8 to 10 years (Coyle-Gilchrist et al., 2016; Kansal et al., 2016). The non-fluent variant of primary progressive aphasia is characterised by the initial degeneration of a restricted region of the frontal lobe, called the inferior frontal gyrus. It represents

about 25% of all FTD patients, with a mean age at onset of approximately 63 years and an average survival of 8 to 9 years. This is the most heterogeneous disorder within the FTD spectrum. The semantic variant of primary progressive aphasia is characterised by initial damage in the temporal lobe. It affects approximately 20% of patients, with a mean age at onset of approximately 60 years and an averaged survival of 11 to 12 years.

2. Clinical presentation

2.1. Behavioural variant

The behavioural variant is characterised by progressive and persistent alterations in personality and behaviour, accompanied by a decline in social skills and executive dysfunction (Piguet and Kumfor, 2020). The symptoms exhibited by patients are highly variable and evolve over time. Nevertheless, a number of core and typical symptoms were identified in the majority of presentations and were classified into six main categories (Rascovsky et al., 2011). These categories are as follows: 1) Social disinhibition, manifested as impulsivity, inappropriate statements and actions, and a childish attitude; 2) Apathy and reduced initiative; 3) Loss of sympathy or empathy; 4) Hyperorality and changes in eating habits; 5) Perseverative, stereotyped and/or compulsive behaviours (for both language and motor behaviours); and 6) Executive dysfunction. In the initial stages of the disease, language and memory functions are typically retained. However, pronounced deficiencies in executive function may lead to impairments in sustained attention span, working memory, planning abilities, verbal fluency, mental flexibility, and problem-solving skills. It is not uncommon to observe in these patients a lack of control, as well as engagement in illegal behaviours and substance abuse. This includes excessive consumption of alcohol and tobacco, gambling, and overspending. In more advanced stages of the disease, a tendency to ingest non-edible objects may also be observed.

2.2. Primary progressive aphasia

The two variants of primary progressive aphasia are characterised by distinct progressive language deficits (Marshall et al., 2018). In the non-fluent variant, patients present with difficulties in the motor programming of speech (apraxia), which is associated with deficits in verbal articulation (Botha and Josephs, 2019). The speech of these patients becomes slow, effortful, and hesitant. The length of the sentences is reduced, and a number of grammatical errors emerge (e.g., errors in verb conjugation, or omissions of prepositions and articles). Patients can comprehend single words but are unable to process complex sentences. In addition, there may be mild deficits in executive functions, particularly in verbal fluency and working memory. In the semantic variant, the language is fluent, but the patients exhibit a progressive decline in their ability to recognise the meaning of words (anomia). It commences with the less commonly used terms and

progresses towards the more frequently used ones. Therefore, patients employ paraphrases to offset their loss of specific terms. Most of these patients demonstrate no significant impairment to their executive functions. However, in advanced stages of the disease, behavioural alterations, including apathy and disinhibition, can be observed in both variants (Harris et al., 2019). In the semantic variant, behavioural deficits also manifest as changes in eating habits, obsessive and compulsive behaviours, irritability, social isolation and emotional detachment.

2.3. Motor symptoms

Up to 40% of patients with FTD present with a range of motor symptoms. The latter can be subtle, manifesting as alterations in fine movements for instance, or frank due to the presence of an overlapping movement disorder syndrome. There is a growing recognition that FTD shares significant clinical, pathological and genetic similarities with progressive supranuclear palsy, corticobasal syndrome, and motor neuron diseases (including ALS). As a consequence, the typical motor dysfunctions associated with these syndromes may be present in FTD patients, particularly in the behavioural variant or non-fluent variant of primary progressive aphasia. This encompasses spontaneous and involuntary muscle contractions and relaxations (fasciculations), muscle atrophy, muscle stiffness (spasticity), and overresponsive reflexes (hyperreflexia) associated with ALS, as well as rigidity and unsteadiness in walking linked to progressive supranuclear palsy, and asymmetric slowness of movements, rigidity or uncontrollable muscle movements linked to corticobasal syndrome. Of note, progressive supranuclear palsy and corticobasal syndrome are sometimes included within the spectrum of FTD.

3. Epidemiology

3.1. Incidence and prevalence

The most recent assessments of FTD incidence and prevalence included patients with progressive supranuclear palsy and corticobasal syndrome and were based on European registries. Hence, the results do not represent the epidemiology of the FTD spectrum in its narrower form (i.e., including only the behavioural variant and both variants of primary progressive aphasia). In light of the aforementioned considerations, the European annual incidence of FTD is currently estimated to be between 1.6 and 2.4 new cases per 100 000 persons (Coyle-Gilchrist et al., 2016; Logroscino et al., 2023). The prevalence is 10.8 cases per 100 000 individuals, and the estimated lifetime risk is 1 in 742. In France, the annual incidence is 2.9 per 100 000 persons. It is noteworthy that the reported prevalence of FTD exhibits worldwide racial and geographic variations. These may be attributed to discrepancies in social norms between cultures, and a lack of medical facilities equipped to diagnose and care for these patients in certain areas.

3.2. Risk factors and identified causes

A. Age and sex

The risk of developing FTD increases with age, reaches a peak around 65 and 70 years, and then declines (Coyle-Gilchrist et al., 2016; Logroscino et al., 2023). Most patients present with initial symptoms at 56 years, with a median survival of 7 to 13 years. However, these parameters are contingent upon the clinical variant under investigation. In addition, approximately 13% of individuals develop symptoms before the age of 50. In patients who inherited a FTD-causing mutation, it is suggested that the age at which their first symptoms manifest is correlated with the age at which the parents (or other family members) exhibited their first symptoms (Moore et al., 2020). However, this observation may not apply to all mutations, and further investigation into the factors influencing the phenotype is required to improve these estimations. It is generally accepted that sex is a risk factor for FTD, as women and men are affected in equal numbers. However, there is evidence suggesting that sex may exert an influence on the clinical phenotype of patients. For instance, the behavioural variant of FTD is overrepresented in men, while primary progressive aphasia is more common in women (Pengo et al., 2022).

B. Environment

The available evidence concerning the potential association between environmental factors and the risk of developing FTD is limited (Rasmussen et al., 2018). It has been proposed that there is an increased risk associated with diabetes, as well as with smoking and being overweight. However, we currently do not know the duration of the prodromal phase in FTD. Hence, it is possible that smoking and overweight represent prodromal symptoms rather than modifiable risk factors. Autoimmune disease may also be associated with an increased risk of primary progressive aphasia. Finally, head injury may elevate the risk of FTD, and the prevalence of traumatic brain injury is significantly higher in patients with FTD than in patients with other forms of dementia (Deutsch et al., 2015).

C. Genetics

A family history of dementia, psychiatric diseases, movement disorders or motor neuron diseases is present in 30 to 50% of patients with FTD (Rohrer et al., 2009). This heritability varies across the different clinical variants, with the behavioural variant being the most commonly inherited (40-45% of patients exhibit a familial form of the disease), followed by the non-fluent variant of primary progressive aphasia (5%) and the semantic variant (< 1%). In familial FTD, approximately 10% of patients demonstrate a clear autosomal dominant inheritance of the mutation. In the remaining cases, the disease manifests in a patient without a documented family history.

4. Diagnosis

An early and accurate diagnosis of FTD is crucial, as it allows for the appropriate therapeutic interventions. The principal diagnostic tool currently employed is the clinical examination. This comprises an evaluation of the medical and family history, neurological examinations with particular focus on the cranial nerves and motor system, and cognitive examinations. A plethora of neuropsychological assessments are available and aim at investigating multiple cognitive domains while being oriented towards the dysfunction of specific brain structures. As previously stated, the behavioural variant of FTD is now understood to be characterised by six core symptoms: disinhibition, apathy, loss of empathy, altered eating behaviour, stereotyped attitude, and impaired executive functions. The diagnostic criteria, which are accepted and used to date, are divided into three levels of certainty: "possible" is based upon the presence of at least three core symptoms; "probable" is based on clinical manifestations supported by a functional decline and neuroimaging showing cortical changes; " definite" is given to patients with a clinical syndrome supported by a causal mutation or histopathological evidence (Rascovsky et al., 2011). The diagnostic criteria for primary progressive aphasia are based on the assessment of specific speech impairments (Mesulam et al., 2012).

The differentiation of FTD from other prevalent neurodegenerative or psychiatric conditions remains a challenge. For instance, young patients exhibiting pronounced personality and behavioural alterations often receive an incorrect initial diagnosis of schizophrenia, bipolar disorder, or depression. The presence of biomarkers that are highly indicative of other neurodegenerative diseases or early memory impairments are regarded as exclusionary criteria for FTD. However, it is becoming increasingly recognised that early memory deficits are a feature of some patients with FTD. Conversely, elevated neurofilament levels are observed in all three variants of FTD and can assist in differentiating them from psychiatric disorders (Ducharme et al., 2020). Finally, neuroimaging can help identify the variants of FTD, as each FTD syndrome is associated with atrophy in specific brain regions (Figure 3). These patterns of atrophy can be observed using magnetic resonance imaging or 18F-fluoro-2-deoxyglucose positron emission tomography to assess decreased metabolism.

5. Prognosis and staging

As symptoms evolve over time and may necessitate adjustments in the therapeutic interventions, it is crucial to periodically reassess the behavioural, cognitive and language alterations of patients. To this aim, a number of neuropsychological assessments are available, including the Mini-Mental-State Examination and Clinical Dementia Rating, which quantifies the severity of cognitive and dementia symptoms, respectively. The progression of the disease can also be evaluated with neuroimaging techniques, as a

progressive atrophy in the brain region initially affected and extension to other regions are observed during the disease course. However, apart from this individual follow-up, there is no tool available to predict the clinical course of FTD, nor are there any clear factors that impact the prognosis of the disease. Recently, it has been proposed that hippocampal atrophy may serve as an effective predictor of disease progression, whereas a number of other factors (including regular alcohol consumption and comorbidities) do not (Ghouri et al., 2023). In addition, elevated levels of neurofilaments light chain in the cerebrospinal fluid and blood seem to correlate with more aggressive disease phenotypes and a shorter survival period (Ljubenkov et al., 2018; Rohrer et al., 2016; Skillbäck et al., 2017). However, the efficacy of the prediction may vary between the clinical variants. In gene carriers followed over a two-year period, a stepwise increase in plasma neurofilament levels was observed, progressing from the asymptomatic phase to the prodromal phase to the complete phenotype (Rojas et al., 2021).

6. Treatments

For the moment, there is no established treatment for FTD that has been demonstrated to be effective. In order to maintain the autonomy and quality of life of the patients, medical facilities offer education to patients and caregivers, as well as a range of physical, occupational and speech therapies (Tsai and Boxer, 2016). In addition, symptomatic therapies may be employed with the objective of controlling symptoms. Selective serotonin reuptake inhibitors represent the most commonly utilised pharmacological therapies, and have been demonstrated to reduce depression, irritability, disinhibition, dietary changes and compulsivity (Huber et al., 2022). Antidepressant, antipsychotic and anticonvulsant medications are also often considered for the treatment of behavioural symptoms, such as severe agitation and disinhibition. However, the evidence supporting their efficacy is limited, and their side effects should restrict their use.

A number of pharmacological trials are currently in progress. Some aim to reduce the toxic effect of mutated genes or proteins by preventing the expression of messenger RNA with antisense oligonucleotides, inhibiting pathogenic post-translational modifications, or promoting the clearance of pathological aggregates with antibodies. Other trials aim to enhance the transcription of wild-type genes or to replace the mutated alleles with viral vectors. Non-invasive brain stimulation techniques, including transcranial electrical and magnetic stimulations, are also the subject of increasing research and may offer a promising avenue for the alleviation of cognitive symptoms. This approach is based on the modulation of neuronal population activity and the induction of specific oscillations, with the objective of restoring brain activity and subsequently alleviating symptoms. The protocols that have been tested to date demonstrated moderate and heterogenous effects, notably on language improvement in primary progressive aphasia (Sanches et al., 2020).

Part 3: ALS-FTD continuum

Despite considerable heterogeneity in the presentation of symptoms, it has been established for a decade now that ALS and FTD exhibit clinical, genetic and histopathological overlaps. One of the earliest indications of this association was the clinical observation that both disorders can manifest within a family or even within an individual. As previously stated, approximately 50% of patients with ALS exhibit behavioural and cognitive deficits, which are all core symptoms of FTD (Pender et al., 2020). Conversely, up to 40% of patients with FTD manifest a range of motor symptoms, including those that are reminiscent of ALS. When these clinical manifestations are severe, patients with ALS meet the diagnostic criteria for FTD, and *vice versa*. In total, 15% of patients receive both diagnoses, although this number may be an underestimate due to the prevalence of one condition over the other. These two neurodegenerative diseases are now considered as part of a single continuum, with pure ALS and pure FTD representing the two extreme ends. Here, I will describe the genetic and neuropathological continuum, while highlighting some shared pathological mechanisms.

1. Genetic continuum

It is now evident that the same genes can lead to either ALS, FTD, or a combination of both, sometimes within the same family. This discovery served to reinforce the idea that ALS and FTD converge into a single spectrum. Currently, a dozen of genes is known to be associated with the ALS-FTD continuum (Figure 4). This includes *C9ORF72*, *TARDBP* and *TBK1*, which will be described briefly here, as well as fused in sarcoma (*FUS*), which will be introduced later (Part 6, page 91). Additionally, there are genes that are exclusively associated with pure ALS, such as *SOD1*, and genes that are exclusively associated with pure FTD, such as *MAPT* and *GRN*. As next-generation sequencing and genome-wide association studies become more accessible, it is reasonable to anticipate that this list will continue to expand in the coming years.

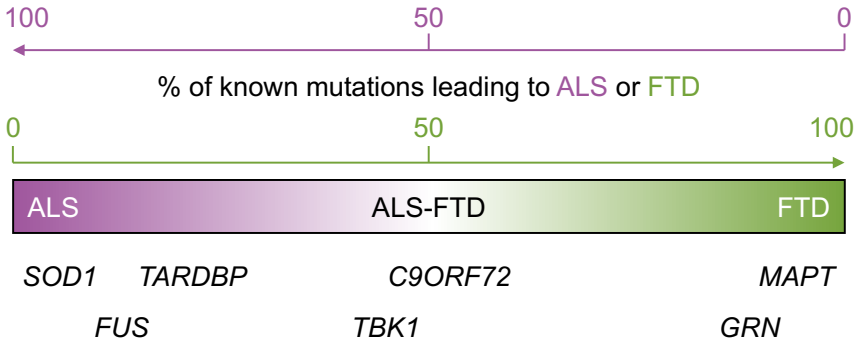


Figure 4: Genetic overlap of ALS and FTD. A number of genes have been identified as the cause of ALS, FTD or both. In this figure, they are plotted according to the ratio of known mutations that lead to ALS or FTD. Adapted from Ling et al., 2013.

1.1. Chromosome 9 open reading frame 72 (*C9ORF72*)

Since 2011, pathogenic hexanucleotide repeat expansions in a non-coding region of the chromosome 9 open reading frame (*C9ORF72*) gene were found to be the most common genetic cause of ALS, FTD, and ALS-FTD (DeJesus-Hernandez et al., 2011; Renton et al., 2011). The threshold for repeat expansion length that would confer pathogenicity remains unclear. Most healthy individuals carry less than 20 repeats, whereas ALS and FTD patients can exhibit between 100 and 1000 repeats. This mutation is responsible for 40% of familial ALS cases, 7% of sporadic ALS (Akçimen et al., 2023), and 25% of familial FTD. We still do not know why some patients develop ALS while others develop FTD or a combination of both, sometimes within the same family.

The majority of *C9ORF72*-related FTD cases are diagnosed with a behavioural variant. However, these patients present with a distinctive set of prominent neuropsychiatric symptoms, including hallucinations, psychosis, and delusions. In ALS, C9ORF72 repeat expansions cause classic symptoms. It is noteworthy that these expansions have also been identified as a rare cause of other neurodegenerative conditions, including Alzheimer's and Parkinson's diseases, progressive supranuclear palsy, corticobasal syndrome, ataxia, Huntington disease-like and Creutzfeldt–Jakob disease.

The functions of the C9ORF72 protein remain incompletely characterised, although it has been associated with the regulation of vesicle trafficking, lysosome homeostasis, and autophagy (Pang and Hu, 2021). Several mechanisms have been proposed to elucidate how repeat expansion causes neurodegeneration (Sellier et al., 2024). This encompasses both a haploinsufficiency of endogenous C9ORF72 protein, and a gain of toxicity due to the formation of RNA aggregates (foci) and/or dipeptide repeat proteins. Subsequent alterations were identified in several cellular mechanisms (Figure 6). The data supporting each of these hypotheses is compelling, and it is possible that multiple mechanisms, acting either simultaneously or sequentially, are responsible for the death of neurons.

1.2. Transactive response DNA binding protein of 43 kDa (*TARDBP*)

In 2008 and 2009, the transactive response DNA binding protein of 43 kDa (*TARDBP*) gene was found to cause ALS (Kabashi et al., 2008; Sreedharan et al., 2008), FTD (Borroni et al., 2009), and ALS-FTD (Benajiba et al., 2009). More than 30 *TARDBP* mutations were identified and are responsible for 4% of familial ALS cases, 1% of sporadic ALS (Akçimen et al., 2023), and 1% of FTD. These mutations result in classic ALS symptoms or FTD with a behavioural variant. However, some patients manifest semantic or non-fluent variants of primary progressive aphasia at the initial stage of the disease (Caroppo et al., 2016).

TARDBP encodes TDP-43, a protein that shares the same nomenclature as the gene. TDP-43 is a DNA and RNA binding protein with functional homology to FUS. In physiological conditions, TDP-43 is predominantly nuclear, and is involved in a number of processes related to RNA metabolism, including transcription, splicing, transport and stabilisation of messenger RNA. In addition to regulating its own messenger RNA expression levels, TDP-43 is crucial for maintaining normal expression levels and splicing patterns of over 1000 messenger RNAs (Polymenidou et al., 2011). It can be reasonably deduced that mutations affecting the function of TDP-43 have the potential to impair a wide range of downstream cellular pathways (Figure 6). In addition, *TARDBP* mutations increase the aggregation potential of the protein. Consequently, two mechanisms have been proposed to explain how mutated TDP-43 induces neurodegeneration (Hergesheimer et al., 2019). Neuronal death could be linked to the nuclear depletion of TDP-43, which is trapped in cytoplasmic aggregates. Alternatively, the aggregates themselves may possess an inherent toxic property. However, the toxicity of aggregated TDP-43 is still under debate.

1.3. TANK-binding kinase 1 (*TBK1*)

In 2015, the TANK-binding kinase 1 (*TBK1*) gene was demonstrated to be associated with ALS (Cirulli et al., 2015), FTD (Pottier et al., 2015), and ALS-FTD (Le Ber et al., 2015). TBK1 is a ubiquitously expressed serine/threonine kinase, which is involved in a number of cellular processes, including autophagy and immune signalling. More than 90 mutations were identified, and were reported to result in loss of function of TBK1 (Figure 6), associated with a decrease in *TBK1* messenger RNA expression and protein levels (Freischmidt et al., 2015). Missense mutations seem to cluster within the domain that is responsible for the interaction between TBK1 and adaptor proteins, thereby preventing TBK1 functions. These mutations are responsible for less than 1% of familial or sporadic ALS cases (Akçimen et al., 2023), and between 0.4 and 1.7% of FTD and ALS-FTD. *TBK1* mutations are associated with bulbar onset ALS and fast-progressing behavioural FTD (Freischmidt et al., 2015).

1.4. Superoxide dismutase 1 (*SOD1*)

The superoxide dismutase 1 (*SOD1*) gene was the first gene discovered in familial ALS in 1993 (Rosen et al., 1993). Since then, more than 200 mutations spanning the entire length of the gene have been identified, and most of the disease-causing variants appear to be missense mutations. Several different mechanisms of neurodegeneration have been proposed (Figure 6), including conformational instability of the mutant SOD1 protein and formation of toxic aggregates, but the exact mechanisms remain unclear. The consensus is that the mutations confer a toxic gain of function, which has led to the development of silencing mutant gene expression as a therapeutic approach (Part 1, Treatments, page 26). These mutations are responsible for 12% of familial ALS cases and 2% of sporadic ALS

(Akçimen et al., 2023). The clinical phenotype is variable across the different *SOD1* mutations, but in general, the initial phase of the disease affects both lower limbs. For some genetic variants, the phenotype can be remarkably stereotypical. This is exemplified by patients with the homozygous D90A mutation, who have a relatively long disease duration (Jonsson et al., 2009).

1.5. Microtubule-associated protein tau (*MAPT*)

In 1994, the microtubule-associated protein tau (*MAPT*) gene was found to be associated with a form of FTD with parkinsonism (Lynch et al., 1994). More than 80 exonic and intronic mutations have now been identified and are associated with different tauopathies. In axons, the tubulin associated unit (tau) protein co-assembles with tubulin and is involved in microtubule assembly and stabilisation, as well as axonal transport, which in turn regulates neuronal activity, neurogenesis, iron transport, and synaptic long-term depression (Wang and Mandelkow, 2016). Three main mechanisms have been proposed to explain how *MAPT* mutations cause neurodegeneration: a loss of function of tau due to its hyperphosphorylation and/or aggregation, a toxic gain of function intrinsic to the mutant, hyperphosphorylated and/or aggregated forms of tau, and synaptic dysfunctions due to the mislocalisation of tau into postsynaptic spines. The first two mechanisms are associated with microtubule disassembly and axonal transport defects (Figure 6). The clinical presentation of patients harbouring *MAPT* variants is heterogeneous even within the same family, and includes both the behavioural variant of FTD and the non-fluent variant of primary progressive aphasia (Snowden et al., 2015).

1.6. Progranulin (*GRN*)

In 2006, the progranulin (*GRN*) gene was identified as a cause of FTD (Cruts et al., 2006). More than 70 different mutations have been described, including frameshift, splice, nonsense and deletion mutations. Progranulin is a glycoprotein expressed by neurons and microglia that is cleaved to produce small proteins called granulins. Both progranulin and granulins act as growth factors, regulating cell cycle and motility. They are involved in several biological processes, including brain development, synaptic function, lysosome homeostasis and inflammation (Paushter et al., 2018). Following its mutation, GRN haploinsufficiency is thought to cause neurodegeneration via lysosomal dysfunction, microglial activation, and excessive complement-dependent synaptic pruning (Figure 6). *GRN* mutations are associated with a wide phenotypic heterogeneity, with the most common clinical diagnoses being the behavioural variant of FTD and the non-fluent variant of primary progressive aphasia.

2. Histopathological continuum

ALS and FTD are both characterised by the aggregation of proteins in neuronal and glial cells. As previously stated, the mutation of *C9ORF72*, *SOD1*, and *MAPT* results in the aggregation of the encoded proteins. Nevertheless, the prominent presence of ubiquitin- and p62-positive inclusions has been observed in ALS-FTD, irrespective of the presence of a mutation. Ubiquitin and p62 are involved in the proteasome and autophagy degradation pathways, which are both altered in ALS-FTD. The precise composition of these inclusions varies according to the cell type and patient, although some key protein components have been identified (Figure 5). These include FUS, which will be introduced later (Part 6, page 91), and TDP43, which represents the most prominent example of histopathological overlaps between ALS and FTD (Arai et al., 2006; Neumann et al., 2006).

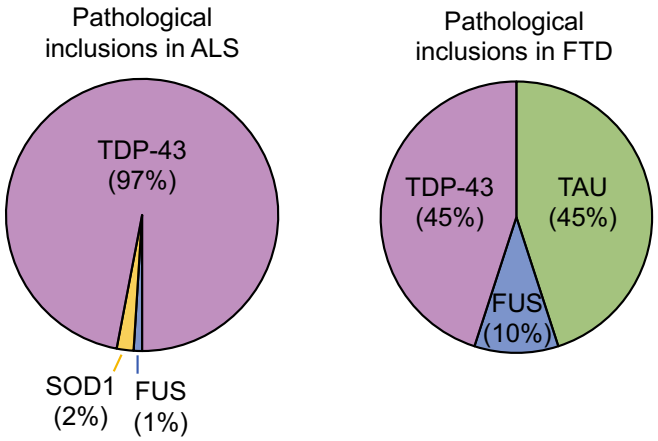


Figure 5: Pathological overlap of ALS and FTD. Major proteins found to be aggregated in ALS and FTD patients. In this figure, they are plotted according to the percentage of patients who exhibit these pathological inclusions. Adapted from Ling et al., 2013.

TDP-43 inclusions are found in 97% of ALS patients and 45% of FTD patients. In ALS, TDP-43 pathology appears to be comparable between sporadic patients and patients exhibiting *TARDBP* mutations (Pamphlett et al., 2009). These inclusions can be observed in the primary motor cortex, brainstem motor nuclei, and spinal cord, as well as outside of the motor cortex, where they may correlate with non-motor systems. In FTD, the inclusions are typically observed in the frontotemporal neocortex and hippocampus, and can be present in any of the major clinical phenotypes (i.e., the behavioural variant and both variants of primary progressive aphasia) (Cairns et al., 2007).

The exact mechanisms linking these inclusions to neurodegeneration are still unclear. Because these inclusions are dense and insoluble, proteins and RNA are sequestered inside them and can no longer fulfil their functions. In addition, these aggregates may themselves be toxic, as they can increase oxidative stress in cells, which in turn increases the propensity to form aggregates, thus creating a vicious cycle.

3. Proposed pathogenic mechanisms

Overall, despite extensive research, the causative pathogenic mechanisms in ALS and FTD are still unclear. It is likely that multiple factors contribute to the development and progression of the diseases. In view of the high genetic and phenotypic variations between patients, it is also possible that the initial pathological events are different between subgroups of patients. Adding a layer of complexity, we also know that several cell types are involved beyond the main degenerating neurons. All of this led to the proposal of a large number of mechanisms (Figure 6). These include disturbances in DNA and RNA metabolism, impaired protein homeostasis, nucleocytoplasmic transport defects, axonal transport defects, vesicular transport defects, oxidative stress, neuroinflammation, mitochondrial dysfunction, excitotoxicity and oligodendrocyte dysfunction. Clarification is now needed on the timing and extent to which each of these mechanisms contributes to the pathogenesis of ALS and FTD.

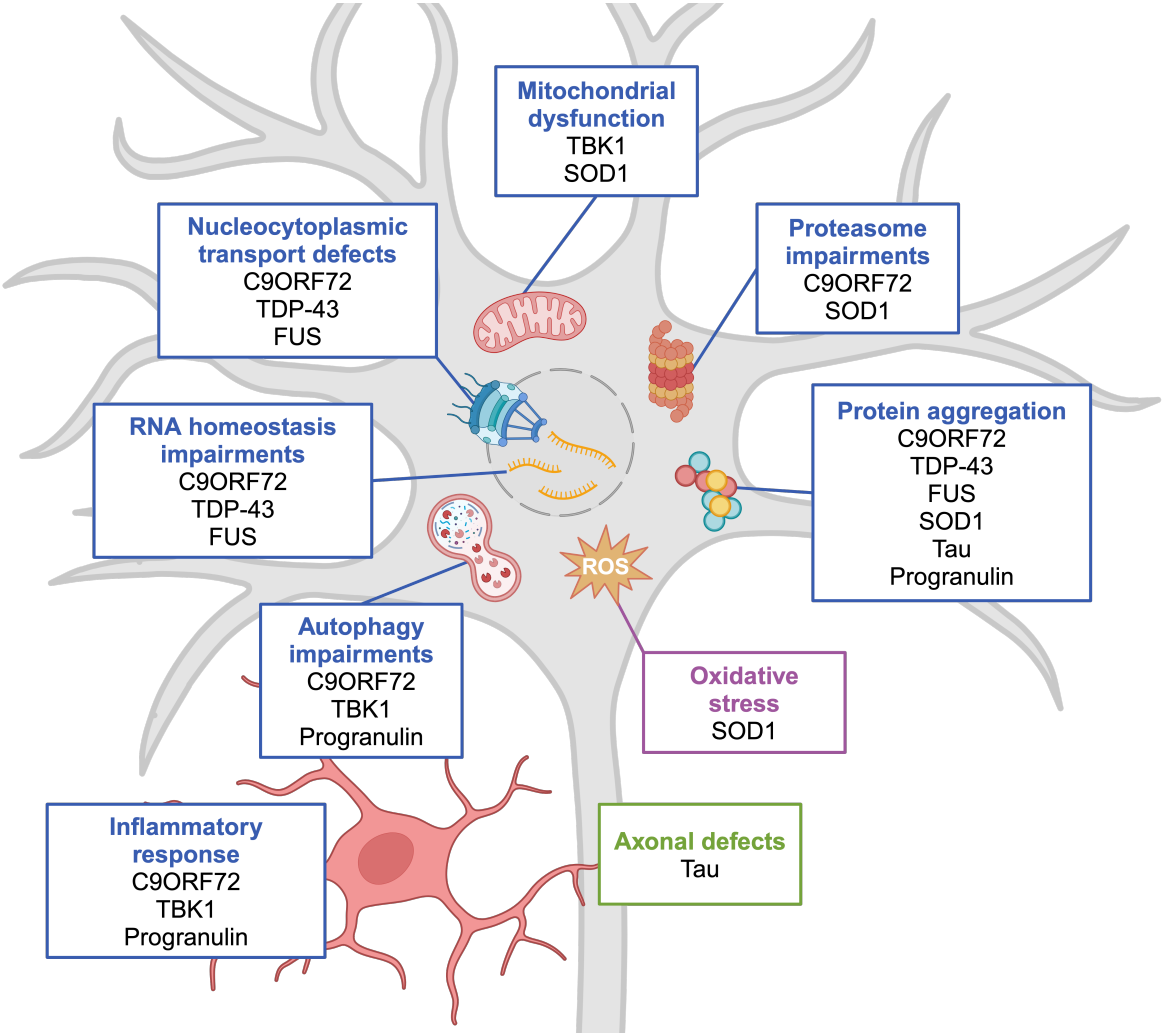


Figure 6: The ALS-FTD continuum is associated with a range of pathogenic cellular pathways. Alterations in blue were reported in ALS and FTD, while alterations in purple were reported in ALS only and alterations in green in FTD. Adapted from Ranganathan et al., 2020.

4. Neuronal circuit dysfunctions

There is now compelling evidence that neuronal circuit dysfunction is an early feature of both ALS and FTD. The development, maintenance and functioning of neuronal circuits depend on several factors. In particular, the activity of a neuronal population is determined by three key factors: the intrinsic excitability of the neurons, the strength of the synapses, and the quantity and timing of excitatory and inhibitory inputs. The intrinsic excitability of a neuron, defined as its propensity to generate action potentials in response to a stimulus, is contingent upon its biophysical properties. These are, to some extent, defined by the composition, affinity and quantity of receptors and ion channels.

Cortical excitability was then defined as "the strength of the response of cortical neurons to a given stimulation, [which] reflects neuron reactivity and response specificity" (Ly et al., 2016). In humans, it is assessed using a combination of transcranial magnetic stimulation and electro-encephalography. Transcranial magnetic stimulation is a non-invasive procedure during which a local magnetic field is applied over the head of the patient to depolarise neurons beyond their firing threshold. In the case of the motor cortex, this stimulation is coupled to a simultaneous recording of the motor-evoked potential in the contralateral innervated muscle.

There is now compelling evidence that cortical excitability is increased is ALS patients compared to healthy controls, and this appears early in the diseases course (Menon et al., 2020, 2015; Shibuya et al., 2017; Van den Bos et al., 2018; Vucic and Kiernan, 2006; Zanette et al., 2002). This increased cortical excitability was also detected in FTD patients (Bae et al., 2016; Benussi et al., 2017; Burrell et al., 2011).

Studies addressing electrophysiological alterations in human bulbar and spinal motor neurons have to be conducted *in vitro*, using induced pluripotent stem cell-derived motor neurons from patient fibroblasts. These motor neurons exhibited increased excitability and activity in early cultures (Devlin et al., 2015; Wainger et al., 2014), followed by a decreased excitability and activity when maintained longer (Devlin et al., 2015).

These alterations in excitability may be attributed to an increased intrinsic excitability and/or an increased excitation and/or a decreased inhibition. In fact, all the components regulating the functioning of neuronal circuits have been reported to be altered in ALS and FTD. This includes altered intrinsic excitability (Gunes et al., 2020), impaired excitatory and inhibitory inputs (Mora and Allodi, 2023), altered neuromodulation (Brunet et al., 2020) and impaired support by the glial cells. Furthermore, these alterations are not isolated but rather influence each other and are potentially accompanied by compensatory or maladaptive mechanisms. Finally, these alterations may be specific to the cell type, area of the central nervous system and stage of the disease.

One potential -but perhaps overly simplistic- model suggests that ALS and FTD are characterised by an imbalance between excitation and inhibition, which is shifted towards unopposed excitation, ultimately becoming pathological.

The use of functional magnetic resonance imaging has produced disparate outcomes in ALS patients. To elucidate this discrepancy, it was proposed that there is an increased functional connectivity at early stages of the disease, followed by a decrease as the disease progresses (Kocar et al., 2021). Electroencephalography (Iyer et al., 2015) and magnetoencephalography (Proudfoot et al., 2018) studies also reported results consistent with an increased functional connectivity in ALS. Two underlying mechanisms may explain this increase: additional brain structures may be recruited to compensate for structural damage, and/or local inhibitory circuitries may be impaired.

Overall, these results prompt the necessity to study the contribution of inhibitory neurons to the amyotrophic lateral sclerosis and frontotemporal dementia continuum.

Part 4: Inhibitory neurons

Over the past two decades, there has been a significant expansion in research on inhibitory neurons. This is largely attributable to advances in molecular genetic techniques for labelling, monitoring and manipulating specific populations of neurons. These techniques have facilitated a deeper understanding of the organisation of neuronal circuits and their role in behaving animals. Most of the studies quoted below were carried out with rodents. Overall, it seems that the same basic inhibitory neurons exist across most mammalian species (Hodge et al., 2019). However, it is important to note that the relative abundance, distribution, gene expression patterns, morphologies, and electrophysiological properties of inhibitory neurons can differ between rodents and primates (Krienen et al., 2020). Therefore, subdivisions and specialisations of these cells may vary. In this manuscript, I used a biochemical definition of inhibitory neurons and gathered data regarding neurons that release the two main inhibitory neurotransmitters: GABA and glycine.

1. Inhibitory neurotransmitters

1.1. GABAergic transmission

Gamma-aminobutyric acid (GABA) is a non-protein amino acid that has many roles in the central nervous system and is distributed in different cellular populations reflecting its multiple functions. It is estimated that at least 40% of inhibitory synapses use GABA. Its ubiquitous presence in the brain and spinal cord means that almost all neurons either release GABA (Figure 7), express GABA receptors, or are innervated by neurons that do. GABA is the principal inhibitory neurotransmitter in the mature brain.

A. Organisation of the synapse

GABA is synthesized from glutamate via the activity of the glutamic acid decarboxylase (GAD), whose two main isoforms are GAD_{65} and GAD_{67}, with molecular weights of 65 and 67kDa, respectively. In inhibitory neurons of the mature neocortex, hippocampus, cerebellum and dorsal horn of the spinal cord, GAD_{67} synthesises approximately 90% of the GABA. In the presynaptic compartment, GABA is loaded into vesicles by the vesicular GABA transporter (VGAT) and is liberated by calcium-dependent exocytosis. GABAergic transmission is terminated by the reuptake of GABA into the presynaptic compartment and the uptake into the surrounding astrocytes. In both cases, it involves plasma membrane GABA transporters (GAT). These transporters depend on the cotransport of sodium and chloride ions to transfer GABA. In GABAergic axons, this uptake is mostly ensured by GAT1, while astrocytic GAT3 provides approximately 20% of the reuptake. In the astrocytes, GABA is degraded and ultimately converted to glutamate and glutamine.

Astrocytic glutamine can then be transported to GABAergic neurons by a glutamine transporter, which may constitute the primary source of glutamate (Bak et al., 2006).

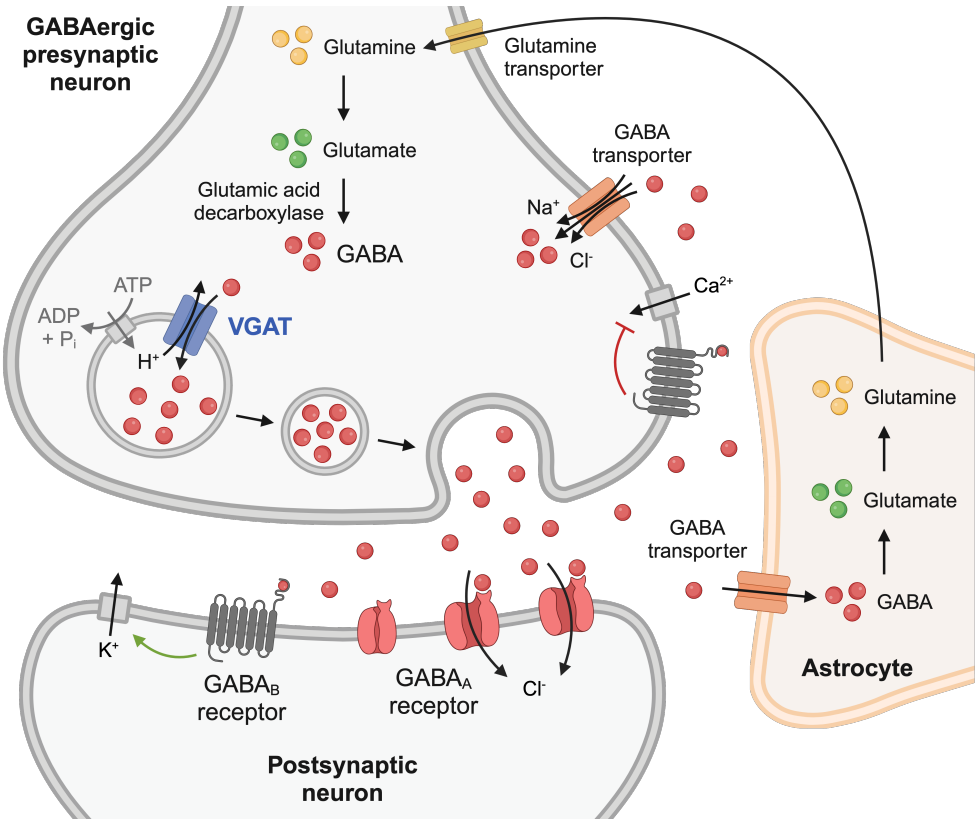


Figure 7: Organisation of a GABAergic synapse. ADP + P_i: adenosine diphosphate and inorganic phosphate; ATP: adenosine triphosphate; Ca^{2+}: calcium; Cl^-: chloride; H^+: proton; K^+: potassium; Na^+: sodium.

B. GABA receptors

GABA activates ionotropic ligand-gated ion channels, called $GABA_A$ receptors, and metabotropic G protein-coupled receptors, called $GABA_B$ receptors. These receptors can be found in the pre- and postsynaptic compartments. In the central nervous system, most of the fast synaptic inhibitory transmission is mediated by $GABA_A$ receptors. These receptors are composed of five heteromeric subunits belonging to seven different subunit families (α1-6, β1-3, γ1-3, δ, ε, π, and θ). $GABA_A$ receptors contain at least one α, one β, and one γ subunit. In the brain, $GABA_A$ receptors are predominantly composed of a combination of α1-2, β1-3 and γ2 subunits. However, this composition varies among the brain regions (Sieghart and Sperk, 2002). In the dorsal horn of the spinal cord, $GABA_A$ receptors mostly consist of α3, β3 and γ2 subunits (Paul et al., 2012). The different subunit compositions exhibit their own pharmacological and electrophysiological properties. Of note, a third GABA receptor, called $GABA_C$, is considered as a variant of $GABA_A$ receptors, and is composed only of single or multiple ρ1-2 subunits. The binding of GABA to the $GABA_A$ and $GABA_C$ receptors induces an influx of chloride ions and mediates

hyperpolarization of the membrane potential. $GABA_B$ receptors are composed of two subunits, $GABA_{B1}$ (1a and 1b) and $GABA_{B2}$. In the spinal cord, $GABA_B$ receptors are found in the dorsal horn and motor neuron pool. The binding of GABA to $GABA_B$ receptors results in a cascade of signalling pathways, which either inhibit neurotransmitter release from the presynaptic compartment (notably by inhibiting the influx of calcium in excitatory or inhibitory synapses) or participates in the inhibition of the postsynaptic potential (notably by activating the efflux of potassium ions).

1.2. Glycinergic transmission

In the brainstem and spinal cord, both GABA and glycine ensure inhibition either in distinct neurons (Figure 8) or in neurons co-expressing them. The latter is especially true in the dorsal horn of the spinal cord (Dougherty et al., 2009), while in the ventral horn, inhibitory neurons are mainly glycinergic.

A. Organisation of the synapse

Prior to synaptic release, glycine is loaded into vesicles via VGAT, just as for GABA. The glycinergic transmission is terminated by the reuptake of glycine into the presynaptic compartment and the uptake into the surrounding astrocytes. In both cases, it involves plasma membrane glycine transporter (GlyT), which depends on the cotransport of sodium and chloride ions to transfer glycine. There are two types of transporters: GlyT1 at the astrocytic membrane and GlyT2 at the axon terminal (Eulenburg et al., 2005). In astrocytes, glycine may be locally degraded. In neurons, the pathway leading to the production of glycine is still unclear. High-affinity uptake systems, mediated by GlyT2, are considered as the main regulators of intracellular glycine concentrations. In addition, serine hydroxymethyltransferase can synthetise glycine. However, the knockout of GlyT2 in mice results in early lethality during the second postnatal week due to a lack of glycine (Gomeza et al., 2003; Latal et al., 2010), which suggests that *de novo* synthesis is not sufficient to ensure glycinergic transmission.

B. Glycine receptors

The glycine receptor is an ionotropic ligand-gated ion channel that consists of five subunits belonging to two different subunit families (α1–3 and β). As for GABA, the subunits composition varies among the regions of the central nervous system and influences the electrophysiological properties of the receptor. The binding of glycine to these receptors induces an influx of chloride ions and mediates hyperpolarization of the postsynaptic membrane potential.

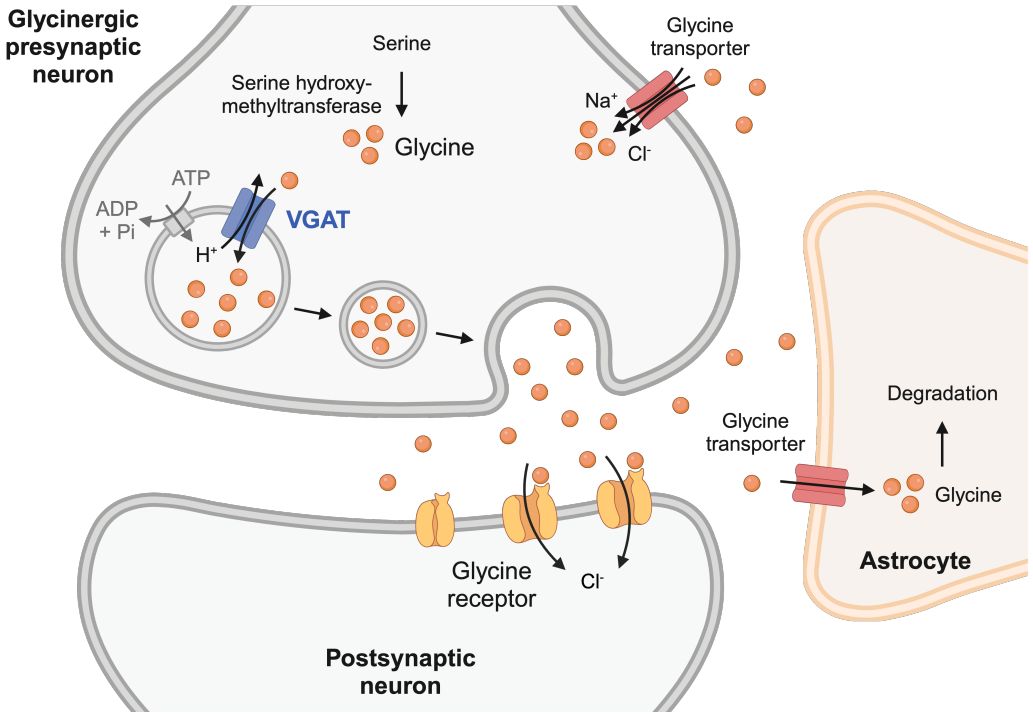


Figure 8: Organisation of a glycinergic synapse. ADP + P_i: adenosine diphosphate and inorganic phosphate; ATP: adenosine triphosphate; Cl^-: chloride; H^+: proton; Na^+: sodium.

1.3. Focus on the shared vesicular transporter

To date, VGAT, also known as vesicular inhibitory amino acid transporter (VIAAT), is the sole identified transporter allowing the filling of synaptic vesicles with GABA and glycine in inhibitory presynaptic compartments (McIntire et al., 1997; Sagné et al., 1997). Hence, the presence of VGAT is considered essential for GABAergic and glycinergic transmissions (Figure 7 and Figure 8). This indicates that VGAT is an optimal candidate for targeting most cerebral and spinal inhibitory neurons. Of note, this proton antiporter is composed of 9 transmembrane domains, and is encoded by *Slc32a1*, but for the sake of simplicity, we will refer to the *Vgat* gene in this manuscript.

In C57BL/6J mice, VGAT expression was detected as soon as embryonic day (E) 11 by immunohistochemistry (Kosaka et al., 2012). The knockout of *Vgat* in mice demonstrated that this transporter is essential for inhibitory neurotransmission and embryonic development. Indeed, these mice died between E18.5 and birth, and exhibited abdominal defects and a cleft palate (Wojcik et al., 2006). In addition, they were completely stiff, immobile and their motor functions were severely impaired (Saito et al., 2010; Wojcik et al., 2006). Electrophysiological recordings revealed minimal to no spontaneous inhibitory postsynaptic currents, resulting in an imbalance between excitation and inhibition. Since then, several transgenic or knock-in mice have been generated to enable the targeting of VGAT-positive neurons, either by expressing diverse recombinases under the control of

the *Vgat* promoter, by allowing the optical activation of these neurons, or by abolishing *Vgat* expression upon recombination.

In addition to sharing a vesicular transporter, GABA and glycine can be co-transmitted by some neurons situated in the cerebellum, brainstem and spinal cord. In these inhibitory neurons, VGAT enables the loading of GABA and glycine into the same vesicles (Wojcik et al., 2006). These cells then mediate pure GABAergic transmission, pure glycinergic transmission, or a combination of both, depending on the receptors present at the postsynaptic membrane. In the cerebellum, it has been demonstrated that an individual inhibitory neuron can perform all three forms of transmission by forming distinct synapses, the characteristics of which depend on the postsynaptic cell type (Dugué et al., 2005). Given that the kinetics of glycine receptors are faster than those of $GABA_A$ receptors, the presence of both results in an inhibitory postsynaptic current with fast and slow components, thereby enabling precise control over postsynaptic firing rates.

2. Inhibitory neuronal populations

2.1. Cerebral neocortex

In the cerebral cortex, two principal types of neurons constitute highly interconnected and dynamic circuits: glutamatergic excitatory neurons, which propagate signals within and among diverse brain regions, and GABAergic inhibitory neurons, which regulate signal flow and shape network dynamics. Despite representing only 10 to 30% of all cortical neurons (with the percentage varying between species, cortical regions and cortical layers) (Meyer et al., 2011), inhibitory neurons have extensive axonal ramification. Moreover, a considerable diversity of GABAergic neurons exists, differing based on their function, morphology, connectivity, electrophysiological properties, and the molecular markers they express. This results in highly specific spatiotemporal inhibitory control of the activity of surrounding neurons and local circuits.

The classification of inhibitory neurons in the cortex is challenging. Here, we will distinguish four major subtypes of GABAergic neurons based on the main non-overlapping markers they express: parvalbumin, somatostatin, and the ionotropic serotonin receptor 5HT3a (5HT3aR) in the presence or absence of vasoactive intestinal polypeptide (VIP) (Tasic et al., 2016; Zeisel et al., 2015). Their typical localisation and connections are depicted in Figure 9.

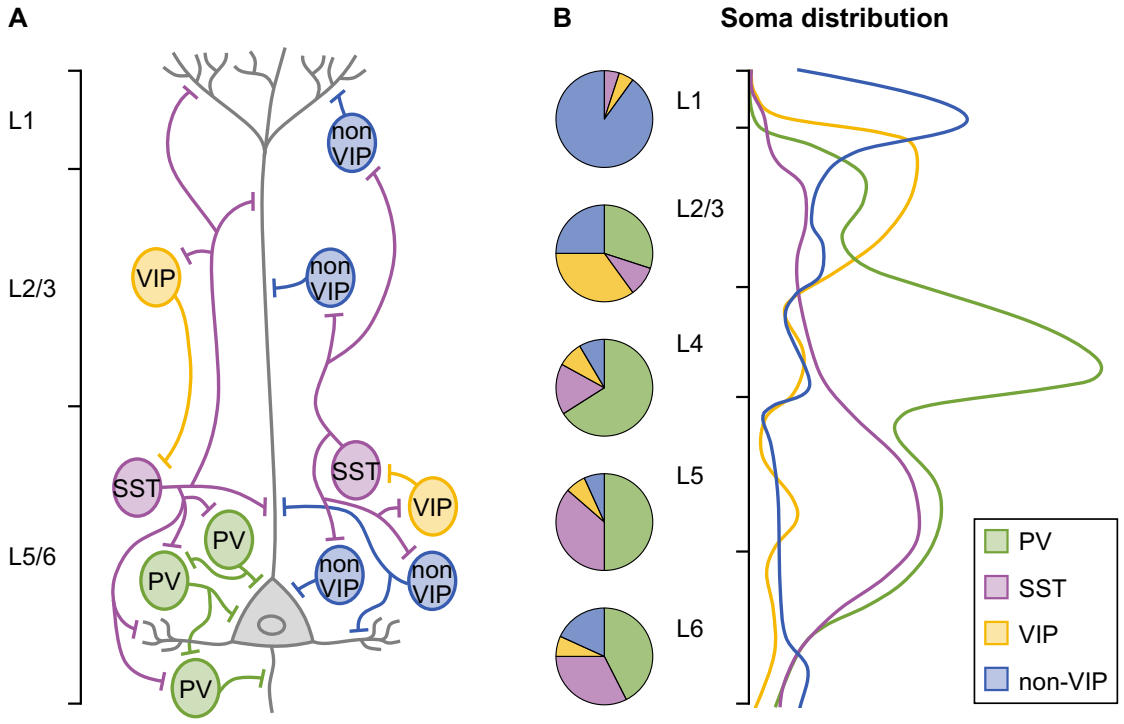


Figure 9: Inhibitory neuronal populations in the neocortex. (A) Schematic representation of the main inhibitory connections onto layer 5/6 pyramidal cells. To facilitate the comprehension of the figure, certain connections have been omitted. This includes inter-connections between inhibitory neurons in layers 1 and 2/3, as well as non-VIP connections onto inhibitory neurons (they form synapses on every other inhibitory neuron, including themselves, in every layer). (B) Distribution of the soma of inhibitory neurons throughout the cortex. Pie charts illustrate the proportion of the different populations of inhibitory neurons in each cortical layer. PV: parvalbumin, SST: somatostatin, VIP: 5HT3aR neurons expressing VIP, non-VIP: 5HT3aR neurons not expressing VIP. Adapted from Tremblay et al., 2016.

A. Parvalbumin neurons

Approximately 40% of all cortical inhibitory cells are parvalbumin neurons, representing the largest population of GABAergic neurons. Their soma is present in every cortical layer, except in layer 1, where there are virtually absent (Figure 9B). These cells can be subdivided into two major, clearly distinct subgroups: the fast-spiking basket cells, which target the soma and proximal dendrites of excitatory and inhibitory neurons (Hu et al., 2014), and the axo-axonic chandelier cells, which target the axon initial segment of pyramidal cells. Both subgroups exert a profound influence on the output of the targeted neurons, as they induce hyperpolarisation and/or shunting inhibition near the site of action potential generation.

B. Somatostatin neurons

Somatostatin neurons represent approximately 30% of all cortical inhibitory cells. Their soma is found in every layer and is most prominently distributed in deep layers 5/6

(infragranular layers). In layers 2/3, somatostatin neurons predominantly inhibit pyramidal cells, while in layer 4, they predominantly target local parvalbumin neurons and thus produce a disinhibition of pyramidal cells (Xu et al., 2013). Of note, these cells can be further divided into two major subgroups: Martinotti cells, which project axons in cortical layer 1 where they target distal dendrites of pyramidal cells, and non-Martinotti cells, which do not project axon in layer 1 (Nigro et al., 2018).

Somatostatin neurons differ from parvalbumin neurons based on two major aspects. First, they target the dendrites of inhibitory and excitatory neurons, including the distal dendrites. Second, excitatory inputs on somatostatin neurons are strongly facilitating (Beierlein et al., 2003; Kapfer et al., 2007; Silberberg and Markram, 2007), while they are moderately or strongly depressing on most other inhibitory neurons. As a result of this opposite dynamics of excitatory inputs, as well as intrinsic membrane properties, parvalbumin and somatostatin neurons do not require the same stimuli to be activated. Parvalbumin neurons require the synchronous firing of many presynaptic cells to fire, while a single high-frequency burst from one presynaptic cell is sufficient to recruit somatostatin neurons and produced feedback inhibition.

C. 5HT3aR neurons

5HT3aR neurons also represent approximately 30% of all cortical inhibitory cells. Their soma is found in every layer, and there are the most numerous inhibitory neurons in superficial layers 1 and 2/3 (supragranular layers). As previously stated, 5HT3aR neurons can be subdivided into two subgroups based on whether they expressed VIP or not. Neurons expressing VIP represent almost 40% of 5HT3aR neurons. They are the largest population in layers 2/3, and preferentially form synapses onto somatostatin neurons, which can produce a disinhibition of pyramidal cells. Because of their relatively high input resistance, these neurons are particularly sensitive to excitatory inputs (SooHyun Lee et al., 2010). Neurons not expressing VIP (non-VIP) represent approximately 60% of 5HT3aR neurons and 90% of all inhibitory neurons in layer 1.

D. Long-range projecting GABAergic neurons

Most cortical GABAergic neurons strictly target nearby cells and control the local network activity. However, some neocortical parvalbumin, somatostatin and VIP neurons also project to other brain regions (Jinno and Kosaka, 2004; Lee et al., 2014; Tamamaki and Tomioka, 2010; Tomioka et al., 2015). This includes neurons projecting both ipsilaterally and contralaterally to the amygdala and striatum. GABAergic long-range projecting cells constitute a heterogeneous population but seem to preferentially target inhibitory neurons in the distant brain regions. Overall, these inhibitory projections could synchronise distant neuronal networks.

2.2. Ventral horn of the lumbar spinal cord

The inhibitory neurons of the ventral horn of the lumbar spinal cord can be divided into three populations: V0, V1 and V2 (Figure 10). These populations are distinguished by the expression of transcription factors regulating cell-type specification during development, and the expression of molecular markers in mature neurons, particularly calcium-binding proteins. Inactivating these neurons in mice has enabled the elucidation of their role in the regulation of locomotion, which will be introduced below.

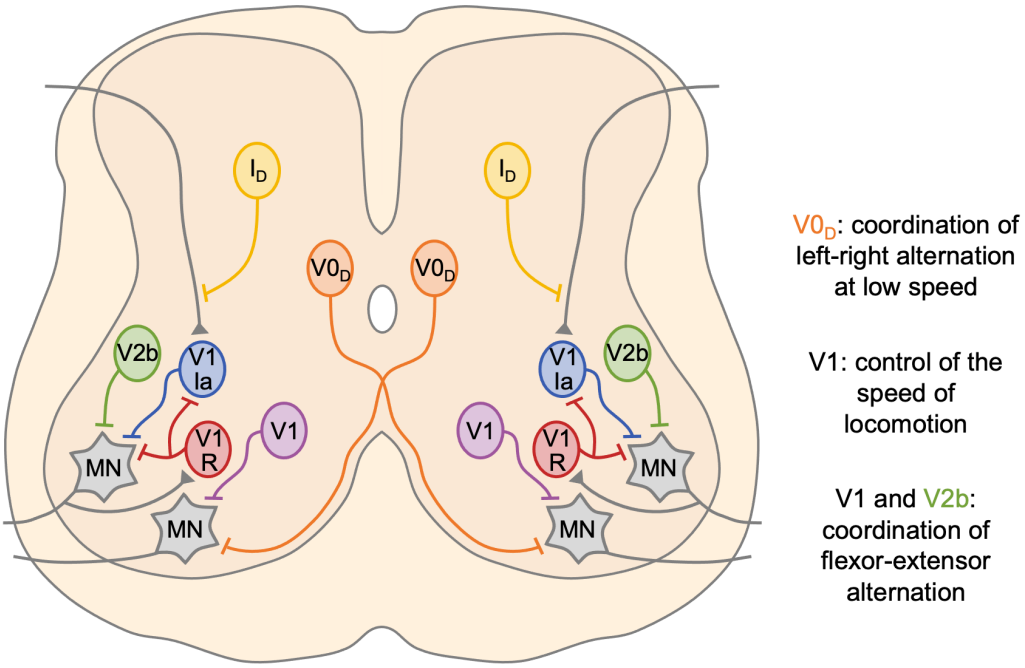


Figure 10: Inhibitory neuronal populations in the ventral spinal cord. Schematic representation of the main inhibitory neurons involved in spinal motor control. In the ventral horn, V1 neurons (which include V1 Renshaw cells in red and V1 Ia neurons in blue) and V2b neurons (green) form ipsilateral connections on motor neurons (grey). Renshaw cells express both parvalbumin and calbindin, while Ia neurons express parvalbumin only. Commissural dorsal $V0_D$ neurons (orange) form contralateral connections on motor neurons. In the dorsal horn, several populations of inhibitory neurons (represented by a single I_D neuron in yellow) are involved in sensory pathways and can form connections on primary sensory afferents.

A. $V0_D$ interneurons

$V0_D$ interneurons are commissural neurons which form monosynaptic contacts with contralateral motor pools. They express developing brain homeobox protein 1 (Dbx1) in the absence of even-skipped homeobox 1 (Evx1). Most of these neurons are glycinergic. Additionally, about half of the $V0_D$ neurons are GABAergic, with a notable subset of these cells co-expressing GABA and glycine (Griener et al., 2015). The selective ablation of these neurons showed that they control left-right coordination at slow speed of locomotion (Lanuza et al., 2004), which corresponds to walking behaviours.

B. V1 interneurons

V1 interneurons are ipsilaterally projecting inhibitory neurons. In the adult mice, 80% of them are glycinergic, although they often co-express GABA (Alvarez et al., 2005). They form a large population of highly heterogeneous neurons, which are defined by the expression of engrailed 1 (En1) (Bikoff et al., 2016). This transcription factor is expressed in V1 neurons from the development to the adulthood in mice and can thus be used as a marker to target this subpopulation of neurons. Altogether, V1 neurons represent more than 50% of the synapses on the soma of motor neurons. They are known to control the speed of locomotion (Gosgnach et al., 2006). Indeed, genetic ablation or silencing of V1 neurons decreases the locomotor speed and intralimb extension, and increases the duration of flexor activation, without disrupting coordination.

Among them, we can distinguish two well-studied populations of inhibitory neurons: the Renshaw cells and Ia inhibitory neurons. Renshaw cells represent less than 10% of V1 neurons (Alvarez et al., 2005). They are glycinergic neurons which receive input from axon collaterals of motor neurons, and mediate recurrent inhibition. In addition, Renshaw cells inhibit other Renshaw cells and Ia inhibitory neurons. Therefore, they exert a feedback modulation on motor neurons, both directly and through the inhibition of other inhibitory neurons, creating a disinhibitory effect. In mouse, these cells express calbindin and parvalbumin. Ia inhibitory neurons represent approximately 15% of V1 neurons. They receive input from Renshaw cells and proprioceptive Ia afferents, and form synapses onto motor neurons to mediate reciprocal inhibition. They express parvalbumin but not calbindin. In addition to V1 neurons, a subpopulation of V2b neurons also constitutes Ia inhibitory interneurons (Zhang et al., 2014). Of note, V1 neurons were also found to be present at cervical and thoracic levels (Sweeney et al., 2018), but it remains unknown whether they are involved in the brainstem circuits controlling rhythmic orofacial actions (e.g., breathing, chewing, swallowing) (Moore et al., 2014).

C. V2b interneurons

V2b interneurons are also ipsilaterally projecting inhibitory neurons. They express GATA-binding factors 2 and 3 (Gata2, Gata3). Of note, a small proportion of V2b neurons are Ia inhibitory neurons. V2b neurons preferentially inhibit extensor motor neurons. Together with V1 neurons, they are required for the coordination of flexor-extensor alternation (Britz et al., 2015; Zhang et al., 2014).

3. Development of the inhibitory system

The development of the central nervous system is a lengthy process, extending over more than two decades in humans. This commences with the generation of complex patterns of

cell fates in embryos and continues through to the pruning of synapses during adolescence (Silbereis et al., 2016). In particular, a series of developmental milestones are crucial for the formation and refinement of neuronal circuits. These milestones represent critical windows, as it has been proposed that even subtle variations in the organisation of neural circuits can have long-lasting effects on the function or dysfunction of the nervous system. Most of our current knowledge regarding neuronal circuit development is derived from studies of the rodent brain. However, it has been suggested that these principles are broadly conserved in primates.

A noteworthy aspect of the development of the inhibitory system is its prolonged duration. The signalling of GABA and glycine commences at an early stage of embryonic development, before the formation of synapses. At this stage, GABA may act as a trophic factor regulating pivotal transitions, including proliferation, migration, differentiation, synapse maturation and programmed cell death (Owens and Kriegstein, 2002; Peerboom and Wierenga, 2021). Moreover, a number of key processes involved in the assembly of neuronal networks may be directly linked to the maturation of inhibitory neurons, including the postnatal switch from depolarisation to hyperpolarisation and the establishment of mature cortical oscillatory rhythms (Figure 11).

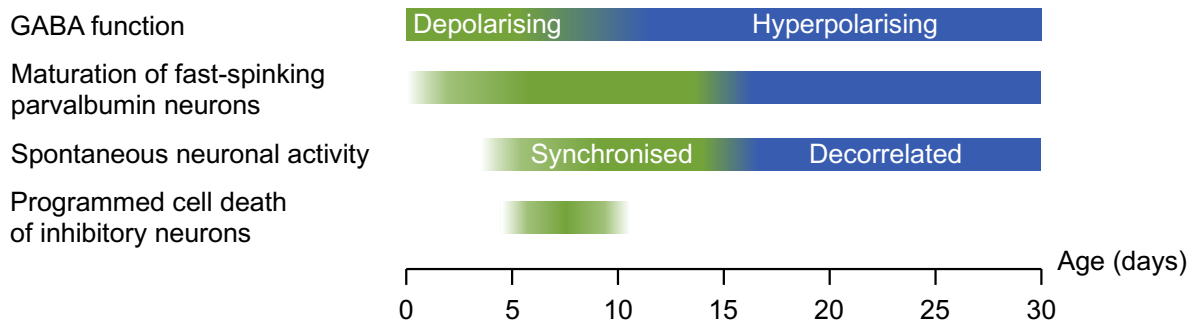


Figure 11: Milestones in the postnatal development of the inhibitory system in the mouse neocortex. Adapted from Marín, 2016.

3.1. Transition from depolarisation to hyperpolarisation

The change in membrane potential exerted by GABA and glycine is determined by the intracellular concentration of chloride ions in the postsynaptic cell (Figure 12). This concentration is regulated by the expression of two different chloride cotransporters at the membranes of neuronal soma and dendrites: sodium-potassium-chloride cotransporter 1 (NKCC1), which increases intracellular concentrations of chloride ions, and potassium-chloride cotransporter 2 (KCC2), which has the opposite effect. During the embryonic development, immature neurons highly express NKCC1 and thereby exhibit high intracellular concentrations of chloride ions. When their GABA and glycine receptors are activated, the efflux of chloride ions is facilitated, which induces the depolarisation of the membrane potential. This was proposed to be an important aspect of the embryonic

development, as the excitatory action of GABA may influence the neurogenesis, migration and morphological development of pyramidal and inhibitory neurons in the developing cortex (Ojeda and Ávila, 2019). During the development, a switch occurs, and mature neurons highly express KCC2, thus exhibiting low intracellular concentrations of chloride ions. When their GABA and glycine receptors are activated, the influx of chloride ions is facilitated, which induces the hyperpolarisation of the membrane potential. This switch occurs around the end of the first postnatal week in the murine cortex, and at E15.5 in the lumbar spinal cord. Altered cerebral ratios of NKCC1 and KCC2 (with an increase in NKCC1 and a decrease in KCC2 expressions) have been associated with epilepsy, as well as several neurodegenerative and neuropsychiatric disorders.

Of note, *in vivo* studies reported that GABA effectively depolarises cortical immature neurons at postnatal day (P) 3 (Kirmse et al., 2015). However, it did not activate voltage-gated calcium channels, nor did it induce firing. In addition, activating $GABA_A$ receptors inhibited spontaneous neuronal activity, whereas the blocking of these receptors had the opposite effect. Hence, it was proposed that GABA is predominantly depolarising at the cellular level, but already has an inhibitory influence at the network level, at least in the cortex (Chini et al., 2022; Kirmse et al., 2015). This effect differs among brain regions, as GABAergic neurons were found to exert an excitatory influence in the hippocampus at P3, and then an inhibitory influence at P7 (Murata and Colonnese, 2020).

In the spinal cord, NKCC1 and KCC2 are present as early as E11.5 and remain detectable until birth (Delpy et al., 2008). However, NKCC1 was found to be inactivated at E15.5. Consequently, after this age, the depolarising activity of GABA failed to trigger action potentials. Hence, the adult inhibitory response to GABA is established earlier in the spinal cord than in the brain (Stein et al., 2004).

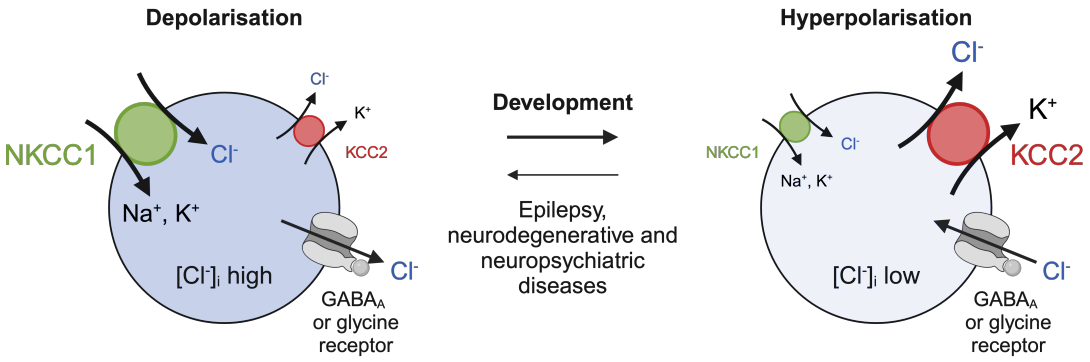


Figure 12: Developmental switch from depolarisation to hyperpolarisation. NKCC1: sodium-potassium-chloride cotransporter 1; KCC2: potassium-chloride cotransporter 2; Cl^-: chloride; $[Cl^-]_i$: intracellular concentrations of chloride ions; K^+: potassium; Na^+: sodium.

3.2. Focus on two aspects of the neocortex postnatal development

A. Programmed cell death of inhibitory neurons

GABAergic cortical interneurons are born from embryonic progenitor cells located in the ventral subpallium, which is far from their final location. All the major subtypes of inhibitory neurons previously introduced can found their origin in two specific regions: the medial ganglionic eminence (MGE), which generate parvalbumin and somatostatin cells, and the caudal ganglionic eminence (CGE), which generate VIP neurons. These regions give rise to different lineages of inhibitory neurons, for which the exact development and maturation differ (Llorca and Deogracias, 2022). The generation of MGE-derived inhibitory neurons commence at E9.5, followed by the generation of CGE-derived interneurons starting at E12.5. To reach the cortex, these neurons migrate tangentially, following external chemical cues that attract or repel them (Marín, 2013). They then migrate radially to populate various cortical regions and ultimately position themselves within the designated cortical layers. It is only after this step that inhibitory neurons commence the process of acquiring their final morphology, integrating into the brain circuitry, and forming synapses onto the surrounding neurons. The functional integration of inhibitory neurons into cortical circuits is a slow process that is initiated by the formation of transient circuits (Anastasiades et al., 2016). Pyramidal neurons may be involved in this process, providing molecular cues that guide the migration of inhibitory neurons, and regulating their survival in an activity-dependent manner.

To ensure the assembly of functional networks in the neocortex, the brain produces an excess of neurons during development and then prunes this excess with waves of programmed cell death which are essential for the correct maturation of the circuits. The death of excitatory neurons precedes and influences the death of inhibitory neurons, which are both dependent on the pro-apoptotic factors Bcl2-associated X protein (Bax) and Bcl2 antagonist/killer 1 (Bak) (Southwell et al., 2012). In mice, most neocortical pyramidal neurons undergo cell death between P2 and P5, during which around 13% of excitatory neurons are lost (Wong et al., 2018). For inhibitory neurons, apoptosis occurs between P5 and P10, and results in the loss of 20 to 30% of neurons depending on their subtype (Priya et al., 2018; Wong et al., 2018). During this critical period, neuronal activity plays a key role in the survival of inhibitory neurons (except for VIP cells). It was shown that active inhibitory neurons are more likely to survive than inactive neurons. Interestingly, *in vitro* experiments suggested that the physical interactions between inhibitory neurons and pyramidal cells are required for their survival, as GABAergic neurons seem to be fated to die in the absence of inputs from excitatory cells (Priya et al., 2018). Indeed, some cortical inhibitory neurons exhibit increasing levels of the phosphate PTEN during the critical period of apoptosis. PTEN is known to inhibit the serine-threonine kinase Akt, which is a critical mediator of neuronal survival, ultimately leading

to cell death. However, increasing the activity of excitatory neurons was found to be sufficient to decrease PTEN levels in inhibitory neurons, which mechanistically explains the survival of activated inhibitory neurons (Wong et al., 2018).

This critical period of cell death is particularly important to ensure the elimination of abnormally wired neurons, as well as to adjust the number of cells or ensure the normal spacing between neurons. Ultimately, this apoptosis plays important roles in the changes in neuronal activity patterns, remodelling of transient connections, and establishment of mature patterns of connectivity and activity, which all occur during the first two weeks of postnatal development in the murine cortex. It is worth noting that inhibiting the expression of the proapoptotic gene *Bax* in mice results in relatively limited neuropathological and morphological alterations, while it impairs a wide range of behaviours, including increased locomotor activity (Krahe et al., 2015) or slightly decreased motor coordination (Jyotika et al., 2007).

Finally, the process of inhibitory synaptogenesis is characterised by a high degree of cell-type specificity, with distinct molecular programmes (Favuzzi et al., 2019) and neural activity (Kepecs and Fishell, 2014) playing a pivotal role in its orchestration. In rodents, the development of inhibitory synapses is not complete until P30.

B. Transition from synchronisation to decorrelation

During the first postnatal week, inhibitory circuits exhibit distinctive characteristics that diverge from those observed in adult circuits. At this developmental stage, cortical circuits are distinguished by highly synchronised activity patterns involving a considerable number of neurons. In particular, this synchronisation may be of significance for the maturation of neuronal circuits (Kirkby et al., 2013; Uhlhaas et al., 2010). During the second postnatal week, the brain transitions towards sparse and decorrelated neuronal activity patterns, which reflect changes in circuit connectivity and characterise a mature state (Golshani et al., 2009). This transition has important functional implications, as the latter state is thought to facilitate more efficient storage, retrieval, and processing of information. The mechanisms underpinning this process remain poorly understood. Theoretical and experimental studies indicated that the balance between excitation and inhibition is of critical importance in establishing sparse neuronal activity. Before the transition, the excitation-inhibition ratio in cortical neurons is higher than that observed in the adult brain. However, during network maturation, this ratio decreases progressively, while the inhibitory influence increases (Zhang et al., 2011). Interestingly, GABA release and inhibitory synaptic inputs onto pyramidal cells were found to influence the spatiotemporal structure of spontaneous activity patterns (Duan et al., 2020) and the decorrelation of neuronal activity (Chini et al., 2022) in young pups. This suggests that the functional integration of inhibitory neurons in developing circuits is involved in the

observed transition. The maturation of somatostatin neurons occurs at a faster rate than that of parvalbumin neurons (Miyamae et al., 2017; Tuncdemir et al., 2016). Consequently, inhibitory circuits during the first postnatal week exhibit a predominance of synapses formed by somatostatin neurons. These are the principal cells influencing cortical dynamics during this period, regulating both spontaneous and evoked synchronous activity patterns (Mòdol et al., 2024). Interestingly, the inhibition of somatostatin neurons was found to accelerate the maturation of parvalbumin neurons and the decorrelation of cortical activity. This indicates that the sequential integration of somatostatin and parvalbumin neurons is also crucial for the transition from synchronisation to decorrelation.

3.3. Focus on two aspects of the spinal cord embryonic development

In general, the development of the spinal cord progresses in the ventral-to-dorsal and rostral-to-caudal directions, and this is also true for the development of the inhibitory system (Sagner and Briscoe, 2019; Shimizu-Okabe et al., 2022). During the early development of inhibitory spinal neurons, twelve progenitor domains are formed in the ventricular zone, and each of them produces distinct neuronal classes. In the cervical spinal cord of rodents, $V0_D$ neurons first appear on the surface of the ventricular zone between E10 and E11. They are followed by V1 neurons, appearing before E11, and V2b neurons arising between E12 and E13. After exiting the cell cycle, these neurons migrate into the grey matter along distinct routes and finally settle in distinct laminae. Their axons then ascend or descend for several segments and enter the contralateral (for $V0_D$ neurons) or ipsilateral (for V1 and V2b neurons) motor neuron pool.

A. Transition from GABAergic to glycinergic synapses

The emergence of GABAergic and glycinergic neurons in the lumbar spinal cord occurs at E12.5, and a couple of studies revealed significant differences in their maturation process. Firstly, it was observed that GABAergic neurons predominantly invade the superficial dorsal horn, whereas glycinergic neurons mostly invade the deep dorsal and ventral horns (Allain et al., 2006, 2004). At this stage, a significant proportion of inhibitory neurons may already co-express GABA and glycine. Secondly, GABAergic synapses are the most prevalent during the embryonic and early postnatal developmental stages, up to P7. However, it has been proposed that a transition occurs during the second week of life, whereby the spinal inhibitory system shifts from predominantly GABAergic to predominantly glycinergic. In the ventral horn, GABAergic terminals were first detected at E13, while glycine receptors were first detected at E16 and localised at GABAergic terminals (Sunagawa et al., 2017). Interestingly, the density of glycinergic synapses was shown to increase progressively, while that of GABAergic synapses decreased, thereby allowing glycinergic terminals to become dominant during the second postnatal week.

B. Influence of inhibitory neurons on motor neuron development

Approximately half of motor neurons are lost between E13 and birth due to programmed cell death. This loss overlaps with the formation of the first synaptic connections between interneurons and motor neurons, and between motor neurons and muscle cells. It was shown that the survival and differentiation of these cells depend on trophic factors secreted from targeted muscle fibres and myelinating cells surrounding motor axons. In particular, when neuromuscular activity is decreased, more motor neurons survive. It was proposed that under these conditions, motor neurons increase their axonal branching, which increases their access to trophic factors, thus increasing their survival (Banks et al., 2003). In addition, inhibitory neurons were found to regulate motor neuron development. Gephyrin is a post-synaptic tubulin-binding protein essential for the clustering and anchoring of glycinergic and $GABA_A$ receptors at the membrane. Gephyrin-deficient mice die at birth but their characterisation at E18.5 showed that the loss of all glycine receptors and some $GABA_A$ receptors affect motor neurons differently depending on their localisation (Banks et al., 2005). In the brainstem, respiratory motor neurons exhibited increased spontaneous activity, decreased axonal branching to the diaphragm and decreased survival. VGAT-deficient and GAD67-deficient mice recapitulated this phenotype which was accompanied, *in vitro*, by decreased inhibitory inputs and increased excitatory inputs (Fogarty et al., 2017, 2013). Conversely, in gephyrin-deficient and VGAT-deficient mice, lumbar motor neurons exhibited decreased spontaneous activity, increased innervation of limb muscles and increased survival (Banks et al., 2005; Fogarty et al., 2015). In GAD67-deficient mice, no alterations were observed for lumbar motor neurons (Fogarty et al., 2013). Overall, GABAergic influence appears to be important for the survival of respiratory motor neurons, but not of locomotor neurons.

4. Physiological functions of inhibitory neurons

The most fundamental role of inhibitory neurons is to regulate the excitability and activity of excitatory neurons, thereby maintaining a stable homeostatic balance and preventing excessive excitation. The challenge in comprehending the physiological functions of inhibitory neurons and their implications in disease lies in their remarkable diversity. This is probably this diversity which allows the inhibitory neurons to constitute a potent and complex regulatory machinery that controls the physiology of neural circuits.

4.1. Balance between excitation and inhibition

Under physiological conditions, neurons and circuits coordinate their excitatory and inhibitory inputs in order to establish and maintain a constant balance between excitation and inhibition. This is thought to be a crucial element to ensure the proper functioning and stability of the circuits. This balance can be studied at the level of the neurons, where

molecular mechanisms regulate the amount of excitatory and inhibitory inputs (along with the regulation of other parameters, such as the intrinsic excitability), thus adapting the produced output. This balance can also be studied at the circuit level, in which balanced and delayed inhibition is important for enabling the progressive recruitment of firing neurons and restricting the spatial and temporal spread of activity. At this level, four core motifs can be distinguished to explain the relationship between excitation and inhibition (Figure 13). With feedforward inhibition, the excitatory source is external and can target both inhibitory and excitatory neurons. In that case, the activation of the inhibitory neuron results in an inhibitory influence on the locally targeted neuron. With feedback inhibition and lateral inhibition, the excitatory source is local. The inhibitory neuron targets either the neuron which provided the excitation (recurrent inhibition) or another neighbouring neuron (lateral inhibition). Finally, with disinhibition, the principal target is another inhibitory neuron, preventing it from inhibiting its own target.

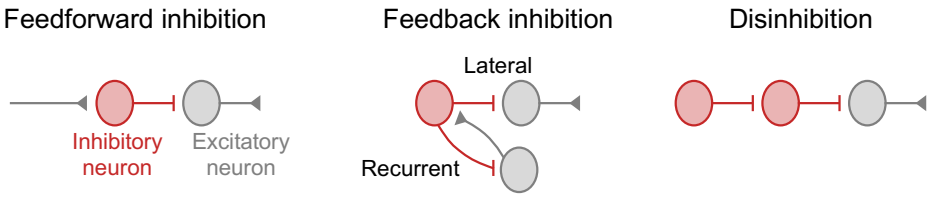


Figure 13: Circuits motifs highlighting the relationship between excitation and inhibition.

4.2. Regulation of behavioural and cognitive processes

The GABAergic system is associated with multiple behavioural and cognitive functions, including perception, attention, learning, memory and anxiety, among others. Inhibitory neurons are of critical importance within cortical local circuits. They exert direct control over pyramidal cell activity, regulate cortical rhythms and generate network oscillations that further determine pyramidal cell activation. In particular, inhibitory neurons were found to synchronise local assemblies of pyramidal cells and to coordinate gamma (30-100 hertz) and theta (4-12 hertz) frequency oscillations, allowing the emergence of functional interactions between brain areas. This synchronisation between brain regions is important for the processing of information, the integration of cognitive functions, as well as the encoding and retrieval of memories. This illustrates why the correct functioning of inhibitory neurons is essential for the generation of specific brain states and the maintenance of cognitive health. For instance, $GABA_A$-mediated inhibition has been demonstrated to synchronise neuronal activity between the hippocampus and the entorhinal cortex, which is essential for successful memory encoding and retrieval (Nakazono et al., 2018). In contrast, it is thought that $GABA_B$-mediated inhibition serves to terminate this coordinated activity, thereby regulating its duration. Furthermore, $GABA_B$ activation may be involved in the transition between theta and gamma oscillations,

which may be associated with memory consolidation. In addition, distinct subpopulations of inhibitory neurons may be responsible for disparate roles. For example, cortical parvalbumin neurons appear to be involved in the generation and maintenance of both gamma and theta oscillations, while somatostatin neurons are involved in theta oscillations (Fanselow et al., 2008; Sohal et al., 2009; Stark et al., 2013). Finally, there is substantial evidence indicating that GABAergic neurons and synapses are subject to plastic changes. It has been demonstrated that the learning process is associated with modifications in inhibitory neurotransmission and reorganisation of cortical activation. In particular, inhibitory synaptic transmission can be increased with learning.

4.3. Control of movements

Execution of movements requires coordinated activation of spinal motor neuron pools for appropriate muscle activation. This activation is mediated by a complex network of inhibitory and excitatory spinal neurons decoding inputs both from the descending motor pathways and the afferent sensory pathways. The neuronal circuits located in the ventral horn of the spinal cord are responsible for the coordination of a wide range of activities, including breathing, walking, running, and producing both voluntary and involuntary movements. Glutamatergic and cholinergic excitatory neurons, as well as GABAergic and glycinergic inhibitory neurons form delimited neuronal networks, called central pattern generators (Frigon, 2012). In mammals, these networks perform two fundamental actions to drive motor neuron outputs in simple rhythmic behaviours, such as respiration, mastication and locomotion. First, they generate the timing, phasing and intensity cues received by motor neurons. Second, they shape and coordinate the pattern of activity of multiple motor neuron pools. The modulation of the central pattern generator activity necessitates a coordinated activity of all constituent neurons, while motor neurons represent the final efferent pathway to muscles. Among this network, interneurons are of particular importance due to the intricate connectivity between them and with motor neurons. At least 11 neuronal subpopulations of interneurons have been identified, most of them being excitatory. Each of these subpopulations has been associated with a specific localisation and function. In the previous sections, I introduced the inhibitory neurons found in the ventral horn of the lumbar spinal cord, as well as their respective roles in the control of locomotion. Of note, cortical inhibitory neurons are also involved in motor functions. For instance, parvalbumin, somatostatin and VIP neurons are differentially engaged in motor learning and movement execution.

4.4. Ageing of the inhibitory system

The precise mechanisms underlying the age-related decline in both cognitive and locomotor functions remain largely unknown. During ageing, both dysregulations of the GABAergic system and modifications of excitatory and inhibitory synapses may result in

an imbalance between excitation and inhibition (Rozycka and Liguz-Lecznar, 2017). The latter can induce dysfunctions within neuronal networks and contribute to cognitive and behavioural declines (Dickstein et al., 2007; Morrison and Baxter, 2012). However, the age-related alterations of intrinsic neuronal properties and the resulting consequences are dependent on both the brain region and the neuronal population under consideration. For instance, it has been suggested that inhibition increases with age in the prefrontal cortex but decreases in the hippocampus.

Overall, it appears that loss and dysfunction of inhibitory synapses have been consistently observed in numerous brain structures, whereas the loss of inhibitory neurons remains a topic of debate. A reduction in the synthesis of GABA has been proposed in the brains of humans and rodents, based on observations of decreased RNA and protein levels of GAD. In rodents, it has been shown that age-related alterations in the composition of GABA receptor subunits may influence the intrinsic characteristics of these receptors (i.e., channel kinetics, ligand binding and ion specificity) and underlie the diverse cognitive and behavioural declines. These findings suggest that the process of ageing, through subtle alterations in the subunit composition of inhibitory receptors, can influence their physiological functions and alter inhibitory synaptic transmission. Little is known about how VGAT expression or activity changes during ageing. Of note, genes associated with GABAergic inhibitory function are significantly more strongly downregulated in aged humans than in aged mice (Loerch et al., 2008). Regarding the spinal cord, it was observed that the efficiency of several reflex pathways is reduced and that their modulation is impaired during the ageing process (Geertsen et al., 2017). This encompasses the pathway responsible for the postsynaptic inhibition of motor neurons by Ia inhibitory neurons (reciprocal inhibition) and the pathway responsible for the inhibition of primary sensory afferents targeting motor neurons (presynaptic inhibition).

Part 5: Involvement of inhibitory neurons in ALS-FTD

In line with their multifaceted functions, the malfunction of inhibitory neurons has been linked to epilepsy, as well as a range of neurodevelopmental disorders (including schizophrenia and autism), psychiatric disorders (including anxiety disorders) and neurodegenerative diseases (including Alzheimer's disease).

A growing body of evidence suggests that inhibitory neurons are impaired in both ALS and FTD and may play a role in the onset and/or progression of symptoms. Interestingly, these impairments may be involved in sporadic patients, as well as in patients exhibiting different mutated genes. Here I will present the current state of knowledge regarding the involvement of inhibitory neurons in the ALS-FTD continuum. The first part corresponds to a review published in Neurobiology of Disease. In this review, I discuss the evidence for inhibitory neuron impairments in ALS and FTD patients, as well as their potential contribution to symptoms. I also assess the mechanisms that have been proposed to explain the decreased inhibitory influence, and I mention the potential therapeutic strategy of targeting these alterations. In the second part, I will summarise the inhibitory neuron impairments that have already been observed in ALS and FTD mouse models.

Review

Impairments of inhibitory neurons in amyotrophic lateral sclerosis and frontotemporal dementia

Félicie Lorenc, Luc Dupuis, Raphaelle Cassel

Neurobiology of Disease, Volume 203, December 2024, 106748
https://doi.org/10.1016/j.nbd.2024.106748

Impairments of inhibitory neurons in amyotrophic lateral sclerosis and frontotemporal dementia

Félicie Lorenc[1], Luc Dupuis[1], Raphaelle Cassel[1*]

[1]Université de Strasbourg, INSERM, UMR-S 1329, Strasbourg Translational Neuroscience and Psychiatry, CRBS, Strasbourg, France

*** Corresponding author**

E-mail addresses:
felicie.lorenc@inserm.fr (F. Lorenc)
ldupuis@unistra.fr (L. Dupuis)
raphaelle.cassel@inserm.fr (R. Cassel)

Abstract

Amyotrophic lateral sclerosis and frontotemporal dementia are two fatal neurodegenerative disorders. They are part of a pathophysiological continuum, displaying clinical, neuropathological, and genetic overlaps. There is compelling evidence that neuronal circuit dysfunction is an early feature of both diseases. Impaired neuronal excitability, imbalanced excitatory and inhibitory influences, and altered functional connectivity have been reported. These phenomena are likely due to combined alterations in the various cellular components involved in the functioning of neuronal networks. This review focuses on one of these cellular components: inhibitory neurons. We assess the evidence for inhibitory neuron impairments in amyotrophic lateral sclerosis and frontotemporal dementia, as well as the mechanisms leading to the loss of inhibition. We also discuss the contributions of these alterations to symptoms, and the potential therapeutic strategies for targeting inhibitory neuron deficits.

Keywords: Amyotrophic lateral sclerosis; Frontotemporal dementia; Inhibition; Inhibitory neurons; Interneurons; GABA; Glycine.

Abbreviations: ALS, Amyotrophic lateral sclerosis; ALSFRS-R, Revised ALS functional rating scale; CSP, Cortical silent period; FTD, Frontotemporal dementia; GABA, γ-aminobutyric acid; GAD, Glutamic acid decarboxylase; KCC2, Potassium-chloride cotransporter 2; LICI, Long-interval intracortical inhibition; NKCC1, Sodium-potassium-chloride cotransporter 1; SICI, Short-interval intracortical inhibition; [^{11}C]flumazenil, Flumazenil labelled with carbon-11.

Introduction

Amyotrophic lateral sclerosis (ALS) and frontotemporal dementia (FTD) are progressive and disabling neurodegenerative disorders. ALS is characterised primarily by the degeneration of upper and lower motor neurons in the cortex, brainstem and spinal cord, which leads to muscle atrophy and progressive paralysis. Patients typically die from respiratory failure 3 to 5 years after diagnosis (reviewed by Feldman et al., 2022; Ilieva et al., 2023). FTD represents a group of clinically diverse disorders characterised by a relatively selective degeneration of the frontal and temporal lobes. This results in significant alterations in behaviour, personality, executive functions, and language skills. Based on these clinical manifestations, patients are classically subdivided into subgroups, including the behavioural variant, and two variants of primary progressive aphasia (semantic or non-fluent). Patients typically die from comorbidities and undernourishment 7 to 13 years after diagnosis (reviewed by Antonioni et al., 2023).

ALS and FTD constitute a pathophysiological *continuum*, displaying clinical, neuropathological and genetic overlaps. Pure ALS and pure FTD represent the two extreme ends of this *continuum*, whereas 15% of patients receive both diagnoses. This number may be underestimated because of the preponderance of one condition. It is now postulated that at least 50% of patients with ALS develop behavioural and cognitive alterations, while up to 40% of FTD patients experience motor impairments (Burrell et al., 2011; Murphy et al., 2016). Beyond this clinical overlap, ALS and FTD display common pathological abnormalities, including inclusions of TDP-43, which are present in most ALS cases and approximately half of FTD cases (Arai et al., 2006; Ling et al., 2013; Neumann et al., 2006). Finally, genes linked to ALS have also been associated with FTD. The most prominent example is *C9ORF72* repeat expansion, which leads to ALS and/or FTD, sometimes within the same family (DeJesus-Hernandez et al., 2011; Renton et al., 2011). Similarly, *TARDBP* mutations or *TBK1* haploinsufficiency are associated with ALS, FTD, or the combination of both (Benajiba et al., 2009; Borroni et al., 2009; Cirulli et al., 2015; Freischmidt et al., 2015; Kabashi et al., 2008; Le Ber et al., 2015; Pottier et al., 2015; Sreedharan et al., 2008). However, this is not the case for all genes. Currently, *SOD1* mutations are known to only cause ALS (Rosen et al., 1993), whereas *GRN* mutations cause FTD (Cruts et al., 2006). As there is no effective treatment available, it is imperative to elucidate the pathological causes and mechanisms to identify therapeutic targets.

There is compelling evidence that neuronal circuit dysfunction is an early feature of both ALS and FTD. A multitude of factors contribute to the precise regulation of neuronal network development, maintenance and functioning. In particular, neuronal activity is contingent upon the intrinsic excitability of the neuronal populations, the strength of synapses, and the quantity and timing of both excitatory and inhibitory inputs. In ALS and FTD, alterations have been reported in multiple components regulating neuronal

networks and activities. These encompass altered intrinsic excitability of neurons (reviewed by Gunes et al., 2020), impaired excitatory and inhibitory synaptic inputs (reviewed by Mora and Allodi, 2023), altered neuromodulation (reviewed by Brunet et al., 2020) and dysfunctional support by the glial cells (reviewed by Xie et al., 2023). This ultimately results in increased cortical excitability in individuals with ALS or FTD (Vucic and Kiernan, 2017, 2006). In the spinal cord of ALS patients, the current results are less conclusive but may point towards an initial increase in the excitability of lower motor neurons (Wainger et al., 2014), which is then followed by a decrease in excitability (Devlin et al., 2015). All of these alterations influence each other and are probably accompanied by compensatory or maladaptive mechanisms. Adding to this complexity, these alterations appear to be specific to the type of cells, region of the central nervous system and stage of the disease. Identifying the initial perturbation and the sequence of events involved in ALS and FTD pathophysiology will thus be extremely challenging. A perhaps overly simplistic model suggests that ALS and FTD are characterised by an imbalance between excitation and inhibition, which is shifted towards a relatively unopposed excitation which ultimately becomes pathological.

The use of functional magnetic resonance imaging –fMRI– has produced contradictory outcomes, with studies demonstrating either increased or decreased functional connectivity in the brains of ALS patients compared with controls (reviewed in Kocar et al., 2021). To elucidate this discrepancy, it has been postulated that functional connectivity may increase at early stages of the disease and then decline as the pathological burden accumulates. Electrophysiological techniques, including electroencephalography –EEG– and magnetoencephalography –MEG–, have also reported results which are consistent with increased functional connectivity in ALS. Two underlying mechanisms may explain this increase: additional brain structures may be recruited to compensate for structural damage, and/or local inhibitory circuitries may be impaired. Interestingly, this disrupted functional connectivity seems to be related to behavioural and cognitive dysfunctions (Basaia et al., 2020). Most studies including FTD patients demonstrated reduced functional connectivity, which was correlated with atrophy patterns (Dev et al., 2021).

This review examines the evidence for inhibitory neuron deficits in ALS and FTD patients, with a focus on the similarities and differences between the two diseases. To this end, we used a biochemical definition of inhibitory neurons and gathered data regarding neurons that release the two main inhibitory neurotransmitters: γ-aminobutyric acid (GABA) and glycine. Based on data obtained from patients and mouse models, we further discuss the mechanisms leading to a reduced inhibition, as well as the contribution of inhibitory neuron alterations to motor, behavioural and cognitive symptoms. Finally, we highlight potential therapeutic strategies for targeting inhibitory neurons.

1. Pathological evidence of inhibitory neuron impairments in the brains of ALS and FTD patients

1.1. Uncertainty regarding the levels of neurotransmitter

Following the initial stages of postnatal development, GABA is the principal inhibitory neurotransmitter in the brain. Given that inhibitory neurons may be affected during the pathogenesis of ALS and FTD, we hypothesise that the levels of this neurotransmitter should decrease. Indeed, significantly lower levels of GABA have been reported in the motor cortex of ALS patients compared with healthy controls using edited proton magnetic resonance spectroscopy (Foerster et al., 2013, 2012). However, this alteration was not observed when more recent protocols were employed (Atassi et al., 2017; Weerasekera et al., 2019). In patients with ALS, Weerasekera et al. reported a significant correlation between the levels of GABA and *N*-acetylaspartate, which is considered a marker of neuronal integrity. In patients with FTD, GABA levels were found to be reduced in a subregion of the frontal cortex (Murley et al., 2020). Nevertheless, the assessment of GABA levels remains challenging because of the superimposition of signals for diverse metabolites and the low concentration of GABA, which results in low spatial resolution.

An alternative approach is to study the levels of key enzymes involved in neurotransmitter synthesis. Glutamic acid decarboxylase (GAD) is expressed predominantly in inhibitory neurons and is the enzyme responsible for the synthesis of GABA from glutamate. GAD mRNA levels were found to be significantly increased in the prefrontal and temporal cortices of ALS patients using in situ hybridisation histochemistry (Petri et al., 2006). This could be interpreted as a compensatory mechanism to counter a decline in inhibitory influences. Another study reported an upregulation of *GAD1*, encoding the GAD_{67} isoform, in the frontal cortex of sporadic ALS patients compared with controls (Andrés-Benito et al., 2017). However, the protein levels of GAD_{67} appeared to be unaltered. Conversely, a decrease in GAD_{67} immunofluorescent labelling was reported in a small number of *SOD1* patients (Khademullah et al., 2020).

In light of the inherent constraints associated with the direct assessment of inhibitory neurotransmitter levels, it remains challenging to ascertain whether ALS and FTD patients exhibit a reduction in these levels.

1.2. Decreased binding to GABA receptors

To circumvent the aforementioned limitations, some studies have employed indirect methods, including positron emission tomography –PET–. In particular, flumazenil labelled with carbon-11 ([^{11}C]flumazenil) is a widely used tracer for the assessment of GABAergic function in the cerebral cortex, as it binds to ionotropic $GABA_A$ receptors

(Andersson et al., 2019). In ALS patients, a marked and widespread decrease in the binding of [^{11}C]flumazenil has been reported in motor and premotor regions (Lloyd et al., 2000; Turner et al., 2005a), as well as prefrontal regions (Lloyd et al., 2000). Moreover, there was a significant negative correlation between impairments in upper motor neurons and a decrease in binding over the dominant hemisphere (Turner et al., 2005a). This reduction in binding may be indicative of a loss of inhibitory and pyramidal neurons that express $GABA_A$ receptors and/or a downregulation of the expression of $GABA_A$ receptors in intact neurons (Figure 14). These two hypotheses are discussed below.

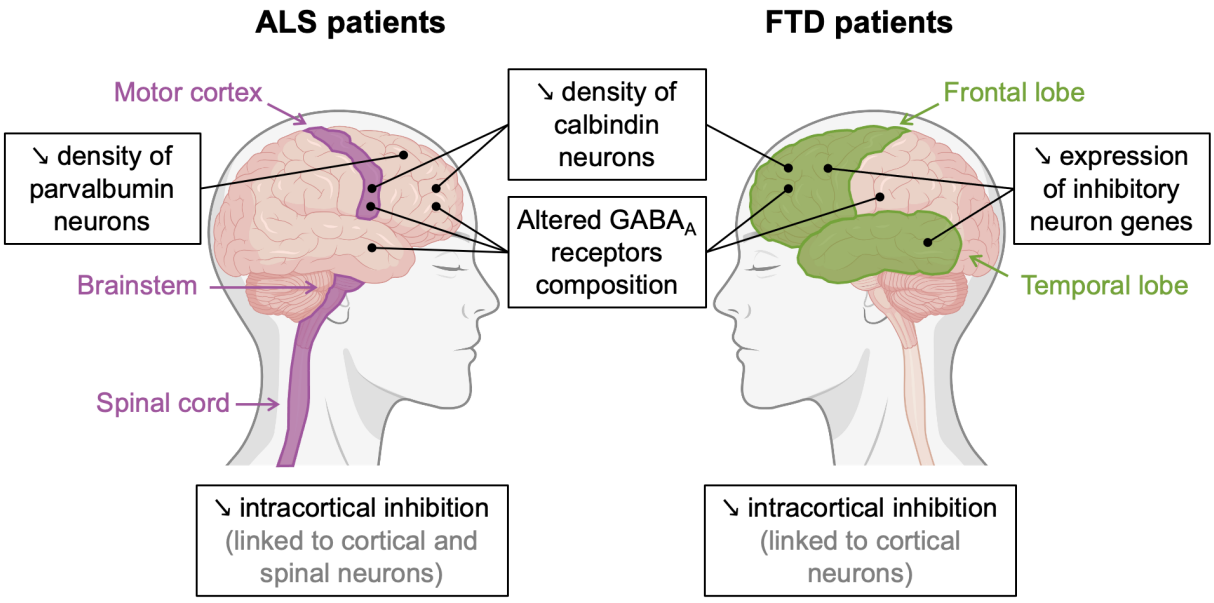


Figure 14: Main inhibitory neuron impairments reported in the brains of ALS and FTD patients. ALS is characterised by the degeneration of motor neurons in the motor cortex, brainstem and spinal cord (in purple), whereas FTD is characterised by a relatively selective degeneration of the frontal and temporal lobes (in green).

SOD1 patients homozygous for the D90A mutation exhibit a characteristic phenotype and relatively long disease duration. Their pattern of decreased [^{11}C]flumazenil was distinct and less extensive than in sporadic patients (Turner et al., 2005a). In particular, no decrease was detected in motor regions when compared to controls. A significant correlation was reported between clusters of reduced [^{11}C]flumazenil binding and disease duration or severity score. The latter was calculated with the revised ALS functional rating scale (ALSFRS-R), a clinical scale designed to evaluate motor impairments and functional deterioration in patients (Gordon et al., 2004). It is therefore tempting to suggest that the relative sparing of inhibitory circuits may be a mechanism contributing to the slower disease progression in patients homozygous for the D90A mutation.

1.3. Loss of neurons and neurites

As an alternative indirect evaluation of inhibitory neurotransmission, several studies have focused on characterising the density and molecular markers of inhibitory neurons in ALS and FTD. The number of calbindin neurons was reported to be reduced by over 60% in deep cortical layers of several brain regions in ALS patients compared with healthy controls (Maekawa et al., 2004). This was notably shown in the primary motor cortex and dorsolateral prefrontal cortex. In previous studies, the density of calbindin neurons was also drastically reduced in the frontal cortex of patients with ALS-FTD (Ferrer et al., 1993) or FTD (Ferrer, 1999). The *post-mortem* analysis conducted by Maekawa et al. further revealed trends towards a reduced density of calretinin and parvalbumin neurons. However, this result is still a topic of debate. Previous studies concluded that the soma of parvalbumin neurons is relatively well preserved in patients with ALS (Ince et al., 1993), ALS-FTD (Ferrer et al., 1993) or FTD (Ferrer, 1999). Nevertheless, a lower expression of the *PVALB* gene, encoding parvalbumin, was observed in the motor cortex of ALS patients in comparison to controls (Lederer et al., 2007). A recent transcriptomic analysis also revealed that neuronal markers, including calbindin, parvalbumin and vasoactive intestinal peptide –VIP–, were downregulated in the frontal and temporal cortices of FTD patients compared with controls (Hasan et al., 2022). A comparison of the estimated cellular compositions showed a significant decrease in the proportion of inhibitory neurons in the frontal and temporal cortices. This was partially associated with the neuronal loss and reduction in cortical thickness observed in the frontal cortex. Finally, the number of parvalbumin neurons was reported to be reduced by 25% in the dorsolateral prefrontal cortex of sporadic and *C9ORF72* ALS patients (Lin et al., 2021) and was found to be reduced in a small number of *SOD1* patients (Khademullah et al., 2020).

To our knowledge, only one study has evaluated the presence of pathological hallmarks in cortical inhibitory neurons (Nolan et al., 2020). The authors reported that, in sporadic ALS patients, aggregates of hyperphosphorylated TDP-43 are only rarely observed in GAD_{67}-positive inhibitory neurons.

1.4. Altered composition of GABA receptors

An additional indirect assessment of inhibitory neurotransmission is the evaluation of the composition of GABA receptors. In the brain, $GABA_A$ receptors are predominantly composed of a combination of α1–2, β1–3 and γ2 subunits. Initial studies demonstrated a significant reduction in the expression of *GABRA1*, encoding the α1 subunit, in the motor (Lederer et al., 2007; Petri et al., 2003), prefrontal and temporal (Petri et al., 2006) cortices of ALS patients compared with controls. This was not observed in the occipital cortex (Petri et al., 2006), which is considered to be preserved in ALS. More recently,

omics studies have revealed deregulation of GABAergic signalling pathways in both ALS (Andrés-Benito et al., 2017; Aronica et al., 2015; Laszlo et al., 2022) and FTD (Jiang et al., 2018; Pottier et al., 2022). Although the findings appear to be heterogeneous, they indicate that the composition of $GABA_A$ receptors is altered in the brains of these patients (Table 1), which may result in changes in the physiological and pharmacological properties of these receptors.

		Transcriptomics analysis of the main $GABA_A$ receptor subunits					
Form of disease	**Brain region**	**α1**	**α2**	**β1**	**β2**	**β3**	**γ2**
ALS	Motor cortex	↘	=	↗	=	=	=
	Frontal cortex	↘	—	=	= ↗	—	=
	Temporal cortex	↘	—	=	=	—	=
FTD with TDP-43 inclusions	Frontal cortex	—	—	—	—	↘	—
	Parietal cortex	—	=	=	=	=	=
FTD with *MAPT* mutations	Insular cortex	—	↘	=	↘	↘	↘
	iPSC-derived cortical neurons	—	↘	↘	↘	↘	↘

		Transcriptomics (or proteomics) analysis of the other $GABA_A$ receptor subunits					
Form of disease	**Brain region**	**α3**	**α4**	**α5**	**γ1**	**γ3**	**δ**
ALS	Motor cortex	=	=	= (↗)	—	=	= (↗)
	Frontal cortex	—	—	—	—	—	↗
	Temporal cortex	—	—	—	—	—	—
FTD with TDP-43 inclusions	Frontal cortex	—	—	=	—	—	—
	Parietal cortex	—	=	=	=	—	—
FTD with *MAPT* mutations	Insular cortex	—	↘	=	=	—	—
	iPSC-derived cortical neurons	—	↘	↘	↘	—	—

Table 1: ALS and FTD patients display broad alterations in the composition of $GABA_A$ receptors. Depending on the group of patients and brain region, the expression of genes encoding the different subunits is either reduced (blue), unaltered (white) or increased (red). This does not necessarily indicate that the expression of proteins is similarly affected. iPSC: induced pluripotent stem cells. References: Andrés-Benito et al., 2017; Jiang et al., 2018; Laszlo et al., 2022; Lederer et al., 2007; Petri et al., 2006, 2003; Pottier et al., 2022.

Interestingly, certain alterations appear to be specific to subgroups of ALS patients. In a transcriptomics study of the motor cortex, an unsupervised hierarchical clustering approach subdivided sporadic patients into two groups associated with distinct deregulated pathways and genes (Aronica et al., 2015). These groups were not related to technical variation or demographic factors (sex, age at onset and death, disease duration). The first subgroup exhibited a downregulation of a gene cluster associated with the life cycle of $GABA_A$ receptors. This was linked to the significant downregulation of *GABRA1*, *GABRB1*, *GABRB2* and *GABRG2*. Conversely, the second group did not exhibit any

deregulation of the GABAergic signalling pathways. Furthermore, a proteomics study of the primary motor cortex of ALS patients revealed increased levels of α5 and δ subunits (Laszlo et al., 2022). Stratifying the data by cognitive performance demonstrated that the δ subunit was upregulated in ALS patients with cognitive impairments compared to those without. Data stratified by *C9ORF72* status displayed an upregulation in the α4 subunit expression in the prefrontal cortex of patients with repeat expansions in comparison to those with no mutation. These results underscore the necessity of developing methods for the identification of ALS subtypes, as considering ALS pathology as a single entity may mask the underlying pathogenic mechanisms.

G protein-coupled $GABA_B$ receptors may be relatively well preserved in ALS and FTD. These receptors are composed of two subunits, $GABA_{B1}$ and $GABA_{B2}$, and are encoded by *GABBR1* and *GABBR2*, respectively. Only two studies reported the deregulation of these genes in the brains of sporadic ALS patients. One study observed a reduction in *GABBR1*expression in the motor cortex (Aronica et al., 2015), while the second study found an upregulation in *GABBR2* in the frontal cortex (Andrés-Benito et al., 2017).

2. Neurophysiological evidence of inhibitory neuron impairments in the brains of ALS and FTD patients

2.1. Reduced inhibitory transmission

The loss of inhibitory neurons and neurites, as well as the altered composition of GABA receptors, can affect inhibitory neurotransmission. Over the past few decades, different protocols of transcranial magnetic stimulation –TMS– have been employed to assess cortical excitability in patients. Several neurophysiological parameters have emerged, including short-interval intracortical inhibition (SICI), long-interval intracortical inhibition (LICI) and cortical silent period (CSP). SICI is commonly associated with cortical inhibitory neurons acting via $GABA_A$ receptors, while LICI is mediated by long-latency inhibitory post-synaptic potentials acting via $GABA_B$ receptors (McDonnell et al., 2006; Vucic et al., 2023). CSP duration is linked to a combination of long-latency inhibitory cortical processes and spinal inhibitory mechanisms. It emerges from the activation of cortical inhibitory neurons acting via $GABA_B$ receptors, as well as glycinergic inhibitory neurons in the ventral horn of the spinal cord (Škarabot et al., 2019).

The reduction in both SICI and CSP duration appears to represent a uniform pathophysiological process in ALS patients (Figure 14, Table 2) (Higashihara et al., 2024). Interestingly, this was also observed in sporadic patients, who presented no clinical or neurophysiological evidence of lower motor neuron dysfunction (Menon et al., 2015), and in patients at the time of symptom onset (Menon et al., 2020). This suggests that cortical disinhibition is an early phenomenon in ALS pathology. Asymptomatic carriers

of *SOD1*mutations or *C9ORF72* repeat expansion exhibited no alterations in SICI or CSP duration when compared to controls (Geevasinga et al., 2015; Vucic et al., 2008). However, Vucic et al. described three presymptomatic *SOD1* mutation carriers in whom both parameters were altered months before the development of the first clinical manifestations of ALS.

Form of disease	Short interval intracortical inhibition	Long interval intracortical inhibition	Cortical silent period	References
Sporadic ALS	Reduced	—	Reduced	Menon et al., 2020; Pavey et al., 2024; Shibuya et al., 2017; Van den Bos et al., 2018; Vucic and Kiernan, 2006
Familial ALS with *SOD1* mutations	Reduced	—	Normal	Vucic et al., 2008
Familial ALS with *FUS* mutations	Reduced	—	Reduced	Blair et al., 2010
Familial ALS with *C9ORF72* repeat expansions	Reduced	—	Reduced	Geevasinga et al., 2015; Williams et al., 2013
FTD with a behavioural variant	Reduced	Reduced	Reduced	Bae et al., 2016; Benussi et al., 2017
FTD with primary progressive aphasia	Reduced	Reduced	Non-significant trend towards a reduction	Benussi et al., 2017; Burrell et al., 2011
FTD with *C9ORF72* or *GRN* mutations	Reduced	Non-significant trend towards a reduction	—	Benussi et al., 2016

Table 2: ALS and FTD patients exhibit common alterations in neurophysiological parameters linked to cortical inhibition.

Two studies reported that SICI declines with time when patients are followed longitudinally (Menon et al., 2020; Shibuya et al., 2017). This highlights the possibility that the dysfunction of inhibitory neuronal circuits evolves with disease progression and is more prominent in the later stages of ALS. However, a previous study observed the opposite phenomenon in their cohort. Patients with a limited peripheral disease burden presented a smaller SICI than patients with advanced disease (Vucic and Kiernan, 2006). Correlation analyses also reported mixed results, with SICI reduction being associated with the progression of motor impairments and functional deterioration (assessed with the ALSFRS-R) (Shibuya et al., 2017; Van den Bos et al., 2018) or not (Menon et al., 2020).

Intracortical inhibition was found to be preserved in *SOD1* patients homozygous for the D90A mutation (Turner et al., 2005b), yet they exhibited similar functional disability (assessed with the ALSFRS-R) as sporadic ALS patients who had reduced intracortical inhibition. This is in line with another study in which the authors concluded that cortical, and possibly spinal, inhibitory circuits are preserved in patients with homozygous D90A mutations compared to sporadic patients (Weber et al., 2000).

In FTD patients, the reduction in both SICI and LICI seems to be a uniform pathophysiological process (Figure 14, Table 2). However, inconsistent results were obtained with asymptomatic carriers of *GRN* mutations compared with controls. A study reported no alterations in intracortical inhibition (Benussi et al., 2016), while a second one reported a significant reduction in SICI (Gazzina et al., 2018). In both studies, the onset of clinical symptoms was estimated from the mean age at symptom onset observed in the family. This showed that SICI assessments were performed 16.8 and 18.5 years before the expected symptom onset, respectively. A third study included both symptomatic and asymptomatic carriers of *GRN* mutations and *C9ORF72* repeat expansion, and stratified them based on the age at symptom onset or estimated years from symptom onset (Benussi et al., 2019b). With this approach, they highlighted that SICI may already be significantly reduced 25 years before the expected symptom onset, followed by a reduction in LICI 5 years later. Both neurophysiological parameters were found to decline over time, and this continued after symptom onset for SICI, while LICI tended to stabilise. The estimation of the age at symptom onset based on family history may not be applicable for all mutations (Moore et al., 2020), so one should exercise caution with the aforementioned observations.

In studies including both ALS and FTD patients, no significant differences in SICI were reported between the two groups, but defects were more pronounced in ALS than FTD (Bae et al., 2016; Burrell et al., 2011). Burrell et al. reported that one-third of FTD patients in their cohort exhibited motor deficits and one-eighth were also diagnosed with motor neuron disease. In these patients, SICI tended to be lower than in FTD patients without motor neuron disease. While inhibitory neurotransmission may be more intensively affected in ALS than in FTD patients, it may be more broadly affected in the latter. Indeed, both SICI and LICI appear to be altered in FTD.

2.2. Altered neuronal oscillations

Finally, a number of studies have used electroencephalography –EEG– and magnetoencephalography –MEG– recordings to assess neuronal oscillations in the brains of ALS and FTD patients. Beta oscillations (15-30Hz), which can be measured at rest or during somatosensory processing and motor control, may reflect inhibitory neuron functions (Barone and Rossiter, 2021). In healthy controls, the enhancement of GABAergic

neurotransmission, achieved by inhibiting the neuronal reuptake of synaptic GABA or activating $GABA_A$ receptors with diazepam, increased baseline beta power at rest, as well as beta desynchronisation during movement preparation (Hall et al., 2011; Muthukumaraswamy et al., 2013). A reduction in beta power has been reported in the sensorimotor cortex of sporadic and *C9ORF72* ALS patients (Dukic et al., 2019; Trubshaw et al., 2024), as well as in the temporal, parietal, occipital and subcortical regions of the brains of FTD patients with a behavioural variant (Govaarts et al., 2022; Lindau et al., 2003). This provides further support for the concept of a diminished inhibitory neurotransmission in patients. In these cohorts, measuring beta desynchronisation during movement preparation did not allow to draw a definitive conclusion, as this parameter was inconsistently found to be reduced (Bizovičar et al., 2014; Hughes et al., 2018), unaltered (Riva et al., 2012), or increased (Proudfoot et al., 2017). Beta resynchronisation after movement may depend on $GABA_B$ receptors, as it was reduced by increased synaptic concentrations of GABA (Muthukumaraswamy et al., 2013), but not upon the activation of $GABA_A$ receptors (Hall et al., 2011). Post-movement beta resynchronisation was observed to be diminished in ALS (Bizovičar et al., 2014; Proudfoot et al., 2017; Riva et al., 2012) and FTD (Hughes et al., 2018) patients compared with controls. In ALS, this reduction was found to be negatively correlated with the extent of corticospinal damage, and may be associated with reduced cortical inhibition (Riva et al., 2012). In particular, the results of these clinical studies have been interpreted as indicating a difficulty in reaching a state of decreased neuronal excitability after movement cessation. In the motor cortex of healthy controls, a positive correlation was identified between post-movement beta resynchronisation and bulk GABA concentrations (Gaetz et al., 2011), which may reflect inhibitory neuron and synapse densities, rather than synaptic activity per se. It may therefore be hypothesised that the diminished resynchronisation is also associated with a reduced density of inhibitory neurons and synapses in patients. Overall, the altered cortical beta oscillations lend support to the idea that inhibitory systems may be dysfunctional in ALS and FTD.

3. Pathological evidence of inhibitory neuron impairments in the spinal cords of ALS patients

3.1. Loss of neurons and neurites

In the lumbar spinal cords of sporadic ALS patients (Figure 15), the density of interneurons was found to be reduced by 53% compared with controls (Stephens et al., 2006). This has been studied in the dorsomedial region of the ventral horn grey matter, where it was not possible to differentiate between excitatory and inhibitory interneurons. Similarly, a variable but substantial loss of synapses was observed in the ventral horn of the spinal cord, but not in the dorsal and intermediate laminae (Aousji et al., 2023). The extent of synaptic loss demonstrated a strong correlation with disease duration; however,

this study did not differentiate between excitatory and inhibitory synapses. A previous study reported a loss of calbindin-positive soma and axons (Ince et al., 1993). In the ventral horn white matter, a significant loss of parvalbumin- and calretinin-positive axons has been found in sporadic ALS patients compared with controls (Hayashi et al., 2013). This reduction was equal to 83% and 74%, respectively. It is noteworthy that the number of calretinin-positive soma was not affected.

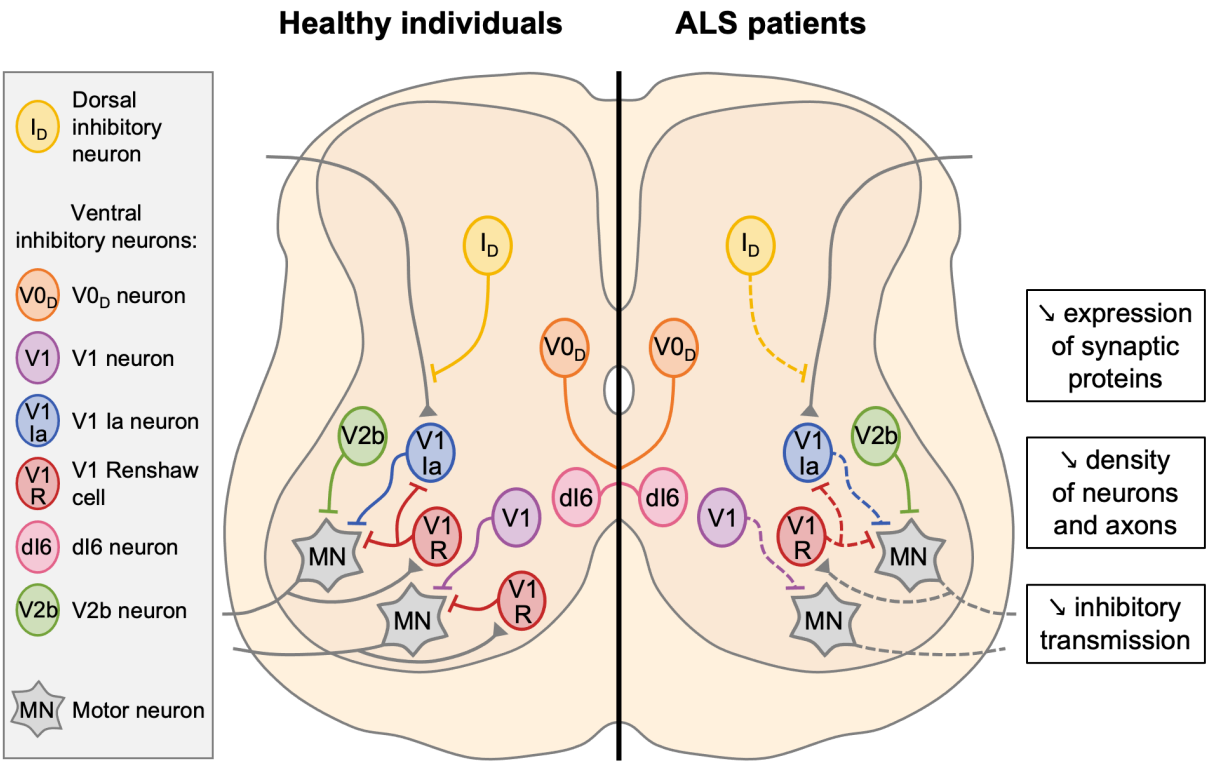


Figure 15: Spinal inhibitory neurons involved in locomotor control, and main alterations reported in ALS patients. In the dorsal horn, several populations of inhibitory neurons (represented by a single I_D neuron in yellow) are involved in sensory pathways, and can form connections with primary sensory afferents. In the ventral horn, V1 neurons (which include V1 Renshaw cells in red and V1 Ia neurons in blue) and V2b neurons (green) form ipsilateral connections with motor neurons (grey). Of note, all V1 neurons express the transcription factor Engrailed-1, while V1 Renshaw cells also express parvalbumin and calbindin, and V1 Ia neurons express parvalbumin. Commissural dorsal $V0_D$ neurons (orange) and dI6 neurons (pink) form contralateral connections with motor neurons. Dashed lines indicate known alterations in ALS patients.

3.2. Altered composition of GABA receptors

Following the initial stages of postnatal development, glycine is the principal inhibitory neurotransmitter in the spinal cord. In particular, dorsal inhibitory neurons largely co-express GABA and glycine, whereas ventral inhibitory neurons are mainly glycinergic. The data currently available on the composition of GABA or glycine receptors in the spinal

cords of ALS patients remain limited and inconsistent. A reduction in *GABRE* expression, encoding the $GABA_A$ receptor δ subunit, was reported in a cohort of patients, which included sporadic cases, one familial case with a *SOD1* mutation, and one familial case with an unidentified mutation (Dangond et al., 2004). However, another study reported the main deregulated gene clusters in the ventral horn of the lumbar spinal cords of sporadic patients, and this did not include GABAergic or glycinergic signalling pathways (Andrés-Benito et al., 2017). More recently, a proteomics analysis revealed a downregulation of pathways linked to synaptic signalling and diverse synapse subtypes, including GABAergic synapses, in the cervical spinal cords of sporadic patients and patients with *C9ORF72* repeat expansions (Aly et al., 2023).

4. Neurophysiological evidence of inhibitory neuron impairments in the spinal cords of ALS patients

The H reflex is a valuable tool for evaluating the excitability of inhibitory neuronal circuits in the spinal cord (Knikou, 2008). Distinct inhibitory circuits can be assessed using different paradigms and were found to be altered in ALS patients (Figure 15). Recurrent inhibition, which is mediated by Renshaw cells and allows negative feedback important for movement control, is significantly decreased in patients compared with controls (Castro et al., 2024). It has been proposed that this inhibition is enhanced at early stages of the disease and serves as a protective mechanism, particularly in patients with slow progression of lower limb dysfunctions (Sangari et al., 2022). Additionally, recurrent inhibition was found to be unaltered in patients with no lower limb dysfunction, while it was reduced in patients with motor weakness in the lower limbs (Özyurt et al., 2020; Sangari et al., 2022). GABAergic neurons located in the dorsal horn mediate the presynaptic inhibition of primary sensory afferents, which has been observed to be reduced in ALS patients (Castro et al., 2024; Howells et al., 2020; Özyurt et al., 2020). Finally, the postsynaptic inhibition induced by cutaneous stimulation is mediated by glycinergic synapses, and was also found to be reduced in ALS (Castro et al., 2024).

5. What is the relationship between impairments in inhibitory neurons and symptoms of ALS and FTD?

Neuronal circuit dysfunction has been proposed as an early feature of both ALS and FTD and may be an important step in the pathogenesis of these diseases. Clinical studies have highlighted correlation between inhibitory neurons impairments and motor, behavioural and cognitive symptoms in patients. However, most of the causal relationships remain to be investigated.

5.1. Inhibitory neurons impairments are associated to specific motor symptoms in ALS patients

The split-hand phenomenon is a specific clinical feature of ALS, characterised by the weakness and wasting of muscles located at the base of the thumb (thenar muscles) and the relative preservation of muscles located at the base of the little finger (hypothenar muscles). It was suggested that the reduction in intracortical inhibition, but not peripheral dysfunctions, contribute to the development of this phenomenon (Menon et al., 2014). Notably, reductions in short-interval intracortical inhibition and cortical silent period duration were observed when motor responses were recorded across all muscles, but were most prominent with recordings over the thenar muscles.

5.2. Inhibitory neurons impairments are correlated with behavioural phenotypes in FTD patients

Behavioural disinhibition is a common feature of FTD and is associated with decreased functional independence and increased mortality. Challenging behaviours probably originate both from a lack of comprehension of the appropriateness of actions in a given social context and an altered motor inhibition. The absence of effective symptomatic treatments reinforces the need to understand the mechanistic links between neuropathology, brain function and behaviour.

A significant correlation was reported between a reduction in intracortical inhibition (assessed with transcranial magnetic stimulation) and an increase in disinhibited and aggressive behaviours in FTD patients with a behavioural variant or primary progressive aphasia (semantic and non-fluent) (Benussi et al., 2020). This correlation was stronger in patients with *GRN* mutations than in those without. Upon detailed examination of the behaviours, SICI reduction was found to be associated with aggressivity, irritability, poor judgement and impulsivity, restlessness, obsessive behaviour, hoarding, excessive jocularity, hyperorality, hypersexuality and incontinence. Conversely, apathetic behaviours were associated with a decrease in intracortical facilitation, which reflects the activity of excitatory glutamatergic circuits. These results thus suggest that disinhibited symptoms may originate from the reduced activity of inhibitory circuits. Another study demonstrated that decreased GABA and glutamate concentrations were associated with increased disinhibited behaviour, characterised by impaired response inhibition measured by a stop-signal task (Murley et al., 2020). However, in this cohort, no associations were found between GABA concentrations and social disinhibition or challenging behaviours reported by carers. This discrepancy may be attributed to the fact that GABA levels are difficult to assess and were evaluated in a specific subregion of the frontal lobe, while numerous other regions are implicated in the behavioural impairments reported by carers.

In FTD patients with a behavioural variant, increased disinhibited behaviours were also strongly associated with reduced movement-related beta desynchronisation and resynchronisation when they needed to generate and inhibit responses during a stop-signal task (Hughes et al., 2018). As stated before, this neurophysiological alteration may be a proxy of inhibitory neuron dysfunctions.

5.3. Inhibitory neurons impairments are correlated with cognitive phenotypes in ALS and FTD patients

In ALS patients, the assessment of [^{11}C]flumazenil binding in specific frontal and temporal areas demonstrated a correlation between reduced binding and decreased performance on a written verbal fluency task and naming task (Wicks et al., 2008). Based on the protocol used and the lumbar onset of motor symptoms, these results appear to be exclusively linked to cognitive alterations, including executive and language defects. A previous study showed that cerebral activation was impaired in ALS patients compared with controls during word retrieval processes (assessed with both letter fluency and naming tasks) (Abrahams et al., 2004). Depending on the region, functional magnetic resonance imaging revealed increased or decreased cerebral activity, but inhibition remains to be more precisely assessed.

A transcriptomics study recently revealed reduced expression of *CPLX1*, encoding complexin-I, in the frontal cortex of FTD patients with TDP-43 inclusions, regardless of the presence of *GRN* mutations (Pottier et al., 2022). Complexin-I is a presynaptic protein relatively enriched in GABAergic inhibitory terminals. It regulates the assembly of SNARE proteins and, in turn, synaptic vesicle exocytosis. In patients with Alzheimer's disease, decreased levels of complexin-I have been linked to lower cognitive performance (Ramos-Miguel et al., 2017) and increased rate of cognitive decline (Boyle et al., 2013). Therefore, it would be interesting to further investigate the consequences of this decrease on the cognitive performance of FTD patients.

6. What are the mechanisms leading to decreased inhibition in ALS and FTD?

Several underlying mechanisms may account for the observed impairments in cortical and spinal inhibitory circuits (Figure 16). Given the complex and multifactorial nature of ALS and FTD, which involve different cell types, it is plausible that a combination of mechanisms is at play, or that specific mechanisms are associated with particular subtypes of ALS and FTD. The following paragraphs present a summary of the mechanisms that have been proposed based on studies conducted with mouse models.

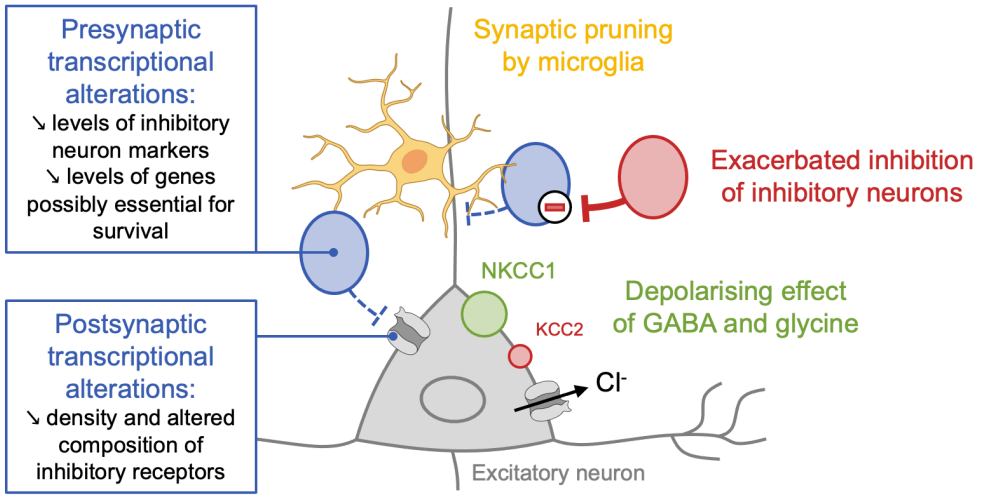


Figure 16: Several mechanisms, likely to be complementary, could account for the decreased inhibition in ALS and FTD. Cl^-: chloride; KCC2: potassium-chloride cotransporter 2; NKCC1: sodium-potassium-chloride cotransporter 1.

6.1. Presynaptic transcriptional alterations leading to inhibitory neuron dysfunction and death

Transcriptional alterations, which have been reported in patients and mouse models, could influence cell fate and neuronal activity in inhibitory neurons. In the spinal cord of *SOD1*^{G93A} mice, early and parallel reductions in the expression of *extended synaptotagmin 1* (Mora et al., 2024) and *engrailed-1* (Montañana-Rosell et al., 2024) were recently reported in V1 inhibitory neurons. This was followed by downregulation of inhibitory neurotransmitter markers (Montañana-Rosell et al., 2024) and cell death (Allodi et al., 2021; Chang and Martin, 2009) at later stages of the disease. Extended synaptotagmin 1 is a presynaptic protein which has been linked to the promotion of synaptic growth when overexpressed, and to reduced neurotransmission when mutated (Kikuma et al., 2017). Engrailed-1 appears to be an essential maintenance factor for the survival of postmitotic dopaminergic and serotoninergic neurons, possibly by preventing apoptosis (Albéri et al., 2004; Fox and Deneris, 2012; Simon et al., 2001). The early loss of these genes may thus contribute to the dysfunction and degeneration of V1 neurons. Of note, in zebrafish carrying a mutant *Sod1* gene, spinal glycinergic neurons were found to be vulnerable at early stages of embryonic development (McGown et al., 2013). These neurons were the first cell type to exhibit translational modifications related to the activation of a stress response, which was followed by dysregulation of glycine release.

6.2. Postsynaptic transcriptional alterations modifying the composition of inhibitory receptors

A number of mouse models have been observed to recapitulate the altered composition of $GABA_A$ receptors, which is a feature present in *post-mortem* brain tissues from ALS and

FTD patients. This may ultimately impair the functionality of these receptors and, thereby, the inhibitory neurotransmission. FUS was found to be localised in both pre- and postsynaptic compartments, where it binds to several RNAs encoding GABA receptor subunits, and may be directly involved in the regulation of protein translation, including the translation of the $GABA_A$ receptor α1 subunit (Sahadevan et al., 2021). In the cortex of *Fus*$^{\Delta NLS/+}$ mice, the authors observed an early synaptic accumulation of FUS, which was accompanied by a downregulation of $GABA_A$ receptor α3 subunit protein levels, followed by a transient upregulation of GABAergic genes and proteins in unstable synapses (Sahadevan et al., 2021; Scekic-Zahirovic et al., 2021). This increased transcription may be seen as a compensatory mechanism that is directly linked to the accumulation of FUS and the stabilisation of RNAs by FUS binding. At late stages of the disease, molecular and ultrastructural alterations of inhibitory synapses have been reported, but the underlying mechanisms remain to be studied.

Similarly, genes encoding subunits of the $GABA_A$ and $GABA_B$ receptors (including *Gabrb2*, *Gabrb3*, *Gabrg2* and *Gabbr1*) were found to be downregulated in the brains of tau^{P301L} mice compared to control mice (Jiang et al., 2018). Restricted expression of a mutant human *MAPT* gene in forebrain excitatory neurons was found to be sufficient to alter inhibitory synapses via non-cell autonomous mechanisms (Shimojo et al., 2020). In particular, a loss of GABAergic synapses was observed in the cortex and hippocampus, and this was accompanied by a reduction in the levels of pre- and postsynaptic GABAergic proteins, including the $GABA_A$ receptor α1 subunit. During the ageing process, these protein levels were comparable between mutant and control mice, indicating that compensatory mechanisms may have occurred.

In addition, inhibitory receptors were found to be altered in the spinal cords of *SOD1*^{G93A} mice. An early reduction in *Gabra5* expression was observed, accompanied by a loss of GABAergic boutons on the membrane of bulbar motor neurons (Venugopal et al., 2023). A previous in vitro study of spinal motor neurons obtained from embryos also proposed that alterations in the expression and functionality of $GABA_A$ receptors may occur (Avossa et al., 2006). However, to date, in vivo studies have not reported significant impairments in spinal GABAergic inhibition. Conversely, alterations in glycinergic inhibition have been documented. The density of glycine-evoked currents was found to be significantly smaller in cultured motor neurons prepared from *SOD1*^{G93A} embryos compared to control motor neurons (Chang and Martin, 2011). This was accompanied by a decreased density of glycine receptors on motor neurons and a reduction in the expression of the gene encoding the α1 subunit.

6.3. Abnormal elimination of inhibitory synapses by microglia

In the brains of *Grn*$^{-/-}$ mice, the loss of progranulin has been linked to an excessive age-dependent activation of microglia (Lui et al., 2016). This was associated with increased production and accumulation of complement proteins in both excitatory and inhibitory synapses, while the enhanced synaptic pruning activity of microglia selectively eliminated inhibitory synapses. Although the underlying mechanisms still need to be studied, two hypotheses have been proposed. It is possible that excitatory and inhibitory synapses exhibit different expression profiles of complement receptors and/or different intrinsic properties, which influences the efficacy of engulfment by microglia.

6.4. Abnormal depolarising action of GABA

In immature neurons, high expression of sodium-potassium-chloride cotransporter 1 (NKCC1) results in a high concentration of intracellular chloride ions (Kaila et al., 2014). This facilitates the efflux of chloride ions when GABA and glycine receptors are activated, thereby inducing depolarisation of the membrane potential. During development, a switch occurs, allowing hyperpolarisation of the membrane potential upon the activation of inhibitory receptors. This is due to the upregulated and abundant expression of potassium-chloride cotransporter 2 (KCC2) in mature neurons, which results in a low concentration of intracellular chloride ions, and an influx of chloride ions when GABA and glycine receptors are activated. An increase in NKCC1 expression and a decrease in KCC2 expression have been associated with epilepsy, as well as several neurodegenerative and neuropsychiatric disorders (Ben-Ari, 2017; Lam et al., 2023).

In the lumbar spinal cords of *SOD1*^{G93A} mice, a reduction in KCC2 expression was observed at the membrane of vulnerable motor neurons (Fuchs et al., 2010). This process started during the late presymptomatic phase and accelerated as the disease progressed. A more recent study reported decreased expression of KCC2 at the membrane of cortical and spinal motor neurons in presymptomatic *SOD1*^{G93A} and *TDP-43*^{A315T} mice (Khademullah et al., 2023). It is noteworthy that the administration of KCC2 enhancers restored its membrane expression and function, postponed the onset of motor deficits, and prolonged the lifespan of *SOD1*^{G93A} mice by 50 days. Additionally, the authors reported that KCC2 expression was diminished at the membrane of cortical motor neurons in *SOD1*, *C9ORF72*, and sporadic ALS patients. These results suggest that a switch could occur from hyperpolarising to depolarising GABA, which would decrease the inhibitory influence of this neurotransmitter.

6.5. Exacerbated inhibition of inhibitory neurons

To allow tight regulation of their influence, inhibitory neurons are interconnected: they can synapse on excitatory motor neurons to provide direct inhibition but can also synapse onto other inhibitory neurons and consequently have an indirect facilitatory effect, which is called a disinhibitory effect (Tremblay et al., 2016). One can thus imagine that the initial impairment of the upstream subpopulation of inhibitory neurons induces a cascade of consequences and an indirect alteration of motor neurons. In line with this hypothesis, the density of somatostatin neurons was found to be decreased, while their activity was increased in the motor cortex of presymptomatic *TDP-43*^{A315T} mice compared with control littermates (Zhang et al., 2016). Conversely, the density of parvalbumin neurons was not altered, but their activity was decreased. As somatostatin neurons are known to regulate parvalbumin activity, the authors proposed that the enhanced activity of somatostatin neurons increased their inhibitory influence on parvalbumin neurons, which, in turn, disinhibited layer 5 pyramidal neurons, leading to their increased excitability and degeneration. Interestingly, the ablation of somatostatin neurons in *TDP-43*^{A315T} mice restored the spiking activity of pyramidal neurons to physiological levels. This was followed by a significant increase in the density of GABAergic synapses on these neurons, and this prevented neuronal loss.

7. Contribution of inhibitory neuron impairments to symptoms

To our knowledge, the causal relationship between inhibition deficits and motor symptoms has been evaluated in mouse models by several research groups, while the contribution of inhibitory neuron impairments to behavioural or cognitive symptoms has yet to be investigated in ALS and FTD models. Mice lack Betz cells and von Economo neurons (Bakken et al., 2021; Seeley et al., 2012), which are the main degenerating neurons in the frontal cortex of ALS and FTD patients, respectively. Additionally, their corticospinal tract is anatomically and functionally different than in humans (Lemon, 2008). However, network activity and degeneration can still be recapitulated in mice.

7.1. Inhibitory neurons influence motor neuron activity and death in ALS mouse models

In ALS, ocular motor neurons are considered resilient because they do not degenerate. Several studies have compared these neurons with vulnerable brainstem and spinal motor neurons to identify potential protective mechanisms. In healthy humans, mice and rats, resilient motor neurons have distinct transcriptional profiles, with marked differences in genes involved in GABAergic synaptic transmission (Brockington et al., 2013). Several genes encoding $GABA_A$ and $GABA_B$ receptor subunits were found to be upregulated in the three species under investigation. In particular, an enrichment of the

$GABA_A$ receptor α1 subunit was observed in resistant motor neurons, while vulnerable motor neurons were enriched in the α2 subunit (Comley et al., 2015; Lorenzo et al., 2006). In addition, resilient motor neurons showed a decreased ratio of glycine receptor density to $GABA_A$ receptor density, as well as an elevated density of extrasynaptic $GABA_A$ receptors in healthy rats (Lorenzo et al., 2006). Finally, resilient motor neurons exhibited reduced susceptibility to excitotoxicity, which was mediated in part through enhanced GABAergic transmission (Brockington et al., 2013). Collectively, these results suggest that inhibitory synaptic transmission differs between resilient and vulnerable motor neurons, and may underlie their differential vulnerability. This hypothesis has recently been supported by the study of a mouse model in which human TDP-43 is mislocalised primarily in forebrain excitatory neurons. In these mice, the increased excitability of upper motor neurons was followed by a degeneration of lower motor neurons in lumbar regions 1 to 3, but not in lumbar regions 4 to 6. Interestingly, an increased inhibitory innervation was observed specifically in lumbar regions 4 to 6, where lower motor neurons were spared, potentially due to protective mechanisms associated with the inhibitory system (Reale et al., 2023).

Moreover, the impairment of inhibitory neurons may directly contribute to the altered activity and degeneration of motor neurons (Figure 17). The density of GABAergic synapses was found to be reduced in the somatic area of layer 5 pyramidal neurons in the motor cortex of presymptomatic *TDP-43*^{A315T} mice compared with control littermates (Zhang et al., 2016). Measurements of miniature and evoked inhibitory postsynaptic currents from pyramidal cells demonstrated a significant reduction, whereas excitatory transmissions remained unaltered. In addition, pyramidal neurons exhibited increased excitability, which could be abolished by blocking $GABA_A$ receptors. This was followed by signs of dendritic alterations and neurodegeneration at the onset of symptoms. Similar observations were reported for presymptomatic *SOD1*^{G93A} mice. In the motor cortex of these mice, decreased density and activity of parvalbumin neurons were found, accompanied by increased excitability of pyramidal motor neurons (Khademullah et al., 2020). Interestingly, increasing the activity of parvalbumin neurons during the late presymptomatic and symptomatic phases normalised pyramidal cell excitability to control levels and effectively delayed the onset of motor impairments, as evidenced by a delayed decline in muscle strength. This ultimately extended survival by almost 20 days.

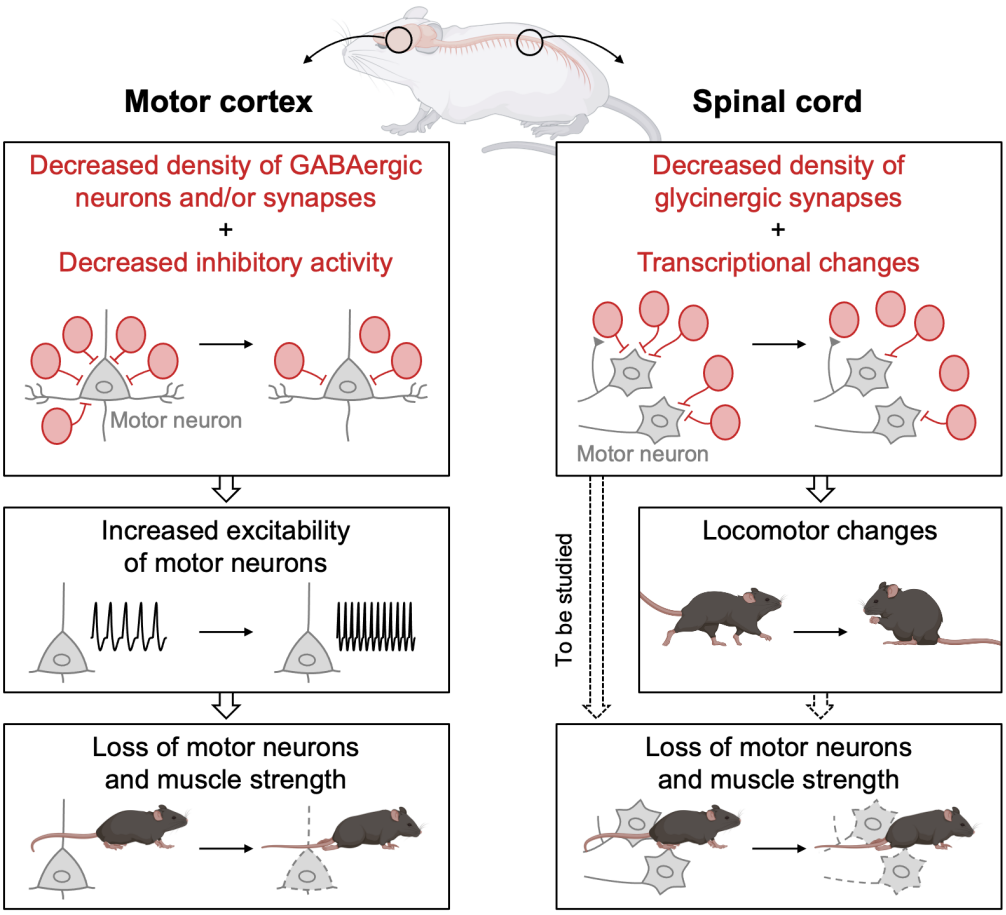


Figure 17: Impairments of inhibitory neurons influence the development of locomotor deficits in ALS mouse models. Impairments of inhibitory neurons (red) result in impairments of cortical and spinal motor neurons (grey) via a proven (solid arrow) or assumed (dashed arrow) cause-and-effect relationship.

In the spinal cords of presymptomatic *SOD1*^{G93A} mice, it was demonstrated that inhibitory neurons undergo transcriptional changes prior to those observed in excitatory neurons (Montañana-Rosell et al., 2024). One of the lost markers is engrailed-1, which is a transcription factor expressed by V1 neurons and transferred from these cells to motor neurons (Lebœuf et al., 2023). Both the decreased expression of *engrailed-1* and the neutralisation of extracellular engrailed-1 resulted in a loss of motor neurons and decreased limb strength. This may therefore be another mechanism linking the loss of inhibitory synapses to the progression of ALS.

7.2. Inhibitory neurons contribute to locomotor phenotype in ALS mouse models

In the spinal cords of presymptomatic *SOD1*^{G93A} mice, a selective loss of glycinergic synapses on fast motor neurons has been reported (Allodi et al., 2021). This was accompanied by a progressive slowing of locomotor speed, an inability to maintain locomotion, and a hyperflexion of the hindlimbs. These phenotypes emerged prior to the

observed decline in grip strength and the degeneration of motor neurons. In addition, the silencing of V1 inhibitory neurons positive for engrailed-1 in wild-type mice resulted in the aforementioned phenotypes. In *SOD1*^{G93A} mice, the stabilisation of V1 inhibitory connections was sufficient to rescue motor neuron loss and ameliorate motor phenotypes, but this did not prevent weight loss or death (Mora et al., 2024). From this, it is evident that other altered neuronal circuits are involved in the pathogenesis of ALS, thereby reinforcing the necessity to develop a combination of therapies to address all symptoms. Nevertheless, these studies strongly indicate that inhibitory neurons play a pivotal role in the initial stages and development of locomotor changes (Figure 17).

8. Future directions: inhibitory neurons as a possible therapeutic target

As detailed in this review, several alterations in inhibitory neurons have been documented in the brains and spinal cords of ALS and FTD patients, as well as in mouse models. Interestingly, these impairments may contribute to the development and/or progression of certain core symptoms that characterise these two neurodegenerative diseases. This hypothesis has been primarily investigated in ALS models, in which a reduction in cortical and spinal inhibitory influences has been linked to alterations in motor neurons and/or changes in locomotor function (Allodi et al., 2021; Khademullah et al., 2020; Zhang et al., 2016). The question of whether alterations in inhibitory neurons can cause behavioural and cognitive deficits in ALS and FTD remains unanswered. This topic is of particular interest given that the reduced intracortical inhibition and altered oscillatory dynamics have been associated with disinhibited and aggressive behaviours (Benussi et al., 2020; Hughes et al., 2018), which has the potential to worsen the prognosis of FTD patients. Overall, the current data justifies the necessity of investigating whether targeting deficits in cortical and spinal inhibition would efficiently alleviate certain symptoms. The development of new therapeutic approaches to stabilise or enhance the inhibitory activity will be challenging owing to the complexity and heterogeneity of inhibitory neuronal populations and circuits. Further investigation is also needed to elucidate all the mechanisms underlying the reduced inhibitory influence in ALS and FTD. Nevertheless, this represents a promising avenue for further research, as discussed below.

In ALS mouse models, enhancing or stabilising the inhibitory activity effectively attenuated locomotor impairments (Figure 18), thus offering an encouraging therapeutic approach. In particular, the fact that analogous mechanisms have been documented in TDP-43 and SOD1 mice suggests that inhibitory neurons may represent a relevant target in ALS cases associated with different causative genes and proteins, and even in patients for whom the aetiology of the disease remains unknown.

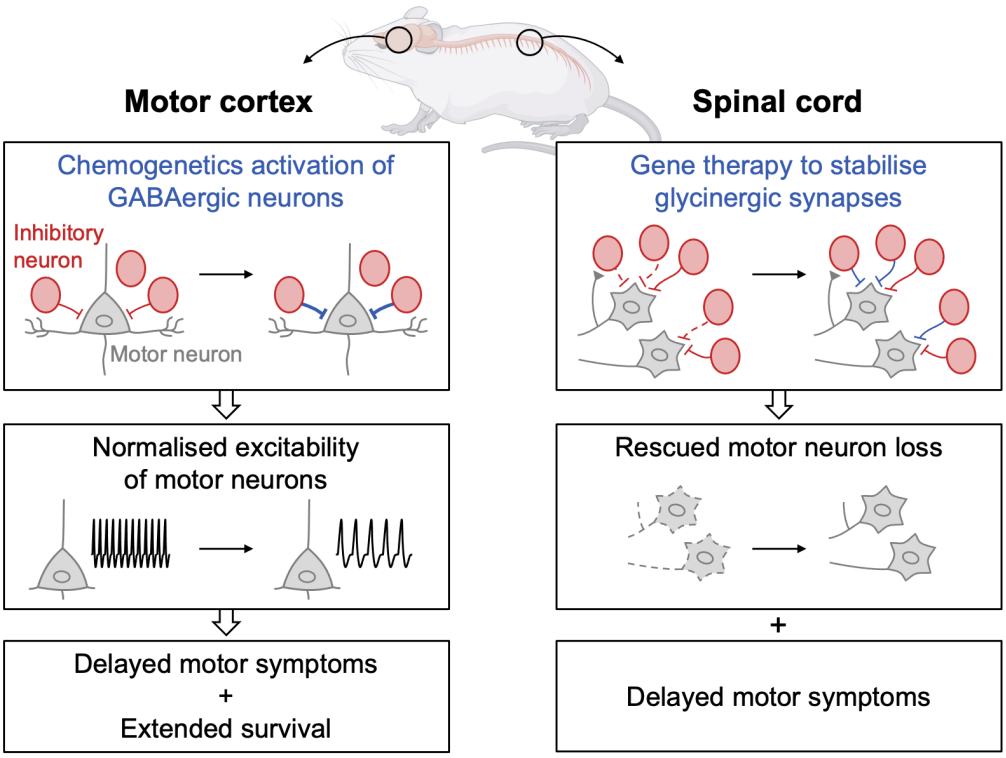


Figure 18: Enhancing or stabilising the inhibitory activity represents a promising therapeutic approach to alleviate locomotor deficits. In ALS mouse models, activating inhibitory neurons (red) or stabilising inhibitory synapses results in the protection of cortical and spinal motor neurons (grey) and delays motor symptoms.

It is noteworthy that the augmentation of cortical, but not spinal, inhibitory activity in ALS mouse models extended their survival (Khademullah et al., 2020; Mora et al., 2024). In sporadic ALS patients within two years of disease onset, reduced short-interval intracortical inhibition has been identified as an independent factor associated with shorter survival (Shibuya et al., 2016). This reduction was not found to be a prognostic factor when including patients at a later disease stage. However, this could be explained by the reduced number of patients with long disease durations and a possible change in intracortical inhibition during disease progression. In the total cohort, the estimated median survival was 28 months for patients with the smallest intracortical inhibition values and 36 months for patients with the highest values.

8.1. Increasing the activity of GABA receptors in ALS patients

A limited number of drugs are currently available to treat ALS, and their effects on disease progression are moderate (Evans et al., 2024). Riluzole was the first pharmaceutical compound approved by the Food and Drug Administration –FDA– in 1995 and the European Medicines Agency –EMA– in 1996. It is now postulated that this sodium channel blocker increases the median survival of patients by 6 to 19 months (Andrews et al., 2020), while exerting neuroprotective effects through several mechanisms of action. In

particular, riluzole is thought to restore the balance between excitation and inhibition, notably by reducing synaptic GABA reuptake (Mantz et al., 1994) and potentiating postsynaptic $GABA_A$ receptor function (He et al., 2002; Jahn et al., 2008). In ALS patients, riluzole partially normalises intracortical inhibition (Vucic et al., 2013), but this effect is transient (Geevasinga et al., 2016).

Retigabine (or ezogabine) is a potassium channel activator which has been approved for the treatment of focal-onset epilepsy (Gunthorpe et al., 2012). This compound has multiple mechanisms of action, including the potentiation of postsynaptic $GABA_A$ receptor responses. In ALS patients, a single dose of retigabine was sufficient to reduce the excitability of motor axons to a greater extent than a single dose of riluzole (Kovalchuk et al., 2018). Recently, retigabine was used in a phase II clinical trial including 55 patients with ALS, resulting in a dose-dependent reduction in the excitability of both cortical and spinal motor neurons and a 53% increase in short-interval intracortical inhibition (Wainger et al., 2021). However, the effect on disease progression remains to be investigated.

Given that none of the aforementioned compounds act solely by increasing the activity of GABA receptors, it is possible that the beneficial effects observed in ALS patients, whether currently or in the future, may be due to other mechanisms of action.

8.2. Regulating neuronal activity in ALS and FTD patients

In ALS patients, the external modulation of excitatory and inhibitory neurotransmission has the potential to mitigate motor impairments, notably by promoting growth factors which enhance neuroplasticity and by possibly slowing the degeneration of neuronal circuits. A two-week course of transcranial direct current stimulation –tDCS– applied to both motor cortices and spinal cords was found to improve global muscle force and quality of life (Benussi et al., 2019a). More recently, this non-pharmacological intervention has yielded encouraging results regarding the patient survival, a potential reduction in neurofilament levels and the modulation of cortical excitation and inhibition (Benussi et al., 2023). This current stimulation may modulate superficial neuronal populations and, in turn, facilitate the increase in short-interval intracortical inhibition while reducing intracortical facilitation (Vignaud et al., 2018).

In FTD patients, the external modulation of inhibitory neuron activity and the induction of gamma oscillations could represent a promising therapeutic approach to slow the neurotoxicity and death of pyramidal cells. An intervention based on 40Hz transcranial alternating current stimulation –tACS– is currently being tested in patients with a behavioural variant (Assogna et al., 2022). This non-invasive brain stimulation is thought to restore altered brain oscillatory patterns and, in turn, to improve working memory,

attention and cognitive functions. In addition, it would be interesting to assess whether a long-term effect on disinhibitory behaviours can be elicited with this approach.

Conclusion

Over the past two decades, a growing body of clinical and experimental evidence has highlighted the contribution of inhibitory neuron impairments to the ALS-FTD continuum. Degeneration of inhibitory neurons and neurites, as well as alterations to pre- and postsynaptic inhibitory markers, have been documented in the brains of patients. However, *post-mortem* investigations remain constrained in their ability to elucidate the temporal sequence and potential functional consequences of these alterations. Interestingly, neurophysiological studies have revealed a reduction in cortical inhibitory transmission, which appears to be an early feature of both ALS and FTD. The precise alterations may differ among patients carrying different pathological mutations and/or exhibiting different forms of the diseases. Nevertheless, it has been proposed that ALS and FTD are both characterised by an imbalance between excitation and inhibition, with the former being relatively unopposed and ultimately becoming pathological. Although this model is arguably overly simplistic, it reinforces the idea that ALS and FTD belongs to a continuum, in which both diseases share pathological mechanisms, as evidenced by the damage to inhibitory neurons. Studies on the spinal cord of ALS patients are less extensive, and the current findings appear to be more heterogeneous. However, some of them also point towards a reduced inhibition. Given that inhibitory neuron alterations have been observed in a number of mouse models of ALS and FTD, several underlying mechanisms have been proposed to explain the impairments in cortical and spinal inhibitory circuits. It remains unclear whether specific mechanisms are associated with subtypes of ALS and FTD, or whether they all combine. More importantly, the alterations in inhibitory neurons may play a pivotal role in the development and/or progression of motor, behavioural and cognitive symptoms, thus becoming potential therapeutic targets. As a consequence, further investigation of inhibitory neurons in ALS and FTD would be beneficial for advancing our understanding of these diseases, and potentially improving their management.

9. Inhibitory neuron impairments in ALS-FTD mouse models

Several studies have documented impairments of inhibitory neurons in mouse models of ALS and FTD. The publications included in the Review enabled the identification of potential mechanisms underlying the alteration of inhibitory neurons, or the contribution of these alterations to locomotor phenotypes. Here, I will present the current understanding of the progression of these impairments in mice, and I will discuss the potential associations with motor and behavioural phenotypes.

9.1. Mutation of *TARDBP* to model ALS and FTD

Inhibitory neuron impairments have been reported in transgenic mice overexpressing wild-type or mutant versions of the human *TARDBP* gene (Tsuiji et al., 2017; Zhang et al., 2016). In particular, it was shown that wild-type TDP-43 accelerates the age-dependent degeneration of hippocampal inhibitory neurons, while mutant TDP-43 induces early alterations of the disinhibitory effects of cortical somatostatin neurons (Figure 16).

However, TDP-43 is a protein able to regulate its own production by influencing the homeostasis of its messenger RNA. Therefore, the use of overexpression paradigm in classical transgenic mice perturbs this autoregulation, which means that the consequences of the mutations are not studied in the presence of a physiological control of TDP-43 production. To circumvent this issue, some groups developed knock-in mouse lines carrying point mutations within the endogenous murine *Tardbp* gene.

TDP-43^{Q331K} knock-in mice were created by introducing a mutation equivalent to the human Q331K mutation (White et al., 2018). Heterozygous and homozygous mice do not recapitulate ALS-like motor impairments, even during aging. However, they exhibit executive dysfunction, memory impairment and hyperphagia, recapitulating FTD at the behavioural level. In 5 to 7-month-old TDP-43$^{Q331K/Q331K}$ mice compared to control mice, the density of parvalbumin neurons was found to be reduced in several brain regions (Lin et al., 2021; White et al., 2018). Using magnetic resonance imaging, an association was made between this loss of parvalbumin neurons and an atrophy of the brain regions, while the number of inhibitory neurons remained unaltered in areas with no volume loss. In the frontal cortex, a 20 to 25% reduction in parvalbumin neuron density was reported. Interestingly, at 12 months of age, these mice exhibited attentional deficits, which may be directly caused by the loss of parvalbumin neurons. Indeed, prefrontal parvalbumin neurons play a direct role in the control of attention (Kim et al., 2016). Of note, no cytoplasmic accumulation of TDP-43 was observed in parvalbumin neurons (White et al., 2018). However, their loss may come from neurodevelopmental alterations as the density of hippocampal parvalbumin was already decreased at 14 days of age (Lin et al., 2021).

Recently, a progressive loss of parvalbumin neurons was reported in the frontal cortex of 12- and 24-month-old TDP-43$^{M323K/M323K}$ knock-in mice (Godoy-Corchuelo et al., 2024). This was observed in the absence of TDP-43 inclusions in these neurons. Of note, the number of parvalbumin neurons was unaltered at 3 months of age, while the mice exhibited structural brain changes, as well as cognitive and behavioural deficits (including apathy and memory deficits). However, the contribution of inhibitory neurons to these early phenotypes cannot be ruled out, as the latter may arise from the impairments of other inhibitory neuron subpopulations or from synaptic dysfunctions in the absence of neurodegeneration. These mice later developed progressive motor deficits, which started at 6 months in males and 9 months in females. Although the M323K mutation has not been identified in patients, it is present within a C-terminal domain in which almost all human ALS-causing mutations are clustered (Fratta et al., 2018).

9.2. Mutation of *SOD1* to model ALS

The most widely used ALS mouse model was developed by expressing high levels of the human *SOD1* gene carrying the G93A mutation (Gurney et al., 1994). This induces both cognitive and motor phenotypes, which are associated with a wide range of inhibitory neuron impairments. Some major steps in the disease progression involve the onset of locomotor deficits around postnatal day 60 (P60), followed by a loss of motor neurons around P90-P100, and a progressive paralysis starting at P120 and ending around P140.

At P56, the density of parvalbumin neurons was found to be reduced in the hippocampus of *SOD1*^{G93A} mice compared to control mice (Quarta et al., 2015). This may, at least partially, explain the increased anxiety and impaired spatial navigation learning observed in these mice. Indeed, it was shown that the acquisition phase of spatial learning is impaired when subpopulations of hippocampal GABAergic neurons are inhibited (Andrews-Zwilling et al., 2012). Around P60 and P85, a decreased density and activity of parvalbumin neurons was observed in the motor cortex of these mice (Khademullah et al., 2020). This was accompanied by an increased excitability of pyramidal motor neurons, which could be reduced by increasing the activity of inhibitory neurons. Interestingly, electrophysiological and morphological alterations were reported in cultured cortical GABAergic neurons prepared from *SOD1*^{G93A} embryos compared to control inhibitory neurons (Clark et al., 2018). This decreased excitability, which may be driven by circuits and/or intrinsic alterations, may contribute to the decreased inhibitory influence observed in the cortex of *SOD1*^{G93A} mice. Around P90 and P100, the excitability of cortical parvalbumin neurons was found to be increased (Kim et al., 2017). It was also the case during the neonatal period, but not during the pre-symptomatic phase (P30). The authors proposed that the functional properties of neurons evolve and are adapted in order to normalise cortical excitability as the disease progresses. Of note, previous studies reported no loss of parvalbumin neurons in the motor cortex of mice at P68 or P120-P140

(Minciacchi et al., 2009; Ozdinler et al., 2011). The density of other subpopulations of cortical inhibitory neurons was found to be reduced. This included NPY neurons around P60, and calretinin neurons around P110 (Clark et al., 2017). Interestingly, the branching complexity of calretinin neurons was already found altered one month before their loss.

A reduction in the density of GABAergic boutons was observed on the membrane of bulbar vulnerable motor neurons during the second postnatal week (Venugopal et al., 2023). This was accompanied by a reduction in persistent GABA inhibition. In addition, the expression of *Gabra5* was decreased, which could directly impair the intrinsic excitability of motor neurons. Indeed, the selective pharmacological blocking of $GABA_A$ receptor α5 subunit disinhibited motor neurons and lowered their recruitment threshold. Similarly, an *in vitro* study of spinal motor neurons obtained from embryos proposed that the expression and functionality of $GABA_A$ receptors are altered, which could contribute to the increased vulnerability of motor neurons (Avossa et al., 2006). However, to date, *in vivo* studies have not reported significant impairments in GABAergic inhibition in the spinal cord of *SOD1*^{G93A} mice. Conversely, alterations in glycinergic inhibition have been documented, which may lead to motor neuron death and motor deficits.

In the ventral horn of the lumbar spinal cord, glycinergic inhibitory neurons were found to be less excitable during the early postnatal development (Cavarsan et al., 2023). The most affected glycinergic neurons were the most ventrally located, where V1 neurons are found. Interestingly, it was shown that, in young adults (P56), there is a selective and progressive loss of glycinergic boutons on the membrane of lumbar motor neurons (Chang and Martin, 2009). For motor neurons innervating fast-fatigable motor units, the loss of glycinergic synapses was first observed at P45, and then worsened at P63 and P84 (Allodi et al., 2021). This included a loss of V1 synapses labelled with engrailed-1 at P42. This was found to be followed by transcriptional alterations and a loss of inhibitory markers, including engrailed-1 and calbindin in Renshaw cells, at P63 (Montañana-Rosell et al., 2024). Around the same time, a loss of engrailed-1-positive V1 neurons (Allodi et al., 2021) and calbindin-positive Renshaw cells (Chang and Martin, 2009) were observed. Of note, a previous study reported no loss of Renshaw cells before P120 (Wootz et al., 2013). However, they demonstrated that the projections of motor neurons on Renshaw cells were already profoundly lost around P90, while the number of projections of Renshaw cells on motor neurons was transiently increased, possibly as an adaptive mechanism to maintain the level of inhibitory influence. In addition, the loss of V1 neurons may be a generalised feature in the spinal cord, as a decreased density of V1 neurons was also reported at the cervical and thoracic levels, but it was only studied in late-stage symptomatic animals (Salamatina et al., 2020). Ultimately, this loss of glycinergic synapses and neurons may impair the inhibitory input received by motor neurons. The density of glycine-evoked currents was found to be significantly smaller in cultured large motor neurons prepared from *SOD1*^{G93A} embryos compared to control motor neurons

(Chang and Martin, 2011). This was accompanied by lower levels of messenger RNA encoding the glycine receptor α1 subunit.

9.3. Mutation of *MAPT* to model FTD

Tau transgenic mice were created by expressing a modified version of the human *MAPT* gene under the control of the promoter of different genes, resulting in distinct pattern of expression of the mutant human tau protein. Given that tau aggregation is associated with Alzheimer's disease in addition to FTD, the hippocampus of these mice was extensively studied, and some alterations of inhibitory neurons were reported.

In tau^{P301L} mice, the mutated human *MAPT* gene is expressed under the control of the promoter of the mouse prion gene, resulting in the presence of mutant tau in the central nervous system. In 12 to 18-month-old mice, a 20% reduction in the density of hippocampal inhibitory neurons was reported, and affected parvalbumin and somatostatin neurons to the same extent (Levenga et al., 2013). Because pathological tau markers were found in the remaining neurons, it was proposed that the accumulation of mutant tau protein can induce the loss of GABAergic neurons, but the underlying mechanisms are yet to be studied. In addition, genes encoding subunits of the $GABA_A$ and $GABA_B$ receptors (including *Gabrb2*, *Gabrb3*, *Gabrg2* and *Gabbr1*) were found to be downregulated in 18-month-old mutant mice compared to control mice (Jiang et al., 2018). These changes were not observed in 8-month-old mice or before, but they suggest that the inhibitory influence of the remaining parvalbumin and somatostatin neurons may be impaired. Interestingly, these mice exhibited impaired prepulse inhibition of startle response when compared to controls (Levenga et al., 2013). This may be caused by the loss of hippocampal inhibitory neurons, as they are involved in the control of the startle reactivity and prepulse inhibition in rodents (Bast et al., 2001). Finally, these mice exhibited an altered hippocampal synaptic plasticity, which was rescued by the use of a $GABA_A$ receptor agonist, and which may underlie the observed memory deficits.

The study of another transgenic mouse line carrying a P301L mutation highlighted that alterations in the GABAergic system can be observed in the absence of major loss of inhibitory neurons (Shimojo et al., 2020). In these mice, the expression of *MAPT* is controlled by the tetracycline transactivator transgene under the calcium/calmodulin-dependent protein kinase IIα (CaMKIIα) promoter, which results in mutant tau expression in forebrain excitatory neurons. In 2- to 3-month-old mice, a decreased binding of [^{11}C]flumazenil was reported, suggesting impaired GABAergic transmission, while excitatory synapses were unaltered. This was confirmed by biochemical and immunohistochemical experiments showing a loss of synaptic constituents without major loss of the soma of GABAergic inhibitory neurons in the neocortex and hippocampus. This included decreased protein levels of GAD67, VGAT and $GABA_A$ receptor α1 subunit.

During the aging process, these protein levels were comparable between mutant and control mice, indicating potential compensatory mechanisms. Interestingly, the absence of mutant tau in GABAergic neurons was confirmed, indicating that non-cell autonomous mechanisms drove the inhibitory synaptic alterations. Ultimately, this was followed by a progressive brain atrophy, which was accompanied by a gradual decline in excitatory synaptic functions and cognitive impairments. It was thus proposed that the early disruption of inhibitory synapses may be a critical event triggering the progressive neurodegeneration.

The appearance of early GABAergic synaptic alterations in mouse models of tauopathies was confirmed by the study of the transgenic VWL mouse line carrying three tau mutations (G272V, P301L and R406W) (Soler et al., 2017). In these mice, the mutated human *MAPT* gene is expressed under the control of the promoter of the Thy1 gene, resulting in the presence of mutant tau exclusively in projection neurons. In 2- and 8-month-old mice, an accumulation of a phosphorylated form of endogenous tau (phosphorylated at residue Thr231) was reported in parvalbumin hippocampal neurons. Interestingly, these mice overexpress mutant tau in hippocampal pyramidal neurons but not in inhibitory neurons (Dávila-Bouziguet et al., 2019). Therefore, it was proposed that this increase in phosphorylation levels in inhibitory neurons is driven by a non-cell autonomous effect, probably linked to the accumulation of mutant tau in pyramidal neurons. GABAergic neurons found in the septum are known to innervate hippocampal inhibitory neurons via the septo-hippocampal pathway. A progressive deterioration of this innervation on parvalbumin neurons with aberrant phosphorylated tau was reported (Soler et al., 2017). This was driven by a reduced number of GABAergic axon terminals, while the number of inhibitory neurons in the septum and hippocampus remained unaltered. Both this altered pathway and the potential dysfunction of hippocampal inhibitory neurons may underlie the cognitive deficits observed in these mice.

9.4. Highlights from the characterisation of ALS-FTD mouse models

In recent years, there has been a growing interest in inhibitory neurons in the context of characterising mouse models of ALS and FTD. The causal relationship between inhibition deficits and the pathogenesis of ALS-FTD is yet to be investigated for most motor, behavioural and cognitive symptoms. Nevertheless, early impairments in inhibitory processes have been associated with a range of symptoms observed in mouse models linked to distinct pathogenic genes and proteins. It is noteworthy that inhibitory synaptic dysfunctions can occur in the absence of major neuronal loss, underscoring the importance of comprehensive assessments of the inhibitory system. In the brain, parvalbumin neurons represent the most extensively studied subpopulation of GABAergic neurons. While they constitute the predominant population of inhibitory neurons in numerous brain regions, this may obscure deficits in other subpopulations.

Part 6: Involvement of fused in sarcoma in ALS-FTD

Fused in sarcoma (FUS), also known as translocated in liposarcoma, was initially identified as an oncoprotein with the potential to undergo chromosomal translocation. These processes result in the fusion of *FUS* with other endogenous transcription factors, leading to the expression of aberrant genes. In 2009, *FUS* mutations were associated with ALS, and shortly after, FUS mislocalisation was associated with FTD. In this last section, I will highlight some of the physiological properties and functions of FUS and demonstrate its involvement in the ALS-FTD continuum. I will conclude with an overview of previous work from the laboratory and colleagues that supports the objectives of my thesis project.

1. Properties

1.1. Structure

The human *FUS* gene comprises 15 exons and is located on chromosome 16. It encodes a protein of 526 amino acids for a molecular weight of 75 kDa. FUS belongs to the FET family, which comprises the TATA-box binding protein associated factor 15 (TAF15) and EWS RNA binding protein 1 (EWSR1). These three DNA/RNA-binding proteins share similar protein domains in terms of structure and function. In addition, FUS shares numerous commonalities with TDP-43. FUS contains an N-terminal low complexity domain, three domains enriched in arginine and glycine motifs (RGG domains), an RNA recognition motif, a zinc finger motif, a nuclear export signal (NES) and an atypical proline-tyrosine nuclear localisation signal (NLS) domain at its C-terminal extremity (Figure 19). Importantly, the NLS sequence is highly conserved during evolution, and is identical in humans and mice, allowing to study its importance in rodents.

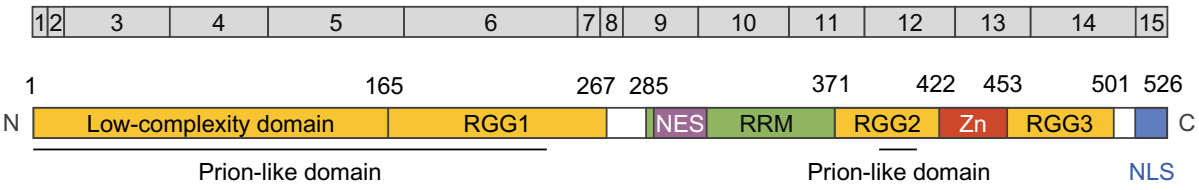


Figure 19: Schematic representation of messenger RNA and protein sequences of FUS. *FUS* gene comprises 15 exons. FUS protein contains a nuclear export signal (NES), a RNA-recognition motif (RRM), a zinc finger motif (Zn), a nuclear localisation sequence (NLS) domain and four domains enriched in glycine (the low-complexity domain is a enriched in glutamine, glycine, serine and tyrosine, RGG domains are enriched in arginine and glycine).

1.2. Nucleocytoplasmic shuttling

FUS is ubiquitously expressed throughout most human organs. In most cell types, FUS is present in both the nucleus and cytoplasm, and shuttles between these two compartments. In neurons, there is proportionally more FUS in the nucleus than in the cytoplasm, and in glia its expression is exclusively nuclear (Andersson et al., 2008). FUS nuclear export is not completely understood but, due to its small size, it has been proposed that the protein passively diffuses across nuclear pore complexes. In addition, FUS contains a nuclear export signal domain, which could be recognised by exportins, thus allowing an active nuclear export. However, the silencing of exportin-1 had no impact on FUS localisation (Ederle et al., 2018). This was further confirmed when no interactions were found between FUS and exportin-1 (Baade et al., 2021).

Conversely, the truncation of the NLS domain of FUS highlighted that this region is required for the nuclear localisation of the protein (Kino et al., 2011). In particular, it was shown that transportin-1 (also called karyopherin-β2), which is a nuclear import receptor, binds to three specific sites of the NLS domain of FUS and to a fourth site located upstream of the NLS domain, to translocate FUS across the nuclear pore complex (Dormann et al., 2012, 2010). More recently, other protein partners were identified and may be involved in this active nuclear import (Baade et al., 2021). This includes transportin-3, whose binding seems to depend on arginine residues within the RGG motifs. Interestingly, several mutations impacting arginine residues in the C-terminal region of the *FUS* gene were identified in ALS patients, and were found to impair the nuclear import of FUS by decreasing the binding of transportin-1 (Niu et al., 2012). In addition, these arginine residues are highly susceptible to methylation, and in pathological conditions, FUS is found to exhibit asymmetrically dimethylated arginines, further preventing the binding of transportin-1 (Dormann et al., 2012).

1.3. Autoregulation

FUS can bind to the exon 7 and introns 6 and 7 of its own pre-messenger RNA (Lagier-Tourenne et al., 2012) to autoregulate its protein levels. Three mechanisms have been proposed to explain this autoregulation (Figure 20). FUS was found to repress the splicing of exon 7 resulting in an exon 7-skipped splice variant, which is subject to nonsense-mediated decay (Zhou et al., 2013). FUS can also upregulate the production of micro-RNA, which in turn inhibits its translation (Dini Modigliani et al., 2014). Finally, FUS can exert a retention of introns 6 and 7, leading to a nuclear accumulation of this pre-messenger RNA (Humphrey et al., 2020). This last mechanism may be the most prominent one. Overall, the following model has been proposed: when FUS levels increase, the protein binds to its own pre-messenger RNA and induces the production of other isoforms, which are either sent for degradation or retained in the nucleus to avoid their translation. This

model can explain the increased production of FUS protein in mutant mice. Indeed, as mutant FUS accumulates in the cytoplasm and cannot reinter the nucleus, then the autoregulation mechanisms cannot occur, leading to increased production of FUS, and ultimately a vicious cycle. Consistent with this idea, the expression of a wild-type human form of FUS in mutant mice was able to elicit autoregulation of the mutant allele, leading to decreased levels of mutant FUS, and mitigated phenotypes (Sanjuan-Ruiz et al., 2021).

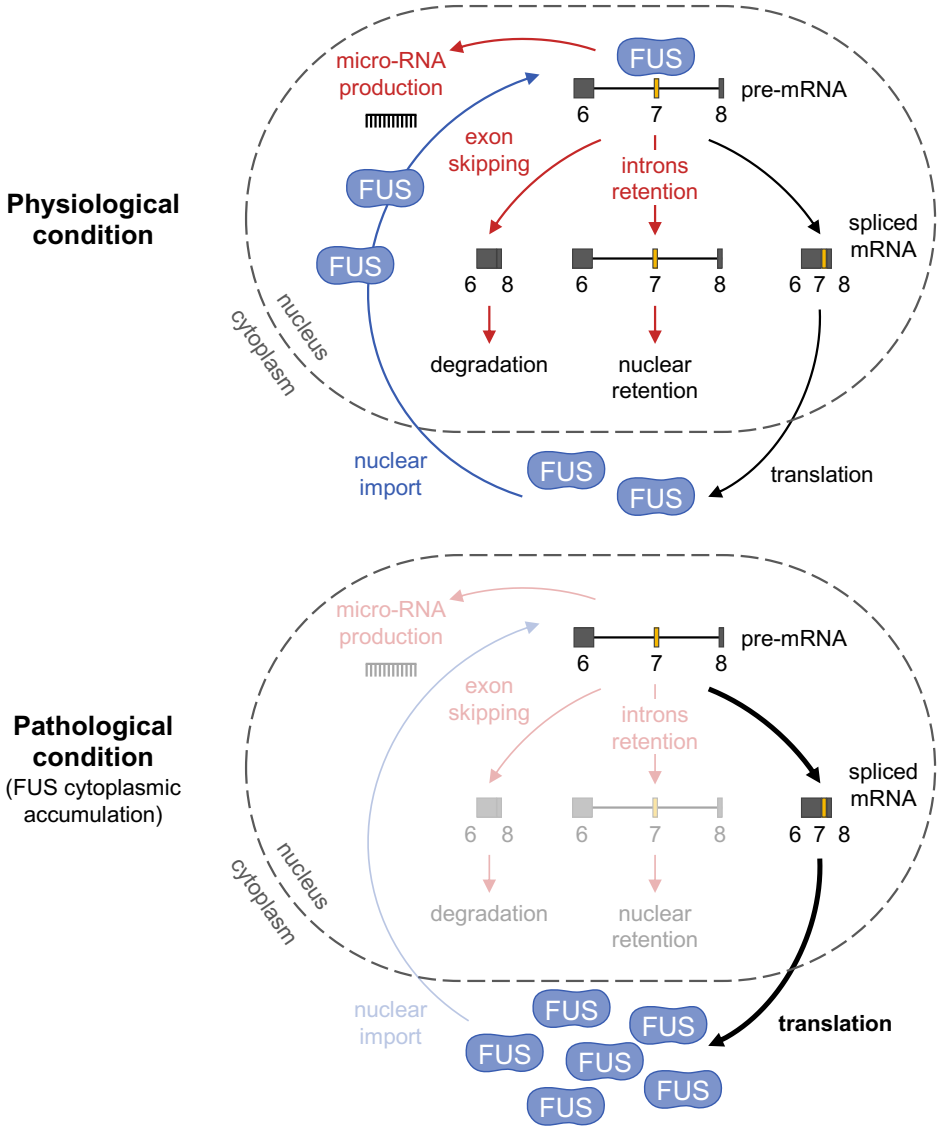


Figure 20: Proposed mechanisms for the autoregulation of FUS. (Top) Elevated nuclear FUS levels activate an autoregulatory loop and ultimately reduce *Fus* translation. (Bottom) In pathological conditions, this autoregulation can be prevented, leading to increased production of FUS. Pre-mRNA: pre-messenger RNA; mRNA: messenger RNA.

1.4. Liquid-liquid phase separation

FUS undergoes liquid-liquid phase separation and can form small spherical membrane-less compartments. These compartments are highly dynamic and reversible structures.

Their formation is notably stimulated by cellular stress, during which RNAs are sequestered to inhibit their translation, which explains why these compartments are also called "stress granules". In physiological conditions, these granules are essential for the cell functioning. For instance, they form nuclear bodies to concentrate DNA repair actors around strand break, or RNA-transporting granules (Levone et al., 2021). The phase separation of FUS is allowed by the presence of the N-terminal low complexity domain, which has prion-like characteristics and is prone to aggregation (Murray et al., 2017). Both post-transcriptional modifications of FUS and surrounding concentrations of FUS protein modulate the propensity to undergo liquid-liquid phase separation. For instance, the methylation of arginines in RGG domains decreases the formation and stabilisation of these granules (Hofweber et al., 2018). In addition, high concentrations of FUS facilitate their formation, while low concentrations of FUS compared to high concentrations of surrounding RNA tend to maintain FUS in a soluble phase (Maharana et al., 2018). Finally, the interaction between FUS and transportin-1 prevents phase separation (Guo et al., 2018; Qamar et al., 2018; Yoshizawa et al., 2018).

2. Physiological functions

FUS is a multifunctional protein (Figure 21), yet its precise functions remain incompletely characterised. Of note, several distinct functional domains of FUS, as well as post-translational modifications of FUS, appear to be required for its interactions with DNA, RNA and protein, but this falls beyond the scope of this manuscript.

2.1. Nuclear functions

In the nucleus, known roles of FUS include DNA repair and maintenance of genomic integrity, control of transcription, RNA processing and regulation of splicing.

DNA repair: DNA damage is a process that accumulates with aging and can eventually lead to cell death. Neurons are particularly sensitive to DNA damage since they are not able to replicate DNA or divide. Different mechanisms allow the reparation of DNA strand breaks, and FUS is involved in these pathways (Sukhanova et al., 2020). In particular, FUS can bind both single-strand and double-strand DNA, and is one of the first proteins recruited to a DNA damage site, where it interacts with several factors, including the histone deacetylase 1 (W.-Y. Wang et al., 2013).

Transcription: FUS can bind the promoter region of certain genes, leading either to the activation or the repression of their transcription. It has been proposed that FUS interacts with RNA polymerase II to modulate the transition from the initiation step to the elongation step. FUS is also involved in the production of microRNA by facilitating the recruitment of the Drosha complex (Morlando et al., 2012).

FUS binds a wide range of RNA, preferentially targeting intronic regions, and its affinity has been correlated with the length of these RNA (Lagier-Tourenne et al., 2012; Wang et al., 2015). Interestingly, the RNA targets of FUS were found to be highly similar in the cortex of mice and humans. These targets are mostly associated with gene transcription, synaptic transmission, glutamate signalling, metabolic process and cell-adhesion.

Splicing: Splicing is an important process to generate several protein isoforms, with potentially different characteristics and functions, from a single pre-messenger RNA. The major player in this mechanism is the spliceosome, a large complex composed of several subunits of nuclear ribonucleoproteins. FUS interacts with these subunits to integrate the spliceosome. In addition, FUS can directly bind the intronic regions of RNA to reduce their accessibility for the spliceosome (Nakaya et al., 2013). Typical examples of splicing controlled by FUS include *Mapt* (Ishigaki et al., 2017, 2012; Orozco et al., 2012) and the gene encoding brain-derived neurotrophic factor (BDNF) (Qiu et al., 2014).

2.2. Cytoplasmic and synaptic functions

In the cytoplasm and at the synapses, FUS is involved in the stabilisation, transport and translation of messenger RNAs, with important roles in the maintenance of synaptic integrity and the regulation of neuronal plasticity. In the brain, FUS is present in both pre- and postsynaptic compartments of excitatory and inhibitory synapses (Aoki et al., 2012; Fujii et al., 2005), with a preferred localisation in the presynaptic compartment, where it can be found in close proximity to synaptic vesicles (Belly et al., 2005; Deshpande et al., 2019; Sahadevan et al., 2021; Schoen et al., 2015). At the neuromuscular junction, FUS is enriched in muscles subsynaptic nuclei where it is involved in the transcription of genes encoding subunits of the acetylcholine receptor (Picchiarelli et al., 2019).

Stabilisation: FUS was found to bind the 3' untranslated region of RNAs (Colombrita et al., 2012) and can control the maintenance of their poly-adenylated tails (Udagawa et al., 2015), thereby mediating their stabilisation. In particular, FUS stabilises RNAs that encode proteins with important synaptic functions. This includes the GluA1 subunit of glutamatergic AMPA receptors, as well as the synaptic Ras GTPase-activating protein (SYNGAP), which is critical for the organisation and function of synapses (Yokoi et al., 2017). Other known RNA targets of FUS may also be stabilised by its binding.

Transport and local translation: In neurons, the transport of RNA is particularly important as it allows the local translation of proteins in dendritic and axonal projections located far from the nucleus. This transport relies on the cytoskeleton, including microtubules and neurofilaments. The motor proteins responsible for the anterograde transport (towards the synapse) are kinesins, while the motor protein responsible for

retrograde transport (towards the soma) is dynein. FUS binds to the kinesin-1 and controls the anterograde transport. In addition, FUS incorporates RNAs into transporting granules, where it recruits ribonucleoproteins to inhibit the translation of these RNAs and prevent their degradation during axonal transport. Following this transport, FUS plays a role in the translation of the RNA found in the transporting granules (Yasuda et al., 2013), and can also inhibit translation when needed (Sévigny et al., 2020).

The synaptic RNA targets of FUS were recently identified in the murine cortex, and included messenger RNAs encoding subunits of GABAergic and ionotropic glutamatergic (AMPA, NMDA) receptors (Sahadevan et al., 2021). This work, with the support of previous studies (Aoki et al., 2012; Husi et al., 2000; Udagawa et al., 2015), thus proposed that, through its involvement in RNA transport, stabilisation and local translation, FUS can regulate the composition of postsynaptic receptors during synaptogenesis.

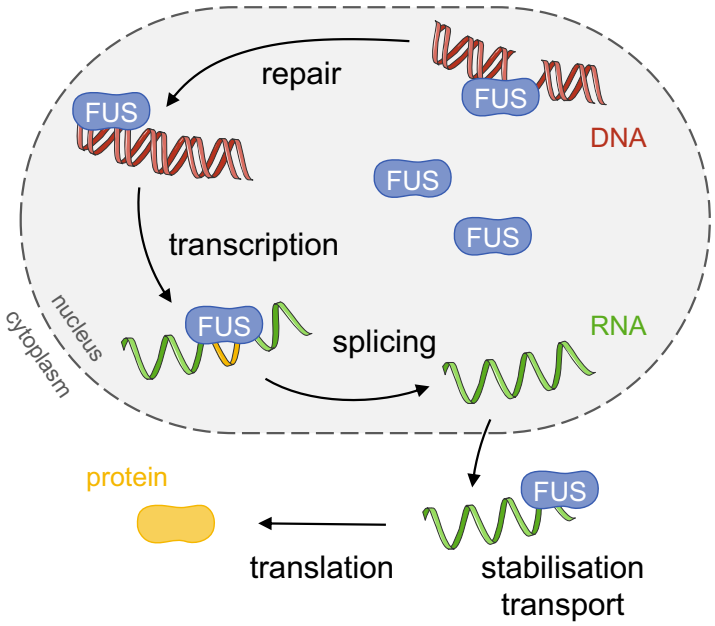


Figure 21: Summary of the main nuclear and cytoplasmic functions of FUS. In the nucleus, FUS is involved in DNA and RNA homeostasis (included DNA repair, DNA transcription, and RNA splicing). In the cytoplasm, FUS is involved messenger RNA homeostasis (including stabilisation, transport and translation).

3. Pathological conditions

Through its involvement in DNA and RNA metabolism, FUS plays a role in multiple physiological mechanisms which are essential for cellular function and survival. Thereby, its alterations (linked to mutations, delocalisation and/or aggregation) are found in a number of diseases affecting the central nervous system, including ALS and FTD.

3.1. Germline mutations in ALS

In 2009, pathogenic mutations in *FUS* were found to cause both familial and sporadic ALS (Belzil et al., 2009; Kwiatkowski et al., 2009; Vance et al., 2009). Up to 50 mutations have been identified, the majority of which is located in exons 12 to 15, which encode the C-terminal domain of FUS (including the NLS domain). These mutations account for 4% of familial and 1% of sporadic ALS cases (Akçimen et al., 2023), and are predominantly associated with autosomal dominant transmission. However, *de novo* mutations have also been reported (Chiò et al., 2011). Importantly, a subset of *FUS* mutations has been associated with juvenile (diagnosis before 25 years) and paediatric (diagnosis before 18 years) forms of ALS. To date, these mutations account for approximately half of the juvenile and paediatric cases (Picher-Martel et al., 2020). Heterozygous truncating mutations and missense variants, which are found in the C-terminal sequence and have a significant impact on the integrity of the NLS domain, are a primary cause of early-onset ALS cases. This includes the P525L and R495X mutations, which are associated with a rapid and aggressive disease course (Hübers et al., 2015; Waibel et al., 2013, 2010). Of note, *FUS* mutations have also been associated with essential tremor disease in one family (Merner et al., 2012). As previously stated, the mutation or complete deletion of the NLS domain prevents the binding of transportin-1, and subsequently the nuclear import of FUS. As a consequence, neuronal and glial cytoplasmic aggregates of FUS are observed in the brain and spinal cord, and occasionally contain components of the ubiquitin-proteasome system (Kwiatkowski et al., 2009; Mackenzie et al., 2011a; Vance et al., 2009). Most of the cells presenting these inclusions show an absence of the normal diffuse nuclear localisation of FUS, with some exceptions. Importantly, the degree of cytosolic mislocalisation of FUS is inversely correlated to the age of onset (Dormann et al., 2010).

3.2. Delocalisation and aggregation in ALS and FTD

Beyond the rare cases exhibiting *FUS* mutations, pathological studies have highlighted FUS cytoplasmic mislocalisation in ALS and FTD patients. FUS aggregates seem to be a pathological hallmark of several sporadic ALS cases in the absence of gene mutation, and are particularly common in spinal motor neurons (Deng et al., 2010). More recently, it has been highlighted that FUS cytoplasmic mislocalisation (without aggregation) may be an underestimated, yet important, feature of ALS, including sporadic cases without mutation (Tyzack et al., 2019). In addition, inclusions immunoreactive for FUS (and negative for TDP-43 and tau proteins) are present in FTD patients exhibiting no mutation. This represents approximately 10% of all FTD cases (Figure 5). These patients generally exhibit neuronal cytoplasmic and intranuclear inclusions, and glial cytoplasmic inclusions (Munoz et al., 2009; Neumann et al., 2009a, 2009b). However, cells with FUS-positive inclusion bodies retain at least some of the normal nuclear and cytoplasmic distribution of FUS staining. Interestingly, FUS inclusions in ALS and FTD patients appear to be

different. FUS was found to be asymmetrically dimethylated at arginine residues in ALS, but unmethylated or monomethylated in FTD (Suárez-Calvet et al., 2016). In addition, inclusions in FTD, but not in ALS, also contain the two other members of the FET family (TAF15 and EWS), as well as transportin-1 (Neumann et al., 2011). Of note, FUS intranuclear inclusions have also been associated with Huntington's disease (Mori et al., 2019) and spinocerebellar ataxia (Doi et al., 2010).

In ALS and FTD, all factors promoting the phase separation of FUS are gathered (Figure 22). The impairment of the nuclear import of FUS induces its cytoplasmic accumulation, where the concentrations of RNA are low. In addition, mutations in ALS patients can prevent the interaction with transportin-1, and methylation levels of arginines are low in FTD patients. Thereby, under pathological conditions, the phase separation process is intensified, and FUS ultimately undergoes a liquid-solid transition (Murakami et al., 2015; Patel et al., 2015). This results in the formation of dense, insoluble and inert aggregates, in which other proteins, such as p62 and ubiquitin, can be trapped.

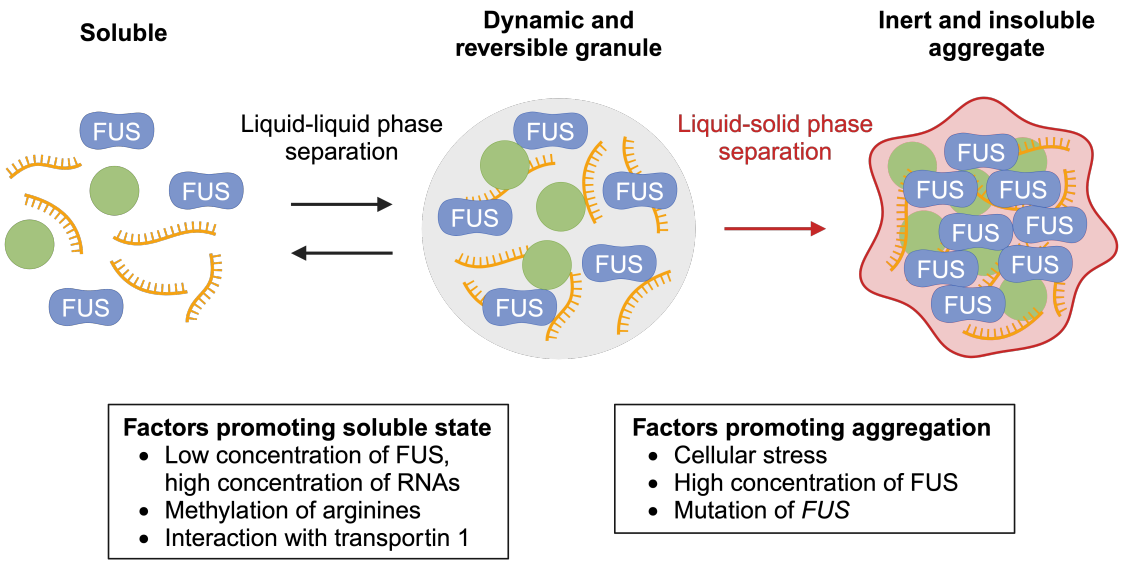


Figure 22: Phase separations and aggregation of FUS. In physiological conditions, the liquid-liquid phase separation of FUS is essential for its roles in the control of DNA and RNA homeostasis. However, in pathological conditions, FUS is prone to aggregation, which results in the sequestration of proteins (in green) and RNA (in yellow), thus impairing their functions.

3.3. Typical ALS and FTD symptoms associated with FUS

ALS patients with FUS pathology generally display severe neuronal loss in the spinal cord with only low or moderate neuronal loss in the motor cortex. However, FUS-related cases exhibit a broad spectrum of phenotypic variability, encompassing individuals of all ages, from the elderly to paediatric populations. The stratification of patients with *FUS* mutations has enabled to identify the age at onset as the most critical prognostic factor, and to propose three subgroups (Grassano et al., 2022). In the case of a mild-to-late onset

of ALS, the classic bulbar or spinal forms are observed, with no major cognitive impairments. Nevertheless, a subset of ALS patients with *FUS* mutations present with FTD symptoms (Blair et al., 2010; Broustal et al., 2010; Yan et al., 2010), while others exhibit neurological and psychiatric symptoms, including chorea (Flies and Veldink, 2020) and schizophrenia (Yan et al., 2010). The prognosis for these patients is comparable to the average survival rate observed in ALS, which is approximately 3 to 5 years after the date of diagnosis. Conversely, in patients whose initial symptoms manifest in early life, the disease progresses at an accelerated rate, with mortality occurring within 1 or 2 years of diagnosis for juvenile and paediatric patients, respectively. These patients also present with a bulbar or spinal form of ALS, but the progression to respiratory failure is rapid in both cases. In addition, intellectual disability appears to be a common feature of early-onset ALS, with studies indicating that this may precede motor symptoms by several years (Goldstein et al., 2022; Yamashita et al., 2012; Yan et al., 2010). A third, albeit rare, phenotype includes patients with a late onset, slow progression and prolonged survival.

FTD patients with FUS pathology can also be further divided into three groups showing overlapping but divergent clinical and neuropathological features. Patients with an atypical frontotemporal lobar degeneration defined by ubiquitin-positive cellular inclusions show a sporadic, early onset, severe and rapidly progressive behavioural variant of FTD, in the absence of significant language or motor deficits. Changes in behaviour and personality include disinhibition with inappropriate social conduct, antisocial behaviour, impairment of judgment and executive skills, poor attention, reduced personal hygiene, and sometimes psychiatric abnormalities (Mackenzie et al., 2011b; Neumann et al., 2009a). Patients with neuronal intermediate filament inclusion disease usually present sporadic, early-onset and rapid FTD with movement disorder (Mackenzie et al., 2011b; Neumann et al., 2009b). Finally, basophilic inclusion body disease cases are more heterogeneous, and phenotypes include pure ALS, pure FTD or a combination of them (Mackenzie et al., 2011b; Munoz et al., 2009).

3.4. Proposed pathogenic mechanisms

The nuclear clearance of FUS and its accumulation in the cytoplasm suggests that the proteinopathy can originate from a gain of toxic functions and/or a loss of physiological functions. For the moment, the exact mechanisms linking FUS to neurodegeneration are still unclear. Given that FUS is both ubiquitous and multifunctional, a wide range of downstream cellular pathways can be impaired by the mutation and/or delocalisation of this protein (Figure 6). A growing body of evidence indicates that both gain and loss of function mechanisms are involved in ALS and FTD, and this may depend on the mutation found in *FUS* and its functional connotations.

A. Gain of function

The concept of toxic gain of function is closely tied to the formation of stress granules which can recruit mutant FUS protein and which could potentially initiate cell death (Bosco et al., 2010; Tradewell et al., 2012). In addition, mutations can aberrantly increase the interactions between FUS and other RNAs and proteins or create new targets. *In vitro*, mutant FUS exhibited increased interaction with cytoplasmic RNAs compared to wild-type FUS, and the transcripts uniquely targeted by mutant FUS were enriched in genes related to the endoplasmic reticulum and ubiquitin-proteasome system (Hoell et al., 2011). In addition, mutant FUS was found to abundantly bind polyribosomes and repress global protein synthesis (Sévigny et al., 2020). In mice, mutant FUS was found to aberrantly bind the messenger RNA encoding the RNA-binding protein HuD, which prevented the inhibition of its transcription, thus increasing HuD levels and functions (Garone et al., 2021). In turn, this induced increased axonal growth and branching. The interaction between survival motor neuron (SMN) and FUS was also found to be increased when the latter is mutated, which impaired SMN functions (Sun et al., 2015; Yamazaki et al., 2012).

It is important to note that the cytoplasmic accumulation of FUS appears to be necessary to cause ALS-like motor neuron defects in mice, even in the absence of FUS aggregates. Our laboratory and others showed that knock-in mice exhibiting a cytoplasmic delocalisation of FUS develop mild and progressive muscle weakness, associated with motor neuron degeneration (Devoy et al., 2017; Ling et al., 2019; López-Erauskin et al., 2018; Sanjuan-Ruiz et al., 2021; Scekic-Zahirovic et al., 2017, 2016), while haploinsufficient *Fus* knockout mice do not develop these phenotypes (Devoy et al., 2017; Scekic-Zahirovic et al., 2017, 2016). In zebrafish and drosophila, the knock-down of *Fus* (or of *caz*, the drosophila orthologue of all three FET proteins) effectively resulted in a decreased motor activity (Armstrong and Drapeau, 2013; Bourefis et al., 2020; Kabashi et al., 2011; Sasayama et al., 2012), highlighting phenotypic discrepancy between species.

B. Loss of function

Nuclear functions of FUS may be affected by either its depletion from the nucleus or its intranuclear aggregation, while cytoplasmic functions can be prevented by the formation of cytoplasmic inclusions (Ishigaki and Sobue, 2018). For instance, *in vitro* FUS depletion was found to impact the splicing of *SNC8A* and *SNC4A*, which encode sodium channel proteins required for the transmission of action potentials in cortical pyramidal cells and skeletal muscles, respectively (Reber et al., 2016). In addition, FUS aggregates can sequester other proteins, ultimately preventing their functions. In particular, subunits of the spliceosome, as well as protein arginine methyltransferase 1 (PRMT1) and SMN protein were found to be sequestered in cytoplasmic FUS inclusions (Groen et al., 2013;

Sun et al., 2015; Tibshirani et al., 2015; Tsuiji et al., 2013). This resulted in a loss of splicing activity, transcriptional repression due to a lack of methylation, and axonal defects, respectively. The same phenomenon of sequestration was reported for kinesin-1, which prevented the localisation of RNA in protrusions (Yasuda et al., 2017). The homeostasis of RNAs is thus highly affected by FUS depletion.

Interestingly, FUS loss of function may be sufficient to induce FTD-like behavioural alterations in mice. The complete deletion of FUS leads to perinatal lethality due to respiratory insufficiency (Scekic-Zahirovic et al., 2016), or impairments in genomic maintenance and chromosomal stability (Hicks et al., 2000). Nevertheless, these mice can survive when raised on a mixed genetic background, and display a reduced body weight but no motor phenotype (Kino et al., 2015), confirming that motor defects depend on FUS cytoplasmic accumulation in mice. However, they exhibited behavioural phenotypes, evidenced by a reduced anxiety and increased locomotor activity. The specific silencing of *Fus* in the hippocampus also led to these phenotypes, accompanied by an increased sociability, a reduced dendritic spines maturation (Udagawa et al., 2015), and an hippocampal atrophy (Ishigaki et al., 2017).

4. *Fus*$^{\Delta NLS/+}$ mouse line as a model of ALS and FTD

As we saw previously, FUS can regulate the homeostasis of its messenger RNA, thereby exerting control over its own protein production. This means that in transgenic mice expressing wild-type or mutant human FUS, the physiological regulation of its expression is disrupted. Furthermore, the overexpression of wild-type human FUS was found to be toxic in a range of cell culture experiments and in mice (Mitchell et al., 2013). In order to study the biology of FUS and its implications in the ALS-FTD continuum, our laboratory decided to work with knock-in mouse models which maintain physiological control of FUS expression. To further elucidate the pathological mechanisms associated with the cytoplasmic accumulation of FUS, our approach does not rely on point mutations but rather on the complete deletion of the NLS domain, which is involved in the nuclear import of FUS. In the first mouse model generated, the NLS domain was truncated in every cell type, since the embryonic development (Scekic-Zahirovic et al., 2016).

This approach effectively induced the cytoplasmic delocalisation of FUS, in the absence of inclusions. Homozygous *Fus*$^{\Delta NLS/\Delta NLS}$ mice die at birth due to respiratory deficiency, thus precluding to study the consequences of FUS truncation in adults. However, heterozygous *Fus*$^{\Delta NLS/+}$ mice survive until adulthood and recapitulate several hallmarks of both ALS and FTD (Figure 23). The disease course is not as rapid or aggressive as that observed in juvenile forms of ALS associated with this truncation. However, *Fus*$^{\Delta NLS/+}$ mice exhibit early alterations of the neuromuscular junctions (Picchiarelli et al., 2019), mild progressive motor deficits (Sanjuan-Ruiz et al., 2021; Scekic-Zahirovic et al., 2017), and

late degeneration of motor neurons (Scekic-Zahirovic et al., 2017), which do not result in paralysis. In addition, they develop behavioural defects, including an increased sociability and an altered remote spatial memory (Scekic-Zahirovic et al., 2021). It is noteworthy that, in recent years, three additional heterozygous knock-in mouse models have been generated by other research groups (Devoy et al., 2017; Korobeynikov et al., 2022). These mouse lines are also based on genetic mutations that mimic the aetiology of juvenile ALS. However, as with the *Fus*$^{\Delta NLS/+}$ mice, they display a cytoplasmic delocalisation of FUS in the absence of inclusions, and motor neuron degeneration occurs at a late stage (12 or 18 months of age, depending on the mouse line) in the absence of paralysis. Therefore, it is possible that the discrepancy between the observed phenotype in ALS patients and that of mice is due to intrinsic biological differences between the two species.

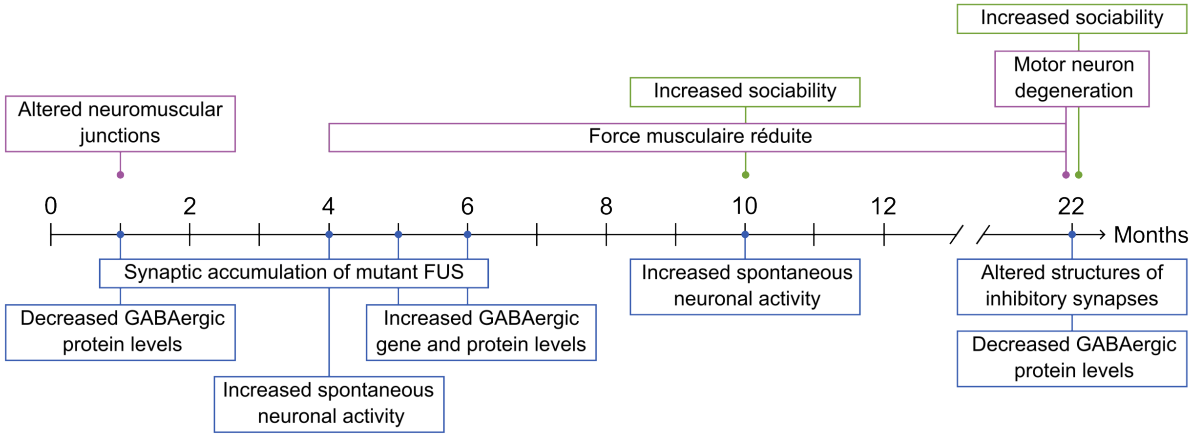


Figure 23: Summary of the main results previously obtained from the characterisation of *Fus*$^{\Delta NLS/+}$ adult mice. Neuronal and synaptic alterations (in blue) were observed in the brain.

In *Fus*$^{\Delta NLS/+}$ mice, motor neurons, oligodendrocytes and skeletal muscles were all found to participate in the pathogenesis of the disease. Interestingly, these mice also exhibited defects in inhibitory neurons. An early and persistent accumulation of mutant FUS and a loss of wild-type FUS were observed in cortical synapses (Sahadevan et al., 2021). At 1 month of age, this was accompanied by an increased synaptic density of the NMDA receptor 1 (GluN1), and a decreased density and cluster size of $GABA_A$ receptors containing the α3 subunit ($GABA_A$ α3 receptors).

At 5 and 6 months of age, levels of genes and proteins associated with GABAergic synapses were found to be increased, potentially as a compensatory mechanism (Sahadevan et al., 2021; Scekic-Zahirovic et al., 2021). With regard to gene expression, this encompassed *Gabra1* and *Gabrb1*, as well as *App*, encoding amyloid precursor protein (APP), which was found to play a role in the regulation of GABA neurotransmission (Dinamarca et al., 2019; Tang, 2019). Regarding protein levels, an augmented cluster size of presynaptic inhibitory boutons (labelled with VGAT antibody) was associated with an increased cluster size of $GABA_A$ α3 receptors. However, this was not accompanied by an increase in gephyrin,

which is a postsynaptic protein responsible for the anchoring of $GABA_A$ receptors (Specht et al., 2013). This suggests that the inhibitory postsynaptic sites may be unstable.

At 10 months of age, spontaneous neuronal activity levels were increased in the frontal cortex of *Fus*$^{\Delta NLS/+}$ mice, while the number of parvalbumin neurons remained unaltered. Finally, at 22 months of age, a potential functional impairment of inhibitory synapses was documented, as evidenced by molecular and ultrastructural alterations. A reduction in the density and cluster size of VGAT, $GABA_A$ α3 receptors and gephyrin was observed, indicating defects in the pre- and postsynaptic compartments. In addition, inhibitory boutons were larger, with longer active zones and increased vesicle numbers, which were abnormally distant from the active zone. Based on these findings, it was proposed that the increased synaptic localisation of FUS at presymptomatic stages causes early alterations in synaptic content and misregulation of the GABAergic network, which evolve as the disease progresses and which may underlie some of the behavioural dysfunctions observed in these mice.

To the best of our knowledge, this is the first observation of inhibitory neuron impairments in an ALS-FTD animal model of FUS pathology. This motivated the investigation of the contribution of inhibitory neurons to ALS-like motor and FTD-like social phenotypes associated with the FUS protein.

Objectives

Scientific question

As previously outlined, amyotrophic lateral sclerosis (ALS) and frontotemporal dementia (FTD) are two fatal neurodegenerative disorders that are characterised by an early dysfunction of neuronal circuits. While this is likely due to combined alterations in various cellular components, an increasing body of clinical and experimental evidence has highlighted impairments of inhibitory neurons, which could play a crucial role in the pathogenesis of ALS and FTD. One area of research is the clarification of the impairments of specific subpopulations of inhibitory neurons, and their subsequent effects on motor, behavioural and cognitive symptoms. To the best of our knowledge, the contribution of inhibitory neurons to phenotypes related to fused in sarcoma (FUS) has yet to be studied.

Our laboratory previously created an ALS-FTD mouse model by truncating the nuclear localisation signal (NLS) domain of *Fus* in every cell type since the embryonic development. In heterozygous mice, this resulted in the cytoplasmic delocalisation of FUS, mild and progressive motor deficits, and behavioural impairments, which were mostly manifested by an increased sociability. Furthermore, molecular and ultrastructural alterations of GABAergic inhibitory synapses have been observed throughout the course of the disease. Following this work, **the objective of my project was to ascertain the role of inhibitory neurons in motor and social defects**.

In particular, we wanted to verify whether the cytoplasmic delocalisation of FUS in inhibitory neurons is a prerequisite for the onset and progression of symptoms. In other words, we aimed to determine whether it is possible to attenuate, or even eliminate, the motor and social deficits by inducing FUS delocalisation in all cell types except inhibitory neurons. In parallel, I developed a complementary approach to determine if the cytoplasmic delocalisation of FUS in inhibitory neurons only is sufficient to cause the aforementioned symptoms. As this represents the first investigation into the impact of FUS subcellular localisation in inhibitory neurons, our objective was to target as many neurons as possible, without distinguishing the involvement of specific subtypes.

Experimental approach

To achieve my primary objective, I created novel mouse lines based on the Cre-Lox recombination technology. To target most cortical and spinal inhibitory neurons, we decided to use a mouse line in which Cre is expressed under the control of the endogenous promoter of the gene encoding the vesicular GABA transporter (VGAT). This transporter is expressed in virtually all GABAergic and glycinergic neurons. Consequently, Cre was expected to be active in most inhibitory neurons in the brain and spinal cord. Two distinct mouse lines expressing LoxP sequences in the *Fus* locus allowed

either the rescue of the expression of the NLS domain or the induction of its truncation upon recombination (Figure 24).

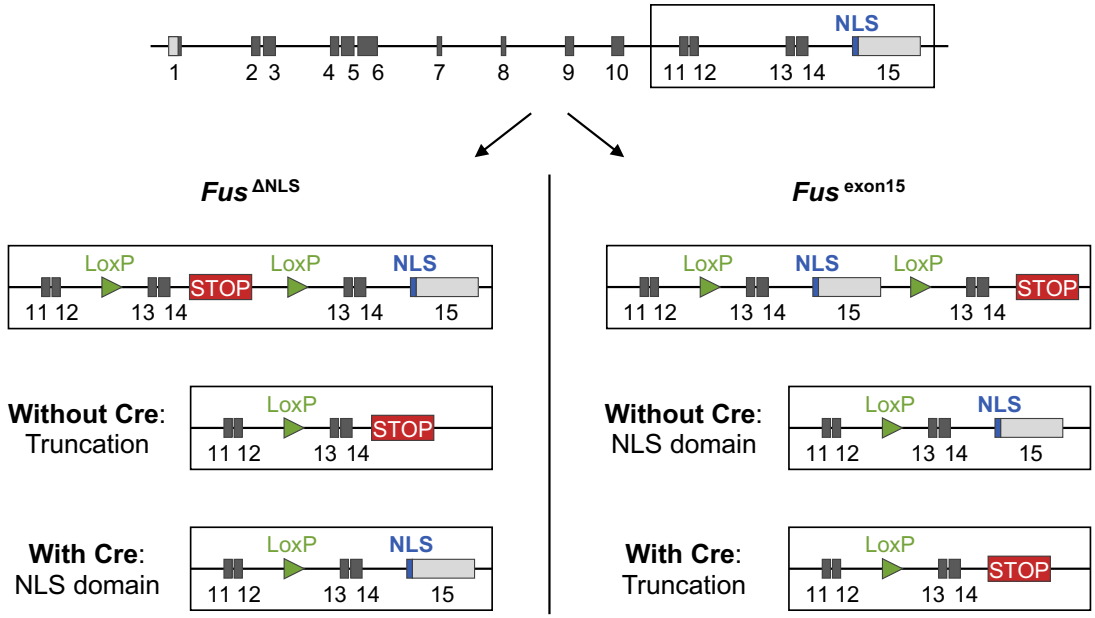


Figure 24: In the *Fus* locus, LoxP sequences allow to manipulate the truncation of the NLS domain. Schematic representation of the *Fus* gene locus. The lower panels depict the last exons in *Fus*$^{\Delta NLS}$ and *Fus*^{exon15} mice. (Left) In *Fus*$^{\Delta NLS}$ mice, the *Fus* locus was engineered to include, in intron 12, a floxed cDNA encoding exons 13 and 14 of *Fus*, followed by three transcription stop cassettes and a poly-adenylation signal. (Right) In *Fus*^{exon15} mice, the *Fus* locus was engineered to add LoxP sequences in intron 12 and downstream of exon 15. In addition, a cDNA encoding exons 13 and 14 of *Fus*, followed by three transcription stop cassettes and a poly-adenylation signal, was added downstream of exon 15. Coding regions are in dark grey, except the NLS domain highlighted in blue. Untranslated transcribed regions are in light grey, LoxP sites (triangles) are in green, and stop cassettes (rectangles) are in red.

In total, I worked with four principal mouse lines (Figure 25), accompanied by their respective controls. ***Fus*$^{\Delta NLS/+}$ mice** have already been studied in the laboratory and thus served as a positive control regarding the appearance of motor and social symptoms. In each cell type, one allele of the *Fus* gene was wild-type, and the other was truncated. ***Fus*$^{Resc/+}$ mice** allowed us to assess whether the motor and social symptoms are alleviated when the nuclear localisation of FUS is restored exclusively in inhibitory neurons. In Vgat-expressing neurons, both copies of *Fus* expressed the NLS domain. In the other cell types, one copy was wild-type, and the other was truncated. ***Fus*$^{Trunc/+}$ mice** (abbreviated Trunc$^{+/-}$) and ***Fus*$^{Trunc/Trunc}$ mice** (abbreviated Trunc$^{-/-}$) were used to determine whether it is possible to cause motor and social symptoms by inducing FUS cytoplasmic delocalisation exclusively in inhibitory neurons. In the *Vgat*-expressing neurons of *Fus*$^{Trunc/+}$ mice, one allele of *Fus* was wild-type, and the other was truncated.

In the *Vgat*-expressing neurons of *Fus*$^{Trunc/Trunc}$ mice, both alleles were truncated. In the other cell types of *Fus*$^{Trunc/+}$ and *Fus*$^{Trunc/Trunc}$ mice, both copies expressed the NLS domain.

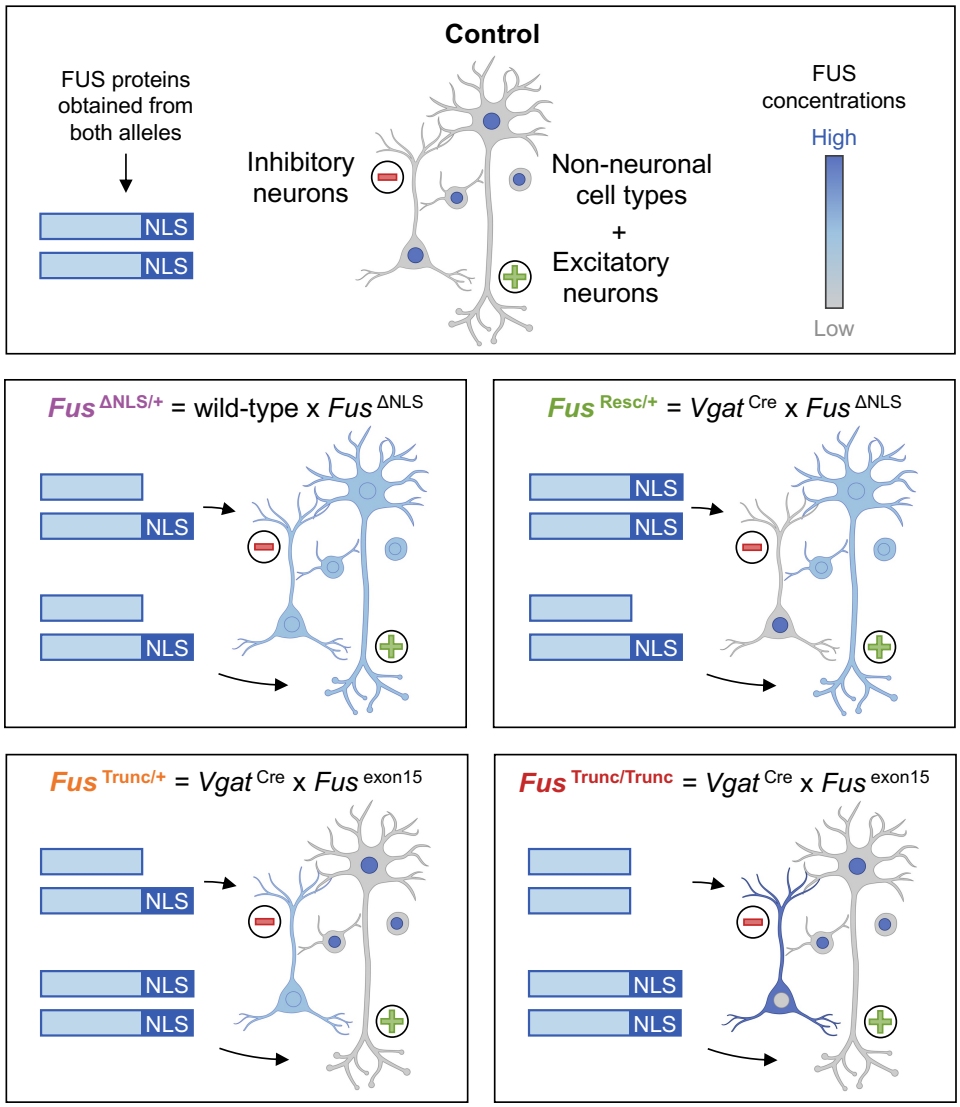


Figure 25: Schematic representation of the main mouse lines included in this project. For each mouse, the anticipation of the subcellular localisation of FUS is based on the presence or absence of the NLS domain.

Following the creation of the novel mouse lines, we observed that *Fus*$^{Trunc/Trunc}$ mice died prior to weaning, in contrast to the other three principal mouse lines. Consequently, we decided to conduct a longitudinal study to characterise adult *Fus*$^{\Delta NLS/+}$, *Fus*$^{Resc/+}$ and *Fus*$^{Trunc/+}$ mice, the results of which will constitute Publication 1. In order to characterise *Fus*$^{Trunc/Trunc}$ mice, we adapted our approach and focused on the postnatal period, the results of which will constitute Publication 2.

Results

Publication 1: Cytoplasmic accumulation of FUS in inhibitory neurons impairs cortical activity and sociability in mice

This first publication details the characterisation of *Fus*$^{\Delta NLS/+}$, *Fus*$^{Resc/+}$ and *Fus*$^{Trunc/+}$ adult mice, as well as their respective controls (Figure 26). Our aim was to ascertain whether it is possible to 1) attenuate, or even eliminate, ALS- and FTD-like deficits by rescuing FUS nuclear localisation exclusively in *Vgat*-expressing neurons, and 2) cause these deficits by inducing FUS cytoplasmic delocalisation exclusively in *Vgat*-expressing neurons.

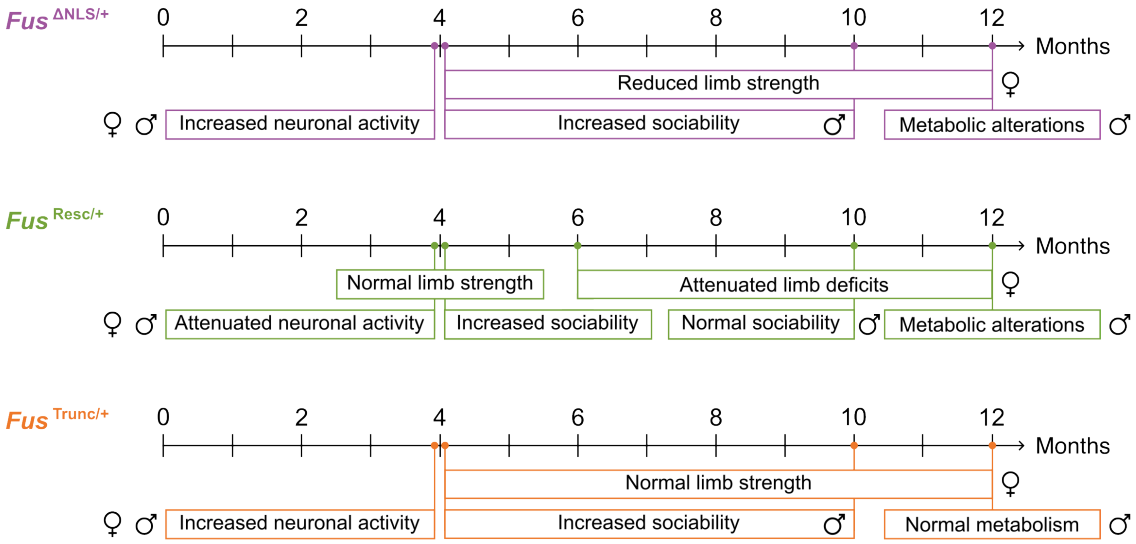


Figure 26: Summary of the main results obtained from the characterisation of *Fus*$^{\Delta NLS/+}$, *Fus*$^{Resc/+}$ and *Fus*$^{Trunc/+}$ adult mice.

Firstly, I verified the specificity and efficacy of the targeting of inhibitory neurons. To do so, I crossed the mice in which Cre is expressed in *Vgat*-positive cells with a reporter line. Conventional immunofluorescence protocols are unable to label all inhibitory neurons. Therefore, I focused on cortical parvalbumin-expressing neurons and showed that almost two third of them expressed Cre. Secondly, I investigated the subcellular localisation of FUS in subpopulations of neurons. As anticipated, in *Fus*$^{\Delta NLS/+}$ mice, I demonstrated that FUS accumulates in the cytoplasm of inhibitory and excitatory cortical neurons. In *Fus*$^{Resc/+}$ mice, FUS was found to be delocalised in excitatory neurons but not in inhibitory neurons, indicating that our rescue strategy was effective. Conversely, in *Fus*$^{Trunc/+}$ mice, FUS was found to be delocalised in inhibitory neurons but not in excitatory neurons, indicating that our truncation strategy was effective.

Then, to evaluate the development and progression of ALS- and FTD-like symptoms, I conducted a longitudinal study from 2 to 12 months of age. I weighed the mice every month, assessed their motor skills every two months, and evaluated their sociability at 4

and 10 months. With *Fus*$^{\Delta NLS/+}$ mice, I found comparable results to those previously documented in the laboratory. Both females and males displayed muscle weakness, while males exhibited increased sociability. Interestingly, the onset of motor symptoms was delayed in female *Fus*$^{Resc/+}$ mice, and social impairments were attenuated in aged male *Fus*$^{Resc/+}$ mice. Inducing the cytoplasmic delocalisation of FUS exclusively in inhibitory neurons did not cause motor symptoms, but increased sociability in male *Fus*$^{Trunc/+}$ mice.

Prior characterisation of *Fus*$^{\Delta NLS/+}$ mice demonstrated both an impairment of their cortical inhibitory synapses and an increase in the activity of cortical pyramidal neurons. We postulated that inhibitory neuron impairments could be the cause of this abnormal neuronal activity. To very this hypothesis, we established a collaboration with Dr Sabine Liebscher (Munich), whose laboratory has expertise in measuring neuronal activity using *in vivo* two-photon calcium imaging. Comparing *Fus*$^{\Delta NLS/+}$ and *Fus*$^{Resc/+}$ mice showed a slight, yet incomplete, attenuation of the phenotype. Conversely, *Fus*$^{Trunc/+}$ mice exhibited heightened neuronal activity in comparison to control mice.

To gain a deeper insight into the transcriptional changes occurring in inhibitory neurons, we established a collaboration with Dr Salim Megat (Strasbourg) and performed single-nucleus RNA sequencing in the frontal cortex of 10-month-old *Fus*$^{\Delta NLS/+}$ female and male mice. The analysis is currently underway, and preliminary findings suggest that parvalbumin neurons are the most affected inhibitory neurons.

Finally, we established a collaboration with Simon J. Guillot and Dr Matei Bolborea (Strasbourg) to evaluate the metabolism of our mouse lines using an indirect calorimetry system. This pilot study exhibited that the metabolism is altered in aged *Fus*$^{\Delta NLS/+}$ male mice. However, *Vgat*-expressing neurons were neither necessary nor sufficient to cause these symptoms. In addition, the housing conditions seemed to influence the metabolism of *Fus*$^{\Delta NLS/+}$ mice. This study will be detailed as supplementary data.

Publication 1

Cytoplasmic accumulation of FUS in inhibitory neurons impairs cortical neuronal activity and sociability in mice

Félicie Lorenc, Vanessa Wing Yin Kan, Salim Megat, Marion Boutry, Aurélie Bombardier, Paul Letellier, Véronique Devignot, Sylvie Grosch, Pascal Kessler, Luc Dupuis, Sabine Liebscher, Raphaelle Cassel

In preparation

Cytoplasmic accumulation of FUS in inhibitory neurons impairs cortical neuronal activity and sociability in mice

Félicie Lorenc[1], Vanessa Wing Yin Kan[2,3], Salim Megat[1], Marion Boutry[1], Aurélie Bombardier[1], Paul Letellier[1], Véronique Devignot[1], Sylvie Grosch[1], Pascal Kessler[4], Luc Dupuis[1], Sabine Liebscher[# 2], Raphaelle Cassel[# 1]

[1] Université de Strasbourg, INSERM, UMR-S 1329, Strasbourg Translational Neuroscience and Psychiatry, CRBS, Strasbourg, France.
[2] Institute of Clinical Neuroimmunology, Klinikum der Universität München, Ludwig Maximilians University Munich, Munich, Germany.
[3] Graduate School of Systemic Neurosciences, Ludwig Maximilians University Munich, Munich, Germany.
[4] Université de Strasbourg, INSERM, UMS 38, Imaging Core Facility PIC-STRA, CRBS, Strasbourg, France.

# Contributed equally.

felicie.lorenc@inserm.fr / https://orcid.org/0009-0003-8551-0981
sabine.liebscher@med.uni-muenchen.de / https://orcid.org/0000-0001-5633-8981
raphaelle.cassel@inserm.fr / https://orcid.org/0000-0002-3157-3798

Abstract

Impairments in inhibitory neurons appear to be an early feature of both amyotrophic lateral sclerosis (ALS) and frontotemporal dementia (FTD). In addition, it may participate in the dysfunction of neuronal circuits and the subsequent clinical symptoms. Fused in sarcoma (FUS) is a DNA/RNA-binding protein involved in the pathogenesis of ALS and FTD. The ubiquitous cytoplasmic accumulation of FUS gives rise to motor and behavioural phenotypes, which are associated with alterations of cortical GABAergic inhibitory synapses. The aim of the present study was to investigate whether the cytoplasmic accumulation of FUS in inhibitory neurons is necessary and/or sufficient for the development of these phenotypes. We generated knock-in mice in which the subcellular localisation of FUS can be manipulated in cells expressing the vesicular GABA transporter (VGAT). We show that rescuing FUS nuclear localisation in these neurons delays ALS-like motor deficits in female mice and attenuates FTD-like social alterations in aged male mice. Conversely, inducing FUS cytoplasmic delocalisation solely in these neurons recapitulates social alterations, which may be linked to the increased spontaneous neuronal activity observed in the frontal cortex of these mice. Collectively, our study emphasises that FUS localisation in inhibitory neurons is critical for the development or progression of ALS- and FTD-like symptoms in mice.

Introduction

Amyotrophic lateral sclerosis (ALS) and frontotemporal dementia (FTD) are progressive, disabling and fatal neurodegenerative diseases which form a pathophysiological continuum with genetic, histological and clinical similarities. The primary feature of ALS is the degeneration of motor neurons in the cortex, brain stem and spinal cord, which results in muscle atrophy and paralysis (Feldman et al., 2022). In FTD, a relatively selective degeneration of the frontal and temporal lobes leads to significant alterations in behaviour, personality, executive functions and language skills (Antonioni et al., 2023). Currently, there is no effective treatment available. It is therefore crucial to gain a deeper understanding of the underlying causes and pathological mechanisms in order to identify potential therapeutic targets.

Fused in sarcoma (FUS) is a multifunctional, ubiquitous, and predominantly nuclear protein which is involved in the ALS-FTD continuum. Pathogenic FUS mutations are primarily located within or in close proximity to the nuclear localisation signal (NLS) domain, and are associated with both sporadic and familial forms of ALS (Belzil et al., 2009; Kwiatkowski et al., 2009; Vance et al., 2009). The mutation or deletion of this domain impairs the nucleocytoplasmic transport of FUS, resulting in a cytoplasmic accumulation of the protein in both neuronal and glial cells. It is noteworthy that this mislocalisation can occur in the absence of mutations. This appears to be an underestimated, yet important pathological feature of sporadic ALS (Deng et al., 2010; Ikenaka et al., 2020; Tyzack et al., 2019). Furthermore, it characterises individuals with FUS-related FTD, who typically exhibit behavioural disorders, occasionally accompanied by motor disorders, but without language deficits (Mackenzie et al., 2011b; Neumann et al., 2009a; Seelaar et al., 2010; Snowden et al., 2011; Urwin et al., 2010). A few exceptions have been described in patients with a dual diagnosis of ALS-FTD and FUS mutations (Blair et al., 2010; Broustal et al., 2010).

We previously generated heterozygous *Fus*$^{\Delta NLS/+}$ mice, in which the nuclear localisation signal (NLS) domain is ubiquitously deleted in one copy of *Fus*, inducing a cytoplasmic accumulation of the protein. These mice exhibited mildly affected lifespan (Sanjuan-Ruiz et al., 2021), denervated neuromuscular junctions (Picchiarelli et al., 2019), as well as mild and progressive motor impairments (Sanjuan-Ruiz et al., 2021; Scekic-Zahirovic et al., 2017). Several months later, this was followed by abnormal electrical activities in the hind limb muscles and degeneration of motor neurons in the lumbar spinal cord (Scekic-Zahirovic et al., 2017). Rescuing FUS localisation in cholinergic neurons prevented aberrant muscle activities and motor neuron degeneration, while only delaying the onset of motor impairments. This suggests that additional cell types are involved in the pathogenesis of motor deficits. Interestingly, *Fus*$^{\Delta NLS/+}$ mice also developed early-onset behavioural abnormalities, which predominantly manifested as an increased sociability

(Scekic-Zahirovic et al., 2021). This was associated with increased cortical neuronal activity levels, as well as molecular and ultrastructural alterations of GABAergic inhibitory synapses (Scekic-Zahirovic et al., 2021). These observations led us to hypothesise that the expression of *Fus* mutations in inhibitory neurons might contribute to neurological and neurodegenerative diseases associated with FUS pathology.

A growing body of evidence suggests that inhibitory neuron impairments contribute to ALS and FTD, both in patients and animal models (see Review, page 59). In particular, this may play a role in the onset and progression of symptoms in cases of ALS and FTD linked to different genes and proteins. To the best of our knowledge, the contribution of inhibitory neurons to FUS-related phenotypes has never been studied before. Here, we created novel mouse lines based on the Cre-Lox recombination technology to manipulate FUS subcellular localisation in cortical and spinal neurons expressing the vesicular GABA transporter (VGAT). With a longitudinal study, we showed that rescuing FUS nuclear localisation in these neurons delayed ALS-like motor deficits in females and attenuated FTD-like social alterations in 10-month-old males. In contrast, inducing FUS cytoplasmic delocalisation solely in these neurons recapitulated social alterations in 4- and 10-month-old males. This may be linked to the increased spontaneous neuronal activity we observed in the frontal cortex of these mice. Together, these results emphasise the contribution of FUS mislocalisation, particularly in inhibitory neurons, on overall network function and the subsequent behavioural effects.

Results

Recombinase activity targets inhibitory neurons in *Vgat*$^{Cre/+}$ mice

To elucidate the role of inhibitory neurons in FUS-related ALS and FTD, we developed novel mouse lines based on the Cre-Lox recombination technology. Our objective was to target as many inhibitory neuron subpopulations as possible. Accordingly, we selected a Cre recombinase which is expressed under the control of the endogenous promoter of the gene encoding VGAT (Vong et al., 2011). This transporter is thought to be expressed in all neurons releasing GABA or glycine as a neurotransmitter, both in the brain and spinal cord. To verify the specificity and efficacy of the recombination, we crossed *Vgat*$^{Cre/Cre}$ mice with the Ai14 reporter mouse line (Fig. 1A). In the progeny, the fluorescent protein tdTomato was expressed after the recombination of the LoxP sequences in cells where Cre was active (Fig. 1B). In the frontal cortex of 2-month-old female and male mice, 94% of the tdTomato-positive cells were NeuN-positive, indicating that Cre is specifically active in neurons (Fig. 1C and 1D, top). Upon examination of all NeuN-positive cells, we found that 10% of them exhibited tdTomato fluorescence (Fig. 1C and 1D, bottom). Given that GABAergic inhibitory neurons constitute between 10 and 15% of all cortical neurons in rodents (Meyer et al., 2011), our results suggest that we effectively targeted the majority of cortical inhibitory neurons with *Vgat*^{Cre} mice. We then

focused on the parvalbumin subpopulation and found that 38% of the tdTomato-positive cells were also parvalbumin-positive (Fig. 1E and 1F, top). Concerning the efficacy of the recombination, 61% of all parvalbumin-positive neurons were tdTomato-positive (Fig. 1E and 1F, bottom). Overall, our results confirm that *Vgat*^{Cre} mice offer good specificity and efficacy to target cortical GABAergic neurons, although further verification is required for spinal inhibitory neurons (analysis in progress).

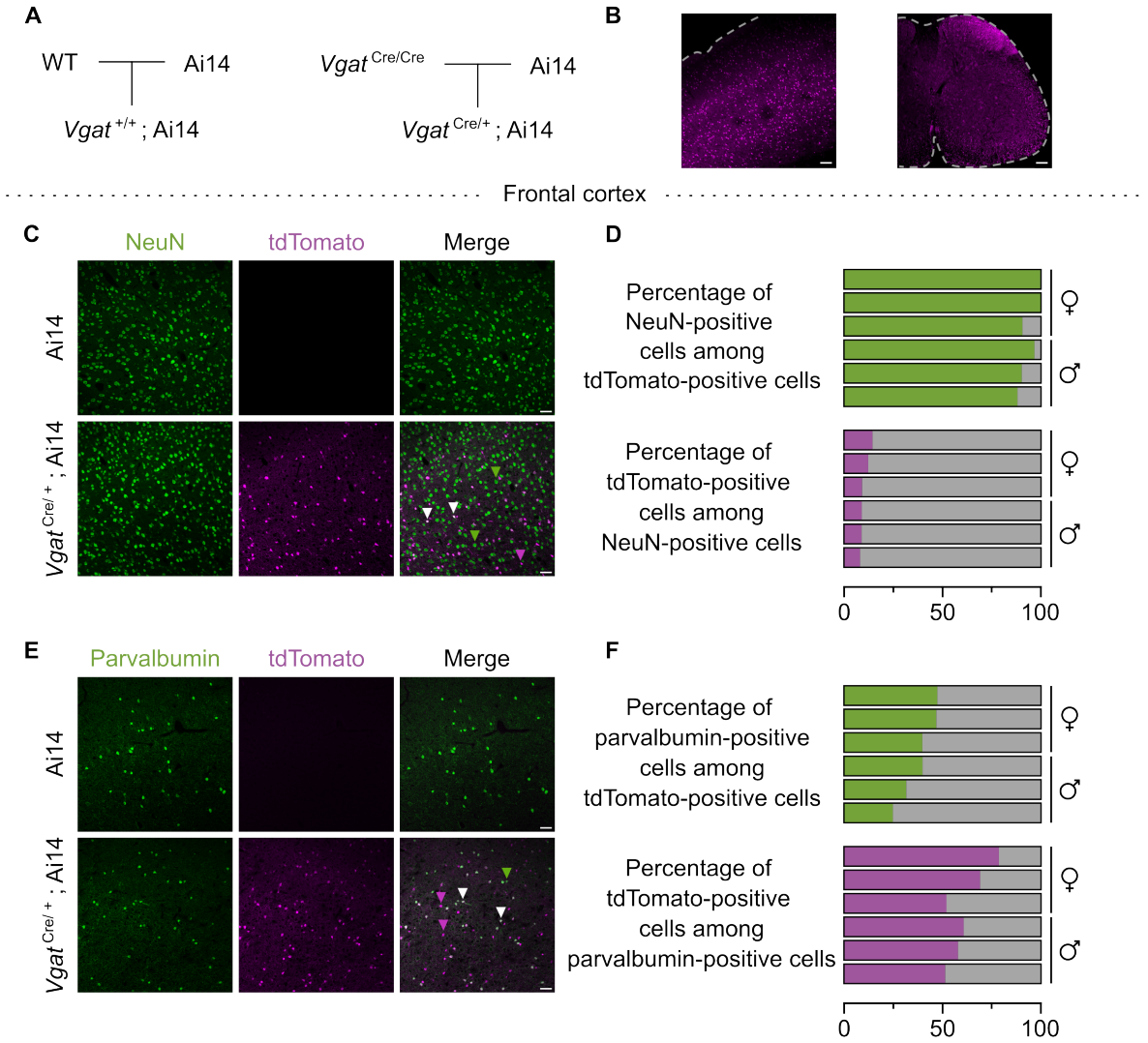


Figure 1: Inhibitory neurons targeting with *Vgat*^{Cre} mice. (**A**) Breeding scheme to generate *Vgat*$^{Cre/+}$; Ai14 mice, as well as age- and sex-matched Ai14 control mice. (**B**) Representative widefield images of the tdTomato fluorescent staining in the motor cortex (left) and lumbar spinal cord (right) of *Vgat*$^{Cre/+}$; Ai14 mice. Scale bar = 100µm. (**C**, **E**) Representative widefield images of the immunofluorescent staining of neurons (C) and inhibitory parvalbumin neurons (E) in the frontal cortex of 2-month-old mice. NeuN and parvalbumin staining were used to identify neurons and inhibitory neurons, respectively. The tdTomato staining was used to identify cells with active Cre recombinase. Scale bar = 50µm. (**D**, **F**) Quantification of cells showing double labelling in *Vgat*$^{Cre/+}$; Ai14 mice. Results are expressed as percentages, n = 3 females and 3 males.

FUS nuclear localisation is rescued exclusively in inhibitory neurons in *Fus*$^{Resc/+}$ mice

To understand whether ALS-like and FTD-like symptoms can be prevented by rescuing the nuclear localisation of FUS exclusively in inhibitory neurons, we created a mouse line in which the NLS domain of *Fus* is truncated in every cell type except inhibitory neurons. We took advantage of the *Fus*$^{\Delta NLS/+}$ mice, in which one copy of *Fus* is wild-type and the other contains a stop cassette surrounded by LoxP sequences in front of the NLS domain. By crossing *Vgat*$^{Cre/Cre}$ mice with *Fus*$^{\Delta NLS/+}$ (Fig. 2A), we obtained germline transmission of the recombinant alleles (Fig. 2B), resulting in the generation of mice designated as *Fus*$^{Resc/+}$. In the inhibitory neurons of these mice, both copies of *Fus* express the NLS domain, whereas in the other cell types, one copy is wild-type and the other is truncated. To verify the specificity of the recombination, we analysed FUS subcellular localisation in the motor cortex of 2-month-old female and male mice (Fig. 2C and 2F). The truncation of the NLS domain in *Fus*$^{\Delta NLS/+}$ mice is known to induce the cytoplasmic delocalisation of FUS (Scekic-Zahirovic et al., 2016). Indeed, we found a decrease in the nuclear-to-cytoplasmic ratio of FUS in both parvalbumin inhibitory neurons (1.3-fold reduction, Fig. 2D) and layer 5 excitatory pyramidal neurons (1.7-fold reduction, Fig. 2G) in *Fus*$^{\Delta NLS/+}$ mice compared to *Fus*$^{+/+}$ and *Vgat*$^{Cre/+}$ control mice. In addition, the nuclear localisation of FUS was successfully restored in parvalbumin inhibitory neurons of *Fus*$^{Resc/+}$ mice, as demonstrated by a significant 1.3-fold increase in the nuclear-to-cytoplasmic ratio of *Fus*$^{Resc/+}$ mice compared to *Fus*$^{\Delta NLS/+}$ mice, reaching levels comparable to those observed in *Fus*$^{+/+}$ and *Vgat*$^{Cre/+}$ mice (Fig. 2D). Conversely, FUS was found to be delocalised in the cytoplasm of excitatory pyramidal neurons. Our preliminary analysis showed that the nuclear-to-cytoplasmic ratio was not different between *Fus*$^{Resc/+}$ and *Fus*$^{\Delta NLS/+}$ mice, and was 1.7-fold decreased compared to *Fus*$^{+/+}$ and *Vgat*$^{Cre/+}$ mice (Fig. 2G). Of note, this cytoplasmic accumulation of FUS was not accompanied by a loss of inhibitory neurons (Fig. 2F), nor a loss of excitatory neurons (preliminary data not shown), as all genotypes exhibited comparable numbers of cells per section. Our findings confirm that in *Fus*$^{Resc/+}$ mice, the nuclear localisation of FUS is restored exclusively in cortical inhibitory neurons, while further verification is required for spinal neurons (analysis in progress).

Legend Figure 2: (**C**, **F**) Images of the immunofluorescent staining of FUS in the primary motor cortex of 2-month-old mice. Hoechst staining was used to delimit nuclei. Parvalbumin staining was used to delimit the cytoplasm of inhibitory neurons (C), while CRYM staining was used to delimit the cytoplasm of layer 5 excitatory pyramidal neurons (F). Scale bar = 10µm (**D**, **G**) Quantification of the nuclear-to-cytoplasmic ratio of FUS in parvalbumin inhibitory neurons (D) and pyramidal excitatory neurons (G). Number of inhibitory neurons analysed: 83 in *Fus*$^{+/+}$, 87 in *Vgat*$^{Cre/+}$, 97 in *Fus*$^{\Delta NLS/+}$, and 87 in *Fus*$^{Resc/+}$ mice. Number of excitatory neurons analysed: 81 in *Fus*$^{+/+}$, 80 in *Vgat*$^{Cre/+}$, 83 in *Fus*$^{\Delta NLS/+}$, and 83 in *Fus*$^{Resc/+}$ mice. (**E**) Averaged number of parvalbumin inhibitory neurons per section. (D, E, G) Kruskal-Wallis test and multiple comparisons were corrected with a two-stage Benjamini, Krieger and Yekutieli false discovery rate procedure, * $p < 0.05$.

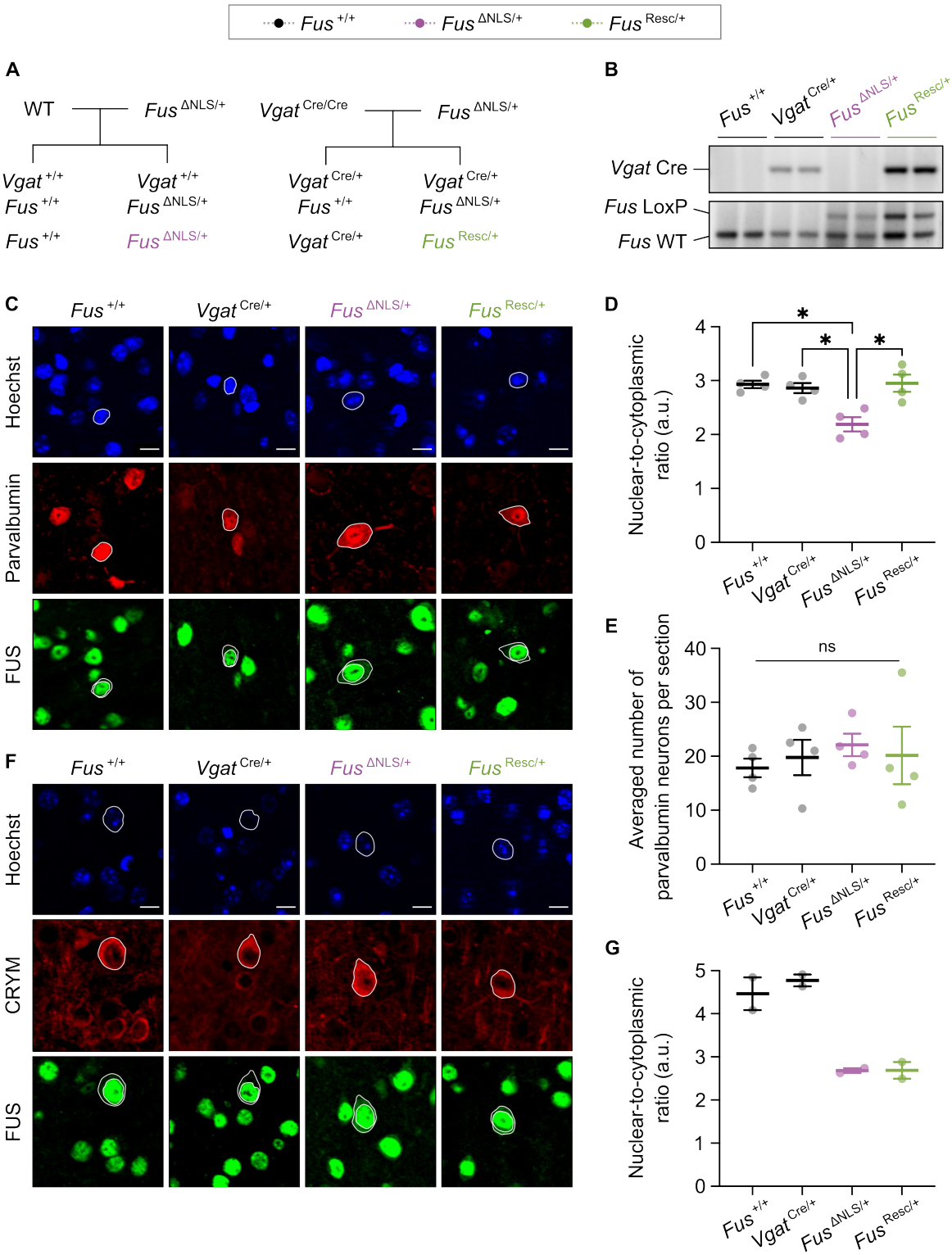


Figure 2: Rescued nuclear localisation of FUS in inhibitory neurons in FusResc/+ mice. Preliminary version. Results are expressed as mean ± SEM, n = 2 *Fus*$^{+/+}$ (black), 2 Cre (black), 2 *Fus*$^{\Delta NLS/+}$ (purple) and 2 *Fus*$^{Resc/+}$ (green) for both females and males (merged in graphs). (**A**) Breeding scheme to generate *Fus*$^{+/+}$ and *Fus*$^{\Delta NLS/+}$ littermates, as well as age- and sex-matched *Vgat*$^{Cre/+}$ and *Fus*$^{Resc/+}$ mice. (**B**) Representative PCR genotyping results.
End of the legend on the previous page.

Rescuing FUS nuclear localisation in inhibitory neurons delays motor deficits in females

To ascertain the involvement of inhibitory neurons in motor deficits, we first investigated whether rescuing the nuclear localisation of FUS in inhibitory neurons could prevent the development of ALS-like motor symptoms seen in *Fus*$^{\Delta NLS/+}$ mice. To this end, we longitudinally monitored *Fus*$^{Resc/+}$ mice, as well as *Fus*$^{\Delta NLS/+}$ and *Fus*$^{+/+}$ control littermates from 2 to 12 months of age (Fig. 3A). Their body weight was measured monthly, and no significant genotype effect was observed during the lifespan of both females (Fig. 3B) and males (Fig. 3C). Muscle weakness was assessed every two months using the four-limb inverted grid test. Although the hanging time did not show major significant differences between the genotypes (Fig. S1A-S1C), the mouse lines exhibited distinct motor performances. These were further assessed by considering the influence of the body weight. From 4 to 12 months of age, *Fus*$^{\Delta NLS/+}$ females exhibited a decreased holding impulse compared to *Fus*$^{+/+}$ females, and this reduction was significant at 4 and 12 months (Fig. 3D). At 4 months of age, the holding impulses of *Fus*$^{Resc/+}$ and *Fus*$^{+/+}$ females were comparable and significantly higher than the holding impulse of *Fus*$^{\Delta NLS/+}$ females. This indicates that muscle strength is altered at 4 months of age in *Fus*$^{\Delta NLS/+}$ females but not in *Fus*$^{Resc/+}$ females. From 6 to 12 months of age, no significant differences were observed between *Fus*$^{Resc/+}$ females and *Fus*$^{+/+}$ or *Fus*$^{\Delta NLS/+}$ females, indicating an intermediate muscle weakness in *Fus*$^{Resc/+}$ females. Similarly, *Fus*$^{\Delta NLS/+}$ males exhibited a significantly decreased holding impulse at 4 and 6 months of age in comparison to *Fus*$^{+/+}$ males (Fig. 3E). However, *Fus*$^{Resc/+}$ males showed no significant difference compared to *Fus*$^{+/+}$ and *Fus*$^{\Delta NLS/+}$ males throughout the study. These findings show that rescuing the nuclear localisation of FUS in inhibitory neurons delays the onset of motor deficits in female mice.

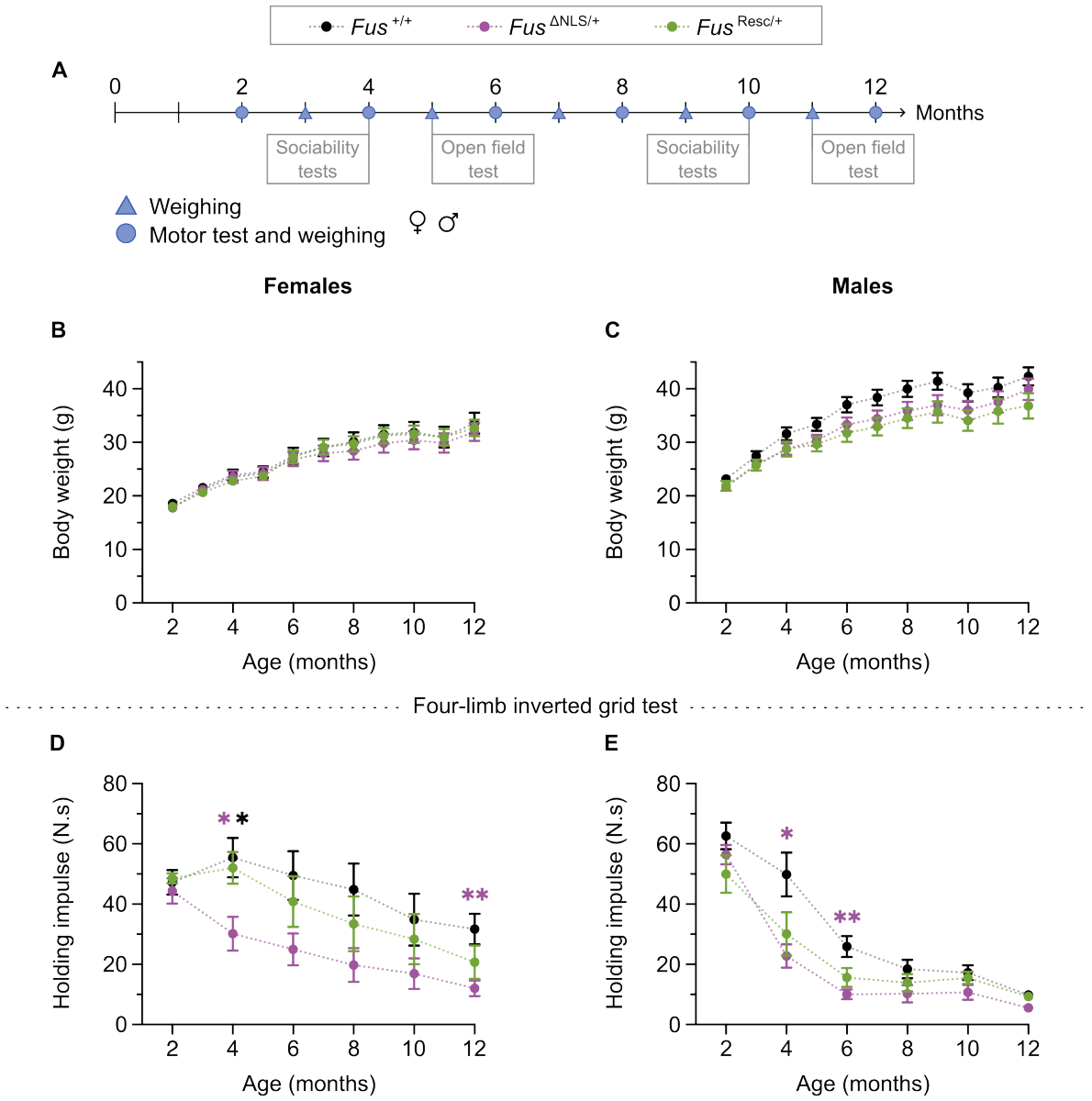


Figure 3: Slight delay of motor deficits in *Fus*$^{Resc/+}$ female mice. Results are expressed as mean ± SEM, n = 11 *Fus*$^{+/+}$ (black), 12 *Fus*$^{\Delta NLS/+}$ (purple) and 8-9 *Fus*$^{Resc/+}$ (green) for both females (left panels) and males (right panels). (**A**) Scheme of the experimental design. (**B**, **C**) Body weight was monitored monthly. (**D**, **E**) Holding impulse was calculated from the hanging time, which was monitored every two months with the four-limb inverted grid test. (B-E) Two-way ANOVA and multiple comparisons were corrected with Tukey's test: *Fus*$^{+/+}$ *vs Fus*$^{\Delta NLS/+}$, * $p < 0.05$ (purple); *Fus*$^{+/+}$ *vs Fus*$^{Resc/+}$, ns $p > 0.05$; *Fus*$^{\Delta NLS/+}$ *vs Fus*$^{Resc/+}$, * $p < 0.05$ (black).

Rescuing FUS nuclear localisation in inhibitory neurons attenuates social impairments in males

More recently, it has been shown that inducing a cytoplasmic delocalisation of FUS in every cell type results in social impairments, potentially due to an increase in neuronal activity levels in the frontal cortex (Scekic-Zahirovic et al., 2021). To understand whether the expression of *Fus* mutation in inhibitory neurons is involved in this phenotype, we evaluated sociability at 4 and 10 months of age using the three-chamber task (Fig. 4A).

At 4 months of age, $Fus^{\Delta NLS/+}$ male mice showed an increased social interest compared to $Fus^{+/+}$ littermates. This was evidenced by a significantly higher total social interaction time for $Fus^{\Delta NLS/+}$ than $Fus^{+/+}$ males (Fig. 4B, mouse). This increase was driven by a significant difference in the behaviour of $Fus^{\Delta NLS/+}$ and $Fus^{+/+}$ mice during the third trial (Fig. 4C, dashed lines). Indeed, $Fus^{+/+}$ mice demonstrated a loss of interest in their conspecifics throughout the task, whereas the interest of $Fus^{\Delta NLS/+}$ mice remained consistent. In both aforementioned graphs, $Fus^{Resc/+}$ mice demonstrated significantly longer social interaction times than $Fus^{+/+}$ mice (Fig. 4B, mouse and 4C, dashed lines). Moreover, there was no significant difference between $Fus^{Resc/+}$ and $Fus^{\Delta NLS/+}$ males. This suggests that FTD-like social symptoms at 4 months of age are not prevented by the rescued nuclear localisation of FUS in inhibitory neurons.

At 10 months of age, $Fus^{\Delta NLS/+}$ males still demonstrated an increased social interest. In particular, their total (Fig. 4F, mouse) and detailed (Fig. 4G, dashed purple line) social interaction times were increased compared to those at 4 months of age (Fig. 4B, mouse and 4C, dashed purple line). This was not the case for $Fus^{+/+}$ and $Fus^{Resc/+}$ mice. As a consequence, $Fus^{\Delta NLS/+}$ mice exhibited a significantly higher total interaction time in comparison to $Fus^{+/+}$ and $Fus^{Resc/+}$ mice (Fig. 4F, mouse). Most of this difference was attributed to a significantly increased interaction time during the third trial (Fig. 4G). At this age, there was no significant difference between $Fus^{Resc/+}$ and $Fus^{+/+}$ males. These findings indicate that the social impairments are attenuated in aged male mice when FUS nuclear localisation is rescued in inhibitory neurons.

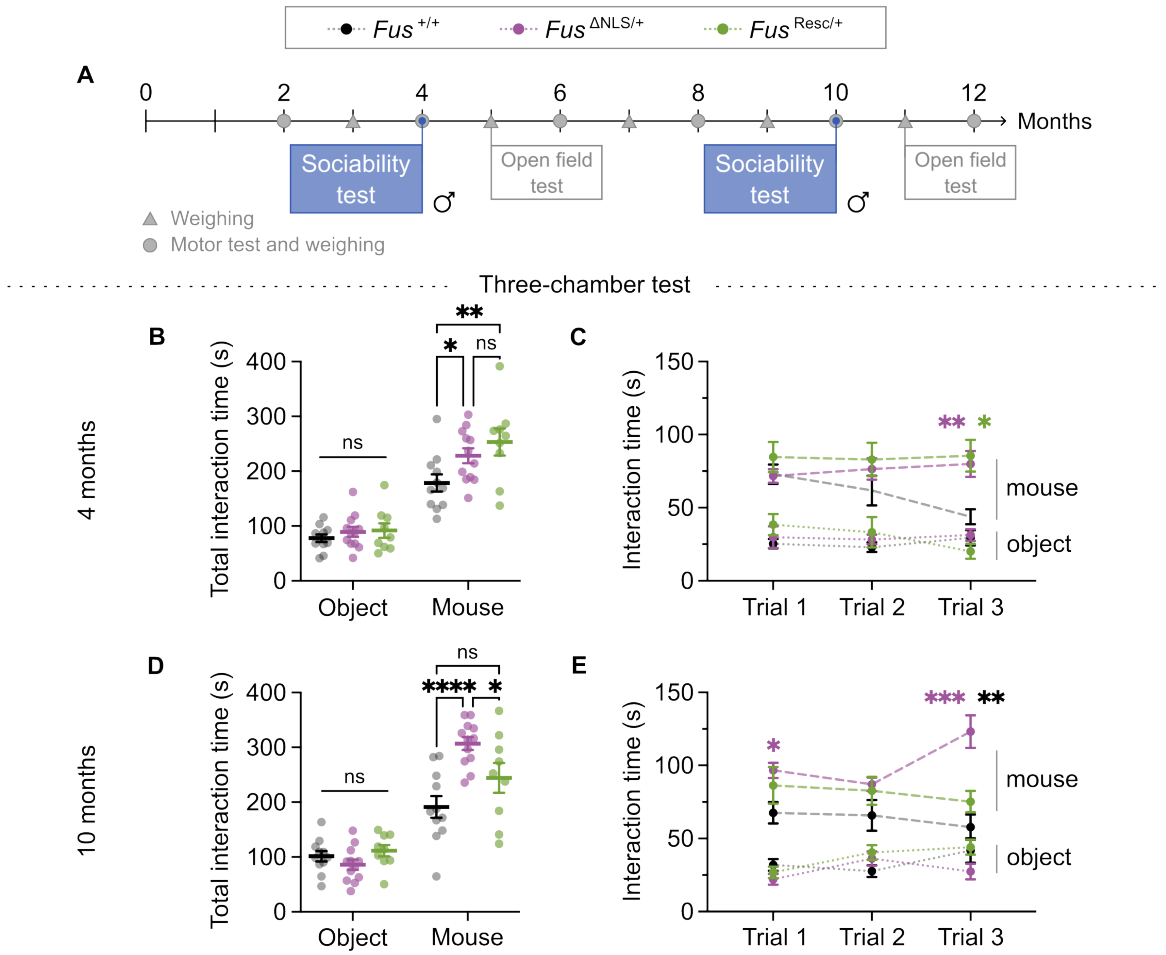


Figure 4: Attenuation of social impairments in *Fus*$^{Resc/+}$ male mice. Results are expressed as mean ± SEM, n = 11 *Fus*$^{+/+}$ (black), 12 *Fus*$^{\Delta NLS/+}$ (purple) and 9 *Fus*$^{Resc/+}$ (green) males. (**A**) Scheme of the experimental design. Sociability was assessed at 4 (B, C) and 10 (D, E) months of age. (**B-E**) Time spent contacting an empty cage (object) or a cage with a mouse (mouse) was measured with the three-chamber task. Social preference was assessed in a novel environment for 15 min (B, D) divided into three 5-minute trials (C, E). Two-way ANOVA and multiple comparisons were corrected with Tukey's test. Comparison of genotypes for the interaction time with the object: ns $p > 0.05$. Comparison of genotypes for the interaction time with the mouse: *Fus*$^{+/+}$ *vs* *Fus*$^{\Delta NLS/+}$, * $p < 0.05$ (purple); *Fus*$^{+/+}$ *vs* *Fus*$^{Resc/+}$, * $p < 0.05$ (green); *Fus*$^{\Delta NLS/+}$ *vs* *Fus*$^{Resc/+}$, ** $p < 0.01$ (black).

At 4 and 10 months of age, the increased social interest was not accompanied by a general increase in curiosity or locomotor exploration. In the three-chamber social task, the interaction times with the empty cage (Fig. 4B-4E, object) and the total distance travelled (Fig. S2B-S2E) were not significantly different between the three genotypes. To validate these results, we performed an open field test at 5 and 11 months of age (Fig. S2A). The tested mouse was allowed to move freely within a novel environment while being recorded. At both ages, the times spent in the periphery and centre (Fig. S2F and S2I), as well as the latency to first enter the centre (Fig. S2G and S2J), were comparable between the genotypes. This indicates that *Fus*$^{\Delta NLS/+}$ and *Fus*$^{Resc/+}$ males did not exhibit a reduction

in anxiety-like behaviour. Similarly, the total distance travelled was not different between the genotypes (Fig. S2H and S2G), thereby confirming that locomotor exploration is not enhanced in *Fus*$^{\Delta NLS/+}$ or *Fus*$^{Resc/+}$ males.

In conclusion, *Fus*$^{\Delta NLS/+}$ male mice exhibited increased sociability at 4 months of age, with this phenotype becoming even more pronounced at 10 months of age. Rescuing FUS localisation in the inhibitory neurons of *Fus*$^{Resc/+}$ males resulted in increased sociability at 4 months of age, although this phenotype was attenuated with age.

Rescuing FUS nuclear localisation in inhibitory neurons reduces spontaneous neuronal activity levels in anaesthetised animals

We previously showed that neuronal activity levels are increased in the frontal cortex of *Fus*$^{\Delta NLS/+}$ mice (Scekic-Zahirovic et al., 2021). To assess whether inhibitory dysfunction could cause this abnormal cortical activity, we performed *in vivo* two-photon calcium imaging in the motor cortex of 4-month-old anesthetised animals, using the genetically encoded calcium indicator GCaMP7s (Fig. 5A and 5B). We did not find a change in the fraction of active neurons when comparing *Fus*$^{\Delta NLS/+}$ and *Fus*$^{Resc/+}$ mice (Fig. 5C). However, we observed a significant decrease in calcium transient frequency in *Fus*$^{Resc/+}$ mice (Fig. 5D), accompanied by an increase in transient amplitude (Fig. 5E). Neuronal activity is tightly correlated, for which inhibitory neurons are indispensable. As a proxy for activity regulations within networks, we assessed the correlation of neuronal activity by computing pairwise neuronal correlation coefficients. This investigation revealed a decrease in the elevated neuronal correlation in *Fus*$^{Resc/+}$ mice both at the level of individual fields of view (Fig. 5G) as well as on individual regions of interest pairs (Fig. 5H). This decrease in the elevated neuronal correlation upon rescue of FUS localisation in inhibitory neurons, in addition to a reduction of the increased neuronal activity levels, emphasises the relevance of FUS mislocalisation, particularly in inhibitory neurons, on overall network function.

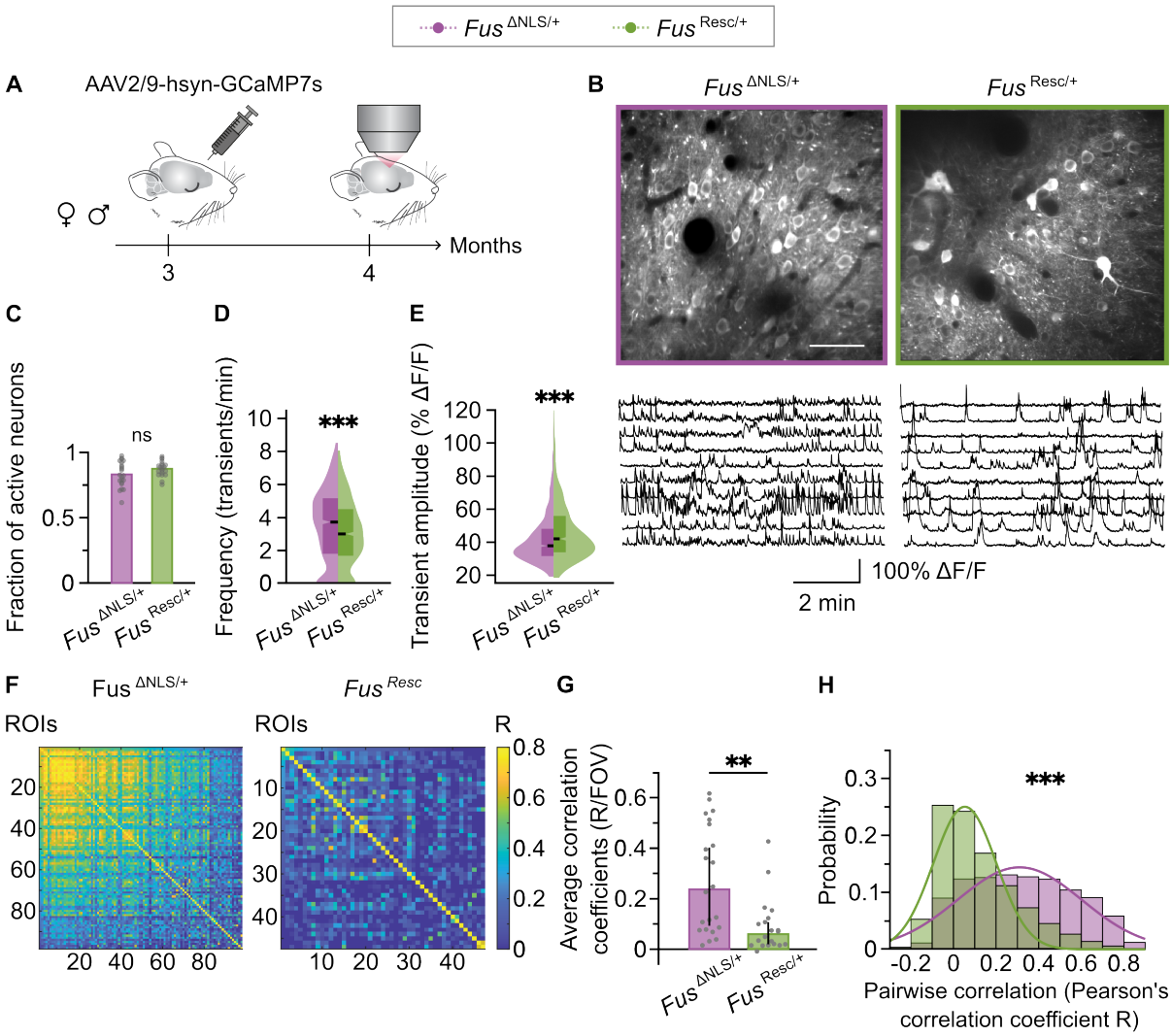


Figure 5: Reduction of spontaneous neuronal activity levels in anaesthetised *Fus*$^{Resc/+}$ mice. Results are expressed as mean ± SEM (C) or median ± 95% confidence interval (G). Data from both sexes are pulled in the graphs. (**A**) Scheme of the experimental design. Mice were injected with AAV2/9-hsyn-jGCaMP7s into the primary motor cortex and imaged four weeks later. (**B**) Exemplary average projection of a field of view (FOV) in a *Fus*$^{\Delta NLS/+}$ and *Fus*$^{Resc/+}$ mouse, and representative calcium traces of selected regions of interest (ROIs). Scale bar = 50µm. (**C**) Fraction of active neurons (n = 22 FOV in *Fus*$^{\Delta NLS/+}$ mice, and 20 FOV in *Fus*$^{Resc/+}$ mice). (**D**) Frequency of calcium transients of analysed ROIS (n = 1613 ROIs in *Fus*$^{\Delta NLS/+}$ mice, and 1348 ROIs in *Fus*$^{Resc/+}$ mice). (**E**) Distribution of calcium transient amplitudes of active ROIs (n = 1359 ROIs in *Fus*$^{\Delta NLS/+}$ mice, and 1178 ROIs in *Fus*$^{Resc/+}$ mice). (**F**) Representative correlograms of pairwise correlations. (**G**) Median Pearson correlation coefficient (R) per FOV (n = 22 FOV in *Fus*$^{\Delta NLS/+}$ mice, and 20 FOV in *Fus*$^{Resc/+}$ mice). (**H**) Distribution of pairwise correlation coefficients superimposed by a Gaussian fit (n = 46335 ROI pairs in *Fus*$^{\Delta NLS/+}$ mice, and 34722 ROI pairs in *Fus*$^{Resc/+}$ mice). (C) Unpaired t-test, ns $p > 0.05$. (D, E, H) Kolmogorov-Smirnov test, *** $p < 0.001$. (G) Mann-Whitney test, ** $p < 0.01$

FUS cytoplasmic delocalisation is induced exclusively in inhibitory neurons in *Fus*$^{Trunc/+}$ mice

As a complementary approach, we created a mouse line in which the NLS domain of *Fus* is truncated exclusively in inhibitory neurons. To do so, we used *Fus*$^{LoxP/LoxP}$ mice in which both copies of *Fus* contain LoxP sequences surrounding the NLS domain (Publication 3, page 295). By crossing *Vgat*$^{Cre/+}$ mice with *Fus*$^{LoxP/LoxP}$ (Fig. 6A), we obtained germline transmission of the recombinant alleles (Fig. 6B), resulting in the generation of mice designated as *Fus*$^{Trunc/+}$. In the inhibitory neurons of these mice, one copy of *Fus* is wild-type and the other is truncated, whereas in the other cell types, both copies express the NLS domain. As previously, we analysed FUS subcellular localisation in the motor cortex of 2-month-old female and male mice (Fig. 6C and 6F). We effectively induced the cytoplasmic accumulation of FUS in inhibitory neurons. In *Fus*$^{Trunc/+}$ mice compared to *Fus*$^{+/+}$, *Vgat*$^{Cre/+}$ and control (Ctrl) mice, we found a tendency towards a significant 1.3-fold decrease in the nuclear-to-cytoplasmic ratio of FUS in parvalbumin inhibitory neurons (Fig. 6D). Surprisingly, our preliminary analysis showed that the nuclear-to-cytoplasmic ratio of FUS in layer 5 excitatory pyramidal neurons was also slightly decreased in *Fus*$^{Trunc/+}$ mice compared to the three other mouse lines (1.3-fold decrease, Fig. 6F). We will have to include a higher number of mice in the analysis to ascertain whether this result is an artefact. Of note, the delocalisation of FUS was not accompanied by a loss of inhibitory neurons (Fig. 6F), nor a loss of excitatory neurons (preliminary data not shown), as all genotypes exhibited comparable numbers of cells per section. Overall, these results confirm that in *Fus*$^{Trunc/+}$ mice, the cytoplasmic delocalisation of FUS is induced, possibly exclusively, in cortical inhibitory neurons, while further verification is required for spinal neurons (analysis in progress).

Legend Figure 6: (**C**, **F**) Images of the immunofluorescent staining of FUS in the primary motor cortex of 2-month-old mice. Hoechst staining was used to delimit nuclei. Parvalbumin staining was used to delimit the cytoplasm of inhibitory neurons (C), while CRYM staining was used to delimit the cytoplasm of layer 5 excitatory pyramidal neurons (F). Scale bar = 10µm (**D**, **G**) Quantification of the nuclear-to-cytoplasmic ratio of FUS in inhibitory parvalbumin neurons (D) and excitatory pyramidal neurons (G). Number of inhibitory neurons analysed: 129 in *Fus*$^{+/+}$, 158 in *Vgat*$^{Cre/+}$, 139 in Ctrl, and 135 in *Fus*$^{Trunc/+}$ mice. Number of excitatory neurons analysed: 81 in *Fus*$^{+/+}$, 72 in *Vgat*$^{Cre/+}$, 80 in Ctrl, and 82 in *Fus*^{Trunc} mice. (**E**) Averaged number of parvalbumin inhibitory neurons per section. (D, E, G) Kruskal-Wallis test and multiple comparisons were corrected with a two-stage Benjamini, Krieger and Yekutieli false discovery rate procedure, ns $p > 0.05$.

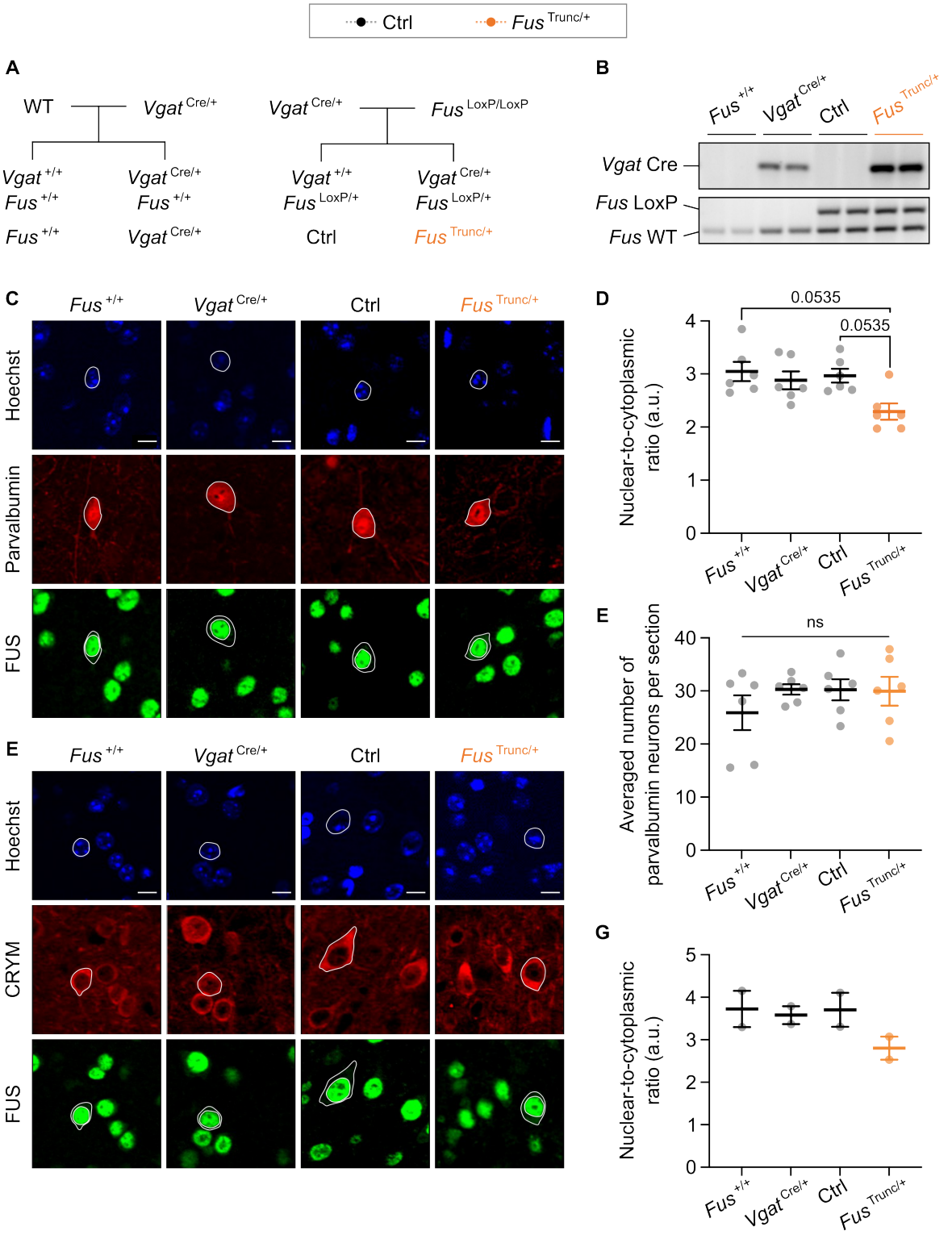


Figure 6: Induced cytoplasmic delocalisation of FUS in inhibitory neurons in *Fus*$^{Trunc/+}$ mice. Preliminary version. Results are expressed as mean ± SEM, n = 3 *Fus*$^{+/+}$ (black), 3 *Vgat*$^{Cre/+}$ (black), 3 Ctrl (black) and 3 *Fus*$^{Trunc/+}$ (green) for both females and males (merged in graphs). (**A**) Breeding scheme to generate Ctrl and *Fus*$^{Trunc/+}$ littermates, as well as age- and sex-matched *Fus*$^{+/+}$ and *Vgat*$^{Cre/+}$ mice. (**B**) Representative PCR genotyping results.
End of the legend on the previous page.

Inducing FUS cytoplasmic delocalisation in inhibitory neurons does not cause motor deficits

ALS-like motor symptoms were assessed as previously described (Fig. 7A). There was no significant difference between *Fus*$^{Trunc/+}$ mice and their Ctrl littermates in terms of body weight (Fig. 7B and 7C), hanging time (Fig. S1D and S1E), and holding impulse (Fig. 7D and 7E) for both females and males. These findings indicate that FUS cytoplasmic delocalisation in inhibitory neurons is not sufficient to cause motor deficits.

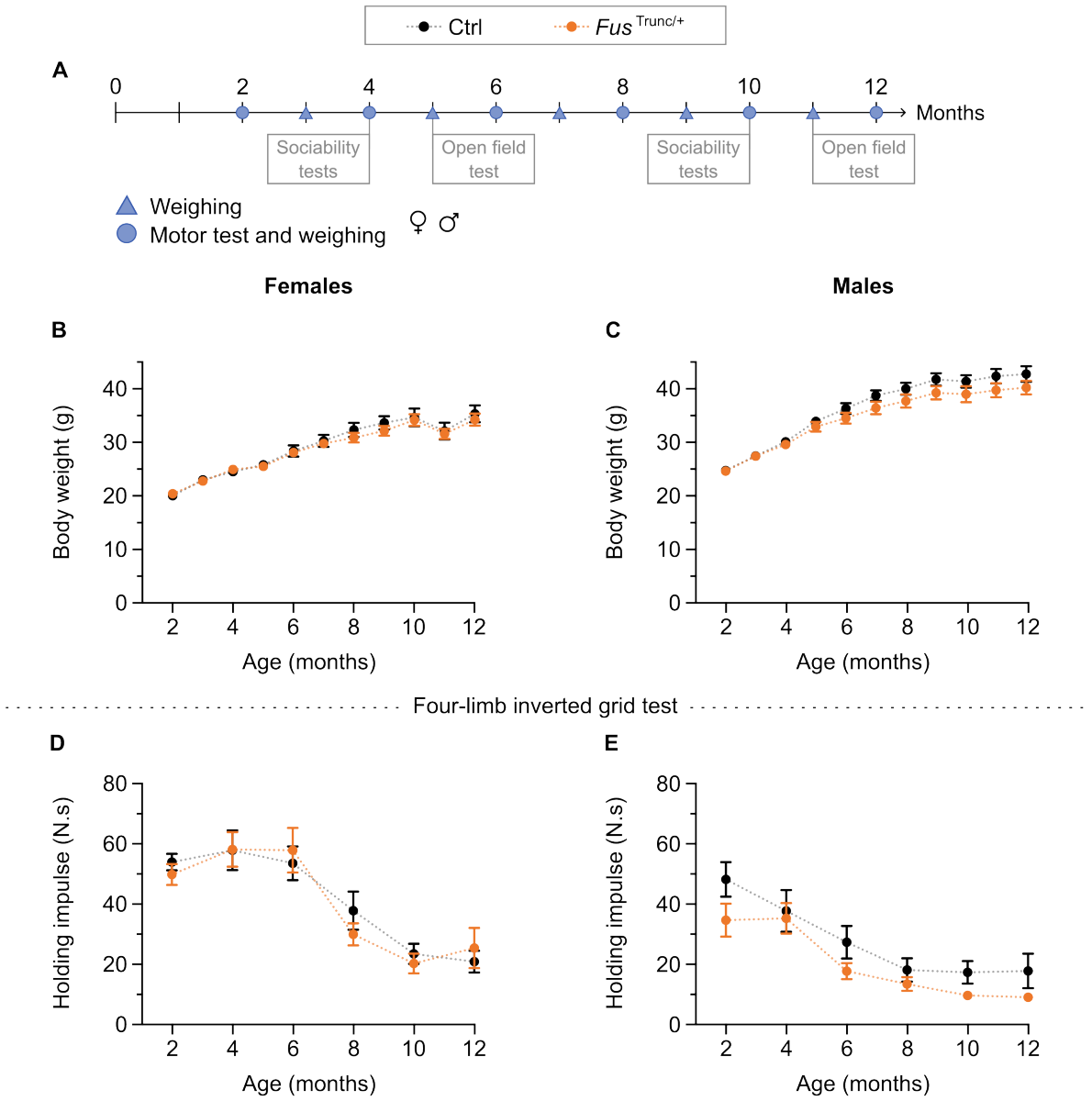


Figure 7: Absence of motor deficits in *Fus*$^{Trunc/+}$ mice. Results are expressed as mean ± SEM, n = 8 Ctrl (black) and 11 *Fus*$^{Trunc/+}$ (orange) females (left panels), n = 14 Ctrl (black) and 14 *Fus*$^{Trunc/+}$ (orange) males (right panels). (**A**) Scheme of the experimental design. (**B**, **C**) Body weight monitored monthly. (**D**, **E**) Holding impulse was calculated from the hanging time monitored every two months with the four-limb inverted grid test. (B-E) Two-way ANOVA and multiple comparisons were corrected with Šidák's test. Comparison of genotypes: ns $p > 0.05$.

Inducing FUS cytoplasmic delocalisation in inhibitory neurons cause social impairments in males

FTD-like social symptoms were assessed as previously described (Fig. 8A). At 4 and 10 months of age, *Fus*$^{Trunc/+}$ male mice exhibited increased social interest compared to their Ctrl littermates. At both ages, we observed a significant increase in the total social interaction time of *Fus*$^{Trunc/+}$ mice (Fig. 8B and 8D, mouse). At 4 months of age, this was predominantly attributable to a significantly increased interaction time during the second trial (Fig. 8C, dashed lines), whereas at 10 months of age, this was due to the third trial (Fig. 8E, dashed lines). These data indicate that FUS cytoplasmic delocalisation in inhibitory neurons is sufficient to cause social impairments in male mice.

The increased social interest in *Fus*$^{Trunc/+}$ mice was not accompanied by an increase in curiosity or locomotor exploration. During the three-chamber social task, the interaction times with the empty cage were comparable between the genotypes (Fig. 8B-8E, object). At 4 and 10 months of age, the total distance travelled appeared to be marginally greater for *Fus*$^{Trunc/+}$ mice than for Ctrl mice (Fig. S3B-S3E). To validate these results, we performed an open field test at 5 and 11 months of age (Fig. S3A) and observed that the times spent in periphery and centre were comparable between the genotypes (Fig. S3F and S3I). At 4 months of age, the latency to first enter the centre was significantly decreased for *Fus*$^{Trunc/+}$ males compared to Ctrl males (Fig. S3G), but this did not affect the other parameters measured with this test. In addition, this latency was comparable between *Fus*$^{Trunc/+}$ and Ctrl littermates at 10 months of age (Fig. S3J). Overall, these results indicate that *Fus*$^{Trunc/+}$ males did not exhibit decreased anxiety. The total distance travelled was not significantly different between the genotypes (Fig. S3H and S3Q), suggesting that locomotor exploration is not markedly enhanced in *Fus*$^{Trunc/+}$ male mice.

To conclude, *Fus*$^{Trunc/+}$ male mice recapitulated the increased social interest of *Fus*$^{\Delta NLS/+}$ mice, with the exception that their phenotype did not appear to worsen with age

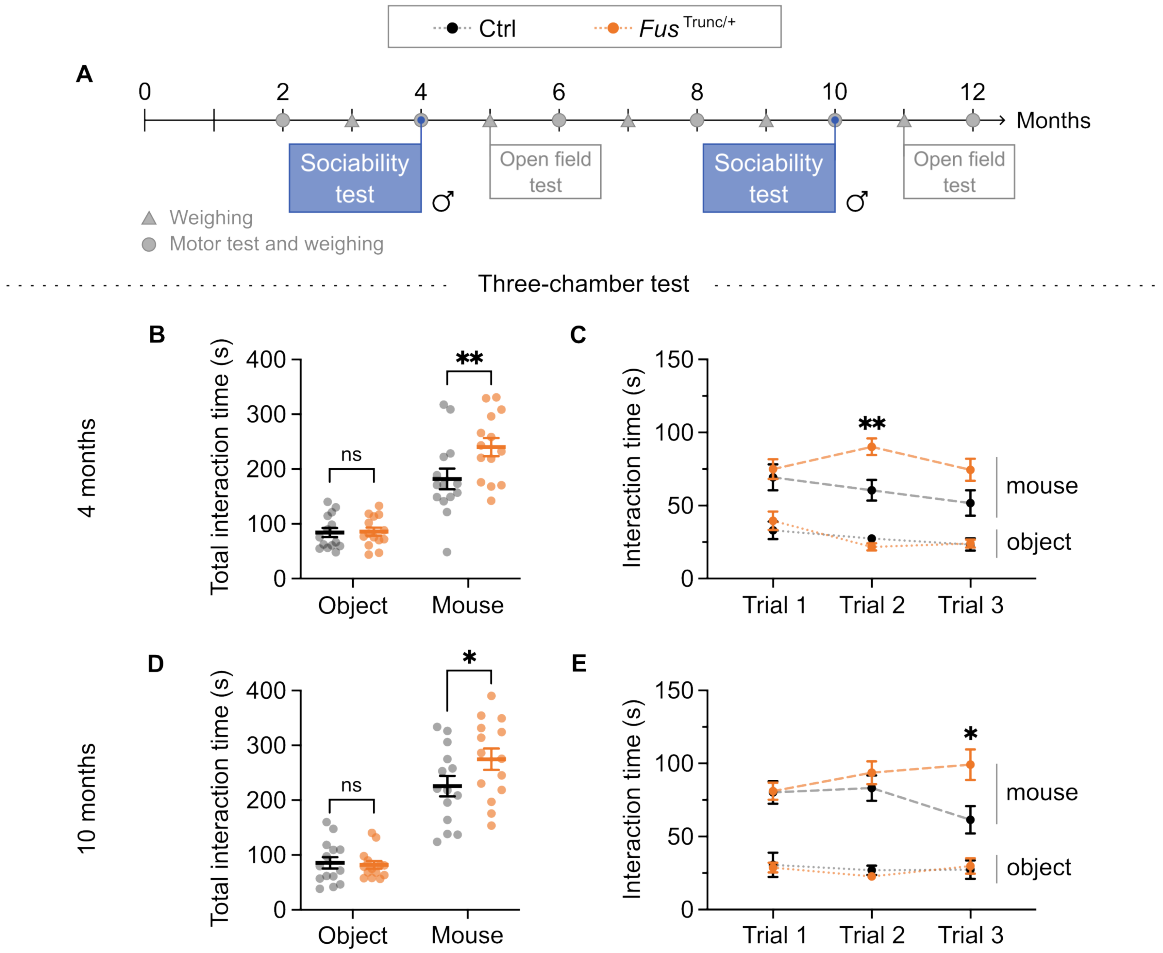


Figure 8: Social impairments in *Fus*$^{Trunc/+}$ male mice. Results are expressed as mean ± SEM, n = 14 Ctrl (black) and 14 *Fus*$^{Trunc/+}$ (orange) males. (**A**) Scheme of the experimental design. Sociability was assessed at 4 (B, C) and 10 (D, E) months of age. (**B-E**) Time spent contacting an empty cage (object) or a cage with a mouse (mouse) was measured with the three-chamber task. Social preference was assessed in a novel environment for 15 min (B, D) divided into three 5-minute trials (C, E). (B, D) Two-way ANOVA and multiple comparisons were corrected with Šidák's test. Comparison of genotypes for the interaction with the object: ns $p > 0.05$. Comparison of genotypes for the interaction time with the mouse: * $p < 0.05$

Inducing FUS cytoplasmic delocalisation in inhibitory neurons increases spontaneous neuronal activity in anaesthetised animals

To assess whether the cytoplasmic mislocalisation of FUS exclusively in inhibitory neurons is sufficient to impair neuronal activity levels, we performed *in vivo* two-photo calcium imaging as previously described (Fig. 9A and 9B). The selective cytoplasmic mislocalisation of FUS in inhibitory neurons caused a significant increase in the fraction of active neurons (Fig. 9C). While the frequency of the detected spontaneous calcium transients did not differ between Ctrl and *Fus*$^{Trunc/+}$ mice (Fig. 9D), we observed higher amplitudes of calcium transients in *Fus*$^{Trunc/+}$ mice (Fig. 9E), indicative of more numerous action potentials underlying individual calcium transients. In addition to an increase in the neuronal activity levels, we also found a decrease in the elevated neuronal correlation in *Fus*^{Trunc} mice (Fig. 9G and 9H), demonstrating higher levels of uncorrelated neuronal activity upon the induction of FUS mislocalisation in inhibitory neurons.

Parvalbumin neurons may be the most affected inhibitory neurons in *Fus*$^{\Delta NLS/+}$ mice

The objective of our genetic approach was to target most inhibitory neurons, both in the brain and spinal cord. This was achieved by targeting *Vgat*-expressing neurons. As a result, it is not possible to determine the contribution of specific subpopulations to the phenotypes described above. To gain a deeper understanding of the underlying mechanisms, we conducted single-nucleus RNA sequencing in the frontal cortex of 10-month-old *Fus*$^{\Delta NLS/+}$ female and male mice. The analysis is currently underway and appears to indicate that parvalbumin neurons are the most affected inhibitory neurons (data not shown**).**

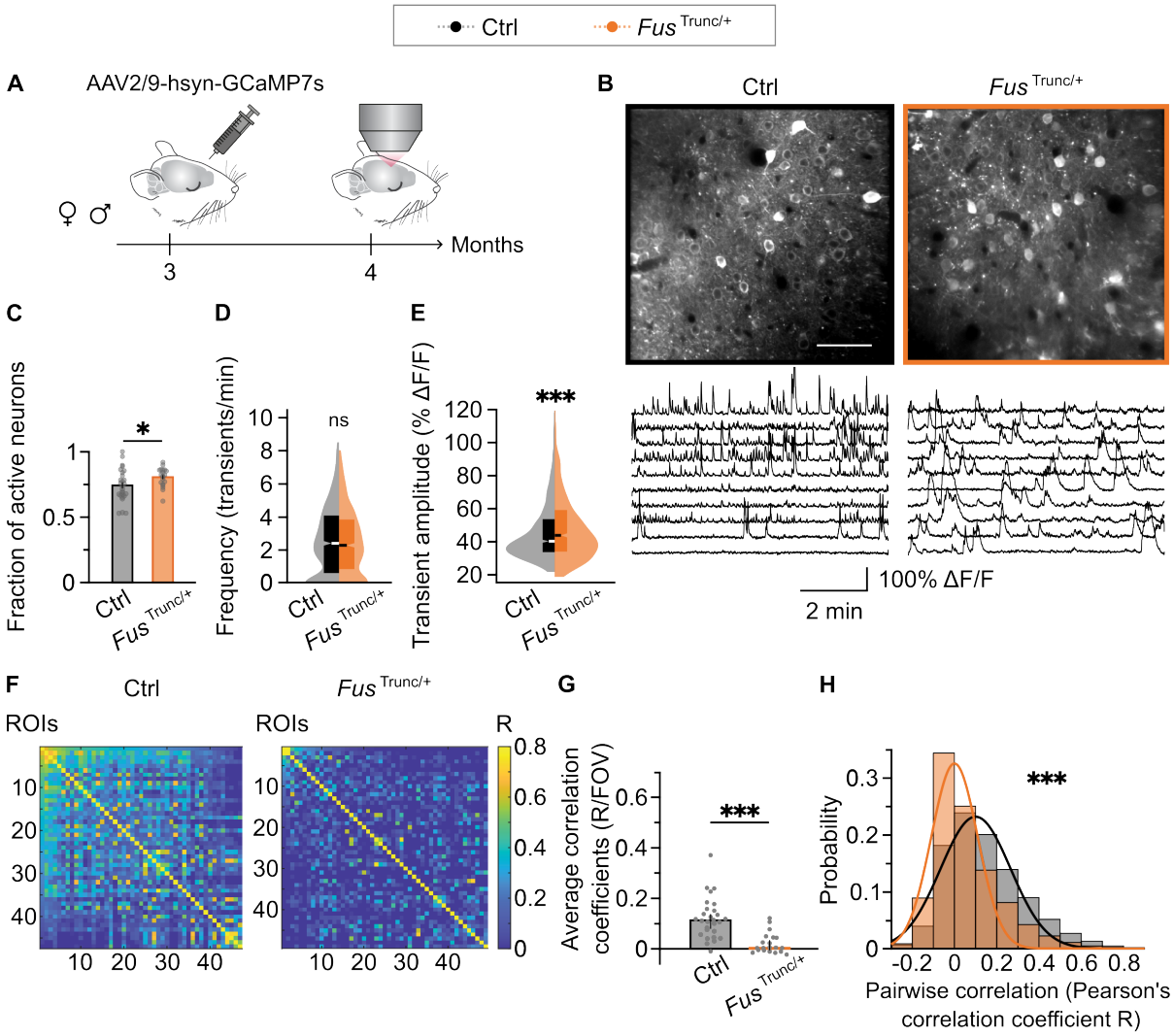


Figure 9: Increase in spontaneous neuronal activity levels in anaesthetised *Fus*$^{Trunc/+}$ mice. Results are expressed as mean ± SEM (C) or median ± 95% confidence interval (G). (**A**) Scheme of the experimental design. Mice were injected with AAV2/9-hsyn-jGCaMP7s into the primary motor cortex and imaged four weeks later. (**B**) Exemplary average projection of a field of view (FOV) in a Ctrl and *Fus*$^{Trunc/+}$ mouse, and representative calcium traces of selected regions of interest (ROIs). Scale bar = 50µm. (**C**) Fraction of active neurons (n = 27 FOV in Ctrl mice, and 20 FOV in *Fus*$^{Trunc/+}$ mice). (**D**) Frequency of calcium transients of analysed ROIS (n = 1597 ROIs in Ctrl mice, and 1273 ROIs in *Fus*^{Trunc} mice). (**E**) Distribution of calcium transient amplitudes of active ROIs (n = 1214 ROIs in Ctrl mice, and 1029 ROIs in *Fus*$^{Trunc/+}$ mice). (**F**) Representative correlograms of pairwise correlations. (**G**) Median Pearson correlation coefficient (R) per FOV (n = 28 FOV in Ctrl mice, and 20 FOV in *Fus*$^{Trunc/+}$ mice). (**H**) Distribution of pairwise correlation coefficients superimposed by a Gaussian fit (n = 31036 ROI pairs in Ctrl mice, and 26746 ROI pairs in *Fus*$^{Trunc/+}$ mice). (C) Unpaired t-test, * $p < 0.05$. (D, E, H) Kolmogorov-Smirnov test, ns $p > 0.05$, *** $p < 0.001$. (G) Mann-Whitney test, *** $p < 0.001$.

Conclusion

With the present study, we demonstrated that the rescue of FUS nuclear localisation in *Vgat*-expressing inhibitory neurons resulted in a delayed onset of ALS-like motor deficits in females and an attenuation of FTD-like social alterations in 10-month-old males. Conversely, the induction of FUS cytoplasmic delocalisation exclusively in these neurons was sufficient to elicit social alterations in 4- and 10-month-old males, as well as to enhance spontaneous neuronal activity in the frontal cortex. Collectively, these findings underscore the role of FUS mislocalisation, particularly in inhibitory neurons, on overall network function and the subsequent behavioural effects.

Materials and methods

Mouse models

Experimental protocols and animal care were conducted in compliance with the European Directive (2010/63/UE) and French Decree (2013/118). The project received approval from the ethical committee of the University of Strasbourg and the French Department of Higher Education, Research and Innovation (reference number 22385 for the behaviour analysis), as well as from the Government of Upper Bavaria.

To generate double mutant mice, Vgat-ires-Cre knock-in mice (The Jackson Laboratory, stock #028862, C57BL/6J background, B6J.129S6(FVB)-*Slc32a1*$^{tm2(cre)Lowl}$/MwarJ) (Vong et al., 2011) were crossed with different knock-in mouse lines containing LoxP sequences: Ai14 (The Jackson Laboratory, stock #007914, C57BL/6J background, B6.Cg-*Gt(ROSA)26Sor*$^{tm14(CAG-tdTomato)Hze}$/J) (Madisen et al., 2010), *Fus*$^{\Delta NLS/+}$ (Mouse Clinical Institute of Strasbourg, C57BL/6J and /6N mix background, B6-*Fus*$^{tm1(\Delta NLS)Ldup}$/Crl) (Scekic-Zahirovic et al., 2016) and *Fus*^{exon15} (Mouse Clinical Institute of Strasbourg, C57BL/6N background, B6-*Fus*$^{tm2(\Delta NLS)Ldup}$/Crl, Publication 3, page 295). When necessary, additional age- and sex-matched control mice were produced with the same genetic background as the other mice of interest. Mice were genotyped by PCR of genomic DNA extracted from ear biopsies (sequences are provided in Table S1).

Mice were bred and housed in the animal facilities of the Faculty of Medicine of Strasbourg and of the Institute of Clinical Neuroimmunology, under constant conditions (22 ± 2°C, 45-65% humidity) and a regular 12-hour light and dark cycle (with lights on at 7:30 am). Food and water were available *ad libitum*, with mice being given a breeding diet before weaning and a maintenance diet afterwards. Animals were housed in groups, unless otherwise specified.

Histological analysis

Mice were anaesthetised with isoflurane and euthanised with an intraperitoneal injection of 230 mg/kg sodium pentobarbital (Euthasol Vet). They were transcardially perfused with 4% paraformaldehyde. After dissection, brains and spinal cords were post-fixed for 24h and then included in 4% agar. Serial cuts (thickness 40µm) were made using a vibratome (Leica Biosystems) and collected in phosphate buffer saline (PBS) with 0.02% azide. Slices were rinsed with PBS and then incubated in 10mM citrate buffer (pH 6) for 30min at 80°C. After three washes in PBS, slices were blocked in PBS with 5% horse serum and 0.3% Triton X-100 for 90min at room temperature. Primary antibodies were incubated in PBS with 1% horse serum and 0.1% Triton-X100 overnight at 4°C or room temperature: goat anti-FUS (Bethyl, 1:250, A303-839A), rabbit anti-FUS (Proteintech, 1:500, 11570-1-AP), guinea pig anti-NeuN (Synaptic Systems, 1:1000, 266-004), mouse anti-parvalbumin (Sigma, 1:1000, P3088), mouse anti-Crym (Abnova, 1:100, H00001428-M03), goat anti-ChAT (Millipore, 1:500, AB114P), rabbit anti-RFP (Rockland, 1:500, 600-401-379). After three washes in PBS, fluorescent conjugated secondary antibodies were incubated in PBS for 90min at room temperature: donkey anti-guinea pig A488 (Jackson, 1:1000, 706-546-148), donkey anti-goat A555 (Invitrogen, 1:1000, A21432), donkey anti-rabbit A555 (Invitrogen, 1:1000, A31572), donkey anti-mouse A647 (Jackson, 1:1000, 715-605-151), donkey anti-goat A647 (Jackson, 1:1000, 705-605-147). Three final washes were performed, and during the second wash, chromatin was stained with Hoechst (sigma, 1:1000, B2261) for 15min at room temperature. Slices were mounted in Mowiol 4-88 (Sigma, 81381), Prolong Diamond (Invitrogen, P36961) or Aqua-Poly/Mount (Polyscience, 18606-5) on microscope slides.

Image acquisition was performed at the Imaging Core Facility of Strasbourg Biomedical Research Centre (University of Strasbourg, INSERM, UMS 38, PIC-STRA,). An upright widefield epifluorescence microscope (Zeiss, Axio Imager M2) was used with an ApoTome module. Data were analysed blind to genotypes. A home-made macro allowed us to study tdTomato labelling in different cell types. Briefly, cellular segmentation was realised with the Cellpose algorithm and one of the following markers: tdTomato, NeuN or parvalbumin. The mean signal intensity of each ROI was then measured for every channel using ImageJ software. For all images, the same threshold was used to consider a ROI as positive or negative for a given marker. ImageJ software was used to study FUS localisation by measuring a mean signal intensity in the nucleus and cytoplasm of cells of interest. The sex and number of mice studied are indicated in the relevant figures.

Behavioural analysis

Mice were carefully handled for a month before the beginning of the longitudinal study to reduce their stress and anxiety. Animals were then monitored from 2 to 12 months of age. Behavioural tests were conducted during the light phase (between 8:00 am and 4:00 pm). Prior to any task, mice were placed in the test room for at least 30 minutes to allow

them to acclimate to the environment. All behavioural tests and data analysis were performed blind to genotypes. Out of the 114 mice produced for this study, four were excluded. One *Fus*$^{+/+}$ female, one *Fus*$^{+/+}$ male and one *Fus*^{Trunc} female were euthanised at 10-11 months of age because of dermatitis. One female was excluded due to a genotyping error. The sex and number of mice included in this study are indicated in the relevant figures. In the end, mice were sacrificed to recover tissues.

Four-limb inverted grid test: The four-limb inverted grid test was used to non-invasively assess the limb strength of mice. The protocol was adapted from Carlson et al., 2010. Each mouse was placed on a grid and allowed to acclimate to the environment for 30 seconds. The grid was then inverted and held 35cm over a cage containing 5cm of wood chips. The test began with the mouse grasping the grid with its four paws. The time necessary for the mouse to fall (referred to as 'hanging time') was measured visually using a stopwatch. Trials lasted a maximum of 5min. In each session, the procedure was repeated three times. The animal was returned to its home cage for 10 minutes between each trial. The body weight was measured just before the test to compute the minimum total sustained force exerted by the mouse to oppose the gravitational force:

$$Holding\ impulse\ (N.s) = averaged\ hanging\ time\ (s) \times\ body\ weight\ (g) \times\ 0.00980665\ (N.g^{-1})$$

At 4 and 10 months of age, male mice were housed individually for three consecutive days. On one of the final two days, they performed the three-chamber social task.

Three-chamber social task: The three-chamber social task was used to evaluate social preference in a novel environment. The protocol was adapted from Gascon et al., 2014. The tested mouse was placed in the middle of a rectangular arena (59 x 39.5cm) consisting of three compartments (18.5 x 39.5cm) bounded by walls with a small opening (Sociability cage, Noldus Information Technology). The central compartment was left empty while the other two contained an openwork cylindrical cage (referred to as 'cage'). For habituation, the tested mouse was placed in the arena containing two empty cages. To assess social preference, the animal was placed three times in the arena containing a cage with a mouse (referred to as 'stranger') and an empty cage. The same stranger was used for all three trials, but the compartment in which it was placed was changed to prevent a potential side bias. For each trial, the tested mice were allowed to explore freely the arena for 5 minutes while being filmed. The animal was returned to its home cage for 15 minutes between two trials. The cages and arena were cleaned with soap after each use to minimise potential odour cues. The strangers were wild-type males of the same age and genetic background as the tested mice. They were housed in groups throughout their lives and had never encountered the tested mice before. Data were analysed with EthoVision XT 17.5 software (Noldus Information Technology). The contacting time was defined as the time during which the nose of the tested mouse was found within 2.5cm of

a cage. Various parameters were measured including total distance travelled, velocity, and time spent contacting cages with strangers or empty cages. The total social interaction time was calculated by adding up the contacting times with the stranger for the three trials, while the total object exploration time was obtained from the contacting times with the empty cage.

Open field test: Male mice were tested at 5 and 11 months without prior isolation. The open field test was used to assess locomotor exploration and anxiety in a novel environment. The protocol was adapted from Kraeuter et al., 2019. The tested mouse was placed in a corner of a square arena (72 x 72cm) and allowed to explore freely the environment for 15 minutes while being filmed. Data were analysed with EthoVision XT 17.0 software (Noldus Information Technology) by dividing the open maze into sixteen squares (18 x 18 cm). Various parameters were measured, including total distance travelled, velocity, time spent in the centre (four central squares), time spent in the periphery (twelve peripheral squares), and latency to first enter the central area.

Neuronal activity analysis

The sex and number of mice included in this study are indicated in the relevant figures.

Craniotomy and window implant: Mice of both sexes were implanted with a cranial window at the age of 3-4 months, and received a stereotaxic injection of adeno-associated viruses (AAVs) encoding the genetically-encoded calcium indicator jGCaMP7s into the primary motor cortex (AAV2/9.syn.jGCaMP7s.WPRE diluted 1:6 in saline, pGP-AAV-syn-jGCaMP7s-WPRE was a gift from Douglas Kim & GENIE Project, Addgene viral prep # 104487-AAV2/9; RRID:Addgene_104487, Dana et al., 2019). Briefly, mice were given Metacam (1 mg/kg) and Metamizol (200 mg/kg) orally 30 minutes prior to surgery and were anaesthetised with Fentanyl (0.05 mg/kg), Midazolam (5.0 mg/kg), and Metedomidine (0.5 mg/kg). A circular craniotomy with a 2mm radius, centred at 1.7mm lateral and 0.8mm anterior to bregma, was performed, followed by the slow injection of a total of ~1µL of the AAV solution into three sites (~150nL at 300µm and ~150nL at 600µm cortical depth per injection site). A 4mm round glass coverslip (Warner Instruments) was placed over the cortex and sealed with UV-curable dental acrylic (Venus Diamond Flow, Heraeus Kulzer GmbH). To enable stable positioning of the mouse during two-photon imaging, a metal head bar was attached to the skull using dental acrylic (Paladur, Heraeus Kulzer GmbH). At the end of the surgery, anaesthesia was antagonized through the intraperitoneal application of Atipamezol (2.5 mg/kg), Flumazenil (0.5 mg/kg) und Naloxon (1.2 mg/kg), and Metacam (1 mg/kg) was then administered orally at 12-, 24-, 36-, 48- and 72-hour post-operation.

Two-photon calcium imaging in anaesthetised mice: Four weeks following the cranial window and head bar implantation, *in vivo* two-photon imaging was performed within

cortical layer II/III using a two-photon microscope (Hyperscope, Scientifica, equipped with an 8 kHz resonant scanner). Using a x16 water-immersion objective (Nikon), stacks consisting of 20 000 frames (equivalent to ~11min) were acquired at a frame rate of 30 Hz and a resolution of 512 × 512 pixels, covering a field of view (FOV) of 300 × 300µm. The light source was a Ti:Sapphire laser with a DeepSee pre-chirp unit (Spectra Physics MaiTai eHP). GCaMP was excited at 910nm, with a laser power not exceeding 40mW (typically 10-40mW) underneath the objective. In each mouse, two to five FOVs at cortical depths of 200 to 300µm were imaged. Mice were initially anaesthetised with 3 volume % isoflurane in pure O2 at a flow rate of ~0.5L/min. The concentration was lowered to 2 volume % for 5min, 1.5 volume % for 15min, and 1 volume % for 30min before the actual experiment was recorded to ensure stable anaesthesia depth. Body temperature was maintained at 37 degrees using a physiological monitoring system (Harvard Apparatus).

Image processing and data analysis: Image analyses were performed in MATLAB (version R2021a, Math Works) using custom-written algorithms (Liebscher et al., 2016; Scekic-Zahirovic et al., 2021). Briefly, stacks of images were corrected for potential x and y brain displacement, and regions of interest (ROIs) were semi-automatically selected based on the maximum and mean projections of all frames. Fluorescence signals of all pixels within a selected ROI were averaged, and the intensity traces were low pass filtered at 10 Hz. Contamination from neuropil signals was accounted for using the following equation adapted from Kerlin et al., 2010:

$$F_{ROI_comp} = F_{ROI} - 0.7 \times F_{neuropil}$$

F_{ROI_comp} represents the neuropil-compensated fluorescence of the ROI, F_{ROI} corresponds to the fluorescence signal of the selected ROI, and $F_{neuropil}$ represents the fluorescence signal within the neuropil surrounding the ROI. A neuron was defined as 'active', if it displayed at least one prominent calcium transient over 30 consecutive frames.

Statistics

The sample size was chosen based on previously published results (Scekic-Zahirovic et al., 2021). At least 8 animal per sex per genotype were studied for the behavioural analysis. Values from all animals were averaged for each genotype group, and data were represented as mean ± standard error of the mean (SEM) unless otherwise stated. When possible, the averaged value from each animal was represented as a single data point. Statistical analysis was performed using GraphPad Prism 9 software with a significant threshold set at $p = 0.05$. Normal distribution was assessed using three different tests (Anderson-Darling, D'Agostino and Pearson, Shapiro-Wilk). Normality was assumed when at least two tests reported $p > 0.05$, and the following statistical tests were chosen accordingly. Sphericity was assessed using the F test to compare two genotypes, and Brown-Forsythe and Bartlett tests to compare three genotypes). For two-way ANOVA, sphericity was not assumed so the Greenhouse-Geisser correction was used. When the

number of animals per genotype was smaller than 8, data was assumed not to follow normal distribution and non-parametric tests were used.

Acknowledgements

The authors would like to thank the technicians of the animal facilities, namely Célian Pitard, Christiane Rieger and Claudia Spielmann, for their care of the mice. We acknowledge the imaging core facility PIC-STRA, particularly Pascal Kessler, for their assistance with project design and data analysis.

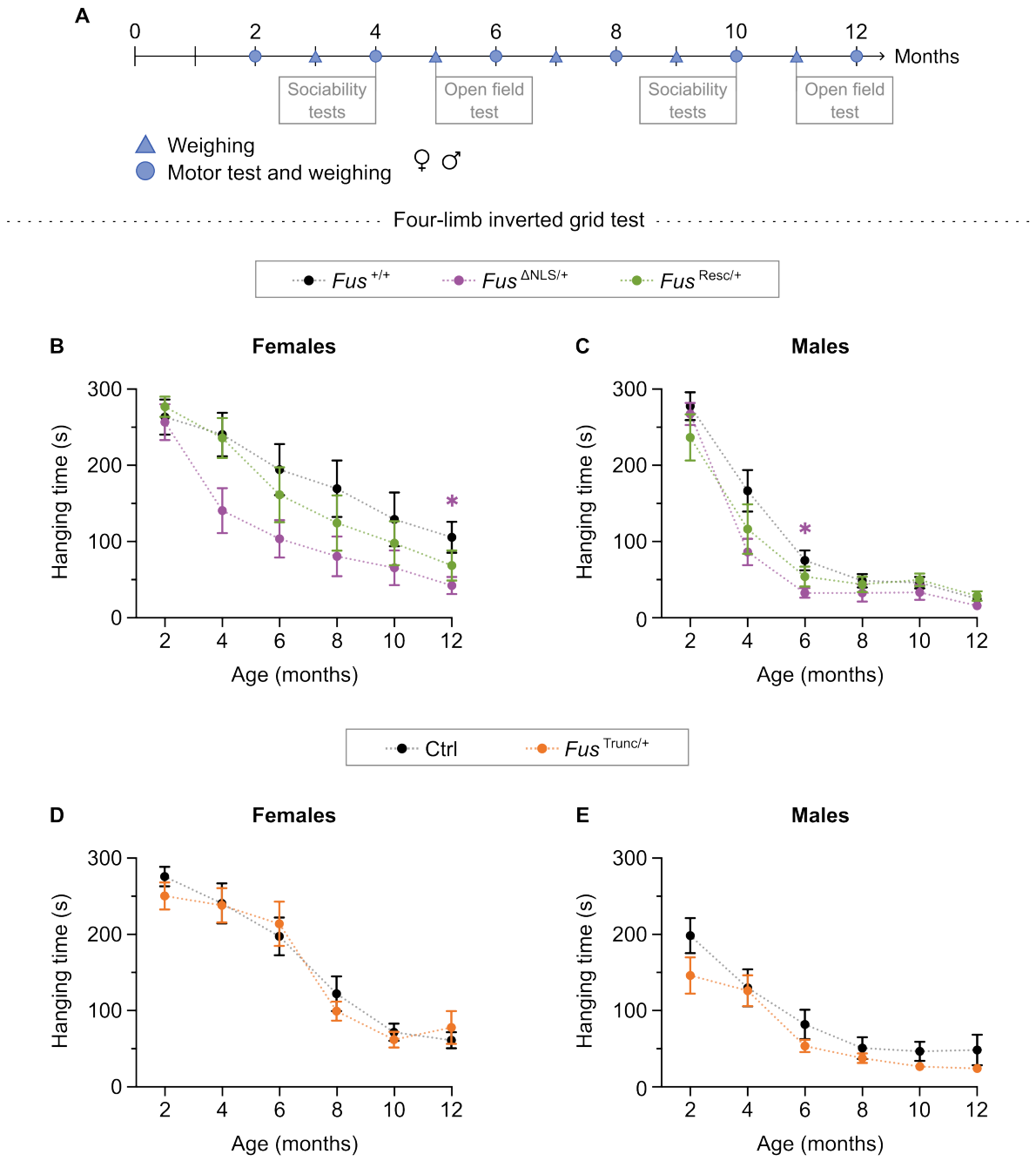
Author contributions

Genotyping was performed by F.L. and P.L. Tissues were processed by F.L., M.B. and A.B. Histological analysis was conducted by F.L., S.G. and V.D., with the assistance of P.K. Behavioural tests were conducted and analysed by F.L. Neuronal activity was assessed by V.W.Y.K., and analysed by V.W.Y.K. and S.L. The manuscript was written by F.L., R.C., L.D. and S.L.

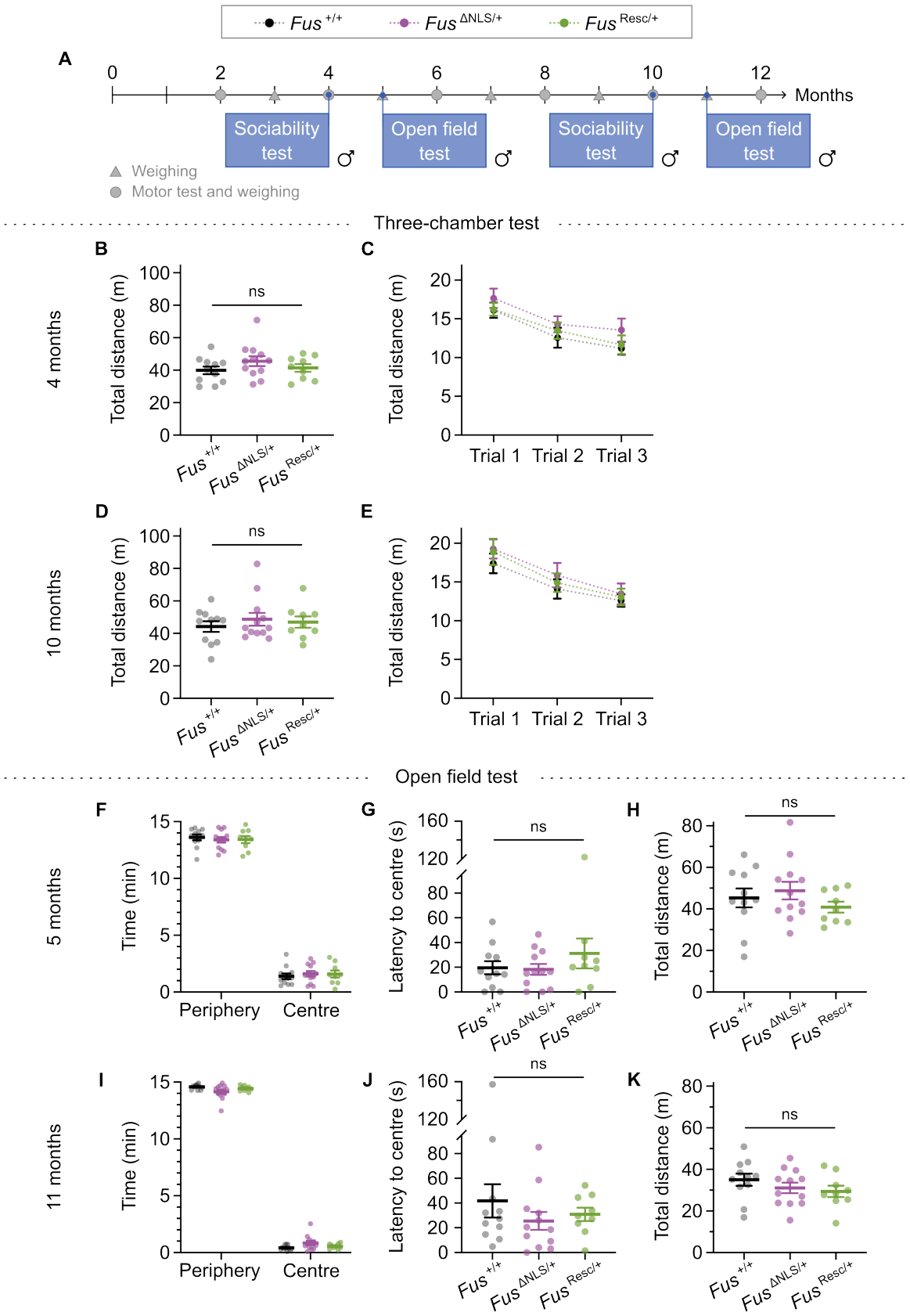
Supplementary data

Gene	Forward	Reverse
Wild-type *Vgat*	CTT CGT CAT CGG CGG CAT CTG	CAG GGC GAT GTG GAA TAG AAA
Mutant *Vgat*	CTT CGT CAT CGG CGG CAT CTG	CCA AAA GAC GGC AAT ATG GT
Wild-type Ai14	AAG GGA GCT GCA GTG GAG TA	CCG AAA ATC TGT GGG AAG TC
Mutant Ai14	CTG TTC CTG TAC GGC ATG G	GGC ATT AAA GCA GCG TAT CC
Fus$^{\Delta NLS}$	GAT TTG AAG TGG GTA GAT AGT GCA GG	CCT TTC CAC ACT TTA GTT TAG TCA CAG
Fus^{exon15}	GCA GAT ACT GAG GAG AGA GAA CTG G	CCA CTG TTA TCT ACA CAT GAT CAC CC

Supplementary Table 1: Oligonucleotides used for the genotyping.

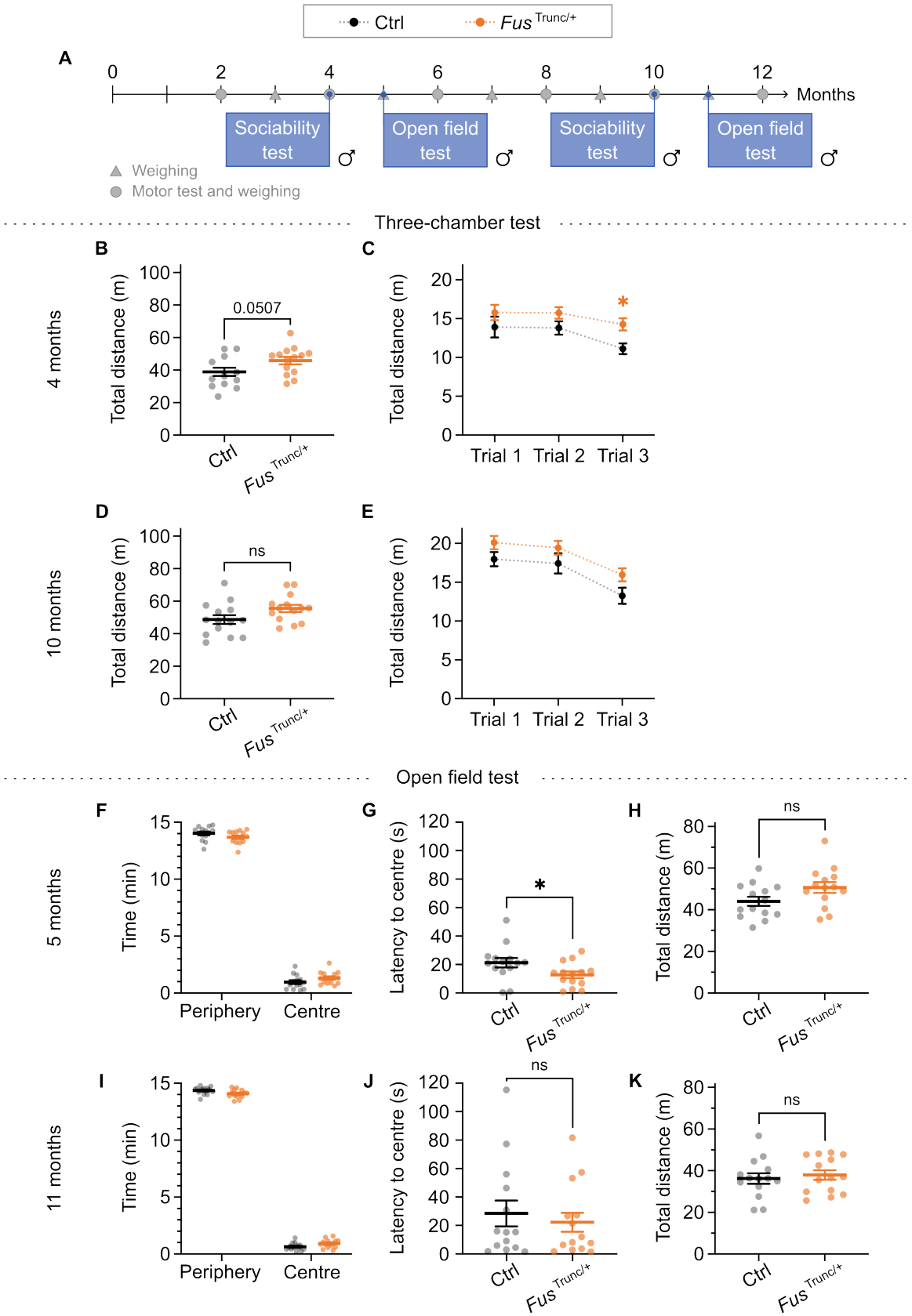


Supplementary Figure 1: Additional data for the four-limb inverted grid test. Results are expressed as mean ± SEM. (B, C) n = 11 *Fus*$^{+/+}$ (black), 12 *Fus*$^{\Delta NLS/+}$ (purple) and 8-9 *Fus*$^{Resc/+}$ (green) for both females (left panels) and males (right panels). (D, E) n = 8 Ctrl (black) and 11 *Fus*^{Trunc} (orange) females (left panels), n = 14 Ctrl (black) and 14 *Fus*$^{Trunc/+}$ (orange) males (right panels). (**A**) Scheme of the experimental design. (**B**-**E**) Hanging time was monitored every two months with the four-limb inverted grid test. (B, C) Two-way ANOVA and multiple comparisons were corrected with Tukey's test: *Fus*$^{+/+}$ *vs* *Fus*$^{\Delta NLS/+}$, * $p < 0.05$ (purple); *Fus*$^{+/+}$ *vs* *Fus*$^{Resc/+}$, ns $p > 0.05$; *Fus*$^{\Delta NLS/+}$ *vs* *Fus*$^{Resc/+}$, ns $p > 0.05$. (D, E) Two-way ANOVA and multiple comparisons were corrected with Šidák's test. Comparison of genotypes: ns $p > 0.05$.



Supplementary Figure 2: FUS localisation in inhibitory neurons did not influence the exploratory behaviour of males. Results are expressed as mean ± SEM, n = 11 *Fus*$^{+/+}$ (black), 12 *Fus*$^{\Delta NLS/+}$ (purple) and 9 *Fus*$^{Resc/+}$ (green) males. (**A**) Scheme of the experimental design. The three-chamber task was used to assess sociability at 4 (B, C) and 10 (D, E)

months of age. The open field test was used to assess locomotor exploration and anxiety in a novel environment at 5 (F-H) and 11 (I-K) months of age. (**B**-**E**) Total distance travelled in the arena. Distance was assessed for 15 min (B, D) divided into three 5-minute trials (C, E). (**F**, **I**) Time spent in the periphery or centre. (**G**, **J**) Latency to first enter the central area. (**H**, **K**) Total distance travelled. (B, D) One-way ANOVA and multiple comparisons were corrected with a two-stage Benjamini, Krieger and Yekutieli false discovery rate procedure, ns $p > 0.05$. (C, E) Two-way ANOVA and multiple comparisons were corrected with Tukey's test: for all comparisons ($Fus^{+/+}$ *vs* $Fus^{\Delta NLS/+}$, $Fus^{+/+}$ *vs* $Fus^{Resc/+}$, $Fus^{\Delta NLS/+}$ *vs* $Fus^{Resc/+}$) ns $p > 0.05$. (F, I) Two-way ANOVA and multiple comparisons were corrected with Tukey's test to compare the time spent in periphery or centre between the three genotypes: for all comparisons, ns $p > 0.05$. (G, J) Kruskal-Wallis test and multiple comparisons were corrected with a two-stage Benjamini, Krieger and Yekutieli false discovery rate procedure, ns $p > 0.05$. (H, K) One-way ANOVA and multiple comparisons were corrected with Tukey's test, ns $p > 0.05$.



Supplementary Figure 3: FUS localisation in inhibitory neurons did not influence the exploratory behaviour of males. Results are expressed as mean ± SEM, n = 14 Ctrl (black) and 14 *Fus*$^{Trunc/+}$ (orange) males. (**A**) Scheme of the experimental design. The three-chamber task was used to assess sociability at 4 (B, C) and 10 (D, E) months of age. The open field

test was used to assess locomotor exploration and anxiety in a novel environment at 5 (F-H) and 11 (I-K) months of age. (**B**-**E**) Total distance travelled in the arena. Distance was assessed for 15 min (B, D) divided into three 5-minute trials (C, E). (**F**, **I**) Time spent in the periphery or centre. (**G**, **J**) Latency to first enter the central area. (**H**, **K**) Total distance travelled. (B, D) Unpaired t-test, ns $p > 0.05$. (C, E) Two-way ANOVA and multiple comparisons were corrected with Šidák's test, * $p < 0.05$. (F, I) Two-way ANOVA and multiple comparisons were corrected with Šidák's test to compare the time spent in periphery or centre between the two genotypes: for all comparisons, ns $p > 0.05$. (G, H, K) Unpaired t-test, * $p < 0.05$. (J) Mann-Whitney test, ns $p > 0.05$.

Supplementary data

1. Social phenotyping of *Fus*$^{Resc/+}$ and *Fus*$^{Trunc/+}$ mice

Context

The increased sociability of 10-month-old *Fus*$^{\Delta NLS/+}$ mice was previously demonstrated using two different tests: the three-chamber task and the home cage social task, also known as the resident-intruder test. We thus decided to assess the sociability of our newly developed mouse lines using both paradigms (Fig. 1A), which differ by two principal factors: the environment and the duration of the test. In the first case, social preference is evaluated in a novel environment over a 15-minute period, comprising three 5-minute trials. In the second case, sociability is assessed in a known environment over a 5-minute period. The results obtained with the three-chamber task are detailed in Publication 1 (pages 122 and 129). In this section, I will present the results obtained with the home cage social task. This includes data that, at first glance, appear to challenge the notion of increased sociability in our mouse lines. I will discuss the potential sources of discrepancies between the two social tests and show that they raised intriguing questions associated with the complexity of FTD symptoms and a potential increased perseverance in mice. Rather than discrediting our previous findings, we posit that this test helped to highlight a potential novel symptom associated with FUS mislocalisation, which warrants further investigation.

Results

At 4 months of age, *Fus*$^{\Delta NLS/+}$ male mice showed an increased social interest in comparison to *Fus*$^{+/+}$ littermates during the home cage task. This was evidenced by a significantly higher total social interaction time (Fig. 10B), which was most apparent towards the end of the recording (Fig. 10C). In these two graphs, there was no significant differences between *Fus*$^{Resc/+}$ and *Fus*$^{\Delta NLS/+}$ males. Moreover, *Fus*$^{Resc/+}$ mice demonstrated longer social interaction times than *Fus*$^{+/+}$ mice, but the difference was not significant. This indicates that rescuing FUS nuclear localisation in inhibitory neurons only is not sufficient to completely rescue the sociability levels of young adult mice, which is in line with the results we obtained with the three-chamber task (Publication 1, Fig. 4B and 4C).

Surprisingly, at 10 months of age, the total (Fig. 10D) and detailed (Fig. 10E) interaction times measured during the home cage task were not significantly different for *Fus*$^{\Delta NLS/+}$, *Fus*$^{Resc/+}$ and *Fus*$^{+/+}$ mice. When comparing the total interaction times at 4 and 10 months of age for each mouse line, we observed a significant 1.5-time increase for *Fus*$^{+/+}$ mice, which was not the case for *Fus*$^{\Delta NLS/+}$ (1.1-time increase, not significant) or *Fus*$^{Resc/+}$ mice (1.1-time decrease, not significant). These results differ from what we observed with the three-chamber task (Publication 1, Fig. 4D and 4E). Indeed, we previously showed that 10-month-old *Fus*$^{\Delta NLS/+}$ male mice exhibited an increased social interest, which was

almost completely rescued to *Fus*$^{+/+}$ mice levels in *Fus*$^{Resc/+}$ mice, and that the sociability of *Fus*$^{\Delta NLS/+}$ males increased with age. These two observations are apparently not confirmed by the home cage task.

Regarding *Fus*$^{Trunc/+}$ male mice, we found that their total social interaction times were significantly higher than those of Ctrl mice at both 4 (Fig. 10F) and 10 (Fig. 10H) months of age. This was due to an overall increase in interaction (Fig. 10G and 10I), although the multiple comparisons did not reveal significant difference in the interaction times analysed in one-minute intervals. This indicates that inducing FUS cytoplasmic delocalisation in inhibitory neurons only is sufficient to cause social impairments in young and old adult mice, which is in line with the results we obtained with the three-chamber task (Publication 1, Fig. 8).

Discussion

Using the home cage task, we showed that *Fus*$^{\Delta NLS/+}$, *Fus*$^{Resc/+}$ and *Fus*$^{Trunc/+}$ male mice exhibited increased social interest at 4 months of age when compared to control mice (Fig. 10B and 10F), which is in line with the results previously reported using the three-chamber task. At 10 months of age, the level of sociability exhibited by *Fus*$^{Resc/+}$ was comparable to that of control mice (Fig. 10D), whereas the social interest displayed by *Fus*$^{Trunc/+}$ mice remained elevated in comparison to control mice (Fig. 10H). These findings are also in accordance with the results obtained using the three-chamber task. However, the home cage task revealed that 10-month-old *Fus*$^{\Delta NLS/+}$ mice did not exhibit increased sociability when compared to control mice, which is inconsistent with our three-chamber task results and previously published results (Scekic-Zahirovic et al., 2021). In addition, the three-chamber task revealed an age-dependent increase in sociability specifically in *Fus*$^{\Delta NLS/+}$ mice, and this effect was not observed with the home cage task.

Several factors may explain these discrepancies. We cannot exclude the possibility that 10-month-old *Fus*$^{\Delta NLS/+}$ mice were not adequately engaged in the home cage social task. However, it should be noted that all these mice also completed the three-chamber task on the day prior to or the day following the home cage task. Yet, with the three-chamber task, they exhibited increased social interest when compared to 10-month-old *Fus*$^{+/+}$ littermates or to their own level of interaction at 4 months. It is also noteworthy that, for unknown reason, *Fus*$^{+/+}$ mice exhibited higher interaction times at 10 months than at 4 months of age during the home cage task (Fig. 10D and 10H) but not during the three-chamber test. This was not expected, as the social interest was reported to remain constant between young 2-month-old and middle age 11-month-old wild-type C57BL/6J male mice (Shoji and Miyakawa, 2019). Thereby, this could be the reason we cannot observe an increased sociability in *Fus*$^{\Delta NLS/+}$ mice with the home cage task.

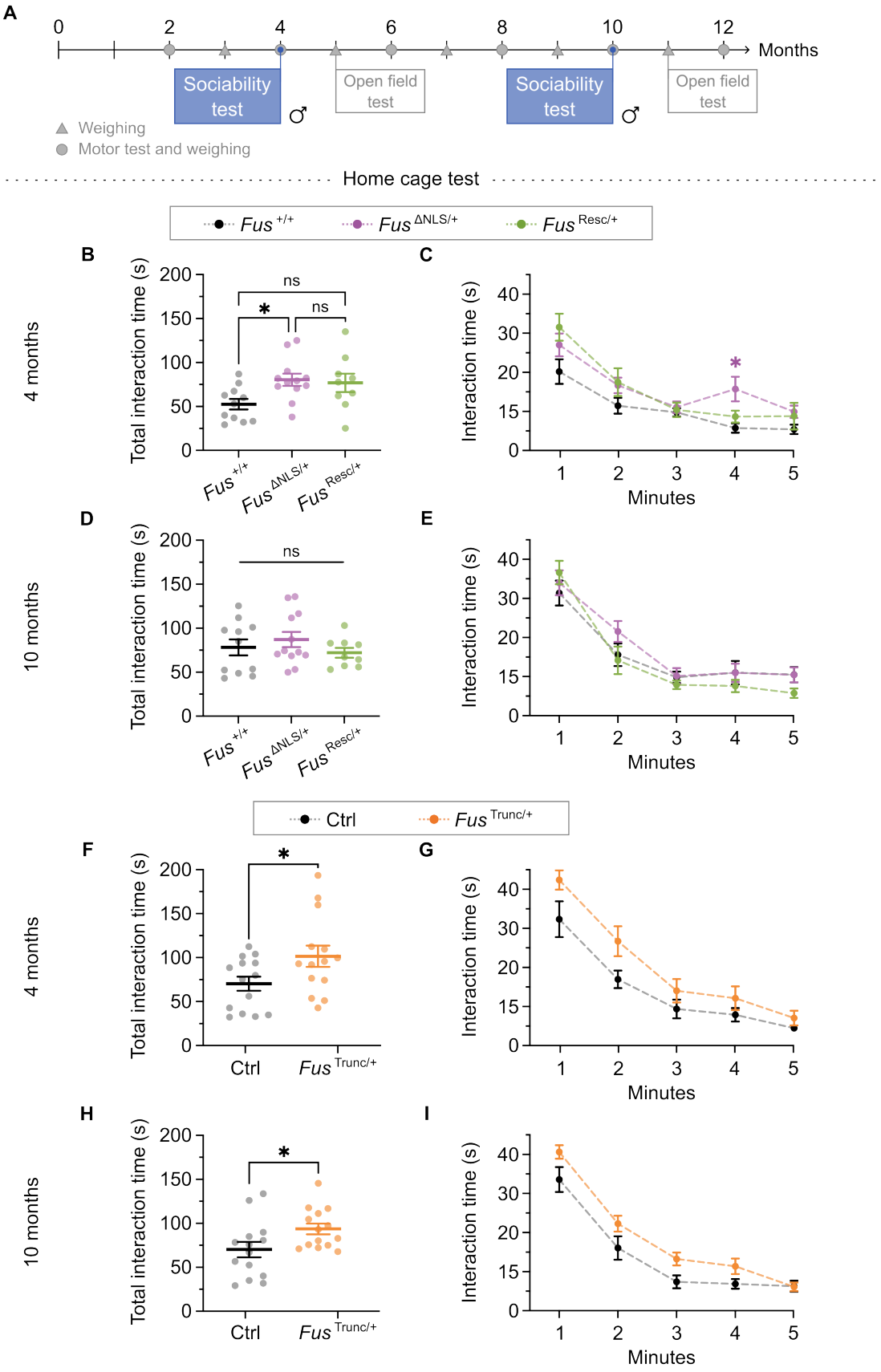


Figure 10: Social phenotyping using the home cage social task. Results are expressed as mean ± SEM. (B-E) n = 11 *Fus*$^{+/+}$ (black), 12 *Fus*$^{\Delta NLS/+}$ (purple) and 9 *Fus*^{Resc} (green) males. (F-I) n = 14 Ctrl (black) and 14 *Fus*^{Trunc} (orange) males. (**A**) Scheme of the experimental

design. Sociability was assessed at 4 (B, C, F, G) and 10 (D, E, H, I) months of age. (**B**, **D**, **F**, **H**) The total time spent contacting a mouse was measured over a 5-minute period. (**C**, **E**, **G**, **I**) The time spent contacting a mouse was measured in 1-minute intervals. (B, D) One-way or (C, E) Two-way ANOVAs and multiple comparisons were corrected with Tukey's test, * $p < 0.05$. (F, H) Unpaired t-test, * $p < 0.05$. (G, I) Two-way ANOVAs and multiple comparisons were corrected with Šidák's test, * $p < 0.05$.

Influence of the environment on sociability: notion of active and passive behaviour

The notion of "sociability" encompasses a wide range of behaviours, including any form of communication and interaction between conspecifics. In our case, we focused our analysis on one main variable: the interaction time. Although it is an efficient and rather easy parameter to measure, it highly limits our understanding of the social behaviours exhibited by mice. Indeed, mice are known to socially and emotionally interact using auditory cues (vocalisation of different frequencies), olfactory cues (body odour, pheromones and urinary scent-marking) and visual cues (facial expression, tail rattling, grooming, freezing, lordosis and paw scratching), in addition to interactive cues (Jabarin et al., 2022). Among the interactive cues, we can further differentiate what could be viewed as active behaviour, which requires the tested mouse to orient its nose towards its conspecific and touch it (e.g., nose-to-nose contact, nose-to-tail contact, and so on), and passive behaviour during which the nose of the tested mouse does not touch its conspecific (e.g., side by side walking, side by side sitting, and so on).

In the three-chamber task, the social stimulus (stranger mouse) is placed in an openwork cylindrical cage, which prevents it to freely move in the arena and thus restricts the range of social behaviours which can occur. This task has the advantage of letting the tested mouse in sole control of the seeking and investigation of the stranger mouse. One limitation is the exposure of the tested mouse to a novel environment, which can create a confounding effect of novelty-induced behavioural change. However, our results and previous results from the lab demonstrated that the exploratory locomotion in a novel environment is not increased in *Fus*$^{\Delta NLS/+}$ male mice compared to *Fus*$^{+/+}$ mice when evaluated with the open field test (Publication 1) (Scekic-Zahirovic et al., 2021). Hence, the increased sociability observed in 10-month-old *Fus*$^{\Delta NLS/+}$ mice using the three-chamber task is unlikely to be due to a novelty-induced behavioural change.

The use of a home cage condition is an interesting alternative to assess sociability in a more naturalistic setting. However, in this task, both the tested mice (residents) and social stimuli (intruders) are free to move and can initiate and stop contacts. Hence, the complexity of the exhibited social behaviours is increased, and includes several approaching and moving away situations. Yet, the analysis we performed was more restrictive for this task than for the three-chamber task. With the home cage social test, we defined the interaction time exclusively as the time during which the nose of the

resident mouse was in direct contact with the body of the intruder mouse. As a consequence, we took into account active, but not passive, behaviours. With the three-chamber task, we defined the interaction time as the time during which the nose of the tested mouse was found within 2.5cm of the openwork cylindrical cage. It means that our analysis encompassed several possible situations, including, but not limited to, direct sniffing of the body of the stranger mouse (active behaviour), sniffing of the olfactory cues let on the cage by the stranger mouse, and sitting next to the stranger mouse (passive behaviour). In young 1-month-old C57BL/6J wild-type male mice, it was reported that the majority of social behaviours exhibited during a home cage task were passive (Fairless et al., 2013). In 2-month-old mice, the proportion of passive behaviour decreased but still represented half of the social behaviours. One could imagine that, at 10 months of age, the increased sociability in *Fus*$^{\Delta NLS/+}$ mice measured with the three-chamber task is driven by passive social behaviours. To test this hypothesis, it would be interesting to reanalyse the data obtained with the home cage social task and to include passive behaviours. Alternatively, we could manually measure interactions in the three-chamber task to be able to differentiate active and passive behaviours.

Influence of the duration of the test on sociability: notion of perseverance

With the protocols we used, social interactions were assessed during 15 minutes with the three-chamber task and during 5 minutes only with the home cage task. Thereby it is possible that the duration of the home cage social test was not long enough to observe an increased sociability in 10-month-old *Fus*$^{\Delta NLS/+}$ mice. This hypothesis is supported by the results we obtained with the three-chamber social test. Indeed, the biggest differences between *Fus*$^{\Delta NLS/+}$ and *Fus*$^{+/+}$ mice were observed during the last trial at both 4 and 10 months of age. In addition, the interaction times of 4-month-old *Fus*$^{\Delta NLS/+}$ and *Fus*$^{+/+}$ mice were identical in the first trial, confirming the idea that more than 5 minutes may be required to observe social impairments in *Fus*$^{\Delta NLS/+}$ mice. The same phenomena were observed in *Fus*$^{Trunc/+}$ mice at both 4 and 10 months of age. To test this hypothesis, we would simply need to conduct the home cage social task over a 15-minute period instead of a 5-minute period. However, it should be noted that at 10 months of age, *Fus*$^{\Delta NLS/+}$ mice exhibited a significantly higher interaction time than *Fus*$^{+/+}$ mice during the first trial, what would suggest that a 5-minute test is enough to observe an increased sociability. In any case, the discrepancy between the two social paradigms raised interesting questions concerning the complexity of symptoms exhibited by our mouse lines. It seems that *Fus*$^{\Delta NLS/+}$ and *Fus*$^{Trunc/+}$ mice have shown increased perseverance in comparison to control mice, which is one of the six criteria for the diagnosis of FTD with a behavioural variant. Thereby, this discrepancy helped to highlight a potential novel symptom associated with FUS mislocalisation in mice. This idea will be detailed in the Discussion (page 204).

Conclusion

In all, the use of the home cage social task at 4 months of age allowed us to corroborate the results obtained with the three-chamber social task. At 10 months of age, *Fus*$^{Trunc/+}$ male mice also exhibited consistent results using both paradigms, which reinforces the notion that FUS accumulation in inhibitory neurons is sufficient to cause social impairments. Conversely, at 10 months of age, *Fus*$^{\Delta NLS/+}$ male mice exhibited contradictory results in the two tasks. Further investigation will be required to understand the cause of this discrepancy, which could be due to an exclusion of passive social behaviour in our analysis and/or which could link increased sociability with increased perseverance in mice with FUS mislocalisation.

Materials and methods

At 4 and 10 months of age, male mice were housed individually for three consecutive days. On one of the final two days, they performed the home cage social task.

Home cage social task: The home cage social task -or resident-intruder test- was used to evaluate the sociability of mice when encountering an intruder in a familiar environment. The home cage (33 x 16cm) of the tested mouse (referred to as 'resident mouse') contained soiled wood chips. The lid of the cage, the nest and environmental enrichment were removed, and the resident mouse was allowed to acclimate to this new setting for 5 minutes. An intruder was then placed in the cage and a 5-minute video was recorded to observe their interactions. The contacting time was defined as the time during which the nose of the resident mouse was in direct contact with the body of the intruder mouse. This was measured visually using a stopwatch for each minute and then added up for the total duration of the test. Aggressive interactions, if occurring, were excluded from the analysis. The intruders were wild-type males of the same age and genetic background as the tested mice. They were housed in groups throughout their lives and had never encountered the tested mice before.

Author contributions

Sociability tests were conducted by F.L. Data from the home cage social task were analysed by Stéphane Dieterlé, and interpreted by F.L.

2. Metabolic phenotyping of *Fus*$^{Resc/+}$ and *Fus*$^{Trunc/+}$ mice

Context

Growing evidence shows that ALS is associated with alterations in energy metabolism, including significant weight loss, increased energy expenditure and augmented use of lipid nutrients at the expense of carbohydrates (Guillot et al., 2021). Weight loss was observed in one to two-thirds of ALS patients (Janse van Mantgem et al., 2020; Marin et al., 2016; Wei et al., 2019, 2021), preceded the onset of motor symptoms (Peter et al., 2017), and was associated with poorer prognostic (Janse van Mantgem et al., 2020; Marin et al., 2016; Shimizu et al., 2019; Wei et al., 2019, 2021). In addition, the hypothalamus, which is the brain region controlling energy homeostasis, was found to be atrophied in ALS patients (Gorges et al., 2017), and exhibited altered connectivity in patients and mice (Bayer et al., 2021). The neuronal mechanisms underlying these hypothalamic alterations are now being investigated by our laboratory and others. Conversely, the metabolic profile of FTD patients was less extensively studied. However, distinct changes in eating behaviour were identified in FTD patients with a behavioural variant (mostly exhibiting hyperphagia) and FTD patients with a semantic primary progressive aphasia (mostly exhibiting impaired preferences in food) (Ahmed et al., 2016). Surprisingly, an atrophy of the hypothalamus has been observed in patients with a behavioural variant only. In FTD, it is likely that a combination of factors, including behavioural and cognitive deficits, changes in the reward system, and alterations of the neuroendocrine systems, contribute to these phenotypes.

Our laboratory recently showed that *Sod1*^{G86R} mice exhibit metabolic alterations (Bolborea et al., 2023), and is now investigating the metabolic profile of *Fus*$^{\Delta NLS/+}$ mice. To ascertain whether *Vgat*-expressing inhibitory neurons are implicated in this phenotype, we sought to determine whether the development of metabolic impairments was rescued in *Fus*$^{Resc/+}$ mice and/or induced in *Fus*$^{Trunc/+}$ mice. To conduct this pilot study, we included mice which were involved in our longitudinal study (Publication 1). The motor and social tests required the mice to remain group-housed throughout their lifespan, whereas the metabolic monitoring required their isolation. Therefore, the mice were isolated after the last motor test, at 12 months of age. A metabolic indirect calorimetry system was then used to monitor various physiological parameters over a 72-hour period. Additionally, we studied a smaller cohort of males which were isolated throughout their life, as is typically done for metabolic studies. These two cohorts will hereafter be referred to as 'group-housed' and 'isolated', respectively.

Results

Inducing FUS cytoplasmic delocalisation in every cell type causes metabolic alterations in group-housed male mice

Group-housed 12-month-old *Fus*$^{\Delta NLS/+}$ male mice showed a significant decrease in food consumption when compared to *Fus*$^{+/+}$ mice (Fig. 11B and 11D). This was driven by a lack of food intake during the nights (Fig. 11C and 11D, dark). Because mice are nocturnal animals, they are typically active during the night (or dark phase) and consume most of their food at that time. Energy expenditure was estimated based on the volume of oxygen consumed and the volume of carbon dioxide produced. Despite a potentially reduced energy intake caused by the lack of food intake, *Fus*$^{\Delta NLS/+}$ exhibited similar energy expenditure as *Fus*$^{+/+}$ mice (Fig. 11E-11G). Therefore, this resulted in a decreased energy balance in *Fus*$^{\Delta NLS/+}$ mice compared to *Fus*$^{+/+}$ mice (Fig. 11H and 11I). We then assessed the respiratory exchange ratio, which represents the source of nutrient mobilisation. During the dark phase, *Fus*$^{+/+}$ mice exhibited a ratio equals to 1 (Fig. 11J and 11K), which corresponds to the oxidation of carbohydrate. In *Fus*$^{\Delta NLS/+}$ mice, this ratio was found to be decreased at night and reached a level corresponding to the use of proteins.

For all the aforementioned physiological parameters, *Fus*$^{Resc/+}$ mice exhibited alterations when compared to *Fus*$^{+/+}$ mice, and no significant differences when compared to *Fus*$^{\Delta NLS/+}$ mice. Therefore, rescuing FUS nuclear localisation in inhibitory neuron did not prevent the development of metabolic alterations. Regarding *Fus*$^{Trunc/+}$ male mice, no alterations were observed, as all the physiological parameters were similar in *Fus*$^{Trunc/+}$ and Ctrl mice (data not shown). Inducing FUS cytoplasmic delocalisation in inhibitory neurons is therefore not sufficient to cause metabolic dysfunctions.

Collectively, these results suggest that 12-month-old *Fus*$^{\Delta NLS/+}$ male mice recapitulate several metabolic alterations which are characteristic of ALS. However, *Vgat*-expressing inhibitory neurons do not seem to be involved in this phenotype.

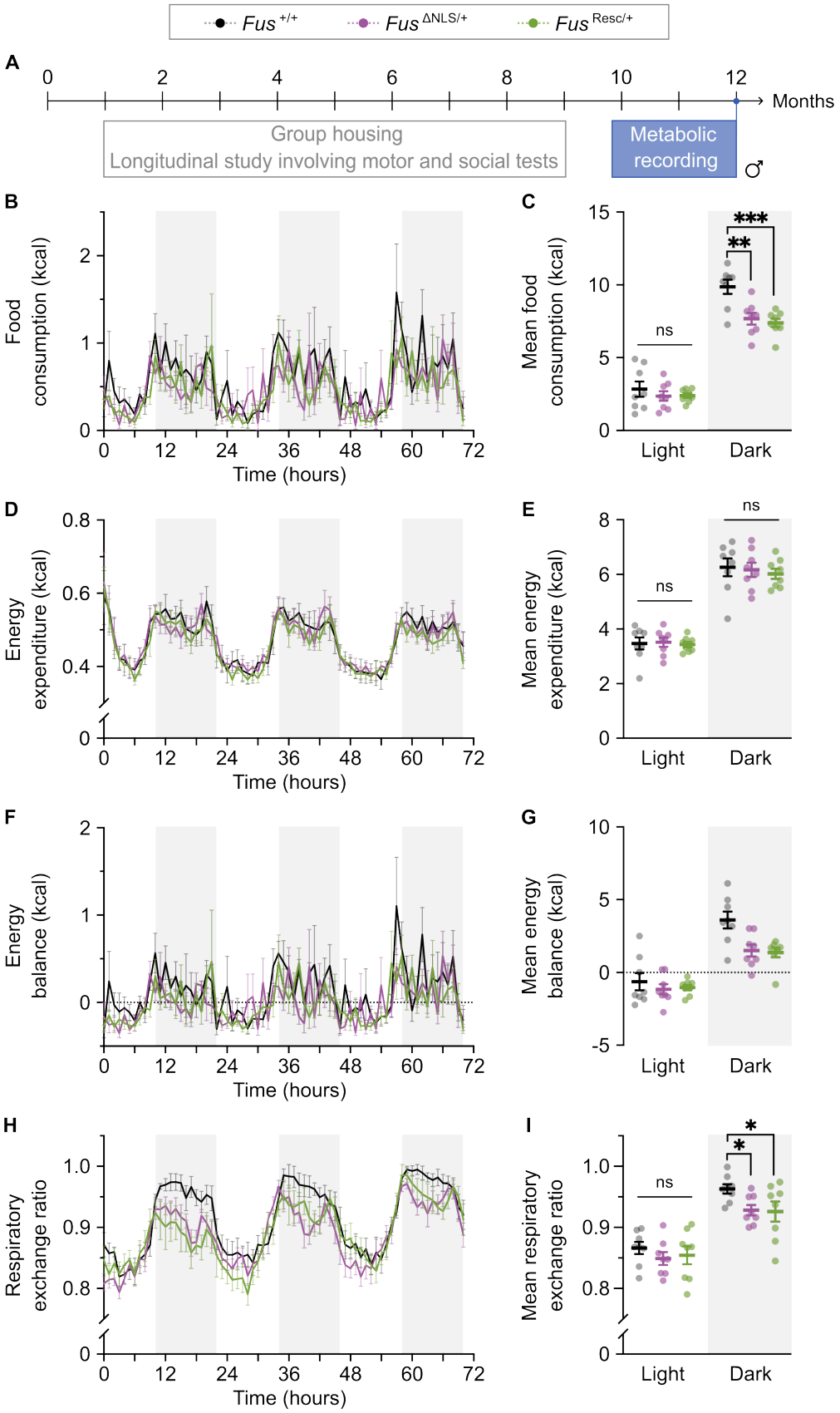


Figure 11: Metabolic alterations in group-housed *Fus*$^{\Delta NLS/+}$ and *Fus*$^{Resc/+}$ mice. Results are expressed as mean ± SEM, n = 8 *Fus*$^{+/+}$ (black), 8 *Fus*$^{\Delta NLS/+}$ (purple) and 8 *Fus*$^{Resc/+}$ (green) males. (**A**) Scheme of the experimental design. (**B**, **C**) Hourly (B) and mean (C) food intake

was monitored by weighing the pellets. (**D**, **E**) Hourly (D) and mean (E) energy expenditure was estimated based on gas exchanges. (**F**, **G**) Hourly (F) and mean (G) energy balance was calculated based on food consumption and energy expenditure. (**H**, **I**) Hourly (H) and mean (I) respiratory exchange ratio. (C, E) Generalised linear model to investigate the genotype and weight effects. Only genotype effect is represented on the graphs (* $p < 0.05$), as weight effect was not significant. (I) One-way ANOVA to investigate the genotype effect, * $p < 0.05$.

Inducing FUS cytoplasmic delocalisation in every cell type may not cause metabolic alterations in isolated male mice

Energy metabolism is usually assessed in animals isolated throughout their entire lifespan. We thus decided to conduct a pilot study with *Fus*$^{\Delta NLS/+}$, *Fus*$^{Resc/+}$ and *Fus*$^{+/+}$ male mice, which were isolated from 3 months of age and analysed at 4 and 12 months of age. To our surprise, no significant differences were observed when the metabolic profiles of *Fus*$^{\Delta NLS/+}$ or *Fus*$^{Resc/+}$ mice were compared to the metabolic profile of *Fus*$^{+/+}$ mice at both 4 (data not shown) and 12 (Fig. 12) months of age. These results suggest that isolated *Fus*$^{\Delta NLS/+}$ males may not exhibit metabolic alterations, although confirmation with a larger cohort is required.

Discussion

With this pilot study, we demonstrated that group-housed 12-month-old *Fus*$^{\Delta NLS/+}$ male mice exhibit alterations which are reminiscent of metabolic defects seen in ALS patients (Fig. 11). These mice showed a decreased energy balance, which was due to a significant reduction in food intake while the energy expenditure remained as high as in *Fus*$^{+/+}$ mice. In addition, *Fus*$^{\Delta NLS/+}$ mice exhibited a decreased respiratory exchange ratio. These alterations were observed in absence of major body weight loss (Publication 1, Fig. 3C). Conversely, isolated 12-month-old *Fus*$^{\Delta NLS/+}$ male mice (Fig. 12) and group-housed 12-month-old *Fus*$^{\Delta NLS/+}$ female mice (data not shown) exhibited an unaltered metabolic profile. However, the number of mice included in these last two cohorts was low (between 3 and 5 mice per genotype), so further confirmation with larger cohorts is required to draw a definite conclusion.

The hypothalamus contains a particularly high diversity of neurons. These can co-release neurotransmitters and neuropeptides, and can engage in task-dependent neurotransmitter switches, thereby increasing the complexity of the neuronal circuits and their contribution to the control of multiple vital behaviours. To date, neurons expressing melanin-concentrating hormone (MCH), orexin or oxytocin were proposed to be involved in the metabolic defects observed in ALS, as their density is decreased in post-mortem tissues (Bolborea et al., 2023; Gabery et al., 2021). In *Fus*$^{\Delta NLS/+}$ mice, a decreased density of MCH neurons was recently reported in the lateral hypothalamus (Bolborea et al., 2023), while preliminary data from our laboratory suggested a preservation of orexin neurons. Other hypothalamic cell populations still need to be investigated.

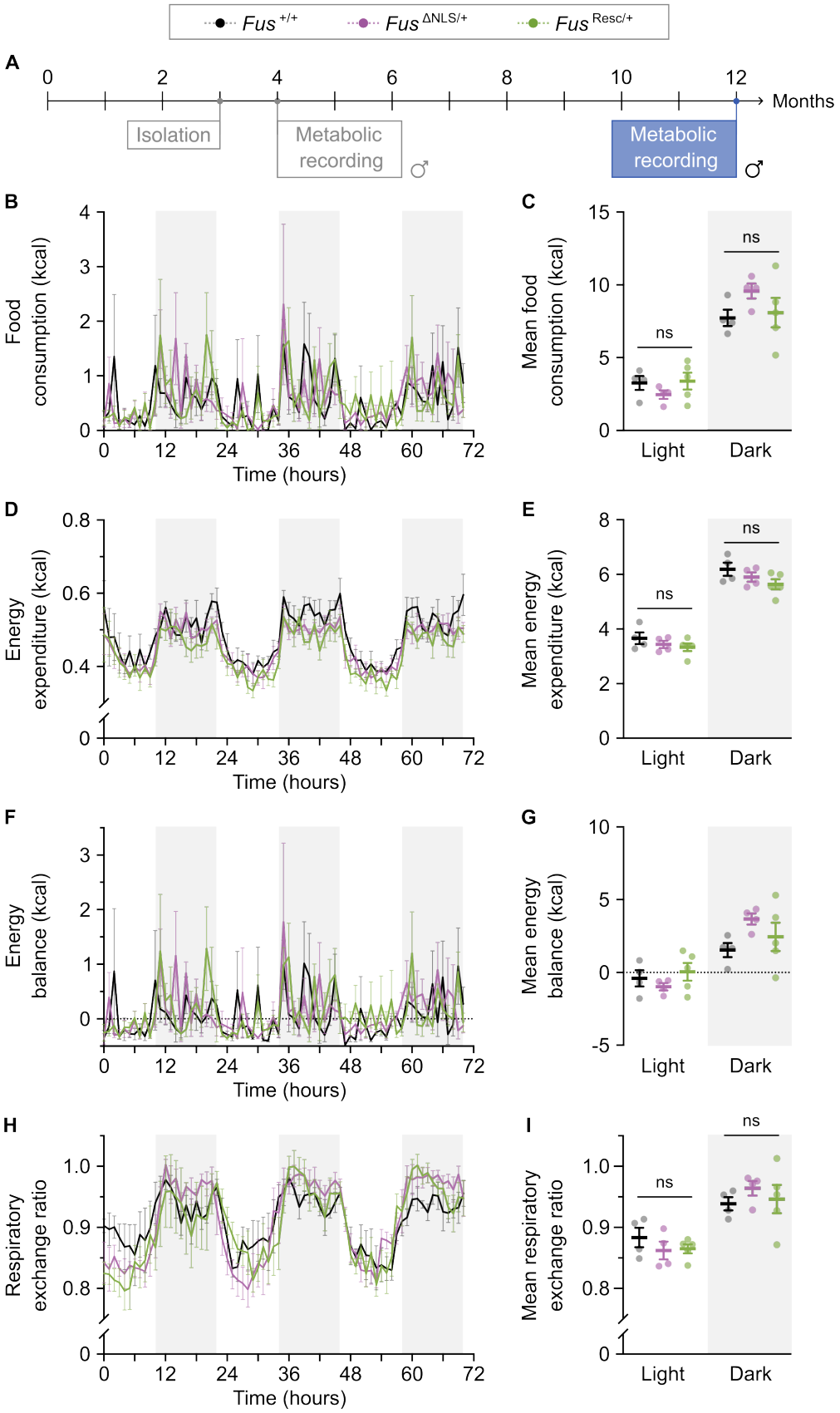


Figure 12: Absence of metabolic alterations in isolated *Fus*$^{\Delta NLS/+}$ male mice. Preliminary results are expressed as mean ± SEM, n = 4 *Fus*$^{+/+}$ (black), 4 *Fus*$^{\Delta NLS/+}$ (purple) and 5 *Fus*$^{Resc/+}$ (green) males. (**A**) Scheme of the experimental design. (**B**, **C**) Hourly (B) and mean (C) food

intake was monitored by weighing the pellets. (**D**, **E**) Hourly (D) and mean (E) energy expenditure was estimated based on gas exchanges. (**F**, **G**) Hourly (F) and mean (G) energy balance was calculated based on food consumption and energy expenditure. (**H**, **I**) Hourly (H) and mean (I) respiratory exchange ratio. (C, E) Generalised linear model to investigate the genotype and weight effects. Only genotype effect is represented on the graphs (ns $p > 0.05$). (I) One-way ANOVA to investigate the genotype effect, ns $p > 0.05$.

Could a loss of MCH neurons underly the metabolic defects in *Fus*$^{\Delta NLS/+}$ mice?

MCH is a neuropeptide involved in the control of energy homeostasis. It stimulates food intake, reduces energy expenditure and locomotor activity, and induces weight gain and peripheral lipid storage (Al-Massadi et al., 2021). Conversely, the loss or inhibition of MCH neurons has been associated with weight loss, decreased food intake and increased energy expenditure in lean, obese and aged mice. Hence, the decreased food consumption in our group-housed 12-month-old *Fus*$^{\Delta NLS/+}$ males (Fig. 11) could be explained by a loss of MCH neurons. However, weight loss and increased energy expenditure were not observed in our cohort.

Our results demonstrate that the altered metabolic profile in *Fus*$^{\Delta NLS/+}$ male mice may not be dependent on *Vgat*-expressing inhibitory neurons. Indeed, alterations were not prevented when we restored the nuclear localisation of FUS in inhibitory neurons (Fig. 11), and they were not induced when we delocalised FUS exclusively in the cytoplasm of inhibitory neurons (data not shown). MCH neurons were found to exert an inhibitory influence on the neurons they contact (Gao and van den Pol, 2001; Rao et al., 2008), and to produce the GABA-synthetising enzyme GAD67 (Elias et al., 2008). Around 6% of their prolongments were reported to express VGAT (Del Cid-Pellitero and Jones, 2012), and 5% to form active gephyrin-positive inhibitory synapses (Del Cid-Pellitero and Jones, 2012). However, Blanco-Centurion *et al*. crossed the non-congenic version of the *Vgat*^{Cre} mouse line we are using with the R26R-EYFP reporter mouse line, and observed an absence of Cre recombinase activity in the MCH neurons of the posterior hypothalamus (Blanco-Centurion et al., 2018). This is in line with other studies showing that, in the lateral hypothalamus, *Vgat*-expressing inhibitory neurons do not contain MCH peptides (Jennings et al., 2015; Venner et al., 2016). In addition, the use of single-cell quantitative polymerase chain reaction to quantify gene expression demonstrated that MCH neurons express the machinery for GABA synthesis in the absence of a vesicular GABA release pathway (Mickelsen et al., 2017). Based on these data, it has been proposed that MCH neurons produce GABA for their local use only. It is important to mention that optogenetic stimulation of MCH terminals was reported to evoke $GABA_A$-mediated inhibitory postsynaptic currents (Jego et al., 2013). However, the particularly high stimulation may have caused this artifact. In all, the absence of *Vgat* expression in MCH neurons could explain why the decreased food consumption was not rescued upon the nuclear relocalisation of FUS in *Fus*$^{Resc/+}$ mice, and why this was not induced upon the cytoplasmic delocalisation of FUS in *Fus*$^{Trunc/+}$ mice.

Are hypothalamic *Vgat*-expressing neurons altered in ALS?

VGAT, GAD65 and GAD67 are all markers of GABAergic neurons, but in the hypothalamus, they are not always co-expressed by neurons, as it was previously illustrated with MCH neurons. For instance, it was demonstrated that only 50% of GAD65-positive neurons contain VGAT, while 20% of VGAT-positive neurons express GAD65 (Kosse et al., 2017). It is important to differentiate *GAD*-expressing GABAergic neurons (i.e., GABA-producing neurons) and *VGAT*-expressing GABAergic neurons (i.e., GABA-releasing neurons). It also means that, by using a $Vgat^{Cre}$ mouse line, we did not target all GABA-producing neurons in the hypothalamus. However, VGAT is considered as an essential component for GABA synaptic transmission, so it is possible that we targeted all GABA-releasing neurons. If this is the case, then we could have expected an altered food intake phenotype in $Fus^{Resc/+}$ and $Fus^{Trunc/+}$ mice. Indeed, the chemogenetic and optogenetic activations of *Vgat*-expressing neurons in the lateral hypothalamus were found to promote wake (Venner et al., 2016), as well as appetitive and consummatory behaviours (Jennings et al., 2015), whereas their inhibition caused the opposite phenotypes. The fact that the food intake levels of $Fus^{Resc/+}$ and $Fus^{Trunc/+}$ mice were similar to those of $Fus^{\Delta NLS/+}$ and control mice, respectively, suggests that the subcellular localisation of FUS in these neurons does not massively alter their function, or that compensatory mechanisms took place.

Further investigations will be needed to say whether hypothalamic *Vgat*-expressing neurons are altered or not in ALS. Firstly, we did not verify the subcellular localisation of FUS in the hypothalamus of our mouse lines. The use of the non-congenic version of the $Vgat^{Cre}$ mouse line by Blanco-Centurion *et al*. suggests that Cre recombinase is effectively active in the lateral hypothalamus. However, the efficiency of *Fus* truncation and subsequent cytoplasmic delocalisation would have to be confirmed. Secondly, if hypothalamic *Vgat*-expressing neurons were to be altered in ALS, it would be more complex than just a global deficit of this cell population. Indeed, inhibiting these neurons in mice attenuated weight gain and food consumption (Jennings et al., 2015), increased food aversion (Jennings et al., 2015) and promoted sleep (Venner et al., 2016). If the weight and food intake phenotypes are in line with the metabolic alterations observed in ALS patients, the promotion of sleep is not, as growing evidence shows that sleep is altered in sporadic and familial cases of ALS (Lo Coco et al., 2011; Sun et al., 2020). Finally, in the hypothalamus, several neuronal populations appear to have redundant functions, so the deficits reported in ALS could be -partially or entirely- explained by the dysfunction of other neurons.

Do housing conditions affect to metabolic profile of $Fus^{\Delta NLS/+}$ mice?

Our pilot study showed that the metabolic profiles of isolated $Fus^{\Delta NLS/+}$ and $Fus^{+/+}$ male mice were similar at both 4 and 12 months of age, while group-housed 12-month-old $Fus^{\Delta NLS/+}$ males clearly exhibited metabolic alterations. Two factors could explain this discrepancy. Firstly, there were half as many animals in the isolated cohort as in the

group-housed cohort. As a consequence, the number of mice included in the isolated cohort was low (4 *Fus*$^{\Delta NLS/+}$ and 4 *Fus*$^{+/+}$ mice). It is probable that the sample size was too small and compromised the observation of genotype effects due to large individual variations. Importantly, this pilot study should not preclude the metabolic phenotyping of isolated *Fus*$^{\Delta NLS/+}$ mice, as our preliminary results may not be representative of what would be observed in a bigger cohort.

Secondly, the housing conditions could have affected the metabolic profile of our mouse lines. Isolating mice can influence their body composition and food consumption, among other things. The effects appear to be dependent on the age of the mice and/or the duration of the isolation. It was shown that wild-type C57BL/6J male mice isolated from 4 to 10 months exhibited a comparable body weight gain as group-housed mice, while their food intake was significantly increased (Benfato et al., 2022). Regarding the body weight gain, the same observation was made for young male mice (aged between 1 and 3 months) after two (Yamada et al., 2015) or eight (Challa et al., 2023; Sun et al., 2014) weeks of isolation. However, in young isolated mice, food intake was found to be either significantly increased (Sakakibara et al., 2012; Yamada et al., 2015) or decreased (Sun et al., 2014) when compared to group-housed mice. In old male mice (aged between 20 and 23 months), two weeks of isolation resulted in a significant body weight loss, with no effect on food intake (Yamada et al., 2015). Conversely, housing mice in social groups can introduce significant bias and variability in a number of physiological parameters, including those linked to energy balance. For instance, group-housed mice can huddle to reduce their thermoregulatory requirements. It was shown that the housing of wild-type C57BL/6J male mice at thermoneutrality (29°C) for three months changed both food intake and energy expenditure in comparison to mice housed at a standard temperature (22°C) (Small et al., 2018). To our knowledge, the impact of social hierarchy on the metabolic profile of C57BL/6J mice has yet to be investigated. One study reported comparable body weight in dominant and submissive 3-month-old male mice (Meloni et al., 2024), but it does not mean that body composition and energy balance are similar in these mice. In addition, social stress was found to induce a significant reduction in body weight in defeated mice (Furman et al., 2022; Iñiguez et al., 2014).

In our cohorts, the cumulative food intake analysis showed that *Fus*$^{\Delta NLS/+}$ mice ate more food in the isolated condition than in the group-housed condition, and the opposite effect was observed for *Fus*$^{+/+}$ mice. Hence, energy intake may be decreased in group-housed *Fus*$^{\Delta NLS/+}$ mice compared to isolated mice. This may enhance a potentially pre-existing metabolic stress in *Fus*$^{\Delta NLS/+}$ mice, thereby allowing the observation of a clearly altered metabolic profile in the group-housed condition, while it was not the case in the isolated condition.

Conclusion

The metabolic profile of *Fus*$^{\Delta NLS/+}$ mice is currently under investigation in our laboratory. The cohorts will involve a higher number of mice, which will be isolated throughout their entire lifespan. This will give us a better view of the metabolic phenotype associated to the cytoplasmic delocalisation of FUS. Our preliminary results suggest a sexual dimorphism, with metabolic alterations being specific to males. Thereby, it seems important to include both females and males in future studies to highlight possible sex differences. One may also want to conduct this study in more ideal environmental conditions. Our mice were housed at 22 ± 2°C, which constitutes a mild thermoregulatory stress and may not mimic the situation in humans, who live much closer to thermoneutral condition. A good alternative would be to house the mice at 30°C, especially when they are isolated. In any case, it seems unlikely that the metabolic phenotype of *Fus*$^{\Delta NLS/+}$ mice is linked to *Vgat*-expressing inhibitory neurons.

Materials and methods

Cohort organisation: Mice were bred and housed in the animal facility of the Faculty of Medicine of Strasbourg, under constant conditions (22 ± 2°C, 45-65% humidity) and a regular 12-hour light and dark cycle (with lights on at 7:30 am). Food and water were available *ad libitum*, with mice being given a breeding diet before weaning and a maintenance diet afterwards. In the first cohort, female and male mice were included in a longitudinal study involving motor and social tests (Publication 1). At 12 months of age, when the study ended, mice were isolated, and their metabolic activity was assessed. In the second cohort, male mice were isolated at 3 months of age and remained isolated throughout their lifespan. Their metabolic activity was assessed at 4 and 12 months of age. After their last assessment, mice were sacrificed to recover tissues. The sex and number of mice are indicated in the relevant figures.

Metabolic assessment: A metabolic indirect calorimetry system (Sable Systems International, Promethion Core) was used to non-invasively assess the physiological parameters of mice. The protocol was adapted from Bolborea et al., 2023. Prior to any recording, mice were housed in the calorimetry system for at least four days to allow them to acclimate to the environment. Recordings then lasted for four days, with the first 24 hours being discarded. Up to eight animals were recorded in parallel, balancing genotypes. Housing conditions were constant (22 ± 2°C) and included a regular 12-hour light and dark cycle (with lights on at 7:00 am). Food and water were available *ad libitum*, with mice being given a maintenance diet. Only food intake was monitored by weighing the pellets. Animals had access to a shelter in which the body weight was monitored. Gas exchanges were measured using a perforated stainless-steel manifold in the cage and were then analysed. A pull-mode negative pressure was set to an incurrent flow rate of 2 L/min, and oxygen consumption (VO_2) and carbon dioxide production (VCO_2) were

captured for 20s every 5min. Reference values from the ambient air were measured on the first cage. Energy expenditure was computed using the Weir equation (Weir, 1949). Energy balance was defined as:

$$Energy\ balance = Food\ consumption - Energy\ expenditure$$

The respiratory exchange ratio (RER) represents the source of nutrient mobilisation. A value of 1 corresponds to the oxidation of carbohydrate while a value of 0.7 corresponds to fat oxidation. RER was computed using the following formula:

$$RER = \frac{volume\ of\ carbon\ dioxide\ produced}{volume\ of\ oxygen\ consumed}$$

Data were retrieved from Sable Promethion system and extracted using Sable Systems Macro Interpreter v2.53.1. Data were analysed with CalR 1.3 web-based tool (Mina et al., 2018).

Statistics: When possible, a total of eight animals per sex and genotype were included in the study, in accordance with a previously established protocol (Bolborea et al., 2023). Preliminary results were also obtained with a smaller number of animals and should be interpreted with caution. Values from each animal were averaged for each genotype group, and the resulting data are expressed as mean ± standard error of the mean (SEM). The statistical analysis was conducted using CalR 1.3 web-based tool (Mina et al., 2018) and a significant threshold of p = 0.05. Metabolic variables were analysed using a generalised linear model, with the body weight serving as a covariate. Both the genotype and weight effects were investigated. The respiratory exchange ratio was considered independent of the body weight and was thus analysed with a one-way ANOVA including the genotype as the only factor. Both analyses were conducted on the complete set of data (full day), as well as on subsets of data categorised by time of day (light and dark phases). For each of the time range, all the data points were averaged into a single value per animal, and the analyses were conducted with these averaged data.

Author contributions

Metabolic assessments were conducted by Simon J. Guillot. Data were analysed and interpreted by F.L., Simon J. Guillot and Matei Bolborea.

Publication 2: Cytoplasmic accumulation of FUS in inhibitory neurons results in postnatal muscle weakness and death in mice

This second publication details the characterisation of *Fus*$^{Trunc/+}$ (abbreviated Trunc$^{+/-}$) and *Fus*$^{Trunc/Trunc}$ (abbreviated Trunc$^{-/-}$) pups, as well as their respective controls. As a reminder, these mice carry one or two truncated alleles of *Fus* exclusively in *Vgat*-expressing neurons (Figure 25). When we created the mouse lines, we observed an abnormal death of Trunc$^{-/-}$ mice before weaning, thereby our aim was to characterise their postnatal development and to identify the cause of this mortality (Figure 27).

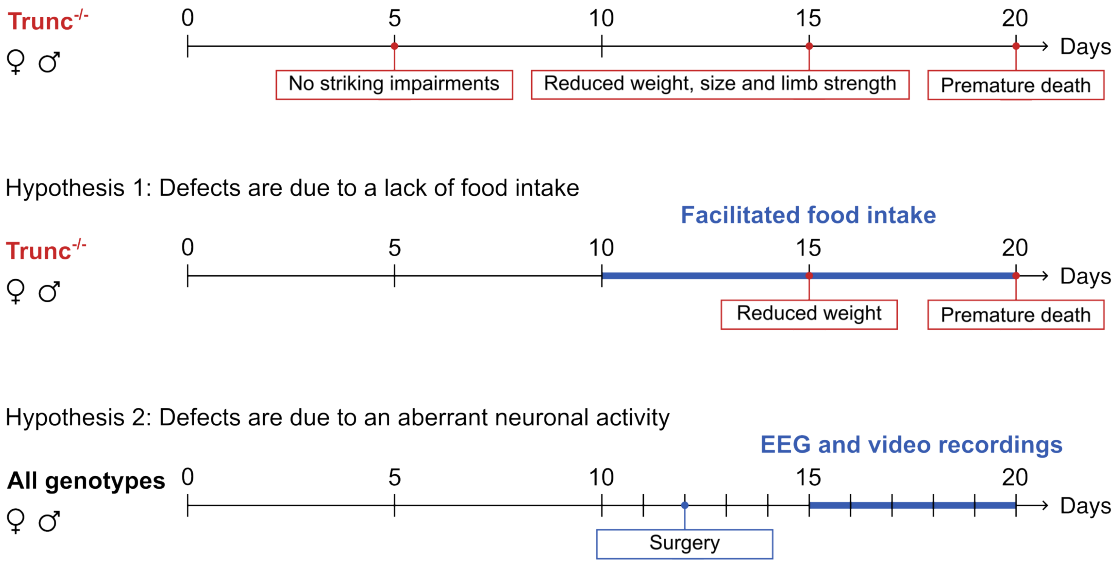


Figure 27: Summary of the main results obtained from the characterisation of Trunc$^{-/-}$ pups. The postnatal development of Trunc$^{+/-}$ pups was also examined, but no alterations were observed, which explains why they are not represented on the figure. EEG: electroencephalographic.

I first investigated the subcellular localisation of FUS in inhibitory neurons. In Trunc$^{+/-}$ pups, I found the same level of cytoplasmic accumulation than in my previous analysis with adult mice. Interestingly, this accumulation was highly enhanced in Trunc$^{-/-}$ pups. I then studied the survival of the mice for a period of 18 months, during which I observed that half of the Trunc$^{-/-}$ pups died three weeks after birth, while the survival of Trunc$^{+/-}$ and control mice was comparable. Given that cortical inhibitory neurons undergo programmed cell death between postnatal day 5 and 10, we hypothesised that FUS delocalisation may have impaired this phenomenon. Thereby, we decided to study our mice before and after this critical period. To this end, I optimised motor tests for pups and demonstrated that no alterations were visible at five days of age. However, at fifteen days of age, Trunc$^{-/-}$ pups were smaller and lighter than Trunc$^{+/-}$ and control littermates,

and this was accompanied by a notable decline in muscle strength across all four limbs. I further verified the subcellular localisation of FUS in spinal motor neuron and demonstrated that the motor phenotype emerges while the physiological nuclear localisation of FUS is maintained in Trunc$^{-/-}$ pups.

Based on our observations, we postulated that the reduced muscle strength may compromise the intake of solid food in mice, which could explain the reduced weight and lethality. To test this hypothesis, I conducted a pilot study in which some of the mice were provided with food that was both more accessible and easier to chew. However, this study highlighted no effect on weight or survival. Our second hypothesis is that these phenotypes are linked to abnormal neuronal activity, which could result in epileptiform activity, or even seizures. To verify this, we established a collaboration with Delphine Roussel (Paris), who will undertake electroencephalographic measurements in the brains of fifteen-day-old pups. Given that adult Trunc$^{+/-}$ mice display elevated neuronal activity levels, this collaboration will also allow us to ascertain whether this aberrant activity already manifests during the postnatal development.

Publication 2

Cytoplasmic accumulation of FUS in inhibitory neurons results in early postnatal muscle weakness and death in mice

Félicie Lorenc, Delphine Roussel, Véronique Devignot, Aurélie Bombardier, Claudia De Tapia, Paul Letellier, Luc Dupuis, Raphaelle Cassel

In preparation

Cytoplasmic accumulation of FUS in inhibitory neurons results in early postnatal muscle weakness and death in mice

Félicie Lorenc[1], Delphine Roussel[2], Véronique Devignot[1], Aurélie Bombardier[1], Claudia De Tapia[1], Paul Letellier[1], Luc Dupuis[# 1], Raphaelle Cassel[# 1]

[1] Université de Strasbourg, INSERM, UMR-S 1329, Strasbourg Translational Neuroscience and Psychiatry, CRBS, Strasbourg, France.
[2] Sorbonne Université, INSERM, CNRS, Electrophysiology Core Facility, Paris Brain Institute, Paris, France.

# Contributed equally.

felicie.lorenc@inserm.fr / https://orcid.org/0009-0003-8551-0981
ldupuis@unistra.fr / https://orcid.org/0000-0002-0902-5824
raphaelle.cassel@inserm.fr / https://orcid.org/0000-0002-3157-3798

Abstract

The cytoplasmic accumulation of fused in sarcoma (FUS), a ubiquitous and multifunctional DNA/RNA-binding protein, is observed in a number of neurological and neurodegenerative diseases, including amyotrophic lateral sclerosis (ALS) and frontotemporal dementia (FTD). Impairments of inhibitory neurons may contribute to the pathogenesis of ALS and FTD. In mice, the partial accumulation of FUS in these cells was found to be sufficient to increase the cortical neuronal activity and trigger a disinhibited behaviour. However, the consequences of a complete delocalisation of FUS in inhibitory neurons remain unknown. Here, we generated knock-in mice that accumulate cytoplasmic FUS specifically in inhibitory neurons expressing the vesicular GABA transporter (VGAT) following the deletion of the nuclear localisation signal (NLS) domain in all copies of *Fus.* This complete mutation of *Fus* in *Vgat*-expressing inhibitory neurons results in an early decline in growth and muscle strength, followed by a premature death for half of the pups. Our study thus emphasises that the delocalisation of FUS in inhibitory neurons impairs the postnatal development in mice.

Introduction

Fused in sarcoma (FUS) is a ubiquitous and multifunctional DNA/RNA-binding protein. In neurons, FUS is predominantly localised within the nucleus. However, it is also found at lower levels in the cytoplasm, as well as at synaptic sites, in which it bind to several RNA species critical for synaptic function in both excitatory and inhibitory neurons (Sahadevan et al., 2021; Scekic-Zahirovic et al., 2021). The nucleocytoplasmic shuttling of FUS is enabled by passive diffusion towards the cytoplasm, and active transport towards the nucleus (Dormann et al., 2010). The latter depends, at least partially, on the nuclear localisation signal (NLS) domain of the protein.

FUS is involved in the pathogenesis of several neurological and neurodegenerative conditions. Mutations in *FUS* have been found in both sporadic and familial forms of amyotrophic lateral sclerosis (ALS) (Belzil et al., 2009; Kwiatkowski et al., 2009; Vance et al., 2009), and can be associated with additional neurological and psychiatric symptoms in these patients, including chorea (Flies and Veldink, 2020), intellectual disability (Goldstein et al., 2022; Yamashita et al., 2012; Yan et al., 2010) or schizophrenia (Yan et al., 2010). Most ALS-associated mutations are located within or close to the NLS domain of FUS, and can impair the nucleocytoplasmic shuttling of FUS, resulting in a cytoplasmic accumulation of the protein. The extent of FUS nuclear import impairment was found to be inversely correlated with the age of onset of ALS (Dormann et al., 2010). In particular, heterozygous mutations resulting in the complete deletion of the NLS domain cause early-onset, rapidly progressive forms of ALS (Hübers et al., 2015; Waibel et al., 2013, 2010). Beyond the rare cases exhibiting *FUS* mutations, pathological studies have observed FUS cytoplasmic mislocalisation in sporadic ALS, as well as in ALS caused by mutations in other genes (Tyzack et al., 2019). In addition, FUS cytoplasmic mislocalisation and/or aggregation have been linked to frontotemporal dementia (FTD) (Mackenzie et al., 2011b; Neumann et al., 2009a; Seelaar et al., 2010; Snowden et al., 2011; Urwin et al., 2010), and FUS intranuclear inclusions have been associated with Huntington's disease (Mori et al., 2019) and spinocerebellar ataxia (Doi et al., 2010).

We previously generated $Fus^{\Delta NLS}$ mice exhibiting a ubiquitous deletion of the NLS domain since the embryonic development. The complete deletion of the NLS domain in homozygous $Fus^{\Delta NLS/\Delta NLS}$ effectively led to a full cytoplasmic delocalisation of FUS in cortical neurons and spinal motor neurons, and a perinatal death due to respiratory insufficiency (Scekic-Zahirovic et al., 2016). Conversely, heterozygous $Fus^{\Delta NLS/+}$ mice exhibited early-onset FTD-like social impairments associated with increased cortical neuronal activity levels (Scekic-Zahirovic et al., 2021), as well as mild late-onset ALS-like motor impairments (Scekic-Zahirovic et al., 2017). In addition, alterations of cortical GABAergic synapses were observed during the disease course (Sahadevan et al., 2021; Scekic-Zahirovic et al., 2021). Recently, we demonstrated that the heterozygous mutation

of *Fus* in inhibitory neurons alone was sufficient to recapitulate social impairments and abnormal cortical activity, but not motor deficits (Publication 1, page 113).

In the present study, we investigated the consequences of the homozygous mutation of *Fus* when induced exclusively in neurons expressing the vesicular GABA transporter (VGAT). We demonstrate that the cytoplasmic delocalisation of FUS in inhibitory neurons severely compromises the postnatal development, with reduced growth and muscle strength at two weeks of age and premature death at three weeks of age. We are now investigating the underlying mechanisms to ascertain whether the contribution of FUS mislocalisation on neuronal network development and function may explain the observed alterations. Ultimately, our study emphasises that FUS cytoplasmic delocalisation in inhibitory neurons plays a role in the postnatal development of mice.

Results

FUS cytoplasmic delocalisation in inhibitory neurons is enhanced in Trunc$^{-/-}$ mice

The aim of this study was to elucidate the consequences of a complete loss of the NLS domain of FUS in inhibitory neurons. To this end, we generated a novel mouse line in which both copies of the *Fus* gene were truncated selectively in *Vgat*-expressing neurons. A two-step breeding process was conducted (Fig. 1A) to achieve germline transmission of the recombinant alleles (Fig. 1B). In brief, mice expressing Cre under the endogenous promoter of *Vgat* (Vong et al., 2011) were crossed with mice in which the *Fus* locus was engineered with LoxP sequences (Publication 3, page 295) in order to permit the deletion of the NLS through Cre-Lox recombination. Mice heterozygous or homozygous for *Fus* truncation will hereafter be referred to as Trunc$^{+/-}$ and Trunc$^{-/-}$, respectively.

We previously demonstrated that 2-month-old Trunc$^{+/-}$ mice exhibit a mild cytoplasmic delocalisation of FUS, which is exclusive to inhibitory neurons, and we reported a 1.3-fold decrease in the nuclear-to-cytoplasmic ratio of FUS when comparing adult Trunc$^{+/-}$ to three different control mouse lines (Publication 1, page 126). In the present study, we investigated FUS subcellular localisation 15 days after birth and observed a similar delocalisation in the parvalbumin inhibitory neurons of Trunc$^{+/-}$ mice (Fig. 1C). Our preliminary results indicated a 1.2-fold decrease in the nuclear-to-cytoplasmic ratio of FUS when comparing Trunc$^{+/-}$ pups to *Fus*$^{LoxP/+}$ or *Fus*$^{LoxP/LoxP}$ control pups (Fig. 1D). This delocalisation was enhanced in Trunc$^{-/-}$ pups, as evidenced by a drastic reduction in the nuclear-to-cytoplasmic ratio of FUS: the later was 2.8 times smaller in Trunc$^{-/-}$ mice than in *Fus*$^{LoxP/+}$ or *Fus*$^{LoxP/LoxP}$ control mice, and 2.3 times smaller in Trunc$^{-/-}$ mice than in Trunc$^{+/-}$ mice (Fig. 1D). Of note, residual amounts of FUS could still be detected in the nucleus of inhibitory neurons, even when the NLS domain of *Fus* was truncated in both copies (Fig. 1C). These results show that there is a dose-dependent effect regarding the cytoplasmic accumulation of FUS and the number of truncated copies.

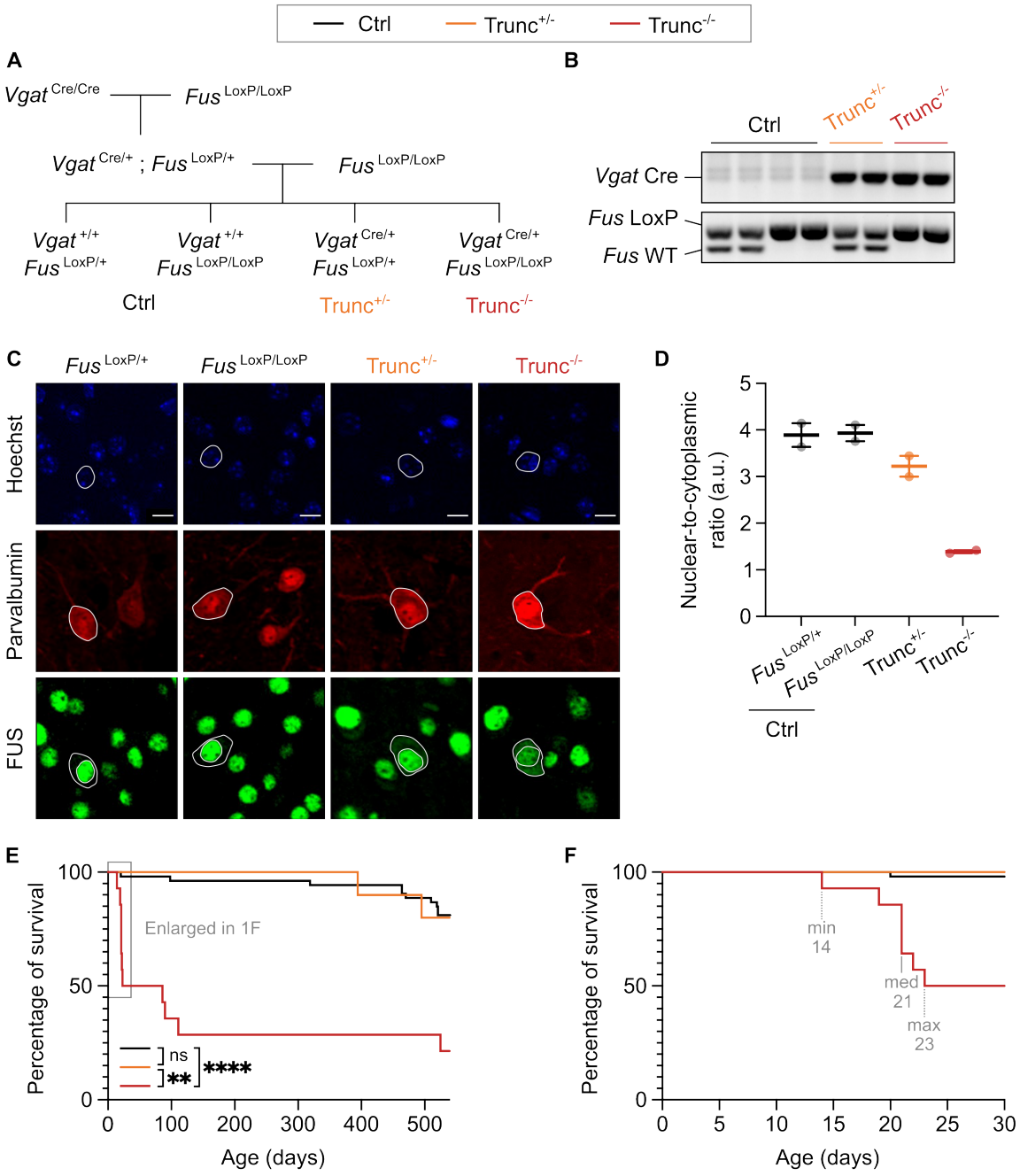


Figure 1: Postnatal lethality in Trunc$^{-/-}$ mice. (**A**) Breeding scheme to generate Ctrl, Trunc$^{+/-}$ and Trunc$^{-/-}$ littermates. (**B**) Representative PCR genotyping results. (**C**) Representative images of the immunofluorescence staining of FUS in the frontal cortex of 15-day-old mice. Hoechst staining was used to delimit nuclei. Parvalbumin staining was used to delimit the cytoplasm of inhibitory neurons. Scale bar = 10µm. (**D**) Quantification of the nuclear-to-cytoplasmic ratio of FUS in inhibitory parvalbumin neurons. Since *Fus*$^{LoxP/+}$ and *Fus*$^{LoxP/LoxP}$ pups exhibited the same nuclear-to-cytoplasmic ratio of FUS in inhibitory neurons, and the same results in the following experiments, they were merged in a control (Ctrl) group. (**E**) The survival curve was obtained by monitoring the mice daily over an 18-month period. (**F**) The previous graph was enlarged for the postnatal period. This shows that half of the homozygous pups die three weeks after birth. (D) Preliminary results are represented as ± SEM, n = 2 *Fus*$^{LoxP/+}$ (black), 2 *Fus*$^{LoxP/LoxP}$ (black), 2 Trunc$^{+/-}$ (orange) and 2 Trunc$^{-/-}$ (green), including 1

female and 1 male per genotype (merged in graphs). Number of inhibitory neurons analysed: 62 in *Fus*$^{LoxP/+}$, 59 in *Fus*$^{LoxP/LoxP}$, 42 in Trunc$^{+/-}$ and 53 in Trunc$^{-/-}$. (E, F) Results are represented as Kaplan-Meier survival curves, n = 53 Ctrl (black), 10 Trunc$^{+/-}$ (orange) and 14 Trunc$^{-/-}$ (red) mice. Control mice included *Vgat*$^{+/+}$; *Fus*$^{+/+}$ and *Vgat*$^{Cre/+}$; *Fus*$^{+/+}$ mice in addition to the genotypes introduced in Fig. 1A. Data from both sexes were merged. Log-rank Mantel-Cox test, ** $p < 0.01$.

FUS cytoplasmic accumulation in inhibitory neurons shortens the lifespan of homozygous pups

Our laboratory previously demonstrated that the truncation of both copies of *Fus* in every cell type results in lethality within the first hour after birth, due to respiratory insufficiency (Scekic-Zahirovic et al., 2016). With this novel mouse line, all pups survived the perinatal period. However, we observed that half of Trunc$^{-/-}$ pups died three weeks after birth (Fig. 1E). This occurred for four females and three males out of the seven females and seven males included in the survival study. The lethality occurred abruptly between 14 and 23 days of age, with a median age of 21 days. (Fig. 1F). This phenomenon was observed regardless of the sex of the pup, size of the litter, genotype and age of the mother, or number of previous litters. In contrast, heterozygous Trunc$^{+/-}$ mice exhibited a survival curve analogous to that of Ctrl mice.

FUS cytoplasmic accumulation in inhibitory neurons alters postnatal growth in homozygous pups

Given that half of the homozygous Trunc$^{-/-}$ pups died three weeks after birth, we decided to assess their postnatal development. In the cerebral cortex, the number of inhibitory neurons derived from the medial ganglionic eminence was reported to remain constant between postnatal days 2 and 5, before declining by 30% between days 5 and 10, and then stabilising between days 10 and 21 (Wong et al., 2018). We thus studied pups at 5 and 15 days of age, before and after the critical period of programmed cell death.

At 5 days of age, there was no significant difference in the body weight and body length of Ctrl, Trunc$^{+/-}$ and Trunc$^{-/-}$ pups (Fig. 2A and 2B). In contrast, at 15 days of age, the body weight and body length of Trunc$^{-/-}$ pups were significantly lower than those of Ctrl and Trunc$^{+/-}$ littermates, whereas no differences were observed between Ctrl and Trunc$^{+/-}$ pups (Fig. 2D and 2E). On average, Trunc$^{-/-}$ pups were 1.94g lighter than their littermates, representing a 26% reduction in body weight. Similarly, Trunc$^{-/-}$ pups were 0.52cm shorter than their littermates, representing a 9% reduction in body length. Apart from that, the overall appearance of the pups at 5 and 15 days of age was comparable between the genotypes. A number of parameters were considered, including skin colour, fur condition, eye opening, and ear and tooth development (data not shown).

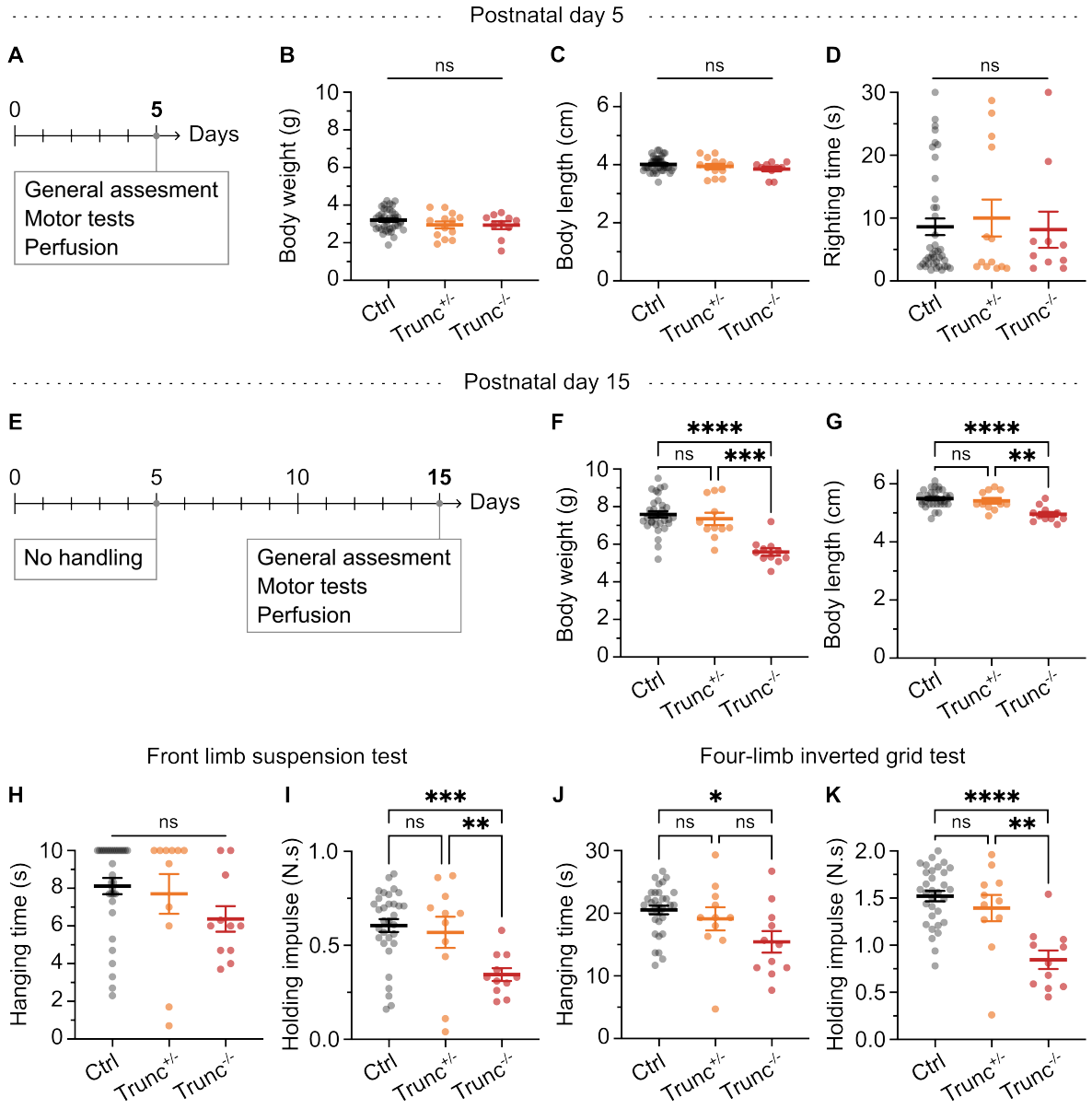


Figure 2: Altered postnatal development in Trunc$^{-/-}$ mice. Results are expressed as mean ± SEM. (**A**, **E**) Scheme of the experimental design. (**B**, **F**) Body weight. (**C**, **G**) Body length was measured from nose-tip to tail-base. (**D**) Righting time was monitored with the righting test. (**H**, **J**) Hanging time was monitored with the front limb suspension test (H) and the four-limb inverted grid test (J). (**I**, **K**) Holding impulse was calculated from the hanging time. (A-D) Study at 5 days of age, n = 40 Ctrl (black), 13 Trunc$^{+/-}$ (orange) and 10 Trunc$^{-/-}$ (red) pups. (E-K) Study at 15 days of age, n = 32 Ctrl (black), 11 Trunc$^{+/-}$ (orange) and 11 Trunc$^{-/-}$ (red) pups. Data from both sexes were merged. (B, F, G, J, K) One-way ANOVA and multiple comparisons were corrected with Tukey's test. (C, D, H, I) Kruskal-Wallis and multiple comparisons were corrected with a two-stage Benjamini, Krieger and Yekutieli false discovery rate procedure.

FUS cytoplasmic accumulation in inhibitory neurons alters muscle strength in homozygous pups

FUS is among the most common genes associated with juvenile ALS cases and induces a rapid motor deterioration. Therefore, our next objective was to assess the muscle strength and motor coordination of these pups. At 5 days of age, the capacity of the pups to control their trunk was evaluated using the righting test, which revealed no significant difference between the genotypes (Fig. 2C). Motor coordination was evaluated using the negative geotaxis test, and the performance of each pup was scored on a five-point scale. No differences were observed between the genotypes for either the rotating time (Fig. S1A) or the score (Fig. S1B). At 15 days of age, muscle strength was evaluated using the front limb suspension test and the four-limb inverted grid test. In both cases, Trunc$^{-/-}$ pups demonstrated a reduced hanging time in comparison to Ctrl and Trunc$^{+/-}$ littermates, although this was overall not significant (Fig. 2F and 2H). We then calculated the holding impulse, defined as the minimum total sustained force exerted by the pup to counteract the gravitational force. This revealed a significant reduction in the holding impulse of Trunc$^{-/-}$ pups compared to Ctrl or Trunc$^{+/-}$ littermates (Fig. 2G and 2I). The negative geotaxis test was also conducted and showed no differences between the genotypes for either the rotating time (Fig. S1C) or the score (Fig. S1D). For all the aforementioned tests, heterozygous Trunc$^{+/-}$ pups showed no significant differences compared to Ctrl pups. These results indicate that while limb strength is affected in 15-day-old Trunc$^{-/-}$ pups, motor coordination is not.

In conclusion, these results demonstrate that the postnatal development of pups is altered when both copies of *Fus* are truncated in inhibitory neurons, which is not the case when only one copy of *Fus* is truncated. This was evidenced by a reduction in body weight, body length and limb strength at 15 days of age, which was not seen at 5 days of age.

Study of the impact of FUS cytoplasmic accumulation in inhibitory neurons on motor units

We next wanted to ascertain whether the observed motor phenotype was attributable to an underlying impairment of the motor units. We first assessed the number of motor neurons present in the lumbar spinal cord (Fig. 3A). Our preliminary analysis did not reveal a deficit in motor neuron density at either 5 (Fig. 3B) or 15 (Fig. 3C) days of age. In *Fus*$^{\Delta NLS/+}$ mice, motor neuron degeneration was observed several months after the decline in muscle strength (Scekic-Zahirovic et al., 2017), while neuromuscular junction defects were already present before the appearance of the motor phenotype (Picchiarelli et al., 2019). Therefore, to complete our analysis, we would like to quantify the number of neuromuscular junctions and the innervation of the hindlimb muscles (Fig. 3D-3F). We also verified the subcellular localisation of FUS in motor neurons (Fig. 3G). As anticipated, the nuclear-to-cytoplasmic ratio of FUS was found to be comparable between 15-day-old Ctrl, Trunc$^{+/-}$ and Trunc$^{-/-}$ pups (Fig. 3H). These results confirm that, if motor neurons or

neuromuscular junctions are impaired in Trunc$^{-/-}$ pups, this will be due to non-cell autonomous mechanisms.

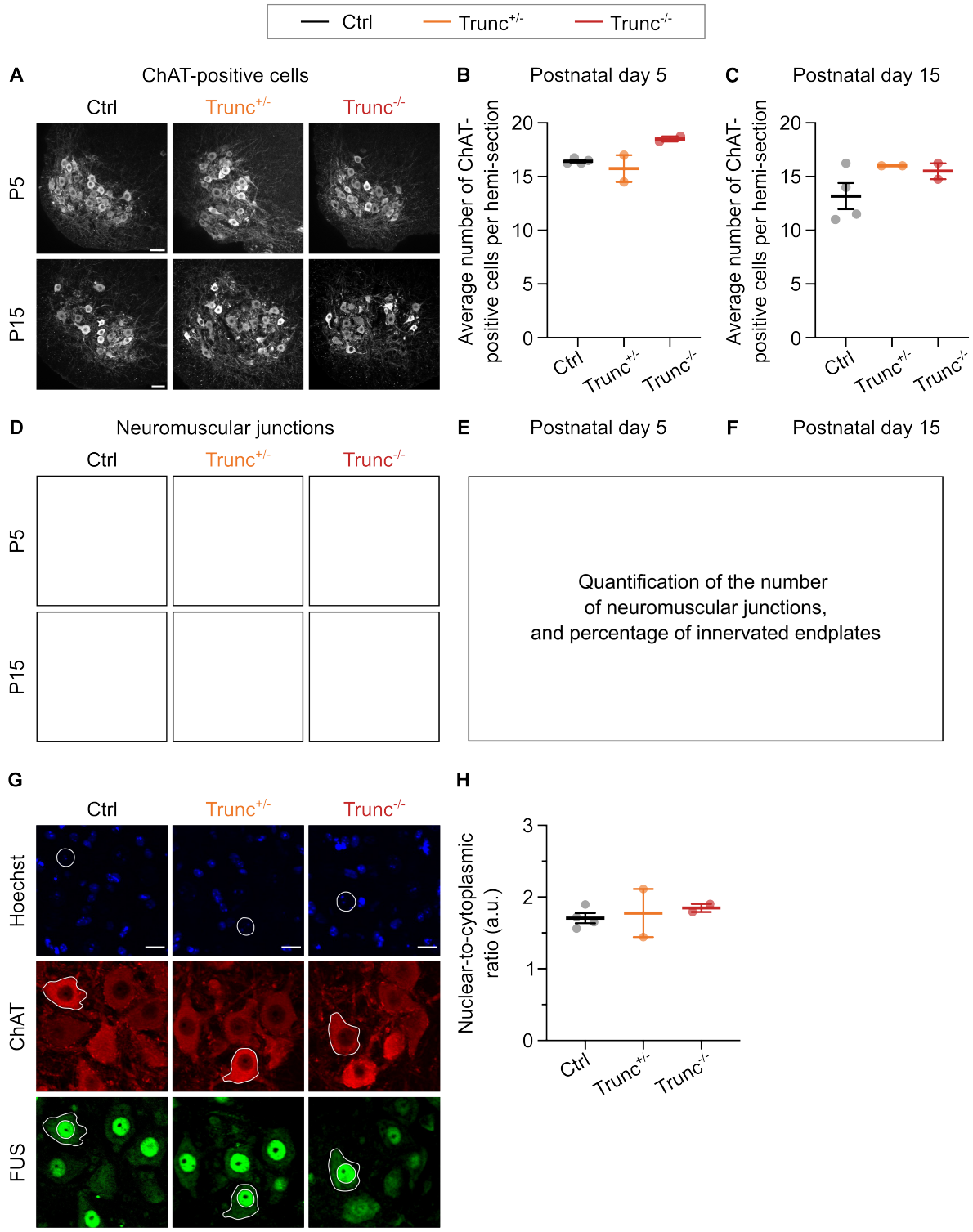


Figure 3: Motor units in Trunc$^{-/-}$ mice. Preliminary results are represented as ± SEM, n = 4 Ctrl (black), 2 Trunc$^{+/-}$ (orange) and 2 Trunc$^{-/-}$ (green), including 1 female and 1 male per genotype (merged in graphs). (**A**) Representative images of the immunofluorescence staining of ChAT in the lumbar spinal cord of 5-day-old (top) and 15-day-old (bottom) mice. Scale

bar = 50µm. (**B** and **C**) Averaged number of ChAT-positive motor neurons per hemi-section in 5-day-old (B) and 15-day-old (C) mice. (**D**-**F**) Analysis of the number of neuromuscular junctions and the innervation of the hindlimb muscles in 5-day-old and 15-day-old mice. (**G**) Representative images of the immunofluorescence staining of FUS in the lumbar spinal cord of 15-day-old mice. Hoechst staining was used to delimit nuclei. ChAT staining was used to delimit the cytoplasm of motor neurons. Scale bar = 10µm. (**H**) Quantification of the nuclear-to-cytoplasmic ratio of FUS in motor neurons. Number of motor neurons analysed: 94 in Ctrl, 44 in Trunc$^{+/-}$ and 61 in Trunc$^{-/-}$.

Facilitating food intake does not prevent the postnatal growth alterations and lethality

Given that Trunc$^{-/-}$ pups exhibited reduced limb strength at 15 days of age, we postulated that the reduced body weight and lifespan might be attributable to a lack of solid food intake. Pups begin to nibble on solid food before postnatal day 15 and are capable of self-feeding by this age (Bailoo et al., 2020). The positioning of the food hopper on the cage lid meant that solid food was only accessible to mice standing in the cage or clinging to the grid of the cage lid. However, the observed reduction in muscle strength may have prevented this behaviour. Additionally, altered jaw strength may also prevent the intake of solid food, as observed in ALS patients. To test this hypothesis, we conducted a pilot study and examined the effect of facilitated food intake on the body weight and survival of pups (Fig. 4A). The litters were divided into two groups. Half of them received solid food pellets on the cage lid (control condition). The other half received solid food pellets, watered powdered food and gel on the bedding, in addition to solid food pellets in the hopper (facilitated food intake condition). The food composition was similar in both conditions.

Facilitating food access and nibbling had no effect on the body weight of pups, regardless of their genotype (Fig. 4B, dashed *versus* solid lines and Fig. 4C). At 15 days of age, we found a 32% and 25% reduction in body weight when comparing Trunc$^{-/-}$ pups to their littermates in the control and facilitated food intake conditions, respectively. While Ctrl and Trunc$^{+/-}$ pups gained weight between 15 and 20 days of age, the body weight of Trunc$^{-/-}$ pups remained stable, thereby increasing the differences. At 20 days of age, we observed a 46% and 38% reduction in body weight when comparing Trunc$^{-/-}$ pups to their littermates in the control and facilitated food intake conditions, respectively. Furthermore, three out of five Trunc$^{-/-}$ pups died between 16 and 20 days of age, despite having a facilitated food intake (Fig. 4D, red dashed line), thereby reproducing the previously observed postnatal lethality (Fig. 1E). In conclusion, our pilot study suggests that the reduced body weight and lifespan of homozygous Trunc$^{-/-}$ pups may not be related to a lack of access to food.

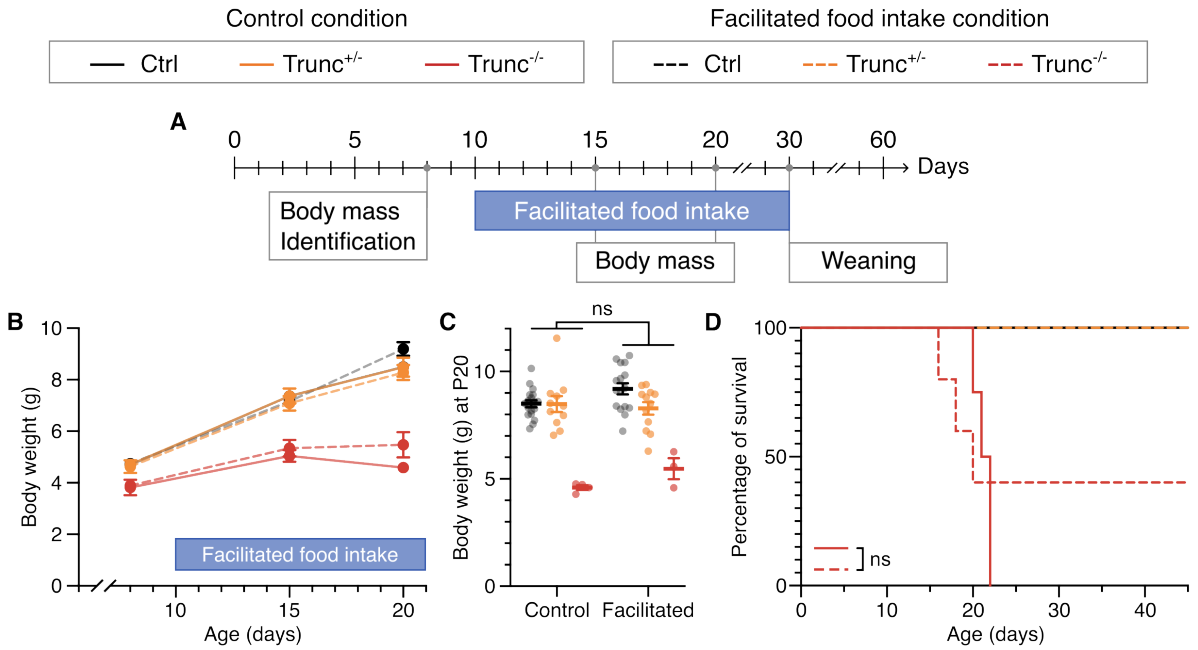


Figure 4: Absence of benefit when food intake is facilitated. (**A**) Scheme of the experimental design. (**B**, **C**) Body weight was monitored over a 12-day period (B), and a detailed representation was made for the final measurement (C). Results are expressed as mean ± SEM. (**D**) The survival curve was obtained by monitoring the mice daily over a 45-day period. Results are represented as Kaplan-Meier survival curves. (B, C) In the control condition, n = 18 Ctrl (black, solid), 11 Trunc$^{+/-}$ (orange, solid) and 4 Trunc$^{-/-}$ (red, solid) mice. In the facilitated food intake condition, n = 16 Ctrl (black, dashed), 12 Trunc$^{+/-}$ (orange, dashed) and 5 Trunc$^{-/-}$ (red, dashed) mice. Data from both sexes were merged. (C) Two-way ANOVA and multiple comparisons were corrected with Šidák's test, ns $p > 0.05$. (D) Log-rank Mantel-Cox test, ns $p > 0.05$.

Conclusion

With the present study, we demonstrated that the cytoplasmic accumulation of FUS exclusively in *Vgat*-expressing inhibitory neurons resulted in an altered postnatal development in homozygous mice, but not in heterozygous mice. This was evidenced by a reduction in growth and muscle strength at 15 days of age, which preceded a premature death at 21 days of age. Given that the observed decrease in muscle strength could have prevented food intake, we attempted to restore the body weight and survival by facilitating food access and nibbling. However, our approach was unsuccessful.

A limitation of our pilot study is that we were unable to control the quantity of food ingested, and thus we cannot provide proof that the pups ate the food available on the bedding. We hypothesised that food intake could be prevented by a lack of muscle strength. However, it is also possible that a lack of appetite is involved. It was demonstrated that silencing *Vgat*-expressing neurons in the hypothalamus attenuate weight gain and food consumption, while increasing food aversion in adult mice (Jennings

et al., 2015). At the moment, we have no evidence to suggest that the cytoplasmic accumulation of FUS impaired these neurons. Indeed, our metabolic phenotyping revealed no defects in food intake in 12-month-old Trunc$^{+/-}$ mice (Publication 1, page 151). However, it remains possible that the complete delocalisation of FUS in homozygous mice affected these *Vgat*-expressing neurons to a greater extent than in heterozygous mice. One solution would be to design a study in which pups would be hand-fed in order to control their food intake. If this approach were to effectively prevent the decline in body weight and premature death, it would allow us to propose that the observed phenotypes are caused by starvation. However, we won't be able to determine which of the lack of muscle strength and/or lack of appetite caused starvation.

When we examined the effect of facilitated food intake on the survival of pups, we observed that all four Trunc$^{-/-}$ pups in the control condition died between 20 and 22 days of age (Fig. 4C, red solid line). This result was not expected as it is not consistent with our first survival study showing that half of the Trunc$^{-/-}$ pups survived up to weaning (Fig. 1E). However, the apparent discrepancy in the reported percentages of survival may be explained by the low number of mice. Indeed, we included four pups in the pilot study compared to fourteen Trunc$^{-/-}$ pups included in the previous survival study.

Materials and methods

Mouse model

Experimental protocols and animal care were conducted in compliance with the European Directive (2010/63/UE) and French Decree (2013/118). The project received approval from the ethical committee of the University of Strasbourg, as well as the French Department of Higher Education, Research and Innovation (reference number 22385).

To generate double mutant breeders, homozygous Vgat-ires-Cre knock-in mice (The Jackson Laboratory, stock #028862, C57BL/6J background, B6J.129S6(FVB)-*Slc32a1*$^{tm2(cre)Lowl}$/MwarJ) (Vong et al., 2011) were crossed with homozygous *Fus*^{exon15} knock-in mice (Mouse Clinical Institute of Strasbourg, C57BL/6N background, B6-*Fus*$^{tm2(\Delta NLS)Ldup}$/Crl, Publication 3, page 295). The resulting double heterozygous mice were then crossed with homozygous *Fus*^{exon15} mice to obtain litters with the four genotypes of interest. When necessary, additional age- and sex-matched control mice were produced by another two-step breeding process. This allowed us to obtain wild-type and heterozygous Vgat-ires-Cre mice with the same genetic background as the other mice of interest. All the mice included in this study have a genetic background that is a combination of C57BL/6J and C57BL/6N. They were genotyped by PCR of genomic DNA extracted from ear biopsies (sequences are provided in Table S1).

Mice were bred and housed in the animal facility of the Faculty of Medicine of Strasbourg, under constant conditions (22 ± 2°C, 45-65% humidity) and a regular 12-hour light and dark cycle (with lights on at 7:30-8:00 am). Food and water were available *ad libitum*, with mice being given a breeding diet before weaning and a maintenance diet afterwards. Animals were housed in groups.

Survival study

Mice were identified and genotyped at 10 days of age. Out of the 85 mice produced for this study, eight were excluded. Six were supernumerary Ctrl males (genotype: *Vgat*$^{+/+}$; *Fus*$^{LoxP/+}$) randomly chosen to be excluded before the beginning of the study. In addition, one Ctrl female (genotype: *Vgat*$^{+/+}$; *Fus*$^{+/+}$) was excluded because the date of its death was not reported, and one female was excluded because its genotyping results were abnormal. All 77 included mice were monitored daily until they died or reached 18 months of age, at which point they were euthanised. Both sexes were studied, and data were merged as they did not show significant differences. Out of the 77 mice, three developed cataracts in one eye, which did not affect their quality of life or lifespan. Six others developed dermatitis at 15-17 months of age and were euthanised. These two health issues were not linked to a given genotype.

Behavioural analysis

Mothers were carefully handled before breeding to reduce their stress and anxiety. Behavioural tests were conducted during the light phase (between 8:00 am and 1:00 pm). Prior to any task, mothers and their litter were placed in the test room for at least 30 minutes to allow them to acclimate to the environment. The entire litter was studied on the same day. Once a pup was separated from the litter, tests and euthanasia were carried out within a 20-minute period to minimise the stress caused by separation and hunger. In addition, isolated pups were kept on a heating pad to prevent any loss of body temperature. All behavioural tests and data analysis were performed blind to genotypes. Both sexes were studied, and data were merged as they did not show significant differences. Out of the 65 pups produced for the study at 5 days of age, two males were excluded as their genotyping results were abnormal. Out of the 56 pups produced for the study at 15 days of age, one male was excluded because of abnormal genotyping results, and one Trunc$^{-/-}$ male was excluded because its general health state was not good enough to conduct the tests. All the remaining pups were studied, but three 5-day-old pups and three 15-day-old pups did not engage in the negative geotaxis test. They were removed from this analysis only. The number of mice included in each experiment is indicated in the relevant figures. At the end of the study, all pups were sacrificed to recover tissues. The following protocols were adapted from Feather-Schussler and Ferguson, 2016, unless otherwise stated.

Righting test: The righting test was used to non-invasively assess the trunk control of pups at 5 days of age. This test relies on an innate motor reflex. Each pup was placed on its back on a heating pad and held in position for 5 seconds. The time necessary for the animal to return to its four feet (referred to as 'righting time') was measured visually using a stopwatch. Trials lasted a maximum of 30 seconds. The procedure was repeated three times, with a 30-second break between each trial.

Negative geotaxis test: The negative geotaxis test was used to assess the motor coordination of pups at 5 and 15 days of age. This non-invasive test relies on an innate sensory reflex. Each pup was placed on an inclined grid (slope of 35° at 5 days of age and 45° at 15 days of age), with its head facing down the slope. After being held in position for 5 seconds, the animal was released and turned to face up the slope due to vestibular cues of gravity. The time necessary for the animal to complete a 180±10° rotation (referred to as 'rotating time') was measured visually using a stopwatch. Following the rotation, the pup was allowed to move freely for 10 seconds. Trials lasted a maximum of 30 seconds. The procedure was repeated three times, with a 2-minute break between each trial. Performance was evaluated after each trial using a five-point scale:

Score	Performance
0	No rotation, ending with or without a fall.
1	Partial rotation ending with a fall.
2	Partial rotation but no fall.
3	Complete rotation (180±10°) ending with a fall.
4	Complete rotation and no fall. The pup did not climb up the slope.
5	Complete rotation, no fall. The pup climbed up the slope (no matter how far).

Front limb suspension test and four-limb inverted grid test: These tests were used to non-invasively assess the limb strength of pups at 15 days of age. During the front limb suspension test, each pup was required to grasp a string with its forepaws. This string was held 25cm above a 10-centimetre-thick towel. The time necessary for the pup to fall (referred to as 'hanging time') was measured visually using a stopwatch. Trials lasted a maximum of 10 seconds. The procedure was repeated three times, with a 1-minute break between each trial. The protocol for the four-limb inverted grid test was adapted from Carlson et al., 2010. Each pup was placed on a grid. Once the animal grasped it with its four paws, the grid was slowly inverted and then held 10cm over a 10-centimetre-thick towel. The hanging time was also measured visually using a stopwatch. Trials lasted a maximum of 45 seconds. The procedure was repeated three times, with a 3-minute break between each trial. The body weight was measured immediately after these tests to compute the minimum total sustained force exerted by the pup to oppose the gravitational force: holding impulse (N.s) = averaged hanging time (s) x body weight (g) x 0.00980665 ($N.g^{-1}$).

Histological analysis

Mice were euthanised at 5 or 15 days of age with an intraperitoneal injection of 230 mg/kg sodium pentobarbital (Euthasol Vet). They were transcardially perfused with 0.1M phosphate buffer saline (PBS) followed by 4% paraformaldehyde. After dissection, brains and spinal cords were post-fixed for 24h and then included in 4% agar. Serial cuts (thickness 40µm) were made using a vibratome (Leica Biosystems) and collected in PBS with 0.02% azide. Slices were rinsed with PBS and then incubated in 10mM citrate buffer (pH 6) for 30min at 80°C. After three washes in PBS, slices were blocked in PBS with 5% horse serum and 0.3% Triton X-100 for 90min at room temperature. Primary antibodies were incubated in PBS with 1% horse serum and 0.1% Triton-X100 overnight at room temperature: goat anti-FUS (Bethyl, 1:250, A303-839A), rabbit anti-FUS (Proteintech, 1:500, 11570-1-AP), guinea pig anti-NeuN (Synaptic Systems, 1:1000, 266-004), mouse anti-parvalbumin (Sigma, 1:1000, P3088), goat anti-ChAT (Millipore, 1:500, AB114P). After three washes in PBS, fluorescent conjugated secondary antibodies were incubated in PBS for 90min at room temperature: donkey anti-guinea pig A488 (Jackson, 1:1000, 706-546-148), donkey anti-goat A555 (Invitrogen, 1:1000, A21432), donkey anti-rabbit A555 (Invitrogen, 1:1000, A31572), donkey anti-mouse A647 (Jackson, 1:1000, 715-605-151), donkey anti-goat A647 (Jackson, 1:1000, 705-605-147). Three final washes were performed, and during the second wash, chromatin was stained with Hoechst (sigma, 1:1000, B2261) for 15min at room temperature. Slices were mounted in Prolong Diamond (Invitrogen, P36961) on microscope slides.

Image acquisition was performed at the Imaging Core Facility of Strasbourg Biomedical Research Centre (University of Strasbourg, INSERM, UMS 38, PIC-STRA,). An upright widefield epifluorescence microscope (Zeiss, Axio Imager M2) was used with an ApoTome module. Data were analysed blind to genotypes. ImageJ software was used to study FUS localisation by measuring a mean signal intensity in the nucleus and cytoplasm of cells of interest. The sex and number of mice studied are indicated in the figures.

Survival study with facilitated food access

Mothers were carefully handled before breeding to reduce their stress and anxiety. Their pups were identified and genotyped at 8 days of age. Out of the 68 mice produced for this study, two mice were excluded. One male was excluded because its genotyping results were abnormal. One Ctrl female (genotype: $Vgat^{+/+}$; $Fus^{LoxP/+}$) was excluded because of growth issues: at 30 days of age, it was showing a 36% reduction in body weight compared to the other Ctrl females. All 66 included mice were monitored daily until they died or reached 45 days of age, at which point they were euthanised. At 10 days of age, the litters were divided into two groups. From this day, five litters received solid food pellets on the cage lid. Five other litters received solid food pellets, watered powdered food and gel on the bedding, in addition to solid food pellets in the hopper. The food composition was similar in both conditions, as the powdered food and gel were obtained

from the solid food pellets. The allocation of each litter to a given experimental condition was based on the number of pups and their genotype, to obtain two groups of similar composition. In both conditions, the average number of pups per litter was 7. The sex was not considered for the allocation, but females and males were studied, and data were merged. The body weight was measured at 8, 15 and 20 days of age. Data were collected blind to genotypes but not to food conditions. Mice were weaned at 30 days of age and from this day, they all received solid food pellets on the cage lid.

Statistics

Values from all animals were averaged for each genotype group, and data were represented as mean ± standard error of the mean (SEM) unless otherwise stated. When possible, the averaged value from each animal was represented as a single data point. Both sexes were merged for the analysis. Statistical analysis was performed using GraphPad Prism 9 software with a significant threshold set at $p = 0.05$. Normal distribution was assessed using three different tests (Anderson-Darling, D'Agostino and Pearson, Shapiro-Wilk). Normality was assumed when at least two tests reported $p > 0.05$, and the following statistical tests were chosen accordingly. Sphericity was assessed using Brown-Forsythe and Bartlett tests. For two-way ANOVA, sphericity was not assumed so the Greenhouse-Geisser correction was used. When the number of animals per genotype was smaller than 8, data was assumed not to follow normal distribution and non-parametric tests were used.

Acknowledgments

The authors would like to thank the technicians of the animal facilities, namely Lénaïc Marczak, Célian Pitard and Christiane Rieger, for their care of the mice. We acknowledge the imaging core facility PIC-STRA.

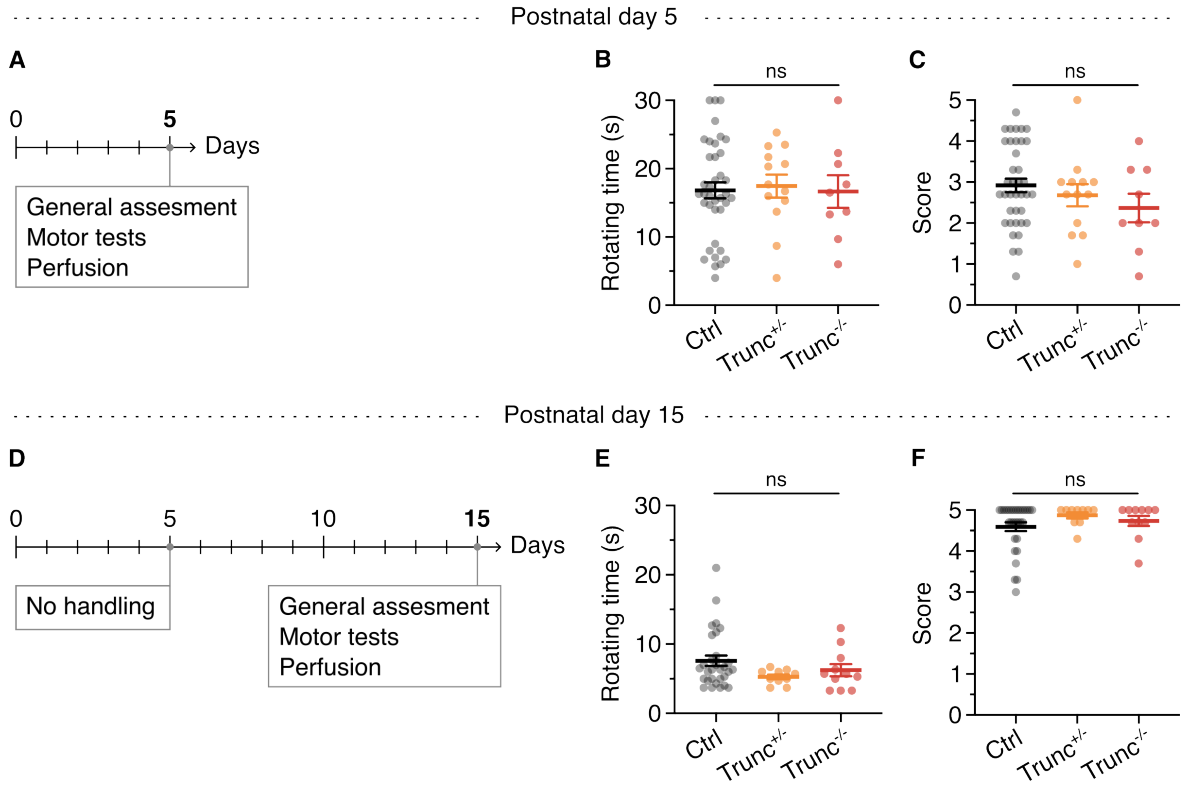
Author contributions

Genotyping was performed by F.L. and P.L. Tissues were processed by F.L. and A.B. Histological analysis was conducted by F.L., with the assistance of V.D. Survival studies were performed by F.L. Behavioural tests were conducted by F.L., R.C. and C.D, while the analysis was performed by F.L. The manuscript was written by F.L., R.C., and L.D.

Supplementary data

Gene	Forward	Reverse
Wild-type *Vgat*	CTT CGT CAT CGG CGG CAT CTG	CAG GGC GAT GTG GAA TAG AAA
Mutant *Vgat*	CTT CGT CAT CGG CGG CAT CTG	CCA AAA GAC GGC AAT ATG GT
Fus^{exon15}	GCA GAT ACT GAG GAG AGA GAA CTG G	CCA CTG TTA TCT ACA CAT GAT CAC CC

Supplementary Table 1: Oligonucleotides used for the genotyping.



Supplementary Figure 1: Motor coordination in Trunc$^{-/-}$ mice. Results are expressed as mean ± SEM. (**A**, **D**) Scheme of the experimental design. (**B**, **E**) Rotating time was monitored with the negative geotaxis test. (**C**, **F**) Score assessing the performance of the pups during the negative geotaxis test. (A-C) Study at 5 days of age, n = 38 Ctrl (black), 13 Trunc$^{+/-}$ (orange) and 9 Trunc$^{-/-}$ (red) pups. (D-F) Study at 15 days of age, n = 30 Ctrl (black), 10 Trunc$^{+/-}$ (orange) and 11 Trunc$^{-/-}$ (red) pups. Data from both sexes were merged. (B, C) One-way ANOVA and multiple comparisons were corrected with Tukey's test. (E, F) Kruskal-Wallis and multiple comparisons were corrected with a two-stage Benjamini, Krieger and Yekutieli false discovery rate procedure.

Supplementary data

Context

The strategy we used to restore the body weight and survival of Trunc$^{-/-}$ pups by facilitating food access and nibbling was unsuccessful. Nevertheless, this pilot study permitted the monitoring of the body weight of the mice prior to their death. Our preliminary results showed that the body weights of the pups were comparable, regardless of whether they succumbed before weaning or survived until adulthood (Fig. 5A). This was observed at 15 days of age, when all the pups were alive, as well as at 20 days of age, when 2 pups had already died. These results suggest that the pups are not dying from starvation. Indeed, one would expect the surviving pups to eat more than the dying ones, and thus to have a greater body weight.

FUS plays a role in the regulation of RNA homeostasis, which is notably crucial for maintaining the integrity and functionality of synapses. For instance, it has been proposed that FUS can modulate the composition of GABAergic receptors during synaptogenesis (Sahadevan et al., 2021). In 1-month-old *Fus*$^{\Delta NLS/+}$ mice, a synaptic accumulation of mutant FUS was observed in the cortex and was accompanied by molecular evidence of an excitatory-inhibitory imbalance in favour of excitation. We also demonstrated that the cytoplasmic accumulation of FUS in inhibitory neurons is sufficient to increase neuronal activity levels in the cortex of 4-month-old Trunc$^{+/-}$ mice (Publication 1, page 131), although the underlying mechanisms are yet to be studied. The precise timing of the onset of this phenotype and its potential exacerbation by the complete delocalisation of FUS in Trunc$^{-/-}$ mice remain unknown. However, we can assume that mutant FUS impaired the activity of inhibitory neurons.

In addition, our pilot study allowed us to observe the behaviour of homozygous pups on a daily basis, providing a greater insight into their phenotype. We saw that some homozygous pups exhibited transient periods of inactivity. They displayed a tendency to cower in on themselves (remaining on their four limbs) and demonstrated a minimal response or lack of response to touch stimuli from their mother or the experimenter. This was not an early indicator of death, as some of these pups were observed to resume normal activity a few hours later. However, this may be indicative of behavioural arrest and unresponsiveness, potentially due to absence seizures, and/or a lethargic phenotype resulting from an unobserved prior stressful event.

Therefore, our second hypothesis to explain the premature death of Trunc$^{-/-}$ pups is that their neuronal activity is increased, and may even exhibit epileptiform discharges or seizures, which would be fatal for half of the pups. To test this hypothesis, we will perform electroencephalographic and video recordings before and during the critical period of lethality (Fig. 5B). This is the most relevant experimental approach to detect a potential

abnormal brain activity and to confirm or refute the epileptic phenotype. We will include both Trunc$^{-/-}$ and Trunc$^{+/-}$ pups, as well as control mice. In addition to investigating the potential cause of death in Trunc$^{-/-}$ pups, this will allow us to determine whether neuronal activity levels are already altered during the postnatal development of Trunc$^{+/-}$ mice.

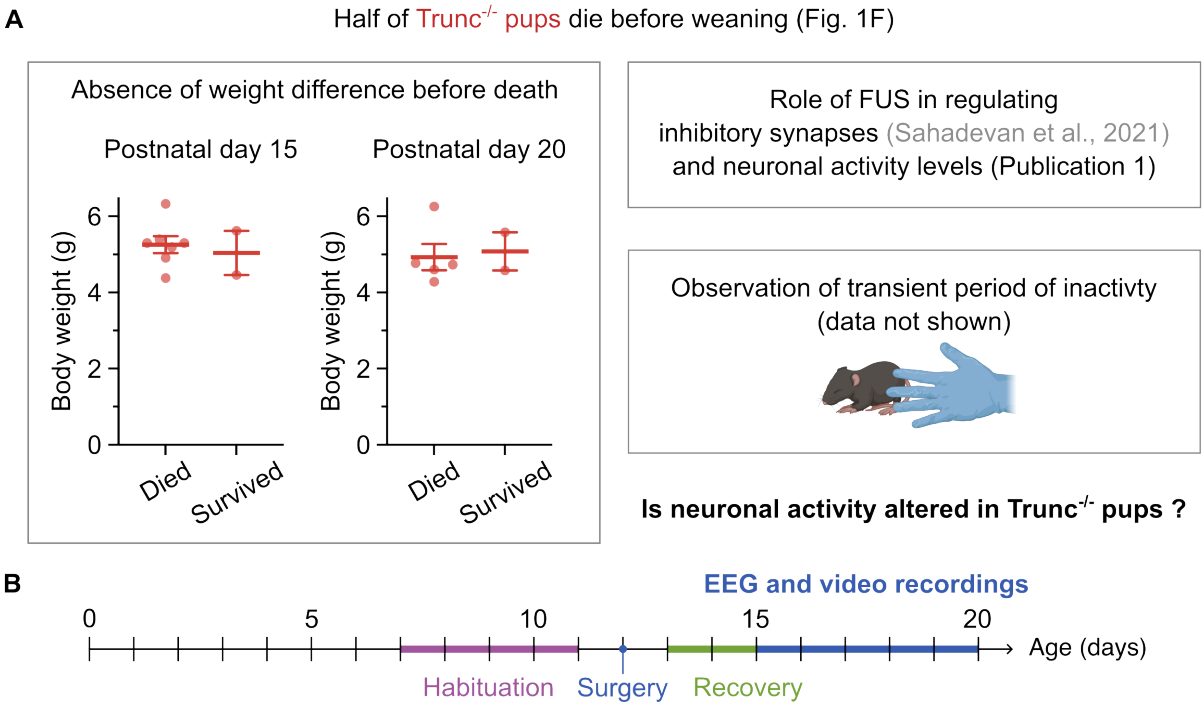


Figure 5: Rationale and experimental design to study neuronal activity in Trunc$^{-/-}$ mice. (A) Body weight of Trunc$^{-/-}$ mice at 15 and 20 days of age. Results are expressed as mean ± SEM, n = 7 pups that died before weaning and 2 pups that survived. (B) Experimental design. The electroencephalographic recordings will enable the identification of potential epileptiform activity in the brain, which are characterised by excessive and synchronous discharges. The simultaneous video recordings will facilitate the subsequent analysis.

Materials and methods

Mouse model

Experimental protocols and animal care will be conducted in compliance with the European Directive (2010/63/UE) and French Decree (2013/118). The project received approval from the ethical committee of Sorbonne University, as well as the French Department of Higher Education, Research and Innovation (reference number 47602). Double mutant mice will be generated as previously described. Mice will be bred and housed in the animal facility of the Paris Brain Institute, under constant conditions (22 ± 2°C, 45-65% humidity) and a regular 12-hour light and dark cycle (with lights on at 7:30-8:00 am). Food and water will be available *ad libitum*, with mice being given a breeding diet before weaning and a maintenance diet afterwards.

Neuronal activity analysis

A total of 20 pups will be included in this study (n = 5 Ctrl, 5 Trunc$^{+/-}$ and 10 Trunc$^{-/-}$ mice), and both sexes will be merged.

Habituation prior to the surgical procedure: Olfactory conditioning will reduce the probability of implant damage and cannibalism by the parents. During the breeding phase, the parents will be habituated to the scent of the implant materials. Five to six days before surgery, the parents and their litter will be habituated to the scent of isoflurane, which will be subsequently employed as the anaesthetic agent.

Implantation of electrodes: Pups of both sexes will be implanted with electrodes at approximately 12 days of age. Briefly, the entire litter will be isolated from the parents and placed in a temperature-controlled cage. No more than one-third of the pups will be implanted. These pups will be administered Buprenorphine (0.1 mg/kg) subcutaneously 30 minutes prior to surgery. They will be anaesthetised with isoflurane (4% for the induction, then 1.5-2% for the surgery) and Lidocaine (2% for cutaneous application, followed by 4 mg/kg for subcutaneous injection). A midline incision of 0.1-0.2 cm will be made in the skin over the skull, after which the skull will be drilled. The electrodes will be positioned in the dura mater or deeper in the hippocampus and then fixed with dental cement. The wound will be sealed with superglue. Subsequently, the litter will be returned to the parents, and the implanted pups will receive Buprenorphine (0.1 mg/kg) subcutaneously every 8 hours for 2 days.

Electroencephalographic and video recordings in awake pups: Two days following the electrode implantation, electroencephalographic and video recordings will be conducted for a period of five consecutive days. Each pup will be isolated in a temperature-controlled cage and recorded for 1 hour, with the recording time gradually extended to 3 hours. The electroencephalographic recordings will enable both the identification of potential epileptiform activity in the brain, characterised by excessive and synchronous discharges of neurons, and the determination of the area of emergence of this activity. The simultaneous video recordings will facilitate the subsequent analysis by allowing for the monitoring of animal behaviour.

Author contributions

Neuronal activity will be assessed and analysed by Delphine Roussel.

Discussion

The principal objective of my thesis project was to ascertain the role of inhibitory neurons in amyotrophic lateral sclerosis (ALS) and frontotemporal dementia (FTD) associated with fused in sarcoma (FUS). In particular, I focused on the contribution of inhibitory neurons to ALS-like motor and FTD-like social phenotypes in mice. To this end, we manipulated the subcellular localisation of FUS in GABAergic and glycinergic neurons expressing the vesicular GABA transporter (VGAT), and we studied the resulting consequences. To induce a pathological cytoplasmic accumulation of FUS, we truncated the nuclear localisation signal (NLS) domain of the *Fus* gene.

Our findings indicate that the rescue of FUS nuclear localisation exclusively in *Vgat*-expressing inhibitory neurons is sufficient to delay the onset of ALS-like motor deficits in female mice and to attenuate FTD-like social alterations in aged male mice (Figure 26). Furthermore, we showed that the induction of FUS cytoplasmic delocalisation exclusively in these inhibitory neurons led to the emergence of distinct phenotypes in heterozygous and homozygous mice. Male mice with a single mutant copy of the *Fus* gene displayed an adult-onset phenotype, characterised by social alterations and elevated spontaneous neuronal activity levels in the frontal cortex, without the presence of motor deficits (Figure 26). In contrast, mice in which both copies of the *Fus* gene were mutated exhibited an altered postnatal development, evidenced by a reduction in growth and muscle strength, which preceded a premature death for half of them (Figure 27).

In this section, I will discuss the specificity and efficacy of our experimental approach for manipulating the subcellular localisation of FUS. Then, I will examine the potential mechanisms through which inhibitory neurons may influence motor and social phenotypes, as well as neuronal activity in our mouse models. This will allow me to evaluate the relevance of some of the tests we conducted and to propose a hypothesis regarding the premature death of homozygous Trunc$^{-/-}$ pups. Finally, I will present a critical analysis of our study, and potential avenues for future research.

Manipulation of FUS localisation in inhibitory neurons

In order to target the majority of cortical and spinal inhibitory neurons, we decided to use a mouse line in which Cre is expressed under the control of the endogenous promoter of the *Vgat* gene (Vong et al., 2011). This transporter is thought to be expressed in most neurons releasing GABA or glycine as a neurotransmitter, both in the brain and spinal cord. I tested the specificity and efficacy of this targeting by crossing these mice with a reporter mouse line (Madisen et al., 2010). In the progeny, the fluorescent protein tdTomato was produced upon recombination of the LoxP sequences in cells where Cre was expressed and active.

1. Was our targeting of inhibitory neurons specific?

A. Did we only target neurons?

In the frontal cortex, 94% of the cells exhibiting an active Cre recombinase were labelled with the neuronal marker NeuN (Publication 1, Fig. 1D), indicating a high degree of specificity for neurons. Two explanations may account for the observation that 6% of the cells labelled with tdTomato were not identified as neurons. Firstly, this discrepancy may be attributed to technical limitations inherent to the histological and imaging processes. The Cre-expressing cells which were not labelled by NeuN may, in fact, be neurons we failed to identify. Secondly, we cannot exclude the possibility that some non-neuronal cells express *Vgat* and, in turn, Cre, at any point of their development.

Growing evidence suggests that astrocytes are capable of releasing GABA, at least in certain regions of the central nervous system. At the moment, two non-vesicular mechanisms have been identified. The GABA-permeable anion channel Best1 appears to drive the release of neurotransmitters from astrocytes with high intracellular concentrations of GABA in the cerebellum and thalamus (Kwak et al., 2020; Soojung Lee et al., 2010). Additionally, astrocytic GABA transporters can operate in reverse mode, releasing GABA in the cerebral cortex, likely due to low extracellular GABA concentrations (Kinney, 2005). In the hippocampus, an elevation of intracellular sodium concentrations is necessary for this process (Héja et al., 2012, 2009). Although these mechanisms appear to be important for regulating the local excitation-inhibition balance, they do not depend on VGAT, indicating that we did not target these astrocytic populations by using the *Vgat*^{Cre} mouse line. However, a vesicular-dependent release of GABA was also proposed in the hypothalamus, where astrocytes exhibited positive labelling for VGAT (Y.-F. Wang et al., 2013). Further investigation is required to ascertain whether astrocytes effectively express *Vgat* in the hypothalamus, and whether this is also the case in other regions of the central nervous system. Our preliminary analysis of astrocytes labelled with an anti-GFAP antibody in the frontal cortex and lumbar spinal

cord revealed no discernible expression of Cre in this cell type, and no GFAP labelling in Cre-expressing cells. Given that GFAP may not be the most relevant marker (for instance, cortical astrocytes are known to express low levels of GFAP), our results should not be regarded as a definitive proof that astrocytes do not express VGAT in the neocortex. Nevertheless, even if we had targeted astrocytes with the Cre-expressing mouse line we selected, this would remain a marginal effect. Therefore, this should not prevent us from inferring the contribution of inhibitory neurons to the phenotypes we studied.

B. Did we only target inhibitory neurons?

Accumulating evidence indicates that subsets of neurons co-release GABA with other neurotransmitters, either by expressing VGAT and the vesicular transporter of the second neurotransmitter, or by expressing the vesicular monoamine transporter VMAT2. A recent study demonstrated that neurons co-expressing VGAT and the vesicular glutamate transporter VGLUT2 are present in 37 different brain regions (Xu et al., 2022). In the adult murine brain, this number is reduced to 19, and the effective co-transmission of GABA and glutamate has yet to be confirmed at the physiological level for most of these regions. To date, the co-release of GABA and glutamate has been convincingly demonstrated in three subcortical regions, including a nucleus in the hypothalamus (supramammillary nucleus) and the ventral tegmental area (Root et al., 2018). It was shown that GABA and glutamate are packaged into separate vesicles, which segregate into distinct presynaptic terminals. In addition, neurons co-expressing VGAT and the vesicular acetylcholine transporter were identified in the basal forebrain and cortex. Notably, a subpopulation of VIP inhibitory neurons was found to express all the necessary genes for synthesising and releasing GABA and acetylcholine (Tasic et al., 2016), and appears to be involved in the control of attention (Obermayer et al., 2019). Overall, these co-releasing neurons can exert an excitatory and/or inhibitory influence. Potential functions for this process include a temporal control over postsynaptic firing, a more precise regulation of neurotransmission, an effective way for a single presynaptic neuron to adapt its transmission based on its target, and an increased control of synaptic plasticity (Wallace and Sabatini, 2023).

As these neurons express *Vgat*, they were likely targeted with the Cre-expressing mouse line we selected. Therefore, when we state that we targeted inhibitory neurons, this is a simplified representation that does not acknowledge the potential for some *Vgat*-expressing neurons to exert an excitatory influence due to the release of other neurotransmitters. However, this simplification is still relevant as most of the neurons we targeted are currently known to exert an inhibitory influence by the sole release of GABA and/or glycine. Of note, the confirmation of co-transmission at the level of individual neurons is often absent, as most of the current studies were conducted at the population level, which may result in erroneous conclusions.

Finally, dopamine neurons of the ventral midbrain were shown to release both dopamine and GABA into the striatum using solely the vesicular monoamine transporter VMAT2 (Tritsch et al., 2012). This GABA co-transmission seems to be involved in reward-based and addiction behaviours (Berrios et al., 2016; Kim et al., 2015). As these neurons do not express VGAT, they were not targeted with the *Vgat*^{Cre} mouse line. Therefore, it is not true to state that we manipulated FUS subcellular localisation in all neurons releasing GABA. However, to our knowledge, the release of GABA in absence of VGAT was confirmed only for this specific co-transmission and remains marginal compared to the number of *Vgat*-expressing neurons releasing GABA or glycine. Of note, these dopaminergic neurons accumulate GABA without synthetising it with glutamic acid decarboxylase (GAD), thereby most classical markers used to identify GABAergic neurons are not useful to visualise or target these cells.

Importantly, we verified the absence of recombination in motor neurons, which are the main degenerating cells in ALS. In layer 5 pyramidal neurons, the nuclear-to-cytoplasmic ratio of FUS was found to be slightly decreased in *Fus*$^{Trunc/+}$ mice compared to control mice (1.3-fold reduction), which could indicate that *Fus* was mutated, and subsequently delocalised, in these neurons (Publication 1, Fig. 6G). However, we believe that this is an artifact caused by the fact that only two mice per genotype were included in this preliminary analysis. Indeed, the nuclear-to-cytoplasmic ratio of FUS was found to be comparable in *Fus*$^{Resc/+}$ and *Fus*$^{\Delta NLS/+}$ mice, and 1.7 times smaller than in control mice (Publication 1, Fig. 2G). This indicates that no recombination prevented the truncation of FUS in these cortical excitatory neurons in *Fus*$^{Resc/+}$ mice. In addition, in the lumbar spinal cord, no motor neurons (identified based on their localisation, size and shape) were found to express Cre, as evidenced with the tdTomato fluorescent protein labelling (Publication 1, Fig. 1B). This was further confirmed by the nuclear-to-cytoplasmic ratios of FUS in the spinal motor neurons of 15-day-old Trunc$^{+/-}$ and Trunc$^{-/-}$ pups, which were similar to the ratio found in control mice (Publication 2, Fig. 3H). It can thus be concluded that in these mice, FUS was not truncated in spinal motor neurons, and this finding is likely to be applicable to cortical motor neurons as well.

2. Was our targeting of inhibitory neurons efficient?

In the frontal cortex, 10% of the cells labelled with a neuronal marker exhibited an active Cre recombinase (Publication 1, Fig. 1D), which is consistent with the observation that GABAergic neurons constitute 10 to 15% of all cortical neurons in rodents (Meyer et al., 2011). Given that conventional immunofluorescence protocols do not allow to label all inhibitory neurons with a single antibody, I focused on neurons expressing parvalbumin, which have been the subject of more extensive study than other populations in the brains of ALS and FTD mouse models. We found that 38% of the Cre-expressing cells were parvalbumin neurons (Publication 1, Fig. 1F). In the mouse neocortex, parvalbumin

neurons represent approximately 40% of all GABAergic inhibitory cells (Tremblay et al., 2016). This suggests that we effectively targeted most of this population.

However, our immunohistological approach revealed that "only" 61% of the parvalbumin neurons underwent effective recombination (Publication 1, Fig. 1F). As previously discussed, this discrepancy may be attributed to various technical limitations. It is possible that both the Cre-expressing and the reporter mouse lines are not entirely reliable, and that they may display some minor irregularities regarding the Cre recombinase activity and the effective production of tdTomato fluorescent protein. The histological and imaging processes can also result in inherent limitations, which preclude the presentation of these data as a precise and definitive investigation of the proportion of parvalbumin neurons in the mouse cortex.

Another alternative explanation is that some of these neurons do not express *Vgat*. A mouse line in which Cre was expressed under the control of the endogenous promoter of the *Pvalb* gene, encoding parvalbumin, was recently characterised (Palicz et al., 2024). In the cortex, Cre was found to be active in a small proportion of cells expressing the vesicular glutamate transporter VGLUT1, which is an acknowledged marker of excitatory neurons. This colocalisation was observed almost exclusively in the cortical layer 5, which was included in our analysis. Whether these neurons express *Vgat* remains to be investigated. If this is not the case, this could explain, at least partially, why some parvalbumin neurons did not display a clear Cre recombinase activity.

It should also be noted that, although Cre is supposed to be active in all *Vgat*-positive cells, there may be variations in its expression and activity within a population of cells. Upon examination of the nuclear-to-cytoplasmic ratio of FUS, we observed a degree of variation within a given animal or section. However, we did not distinguish two distinct populations in which the recombination would have been effective for a subset of neurons but not for the others. In addition, in cell types where *Fus* was not mutated, we also observed intra-individual variations in the nuclear-to-cytoplasmic ratio of the protein, indicating that FUS expression and localisation are also variable.

The specificity and efficacy of the targeting of inhibitory neurons in the lumbar spinal cord are currently under analysis. Our preliminary results show that the localisation of neurons exhibiting an active Cre recombinase is consistent with the expected localisation of inhibitory neurons in the murine spinal cord. Although the specificity and efficacy of a Cre-Lox recombination approach are never 100% reliable, our results indicate that this remains a relevant experimental design to assess the contribution of inhibitory neurons to motor and social phenotypes in mice.

3. Was FUS completely depleted from the nucleus in Trunc$^{-/-}$ pups?

The NLS domain of FUS is thought to be necessary for the nuclear import of the protein (Dormann et al., 2012, 2010; Kino et al., 2011). As a consequence, deleting exon 15, which encodes the NLS domain, in the murine *Fus* gene is sufficient to induce the cytoplasmic accumulation of the protein. However, in our homozygous Trunc$^{-/-}$ pups, low concentrations of FUS were still detected in the nucleus (Publication 2, Fig. 1C). Previous studies also reported that despite the total loss of the NLS domain, FUS is not completely depleted from the nucleus in cell culture experiments (Gonzalez et al., 2021; Kino et al., 2011) and in mice (Ali et al., 2023). In particular, it was shown that transportin-1 can still bind FUS with moderate affinity when the NLS domain is completely absent (Gonzalez et al., 2021). Arginine residues in two domains enriched in arginine and glycine motifs (RGG2 and RGG3) play important roles in this weak and transient binding, and these are still present in our mouse models. Hence, the nuclear import of mutant FUS is still possible, and is likely mediated by transportin-1, but also possibly by other importins. This means that our approach does not allow us to study the consequences of a total loss of FUS nuclear functions, even in homozygous pups. However, the nuclear-to-cytoplasmic ratio of FUS was greatly decreased in Trunc$^{-/-}$ mice compared to heterozygous Trunc$^{+/-}$ mice (Publication 2, Fig. 1D), and this was driven both by a loss of the normal nuclear localisation and a cytoplasmic accumulation. Of note, in ALS and FTD patients, cells retain at least some of the normal diffuse nuclear localisation of FUS, even when FUS inclusions are present in the nucleus (in FTD) and/or the cytoplasm (in ALS and FTD).

4. Does FUS cytoplasmic accumulation alter neuronal density?

A previous characterisation of *Fus*$^{\Delta NLS/+}$ mice reported that the density of cortical parvalbumin neurons remains unaltered at 10 months of age (Scekic-Zahirovic et al., 2021). In the present study, we took advantage of our immunohistological analysis of FUS subcellular localisation to assess the density of excitatory and inhibitory neurons at earlier time points. In 2-month-old *Fus*$^{\Delta NLS/+}$ and *Fus*$^{Resc/+}$ mice compared to control mice, the cytoplasmic accumulation of FUS was not accompanied by a loss of cortical parvalbumin neurons (Publication 1, Fig. 2F), nor a loss of layer 5 excitatory pyramidal neurons (data not shown). The same observation was made for 15-day-old heterozygous and homozygous *Fus*^{Trunc} mice compared to control mice, as comparable numbers of parvalbumin cells were observed (data not shown). In heterozygous *Fus*$^{Trunc/+}$ mice, this was further confirmed by an absence of inhibitory neuron loss at 2 months of age (Publication 1, Fig. 6F), which was also accompanied by an unaltered number of excitatory neurons (data not shown). All these results are preliminary because only two to four mice per genotype were included in most experiments.

To draw a definitive conclusion regarding the consequences of FUS cytoplasmic accumulation on neurogenesis and/or neuronal loss, it will be necessary to increase the number of mice under investigation. This is particularly true for homozygous Trunc$^{-/-}$ pups. Given that half of these pups die before weaning, whereas the other half survive, it is plausible that some pathogenic mechanisms occur in the former but not in the latter. As a consequence, we may identify two distinct subgroups of Trunc$^{-/-}$ pups in our immunohistological analyses. An additional analysis at a later stage may also prove beneficial for heterozygous mice. To this end, I recovered tissues at 12 months of age, after the end of the longitudinal studies. With all these tissues, it would be interesting to verify the density of neurons using a general marker such as NeuN and then proceed to examine more precisely subpopulations of excitatory and inhibitory neurons. As discussed in the following section, it would also be interesting to assess alterations in the spinal cord. Of note, the density of NeuN-positive cells in the frontal cortex, as well as the thickness and lamination of the cortex, were reported unaltered in *Fus*$^{\Delta NLS/+}$ mice at 10 and 22 months of age (Scekic-Zahirovic et al., 2021). Conversely, it was proposed that FUS is involved in the neurodevelopment of the human central nervous system (Zou et al., 2022). The complete deletion of *FUS* in organoids derived from human induced pluripotent stem cells was observed to increase neural proliferation and differentiation in the brain, a decrease neural development in the spinal cord. It appears that the partial loss of function and toxic gain of function associated with the cytoplasmic accumulation of FUS do not recapitulate this phenotype in our mouse lines. This discrepancy may be attributed to the fact that both the underlying mechanisms and species are different.

In line with this observation, our laboratory and others proposed that mutant FUS induces a synaptopathy rather than major neuronal loss (Sephton et al., 2014). In particular, throughout the disease course, alterations of the GABAergic network were observed both in the pre- and postsynaptic compartments in *Fus*$^{\Delta NLS/+}$ mice (Sahadevan et al., 2021; Scekic-Zahirovic et al., 2021). It has been suggested that the synaptic accumulation of mutant FUS is the cause of these impairments. Therefore, it may be more relevant to assess potential synaptic alterations in our novel mouse models. To this end, immunohistological analyses could be performed to quantify the density of synaptic markers, which is of particular interest, given the growing evidence that ALS and FTD are characterised by synaptic dysfunctions (Mora and Allodi, 2023), while major neuronal loss may be a feature of the end stage of the diseases.

Mechanisms underlying the observed motor deficits

To assess motor deficits in our adult mice, we decided to conduct the four-limb inverted grid test every two months from 2 to 12 months of age. This decision was based on previous characterisations of the *Fus*$^{\Delta NLS/+}$ mouse line by our laboratory. The initial characterisation of these mice revealed that until 22 months of age, male mice do not exhibit altered performances in the rotarod or grip strength tests (Scekic-Zahirovic et al., 2017). However, a reduction in muscle strength was effectively observed at 10 months of age using the four-limb inverted grid test. A subsequent longitudinal study of *Fus*$^{\Delta NLS/+}$ mice demonstrated that this mild phenotype manifests progressively with age (Sanjuan-Ruiz et al., 2021). Following minor adaptations, this test was also applicable to 15-day-old pups. Overall, in our study, we observed that the rescue of FUS nuclear localisation in *Vgat*-expressing inhibitory neurons delayed the onset of motor deficits in female mice but not in male mice. Conversely, the heterozygous mutation of *Fus* in these neurons was not sufficient to induce motor deficits in mice, irrespective of their sex. However, the homozygous mutation of *Fus* in inhibitory neurons induced muscle strength deficits at 15 days of age in both females and males. From these results, it appears that the contribution of inhibitory neurons to ALS-like motor defects is complex to ascertain, and likely contingent on the extent of FUS delocalisation and sex.

1. Do inhibitory neurons contribute to FUS-related motor defects?

In *Fus*$^{\Delta NLS/+}$ mice, both motor neuron autonomous and non-autonomous mechanisms contribute to muscle weakness. Indeed, the rescue of FUS nuclear localisation in cholinergic neurons was shown to be sufficient to prevent motor neuron degeneration, yet only delayed the onset of motor impairments, as evaluated with the four-limb inverted grid test (Scekic-Zahirovic et al., 2017). This indicates that additional cell types are involved in the progression of this phenotype. Our analysis of adult heterozygous mice suggests that the expression of mutant *Fus* in inhibitory neurons is not sufficient to cause motor defects. Indeed, no impairment of muscle strength was observed in *Fus*$^{Trunc/+}$ female and male mice during their postnatal development (Publication 2, Fig. 2H-2K) or in adulthood (Publication 1, Fig. 7D and 7E). However, when both copies of *Fus* were mutated in inhibitory neurons, muscle weakness was observed two weeks after birth.

We cannot exclude that motor impairments may manifest at a later age in *Fus*$^{Trunc/+}$ mice. An alternative hypothesis is that the heterozygous mutation of *Fus* does not induce inhibitory neuron impairments with subsequent effects on the motor phenotype. Interestingly, the delayed onset of motor defects in *Fus*$^{Resc/+}$ females (Publication 1, Fig. 3D and 3E) suggests that the expression of mutant *Fus* in inhibitory neurons is required to the onset of the phenotype. One potential explanation for this discrepancy is that FUS-related motor defects may be caused by a synergistic effect of

alterations in multiple cell types. In *Fus*$^{Resc/+}$ mice, most cell types display FUS delocalisation and may therefore accumulate sufficient alterations to trigger motor deficits, which may not occur in *Fus*$^{Trunc/+}$ mice.

In *Fus*$^{\Delta NLS/+}$ mice, it was previously proposed that impairments of myelinating cells, in the spinal cord and/or periphery, contribute to the observed motor deficits (Scekic-Zahirovic et al., 2017). However, the cytoplasmic accumulation of FUS in mature oligodendrocytes was insufficient to induce a reduction in performance in the four-limb inverted grid test in heterozygous and homozygous mice up to 10 months of age (Jamet al., in preparation). A similar observation was made when FUS delocalisation was induced exclusively in adult projection neurons (Publication 3). In TDP-43^{Q331K} mice, the removal of mutant TDP-43 from motor neurons also prevented their loss, although this only delayed the onset of motor symptoms, as evaluated with the rotarod test (Ditsworth et al., 2017). In *SOD1*^{G73R} mice, the disease onset and progression can be accurately evaluated by monitoring the loss of body weight. This demonstrated that the removal of mutant SOD1 from motor neurons or oligodendrocytes delays the disease onset (Boillée et al., 2006; Kang et al., 2013), whereas the removal from astrocytes or microglia slows the disease progression (Boillée et al., 2006; Yamanaka et al., 2008). The consequences of removing mutant TDP-43 or SOD1 from inhibitory neurons have yet to be investigated. Nevertheless, the current results collectively point towards multicellular alterations in ALS (Crabé et al., 2020). It remains unclear whether the alterations to a specific cell type are the initial event that triggers the disease. In *Fus*$^{\Delta NLS/+}$ mice, the relatively mild and difficult-to-observe motor defects may limit our comprehension of the involvement of different cell populations when characterising cell-type-specific knock-in mice.

Indeed, it is important to note that the evaluation of motor deficits was limited to the four-limb inverted grid test, which may not have provided a comprehensive assessment of the phenotype. The methodology I employed followed the established protocol for the evaluation of muscular strength and endurance in mouse models. However, a potential lack of engagement of the mice may have introduced a bias in the results. Our control mice displayed a gradual decline in hanging time and holding impulse with age. This phenomenon has been previously observed by our laboratory (Sanjuan-Ruiz et al., 2021) and others (Yanai and Endo, 2021). In particular, in C57BL/6J wild-type male mice, it was shown that hanging time begins to decline at 6 months of age. However, the underlying cause of this decrease remains a topic of contention. Although this may indicate a gradual decline in motor functions, other parameters can cause, or at least influence, this phenotype. For instance, the age-related increase in body weight and a progressive loss of motivation may result in a decreased hanging time, while the motor function of the mice remains intact. Following this hypothesis, the use of the rotarod or grip strength tests has suggested that the motor functions commence to decline at a later stage in wild-type mice (Börsch et al., 2021; Noda et al., 2020; Shoji and Miyakawa, 2019; Yanai and

Endo, 2021). Furthermore, aged C57BL/6J wild-type males were shown to exhibit reduced motivation compared to their younger counterparts (Jackson et al., 2021). In our cohort, we observed that, with age and/or the repetition of the test, mice were more likely to jump from the grid, even at the outset of the test. This may reflect a lack of engagement rather than muscle fatigue, as these mice were able to hang onto the grid of their home cage for a longer time. This was especially true for males, which were more prone to jumping than females. Therefore, our current results may not be sufficient to draw a definitive conclusion about the contribution (or lack of contribution) of FUS delocalisation in inhibitory neurons to motor phenotypes.

The initial characterisation of the *Fus*$^{\Delta NLS/+}$ mice compared to control mice revealed no discernible difference when their body weight was monitored (Sanjuan-Ruiz et al., 2021) or when the grip strength test was used (Scekic-Zahirovic et al., 2017). This indicates that more sensitive tests are necessary to monitor motor defects in this mouse line. No motor test is without flaws, as they rely on the engagement of the mice (which may decline with the repetition of the tests and the age of the mice) and/or the experimenters. Nevertheless, it may be worthwhile to try a modified version of the grip strength test, which was reported to enhance the validity, consistency, and sensitivity of the test (Takeshita et al., 2017). In addition, it would be beneficial to identify molecular alterations relevant for the observed motor defects. The examination of neuromuscular junction alterations appears to be more pertinent than the observation of motor neuron loss, given that the latter only becomes apparent several months after the onset of motor defects (Scekic-Zahirovic et al., 2017), whereas the former can be observed several months prior to this onset (Picchiarelli et al., 2019). As a result, I recovered the hindlimb muscles of 2- and 12-month-old mice, and it may be of interest to ascertain whether denervation is less pronounced in *Fus*$^{Resc/+}$ females compared to *Fus*$^{\Delta NLS/+}$ mice.

2. Are cortical inhibitory neurons impaired in *Fus*$^{\Delta NLS/+}$ mice?

In ALS patients, a reduction in cortical inhibition may be associated with increased motor dysfunction. In particular, the decreased binding of [^{11}C]flumazenil in the dominant hemisphere was correlated with increased impairments of upper motor neurons (Turner et al., 2005a). The reduced short intracortical inhibition was also correlated with the progression of motor impairments and functional deterioration (Shibuya et al., 2017; Van den Bos et al., 2018), but not in all studies (Menon et al., 2020). In addition, FTD patients with motor deficits exhibited lower short intracortical inhibition than patients without motor neuron disease (Burrell et al., 2011). In other pathological conditions, reduced GABA concentrations and the potential subsequent lack of inhibition were proposed to cause motor impairments. In patients with multiple sclerosis, lower GABA concentrations in the sensorimotor cortex was associated with reduced function in the upper and lower contralateral limbs, including a decrease in grip and muscle strength (Cawley et al., 2015).

In chronic stroke survivors, reduced short intracortical inhibition during a manual dexterity task was associated with decreased motor functions (Ding et al., 2018).

In mice, the loss of cortical and cerebellar inhibitory neurons (resulting from elevated apoptosis during the postnatal period of programmed cell death) was associated with early motor deficits (Carriere et al., 2020). This was not assessed in adult mice but the appearance of spontaneous seizures and decline in body weight may bias the evaluation of the motor phenotype in this mouse line. In the *SOD1*^{G93A} mouse model, it was demonstrated that a reduction in inhibitory inputs from cortical parvalbumin neurons results in an increased excitability of pyramidal neurons, which may be responsible for the observed motor defects (Khademullah et al., 2020). Indeed, increasing the activity of inhibitory neurons normalised the excitability of motor neurons and delayed the onset of motor impairments. The latter was evaluated through a series of tests including the grip strength, rotarod and four-limb inverted grid tests, as well as footprint analysis. In *TDP-43*^{A315T} mice, it was also shown that GABAergic neurons impairments contribute to the increased excitability of pyramidal neurons (Zhang et al., 2016), but the direct effect on motor defects is yet to be investigated.

In *Fus*$^{\Delta NLS/+}$ mice, motor defects appear around 4 months of age, as demonstrated in the present study (Publication 1, Fig. 3D and 3E) and in a previous one (Sanjuan-Ruiz et al., 2021). At that time, GABAergic gene and protein levels are increased in the brain (Sahadevan et al., 2021; Scekic-Zahirovic et al., 2021). However, we do not know if GABAergic synapses are stable, and if GABAergic transmission is altered. It would be interesting to perform electrophysiological recordings to investigate the activity of inhibitory and motor neurons in *Fus*$^{\Delta NLS/+}$ mice, and to verify if the subcellular localisation of FUS influences the results in our novel mouse lines. In addition, it would be interesting to silence or activate inhibitory neurons before the appearance of motor defects in *Fus*$^{\Delta NLS/+}$ mice (via chemogenetic tools for instance) to evaluate the consequences on motor impairments. However, to perform such an experiment, one would need to be sure to have a sensitive and consistent test to evaluate motor deficits.

3. Are spinal inhibitory neurons impaired in *Fus*$^{\Delta NLS/+}$ mice?

One limitation of our study is that we focused our evaluation of motor deficits on muscle strength. Yet, spinal inhibitory neurons were convincingly involved in the control of locomotion (Britz et al., 2015; Gosgnach et al., 2006; Lanuza et al., 2004; Zhang et al., 2014). Furthermore, in the *SOD1*^{G93A} mouse model, it was shown that an early and selective loss of glycinergic synapses on motor neurons innervating fast-twitch fatigable fibres was accompanied by specific locomotor alterations (Allodi et al., 2021). This could be recapitulated by silencing V1 inhibitory neurons, and effectively rescued by stabilising V1 inhibitory connections on motor neurons (Mora et al., 2024).

Could a loss of V1 inhibitory synapses underly locomotor defects in *Fus*$^{\Delta NLS/+}$ mice? The genetic ablation or silencing of V1 neurons was shown to decrease locomotor speed and intralimb extension, without disrupting coordination (Gosgnach et al., 2006). In *SOD1*^{G93A} mice, locomotor defects were evaluated using a treadmill with a defined constant speed and videos to track the movements of the mice (Allodi et al., 2021). This showed that over time, these mice were progressively incapable to cope with the speed of the belt. These mice also exhibited decreased capability of accelerating, decreased step frequency, and reduced stride length (i.e., shorter steps). This phenotype was not associated with alterations in the left-right hindlimb coordination, but a mild alteration of the homolateral interlimb coordination (right forelimb versus right hindlimb or left forelimb versus left hindlimb) was noted. Such evaluation of the locomotor phenotype in *Fus*$^{\Delta NLS/+}$ mice was not performed. However, a CatWalk analysis was previously used to assess the gait parameters of freely moving mice (Scekic-Zahirovic et al., 2017). At 10 months of age, this revealed a reduction in the hind limb stride length and an increase in the variation of the speed of the walk. At 22 months of age, this was accompanied by a decreased body and swing speed. Overall, *Fus*$^{\Delta NLS/+}$ mice demonstrated an irregular walking pattern with phases of fast walking interrupted by standing phases. This locomotor phenotype may be reminiscent of an impairment of V1 inhibitory neurons.

Interestingly, In *SOD1*^{G93A} mice, the loss of V1 synapses on motor neurons was proposed as the direct cause of the observed locomotor phenotype, which could be an early indicator of ALS progression, as this appeared before the loss of motor neurons and grip strength (Allodi et al., 2021). The assessment of inhibitory neurons in the spinal cord of *Fus*$^{\Delta NLS/+}$ mice is yet to be conducted. It would be interesting to verify whether V1 inhibitory synapses and somas are also lost in this mouse model. If this were to be the case, then we could use the novel mouse lines we created to assess the contribution of the cytoplasmic accumulation of FUS to this phenotype. Of note, a RNAseq analysis was conducted on the lumbar spinal cord of a different knock-in mouse model in which the NLS domain is removed upon *Fus* mutation (Devoy et al., 2017). In these mice, the loss of motor neurons was observed at 12 months of age. Concurrently, the analysis of the dysregulated genes revealed an enrichment for genes encoding mitochondrial and ribosomal proteins, as well as the catalytic subunits of the proteasome. However, no marked alterations in inhibitory neurons were observed. Among the downregulated genes (log2 fold change ≃ -0.6, adjusted p value ≃ 0.09) were *Pvalb*, *Gabra4* and *Gabrg1*.

4. Could Trunc$^{-/-}$ pups model a juvenile motor neuron disease?

In Trunc$^{-/-}$ pups, early deficits in muscular strength and endurance were observed using two hanging tests (Publication 2, Fig. 2H-2K). This was not accompanied by alterations in motor coordination, as their performance during the negative geotaxis test was comparable to that of control pups (Publication 2, Fig. S1D-S1F). However, this was

followed by the death of half of the pups before weaning (Publication 2, Fig. 1F). The extent of FUS delocalisation was found to be inversely correlated to the age of onset of ALS (Dormann et al., 2010). When comparing Trunc$^{+/-}$ mice to control mice, we observed a 1.2- to 1.3-fold decrease in the nuclear-to-cytoplasmic ratio of FUS in inhibitory neurons (Publication 1, Fig. 6D and Publication 2, Fig. 1D). This cytoplasmic accumulation was further enhanced in Trunc$^{-/-}$ pups, for which the ratio was 2.8 times smaller than in control pups, and 2.3 times smaller than in Trunc$^{+/-}$ pups. Motor defects were not observed in Trunc$^{+/-}$ mice up to 1 year, while they were present 15 days after birth in Trunc$^{-/-}$ pups. It is tempting to suggest that the age of onset was decreased due to an increased delocalisation of FUS, but could Trunc$^{-/-}$ pups recapitulate juvenile ALS?

Juvenile ALS (diagnosis before 25 years) is a very rare disorder, and paediatric ALS (diagnosis before 18 years) is even more uncommon. To date, *FUS* mutations have been identified in approximately half of juvenile and paediatric cases (Picher-Martel et al., 2020). The other half is associated with mutations in other genes or unknown causes. *FUS* mutations were found in the C-terminal region of the protein, including the NLS domain, and are thought to impair its nuclear import. Of note, some of these mutations result in the partial or complete deletion of the NLS domain. For instance, the R495X mutation creates a premature stop codon resulting in the complete loss of the NLS domain, and has been associated with a severe phenotype (Bosco et al., 2010; Waibel et al., 2010). In Trunc$^{-/-}$ pups, we induced a complete truncation of the NLS domain, and effectively impaired FUS nuclear import resulting in the cytoplasmic accumulation of the protein (Publication 2, Fig. 1C and 1D). However, this was exclusive to inhibitory neurons, which is not the case in patients. In addition, early-onset and aggressive ALS cases are characterised by neuronal cytoplasmic inclusions of FUS in the primary motor cortex, brainstem and spinal cord, while glial cytoplasmic inclusions are absent or sparse (Mackenzie et al., 2011a). Given that this histological hallmark is not recapitulated in mouse models (Devoy et al., 2017; López-Erauskin et al., 2018; Scekic-Zahirovic et al., 2017), we did not evaluate inclusions in Trunc$^{-/-}$ pups. Overall, this novel mouse does not directly recapitulate the aetiology of juvenile ALS but allows to study some of the biological processes in which FUS is involved, which was our objective.

In early-onset ALS cases associated with *FUS* mutations, the first symptoms manifest during the adolescence, and progress at an extremely rapid rate. The median disease duration is approximately 1 year for juvenile patients with *FUS* mutations and 2 years for paediatric patients with *FUS* mutations, while it is more than 12.5 years for the other juvenile cases (Chen, 2021; Picher-Martel et al., 2020). Comparing human and mouse ages is complicated, because maturation and aging occurs at different rates in the two species, and these processes are still the focus of ongoing research. However, using a survival curve based on a large cohort of C57BL/6J female and male mice, it was proposed that mice between 1 and 3 months of age correspond to adolescent humans between 12.5 and

20 years of age (Flurkey et al., 2007). Given that the motor deficits are observed 15 days after birth in Trunc$^{-/-}$ pups and are followed by premature death 20 days after birth, this phenotype arises too early to be representative of ALS with an adolescent onset.

Juvenile and paediatric patients present either a spinal or a bulbar onset, with respiratory failure (Chen, 2021; Picher-Martel et al., 2020). The hanging tests were effective in evaluating motor deficits related to alterations in limb muscles. It would be interesting to complete this phenotyping by evaluating potential alterations in bulbar muscles. More importantly, this could explain the reduced body weight if feeding behaviours are prevented by diminished muscle strength in the jaw and/or dysphagia. Two tests have been employed in *SOD1*^{G93A} mice to assess tongue motility and force (Smittkamp et al., 2008) or swallowing (Osman et al., 2020) when drinking a liquid solution. However, these tests were developed in adult mice and seem difficult to adapt to 15-day-old pups. An alternative approach would be to assess the density of motor neurons in the brainstem. Our preliminary analysis indicated that there was no loss of motor neurons in the lumbar spinal cord at 15 days of age (Publication 3, Fig. 3C). In *Fus*$^{\Delta NLS/+}$ mice, as in other mouse models of ALS, it is established that motor neuron loss appears after the onset of motor deficits (Scekic-Zahirovic et al., 2017). Therefore, it may be relevant to evaluate motor neuron density in end-stage pups. This is not a time point we included in the present study, because no early criteria have yet been identified to predict which homozygous pups will die and which will survive, or when the death will occur. In addition, it was not possible to recover tissues after death, due to extended *post-mortem* durations.

Some juvenile patients carrying *FUS* mutations exhibit intellectual disabilities (Goldstein et al., 2022; Yamashita et al., 2012; Yan et al., 2010; Yu et al., 2018). However, this phenotype is difficult to assess in pups. The cognitive tests and learning paradigms were developed for adult mice, and most of them cannot be adapted to young pups. Indeed, the behavioural repertoire is constrained in pups younger than two weeks of age. The most prevalent experimental strategy currently used to phenotype mouse models of neurodevelopmental disorders is the evaluation of ultrasonic vocalisations. This is a reliable tool to assess neonatal alterations, notably those associated with communicative and social deficits, during the first two weeks after birth (Scattoni et al., 2009). The homing test and social odour preferences paradigms can also be used (Schaal et al., 2013), although they are contingent upon a number of functions that extend beyond those associated with intellectual disabilities. Indeed, associative and discriminative capabilities, as well as adequate olfactory and motor capabilities are required. All of these protocols remain to be tested in ALS mouse models. They may reveal alterations in Trunc$^{-/-}$ pups, but the link with intellectual disabilities would be weak. When mice are older than three weeks of age, a wide range of cognitive and learning tests are available. However, in our case, it would mean that only surviving Trunc$^{-/-}$ pups are tested, which may induce a bias in the results.

Mechanisms underlying the increased sociability

To assess social impairments in our adult male mice, we decided to conduct the three-chamber and home cage social tasks at 4 and 10 months of age. This decision was based on a previous characterisation of the *Fus*$^{\Delta NLS/+}$ mouse line by our laboratory, which revealed a tendency towards increased sociability at 4 months and a significant increase at 10 months (Scekic-Zahirovic et al., 2021). In our study, we observed that the rescue of FUS nuclear localisation in *Vgat*-expressing inhibitory neurons did not prevent the appearance of this phenotype at 4 months of age but restored social interest to control level at 10 months. The heterozygous mutation of *Fus* in these neurons was sufficient to induce increased social interest at 4 and 10 months of age. From these results, we can propose that inhibitory neurons contribute to FTD-like social defects in males. Due to logistic constraints, we could not conduct this analysis in females, so further investigation is needed to determine whether this phenomenon is common to both sexes.

It is noteworthy that a reduction in intracortical inhibition has been associated with disinhibited behaviours in FTD patients (Benussi et al., 2020; Murley et al., 2020). These can manifest in various ways, including social disinhibition with inappropriate statements and actions, impulsivity, perseverative, stereotyped and/or obsessive behaviour, to mention just a few. In adult mice, a number of tests are available for the evaluation of analogous behaviours (Vernay et al., 2016), although these remain to be used with our mouse models. For instance, it would be interesting to ascertain whether our models exhibit impulsive behaviours in the elevated plus maze or light/dark test, while compulsive behaviours may be evaluated with the marble burying test.

1. Which mechanisms could underlie the increased sociability?

In this study we focused on social behaviours as we already knew that they are impaired by the cytoplasmic accumulation of FUS (Scekic-Zahirovic et al., 2021). In addition, there is an extensive literature concerning the role of the excitation-inhibition balance in the regulation of sociability, even though most of the underlying mechanisms remain unknown. In particular, it was proposed that the "deterioration of inhibitory synapses may be an essential neurological basis underlying abnormal social behaviours" (Ju et al., 2023). However, in several pathological conditions, higher levels of excitation and/or lower levels of inhibition have been associated with decreased social interest. This is the case, for instance, in mouse models of autism (Parrella et al., 2024) or schizophrenia (Liu et al., 2021). In FTD patients, social impairments can manifest either as a loss of sympathy and empathy or as a disinhibited behaviour, but in mice, a decreased sociability was almost exclusively reported (Vernay et al., 2016). We observed the opposite phenotype in our mouse models, and interestingly this increased sociability was also detected when *Fus* was silenced specifically in the hippocampus (Udagawa et al., 2015).

How could impairments in inhibitory neurons explain the increased sociability related to FUS? The characterisation of mouse lines with increased social interest and inhibitory neuron impairments allowed to propose two potential underlying mechanisms: the alteration of GABAergic gene expression, and the alteration of GABAergic synapses and circuits. One of these models was based on the decreased expression of *Dlx* genes (Fazel Darbandi et al., 2021). These genes encode homeodomain transcription factors which are notably necessary for the development and differentiation of GABAergic neurons. In these mice, a transient decrease in the expression of genes related to GABA synthesis and a transient reduction in the number of GABAergic neurons were observed during the embryonic development. It was then proposed that this disruption or delay in GABAergic neuronal development could have long-lasting effect on neural circuits, which could underlie the increased sociability observed in young adults. However, this hypothesis remains to be tested. Patients with mutations in the *POGZ* gene, which encodes a protein involved in transcriptional silencing and modulation of chromatin architecture, sometimes exhibit overly social and overly friendly behaviours (Stessman et al., 2016). In a mouse model carrying a homozygous deletion of this gene, several transcriptomic alterations were reported in genes involved in neurogenesis, metabolism and synaptic processes (Suliman-Lavie et al., 2020). This included an upregulation of GABAergic genes in the cerebellum, which was the cerebral region of interest in this study. The authors then proposed that this could underlie the increased sociability. To finish, mutations in the *CYLD* gene were recently associated to ALS and FTD (Dobson-Stone et al., 2020). In the mammalian brain, CYLD has important roles at the synapses. It promotes their remodelling and plasticity, notably by inhibiting the Akt-mTOR pathway which, in turn, enhances autophagy. In knockout mice, this upstream control of the Akt-mTOR pathway was lost, and the resulting decrease in autophagy caused impaired synaptic number, efficacy and plasticity (Zajicek et al., 2022). The authors proposed that this may explain the increased sociability observed in these mice.

In the brain of *Fus*$^{\Delta NLS/+}$ mice, both GABAergic gene expression and GABAergic synapses were found to be altered (Sahadevan et al., 2021; Scekic-Zahirovic et al., 2021). Briefly, the protein levels of $GABA_A$ receptors containing the α3 subunit were found to be decreased at 1 month of age. At 6 months of age, there was an increased expression of two genes encoding subunits of $GABA_A$ receptors (*Gabra1* and *Gabrb1*). This was accompanied by increased expression of GABAergic proteins in potentially unstable inhibitory synapses. In particular, the absence of increased expression of gephyrin, a postsynaptic protein responsible for the anchoring of $GABA_A$ receptors (Specht et al., 2013), suggests a disorganisation of the postsynaptic compartment, which in turn can decrease inhibitory transmission. At 10 months of age, an increase in spontaneous neuronal activity levels was observed and was proposed as the potential cause of the altered sociability (Scekic-Zahirovic et al., 2021). At 22 months of age, GABAergic protein levels were decreased, which may directly decrease inhibitory transmission. Finally, the

ultrastructure of inhibitory synapses was abnormal, with an increased size and number of vesicles, which could be compensatory to their decreased density.

In our study, the increased social interest in 4-month-old *Fus*$^{Trunc/+}$ males was also accompanied by increased neuronal activity in comparison to control mice (Publication 1, Fig. 8B, 8C and 9). At the same age, we observed an increased sociability in *Fus*$^{Resc/+}$ males, reaching levels comparable to those of *Fus*$^{\Delta NLS/+}$ males (Publication 1, Fig. 4B and 4C). However, the spontaneous neuronal activity levels were reduced in *Fus*$^{Resc/+}$ mice compared to *Fus*$^{\Delta NLS/+}$ mice (Publication 1, Fig. 5). This suggests that other mechanisms are involved in the observed social phenotype. It would be interesting to investigate synaptic gene and protein levels in *Fus*$^{\Delta NLS/+}$ and *Fus*$^{Resc/+}$ mice to see if they share some alterations, which may underlie the increased sociability. However, for the moment, no tissues were recovered at this age, as the mice were included in longitudinal studies. At 10 months of age, we observed an increased social interest in *Fus*$^{Trunc/+}$ and *Fus*$^{\Delta NLS/+}$ males, but not in *Fus*$^{Resc/+}$ males for which the interest was similar to those of control mice (Publication 1, Fig. 4D, 4E, 8D and 8E). It suggests that rescuing FUS nuclear localisation in inhibitory neurons is sufficient to attenuate social impairments in aged male mice. Given that we recovered tissues at 12 months of age, an alternative approach would be to assess synaptic gene and protein levels at this age, and to focus on the alterations which would differ between *Fus*$^{\Delta NLS/+}$ and *Fus*$^{Resc/+}$ mice. This may highlight molecular mechanisms potentially linked to the increased sociability in *Fus*$^{\Delta NLS/+}$ mice, as well as protective mechanisms in *Fus*$^{Resc/+}$ mice.

Interestingly, inhibitory neurons were also found to be involved in the social reward system, which plays a critical role in prosocial interaction behaviours. In particular, dopaminergic neurons projecting from the midbrain ventral tegmental area to the nucleus accumbens were found to produce a rewarding effect, and to mediate prosocial behaviours (Gunaydin et al., 2014). It was shown that somatostatin neurons projecting from the basal forebrain to GABAergic neurons localised in the ventral tegmental area exert an inhibitory influence on these neurons, which in turn disinhibits local dopaminergic neurons during social interaction (J. Wang et al., 2021). In particular, the optogenetic inhibition of these somatostatin neurons decreased the release of dopamine and abolished social preference. At the same time, another study demonstrated that the activation of *Vgat*-expressing neurons in the medial amygdala promotes dopamine release in the nucleus accumbens (Hu et al., 2021). This effect was both necessary and sufficient to promote positive reinforcement of social interactions. Although the underlying circuit explaining how these GABAergic neurons promote dopamine release remains to be identified, we can posit that disinhibitory mechanisms may be involved. From these studies, we can also hypothesise that a loss of inhibitory influence on these dopaminergic neurons would result in increased social reward and prosocial behaviours.

It was proposed that FTD patients with a behavioural variant are indifferent to social reward (Perry et al., 2015). However, a more recent study highlighted that high emotional apathy is indeed associated with impaired social reward in patients with dementia, including FTD and Alzheimer's disease patients (Wong et al., 2023). Conversely, learning of social rewards was not impaired in patients exhibiting low emotional apathy. Hence, we would need to assess social reward in overly friendly FTD patients and mouse models to verify if this phenotype is associated with increased reward.

2. Does this highlight an increased perseverance?

As previously outlined in the Results (page 148), the use of the three-chamber social task may have highlighted an increased perseverance in our mouse models. Indeed, the increased social phenotype was predominantly attributable to augmented interaction durations during the second or third trial (Publication 1, Fig. 4C, 4E, 8C and 8E). This indicates that during the initial five minutes of the test (first trial), the social phenotype of the mouse lines of interest was not markedly different from that of control mice. Furthermore, in 10-month-old *Fus*$^{\Delta NLS/+}$ males, the 5-minute home cage social task did not reveal increased sociability (Publication 1, Fig. 10D and 10E), potentially due to the test duration being insufficient.

In FTD patients, perseverative behaviours are rather common, irrespective of the clinical variants or pathological inclusions observed in these patients (Scarioni et al., 2020). In the classification of the core behavioural symptoms of FTD, they are associated with stereotyped and compulsive behaviours (Rascovsky et al., 2011), which can manifest as simple repetitive movements or more complex rituals, such as hoarding and collecting (Moheb et al., 2019). Interestingly, in FTD patients with a behavioural variant, the repetitive behaviours are always associated with disinhibited or impulsive behaviours. These symptoms tend to worsen until intermediate stages of the disease course, and then progressively decrease in severity in more advanced stages (Cosseddu et al., 2020). In *Fus*$^{\Delta NLS/+}$ males, we effectively observed a worsening of the disinhibited social phenotype between 4 and 10 months of age, but for unknown reasons it was not the case in *Fus*$^{Trunc/+}$ males. Of note, perseverative and compulsive behaviours can also be observed in ALS patients with behavioural deficits (Trucco et al., 2024).

In mice, perseverative phenotypes can be evaluated using different paradigms (Silverman et al., 2010; Simmons et al., 2021). For instance, repetitive behaviours, such as self-grooming, can be scored, while the marble burying test can be interpreted as a repetitive digging behaviour (Thomas et al., 2009). In addition, the flexibility to switch from an established habit to a new one can be measured with reversal learning tasks. A spatial habit can be established by reinforcing entries into a specific arm of a maze with a reward, or by locating a hidden escape platform in the Morris water maze. When the

reward or hidden platform is moved to another location, the capacity of the mouse to learn this new location is assessed. Mice which perform well on the initial acquisition but fail on the reversal phase exhibit either increased perseveration or specific alterations in reversal learning. Finally, mice tend to explore all aspects of a novel environment, therefore it has been proposed that the perseverative exploration of only few available objects in an open field may be analogous to restricted interests. It is important to note that the observed behaviours during some of these tests may be influenced by other factors, such as anxiety or learning deficits. Accordingly, the assessment of perseverance may require the use of a range of distinct paradigms.

To our knowledge, abnormal perseverance was suggested in two FTD mouse models. In TDP-43^{Q331K} males, a touchscreen apparatus was used to deliver a panel of behavioural tasks (Kim et al., 2020). In the progressive ratio task, mice were required to meet an increasing level of expectation when facing a given stimulus in order to earn a constant reward. Each session consisted of several trials, and the response decay rate between these trials was computed. When the decay rate is high, it means that with the increasing number of trials, mice become slower to engage in the task. TDP-43^{Q331K} mice exhibited a slower decay than control mice, suggesting a perseverative behavioural phenotype. In addition, during a visual discrimination and reversal learning task, TDP-43^{Q331K} mice required more trials to learn the new stimuli leading to a reward, and made more perseverative errors than control mice, indicating cognitive inflexibility manifested as stimulus-bound perseveration. In *SOD1*^{G93A} males, the Barnes maze was used to evaluate spatial navigation learning (Quarta et al., 2015). Over four days, the mice were placed in the maze and required to locate the target hole, which remained in the same position throughout the acquisition phase. On the fifth day, the target hole was closed to ascertain whether the mice had learned its location. *SOD1*^{G93A} mice spent a significantly greater amount of time in the vicinity of the closed target hole than control mice, which could be interpreted as impaired behavioural flexibility due to perseveration. This hypothesis is supported by a previous study, in which deficits in a fear extinction paradigm may also be caused by an increase in perseverance (Sgobio et al., 2008).

In *Fus*$^{\Delta NLS/+}$ mice, perseverative behaviours remain to be evaluated. However, previous characterisation using the Morris water maze showed that during the extinction phases, these mice do not spend more time in the location where the platform was previously hidden relative to other locations (Scekic-Zahirovic et al., 2021). This suggests that they may not display a tendency towards perseveration. In this cohort, both females and males were included. To date, our social tasks suggest an increased social perseverance in males only, as we did not include females in these experiments. As we are unaware of whether and how sociability is altered in *Fus*$^{\Delta NLS/+}$ females, it would be interesting to assess perseverance separately for both sexes. In addition, for females, it would be interesting to assess sociability first, as their results may differ from those obtained with males.

Contribution of FUS in the regulation of neuronal activity

To assess the role of FUS in the regulation of neuronal activity, our collaborators conducted *in vivo* two-photon calcium imaging in the motor cortex of 4-month-old anesthetised mice. This approach revealed that rescuing FUS nuclear localisation in *Vgat*-expressing inhibitory neurons is sufficient to reduce spontaneous neuronal activity levels in $Fus^{Resc/+}$ mice compared to $Fus^{\Delta NLS/+}$ mice. Conversely, inducing FUS cytoplasmic delocalisation in *Vgat*-expressing neurons is sufficient to increase activity levels in $Fus^{Trunc/+}$ mice compared to control mice. These results suggest that the subcellular localisation of FUS in inhibitory neurons influence the overall neuronal activity. This is in line with a previous characterisation of 10-month-old $Fus^{\Delta NLS/+}$ mice, in which the spontaneous neuronal activity levels were found to be significantly increased in comparison to control mice (Scekic-Zahirovic et al., 2021).

1. Which mechanisms could underlie the increased spontaneous neuronal activity?

Spontaneous neuronal activity corresponds to the firing of excitatory and inhibitory neurons in the absence of external stimuli. This non-evoked form of calcium-dependent synaptic transmission is a fundamental property of the nervous system (Kavalali, 2015). Given that FUS can regulate the organisation, integrity and functioning of excitatory and inhibitory synapses in mice (Husi et al., 2000; Sahadevan et al., 2021; Scekic-Zahirovic et al., 2021; Udagawa et al., 2015; Yokoi et al., 2017), this could ultimately influence spontaneous activity. In $Fus^{\Delta NLS/+}$ mice, previous results pointed towards major defects in both pre- and postsynaptic compartments of inhibitory synapses, which were recapitulated in the previous section (page 200). It was proposed that these transcriptomic, histological and ultrastructural alterations may underlie defective inhibitory neurotransmission, which in turn could explain the increase in spontaneous neuronal activity. However, with these data alone, it is not possible to know whether the increased neuronal activity is driven by excitatory and/or inhibitory neurons, and whether this is due to cell autonomous alterations in the intrinsic excitability of these neurons and/or to neural circuit defects.

To provide some answers, our collaborators conducted two-photon calcium imaging in 4-month-old $Fus^{\Delta NLS/+}$, $Fus^{Resc/+}$ and $Fus^{Trunc/+}$ mice. It should be noted that this study is subject to certain limitations due to technical constraints. The first limitation is linked to the restricted number of genotypes that could be included. As a result, $Fus^{Resc/+}$ mice were compared to $Fus^{\Delta NLS/+}$ mice in the absence of $Fus^{+/+}$ control mice. We observed a reduction in spontaneous neuronal activity levels in $Fus^{Resc/+}$ mice, as evidenced by a significant decrease in calcium transient frequency (Publication 1, Fig. 5D). Although it is not

possible to ascertain whether these levels would be comparable to those of wild-type mice, we posit that this observed reduction is due to heightened activity levels in *Fus*$^{\Delta NLS/+}$ mice, as previously observed (Scekic-Zahirovic et al., 2021). However, we recognise that this experiment is insufficient to substantiate such a conclusion. In comparison to control mice, the neuronal activity in *Fus*$^{Trunc/+}$ mice was significantly increased, as evidenced by a higher fraction of active neurons (Publication 1, Fig. 9C) and higher amplitudes of calcium transients (Publication 1, Fig. 9E). This suggests that the cytoplasmic accumulation of FUS in inhibitory neurons is sufficient to drive this phenotype.

The calcium sensor expression was under the control of the human Synapsin 1 promoter, which allows to selectively target neurons. Nevertheless, it was demonstrated that the ratio of excitatory to inhibitory neurons targeted is dependent on the tropism of the adeno-associated virus (AAV) and on its dilution. For instance, in the murine cortex, low doses of AAV2/1 were shown to induce transcription activity preferentially in inhibitory neurons, whereas high doses efficiently targeted both excitatory and inhibitory neurons (Nathanson et al., 2009). In the present study, AAV2/9 was used, and it is postulated that this vector targets excitatory neurons to a greater extent than inhibitory neurons (Sabine Liebscher, personal communication). Therefore, it can be proposed that the increased neuronal activity observed in *Fus*$^{Trunc/+}$ mice reflects an increased activity of excitatory neurons, resulting from alterations in inhibitory neurons. In particular, the cytoplasmic accumulation of FUS in *Vgat*-expressing neurons may have reduced their activity, which in turn would have led to a decrease in inhibitory transmissions in the brain. In addition, altered inhibitory neurons may have exerted a direct influence on the excitability of excitatory neurons. Indeed, in *SOD1*^{G93A} and *TDP-43*^{A315T} mice, the reduced activity and inhibitory influence of cortical parvalbumin neurons were shown to increase the excitability of pyramidal neurons (Khademullah et al., 2020; Zhang et al., 2016). This was attributable to a decrease in the number of parvalbumin neurons in *SOD1*^{G93A} mice and of GABAergic synapses in *TDP-43*^{A315T} mice. Interestingly, increasing the activity of parvalbumin neurons in *SOD1*^{G93A} mice was effective in normalising the excitability of pyramidal cells. To verify our hypotheses, it will be necessary to assess spontaneous inhibitory transmissions in *Fus*$^{Trunc/+}$ mice using a calcium sensor expressed selectively in inhibitory neurons. Alternatively, electrophysiological studies could assess excitatory and inhibitory neurotransmissions, as well as intrinsic excitability.

The second limitation of our study is that we did not include control mice expressing Cre in the absence of LoxP sequences (*Vgat*$^{Cre/+}$; *Fus*$^{+/+}$). Yet, the genetic manipulation of the endogenous *Vgat* locus may have unintended consequences on *Vgat* expression and, subsequently, on inhibitory transmission. This idea will be further discussed in the following section (page 216). Briefly, the knockout of *Vgat* in mice results in a reduced synaptic release of GABA and glycine, or in a complete absence of spontaneous inhibitory postsynaptic currents in homozygous embryos (Saito et al., 2010; Yamada et al., 2012),

confirming the importance of VGAT for inhibitory transmission. In homozygous *Vgat*$^{Cre/Cre}$ mice, a reduction in VGAT RNA and protein levels was observed, and this was accompanied by a decrease in spontaneous inhibitory postsynaptic currents (Straub et al., 2020). This was not tested in heterozygous *Vgat*$^{Cre/+}$ mice, but we can assume that a similar, though perhaps less pronounced, effect may also occur in these mice. Therefore, if inhibitory neurons were found to be less active in *Fus*$^{Trunc/+}$ mice, it would be necessary to ascertain if this is, at least in part, attributable to a reduction in VGAT function, or if this is entirely due to the cytoplasmic accumulation of FUS in these neurons.

2. Is there a link between seizures and the ALS-FTD continuum?

Seizures are defined as sudden, uncontrolled bursts of electrical activity in the brain. There are numerous types of seizures, which vary according to their area of origin in the brain and the extent to which they propagate. This can result in a range of symptoms and severity, including changes in behaviour, movement, sensation, emotion and level of consciousness. However, it is important to note that seizures are not always associated with epilepsy. The latter is typically diagnosed when an individual experiences two seizures at least 24 hours apart without a known cause. Neuronal circuit dysfunction represents an early feature of both ALS and FTD. In particular, an increased cortical excitability has been extensively observed in ALS (Menon et al., 2020, 2015; Shibuya et al., 2017; Van den Bos et al., 2018; Vucic and Kiernan, 2006; Zanette et al., 2002), and was also detected in FTD (Bae et al., 2016; Benussi et al., 2017; Burrell et al., 2011).

To our knowledge, the potential occurrence of seizures before or after the diagnosis of ALS remains to be investigated. Interestingly, epilepsy is associated with a reduction in the expression and/or activity of subunits of the $GABA_A$ receptor, and particularly the α1 subunit. Yet, the *GABRA1* gene encoding this subunit was found to be downregulated in the motor, prefrontal and temporal cortex of symptomatic ALS patients compared to healthy controls (Aronica et al., 2015; Lederer et al., 2007; Petri et al., 2006, 2003). Of note, an analysis of large genome-wide association study datasets reported no common genetic risk between ALS and epilepsy (Schijven et al., 2020). Conversely, studies on the relationships between FTD and seizures or epilepsy are recent and rare, but general tendencies can be observed. Prior to the age of 70, the seizure incidence rate was found to be higher in FTD patients than in age-matched control populations (Beagle et al., 2017). The exact incidence rates of seizures vary between studies. To date, the largest clinic-based study reported that among 348 patients with FTD, 2.6% of them experienced a new-onset seizure (i.e., the first occurrence of a seizure in a lifetime) between 3 years before the onset of cognitive decline and up to 7 years after (Beagle et al., 2017). Of note, in 2.3% of these 348 FTD patients, seizures were suspected but unconfirmed, so they were not included in the previous count. In smaller studies, higher rates of seizures were reported: 5.8% among 104 patients (X. Wang et al., 2021), 7.1% among 84 patients

(Muroni et al., 2022), 11.3% among 53 patients (Vöglein et al., 2022). This incidence rate was found to be significantly elevated in FTD patients under the age of 50 in comparison to older patients (Beagle et al., 2017). However, only 11 patients were included in the youngest group, which may bias this observation. Finally, the occurrence of seizures was found to vary among patient subgroups (Table 1).

	Incidence rate of seizures		References
Behavioural variant	3.3% 3.5%	(n = 61) (n = 115)	Beagle et al., 2017; Muroni et al., 2022
Primary progressive aphasia - with a non-fluent variant - with a semantic variant	17.4% 5.4% 0%	(n = 23) (n = 37) (n = 82)	Beagle et al., 2017; Muroni et al., 2022
TDP-43 status - with pathological hallmark - without TDP-43 hallmark	 5.1% 28.6%	 (n = 39) (n = 14)	Beagle et al., 2017
C9ORF-72 status - with repeat expansion - without mutation	 10% 6.25%	 (n = 20) (n = 64)	Muroni et al., 2022

Table 3: In FTD patients classified according to their clinical diagnosis or underlying aetiology, the incidence rate of seizures is variable. The proportion of patients who have experienced seizure manifestations is reported as a percentage and is accompanied by the total number of patients included in the subgroup of interest.

Of note, a small number of case reports have described patients with FTD and epilepsy. The latter was diagnosed either before or after the occurrence of behavioural impairments, depending on the patient. Furthermore, while some patients exhibited an identified genetic cause, this was not the case for all of them. Finally, the type of seizures also seems to vary among the cases. Report 1: The patient presented with behavioural and motor impairments, as well as focal unaware seizures. This led to the diagnosis of epilepsy, followed by a possible diagnosis of FTD (Saint et al., 2021). Report 2: The patient was diagnosed with FTD with a behavioural variant. He experienced an isolated episode of generalised tonic-clonic seizure 10 years before this diagnosis, while multiple additional seizure episodes occurred one year after the diagnosis and led to a clinical worsening (Valls-Carbó et al., 2020). Report 3: A family carrying the P301S mutation in the *MAPT* gene was characterised by an early-onset and rapidly progressive FTD, with motor impairments and epileptic seizures (Sperfeld et al., 1999). The most extensively studied case involved an individual who presented with a range of seizure types, including both focal and generalised tonic-clonic seizures complicated by convulsive status epilepticus. These seizures appeared one year after the diagnosis, while the first indications of behavioural abnormalities were observed 6 years before the diagnosis. At that time, status epilepticus was defined as a seizure lasting more than 30 minutes or as a series of seizures during which the patient does not regain normal mental status. In the family, another patient also developed tonic-clonic seizures after the onset of behavioural symptoms and died during status epilepticus. A third patient probably died from status

epilepticus, but a proper evaluation was not performed. Report 4: A patient presented with a history of focal epilepsy and, a few years later, rapidly progressive FTD associated with a mutation of the valosin-containing protein (Carlucci et al., 2024). Finally, four additional reports proposed a link between *C9ORF72* repeat expansions and epilepsy. In three of these reports, patients exhibited cognitive symptoms (Janssen et al., 2016; Melis et al., 2022; van den Ameele et al., 2018), whereas the fourth one described 4 patients diagnosed with ALS and exhibiting abnormal electroencephalographic recordings (Capasso et al., 2017).

In light of these observations, investigating a potential link between seizures and the ALS-FTD continuum seems warranted, particularly given the necessity of early detection and treatment of seizures to prevent any clinical worsening. For instance, in patients with Alzheimer's disease, the occurrence of seizures, or even subclinical epileptiform activity, has been associated with a worse prognosis and accelerated decline in cognitive function (Yang et al., 2022). To date, epileptiform activity has been reported in two FTD mouse models overexpressing mutant tau protein, but not in other mouse strains. In particular, transgenic VWL mice carrying three tau mutations (G272V, P301L and R406W) showed spontaneous epileptiform activity and seizures during electroencephalographic recordings at 5.5 months (the first age examined in this study) and thereafter (García-Cabrero et al., 2013). In addition, 4- to 9-month-old transgenic mice expressing human tau with the A152T mutation exhibited more epileptiform spikes than control mice (Maeda et al., 2016). Of note, this mutation is linked to several tauopathies, including FTD and Alzheimer's disease. To our knowledge, the effect of this aberrant neuronal activity on the disease course remains to be investigated in mice, as well as in FTD patients.

3. Could Trunc$^{-/-}$ pups die from fatal seizures?

Our characterisation of the postnatal development of Trunc$^{-/-}$ pups demonstrated that half of the pups die suddenly three weeks after birth (Publication 2, Fig. 1F). We are still investigating the cause of this lethality, and the protective mechanisms occurring in the surviving pups. Interestingly, this occurs after a period of important changes in the maturation of the cortical inhibitory system (Figure 28). By the end of the second postnatal week, both the inhibitory circuits and spontaneous neuronal activity are expected to resemble those observed in adult mice. One could thus imagine that a delay or an alteration in this postnatal development may underlie at least some of the observed phenotypes. In particular, we postulate that these mice may exhibit increased neuronal activity levels and potential epileptiform discharges. To test this hypothesis, we will perform electroencephalographic and video recordings before and during the critical period of lethality (Publication 2, Fig. 5). If Trunc$^{-/-}$ pups, or at least some of them, were to exhibit seizures, this could explain the transient periods of inactivity we observed.

Indeed, such episode may be indicative of behavioural arrest and unresponsiveness due to an ongoing absence seizure and/or a lethargic phenotype observed after a seizure.

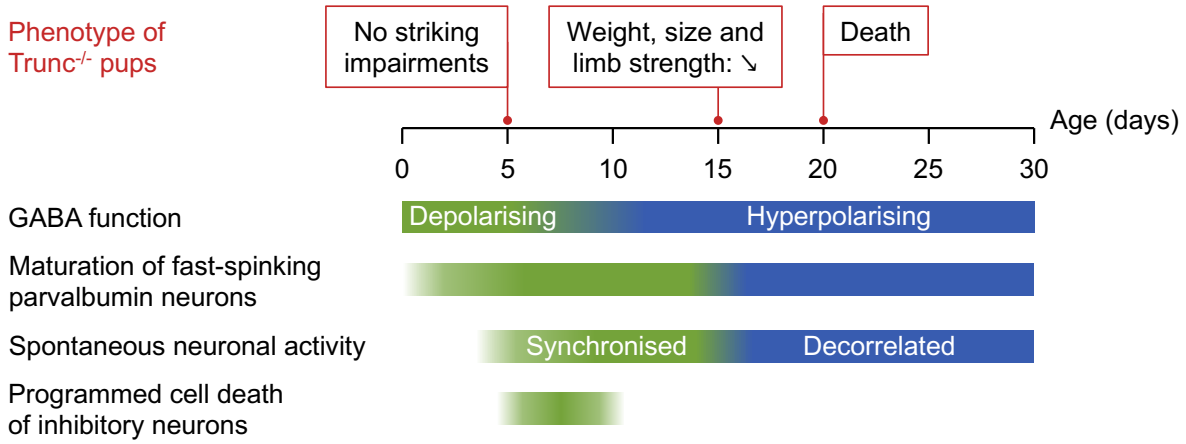


Figure 28: Main results obtained from the characterisation of Trunc$^{-/-}$ pups and comparison with the postnatal development of the cortical inhibitory system.

To date, no manifestations of seizures or epilepsy have been reported in FTD patients with FUS proteinopathy, and only one ALS patient was described with myoclonic seizures (Dodd et al., 2019). This juvenile patient was found to carry a heterozygous nonsense mutation in exon 14 of the *FUS* gene, which resulted in the rapid progression of bulbar and respiratory failure. This was associated with frequent myoclonic jerks (defined as sudden and brief involuntary twitching of a muscle or group of muscles that cannot be stopped or controlled by the patient), predominantly in the upper limbs. Electro-encephalographic recordings revealed the presence of multiple generalised spike and wave discharges, which are typically seen during myoclonic seizures and possibly during generalised epilepsies. In addition, recent histological studies found evidence of Alzheimer's disease-like pathological hallmarks in brain tissues surgically resected from epilepsy patients. Three studies reported the presence of hyperphosphorylated tau protein aggregates, which correlated with cognitive impairments in the first two studies (Gourmaud et al., 2020; Tai et al., 2016) but not in the last one (Aroor et al., 2023). A fourth study reported the presence of sparse phosphorylated tau proteins, which did not correlate with cognitive deficits (Silva et al., 2021). FUS inclusions have been observed in other neurological conditions, including Huntington's disease (Mori et al., 2019) and spinocerebellar ataxia (Doi et al., 2010). Hence, if a link is established between FUS cytoplasmic delocalisation and epileptiform spikes in mice, it would be interesting to ascertain whether FUS inclusions can be observed in brain tissues of epilepsy patients.

The truncation of both copies of *Fus* in every cell type induces perinatal death due to respiratory insufficiency (Scekic-Zahirovic et al., 2016). However, another research group used a mixed genetic background and was able to produce viable offspring with a homozygous deletion of the NLS of *Fus* (Ali et al., 2023). These mice displayed reduced

body weight at birth and throughout their lifespan, as well as a shortened survival. Fatal seizures were reported to occur from 3 months of age. In addition, the authors mentioned fatal seizures in older heterozygous mice with a mixed or pure (C57BL/6J or DBA/2J) genetic background. Seizures were also outlined in two other knock-in mouse models, but only when both copies of *Fus* were mutated (Korobeynikov et al., 2022). The first mouse model was characterised by a homozygous deletion of the NLS of *Fus*, which resulted in a shortened lifespan. Half of the pups died within the first few days after birth, while half of the remaining pups died at approximately 21 days of age. The second mouse model carried a mutant allele (point mutation in the NLS domain) and a knockout allele. This resulted in a shortened lifespan with a median survival of 21 days. However, the percentage of survival declined progressively throughout the entire period between birth and postnatal day (P) 40. The lack of information regarding the assessment of seizures limits our ability to draw conclusions from these two studies. However, they appear to support the hypothesis that FUS cytoplasmic accumulation may alter neuronal activity to the extent of epileptiform discharges.

When looking at mouse models exhibiting spontaneous seizures and similar phenotypes to those of Trunc$^{-/-}$ pups (i.e., altered postnatal development and sudden death around the third weeks of age), we found two studies in which different underlying mechanisms have been proposed as a probable contributing factor to the observed seizures. Interestingly, in both cases, a decreased inhibitory neurotransmission was reported.

The first model was based on the knockout of distinct isoforms of the gene encoding synaptic vesicle protein 2: either the isoform A alone (SV2A), the isoform B alone (SV2B) or a combination of both (SV2A/SV2B) (Venkatesan et al., 2012). These proteins play an essential role in the calcium-dependent secretion of vesicles from presynaptic compartments. SV2A is expressed in nearly all neurons, while SV2B is principally expressed in glutamatergic neurons. In mice, the deletion of SV2A and SV2A/SV2B resulted in a reduced body weight and severe seizures one week after birth, as well as premature death between P14 and P23. In the hippocampus of these mice, both increased spontaneous excitatory postsynaptic currents and decreased spontaneous inhibitory currents were observed and may underlie the appearance of seizures. None of these phenotypes were observed upon the deletion SV2B alone.

The second mouse model was generated through the removal of the *Sox6* gene from inhibitory neurons derived from the medial ganglionic eminence (i.e., parvalbumin and somatostatin cortical neurons) (Batista-Brito et al., 2009). Sox6 is a transcription factor with essential functions during the development. As a result, the positioning and maturation of inhibitory neurons were affected in the knockout mice. However, the mice exhibited no discernible differences in appearance or behaviour from their control littermates until approximately 15 days of age. By P16, they displayed increased

withdrawal and developed spontaneous seizures. They died between P17 and P19 due to prolonged seizures and dehydration. It is noteworthy that fast-spiking parvalbumin neurons undergo significant changes after the second postnatal week (Figure 28). In particular, excitatory synaptic inputs on these neurons were demonstrated to reach their maximal level at P15 (Okaty et al., 2009). This network activity coincides with developmental changes in parvalbumin neurons during the third and fourth postnatal week. These changes include the maturation of their intrinsic cell firing properties, an improved reliability of GABA release, the development of perineural nets, and a significant increase in axonal arborisation around pyramidal neurons (Doischer et al., 2008). Our preliminary data indicate that the density of parvalbumin neurons at P15 is unchanged in Trunc$^{-/-}$ pups. Should this result be confirmed by further investigation, it would be of interest to verify the levels of parvalbumin and the density of perineural nets by immunohistological analyses, as a proxy of the maturation of these cells.

It is interesting to see that other mouse models exhibit a critical period of death that is strikingly similar to that observed in Trunc$^{-/-}$ pups, which commenced at P14 and ended at P23, with a median age of 21 days (Publication 2, Fig. 1F). This suggests that this time window may be of particular importance in pups with alterations in inhibitory neurons. Of note, this is not the case when the inhibitory system is severely disrupted. Indeed, the complete knockout of VGAT or GAD67 has been demonstrated to induce major developmental abnormalities, resulting in death during the embryonic development or shortly after birth (Wojcik et al., 2006). In line with this idea, it was intriguing to see that in a mouse model susceptible to audiogenic seizures, the incidence of seizures (assessed through behavioural observation) and mortality exhibited an age-dependent trend (Wengert et al., 2021). One quarter of the mice were sensitive to seizures at P15, while at P20 and beyond, all the mice became sensitive. In addition, these induced seizures were lethal at P20-P21 due to a lack of respiratory recovery following the tonic phase. However, they were not lethal anymore at P25 or later. In a mouse model with a delay in the maturation of the GABAergic system (due to the mutation of potassium-chloride cotransporter 2), increased excitatory transmission and decreased inhibitory transmission were observed at P15-P20 but not later (Pisella et al., 2019). Therefore, young pups (P15-P20) were more vulnerable to seizures triggered by an anticonvulsant agent than control mice, whereas this was not the case for adult mutant mice (P30). We can then imagine that a similar phenomenon occurs in Trunc$^{-/-}$ mice, with a high susceptibility to seizures and death from seizures in juvenile mice, which is absent in adult mice. This could explain why the surviving Trunc$^{-/-}$ mice do not exhibit overtly deleterious phenotypes.

Validity and limitation of the study

4. Relevance of the choice of mouse lines

In this project, we used *Fus*$^{\Delta NLS/+}$ mice to model ALS and FTD, and *Vgat*^{Cre} mice to target inhibitory neurons. In the following paragraphs, I will discuss the advantages and limitations associated with these choices. It should be noted that when working with double mutant mouse lines, a substantial number of control genotypes is required. Ideally, one would need to assess the endogenous effect of every genetic manipulation by including wild-type mice, mice expressing Cre in the absence of LoxP sequences (*Vgat*$^{Cre/+}$; *Fus*$^{+/+}$), and mice carrying LoxP sequences in the absence of Cre recombinase (*Vgat*$^{+/+}$; *Fus*$^{LoxP/+}$, and *Vgat*$^{+/+}$; *Fus*$^{LoxP/LoxP}$ when needed). In our case, this would have resulted in 10 different genotypes, which would have constituted an excessive number of mice for most of the analyses we conducted.

As a result, we decided to exclude *Vgat*$^{Cre/+}$; *Fus*$^{+/+}$ control mice from our experiments, except for the histological analysis conducted in 2-month-old mice. We acknowledge that this constitutes a significant limitation in the interpretation of our results, as stated in the previous section and further discussed below. In addition, no wild-type mice were included in the study of *Fus*$^{Trunc/+}$ or *Fus*$^{Trunc/Trunc}$ mice. The control mice carried LoxP sequences (on one or two copies of the *Fus* gene) in the absence of Cre recombinase. While our histological study demonstrated no impact of this genetic manipulation, the potential consequences on motricity, behaviour, neuronal activity or metabolism remain unassessed by our laboratory or others.

A. *Fus*$^{\Delta NLS/+}$ mice as a model of ALS and FTD

The precise mechanisms by which FUS contributes to neurodegeneration, and to the symptoms of ALS and FTD, remain unclear. An increasing body of evidence suggests that both gain and loss of function mechanisms may be involved. Investigating the consequences of FUS loss of function in mice is challenging. Indeed, the complete knockout of *Fus* results in perinatal lethality (Hicks et al., 2000; Scekic-Zahirovic et al., 2016). In heterozygous mice, or in homozygous mice maintained on a mixed genetic background, FUS loss of function is not sufficient to induce ALS-like motor phenotypes (Devoy et al., 2017; Kino et al., 2015; Scekic-Zahirovic et al., 2017), but may be relevant to investigate FTD-like behavioural phenotypes (Kino et al., 2015). Evaluating the consequences of *FUS* mutations in mice is also challenging. The levels of FUS protein are tightly autoregulated by mechanisms involving the binding of FUS to its own pre-messenger RNA (Dini Modigliani et al., 2014; Humphrey et al., 2020; Zhou et al., 2013). It has been demonstrated that this autoregulation is highly sensitive to the concentration of FUS in the nucleus. Consequently, even minimal overexpression of wild-type or mutant

human FUS in transgenic mice can result in modifications to this physiological autoregulation, thereby precipitating a cascade of impairments. Furthermore, the overexpression of wild-type human FUS is known to be toxic in mice (Mitchell et al., 2013). Overall, it is difficult to determine the relevance of these impairments for our understanding of the pathological mechanisms occurring in patients.

To address this issue, our laboratory has developed a knock-in mouse model in which the NLS domain of the endogenous *Fus* gene is deleted in every cell type since the embryonic development (*Fus*$^{\Delta NLS/+}$, Scekic-Zahirovic et al., 2016). This enables to evaluate the impact of FUS cytoplasmic accumulation in a physiological context, in the absence of confounding effects of ectopically expressed transgenes. However, this approach alone does not allow to distinguish whether the observed phenotypes result from a loss of physiological functions of FUS and/or a gain of toxic functions.

Although this mouse line does not permit to study the consequences of a specific mutation identified in ALS patients, it encompasses all mutations resulting in alterations of FUS nuclear import, including mutations that lead to the complete deletion of the NLS domain. In addition, *Fus*$^{\Delta NLS/+}$ mice recapitulates the abnormal cytoplasmic accumulation observed in ALS and FTD patients, irrespective of whether *FUS* is mutated or not (Deng et al., 2010; Kwiatkowski et al., 2009; Munoz et al., 2009; Neumann et al., 2009a, 2009b; Tyzack et al., 2019; Vance et al., 2009). Finally, the study of heterozygous mice is of particular significance given that ALS patients present with heterozygous mutations, and some of the normal diffuse nuclear distribution of FUS is retained in the cells of ALS and FTD patients. Overall, these mice offer a good recapitulation of the aetiology of both ALS and FTD, in the absence of FUS inclusions, as this hallmark is not recapitulated in mice (Devoy et al., 2017; López-Erauskin et al., 2018; Scekic-Zahirovic et al., 2017).

Fus$^{\Delta NLS/+}$ mice recapitulate several ALS- and FTD-like phenotypes, including a decline in muscle strength and an increase in sociability. However, as stated before, some of these symptoms are mild and difficult to observe, particularly regarding motor symptoms. Of note, the cytoplasmic accumulation of FUS also appears to be mild in these mice. In comparison to control mice, we observed a 1.3-fold reduction in the nuclear-to-cytoplasmic ratio of FUS in cortical parvalbumin neurons and a 1.7-fold reduction in layer 5 pyramidal neurons (Publication 1, Fig. 2D and 2G). Hence, the toxicity associated with this delocalisation may be restricted. In addition, FUS is still present in the nucleus, so the loss of nuclear and cytoplasmic functions may be limited.

To date, one other *Fus* knock-in mouse model has been characterised (*Fus*$^{\Delta 14}$, Devoy et al., 2017) and is based on a genetic manipulation mimicking a truncating mutation observed in juvenile ALS cases. In these mice, a point mutation has been introduced before exon 14, resulting in the skipping of this exon during splicing and an out-of-frame translation

of exon 15, which generates an aberrant C-terminal sequence. This results in a loss of motor neurons at 12 months of age, which occurs at 22 months of age in *Fus*$^{\Delta NLS/+}$ mice (Scekic-Zahirovic et al., 2017). Although, the muscle strength remains to be longitudinally investigated in *Fus*$^{\Delta 14}$ mice, the reported motor phenotypes suggest that ALS-like symptoms are as mild as in *Fus*$^{\Delta NLS/+}$ mice. Two additional heterozygous knock-in mice are now available (*Fus*$^{\Delta ex14}$ and *Fus*^{P517L}, Korobeynikov et al., 2022). *Fus*$^{\Delta ex14}$ mice are based on the same genetic manipulation than the one described above. In *Fus*^{P517L} mice, a point mutation was introduced in exon 15 to mimic the P525L mutation observed in humans. For both mouse lines, the loss of lumbar motor neurons was observed at 18 months of age, and motor phenotypes remain to be assessed. However, none of these mouse lines exhibited paralysis, indicating that the discrepancy between the observed phenotype in ALS patients and that of mice is possibly due to intrinsic biological differences between the two species. Overall, to further investigate the contribution of inhibitory neurons to FUS-related phenotypes, the choice of knock-in mouse lines is limited. This highlights the necessity to develop more precise and reliable tests to elucidate the underlying mechanisms in the currently available mouse lines.

To finish, the genetic manipulations of the *Fus* locus in the mouse lines generated in Strasbourg permit the deletion of the NLS domain (*Fus*^{exon15}, Publication 3) or the rescue of the mutation (*Fus*$^{\Delta NLS}$, Scekic-Zahirovic et al., 2016) upon recombination. This is of particular interest to develop cell-specific approaches and to ascertain the consequences of *Fus* mutation in different cell types. To our knowledge, these are the only available *Fus* knock-in mouse lines allowing these two opposing, but complementary, manipulations.

B. *Vgat*^{Cre} mice to target inhibitory neurons

For this project, we wanted to target as many inhibitory neurons as possible, both in the brain and spinal cord, since the embryonic development. In order to achieve this objective, *Vgat*^{Cre} mice (The Jackson Laboratory, stock #028862, C57BL/6J background, Vong et al., 2011) were identified as the most appropriate mouse line, as they met a significant number of our criteria. Firstly, we wanted to use knock-in mice, thereby ensuring that Cre expression would precisely and reliably recapitulate the endogenous gene expression. Secondly, we wanted to use a constitutive Cre driver, thereby enabling recombination to occur without the need for further intervention.

One potential limitation of this approach is that the recombination patterns may not correspond precisely to the endogenous expression in the adult central nervous system. Indeed, the final recombination patterns reflect the cumulative expression of *Vgat* throughout the embryonic development and entire life. Therefore, one may imagine that some cells only transiently express *Vgat*, while recombination would still occur in them. However, our analysis of Cre activity revealed both high levels of specificity and efficacy

in the frontal cortex (see the first part of this Discussion), suggesting that our results can be effectively interpreted in terms of inhibitory neuron contribution to the phenotypes. A second limitation is that *Vgat*^{Cre} mice do not express a fluorescent reporter in addition to Cre. This would have helped investigating all the inhibitory neurons in which FUS subcellular localisation was manipulated instead of relying on immunohistological labelling and focusing on parvalbumin neurons only.

The last limitation is directly linked to the construction of the mouse line. Despite the insertion of the Cre cassette downstream of the endogenous *Vgat* stop codon, this can still result in a reduced expression of the endogenous *Vgat* gene. The initial characterisation of this mouse line reported no discernible effects on phenotype when the alleles were used in a heterozygous state (Vong et al., 2011). More recently, another laboratory characterised homozygous *Vgat*$^{Cre/Cre}$ mice by comparing them to wild-type C57BL/6J mice (Straub et al., 2020). Upon evaluation of *Vgat* RNA levels in forebrains through quantitative reverse transcription polymerase chain reaction (RT-qPCR), it was observed that, on average, one additional cycle was necessary in *Vgat*$^{Cre/Cre}$ mice compared to control mice, indicating a 50% reduction in *Vgat* RNA. This was accompanied by a 40 to 50% reduction in VGAT protein levels in the hippocampus, evaluated by Western blot analysis and immunohistological labelling followed by the analysis of the fluorescent signal intensity. Finally, their electrophysiological analysis demonstrated a 20% reduction in spontaneous inhibitory postsynaptic currents in the hippocampus. In our double mutant mice, at least one allele of *Vgat* remained in a wild-type state. It can be postulated that, if *Vgat* expression was altered, the observed reduction would have been less pronounced than in homozygous mice. Nevertheless, this hypothesis requires further investigation to be confirmed. To this end, we conducted a preliminary study in which we assessed *Vgat* RNA levels in the frontal cortex of 4-month-old mice using RT-qPCR. We observed reduced *Vgat* levels in heterozygous *Vgat*$^{Cre/+}$ (30% decrease) and *Fus*$^{Trunc/+}$ (40% decrease) mice compared to wild-type mice.

Although *Vgat*^{Cre} mice exhibit inherent limitations, this remains the only mouse line that allows to target a significant number of cerebral and spinal inhibitory neurons. Indeed, the other mouse lines currently available were developed to express Cre in subpopulations of inhibitory neurons (Taniguchi et al., 2011). For instance, the use of the endogenous promoter of the gene encoding GAD65 allows to target GABA-producing neurons only, while the promoter of the gene encoding GlyT2 allows to target glycinergic neurons. Other mouse lines were developed by taking advantages of enhancers of genes expressed in progenitors and developing inhibitory neurons. This includes several members of the Dlx family, which encode homeodomain transcription factors, and allow to target different subpopulations of cortical GABAergic neurons.

5. Relevance of the follow-up of disease progression

In the previous sections, we discussed the relevance of the choice of tests, their inherent limits, and the other tests that could be employed to gain deeper insights into the role of inhibitory neurons in ALS- and FTD-like phenotypes related to FUS. Here I will briefly discuss the time points we decided to study. In adult heterozygous mice, the evaluation of motor deficits was conducted every two months up to 12 months of age to encompass the progressive decline. Conversely, social impairments were studied at two time points: in mature adult mice at 4 months of age, and in middle-aged mice at 10 months of age. Both time points precede the loss of motor neurons. The first one is considered as the approximate onset of muscle strength defects evaluated with the four-limb inverted grid test (Sanjuan-Ruiz et al., 2021), while the second is in the symptomatic phase, both in terms of motor deficits and altered sociability (Scekic-Zahirovic et al., 2021). Due to logistic constraints, we could not study old mice at 20-22 months of age. Our approach proved to be effective, as the *Fus*$^{\Delta NLS/+}$ mice included in this study recapitulated phenotypes that were previously published by our laboratory. Consequently, they were used as positive controls to interpret the results obtained with the novel mouse lines. Of note, the previously characterised *Fus*$^{\Delta NLS/+}$ mice had a pure C57BL/6J genetic background, whereas in our study, their genetic background was a mix of C57BL/6J and 6N. Despite known phenotypic differences between these two substrains (Simon et al., 2013), this had no significant impact on the motor and social phenotypes we investigated.

In this study, we observed various degrees of heterogeneity in the data we obtained. Although this may be attributed to intrinsic behavioural variabilities in mice of the same age, sex and genotype, it may also reflect the heterogeneous effects of FUS cytoplasmic accumulation in individuals. In ALS and FTD patients, the age at which symptoms first manifest, the rate of progression, and the duration of the disease are subject to significant inter-individual variabilities. We can therefore posit that this is also the case in mice. It would be beneficial to identify a biomarker associated with disease progression, which would allow us to distinguish between potential slow and fast progressors within our cohorts. Furthermore, it may corroborate the interpretation of certain tests. For example, female *Fus*$^{Recs/+}$ mice with delayed motor symptom onset may also exhibit delayed disease progression according to biomolecular analyses. In ALS patients, the levels of neurofilament light chain in the cerebrospinal fluid and blood are considered as effective predictor of disease progression (Benatar et al., 2024; Lu et al., 2015). In particular, elevated levels were found to correlate with faster and more aggressive phenotypes, and a shorter survival (Shahim et al., 2024). Interestingly, it was recently proposed that the use of neurofilament light chain has a high translational value, as it seems to correlate with disease progression in TDP-43 and SOD1 mice (Buck et al., 2022; Loeffler et al., 2020). It would be interesting to verify if this is also true for *Fus*$^{\Delta NLS/+}$ mice, and whether FUS subcellular localisation in *Vgat*-expressing neurons affects this biomarker.

Inhibitory neurons as a possible therapeutic target

As detailed in the Introduction (Part 5, page 60), several inhibitory neuron alterations have been documented in the brains and spinal cords of ALS and FTD patients, and this phenomenon has also been observed in mouse models. Interestingly, some of these impairments may contribute to the onset and/or progression of symptoms. Briefly, in ALS patients, the reduction in intracortical inhibition levels has been associated with muscle weakness and wasting in the hand (Menon et al., 2014), as well as the extent of motor impairments and functional deterioration (Burrell et al., 2011; Shibuya et al., 2017; Van den Bos et al., 2018). The contribution of inhibitory neurons to motor phenotypes was corroborated by the investigation of mouse models. In particular, the loss of cortical inhibitory influence has been demonstrated to result in an increase in motor neuron activity and death in TDP-43 and SOD1 mice (Khademullah et al., 2020; Zhang et al., 2016). In addition, it was proposed that the loss of spinal inhibitory inputs on motor neurons contributes to the development of subtle locomotor changes in SOD1 mice (Allodi et al., 2021), which may serve as an early indicator of ALS progression prior to the onset of muscle strength deficits.

In FTD patients, the reduced intracortical inhibition and altered oscillatory dynamics (which are at least partly regulated by inhibitory neurons) have been associated with disinhibited and aggressive behaviours (Benussi et al., 2020; Hughes et al., 2018). However, the question of whether alterations in inhibitory neurons can cause behavioural or cognitive deficits remains unanswered. To date, it was proposed that the loss of cortical inhibitory neurons may underlie attentional deficits in TDP-43 mice (White et al., 2018), as well as anxiety and spatial navigation learning deficits in SOD1 mice (Quarta et al., 2015). With our study, we demonstrate that the cytoplasmic accumulation of FUS in inhibitory neurons is sufficient to induce behavioural phenotypes, as evidenced by the increased sociability observed at the beginning and middle of the disease course. While the precise mechanisms remain to be elucidated, the data obtained from *Fus*$^{\Delta NLS/+}$ mice (Sahadevan et al., 2021; Scekic-Zahirovic et al., 2021), along with the increased neuronal activity observed in *Fus*$^{Trunc/+}$ mice (Publication 1), suggest that alterations in inhibitory neurons may result in a reduced inhibitory transmission, which in turn may underlie the social defects.

The involvement of inhibitory neurons in motor, behavioural and cognitive symptoms justifies the necessity to investigate whether targeting the deficit in cortical and spinal inhibition would efficiently alleviate certain symptoms. In particular, the fact that analogous mechanisms have been documented in TDP-43 and SOD1 mice suggests that inhibitory neurons may represent a therapeutic target in cases associated with different causative genes and proteins, and even in patients for whom the aetiology of the disease remains unknown. This is of particular importance given that the cause of ALS and FTD

is not identified in most cases, and only *post-mortem* studies currently allow to assess the pathological inclusions characterising a patient. For instance, it has been estimated that in approximately 30% of familial cases and 85% of sporadic ALS cases, the cause of the disease remains unknown. This renders the development of a curative treatment a highly challenging endeavour, which explains why symptomatic treatments are required to maintain the autonomy and quality of life of patients.

Among the symptomatic treatments prescribed to patients with ALS, diazepam (a $GABA_A$ receptor agonist) and baclofen (a $GABA_B$ receptor agonist) are employed to alleviate cramps, fasciculations (spontaneous and involuntary muscle contractions and relaxations) and spasticity (increased muscle tone resulting in muscle stiffness). However, these agents do not act solely on the activity of GABA receptors, so their efficacy may be due to other mechanisms of action. Similarly, Riluzole (the only pharmaceutical compound approved worldwide for the treatment of ALS) and Retigabine (currently tested in patients) have multiple mechanisms of action, including the activation of $GABA_A$ receptors. It was suggested that these compounds restore the balance between excitation and inhibition (Vucic et al., 2013; Wainger et al., 2021), but this effect may be only transient (Geevasinga et al., 2016). In addition, their effect on disease progression and survival is either limited (for Riluzole) or to be tested (for Retigabine).

In patients with FTD, a promising therapeutic approach is based on a non-invasive brain stimulation to modulate the inhibitory neuron activity and induce gamma oscillations (Assogna et al., 2022). In healthy volunteers, this technique was found to be safe and to induce transient improvement of cognitive performances, which depended on the sites of stimulation. Therefore, the authors propose that this may improve working memory, attention and cognitive functions in FTD patients. In addition, it would be interesting to see if a long-term effect on disinhibitory behaviours can be elicited with this approach.

In recent years, the imbalance between excitation and inhibition, as well as deficits in inhibition, have been regarded as a potential therapeutic target for a number of neurodevelopmental and neurodegenerative diseases, including schizophrenia, autism and Alzheimer's disease. A wide range of symptoms commonly associated with reduced inhibition and/or abnormal neural oscillations may be alleviated with this approach, which encompasses cognitive symptoms, as well as anxiety and decreased sociability. However, regarding the increased sociability and disinhibitory behaviours, which characterise some FTD patients, the association with the GABAergic system remain to be understood, and as a result, no such therapeutic approaches have been proposed.

Overall, there already exist a wide range of compounds that can be employed to target the inhibitory system, particularly the cerebral GABAergic system. The primary objective is to enhance inhibitory neurotransmission, which can be achieved by acting on several

aspects of inhibitory synapses. For instance, some pharmacological compounds bind to specific subunits of GABA receptors, thereby modulating their action. It is noteworthy that different $GABA_A$ receptor subunits have distinct functions, and their specific targeting may allow to decrease the risk of adverse effects, including sedation. For instance, it has been demonstrated that targeting α2 and α3 subunits reduces anxiety, while targeting α5 subunit may be relevant to increase inhibitory transmission in the hippocampus and enhance cognitive performances (Maramai et al., 2020). Other pharmacological compounds interfere with the synaptic re-uptake of GABA, resulting in increased concentrations of the neurotransmitter in the synaptic cleft. It is also possible to selectively target the chloride cotransporters located at the membrane of postsynaptic neurons. In this case, the aim is to reduce the intracellular concentrations of chloride ions to enhance the hyperpolarising effect of GABA and glycine.

The advantage of selecting compounds from this list is that some of the mode of action, benefits, and adverse effects may have already been documented, thus providing a foundation for further testing in FTD and facilitating potential treatment access to patients. However, due to their high specificity for a given molecular alteration in the GABAergic synapse, it is first necessary to identify the precise mechanisms which underlie a given symptom in order to select an appropriate therapeutic approach. This may prove challenging, particularly in patients. In addition, it is possible that the underlying mechanisms vary among subgroups of patients, thus complicating the development and testing of treatments. An alternative approach may be to target the neuronal activity with non-invasive brain stimulation, which may prove more readily adaptable to several subgroups of patients, irrespective of the precise underlying mechanisms. Nevertheless, it would be necessary to demonstrate that this has a positive effect on behavioural deficits characterising FTD patients.

Conclusion

Our study demonstrated that the subcellular localisation of FUS in inhibitory neurons influences motor and social phenotypes, as well as spontaneous neuronal activity, in mice. It would be of interest to ascertain the contribution of inhibitory neurons to other symptoms. Regarding ALS, we could evaluate locomotor symptoms associated with spinal V1 inhibitory neurons. Regarding FTD, we could assess additional disinhibitory behaviours, such as impulsivity, perseverative and stereotyped compulsive behaviours. Understanding the contribution of inhibitory neurons to the onset and/or progression of symptoms will be necessary to support the necessity to develop therapeutic approaches targeting these neurons. However, for this targeting to be efficient, it is also necessary to gain insight into the mechanisms by which inhibitory neurons are impaired.

To date, one major unanswered question is how FUS cytoplasmic accumulation affects inhibitory neurons. Previous characterisations of *Fus*$^{\Delta NLS/+}$ mice have demonstrated transcriptomic, histological and ultrastructural alterations in the pre- and postsynaptic compartments (Sahadevan et al., 2021; Scekic-Zahirovic et al., 2021). This indicates that both cell autonomous and non-cell autonomous mechanisms may alter inhibitory synapses. To complete this observation, we conducted single-nucleus RNA sequencing in the frontal cortex of *Fus*$^{\Delta NLS/+}$ mice, and we will further assess the transcriptomic alterations specific to inhibitory neurons. The observed synaptic alterations seem to be directly linked to the synaptic accumulation of mutant FUS, but the underlying mechanisms remain to be explored. It was notably proposed that FUS may influence the homeostasis of key synaptic RNAs by increasing their stability and regulating their local synaptic translation. Further transcriptomic and histological analysis of *Fus*$^{Resc/+}$ and *Fus*$^{Trunc/+}$ mice will be required, notably to understand whether the rescue of FUS nuclear localisation in inhibitory neurons prevented the appearance of presynaptic defects.

Ultimately, this synaptopathy may give rise to impaired neuronal intrinsic excitability as well as an imbalance in excitatory and inhibitory transmissions, which are part of the early neuronal circuit dysfunctions observed in ALS and FTD patients. In *Fus*$^{\Delta NLS/+}$ mice, increased neuronal activity levels were observed using *in vivo* two-photon calcium imaging, and this phenotype was recapitulated when *Fus* was mutated exclusively in inhibitory neurons. However, further calcium imaging or electrophysiological studies will be necessary to assess whether excitatory transmissions are increased and/or inhibitory transmissions are decreased in these mice. Overall, the characterisations of other ALS and FTD mouse models tend to show a reduced inhibitory influence both in the brain and spinal cord, and this seems to occur irrespective of the causative gene. It is therefore possible that the same observation will be made in *Fus*$^{\Delta NLS/+}$ mice. However, in patients and mouse models, some alterations appear to depend on the underlying proteinopathy, region of the central nervous system and neuronal subpopulations. This highlights the

need to characterise changes in inhibitory neurons in different mouse models, and to further investigate this cell type in FUS-related mice, as it has been overlooked.

This also questions the relevance of our approach in which we cannot distinguish the contribution of specific subpopulations of inhibitory neurons. There exist several mouse lines expressing Cre recombinase in restricted populations of inhibitory neurons, hence similar studies could be conducted to assess the contribution of these cells. Alternatively, one could use viral strategies to target and manipulate subpopulations of neurons (Mehta et al., 2019). Their activation or stabilisation may mitigate or delay ALS- and FTD-like symptoms, whereas their ablation or silencing may recapitulate some of these symptoms. In addition, it may facilitate a more profound comprehension of the function of specific populations of inhibitory neurons under physiological conditions. However, when modelling ALS and FTD, the induction of a proteinopathy in most inhibitory neurons may be a more accurate representation of the processes occurring in patients. Although subpopulations of inhibitory neurons may be differentially affected in these diseases, the overall pathogenic mechanism tends towards a decreased inhibitory influence, and alterations in several major subpopulations have already been reported. It is worth noting that, to our knowledge, the subcellular localisation of FUS in inhibitory neurons has yet to be evaluated in *post-mortem* tissues of patients. Ultimately, a potential limitation may reside in the fact that the relative abundance, distribution, gene expression patterns, morphologies, and electrophysiological properties of subpopulations of inhibitory neurons differ between rodents and humans.

In conclusion, further investigation of inhibitory neurons in ALS and FTD would be beneficial for advancing our understanding of these diseases, and potentially for improving their management. Stabilising or enhancing cortical and spinal inhibitory activity will be challenging due to the inherent complexity and heterogeneity of neuronal populations and circuits. However, this represents a promising avenue for alleviating some motor and behavioural symptoms. Although the rescue of FUS nuclear localisation in inhibitory neurons did not result in a significant prevention of motor and social symptoms, it is possible that inhibitory transmission remains impaired in these mice due to postsynaptic alterations. Therefore, the question of whether rescuing the function of inhibitory synapses could represent an effective therapeutic strategy in FUS-related ALS and FTD remains open. It is also important to note that these two diseases are characterised by alterations in a vast number of cell types, which certainly influence each other. It will be essential to integrate the study of inhibitory neurons into broader investigations of other cells. In this regard, our mouse models may prove to be a valuable tool to decipher if FUS cytoplasmic accumulation in inhibitory neurons influences other cell types, and *vice versa*.

Résumé en français

Introduction

La sclérose latérale amyotrophique (SLA) et la démence frontotemporale (DFT) sont deux maladies neurodégénératives progressives et invalidantes. La SLA se caractérise principalement par la dégénérescence des neurones moteurs présents dans le cortex, le tronc cérébral et la moelle épinière, ce qui entraine une atrophie musculaire et une paralysie progressive (Feldman et al., 2022). La plupart des malades décède 3 à 5 ans après leur diagnostic en raison d'une insuffisance respiratoire. La DFT regroupe différentes pathologies caractérisées par une dégénérescence relativement sélective des lobes frontaux et temporaux (Antonioni et al., 2023). Cela induit d'importantes altérations du comportement, de la personnalité, des fonctions exécutives et des compétences linguistiques. Les malades décèdent en moyenne 7 à 13 ans après leur diagnostic, le plus souvent à cause de comorbidités et de problèmes de sous-alimentation. La SLA et la DFT forment un continuum physiopathologique dans lequel nous retrouvons des similitudes cliniques, génétiques et histologiques. La SLA pure et la DFT pure représentent les deux extrémités de ce continuum, tandis qu'au moins 50% des personnes atteintes de SLA ont des altérations comportementales, et jusqu'à 40% des personnes atteintes de DFT ont des troubles moteurs (Pender et al., 2020). Au total, 15% des malades reçoivent un diagnostic de SLA-DFT, bien que ce chiffre puisse être sous-estimé en raison de la prévalence d'une condition par rapport à l'autre. À ce jour, il n'existe aucun traitement curatif pour ces maladies. Il est dès lors important de mieux comprendre les causes et mécanismes pathologiques, qui unissent et distinguent ces deux maladies, afin d'identifier des cibles thérapeutiques.

La protéine *fused in sarcoma* (FUS) est impliquée dans ce continuum. Il s'agit d'une protéine multifonctionnelle, ubiquitaire et majoritairement nucléaire. Le transport de FUS du cytoplasme au noyau est possible grâce à l'expression d'un domaine de localisation nucléaire (abrégé NLS en anglais). Les mutations pathogéniques de *FUS* sont principalement situées dans ce domaine, et induisent des formes sporadiques et familiales de SLA (Belzil et al., 2009; Kwiatkowski et al., 2009; Vance et al., 2009). Les formes les plus précoces, rapides et agressives sont d'ailleurs consécutives à des mutations hétérozygotes entrainant une délétion du domaine de localisation nucléaire (Bosco et al., 2010; Waibel et al., 2013, 2010; Yan et al., 2010). L'absence ou la mutation de ce domaine compromet le transport nucléocytoplasmique de FUS. Ainsi, une délocalisation cytoplasmique de FUS a été observée aussi bien dans les cellules neuronales que gliales (Kwiatkowski et al., 2009; Vance et al., 2009). Il est intéressant de noter que cette délocalisation peut être observée en l'absence de mutation de *FUS*. Cela semble être une caractéristique pathologique sous-estimée, mais importante, des cas de SLA sporadique (Tyzack et al., 2019). En outre, cela caractérise les personnes atteintes de DFT liée à FUS, qui ont en général une pathologie sporadique, précoce, sévère et rapide (Mackenzie et al., 2011b; Munoz et al., 2009; Neumann et al., 2009a, 2009b). Ces malades

présentent des troubles comportementaux sans déficit linguistique, parfois associés à des troubles moteurs. Quelques exceptions ont été décrites chez des personnes ayant un double diagnostic de SLA-DFT et une mutation de *FUS* (Blair et al., 2010; Broustal et al., 2010; Yan et al., 2010).

Avant mon arrivée en thèse, le laboratoire a développé un modèle murin de SLA-DFT en tronquant le domaine de localisation nucléaire du gène *Fus* dans l'ensemble des cellules, et ce depuis le développement embryonnaire. Cette approche permet d'induire une accumulation cytoplasmique de FUS, modélisant de ce fait les deux maladies au centre de ce projet. Les souris homozygotes ($Fus^{\Delta NLS/\Delta NLS}$) meurent à la naissance en raison d'une insuffisance respiratoire, ce qui empêche d'étudier les conséquences de la troncation de FUS à l'âge adulte (Scekic-Zahirovic et al., 2016). En revanche, les souris hétérozygotes ($Fus^{\Delta NLS/+}$), survivent jusqu'à l'âge adulte et récapitulent plusieurs caractéristiques de la SLA et la DFT (Figure 29). Bien que l'évolution de la maladie ne soit pas aussi rapide ou agressive que celle observée dans les formes juvéniles de SLA associées à cette troncation, les souris présentent des altérations précoces des jonctions neuromusculaires (Picchiarelli et al., 2019), des déficits moteurs légers et progressifs (Sanjuan-Ruiz et al., 2021; Scekic-Zahirovic et al., 2017), et une dégénérescence tardive des neurones moteurs (Scekic-Zahirovic et al., 2017). En outre, elles développent des défauts comportementaux se caractérisant notamment par une sociabilité accrue (Scekic-Zahirovic et al., 2021). Chez ces souris, les neurones moteurs, les oligodendrocytes et les muscles squelettiques participent tous à la pathogenèse de la maladie. Il est intéressant de noter que ces souris présentent également des défauts des neurones inhibiteurs. En effet, des modifications moléculaires et ultra-structurales des synapses inhibitrices GABAergiques ont pu être documentées tout au long de la vie de ces souris (Sahadevan et al., 2021; Scekic-Zahirovic et al., 2021).

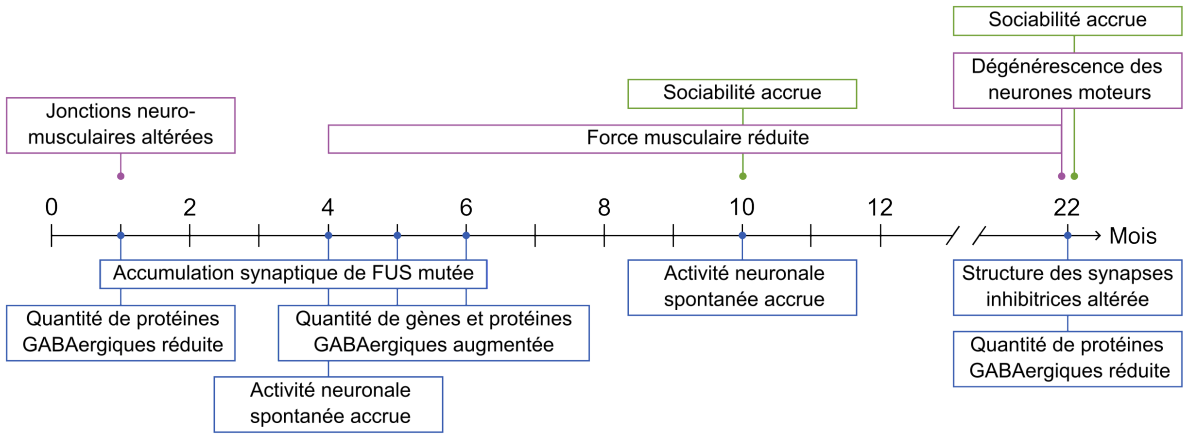


Figure 29: Résumé des principaux résultats précédemment obtenus lors de la caractérisation des souris *Fus*$^{\Delta NLS/+}$ adultes. Les altérations neuronales et synaptiques (en bleu) ont été observées dans le cerveau.

À notre connaissance, il s'agit de la première observation d'altérations des neurones inhibiteurs dans un modèle murin de SLA et DFT associées à FUS. Dans la littérature, de nombreux déficits des neurones inhibiteurs ont été rapportés dans ces deux maladies, que ce soit chez des patient·es ou dans des modèles animaux. Ces altérations pourraient participer à l'apparition et à l'évolution des symptômes, et ce pour des cas de SLA et de DFT liés à différents gènes et protéines. Ces constats sont à l'origine du projet que j'ai réalisé durant ma thèse, et lors duquel j'ai étudié la contribution des neurones inhibiteurs aux phénotypes moteurs (de type SLA) et sociaux (de type DFT) associés à la délocalisation cytoplasmique de la protéine FUS.

Objectifs

L'objectif de mon projet de thèse a été de **caractériser l'implication des neurones inhibiteurs dans la SLA et la DFT liées à la protéine FUS**. En particulier, il s'agissait de vérifier si la délocalisation cytoplasmique de FUS dans les neurones inhibiteurs était nécessaire à l'apparition et la progression des phénotypes moteurs et comportementaux. En d'autres termes, nous voulions savoir s'il est possible d'atténuer, voire de supprimer, ces symptômes en induisant une délocalisation de FUS dans l'ensemble des types cellulaires à l'exception des neurones inhibiteurs. En parallèle, j'ai développé une approche complémentaire permettant de savoir si l'accumulation cytoplasmique de FUS dans les neurones inhibiteurs est suffisante pour causer les symptômes.

Approche expérimentale

Pour remplir mon objectif principal, j'ai développé de nouvelles lignées de souris en me basant sur la technologie de recombinaison Cre-Lox. J'ai sélectionné des souris chez qui la Cre recombinase était exprimée sous le contrôle du promoteur endogène du gène codant pour le transporteur vésiculaire du GABA. Ce transporteur (abrégé VGAT en anglais) est exprimé dans la grande majorité des neurones GABAergiques et glycinergiques situés dans le cerveau et la moelle épinière. Les séquences LoxP se trouvaient dans le gène *Fus* et permettaient, selon la lignée utilisée, d'exprimer le domaine de localisation nucléaire ou d'induire sa troncation (Figure 30).

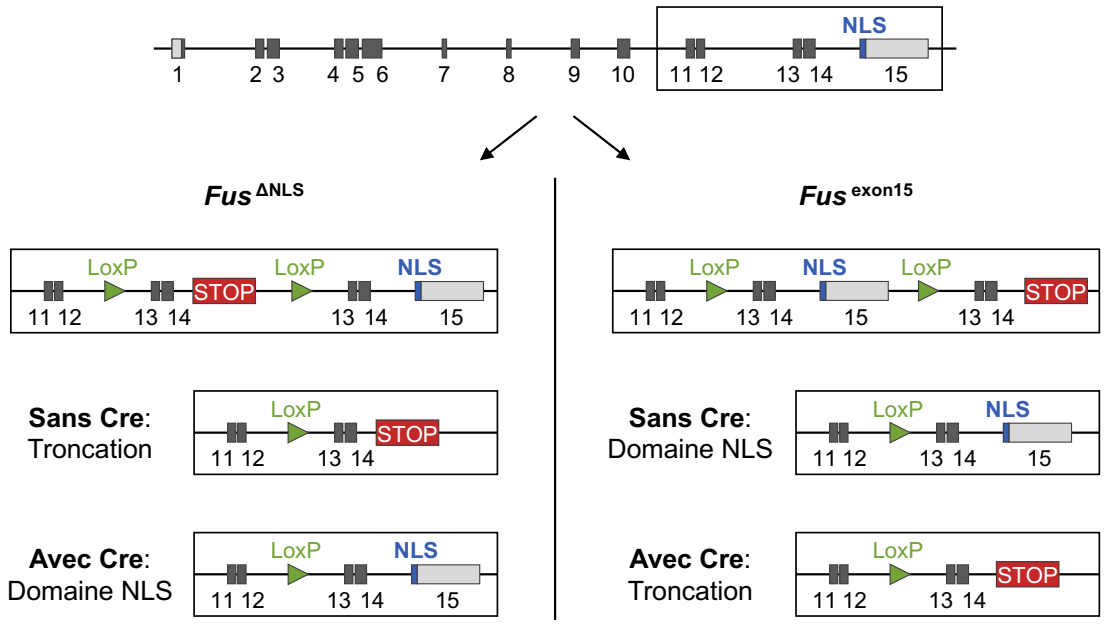


Figure 30: Dans le gène *Fus*, les séquences LoxP permettent de manipuler la troncation du domaine NLS. Représentation schématique du gène *Fus*. Les encadrés situés dans la partie inférieure de la figure représentent les derniers exons chez les souris *Fus*$^{\Delta NLS}$ et *Fus*^{exon15}. (Gauche) Chez les souris *Fus*$^{\Delta NLS}$, le gène a été modifié pour inclure, dans l'intron 12, un ADN complémentaire qui code pour les exons 13 et 14 de *Fus*, suivis de trois cassettes d'arrêt de la transcription et d'un signal de polyadénylation. Cette portion d'ADN est entourée de séquences LoxP. (Droite) Chez les souris *Fus*^{exon15}, le gène a été modifié pour ajouter des séquences LoxP dans l'intron 12 et en aval de l'exon 15. En outre, un ADN complémentaire codant pour les exons 13 et 14 de *Fus*, suivis de trois cassettes d'arrêt de la transcription et d'un signal de polyadénylation, a été ajouté en aval de l'exon 15. Les régions codantes sont en gris foncé, à l'exception du domaine NLS qui est en bleu. Les régions transcrites mais non traduites sont en gris clair, les sites LoxP (triangles) sont en vert, et les cassettes d'arrêt (rectangles) sont en rouge.

J'ai travaillé avec quatre lignées principales (Figure 31), accompagnées de leurs contrôles respectifs. **Souris *Fus*$^{\Delta NLS/+}$** : Ces souris, déjà caractérisées dans le laboratoire, étaient un contrôle positif concernant l'apparition des symptômes moteurs et sociaux. Dans tous les types cellulaires, une copie du gène *Fus* était sauvage, l'autre était tronquée. **Souris *Fus*$^{Resc/+}$** : Ces souris nous ont permis d'évaluer s'il est possible d'atténuer les symptômes en restaurant la localisation nucléaire de FUS exclusivement dans les neurones inhibiteurs. Dans ces neurones, les deux copies de *Fus* exprimaient le domaine NLS. Dans les autres types cellulaires, une copie était sauvage, l'autre était tronquée.

Souris ***Fus***$^{Trunc/+}$ (aussi abrégé Trunc$^{+/-}$) : Dans les neurones inhibiteurs, une copie de *Fus* était sauvage, l'autre était tronquée. Dans les autres types cellulaires, les deux copies exprimaient le domaine de localisation nucléaire. Souris ***Fus***$^{Trunc/Trunc}$ (aussi abrégé Trunc$^{-/-}$) : Dans les neurones inhibiteurs, les deux copies de *Fus* étaient tronquées. Dans les autres types cellulaires, les deux copies exprimaient le domaine de localisation nucléaire.

Ces deux dernières lignées nous ont permis d'évaluer s'il est possible d'induire des symptômes en délocalisant FUS exclusivement dans les neurones inhibiteurs.

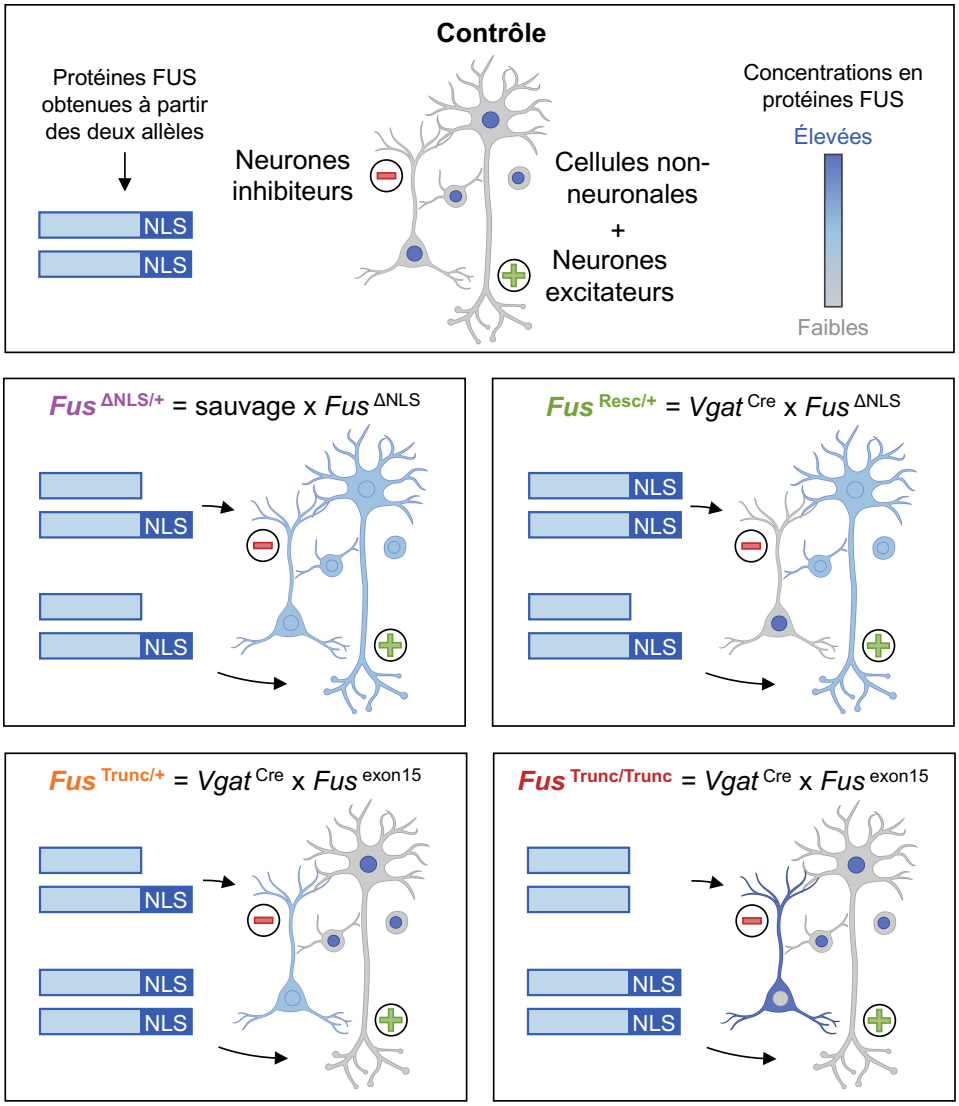


Figure 31: Représentation schématique des principales lignées de souris inclues dans ce projet. Pour chaque souris, l'anticipation de la localisation subcellulaire de FUS est basée sur la présence ou l'absence du domaine NLS.

Suite à la création de ces nouvelles lignées, nous avons observé qu'une partie des souris *Fus*$^{Trunc/Trunc}$ mouraient avant le sevrage, contrairement aux trois autres lignées introduites ci-dessus. Par conséquent, nous avons décidé de mener une étude longitudinale pour caractériser les souris adultes *Fus*$^{\Delta NLS/+}$, *Fus*$^{Resc/+}$ et *Fus*$^{Trunc/+}$. Afin de caractériser les souris *Fus*$^{Trunc/Trunc}$, nous avons adapté notre approche et nous nous sommes concentrées sur la période postnatale.

Résultats

Afin de valider l'approche expérimentale choisie, j'ai vérifié la spécificité et l'efficacité du ciblage des neurones inhibiteurs. Pour cela, j'ai croisé les souris exprimant la Cre recombinase avec une lignée rapportrice. Dans la descendance, la protéine fluorescente tdTomato était exprimée après recombinaison des séquences LoxP, dans les cellules où la Cre recombinase était active. En particulier, dans le cortex frontal de souris de 2 mois, 94% des cellules exprimant tdTomato étaient également positives pour un marquage neuronal, indiquant que Cre est spécifiquement active dans les neurones. Par ailleurs, 10% des neurones exprimaient TdTomato. Or, dans le cortex murin, entre 10 et 15% des neurones sont GABAergiques (Meyer et al., 2011), ce qui suggère que nous avons ciblé la majorité des neurones inhibiteurs. Les protocoles classiques d'immunofluorescence ne permettant pas de marquer l'ensemble des neurones inhibiteurs, je me suis concentrée sur les neurones exprimant la parvalbumine. Ce marqueur est présent dans 40% des neurones inhibiteurs du cerveau, et dans différentes populations de neurones inhibiteurs de la moelle épinière. Mes résultats préliminaires montrent que 38% des cellules exprimant tdTomato étaient également positives pour la parvalbumine, tandis que 61% des neurones parvalbumines exprimaient tdTomato. Dans l'ensemble, ces résultats confirment que les souris exprimant la Cre recombinase offrent une bonne spécificité et une bonne efficacité pour cibler les neurones GABAergiques corticaux, tandis que l'analyse est en cours pour les neurones inhibiteurs spinaux.

Pour compléter cette caractérisation, je me suis intéressée à la localisation subcellulaire de FUS dans des sous-populations de neurones inhibiteurs et excitateurs dans le cortex moteur de souris de 2 mois. Les résultats préliminaires valident que chez les souris $Fus^{\Delta NLS/+}$, la protéine FUS est délocalisée dans le cytoplasme des neurones parvalbumines et des neurones pyramidaux de la couche 5 du cortex. À l'inverse, dans les neurones inhibiteurs, la localisation de FUS était similaire chez les souris $Fus^{Resc/+}$ et les souris contrôles, tandis que dans les neurones excitateurs, la protéine était autant délocalisée chez les souris $Fus^{Resc/+}$ que chez les souris $Fus^{\Delta NLS/+}$. Cela indique que notre stratégie de sauvetage de la localisation nucléaire de FUS spécifiquement dans les neurones exprimant *Vgat* a fonctionnée. Chez les souris $Fus^{Trunc/+}$, une accumulation cytoplasmique de la protéine dans les neurones parvalbumines a été observée chez des souris de 2 mois, et a été confirmée chez des souriceaux de 15 jours. Cette délocalisation était accentuée chez les souriceaux $Fus^{Trunc/Trunc}$ de 15 jours. En revanche, chez les souriceaux $Fus^{Trunc/+}$ et $Fus^{Trunc/Trunc}$, la localisation de FUS dans les neurones moteurs de la moelle épinière lombaire était identique à celle observée chez les souriceaux contrôles. Ainsi, notre stratégie d'induire la délocalisation cytoplasmique de FUS exclusivement dans les neurones exprimant *Vgat* a, elle aussi, fonctionnée.

Pour évaluer l'apparition et la progression des symptômes liés à la SLA et la DFT, j'ai phénotypé les souris *Fus*$^{\Delta NLS/+}$, *Fus*$^{Resc/+}$, *Fus*$^{Trunc/+}$ et leurs contrôles respectifs en réalisant une étude longitudinale de leurs 2 mois à leurs 12 mois (Figure 32). J'ai pesé les souris tous les mois, évalué leur capacité motrice tous les deux mois, et évalué leur sociabilité à 4 et 10 mois. Avec les souris *Fus*$^{\Delta NLS/+}$, j'ai retrouvé des résultats similaires à ce qui a été précédemment décrit dans le laboratoire. Les femelles et mâles présentaient une masse corporelle semblable aux souris contrôles, et des défauts de force musculaire ont été observés à partir de 4 mois avec le test de la grille inversée. Les mâles présentaient une sociabilité accrue à 4 et 10 mois, qui a été observée avec les tests d'interaction en trois chambres et en cage d'hébergement. Cette sociabilité s'intensifiait avec l'âge.

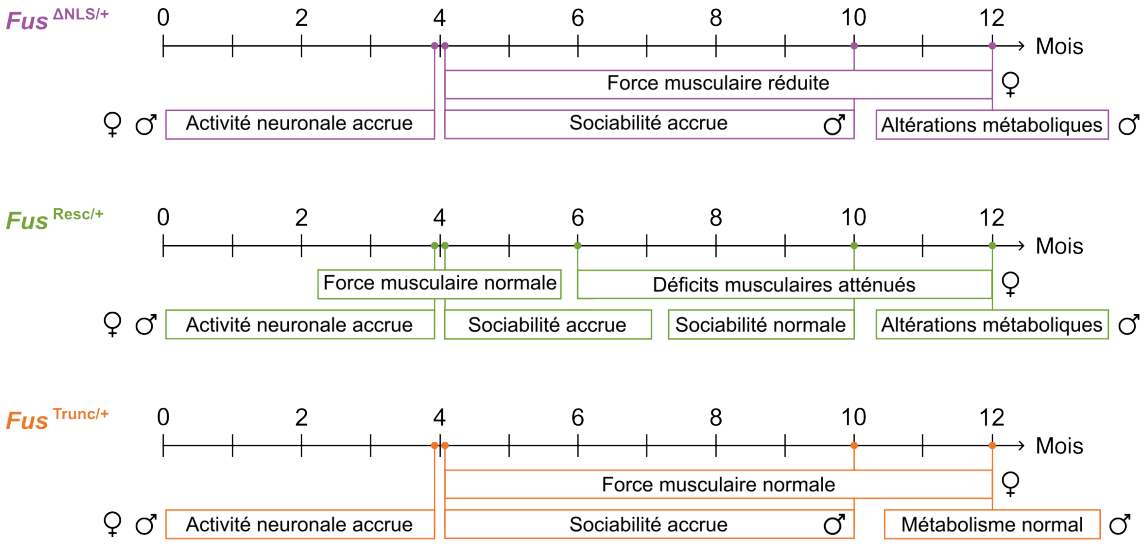


Figure 32: Résumé des principaux résultats obtenus lors de la caractérisation des souris adultes *Fus*$^{\Delta NLS/+}$, *Fus*$^{Resc/+}$ et *Fus*$^{Trunc/+}$.

Relocaliser la protéine FUS exclusivement dans les neurones inhibiteurs a retardé l'apparition des symptômes moteurs chez les femelles, et a atténué les altérations sociales chez les mâles âgés. En effet, à 4 mois les femelles *Fus*$^{Resc/+}$ présentaient une force musculaire similaire à celle des souris contrôles, et significativement supérieure à celles des souris *Fus*$^{\Delta NLS/+}$. Par ailleurs, leurs performances motrices étaient meilleures que celles des souris *Fus*$^{\Delta NLS/+}$ jusqu'à 12 mois. À 4 mois, les mâles *Fus*$^{Resc/+}$ présentaient une sociabilité accrue et similaire à celle des souris *Fus*$^{\Delta NLS/+}$. Il est cependant intéressant de noter que l'accentuation de l'atteinte sociale, observée à 10 mois chez les souris *Fus*$^{\Delta NLS/+}$, n'a pas eu lieu chez les mâles *Fus*$^{Resc/+}$. Au contraire, les mâles *Fus*$^{Resc/+}$ âgés présentaient une sociabilité équivalente à celle des mâles contrôles, et donc significativement moins élevée que celle des souris *Fus*$^{\Delta NLS/+}$. En conclusion, le retrait de la mutation de *Fus* dans les neurones inhibiteurs a permis d'atténuer les symptômes, sans les abolir intégralement.

Délocaliser la protéine FUS exclusivement dans les neurones inhibiteurs n'a pas causé de symptômes moteurs, mais a induit une altération de la sociabilité chez les mâles. En effet, quel que soit l'âge étudié, j'ai observé que les femelles et mâles *Fus*$^{Trunc/+}$ présentaient une force musculaire semblable à celle des souris contrôles. En revanche, les mâles *Fus*$^{Trunc/+}$ présentaient une sociabilité accrue à 4 et 10 mois, sans que celle-ci ne s'intensifie avec l'âge. Ainsi, induire la mutation de *Fus* dans les neurones inhibiteurs est suffisant pour que des altérations sociales apparaissent.

Les travaux précédents du laboratoire ont montré à la fois une atteinte des synapses inhibitrices et une augmentation de l'activité neuronale spontanée dans le cortex frontal des souris *Fus*$^{\Delta NLS/+}$ (Scekic-Zahirovic et al., 2021). Nous nous sommes demandé si l'atteinte inhibitrice pouvait causer cette activité corticale anormale. Pour cela, nous avons mis en place une collaboration avec Dr Sabine Liebscher (Munich), dont le laboratoire est expert en mesure de l'activité neuronale par imagerie calcique *in vivo*. Comme nous savons que les souris *Fus*$^{\Delta NLS/+}$ ont une activité neuronale accrue, nous avons comparé l'activité neuronale de souris *Fus*$^{Resc/+}$ à celle de souris *Fus*$^{\Delta NLS/+}$. Les résultats obtenus chez des souris anesthésiées de 4 mois montrent une atténuation du phénotype. Cependant, l'absence de souris contrôles dans cette expérience nous empêche de savoir si les niveaux d'activité chez les souris *Fus*$^{Resc/+}$ seraient équivalents à ceux de souris sauvages. En revanche, les souris *Fus*$^{Trunc/+}$ présentaient une activité neuronale accrue dans le cortex frontal en comparaison des souris contrôles. Ainsi, la délocalisation cytoplasmique de FUS dans les neurones inhibiteurs est suffisante, et peut-être partiellement nécessaire, à l'altération de l'activité neuronale spontanée au niveau du cortex frontal.

Afin de mieux comprendre l'impact de l'accumulation cytoplasmique de FUS sur les neurones inhibiteurs, nous nous sommes intéressées à son rôle dans le contrôle de l'homéostasie des ARNs. Pour ce faire, nous avons mis en place une seconde collaboration (interne au laboratoire) lors de laquelle j'ai constitué une cohorte de souris *Fus*$^{\Delta NLS/+}$ afin que Dr Salim Megat étudie l'expression des gènes dans le cortex frontal après isolement des noyaux cellulaires et séquençage de l'ARN. Cette analyse est en cours, et confirme que plusieurs types cellulaires, dont les neurones inhibiteurs, sont altérés dans la SLA-DFT. Une étude plus précise de l'altération transcriptomique des neurones inhibiteurs sera réalisée. Si nous identifions des gènes d'intérêt différentiellement exprimés dans les neurones inhibiteurs des souris *Fus*$^{\Delta NLS/+}$, nous pourrons vérifier leur expression dans les tissus des souris *Fus*$^{Resc/+}$ et *Fus*$^{Trunc/+}$, et voir si ces modifications dépendent de la localisation subcellulaire de FUS ou non.

La SLA est associée à des anomalies du métabolisme énergétique, incluant une perte de poids importante, une augmentation des dépenses énergétiques, et une utilisation accrue des nutriments lipidiques au détriment des glucides (Guillot et al., 2021). Afin d'étudier le métabolisme de nos différentes lignées, nous avons réalisé une collaboration (interne

au laboratoire) avec Simon J. Guillot et Dr Matei Bolborea afin de réaliser une étude pilote en utilisant une chambre calorimétrique. Mon analyse des résultats montre que le métabolisme des mâles *Fus*$^{\Delta NLS/+}$ semble dépendre de leur condition d'hébergement. En effet, les mâles isolés tout au long de leur vie présentaient un métabolisme similaire aux souris contrôles isolées. En revanche, les mâles *Fus*$^{\Delta NLS/+}$ vivant en groupes sociaux (et isolées seulement pour l'évaluation de leur métabolisme) présentaient une diminution de la prise alimentaire, une diminution de la balance énergétique, et une augmentation de l'utilisation des lipides au détriment des glucides. Dans cette condition d'hébergement, les mâles *Fus*$^{Resc/+}$ présentaient les mêmes altérations métaboliques que les souris *Fus*$^{\Delta NLS/+}$, tandis que les mâles *Fus*$^{Trunc/+}$ ne présentaient pas d'altérations. Ainsi, les neurones inhibiteurs ciblés ne sont ni nécessaires, ni suffisants pour causer les symptômes métaboliques observés.

Enfin, comme précédemment expliqué, une partie des souris Trunc$^{-/-}$ décèdent avant leur sevrage, nous amenant à adapter notre approche pour nous concentrer sur la période postnatale (Figure 33). J'ai d'abord étudié la survie des souris pendant une période de 18 mois, au cours de laquelle j'ai observé que la moitié des souriceaux Trunc$^{-/-}$ mouraient trois semaines après la naissance, alors que la survie des souris Trunc$^{+/-}$ et des souris contrôles était comparable. Étant donné que la maturation des réseaux corticaux est en partie permise par une mort cellulaire programmée des neurones inhibiteurs entre le 5ème et le 10ème jour postnatal (Wong et al., 2018), nous avons émis l'hypothèse que la délocalisation de FUS pouvait altérer ce phénomène. Nous avons donc décidé d'étudier nos souris avant et après cette période critique. Pour cela, j'ai optimisé et mis en place de nouveaux tests moteurs, et j'ai montré qu'aucune altération n'était visible à l'âge de cinq jours. En revanche, quinze jours après la naissance, les souriceaux Trunc$^{-/-}$ étaient plus petits et plus légers que les souriceaux Trunc$^{+/-}$ et contrôles appartenant aux mêmes portées. Ces souriceaux Trunc$^{-/-}$ avaient également une force musculaire amoindrie dans leurs quatre membres.

Sur la base de ces observations, nous avons fait l'hypothèse qu'une force musculaire amoindrie pourrait compromettre la prise alimentaire des souriceaux, ce qui expliquerait le poids réduit et leur mort prématurée. Pour vérifier cela, j'ai réalisé une étude pilote durant laquelle une partie des souriceaux recevait une nourriture à la fois plus facilement accessible et plus facile à mastiquer. Cette étude n'a pas montré d'effet sur le poids ou la survie. En particulier, les souriceaux qui sont décédés et ceux qui ont survécu présentaient des poids comparables, suggérant que ces souris ne meurent pas de faim.

Nous savons que FUS régule l'homéostasie d'ARNs qui sont importants pour l'intégrité et le fonctionnement des synapses. En particulier, il a été proposé que FUS module la composition des récepteurs GABAergiques dans le cerveau (Sahadevan et al., 2021), ce qui pourrait altérer leur activité. Par ailleurs, notre présente étude a mis en évidence que

l'accumulation cytoplasmique de FUS dans les neurones inhibiteurs est suffisante pour augmenter l'activité neuronale spontanée dans le cortex frontal. Cela suggère que FUS mutée peut modifier le fonctionnement des neurones inhibiteurs. Enfin, notre étude pilote m'a permis d'observer quotidiennement le comportement des souriceaux et de voir que certains d'entre eux présentaient des phases transitoires d'inactivité. Ils adoptaient une position voutée, et réagissaient peu ou pas aux stimuli tactiles. Cela pourrait être le signe d'un arrêt comportemental, potentiellement dû à une absence épileptique et/ou un phénotype léthargique résultant d'un évènement stressant. Ainsi, notre seconde hypothèse est que les phénotypes observés chez les souriceaux Trunc$^{-/-}$ sont liés à une activité neuronale anormale, pouvant aller jusqu'à des crises de type épileptique. Pour vérifier cela, nous avons mis en place une collaboration avec Delphine Roussel (Paris) qui va réaliser des mesures électroencéphalographiques dans le cerveau des souriceaux âgés de 15 à 20 jours.

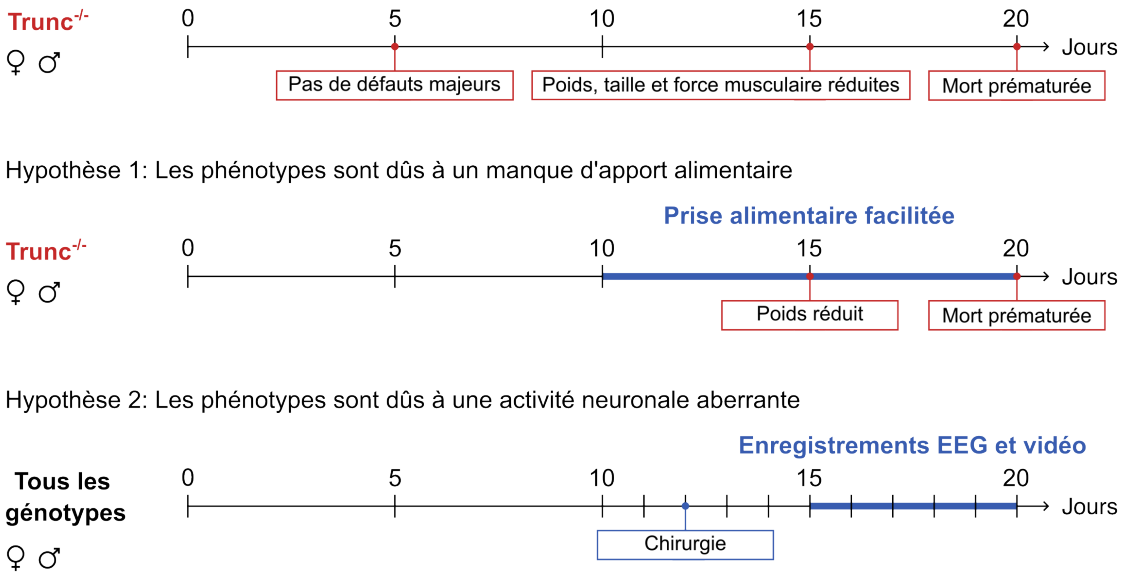


Figure 33: Résumé des principaux résultats obtenus lors de la caractérisation des souriceaux Trunc$^{-/-}$. Le développement postnatal des souriceaux Trunc$^{+/-}$ a également été évalué, mais aucune altération n'a été observée, ce qui explique qu'ils ne soient pas représentés sur la figure. EEG : électroencéphalographiques.

Discussion

1. Mécanismes sous-jacents aux déficits moteurs

La caractérisation initiale des souris *Fus*$^{\Delta NLS/+}$ a révélé que, jusqu'à l'âge de 22 mois, les performances des mâles lors des tests du rotarod ou de la force de préhension ne sont pas altérées (Scekic-Zahirovic et al., 2017). Cependant, une réduction de la force musculaire a effectivement été observée à l'âge de 10 mois en utilisant le test de la grille inversée. Une étude longitudinale a ensuite montré que ce phénotype léger évolue progressivement avec l'âge (Sanjuan-Ruiz et al., 2021). Après quelques adaptations, nous avons pu réaliser ce test avec des souriceaux âgés de 15 jours. Globalement, dans notre étude, nous avons observé que le sauvetage de la localisation nucléaire de FUS dans les neurones inhibiteurs exprimant *Vgat* retardait l'apparition des déficits moteurs chez les souris femelles mais pas chez les souris mâles. À l'inverse, la mutation hétérozygote de *Fus* dans ces neurones n'a pas été suffisante pour induire des déficits moteurs chez les souris, quel que soit leur sexe. En revanche, la mutation homozygote de *Fus* dans les neurones inhibiteurs a induit des déficits de force musculaire à l'âge de 15 jours, chez les femelles comme chez les mâles. À partir de ces résultats, il apparait que la contribution des neurones inhibiteurs aux déficiences motrices de type SLA est complexe à déterminer, et dépend probablement d'ampleur de la délocalisation de FUS et du sexe.

Les neurones inhibiteurs contribuent-ils aux défauts moteurs liés à FUS ? Chez les souris *Fus*$^{\Delta NLS/+}$, des mécanismes autonomes et non autonomes des neurones moteurs contribuent à la faiblesse musculaire. En effet, le sauvetage de la localisation nucléaire de FUS dans les neurones cholinergiques s'est avéré suffisant pour prévenir la dégénérescence des neurones moteurs, mais n'a fait que retarder l'apparition des déficits moteurs, évalués avec le test de la grille inversée (Scekic-Zahirovic et al., 2017). Cela indique que d'autres types cellulaires sont impliqués dans la progression de ce phénotype. Notre analyse des souris hétérozygotes adultes suggère que les neurones inhibiteurs ne jouent pas un rôle significatif dans la pathogenèse du phénotype moteur. En effet, aucune altération de la force musculaire n'a été observée chez les souris *Fus*$^{Trunc/+}$ femelles et mâles au cours de leur développement postnatal ou à l'âge adulte (Figure 32). Cependant, lorsque les deux copies de *Fus* étaient mutées dans les neurones inhibiteurs, une faiblesse musculaire a été observée deux semaines après la naissance.

Nous ne pouvons pas exclure la possibilité que les souris *Fus*$^{Trunc/+}$ pourraient développer des déficits moteurs plus tard au cours de leur vie. Une autre hypothèse est que la mutation hétérozygote de *Fus* n'induit pas d'altérations des neurones inhibiteurs ayant des effets conséquents sur le phénotype moteur. À l'inverse, l'apparition retardée des défauts moteurs chez les femelles *Fus*$^{Resc/+}$ suggère que les neurones inhibiteurs contribuent à l'apparition du phénotype (Figure 32). Une explication possible de cette

divergence est que les anomalies motrices liées à FUS sont causées par un effet synergique d'altérations dans plusieurs types cellulaires. Chez les souris *Fus*$^{Resc/+}$, la grande majorité des types cellulaires présentent une délocalisation de FUS et peuvent donc accumuler suffisamment d'altérations pour déclencher des déficits moteurs, ce qui ne se produit pas nécessairement chez les souris *Fus*$^{Trunc/+}$

Chez les souris *Fus*$^{\Delta NLS/+}$, il a été précédemment proposé que les altérations des cellules myélinisantes, dans la moelle épinière et/ou en périphérie, contribuent aux déficits moteurs (Scekic-Zahirovic et al., 2017). Cependant, l'accumulation cytoplasmique de FUS dans les oligodendrocytes matures n'est pas suffisante pour induire une réduction des performances au test de la grille inversée chez des souris hétérozygotes et homozygotes jusqu'à l'âge de 10 mois (Jamet al., en préparation). Une observation similaire a été faite lorsque la délocalisation de FUS a été induite exclusivement dans les neurones à projection à l'âge adulte (Publication 3). Chez les souris TDP-43^{Q331K}, le retrait de TDP-43 mutant des neurones moteurs a empêché leur dégénérescence, bien que cela n'ait fait que retarder l'apparition des symptômes moteurs, évalués à l'aide du test du rotarod (Ditsworth et al., 2017). Chez les souris *SOD1*^{G73R}, l'apparition et la progression de la maladie peuvent être évaluées avec précision en surveillant la perte de poids. Cela a permis de démontrer que l'élimination de SOD1 mutant des neurones moteurs ou des oligodendrocytes retarde l'apparition de la maladie (Boillée et al., 2006; Kang et al., 2013), tandis que son élimination des astrocytes ou de la microglie ralentit la progression de la maladie (Boillée et al., 2006; Yamanaka et al., 2008). Les conséquences de l'élimination de TDP-43 ou de SOD1 mutants des neurones inhibiteurs n'ont pas encore été étudiées. Néanmoins, les résultats actuels pointent collectivement vers des altérations multicellulaires dans la SLA (Crabé et al., 2020). Nous ne savons toujours pas si l'altération d'un type cellulaire spécifique constitue l'événement initial qui déclenche la maladie. Chez les souris *Fus*$^{\Delta NLS/+}$, les défauts moteurs légers et difficiles à observer peuvent limiter notre compréhension de l'implication des différentes populations cellulaires lors de la caractérisation des souris knock-in spécifiques à un type cellulaire.

En effet, il est important de noter que notre évaluation des déficits moteurs s'est limitée au test de la grille inversée, qui n'a peut-être pas fourni une appréciation complète du phénotype. J'ai suivi le protocole communément établi pour l'évaluation de la force et de l'endurance musculaires chez les modèles murins. Cependant, un manque potentiel d'engagement des souris peut avoir introduit un biais dans les résultats. Nos souris contrôles présentaient un déclin progressif du temps de suspension et de l'impulsion de maintien avec l'âge. Ce phénomène a déjà été observé par notre laboratoire (Sanjuan-Ruiz et al., 2021) et d'autres (Yanai and Endo, 2021). En particulier, chez les souris mâles sauvages C57BL/6J, il a été montré que le temps de suspension commence à diminuer à l'âge de 6 mois. Cependant, la cause sous-jacente de cette diminution reste un sujet de controverse. Bien que cela puisse indiquer un déclin progressif des fonctions motrices,

d'autres paramètres peuvent causer, ou du moins influencer, ce phénotype. Par exemple, l'augmentation du poids corporel liée à l'âge et une perte progressive de motivation peuvent entraîner une diminution du temps de suspension, alors que la fonction motrice des souris reste intacte. Conformément à cette hypothèse, l'utilisation des tests du rotarod ou de force de préhension a suggéré que les fonctions motrices commencent à décliner à un stade plus avancé chez les souris sauvages (Börsch et al., 2021; Noda et al., 2020; Shoji and Miyakawa, 2019; Yanai and Endo, 2021). En outre, il a été montré que les mâles sauvages C57BL/6J âgés présentaient une motivation réduite par rapport à leurs homologues plus jeunes (Jackson et al., 2021). Dans notre cohorte, nous avons observé qu'avec l'âge et/ou la répétition du test, les souris étaient plus susceptibles de sauter de la grille, même au début du test. Cela peut refléter un manque d'engagement plutôt qu'une fatigue musculaire, car ces souris étaient capables de s'accrocher plus longtemps à la grille de leur cage d'hébergement. Cela était particulièrement vrai pour les mâles, qui étaient plus enclins à sauter que les femelles. Par conséquent, nos résultats actuels ne sont peut-être pas suffisants pour tirer une conclusion définitive sur la contribution de la délocalisation du FUS dans les neurones inhibiteurs aux phénotypes moteurs.

La caractérisation initiale des souris *Fus*$^{\Delta NLS/+}$ par rapport aux souris contrôles n'a révélé aucune différence perceptible lors du suivi longitudinal de leur poids (Sanjuan-Ruiz et al., 2021) ou lors de l'utilisation du test de force de préhension (Scekic-Zahirovic et al., 2017). Cela indique que des tests plus sensibles sont nécessaires pour surveiller les défauts moteurs dans cette lignée de souris. Aucun test moteur n'est sans faille, car ils dépendent de l'engagement des souris (qui peut diminuer avec la répétition des tests et l'âge des souris) et/ou des expérimentatrices. Néanmoins, il pourrait être intéressant d'essayer une version modifiée du test de force de préhension, qui a été décrite comme améliorant la validité, la cohérence et la sensibilité du test (Takeshita et al., 2017). En outre, il serait bénéfique d'identifier des altérations moléculaires pertinentes vis-à-vis des défauts moteurs observés. Il semble plus pertinent d'évaluer l'altération des jonctions neuromusculaires que d'observer la dégénérescence des neurones moteurs, car cette dernière ne devient apparente que plusieurs mois après l'apparition des défauts moteurs (Scekic-Zahirovic et al., 2017), alors que la première peut être observée plusieurs mois avant cette apparition (Picchiarelli et al., 2019). Par conséquent, j'ai récupéré les muscles des membres postérieurs de souris âgées de 2 mois et de 12 mois, et il pourrait être intéressant de vérifier si la dénervation des muscles est moins prononcée chez les femelles *Fus*$^{Resc/+}$ que chez les souris *Fus*$^{\Delta NLS/+}$.

2. Mécanismes sous-jacents à la sociabilité accrue

Une précédente caractérisation de la lignée *Fus*$^{\Delta NLS/+}$ a révélé une augmentation légère de la sociabilité à 4 mois et une augmentation significative à 10 mois (Scekic-Zahirovic et al., 2021). Dans notre étude, nous avons observé que le sauvetage de la localisation nucléaire

de FUS dans les neurones inhibiteurs exprimant *Vgat* n'empêchait pas l'apparition de ce phénotype à l'âge de 4 mois, mais restaurait l'intérêt social au même niveau que celui des souris contrôles à 10 mois. La mutation hétérozygote de *Fus* dans ces neurones a été suffisante pour induire un intérêt social accru à 4 et 10 mois. Sur la base de ces résultats, nous pouvons proposer que les neurones inhibiteurs contribuent aux défauts sociaux de type DFT chez les souris mâles. En raison de contraintes logistiques, nous n'avons pas pu effectuer cette analyse chez les femelles, et des investigations supplémentaires sont donc nécessaires pour déterminer si ce phénomène est commun aux deux sexes.

Il est intéressant de noter qu'une réduction de l'inhibition intracorticale a été associée à des comportements désinhibés chez les personnes atteintes de DFT (Benussi et al., 2020; Murley et al., 2020). Ces comportements peuvent se manifester de différentes manières, notamment par une désinhibition sociale avec des propos et des actions inappropriées, une impulsivité, des comportements persévérants, stéréotypés et/ou obsessionnels, pour n'en citer que quelques-uns. Chez les souris adultes, un certain nombre de tests sont disponibles pour l'évaluation de comportements analogues (Vernay et al., 2016), bien qu'ils restent à utiliser avec nos modèles murins. Par exemple, il serait intéressant de vérifier si nos lignées présentent des comportements impulsifs dans un labyrinthe en croix surélevé ou lors d'un test clair/obscur, tandis que les comportements compulsifs pourraient être évalués avec le test d'enfouissement des billes.

Quels mécanismes pourraient expliquer l'augmentation de la sociabilité ? Nous nous sommes concentrées sur les comportements sociaux car nous savions qu'ils sont altérés par l'accumulation cytoplasmique de FUS (Scekic-Zahirovic et al., 2021). De plus, il existe une littérature abondante concernant le rôle de la balance excitation-inhibition dans la régulation de la sociabilité, même si la plupart des mécanismes sous-jacents restent inconnus. Il a notamment été proposé que la « détérioration des synapses inhibitrices puisse être une base neurologique essentielle sous-tendant les comportements sociaux anormaux » (Ju et al., 2023). Cependant, dans plusieurs conditions pathologiques, des niveaux plus élevés d'excitation et/ou des niveaux plus faibles d'inhibition ont été associés à une diminution de l'intérêt social. C'est le cas, par exemple, dans les modèles murins d'autisme (Parrella et al., 2024) ou de schizophrénie (Liu et al., 2021). Chez les personnes atteintes de DFT, les déficiences sociales peuvent se manifester soit par une perte de sympathie et d'empathie, soit par un comportement désinhibé, mais chez les souris, une diminution de la sociabilité a été presque exclusivement rapportée (Vernay et al., 2016). Nous avons observé le phénotype inverse dans nos modèles, et il est intéressant de noter qu'une sociabilité accrue a aussi été rapportée après l'inhibition de l'expression de *Fus* spécifiquement dans l'hippocampe (Udagawa et al., 2015).

Comment l'altération des neurones inhibiteurs pourraient expliquer l'augmentation de la sociabilité liée à FUS ? La caractérisation de lignées de souris présentant à la fois un

intérêt social accru et des altérations des neurones inhibiteurs a permis de proposer deux mécanismes sous-jacents potentiels : l'altération de l'expression des gènes GABAergiques et l'altération des synapses et circuits GABAergiques. L'un de ces modèles est basé sur la diminution de l'expression de gènes Dlx (Fazel Darbandi et al., 2021). Ces gènes codent pour des facteurs de transcription qui sont notamment nécessaires au développement et à la différentiation des neurones GABAergiques. Chez ces souris, une diminution transitoire de l'expression des gènes liés à la synthèse du GABA et une réduction transitoire du nombre de neurones GABAergiques ont été observées au cours du développement embryonnaire. Il a ensuite été proposé que cette perturbation ou ce retard du développement des neurones GABAergiques puisse avoir un effet durable sur les circuits neuronaux, ce qui pourrait expliquer la sociabilité accrue observée chez les jeunes adultes. Cette hypothèse reste toutefois à vérifier. Les personnes présentant des mutations du gène *POGZ*, qui code pour une protéine impliquée dans l'inhibition de la transcription et la modulation de l'architecture de la chromatine, présentent parfois des comportements trop sociaux et amicaux (Stessman et al., 2016). Dans un modèle de souris arborant une délétion homozygote de ce gène, des altérations transcriptomiques ont été observées pour des gènes impliqués dans la neurogénèse, le métabolisme et les processus synaptiques (Suliman-Lavie et al., 2020). Cela incluait une augmentation de gènes GABAergiques dans le cervelet, qui était la région cérébrale d'intérêt dans cette étude. Il a alors été proposé que cela puisse être à l'origine de la sociabilité accrue. Enfin, des mutations du gène *CYLD* ont récemment été associées à la SLA et la DFT (Dobson-Stone et al., 2020). Dans le cerveau, CYLD est important au niveau des synapses. Il favorise leur remodelage et leur plasticité, notamment en inhibant la voie Akt-mTOR qui, à son tour, renforce l'autophagie. Chez les souris ayant une suppression complète de ce gène, il a été observé que ce contrôle en amont de la voie Akt-mTOR est perdu, et la diminution de l'autophagie qui en a résulté a entrainé une altération du nombre, de l'efficacité et de la plasticité des synapses (Zajicek et al., 2022). Ainsi, cela a été proposé comme une explication possible de la sociabilité accrue observée chez ces souris.

Dans le cerveau des souris *Fus*$^{\Delta NLS/+}$, des altérations à la fois de l'expression de gènes GABAergiques et des synapses GABAergiques ont été documentées (Sahadevan et al., 2021; Scekic-Zahirovic et al., 2021). En particulier, une diminution de la quantité de sous-unités α3 des récepteurs $GABA_A$ a été rapportée à 1 mois. À l'inverse, à l'âge de 6 mois, l'expression de deux gènes codant pour des sous-unités de récepteurs $GABA_A$ (*Gabra1* et *Gabrb1*) était augmentée. Cela s'est accompagné d'une augmentation de l'expression de protéines GABAergiques dans des synapses inhibitrices qui étaient potentiellement instables. En effet, l'absence d'augmentation de l'expression de la géphyrine, une protéine postsynaptique responsable de l'ancrage des récepteurs $GABA_A$ (Specht et al., 2013), suggère une désorganisation du compartiment postsynaptique, ce qui pourrait diminuer la transmission inhibitrice. À 10 mois, une augmentation de l'activité neuronale spontanée a été observée et a été proposée comme une cause potentielle de l'altération

de la sociabilité (Scekic-Zahirovic et al., 2021). À l'âge de 22 mois, les niveaux de protéines GABAergiques étaient diminués, ce qui peut directement altérer la transmission inhibitrice. Enfin, l'ultrastructure des synapses inhibitrices était anormale, avec une augmentation de la taille et du nombre de vésicules, ce qui pourrait être un phénomène compensant la diminution de leur densité.

Dans notre étude, l'augmentation de l'intérêt social chez les mâles *Fus*$^{Trunc/+}$ âgés de 4 mois s'est également accompagnée d'une augmentation de l'activité neuronale par rapport aux souris contrôles (Figure 32). Chez les mâles *Fus*$^{Resc/+}$ du même âge, nous avons observé une sociabilité accrue atteignant des niveaux similaires à ceux des mâles *Fus*$^{\Delta NLS/+}$. En revanche, l'activité neuronal spontanée était réduite chez les souris *Fus*$^{Resc/+}$ par rapport aux souris *Fus*$^{\Delta NLS/+}$. Cela suggère que d'autres mécanismes sont impliqués dans le phénotype social observé. Il serait intéressant d'étudier l'expression de gènes et protéines synaptiques chez les souris *Fus*$^{\Delta NLS/+}$ et *Fus*$^{Resc/+}$ pour voir quelles altérations communes ressortent et pourraient être à l'origine de l'augmentation de la sociabilité. Cependant, pour le moment, nous n'avons pas récupéré de tissus à cet âge-là, car les souris étaient incluses dans des études longitudinales. À l'âge de 10 mois, nous avons observé un intérêt social accru chez les mâles *Fus*$^{Trunc/+}$ et *Fus*$^{\Delta NLS/+}$, mais pas chez les mâles *Fus*$^{Resc/+}$ pour lesquels l'intérêt était similaire à celui des souris contrôles. Cela suggère que le sauvetage de la localisation nucléaire de FUS dans les neurones inhibiteurs est suffisant pour atténuer les altérations sociales chez les souris mâles âgées. Étant donné que nous avons récupéré des tissus à 12 mois, une autre approche consisterait à évaluer l'expression de gènes et protéines synaptiques à cet âge en se concentrant sur les différences entre les souris *Fus*$^{\Delta NLS/+}$ et *Fus*$^{Resc/+}$. Cela pourrait mettre en évidence des mécanismes moléculaires protecteurs chez les souris *Fus*$^{Resc/+}$.

Conclusion

Pour conclure, j'ai montré que les neurones inhibiteurs sont impliqués dans la temporalité d'apparition du phénotype moteur et dans la progression du phénotype comportemental chez les souris. En effet, retirer la mutation de *Fus* dans les neurones inhibiteurs a permis d'atténuer les symptômes, mais sans les abolir intégralement. Ce dernier point indique que d'autres types cellulaires contribuent au développement de la SLA et la DFT. De manière intéressante, la délocalisation de FUS dans les neurones inhibiteurs est suffisante pour induire des symptômes comportementaux et une augmentation de l'activité neuronale spontanée dans le cortex frontal. De plus, un autre point clé de ma thèse est la découverte d'une altération du développement postnatal des souriceaux lorsque nous induisons une mutation homozygote de *Fus* dans les neurones inhibiteurs. Les mécanismes sous-jacents sont en train d'être étudiés.

Il serait intéressant de vérifier l'implication des neurones inhibiteurs dans l'apparition et/ou la progression d'autres symptômes. En ce qui concerne la SLA, nous pourrions évaluer les phénotypes locomoteurs associés aux neurones inhibiteurs de la moelle épinière. Pour la DFT, nous pourrions évaluer d'autres comportements caractéristiques d'une désinhibition, tels que l'impulsivité, la persévérance et les comportements compulsifs stéréotypés. Une meilleure compréhension de la contribution des neurones inhibiteurs à l'apparition et/ou à la progression des symptômes est nécessaire pour étayer la nécessité de développer des approches thérapeutiques ciblant ces neurones. Cependant, pour que ce ciblage soit efficace, il est également nécessaire de comprendre les mécanismes par lesquels les neurones inhibiteurs sont altérés.

A ce jour, une question majeure reste sans réponse : comment l'accumulation cytoplasmique de FUS affecte-t-elle les neurones inhibiteurs ? Les caractérisations précédentes des souris $Fus^{\Delta NLS/+}$ ont démontré des altérations transcriptomiques, histologiques et ultrastructurales dans les compartiments pré- et postsynaptiques (Sahadevan et al., 2021; Scekic-Zahirovic et al., 2021). Cela indique que des mécanismes intrinsèques aux neurones inhibiteurs, ainsi que des mécanismes extrinsèques peuvent altérer les synapses inhibitrices. Pour compléter cette observation, nous avons réalisé un séquençage de l'ARN à noyau unique dans le cortex frontal des souris $Fus^{\Delta NLS/+}$, et nous évaluerons plus les altérations transcriptomiques spécifiques aux neurones inhibiteurs. Les modifications synaptiques observées semblent être directement liées à l'accumulation synaptique de FUS mutée, mais les mécanismes sous-jacents restent à explorer. Il a notamment été proposé que FUS puisse influencer l'homéostasie d'ARNs synaptiques clés en augmentant leur stabilité et en régulant leur traduction locale. D'autres analyses transcriptomiques et histologiques des souris $Fus^{Resc/+}$ et $Fus^{Trunc/+}$ seront nécessaires, notamment pour comprendre si le sauvetage de la localisation

nucléaire de FUS dans les neurones inhibiteurs a empêché l'apparition de défauts dans le compartiment présynaptique.

Finalement, cette synaptopathie peut entraîner une altération de l'excitabilité intrinsèque des neurones, ainsi qu'un déséquilibre entre les transmissions excitatrices et inhibitrices, qui font partie des dysfonctionnements précoces des circuits neuronaux observés chez les personnes atteintes de SLA et/ou DFT. Chez les souris *Fus*$^{\Delta NLS/+}$, une augmentation de l'activité neuronale spontanée a été observée par imagerie calcique à deux photons, et nous avons retrouvé ce phénotype lorsque *Fus* était muté exclusivement dans les neurones inhibiteurs. Cependant, d'autres études d'imagerie calcique ou électrophysiologiques seront nécessaires pour évaluer si les transmissions excitatrices sont augmentées et/ou si les transmissions inhibitrices sont diminuées chez ces souris. Dans l'ensemble, la caractérisation d'autres modèles murins de SLA et DFT tend à démontrer une réduction de l'inhibition à la fois dans le cerveau et dans la moelle épinière, et cela semble se produire indépendamment du gène muté. Il est donc possible que la même observation soit faite chez les souris *Fus*$^{\Delta NLS/+}$. Cependant, chez les malades et modèles murins, certaines altérations semblent dépendre de la protéinopathie sous-jacente, de la région du système nerveux central et des sous-populations neuronales. Cela souligne la nécessité de caractériser les altérations des neurones inhibiteurs dans différents modèles de souris, et d'étudier davantage ce type cellulaire chez les souris portant des mutations de *Fus*, car ces neurones ont longtemps été négligés.

La pertinence de notre approche, avec laquelle nous ne pouvons pas distinguer la contribution de sous-populations spécifiques de neurones inhibiteurs, pourrait être remise en question. Il existe plusieurs lignées de souris exprimant la recombinase Cre dans des populations restreintes de neurones inhibiteurs, et des études similaires pourraient donc être menées pour évaluer la contribution de ces cellules. Il est également possible d'utiliser des stratégies virales pour cibler et manipuler des sous-populations de neurones (Mehta et al., 2019). Leur activation ou leur stabilisation pourrait atténuer ou retarder les symptômes semblables à ceux de la SLA et de la DFT, tandis que leur ablation ou leur inactivation pourrait récapituler certains de ces symptômes. En outre, cela pourrait faciliter une compréhension plus approfondie de la fonction de populations spécifiques de neurones inhibiteurs dans des conditions physiologiques. Toutefois, en ce qui concerne la modélisation de la SLA et de la DFT, l'induction d'une protéinopathie dans la grande majorité des neurones inhibiteurs pourrait être une représentation plus précise des processus qui se produisent chez les malades. Bien que des sous-populations de neurones inhibiteurs puissent être affectées de manière différentielle dans ces maladies, le mécanisme pathogénique global tend vers une diminution de l'inhibition, et des altérations dans plusieurs sous-populations majeures ont déjà été rapportées. Il convient de noter qu'à notre connaissance, la localisation subcellulaire de FUS dans les neurones inhibiteurs n'a pas encore été évaluée dans les tissus *post-mortem* de malades. Enfin, une

limitation potentielle pourrait résider dans le fait que l'abondance relative, la distribution, les profils d'expression génétique, les morphologies et les propriétés électrophysiologiques des sous-populations de neurones inhibiteurs diffèrent entre les rongeurs et les humains.

En conclusion, une étude plus approfondie des neurones inhibiteurs dans la SLA et la DFT serait bénéfique pour faire progresser notre compréhension de ces maladies, et potentiellement améliorer leur prise en charge. Stabiliser ou accroitre l'activité inhibitrice dans le cortex et la moelle épinière sera un défi en raison de la complexité et de l'hétérogénéité inhérentes des populations et des circuits neuronaux. Cependant, cela représente une voie prometteuse pour soulager certains symptômes moteurs et comportementaux. Bien que le sauvetage de la localisation nucléaire de FUS dans les neurones inhibiteurs n'ait pas entraîné une prévention significative des symptômes moteurs et sociaux, il est possible que la transmission inhibitrice reste altérée chez ces souris en raison de problèmes post-synaptiques. Par conséquent, la question de savoir si le sauvetage de la fonction des synapses inhibitrices pourrait représenter une stratégie thérapeutique efficace dans la SLA et la DFT liées à FUS reste ouverte. Il est également important de noter que ces deux maladies sont caractérisées par des altérations dans un grand nombre de types cellulaires qui, certainement, s'influencent mutuellement. Il sera essentiel d'intégrer l'étude des neurones inhibiteurs dans des recherches plus larges s’intéressant aussi à d'autres cellules. À cet égard, nos modèles de souris pourraient s'avérer être un outil précieux pour déterminer si l'accumulation cytoplasmique de FUS dans les neurones inhibiteurs influence d'autres types cellulaires, et *vice versa*.

References

- A -

Abrahams, S., Goldstein, L.H., Simmons, A., Brammer, M., Williams, S.C.R., Giampietro, V., Leigh, P.N., 2004. Word retrieval in amyotrophic lateral sclerosis: a functional magnetic resonance imaging study. Brain 127, 1507–1517.

Abrahams, S., Newton, J., Niven, E., Foley, J., Bak, T.H., 2014. Screening for cognition and behaviour changes in ALS. Amyotroph Lateral Scler Frontotemporal Degener 15, 9–14.

Ahmed, R.M., Irish, M., Piguet, O., Halliday, G.M., Ittner, L.M., Farooqi, S., Hodges, J.R., Kiernan, M.C., 2016. Amyotrophic lateral sclerosis and frontotemporal dementia: distinct and overlapping changes in eating behaviour and metabolism. Lancet Neurol 15, 332–342.

Akçimen, F., Lopez, E.R., Landers, J.E., Nath, A., Chiò, A., Chia, R., Traynor, B.J., 2023. Amyotrophic lateral sclerosis: translating genetic discoveries into therapies. Nat Rev Genet 24, 642–658.

Albéri, L., Sgadò, P., Simon, H.H., 2004. Engrailed genes are cell-autonomously required to prevent apoptosis in mesencephalic dopaminergic neurons. Development 131, 3229–3236.

Al-Chalabi, A., Hardiman, O., 2013. The epidemiology of ALS: a conspiracy of genes, environment and time. Nat Rev Neurol 9, 617–628.

Al-Chalabi, A., Lewis, C.M., 2011. Modelling the effects of penetrance and family size on rates of sporadic and familial disease. Hum Hered 71, 281–288.

Ali, Z., Godoy-Corchuelo, J.M., Martins-Bach, A.B., Garcia-Toledo, I., Fernández-Beltrán, L.C., Nair, R.R., Spring, S., Nieman, B.J., Jimenez-Coca, I., Bains, R.S., Forrest, H., Lerch, J.P., Miller, K.L., Fisher, E.M.C., Cunningham, T.J., Corrochano, S., 2023. Mutation in the FUS nuclear localisation signal domain causes neurodevelopmental and systemic metabolic alterations. Dis Model Mech 16.

Allain, A.-E., Baïri, A., Meyrand, P., Branchereau, P., 2006. Expression of the glycinergic system during the course of embryonic development in the mouse spinal cord and its co-localization with GABA immunoreactivity. J Comp Neurol 496, 832–846.

Allain, A.-E., Baïri, A., Meyrand, P., Branchereau, P., 2004. Ontogenic changes of the GABAergic system in the embryonic mouse spinal cord. Brain Res 1000, 134–147.

Allodi, I., Montañana-Rosell, R., Selvan, R., Löw, P., Kiehn, O., 2021. Locomotor deficits in a mouse model of ALS are paralleled by loss of V1-interneuron connections onto fast motor neurons. Nat Commun 12, 3251.

Al-Massadi, O., Dieguez, C., Schneeberger, M., López, M., Schwaninger, M., Prevot, V., Nogueiras, R., 2021. Multifaceted actions of melanin-concentrating hormone on mammalian energy homeostasis. Nat Rev Endocrinol 17, 745–755.

Alvarez, F.J., Jonas, P.C., Sapir, T., Hartley, R., Berrocal, M.C., Geiman, E.J., Todd, A.J., Goulding, M., 2005. Postnatal phenotype and localization of spinal cord V1 derived interneurons. J Comp Neurol 493, 177–192.

Aly, A., Laszlo, Z.I., Rajkumar, S., Demir, T., Hindley, N., Lamont, D.J., Lehmann, J., Seidel, M., Sommer, D., Franz-Wachtel, M., Barletta, F., Heumos, S., Czemmel, S., Kabashi, E., Ludolph, A., Boeckers, T.M., Henstridge, C.M., Catanese, A., 2023. Integrative proteomics highlight presynaptic alterations and c-Jun misactivation as convergent pathomechanisms in ALS. Acta Neuropathol 146, 451–475.

Anastasiades, P.G., Marques-Smith, A., Lyngholm, D., Lickiss, T., Raffiq, S., Kätzel, D., Miesenböck, G., Butt, S.J.B., 2016. GABAergic interneurons form transient layer-specific circuits in early postnatal neocortex. Nat Commun 7, 10584.

Andersson, J.D., Matuskey, D., Finnema, S.J., 2019. Positron emission tomography imaging of the γ-aminobutyric acid system. Neurosci Lett 691, 35–43.

Andersson, M.K., Ståhlberg, A., Arvidsson, Y., Olofsson, A., Semb, H., Stenman, G., Nilsson, O., Aman, P., 2008. The multifunctional FUS, EWS and TAF15 proto-oncoproteins show cell type-specific expression patterns and involvement in cell spreading and stress response. BMC Cell Biol 9, 37.

Andrés-Benito, P., Moreno, J., Aso, E., Povedano, M., Ferrer, I., 2017. Amyotrophic lateral sclerosis, gene deregulation in the anterior horn of the spinal cord and frontal cortex area 8: implications in frontotemporal lobar degeneration. Aging 9, 823–851.

Andrews, J.A., Jackson, C.E., Heiman-Patterson, T.D., Bettica, P., Brooks, B.R., Pioro, E.P., 2020. Real-world evidence of riluzole effectiveness in treating amyotrophic lateral sclerosis. Amyotroph Lateral Scler Frontotemporal Degener 21, 509–518.

Andrews-Zwilling, Y., Gillespie, A.K., Kravitz, A.V., Nelson, A.B., Devidze, N., Lo, I., Yoon, S.Y., Bien-Ly, N., Ring, K., Zwilling, D., Potter, G.B., Rubenstein, J.L.R., Kreitzer, A.C., Huang, Y., 2012. Hilar GABAergic interneuron activity controls spatial learning and memory retrieval. PLoS One 7.

Antonioni, A., Raho, E.M., Lopriore, P., Pace, A.P., Latino, R.R., Assogna, M., Mancuso, M., Gragnaniello, D., Granieri, E., Pugliatti, M., Di Lorenzo, F., Koch, G., 2023. Frontotemporal Dementia, Where Do We Stand? A Narrative Review. Int J Mol Sci 24, 11732.

Aoki, N., Higashi, S., Kawakami, I., Kobayashi, Z., Hosokawa, M., Katsuse, O., Togo, T., Hirayasu, Y., Akiyama, H., 2012. Localization of fused in sarcoma (FUS) protein to the post-synaptic density in the brain. Acta Neuropathol 124, 383–394.

Aousji, O., Feldengut, S., Antonucci, S., Schön, M., Boeckers, T.M., Matschke, J., Mawrin, C., Ludolph, A.C., Del Tredici, K., Roselli, F., Braak, H., 2023. Patterns of synaptic loss in human amyotrophic lateral sclerosis spinal cord: a clinicopathological study. Acta Neuropathol Commun 11, 120.

Arai, T., Hasegawa, M., Akiyama, H., Ikeda, K., Nonaka, T., Mori, H., Mann, D., Tsuchiya, K., Yoshida, M., Hashizume, Y., Oda, T., 2006. TDP-43 is a component of ubiquitin-positive tau-negative inclusions in frontotemporal lobar degeneration and amyotrophic lateral sclerosis. Biochem Biophys Res Commun 351, 602–611.

Armstrong, G.A.B., Drapeau, P., 2013. Loss and gain of FUS function impair neuromuscular synaptic transmission in a genetic model of ALS. Hum Mol Genet 22, 4282–4292.

Aronica, E., Baas, F., Iyer, A., ten Asbroek, A.L.M.A., Morello, G., Cavallaro, S., 2015. Molecular classification of amyotrophic lateral sclerosis by unsupervised clustering of gene expression in motor cortex. Neurobiol Dis 74, 359–376.

Aroor, A., Nguyen, P., Li, Y., Das, R., Lugo, J.N., Brewster, A.L., 2023. Assessment of tau phosphorylation and β-amyloid pathology in human drug-resistant epilepsy. Epilepsia Open 8, 609–622.

Arthur, K.C., Calvo, A., Price, T.R., Geiger, J.T., Chiò, A., Traynor, B.J., 2016. Projected increase in amyotrophic lateral sclerosis from 2015 to 2040. Nat Commun 7, 12408.

Assogna, M., Sprugnoli, G., Press, D., Dickerson, B., Macone, J., Bonnì, S., Borghi, I., Connor, A., Hoffman, M., Grover, N., Wong, B., Shen, C., Martorana, A., O'Reilly, M., Ruffini, G., El Fakhri, G., Koch, G., Santarnecchi, E., 2022. Gamma-induction in frontotemporal dementia (GIFTeD) randomized placebo-controlled trial: Rationale, noninvasive brain stimulation protocol, and study design. Alzheimers Dement 7.

Atassi, N., Xu, M., Triantafyllou, C., Keil, B., Lawson, R., Cernasov, P., Ratti, E., Long, C.J., Paganoni, S., Murphy, A., Salibi, N., Seethamraju, R., Rosen, B., Ratai, E.-M., 2017. Ultra high-field (7tesla) magnetic resonance spectroscopy in Amyotrophic Lateral Sclerosis. PLoS One 12.

Avossa, D., Grandolfo, M., Mazzarol, F., Zatta, M., Ballerini, L., 2006. Early signs of motoneuron vulnerability in a disease model system: Characterization of transverse slice cultures of spinal cord isolated from embryonic ALS mice. Neuroscience 138, 1179–1194.

- B -

Baade, I., Hutten, S., Sternburg, E.L., Pörschke, M., Hofweber, M., Dormann, D., Kehlenbach, R.H., 2021. The RNA-binding protein FUS is chaperoned and imported into the nucleus by a network of import receptors. J Biol Chem 296, 100659.

Bae, J.S., Ferguson, M., Tan, R., Mioshi, E., Simon, N., Burrell, J., Vucic, S., Hodges, J.R., Kiernan, M.C., Hornberger, M., 2016. Dissociation of Structural and Functional Integrities of the Motor System in Amyotrophic Lateral Sclerosis and Behavioral-Variant Frontotemporal Dementia. J Clin Neurol 12, 209–217.

Bailoo, J.D., Voelkl, B., Varholick, J., Novak, J., Murphy, E., Rosso, M., Palme, R., Würbel, H., 2020. Effects of weaning age and housing conditions on phenotypic differences in mice. Sci Rep 10, 11684.

Bak, L.K., Schousboe, A., Waagepetersen, H.S., 2006. The glutamate/GABA-glutamine cycle: aspects of transport, neurotransmitter homeostasis and ammonia transfer. J Neurochem 98, 641–653.

Bakken, T.E., Jorstad, N.L., Hu, Q., Lake, B.B., Tian, W., Kalmbach, B.E., Crow, M., Hodge, R.D., Krienen, F.M., Sorensen, S.A., Eggermont, J., Yao, Z., Aevermann, B.D., Aldridge, A.I., Bartlett, A., Bertagnolli, D., Casper, T., Castanon, R.G., Crichton, K., Daigle, T.L., Dalley, R., Dee, N., Dembrow, N., Diep, D., Ding, S.-L., Dong, W., Fang, R., Fischer, S., Goldman, M., Goldy, J., Graybuck, L.T., Herb, B.R., Hou, X., Kancherla, J., Kroll, M., Lathia, K., van Lew, B., Li, Y.E., Liu, C.S., Liu, H., Lucero, J.D., Mahurkar, A., McMillen, D., Miller, J.A., Moussa, M., Nery, J.R., Nicovich, P.R., Niu, S.-Y., Orvis, J., Osteen, J.K., Owen, S., Palmer, C.R., Pham, T., Plongthongkum, N., Poirion, O., Reed, N.M., Rimorin, C., Rivkin, A., Romanow, W.J., Sedeño-Cortés, A.E., Siletti, K., Somasundaram, S., Sulc, J., Tieu, M., Torkelson, A., Tung, H., Wang, X., Xie, F., Yanny, A.M., Zhang, R., Ament, S.A., Behrens, M.M., Bravo, H.C., Chun, J., Dobin, A., Gillis, J., Hertzano, R., Hof, P.R., Höllt, T., Horwitz, G.D., Keene, C.D., Kharchenko, P.V., Ko, A.L., Lelieveldt, B.P., Luo, C., Mukamel, E.A., Pinto-Duarte, A., Preissl, S., Regev, A., Ren, B., Scheuermann, R.H., Smith, K., Spain, W.J., White, O.R., Koch, C., Hawrylycz, M., Tasic, B., Macosko, E.Z., McCarroll, S.A., Ting, J.T., Zeng, H., Zhang, K., Feng, G., Ecker, J.R., Linnarsson, S., Lein, E.S., 2021. Comparative cellular analysis of motor cortex in human, marmoset and mouse. Nature 598, 111–119.

Bakker, L.A., Schröder, C.D., van Es, M.A., Westers, P., Visser-Meily, J.M.A., van den Berg, L.H., 2017. Assessment of the factorial validity and reliability of the ALSFRS-R: a revision of its measurement model. J Neurol 264, 1413–1420.

Banks, G.B., Choy, P.T., Lavidis, N.A., Noakes, P.G., 2003. Neuromuscular synapses mediate motor axon branching and motoneuron survival during the embryonic period of programmed cell death. Dev Biol 257, 71–84.

Banks, G.B., Kanjhan, R., Wiese, S., Kneussel, M., Wong, L.M., O'Sullivan, G., Sendtner, M., Bellingham, M.C., Betz, H., Noakes, P.G., 2005. Glycinergic and GABAergic synaptic activity differentially regulate motoneuron survival and skeletal muscle innervation. J Neurosci 25, 1249–1259.

Barone, J., Rossiter, H.E., 2021. Understanding the Role of Sensorimotor Beta Oscillations. Front Syst Neurosci 15, 655886.

Basaia, S., Agosta, F., Cividini, C., Trojsi, F., Riva, N., Spinelli, E.G., Moglia, C., Femiano, C., Castelnovo, V., Canu, E., Falzone, Y., Monsurrò, M.R., Falini, A., Chiò, A., Tedeschi, G., Filippi, M., 2020. Structural and functional brain connectome in motor neuron diseases: A multicenter MRI study. Neurology 95, 2552–2564.

Bast, T., Zhang, W.N., Feldon, J., 2001. Hyperactivity, decreased startle reactivity, and disrupted prepulse inhibition following disinhibition of the rat ventral hippocampus by the GABA(A) receptor antagonist picrotoxin. Psychopharmacology 156, 225–233.

Batista-Brito, R., Rossignol, E., Hjerling-Leffler, J., Denaxa, M., Wegner, M., Lefebvre, V., Pachnis, V., Fishell, G., 2009. The cell-intrinsic requirement of Sox6 for cortical interneuron development. Neuron 63, 466–481.

Bayer, D., Antonucci, S., Müller, H.-P., Saad, R., Dupuis, L., Rasche, V., Böckers, T.M., Ludolph, A.C., Kassubek, J., Roselli, F., 2021. Disruption of orbitofrontal-hypothalamic projections in a murine ALS model and in human patients. Transl Neurodegener 10, 17.

Beagle, A.J., Darwish, S.M., Ranasinghe, K.G., La, A.L., Karageorgiou, E., Vossel, K.A., 2017. Relative Incidence of Seizures and Myoclonus in Alzheimer's Disease, Dementia with Lewy Bodies, and Frontotemporal Dementia. J Alzheimers Dis 60, 211–223.

Beeldman, E., Govaarts, R., de Visser, M., Klein Twennaar, M., van der Kooi, A.J., van den Berg, L.H., Veldink, J.H., Pijnenburg, Y.A.L., de Haan, R.J., Schmand, B.A., Raaphorst, J., 2020. Progression of cognitive and behavioural impairment in early amyotrophic lateral sclerosis. J Neurol Neurosurg Psychiatry 91, 779–780.

Beierlein, M., Gibson, J.R., Connors, B.W., 2003. Two dynamically distinct inhibitory networks in layer 4 of the neocortex. J Neurophysiol 90, 2987–3000.

Belly, A., Moreau-Gachelin, F., Sadoul, R., Goldberg, Y., 2005. Delocalization of the multifunctional RNA splicing factor TLS/FUS in hippocampal neurones: exclusion from the nucleus and accumulation in dendritic granules and spine heads. Neuroscience Letters 379, 152–157.

Belzil, V.V., Valdmanis, P.N., Dion, P.A., Daoud, H., Kabashi, E., Noreau, A., Gauthier, J., S2D team, Hince, P., Desjarlais, A., Bouchard, J.-P., Lacomblez, L., Salachas, F., Pradat, P.-F., Camu, W., Meininger, V., Dupré, N., Rouleau, G.A., 2009. Mutations in FUS cause FALS and SALS in French and French Canadian populations. Neurology 73, 1176–1179.

Benajiba, L., Le Ber, I., Camuzat, A., Lacoste, M., Thomas-Anterion, C., Couratier, P., Legallic, S., Salachas, F., Hannequin, D., Decousus, M., Lacomblez, L., Guedj, E., Golfier, V., Camu, W., Dubois, B., Campion, D., Meininger, V., Brice, A., French Clinical and Genetic Research Network on Frontotemporal Lobar Degeneration/Frontotemporal Lobar Degeneration with Motoneuron Disease, 2009. TARDBP mutations in motoneuron disease with frontotemporal lobar degeneration. Ann Neurol 65, 470–473.

Ben-Ari, Y., 2017. NKCC1 Chloride Importer Antagonists Attenuate Many Neurological and Psychiatric Disorders. Trends Neurosci 40, 536–554.

Benatar, M., Granit, V., Andersen, P.M., Grignon, A.-L., McHutchison, C., Cosentino, S., Malaspina, A., Wuu, J., 2022. Mild motor impairment as prodromal state in amyotrophic lateral sclerosis: a new diagnostic entity. Brain 145, 3500–3508.

Benatar, M., Ostrow, L.W., Lewcock, J.W., Bennett, F., Shefner, J., Bowser, R., Larkin, P., Bruijn, L., Wuu, J., 2024. Biomarker Qualification for Neurofilament Light Chain in Amyotrophic Lateral Sclerosis: Theory and Practice. Ann Neurol 95, 211–216.

Benatar, M., Wuu, J., Andersen, P.M., Lombardi, V., Malaspina, A., 2018. Neurofilament light: A candidate biomarker of presymptomatic amyotrophic lateral sclerosis and phenoconversion. Ann Neurol 84, 130–139.

Benfato, I.D., Quintanilha, A.C.S., Henrique, J.S., Souza, M.A., Rosário, B.D.A., Beserra Filho, J.I.A., Santos, R.L.O., Ribeiro, A.M., Le Sueur Maluf, L., de Oliveira, C.A.M., 2022. Effects of long-term social isolation on central, behavioural and metabolic parameters in middle-aged mice. Behav Brain Res 417, 113630.

Benussi, A., Alberici, A., Cotelli, M.S., Dell'Era, V., Cantoni, V., Bonetta, E., Manenti, R., Filosto, M., Morini, R., Datta, A., Thomas, C., Padovani, A., Borroni, B., 2019a. Cortico-spinal tDCS in ALS: A randomized, double-blind, sham-controlled trial. Brain Stimul 12, 1332–1334.

Benussi, A., Cantoni, V., Grassi, M., Libri, I., Cotelli, M.S., Tarantino, B., Datta, A., Thomas, C., Huber, N., Kärkkäinen, S., Herukka, S.-K., Haapasalo, A., Filosto, M., Padovani, A., Borroni, B., 2023. Cortico-spinal tDCS in amyotrophic lateral sclerosis: A randomized, double-blind, sham-controlled trial followed by an open-label phase. Brain Stimul 16, 1666–1676.

Benussi, A., Cosseddu, M., Filareto, I., Dell'Era, V., Archetti, S., Sofia Cotelli, M., Micheli, A., Padovani, A., Borroni, B., 2016. Impaired long-term potentiation-like cortical plasticity in presymptomatic genetic frontotemporal dementia. Ann Neurol 80, 472–476.

Benussi, A., Dell'Era, V., Cantoni, V., Cotelli, M.S., Cosseddu, M., Spallazzi, M., Alberici, A., Padovani, A., Borroni, B., 2020. Neurophysiological Correlates of Positive and Negative Symptoms in Frontotemporal Dementia. J Alzheimers Dis 73, 1133–1142.

Benussi, A., Di Lorenzo, F., Dell'Era, V., Cosseddu, M., Alberici, A., Caratozzolo, S., Cotelli, M.S., Micheli, A., Rozzini, L., Depari, A., Flammini, A., Ponzo, V., Martorana, A., Caltagirone, C., Padovani, A., Koch, G., Borroni, B., 2017. Transcranial magnetic stimulation distinguishes Alzheimer disease from frontotemporal dementia. Neurology 89, 665–672.

Benussi, A., Gazzina, S., Premi, E., Cosseddu, M., Archetti, S., Dell'Era, V., Cantoni, V., Cotelli, M.S., Alberici, A., Micheli, A., Benussi, L., Ghidoni, R., Padovani, A., Borroni, B., 2019b. Clinical and biomarker changes in presymptomatic genetic frontotemporal dementia. Neurobiol Aging 76, 133–140.

Berrios, J., Stamatakis, A.M., Kantak, P.A., McElligott, Z.A., Judson, M.C., Aita, M., Rougie, M., Stuber, G.D., Philpot, B.D., 2016. Loss of UBE3A from TH-expressing neurons suppresses GABA co-release and enhances VTA-NAc optical self-stimulation. Nat Commun 7, 10702.

Bersano, E., Sarnelli, M.F., Solara, V., Iazzolino, B., Peotta, L., De Marchi, F., Facchin, A., Moglia, C., Canosa, A., Calvo, A., Chiò, A., Mazzini, L., 2020. Decline of cognitive and behavioral functions in amyotrophic lateral sclerosis: a longitudinal study. Amyotroph Lateral Scler Frontotemporal Degener 21, 373–379.

Bikoff, J.B., Gabitto, M.I., Rivard, A.F., Drobac, E., Machado, T.A., Miri, A., Brenner-Morton, S., Famojure, E., Diaz, C., Alvarez, F.J., Mentis, G.Z., Jessell, T.M., 2016. Spinal Inhibitory Interneuron Diversity Delineates Variant Motor Microcircuits. Cell 165, 207–219.

Bizovičar, N., Dreo, J., Koritnik, B., Zidar, J., 2014. Decreased movement-related beta desynchronization and impaired post-movement beta rebound in amyotrophic lateral sclerosis. Clin Neurophysiol 125, 1689–1699.

Bjornevik, K., O'Reilly, E.J., Molsberry, S., Kolonel, L.N., Le Marchand, L., Paganoni, S., Schwarzschild, M.A., Benkert, P., Kuhle, J., Ascherio, A., 2021. Prediagnostic Neurofilament Light Chain Levels in Amyotrophic Lateral Sclerosis. Neurology 97, 1466–1474.

Blair, I.P., Williams, K.L., Warraich, S.T., Durnall, J.C., Thoeng, A.D., Manavis, J., Blumbergs, P.C., Vucic, S., Kiernan, M.C., Nicholson, G.A., 2010. FUS mutations in amyotrophic lateral sclerosis: clinical, pathological, neurophysiological and genetic analysis. Journal of Neurology, Neurosurgery & Psychiatry 81, 639–645.

Blanco-Centurion, C., Bendell, E., Zou, B., Sun, Y., Shiromani, P.J., Liu, M., 2018. VGAT and VGLUT2 expression in MCH and orexin neurons in double transgenic reporter mice. IBRO Rep 4, 44–49.

Boillée, S., Yamanaka, K., Lobsiger, C.S., Copeland, N.G., Jenkins, N.A., Kassiotis, G., Kollias, G., Cleveland, D.W., 2006. Onset and progression in inherited ALS determined by motor neurons and microglia. Science 312, 1389–1392.

Bolborea, M., Vercruysse, P., Daria, T., Reiners, J.C., Alami, N.O., Guillot, S.J., Dieterlé, S., Sinniger, J., Scekic-Zahirovic, J., Londo, A., Arcay, H., Goy, M.-A., de Tapia, C.N., Thal, D.R., Shibuya, K., Otani, R., Arai, K., Kuwabara, S., Ludolph, A.C., Roselli, F., Yilmazer-Hanke, D., Dupuis, L., 2023. Loss of hypothalamic MCH decreases food intake in amyotrophic lateral sclerosis. Acta Neuropathol 145, 773–791.

Borroni, B., Bonvicini, C., Alberici, A., Buratti, E., Agosti, C., Archetti, S., Papetti, A., Stuani, C., Di Luca, M., Gennarelli, M., Padovani, A., 2009. Mutation within TARDBP leads to frontotemporal dementia without motor neuron disease. Hum Mutat 30, E974-983.

Börsch, A., Ham, D.J., Mittal, N., Tintignac, L.A., Migliavacca, E., Feige, J.N., Rüegg, M.A., Zavolan, M., 2021. Molecular and phenotypic analysis of rodent models reveals conserved and species-specific modulators of human sarcopenia. Commun Biol 4, 194.

Bosco, D.A., Lemay, N., Ko, H.K., Zhou, H., Burke, C., Kwiatkowski, T.J., Sapp, P., McKenna-Yasek, D., Brown, R.H., Hayward, L.J., 2010. Mutant FUS proteins that cause amyotrophic lateral sclerosis incorporate into stress granules. Hum Mol Genet 19, 4160–4175.

Botha, H., Josephs, K.A., 2019. Primary Progressive Aphasias and Apraxia of Speech. Continuum 25, 101–127.

Bourefis, A.-R., Campanari, M.-L., Buee-Scherrer, V., Kabashi, E., 2020. Functional characterization of a FUS mutant zebrafish line as a novel genetic model for ALS. Neurobiol Dis 142, 104935.

Boyle, P.A., Wilson, R.S., Yu, L., Barr, A.M., Honer, W.G., Schneider, J.A., Bennett, D.A., 2013. Much of late life cognitive decline is not due to common neurodegenerative pathologies. Ann Neurol 74, 478–489.

Britz, O., Zhang, J., Grossmann, K.S., Dyck, J., Kim, J.C., Dymecki, S., Gosgnach, S., Goulding, M., 2015. A genetically defined asymmetry underlies the inhibitory control of flexor-extensor locomotor movements. Elife 4, 04718.

Brockington, A., Ning, K., Heath, P.R., Wood, E., Kirby, J., Fusi, N., Lawrence, N., Wharton, S.B., Ince, P.G., Shaw, P.J., 2013. Unravelling the enigma of selective vulnerability in neurodegeneration: motor neurons resistant to degeneration in ALS show distinct gene expression characteristics and decreased susceptibility to excitotoxicity. Acta Neuropathol 125, 95–109.

Brooks, B.R., Miller, R.G., Swash, M., Munsat, T.L., World Federation of Neurology Research Group on Motor Neuron Diseases, 2000. El Escorial revisited: revised criteria for the diagnosis of amyotrophic lateral sclerosis. Amyotroph Lateral Scler Other Motor Neuron Disord 1, 293–299.

Broustal, O., Camuzat, A., Guillot-Noël, L., Guy, N., Millecamps, S., Deffond, D., Lacomblez, L., Golfier, V., Hannequin, D., Salachas, F., Camu, W., Didic, M., Dubois, B., Meininger, V., Le Ber, I., Brice, A., French clinical and genetic research network on FTD/FTD-MND, 2010. FUS mutations in frontotemporal lobar degeneration with amyotrophic lateral sclerosis. J Alzheimers Dis 22, 765–769.

Brunet, A., Stuart-Lopez, G., Burg, T., Scekic-Zahirovic, J., Rouaux, C., 2020. Cortical Circuit Dysfunction as a Potential Driver of Amyotrophic Lateral Sclerosis. Front Neurosci 14, 363.

Buck, E., Oeckl, P., Grozdanov, V., Bopp, V., Kühlwein, J.K., Ruf, W.P., Wiesner, D., Roselli, F., Weishaupt, J.H., Ludolph, A.C., Otto, M., Danzer, K.M., 2022. Increased NF-L levels in the TDP-43G298S ALS mouse model resemble NF-L levels in ALS patients. Acta Neuropathol 144, 161–164.

Burrell, J.R., Kiernan, M.C., Vucic, S., Hodges, J.R., 2011. Motor neuron dysfunction in frontotemporal dementia. Brain 134, 2582–2594.

- C -

Cady, J., Allred, P., Bali, T., Pestronk, A., Goate, A., Miller, T.M., Mitra, R.D., Ravits, J., Harms, M.B., Baloh, R.H., 2015. Amyotrophic lateral sclerosis onset is influenced by the burden of rare variants in known amyotrophic lateral sclerosis genes. Ann Neurol 77, 100–113.

Cairns, N.J., Neumann, M., Bigio, E.H., Holm, I.E., Troost, D., Hatanpaa, K.J., Foong, C., White, C.L., Schneider, J.A., Kretzschmar, H.A., Carter, D., Taylor-Reinwald, L., Paulsmeyer, K., Strider, J., Gitcho, M., Goate, A.M., Morris, J.C., Mishra, M., Kwong, L.K., Stieber, A., Xu, Y., Forman, M.S., Trojanowski, J.Q., Lee, V.M.-Y., Mackenzie, I.R.A., 2007. TDP-43 in familial and sporadic frontotemporal lobar degeneration with ubiquitin inclusions. Am J Pathol 171, 227–240.

Capasso, M., Anzellotti, F., Di Giacomo, R., Onofrj, M., 2017. Epilepsy and electroencephalographic abnormalities in C9orf72 repeat expansion. Amyotroph Lateral Scler Frontotemporal Degener 18, 140–141.

Carlson, C.G., Rutter, J., Bledsoe, C., Singh, R., Hoff, H., Bruemmer, K., Sesti, J., Gatti, F., Berge, J., McCarthy, L., 2010. A simple protocol for assessing inter-trial and inter-examiner reliability for two noninvasive measures of limb muscle strength. J Neurosci Methods 186, 226–230.

Carlucci, V., Salvalaggio, A., Riguzzi, P., Fasolato, D., Bussè, C., Cecchin, D., Cagnin, A., 2024. Focal epilepsy followed by rapidly progressive frontotemporal dementia: a rare manifestation of VCP mutation. Amyotroph Lateral Scler Frontotemporal Degener 1–3.

Caroppo, P., Camuzat, A., Guillot-Noel, L., Thomas-Antérion, C., Couratier, P., Wong, T.H., Teichmann, M., Golfier, V., Auriacombe, S., Belliard, S., Laurent, B., Lattante, S., Millecamps, S., Clot, F., Dubois, B., van Swieten, J.C., Brice, A., Le Ber, I., 2016. Defining the spectrum of frontotemporal dementias associated with TARDBP mutations. Neurol Genet 2, 80.

Carriere, C.H., Wang, W.X., Sing, A.D., Fekete, A., Jones, B.E., Yee, Y., Ellegood, J., Maganti, H., Awofala, L., Marocha, J., Aziz, A., Wang, L.-Y., Lerch, J.P., Lefebvre, J.L., 2020. The γ-Protocadherins Regulate the Survival of GABAergic Interneurons during Developmental Cell Death. J Neurosci 40, 8652–8668.

Castro, J., Oliveira Santos, M., Swash, M., de Carvalho, M., 2024. Segmental motor neuron dysfunction in amyotrophic lateral sclerosis: Insights from H reflex paradigms. Muscle Nerve 69, 303–312.

Cavarsan, C.F., Steele, P.R., Genry, L.T., Reedich, E.J., McCane, L.M., LaPre, K.J., Puritz, A.C., Manuel, M., Katenka, N., Quinlan, K.A., 2023. Inhibitory interneurons show early dysfunction in a SOD1 mouse model of amyotrophic lateral sclerosis. The Journal of Physiology 601, 647–667.

Cawley, N., Solanky, B.S., Muhlert, N., Tur, C., Edden, R.A.E., Wheeler-Kingshott, C.A.M., Miller, D.H., Thompson, A.J., Ciccarelli, O., 2015. Reduced gamma-aminobutyric acid concentration is associated with physical disability in progressive multiple sclerosis. Brain 138, 2584–2595.

Challa, S.R., Fornal, C.A., Wang, B.C., Boyineni, J., DeVera, R.E., Unnam, P., Song, Y., Soares, M.B., Malchenko, S., Gyarmati, P., Veeravalli, K.K., 2023. The Impact of Social Isolation and Environmental Deprivation on Blood Pressure and Depression-Like Behavior in Young Male and Female Mice. Chronic Stress 7, 24705470231207010.

Chang, Q., Martin, L.J., 2011. Glycine Receptor Channels in Spinal Motoneurons Are Abnormal in a Transgenic Mouse Model of Amyotrophic Lateral Sclerosis. J Neurosci 31, 2815–2827.

Chang, Q., Martin, L.J., 2009. Glycinergic innervation of motoneurons is deficient in amyotrophic lateral sclerosis mice: a quantitative confocal analysis. Am J Pathol 174, 574–585.

Chen, L., 2021. FUS mutation is probably the most common pathogenic gene for JALS, especially sporadic JALS. Rev Neurol 177, 333–340.

Chini, M., Pfeffer, T., Hanganu-Opatz, I., 2022. An increase of inhibition drives the developmental decorrelation of neural activity. Elife 11, 78811.

Chiò, A., Calvo, A., Moglia, C., Ossola, I., Brunetti, M., Sbaiz, L., Lai, S., Abramzon, Y., Traynor, B.J., Restagno, G., 2011. A de novo missense mutation of the FUS gene in a "true" sporadic ALS case. Neurobiol Aging 32, 23–26.

Chiò, A., Moglia, C., Canosa, A., Manera, U., D'Ovidio, F., Vasta, R., Grassano, M., Brunetti, M., Barberis, M., Corrado, L., D'Alfonso, S., Iazzolino, B., Peotta, L., Sarnelli, M.F., Solara, V., Zucchetti, J.P., De Marchi, F., Mazzini, L., Mora, G., Calvo, A., 2020. ALS phenotype is influenced by age, sex, and genetics: A population-based study. Neurology 94, 802–810.

Cirulli, E.T., Lasseigne, B.N., Petrovski, S., Sapp, P.C., Dion, P.A., Leblond, C.S., Couthouis, J., Lu, Y.-F., Wang, Q., Krueger, B.J., Ren, Z., Keebler, J., Han, Y., Levy, S.E., Boone, B.E., Wimbish, J.R., Waite, L.L., Jones, A.L., Carulli,

J.P., Day-Williams, A.G., Staropoli, J.F., Xin, W.W., Chesi, A., Raphael, A.R., McKenna-Yasek, D., Cady, J., Vianney de Jong, J.M.B., Kenna, K.P., Smith, B.N., Topp, S., Miller, J., Gkazi, A., FALS Sequencing Consortium, Al-Chalabi, A., van den Berg, L.H., Veldink, J., Silani, V., Ticozzi, N., Shaw, C.E., Baloh, R.H., Appel, S., Simpson, E., Lagier-Tourenne, C., Pulst, S.M., Gibson, S., Trojanowski, J.Q., Elman, L., McCluskey, L., Grossman, M., Shneider, N.A., Chung, W.K., Ravits, J.M., Glass, J.D., Sims, K.B., Van Deerlin, V.M., Maniatis, T., Hayes, S.D., Ordureau, A., Swarup, S., Landers, J., Baas, F., Allen, A.S., Bedlack, R.S., Harper, J.W., Gitler, A.D., Rouleau, G.A., Brown, R., Harms, M.B., Cooper, G.M., Harris, T., Myers, R.M., Goldstein, D.B., 2015. Exome sequencing in amyotrophic lateral sclerosis identifies risk genes and pathways. Science 347, 1436–1441.

Clark, R.M., Blizzard, C.A., Young, K.M., King, A.E., Dickson, T.C., 2017. Calretinin and Neuropeptide Y interneurons are differentially altered in the motor cortex of the SOD1G93A mouse model of ALS. Sci Rep 7, 44461.

Clark, R.M., Brizuela, M., Blizzard, C.A., Dickson, T.C., 2018. Reduced Excitability and Increased Neurite Complexity of Cortical Interneurons in a Familial Mouse Model of Amyotrophic Lateral Sclerosis. Front Cell Neurosci 12, 328.

Colombrita, C., Onesto, E., Megiorni, F., Pizzuti, A., Baralle, F.E., Buratti, E., Silani, V., Ratti, A., 2012. TDP-43 and FUS RNA-binding proteins bind distinct sets of cytoplasmic messenger RNAs and differently regulate their post-transcriptional fate in motoneuron-like cells. J Biol Chem 287, 15635–15647.

Comley, L., Allodi, I., Nichterwitz, S., Nizzardo, M., Simone, C., Corti, S., Hedlund, E., 2015. Motor neurons with differential vulnerability to degeneration show distinct protein signatures in health and ALS. Neuroscience 291, 216–229.

Cosseddu, M., Benussi, A., Gazzina, S., Alberici, A., Dell'Era, V., Manes, M., Cristillo, V., Borroni, B., Padovani, A., 2020. Progression of behavioural disturbances in frontotemporal dementia: a longitudinal observational study. Eur J Neurol 27, 265–272.

Couratier, P., Corcia, P., Lautrette, G., Nicol, M., Preux, P.-M., Marin, B., 2016. Epidemiology of amyotrophic lateral sclerosis: A review of literature. Rev Neurol 172, 37–45.

Coyle-Gilchrist, I.T.S., Dick, K.M., Patterson, K., Vázquez Rodríquez, P., Wehmann, E., Wilcox, A., Lansdall, C.J., Dawson, K.E., Wiggins, J., Mead, S., Brayne, C., Rowe, J.B., 2016. Prevalence, characteristics, and survival of frontotemporal lobar degeneration syndromes. Neurology 86, 1736–1743.

Crabé, R., Aimond, F., Gosset, P., Scamps, F., Raoul, C., 2020. How Degeneration of Cells Surrounding Motoneurons Contributes to Amyotrophic Lateral Sclerosis. Cells 9, 2550.

Crockford, C., Newton, J., Lonergan, K., Chiwera, T., Booth, T., Chandran, S., Colville, S., Heverin, M., Mays, I., Pal, S., Pender, N., Pinto-Grau, M., Radakovic, R., Shaw, C.E., Stephenson, L., Swingler, R., Vajda, A., Al-Chalabi, A., Hardiman, O., Abrahams, S., 2018. ALS-specific cognitive and behavior changes associated with advancing disease stage in ALS. Neurology 91, 1370–1380.

Cruts, M., Gijselinck, I., van der Zee, J., Engelborghs, S., Wils, H., Pirici, D., Rademakers, R., Vandenberghe, R., Dermaut, B., Martin, J.-J., van Duijn, C., Peeters, K., Sciot, R., Santens, P., De Pooter, T., Mattheijssens, M., Van den Broeck, M., Cuijt, I., Vennekens, K., De Deyn, P.P., Kumar-Singh, S., Van Broeckhoven, C., 2006. Null mutations in progranulin cause ubiquitin-positive frontotemporal dementia linked to chromosome 17q21. Nature 442, 920–924.

- D -

Dana, H., Sun, Y., Mohar, B., Hulse, B.K., Kerlin, A.M., Hasseman, J.P., Tsegaye, G., Tsang, A., Wong, A., Patel, R., Macklin, J.J., Chen, Y., Konnerth, A., Jayaraman, V., Looger, L.L., Schreiter, E.R., Svoboda, K., Kim, D.S., 2019. High-performance calcium sensors for imaging activity in neuronal populations and microcompartments. Nat Methods 16, 649–657.

Daneshvar, D.H., Mez, J., Alosco, M.L., Baucom, Z.H., Mahar, I., Baugh, C.M., Valle, J.P., Weuve, J., Paganoni, S., Cantu, R.C., Zafonte, R.D., Stern, R.A., Stein, T.D., Tripodis, Y., Nowinski, C.J., McKee, A.C., 2021. Incidence of and Mortality From Amyotrophic Lateral Sclerosis in National Football League Athletes. JAMA Netw Open 4, 2138801.

Dangond, F., Hwang, D., Camelo, S., Pasinelli, P., Frosch, M.P., Stephanopoulos, Gregory, Stephanopoulos, George, Brown, R.H., Gullans, S.R., 2004. Molecular signature of late-stage human ALS revealed by expression profiling of postmortem spinal cord gray matter. Physiol Genomics 16, 229–239.

Dávila-Bouziguet, E., Targa-Fabra, G., Ávila, J., Soriano, E., Pascual, M., 2019. Differential accumulation of Tau phosphorylated at residues Thr231, Ser262 and Thr205 in hippocampal interneurons and its modulation by Tau mutations (VLW) and amyloid-β peptide. Neurobiol Dis 125, 232–244.

DeJesus-Hernandez, M., Mackenzie, I.R., Boeve, B.F., Boxer, A.L., Baker, M., Rutherford, N.J., Nicholson, A.M., Finch, N.A., Flynn, H., Adamson, J., Kouri, N., Wojtas, A., Sengdy, P., Hsiung, G.-Y.R., Karydas, A., Seeley, W.W., Josephs, K.A., Coppola, G., Geschwind, D.H., Wszolek, Z.K., Feldman, H., Knopman, D.S., Petersen, R.C., Miller, B.L., Dickson, D.W., Boylan, K.B., Graff-Radford, N.R., Rademakers, R., 2011. Expanded GGGGCC hexanucleotide repeat in noncoding region of C9ORF72 causes chromosome 9p-linked FTD and ALS. Neuron 72, 245–256.

Del Cid-Pellitero, E., Jones, B.E., 2012. Immunohistochemical evidence for synaptic release of GABA from melanin-concentrating hormone containing varicosities in the locus coeruleus. Neuroscience 223, 269–276.

Delpy, A., Allain, A.-E., Meyrand, P., Branchereau, P., 2008. NKCC1 cotransporter inactivation underlies embryonic development of chloride-mediated inhibition in mouse spinal motoneuron. J Physiol 586, 1059–1075.

Deng, H.-X., Zhai, H., Bigio, E.H., Yan, J., Fecto, F., Ajroud, K., Mishra, M., Ajroud-Driss, S., Heller, S., Sufit, R., Siddique, N., Mugnaini, E., Siddique, T., 2010. FUS-immunoreactive inclusions are a common feature in sporadic and non-SOD1 familial amyotrophic lateral sclerosis. Ann Neurol. 67, 739–748.

Deshpande, D., Higelin, J., Schoen, M., Vomhof, T., Boeckers, T.M., Demestre, M., Michaelis, J., 2019. Synaptic FUS Localization During Motoneuron Development and Its Accumulation in Human ALS Synapses. Front Cell Neurosci 13, 256.

Deutsch, M.B., Mendez, M.F., Teng, E., 2015. Interactions between traumatic brain injury and frontotemporal degeneration. Dement Geriatr Cogn Disord 39, 143–153.

Dev, S.I., Dickerson, B.C., Touroutoglou, A., 2021. Neuroimaging in Frontotemporal Lobar Dementia: Research and Clinical Utility. Adv Exp Med Biol 1281, 93–112.

Devlin, A.-C., Burr, K., Borooah, S., Foster, J.D., Cleary, E.M., Geti, I., Vallier, L., Shaw, C.E., Chandran, S., Miles, G.B., 2015. Human iPSC-derived motoneurons harbouring TARDBP or C9ORF72 ALS mutations are dysfunctional despite maintaining viability. Nat Commun 6, 5999.

Devoy, A., Kalmar, B., Stewart, M., Park, H., Burke, B., Noy, S.J., Redhead, Y., Humphrey, J., Lo, K., Jaeger, J., Mejia Maza, A., Sivakumar, P., Bertolin, C., Soraru, G., Plagnol, V., Greensmith, L., Acevedo Arozena, A., Isaacs, A.M., Davies, B., Fratta, P., Fisher, E.M.C., 2017. Humanized mutant FUS drives progressive motor neuron degeneration without aggregation in 'FUSDelta14' knockin mice. Brain 140, 2797–2805.

Dickstein, D.L., Kabaso, D., Rocher, A.B., Luebke, J.I., Wearne, S.L., Hof, P.R., 2007. Changes in the structural complexity of the aged brain. Aging Cell 6, 275–284.

Dinamarca, M.C., Raveh, A., Schneider, A., Fritzius, T., Früh, S., Rem, P.D., Stawarski, M., Lalanne, T., Turecek, R., Choo, M., Besseyrias, V., Bildl, W., Bentrop, D., Staufenbiel, M., Gassmann, M., Fakler, B., Schwenk, J., Bettler, B., 2019. Complex formation of APP with GABAB receptors links axonal trafficking to amyloidogenic processing. Nat Commun 10, 1331.

Ding, Q., Triggs, W.J., Kamath, S.M., Patten, C., 2018. Short Intracortical Inhibition During Voluntary Movement Reveals Persistent Impairment Post-stroke. Front Neurol 9, 1105.

Dini Modigliani, S., Morlando, M., Errichelli, L., Sabatelli, M., Bozzoni, I., 2014. An ALS-associated mutation in the FUS 3′-UTR disrupts a microRNA–FUS regulatory circuitry. Nat Commun 5, 4335.

Ditsworth, D., Maldonado, M., McAlonis-Downes, M., Sun, S., Seelman, A., Drenner, K., Arnold, E., Ling, S.-C., Pizzo, D., Ravits, J., Cleveland, D.W., Da Cruz, S., 2017. Mutant TDP-43 within motor neurons drives disease onset but not progression in amyotrophic lateral sclerosis. Acta Neuropathol 133, 907–922.

Dobson-Stone, C., Hallupp, M., Shahheydari, H., Ragagnin, A.M.G., Chatterton, Z., Carew-Jones, F., Shepherd, C.E., Stefen, H., Paric, E., Fath, T., Thompson, E.M., Blumbergs, P., Short, C.L., Field, C.D., Panegyres, P.K., Hecker, J., Nicholson, G., Shaw, A.D., Fullerton, J.M., Luty, A.A., Schofield, P.R., Brooks, W.S., Rajan, N., Bennett, M.F., Bahlo, M., Landers, J.E., Piguet, O., Hodges, J.R., Halliday, G.M., Topp, S.D., Smith, B.N., Shaw, C.E., McCann, E., Fifita, J.A., Williams, K.L., Atkin, J.D., Blair, I.P., Kwok, J.B., 2020. CYLD is a causative gene for frontotemporal dementia - amyotrophic lateral sclerosis. Brain 143, 783–799.

Dodd, K.C., Power, R., Ealing, J., Hamdalla, H., 2019. FUS-ALS presenting with myoclonic jerks in a 17-year-old man. Amyotroph Lateral Scler Frontotemporal Degener 20, 278–280.

Doi, H., Koyano, S., Suzuki, Y., Nukina, N., Kuroiwa, Y., 2010. The RNA-binding protein FUS/TLS is a common aggregate-interacting protein in polyglutamine diseases. Neurosci Res 66, 131–133.

Doischer, D., Hosp, J.A., Yanagawa, Y., Obata, K., Jonas, P., Vida, I., Bartos, M., 2008. Postnatal differentiation of basket cells from slow to fast signaling devices. J Neurosci 28, 12956–12968.

Dormann, D., Madl, T., Valori, C.F., Bentmann, E., Tahirovic, S., Abou-Ajram, C., Kremmer, E., Ansorge, O., Mackenzie, I.R.A., Neumann, M., Haass, C., 2012. Arginine methylation next to the PY-NLS modulates Transportin binding and nuclear import of FUS. EMBO J 31, 4258–4275.

Dormann, D., Rodde, R., Edbauer, D., Bentmann, E., Fischer, I., Hruscha, A., Than, M.E., Mackenzie, I.R.A., Capell, A., Schmid, B., Neumann, M., Haass, C., 2010. ALS-associated fused in sarcoma (FUS) mutations disrupt Transportin-mediated nuclear import. EMBO J 29, 2841–2857.

Dougherty, K.J., Sawchuk, M.A., Hochman, S., 2009. Phenotypic diversity and expression of GABAergic inhibitory interneurons during postnatal development in lumbar spinal cord of glutamic acid decarboxylase 67-green fluorescent protein mice. Neuroscience 163, 909–919.

Duan, Z.R.S., Che, A., Chu, P., Modol, L., Bollmann, Y., Babij, R., Fetcho, R.N., Otsuka, T., Fuccillo, M.V., Liston, C., Pisapia, D.J., Cossart, R., De Marco García, N.V., 2020. GABAergic Restriction of Network Dynamics Regulates Interneuron Survival in the Developing Cortex. Neuron 105, 75-92.

Ducharme, S., Dols, A., Laforce, R., Devenney, E., Kumfor, F., van den Stock, J., Dallaire-Théroux, C., Seelaar, H., Gossink, F., Vijverberg, E., Huey, E., Vandenbulcke, M., Masellis, M., Trieu, C., Onyike, C., Caramelli, P., de Souza, L.C., Santillo, A., Waldö, M.L., Landin-Romero, R., Piguet, O., Kelso, W., Eratne, D., Velakoulis, D., Ikeda, M., Perry, D., Pressman, P., Boeve, B., Vandenberghe, R., Mendez, M., Azuar, C., Levy, R., Le Ber, I., Baez, S., Lerner, A., Ellajosyula, R., Pasquier, F., Galimberti, D., Scarpini, E., van Swieten, J., Hornberger, M., Rosen, H., Hodges, J., Diehl-Schmid, J., Pijnenburg, Y., 2020. Recommendations to distinguish behavioural variant frontotemporal dementia from psychiatric disorders. Brain 143, 1632–1650.

Dugué, G.P., Dumoulin, A., Triller, A., Dieudonné, S., 2005. Target-dependent use of co-released inhibitory transmitters at central synapses. J Neurosci 25, 6490–6498.

Dukic, S., McMackin, R., Buxo, T., Fasano, A., Chipika, R., Pinto-Grau, M., Costello, E., Schuster, C., Hammond, M., Heverin, M., Coffey, A., Broderick, M., Iyer, P.M., Mohr, K., Gavin, B., Pender, N., Bede, P., Muthuraman, M., Lalor, E.C., Hardiman, O., Nasseroleslami, B., 2019. Patterned functional network disruption in amyotrophic lateral sclerosis. Hum Brain Mapp 40, 4827–4842.

- E -

Ederle, H., Funk, C., Abou-Ajram, C., Hutten, S., Funk, E.B.E., Kehlenbach, R.H., Bailer, S.M., Dormann, D., 2018. Nuclear egress of TDP-43 and FUS occurs independently of Exportin-1/CRM1. Sci Rep 8, 7084.

Elias, C.F., Sita, L.V., Zambon, B.K., Oliveira, E.R., Vasconcelos, L. a. P., Bittencourt, J.C., 2008. Melanin-concentrating hormone projections to areas involved in somatomotor responses. J Chem Neuroanat 35, 188–201.

Eulenburg, V., Armsen, W., Betz, H., Gomeza, J., 2005. Glycine transporters: essential regulators of neurotransmission. Trends Biochem Sci 30, 325–333.

Evans, L.J., O'Brien, D., Shaw, P.J., 2024. Current neuroprotective therapies and future prospects for motor neuron disease. Int Rev Neurobiol 176, 327–384.

- F -

Fairless, A.H., Katz, J.M., Vijayvargiya, N., Dow, H.C., Kreibich, A.S., Berrettini, W.H., Abel, T., Brodkin, E.S., 2013. Development of home cage social behaviors in BALB/cJ vs. C57BL/6J mice. Behav Brain Res 237, 338–347.

Falcão de Campos, C., Gromicho, M., Uysal, H., Grosskreutz, J., Kuzma-Kozakiewicz, M., Oliveira Santos, M., Pinto, S., Petri, S., Swash, M., de Carvalho, M., 2022. Trends in the diagnostic delay and pathway for amyotrophic lateral sclerosis patients across different countries. Front Neurol 13, 1064619.

Fang, T., Jozsa, F., Al-Chalabi, A., 2017. Nonmotor Symptoms in Amyotrophic Lateral Sclerosis: A Systematic Review. Int Rev Neurobiol 134, 1409–1441.

Fanselow, E.E., Richardson, K.A., Connors, B.W., 2008. Selective, state-dependent activation of somatostatin-expressing inhibitory interneurons in mouse neocortex. J Neurophysiol 100, 2640–2652.

Favuzzi, E., Deogracias, R., Marques-Smith, A., Maeso, P., Jezequel, J., Exposito-Alonso, D., Balia, M., Kroon, T., Hinojosa, A.J., F Maraver, E., Rico, B., 2019. Distinct molecular programs regulate synapse specificity in cortical inhibitory circuits. Science 363, 413–417.

Fazel Darbandi, S., Esau, C., Lesage-Pelletier, C., Monis, S., Poitras, L., Yu, M., Perin, S., Hatch, G., Ekker, M., 2021. Increased Sociability in Mice Lacking Intergenic Dlx Enhancers. Front Neurosci 15, 718948.

Feather-Schussler, D.N., Ferguson, T.S., 2016. A Battery of Motor Tests in a Neonatal Mouse Model of Cerebral Palsy. J Vis Exp 53569.

Feldman, E.L., Goutman, S.A., Petri, S., Mazzini, L., Savelieff, M.G., Shaw, P.J., Sobue, G., 2022. Amyotrophic lateral sclerosis. Lancet 400, 1363–1380.

Ferrer, I., 1999. Neurons and their dendrites in frontotemporal dementia. Dement Geriatr Cogn Disord 10 Suppl 1, 55–60.

Ferrer, I., Tuñón, T., Serrano, M.T., Casas, R., Alcántara, S., Zújar, M.J., Rivera, R.M., 1993. Calbindin D-28k and parvalbumin immunoreactivity in the frontal cortex in patients with frontal lobe dementia of non-Alzheimer type associated with amyotrophic lateral sclerosis. J Neurol Neurosurg Psychiatry 56, 257–261.

Figueroa-Romero, C., Mikhail, K.A., Gennings, C., Curtin, P., Bello, G.A., Botero, T.M., Goutman, S.A., Feldman, E.L., Arora, M., Austin, C., 2020. Early life metal dysregulation in amyotrophic lateral sclerosis. Ann Clin Transl Neurol 7, 872–882.

Flies, C.M., Veldink, J.H., 2020. Chorea is a pleiotropic clinical feature of mutated fused-in-sarcoma in amyotrophic lateral sclerosis. Amyotroph Lateral Scler Frontotemporal Degener 21, 309–311.

Flurkey, K., M. Currer, J., Harrison, D.E., 2007. Chapter 20 - Mouse Models in Aging Research, in: Fox, J.G., Davisson, M.T., Quimby, F.W., Barthold, S.W., Newcomer, C.E., Smith, A.L. (Eds.), The Mouse in Biomedical Research (Second Edition), American College of Laboratory Animal Medicine. Academic Press, 637–672.

Foerster, B.R., Callaghan, B.C., Petrou, M., Edden, R.A.E., Chenevert, T.L., Feldman, E.L., 2012. Decreased motor cortex γ-aminobutyric acid in amyotrophic lateral sclerosis. Neurology 78, 1596–1600.

Foerster, B.R., Pomper, M.G., Callaghan, B.C., Petrou, M., Edden, R.A.E., Mohamed, M.A., Welsh, R.C., Carlos, R.C., Barker, P.B., Feldman, E.L., 2013. 3T MR Spectroscopy Reveals an Imbalance between Excitatory and Inhibitory Neurotransmitters in Amyotrophic Lateral Sclerosis. JAMA Neurol 70, 1009–1016.

Fogarty, M.J., Kanjhan, R., Yanagawa, Y., Noakes, P.G., Bellingham, M.C., 2017. Alterations in hypoglossal motor neurons due to GAD67 and VGAT deficiency in mice. Exp Neurol 289, 117–127.

Fogarty, M.J., Smallcombe, K.L., Yanagawa, Y., Obata, K., Bellingham, M.C., Noakes, P.G., 2013. Genetic deficiency of GABA differentially regulates respiratory and non-respiratory motor neuron development. PLoS One 8, 56257.

Fogarty, M.J., Yanagawa, Y., Obata, K., Bellingham, M.C., Noakes, P.G., 2015. Genetic absence of the vesicular inhibitory amino acid transporter differentially regulates respiratory and locomotor motor neuron development. Brain Struct Funct 220, 525–540.

Fontana, A., Marin, B., Luna, J., Beghi, E., Logroscino, G., Boumédiene, F., Preux, P.-M., Couratier, P., Copetti, M., 2021. Time-trend evolution and determinants of sex ratio in Amyotrophic Lateral Sclerosis: a dose-response meta-analysis. J Neurol 268, 2973–2984.

Fox, S.R., Deneris, E.S., 2012. Engrailed is required in maturing serotonin neurons to regulate the cytoarchitecture and survival of the dorsal raphe nucleus. J Neurosci 32, 7832–7842.

Fratta, P., Sivakumar, P., Humphrey, J., Lo, K., Ricketts, T., Oliveira, H., Brito-Armas, J.M., Kalmar, B., Ule, A., Yu, Y., Birsa, N., Bodo, C., Collins, T., Conicella, A.E., Mejia Maza, A., Marrero-Gagliardi, A., Stewart, M., Mianne, J., Corrochano, S., Emmett, W., Codner, G., Groves, M., Fukumura, R., Gondo, Y., Lythgoe, M., Pauws, E., Peskett, E., Stanier, P., Teboul, L., Hallegger, M., Calvo, A., Chiò, A., Isaacs, A.M., Fawzi, N.L., Wang, E., Housman, D.E., Baralle, F., Greensmith, L., Buratti, E., Plagnol, V., Fisher, E.M., Acevedo-Arozena, A., 2018. Mice with endogenous TDP-43 mutations exhibit gain of splicing function and characteristics of amyotrophic lateral sclerosis. EMBO J 37, 98684.

Freischmidt, A., Wieland, T., Richter, B., Ruf, W., Schaeffer, V., Müller, K., Marroquin, N., Nordin, F., Hübers, A., Weydt, P., Pinto, S., Press, R., Millecamps, S., Molko, N., Bernard, E., Desnuelle, C., Soriani, M.-H., Dorst, J., Graf, E., Nordström, U., Feiler, M.S., Putz, S., Boeckers, T.M., Meyer, T., Winkler, A.S., Winkelman, J., de Carvalho, M., Thal, D.R., Otto, M., Brännström, T., Volk, A.E., Kursula, P., Danzer, K.M., Lichtner, P., Dikic, I., Meitinger, T., Ludolph, A.C., Strom, T.M., Andersen, P.M., Weishaupt, J.H., 2015. Haploinsufficiency of TBK1 causes familial ALS and fronto-temporal dementia. Nat Neurosci 18, 631–636.

Frigon, A., 2012. Central pattern generators of the mammalian spinal cord. Neuroscientist 18, 56–69.

Fuchs, A., Ringer, C., Bilkei-Gorzo, A., Weihe, E., Roeper, J., Schütz, B., 2010. Downregulation of the Potassium Chloride Cotransporter KCC2 in Vulnerable Motoneurons in the SOD1-G93A Mouse Model of Amyotrophic Lateral Sclerosis. Journal of Neuropathology & Experimental Neurology 69, 1057–1070.

Fujii, R., Okabe, S., Urushido, T., Inoue, K., Yoshimura, A., Tachibana, T., Nishikawa, T., Hicks, G.G., Takumi, T., 2005. The RNA Binding Protein TLS Is Translocated to Dendritic Spines by mGluR5 Activation and Regulates Spine Morphology. Current Biology 15, 587–593.

Furman, O., Tsoory, M., Chen, A., 2022. Differential chronic social stress models in male and female mice. Eur J Neurosci 55, 2777–2793.

- G -

Gabery, S., Ahmed, R.M., Caga, J., Kiernan, M.C., Halliday, G.M., Petersén, Å., 2021. Loss of the metabolism and sleep regulating neuronal populations expressing orexin and oxytocin in the hypothalamus in amyotrophic lateral sclerosis. Neuropathol Appl Neurobiol 47, 979–989.

Gaetz, W., Edgar, J.C., Wang, D.J., Roberts, T.P.L., 2011. Relating MEG measured motor cortical oscillations to resting γ-aminobutyric acid (GABA) concentration. Neuroimage 55, 616–621.

Gao, X.B., van den Pol, A.N., 2001. Melanin concentrating hormone depresses synaptic activity of glutamate and GABA neurons from rat lateral hypothalamus. J Physiol 533, 237–252.

García-Cabrero, A.M., Guerrero-López, R., Giráldez, B.G., Llorens-Martín, M., Avila, J., Serratosa, J.M., Sánchez, M.P., 2013. Hyperexcitability and epileptic seizures in a model of frontotemporal dementia. Neurobiol Dis 58, 200–208.

Garone, M.G., Birsa, N., Rosito, M., Salaris, F., Mochi, M., de Turris, V., Nair, R.R., Cunningham, T.J., Fisher, E.M.C., Morlando, M., Fratta, P., Rosa, A., 2021. ALS-related FUS mutations alter axon growth in motoneurons and affect HuD/ELAVL4 and FMRP activity. Commun Biol 4, 1025.

Gascon, E., Lynch, K., Ruan, H., Almeida, S., Verheyden, J.M., Seeley, W.W., Dickson, D.W., Petrucelli, L., Sun, D., Jiao, J., Zhou, H., Jakovcevski, M., Akbarian, S., Yao, W.-D., Gao, F.-B., 2014. Alterations in microRNA-124 and AMPA receptors contribute to social behavioral deficits in frontotemporal dementia. Nat Med 20, 1444–1451.

Gazzina, S., Benussi, A., Premi, E., Paternicò, D., Cristillo, V., Dell'Era, V., Cosseddu, M., Archetti, S., Alberici, A., Gasparotti, R., Padovani, A., Borroni, B., 2018. Neuroanatomical Correlates of Transcranial Magnetic Stimulation in Presymptomatic Granulin Mutation Carriers. Brain Topogr 31, 488–497.

Geertsen, S.S., Willerslev-Olsen, M., Lorentzen, J., Nielsen, J.B., 2017. Development and aging of human spinal cord circuitries. J Neurophysiol 118, 1133–1140.

Geevasinga, N., Menon, P., Ng, K., Van Den Bos, M., Byth, K., Kiernan, M.C., Vucic, S., 2016. Riluzole exerts transient modulating effects on cortical and axonal hyperexcitability in ALS. Amyotroph Lateral Scler Frontotemporal Degener 17, 580–588.

Geevasinga, N., Menon, P., Nicholson, G.A., Ng, K., Howells, J., Kril, J.J., Yiannikas, C., Kiernan, M.C., Vucic, S., 2015. Cortical Function in Asymptomatic Carriers and Patients With C9orf72 Amyotrophic Lateral Sclerosis. JAMA Neurol 72, 1268–1274.

Ghouri, R., Öksüz, N., Taşdelen, B., Özge, A., 2023. Factors affecting progression of non-Alzheimer dementia: a retrospective analysis with long-term follow-up. Front Neurol 14, 1240093.

Godoy-Corchuelo, J.M., Ali, Z., Brito Armas, J.M., Martins-Bach, A.B., García-Toledo, I., Fernández-Beltrán, L.C., López-Carbonero, J.I., Bascuñana, P., Spring, S., Jimenez-Coca, I., Muñoz de Bustillo Alfaro, R.A., Sánchez-Barrena, M.J., Nair, R.R., Nieman, B.J., Lerch, J.P., Miller, K.L., Ozdinler, H.P., Fisher, E.M.C., Cunningham, T.J., Acevedo-Arozena, A., Corrochano, S., 2024. TDP-43-M323K causes abnormal brain development and progressive cognitive and motor deficits associated with mislocalised and increased levels of TDP-43. Neurobiol Dis 193, 106437.

Goldstein, O., Inbar, T., Kedmi, M., Gana-Weisz, M., Abramovich, B., Orr-Urtreger, A., Drory, V.E., 2022. FUS-P525L Juvenile Amyotrophic Lateral Sclerosis and Intellectual Disability: Evidence for Association and Oligogenic Inheritance. Neurol Genet 8, 200009.

Golshani, P., Gonçalves, J.T., Khoshkhoo, S., Mostany, R., Smirnakis, S., Portera-Cailliau, C., 2009. Internally mediated developmental desynchronization of neocortical network activity. J Neurosci 29, 10890–10899.

Gomeza, J., Ohno, K., Hülsmann, S., Armsen, W., Eulenburg, V., Richter, D.W., Laube, B., Betz, H., 2003. Deletion of the mouse glycine transporter 2 results in a hyperekplexia phenotype and postnatal lethality. Neuron 40, 797–806.

Gonzalez, A., Mannen, T., Çağatay, T., Fujiwara, A., Matsumura, H., Niesman, A.B., Brautigam, C.A., Chook, Y.M., Yoshizawa, T., 2021. Mechanism of karyopherin-β2 binding and nuclear import of ALS variants FUS(P525L) and FUS(R495X). Sci Rep 11, 3754.

Gordon, P.H., Miller, R.G., Moore, D.H., 2004. ALSFRS-R. Amyotroph Lateral Scler Other Motor Neuron Disord 5 Suppl 1, 90–93.

Gorges, M., Vercruysse, P., Müller, H.-P., Huppertz, H.-J., Rosenbohm, A., Nagel, G., Weydt, P., Petersén, Å., Ludolph, A.C., Kassubek, J., Dupuis, L., 2017. Hypothalamic atrophy is related to body mass index and age at onset in amyotrophic lateral sclerosis. J Neurol Neurosurg Psychiatry 88, 1033–1041.

Gosgnach, S., Lanuza, G.M., Butt, S.J.B., Saueressig, H., Zhang, Y., Velasquez, T., Riethmacher, D., Callaway, E.M., Kiehn, O., Goulding, M., 2006. V1 spinal neurons regulate the speed of vertebrate locomotor outputs. Nature 440, 215–219.

Gosselt, I.K., Nijboer, T.C.W., Van Es, M.A., 2020. An overview of screening instruments for cognition and behavior in patients with ALS: selecting the appropriate tool for clinical practice. Amyotroph Lateral Scler Frontotemporal Degener 21, 324–336.

Gourmaud, S., Shou, H., Irwin, D.J., Sansalone, K., Jacobs, L.M., Lucas, T.H., Marsh, E.D., Davis, K.A., Jensen, F.E., Talos, D.M., 2020. Alzheimer-like amyloid and tau alterations associated with cognitive deficit in temporal lobe epilepsy. Brain 143, 191–209.

Goutman, S.A., Boss, J., Patterson, A., Mukherjee, B., Batterman, S., Feldman, E.L., 2019. High plasma concentrations of organic pollutants negatively impact survival in amyotrophic lateral sclerosis. J Neurol Neurosurg Psychiatry 90, 907–912.

Govaarts, R., Beeldman, E., Fraschini, M., Griffa, A., Engels, M.M.A., van Es, M.A., Veldink, J.H., van den Berg, L.H., van der Kooi, A.J., Pijnenburg, Y.A.L., de Visser, M., Stam, C.J., Raaphorst, J., Hillebrand, A., 2022. Cortical and subcortical changes in resting-state neuronal activity and connectivity in early symptomatic ALS and advanced frontotemporal dementia. Neuroimage Clin 34, 102965.

Grassano, M., Brodini, G., De Marco, G., Casale, F., Fuda, G., Salamone, P., Brunetti, M., Sbaiz, L., Gallone, S., Cugnasco, P., Bombaci, A., Vasta, R., Manera, U., Canosa, A., Moglia, C., Calvo, A., Traynor, B.J., Chio, A., 2022. Phenotype Analysis of Fused in Sarcoma Mutations in Amyotrophic Lateral Sclerosis. Neurol Genet 8, 200011.

Griener, A., Zhang, W., Kao, H., Wagner, C., Gosgnach, S., 2015. Probing diversity within subpopulations of locomotor-related V0 interneurons. Dev Neurobiol 75, 1189–1203.

Groen, E.J.N., Fumoto, K., Blokhuis, A.M., Engelen-Lee, J., Zhou, Y., van den Heuvel, D.M.A., Koppers, M., van Diggelen, F., van Heest, J., Demmers, J.A.A., Kirby, J., Shaw, P.J., Aronica, E., Spliet, W.G.M., Veldink, J.H., van den Berg, L.H., Pasterkamp, R.J., 2013. ALS-associated mutations in FUS disrupt the axonal distribution and function of SMN. Human Molecular Genetics 22, 3690–3704.

Guillot, S.J., Bolborea, M., Dupuis, L., 2021. Dysregulation of energy homeostasis in amyotrophic lateral sclerosis. Curr Opin Neurol 34, 773–780.

Gunaydin, L.A., Grosenick, L., Finkelstein, J.C., Kauvar, I.V., Fenno, L.E., Adhikari, A., Lammel, S., Mirzabekov, J.J., Airan, R.D., Zalocusky, K.A., Tye, K.M., Anikeeva, P., Malenka, R.C., Deisseroth, K., 2014. Natural neural projection dynamics underlying social behavior. Cell 157, 1535–1551.

Gunes, Z.I., Kan, V.W.Y., Ye, X., Liebscher, S., 2020. Exciting Complexity: The Role of Motor Circuit Elements in ALS Pathophysiology. Front Neurosci 14, 573.

Gunthorpe, M.J., Large, C.H., Sankar, R., 2012. The mechanism of action of retigabine (ezogabine), a first-in-class K+ channel opener for the treatment of epilepsy. Epilepsia 53, 412–424.

Guo, L., Kim, H.J., Wang, H., Monaghan, J., Freyermuth, F., Sung, J.C., O'Donovan, K., Fare, C.M., Diaz, Z., Singh, N., Zhang, Z.C., Coughlin, M., Sweeny, E.A., DeSantis, M.E., Jackrel, M.E., Rodell, C.B., Burdick, J.A., King, O.D., Gitler, A.D., Lagier-Tourenne, C., Pandey, U.B., Chook, Y.M., Taylor, J.P., Shorter, J., 2018. Nuclear-Import Receptors Reverse Aberrant Phase Transitions of RNA-Binding Proteins with Prion-like Domains. Cell 173, 677-692.

Gurney, M.E., Pu, H., Chiu, A.Y., Dal Canto, M.C., Polchow, C.Y., Alexander, D.D., Caliendo, J., Hentati, A., Kwon, Y.W., Deng, H.X., 1994. Motor neuron degeneration in mice that express a human Cu,Zn superoxide dismutase mutation. Science 264, 1772–1775.

- H -

Hall, S.D., Stanford, I.M., Yamawaki, N., McAllister, C.J., Rönnqvist, K.C., Woodhall, G.L., Furlong, P.L., 2011. The role of GABAergic modulation in motor function related neuronal network activity. Neuroimage 56, 1506–1510.

Harris, J.M., Saxon, J.A., Jones, M., Snowden, J.S., Thompson, J.C., 2019. Neuropsychological differentiation of progressive aphasic disorders. J Neuropsychol 13, 214–239.

Hasan, R., Humphrey, J., Bettencourt, C., Newcombe, J., NYGC ALS Consortium, Lashley, T., Fratta, P., Raj, T., 2022. Transcriptomic analysis of frontotemporal lobar degeneration with TDP-43 pathology reveals cellular alterations across multiple brain regions. Acta Neuropathol 143, 383–401.

Hayashi, S., Amari, M., Okamoto, K., 2013. Loss of calretinin- and parvalbumin-immunoreactive axons in anterolateral columns beyond the corticospinal tracts of amyotrophic lateral sclerosis spinal cords. J Neurol Sci 331, 61–66.

He, Y., Benz, A., Fu, T., Wang, M., Covey, D.F., Zorumski, C.F., Mennerick, S., 2002. Neuroprotective agent riluzole potentiates postsynaptic GABA(A) receptor function. Neuropharmacology 42, 199–209.

Héja, L., Barabás, P., Nyitrai, G., Kékesi, K.A., Lasztóczi, B., Toke, O., Tárkányi, G., Madsen, K., Schousboe, A., Dobolyi, A., Palkovits, M., Kardos, J., 2009. Glutamate uptake triggers transporter-mediated GABA release from astrocytes. PLoS One 4, 7153.

Héja, L., Nyitrai, G., Kékesi, O., Dobolyi, A., Szabó, P., Fiáth, R., Ulbert, I., Pál-Szenthe, B., Palkovits, M., Kardos, J., 2012. Astrocytes convert network excitation to tonic inhibition of neurons. BMC Biol 10, 26.

Hergesheimer, R.C., Chami, A.A., de Assis, D.R., Vourc'h, P., Andres, C.R., Corcia, P., Lanznaster, D., Blasco, H., 2019. The debated toxic role of aggregated TDP-43 in amyotrophic lateral sclerosis: a resolution in sight? Brain 142, 1176–1194.

Hicks, G.G., Singh, N., Nashabi, A., Mai, S., Bozek, G., Klewes, L., Arapovic, D., White, E.K., Koury, M.J., Oltz, E.M., Van Kaer, L., Ruley, H.E., 2000. Fus deficiency in mice results in defective B-lymphocyte development and activation, high levels of chromosomal instability and perinatal death. Nat Genet 24, 175–179.

Higashihara, M., Pavey, N., Menon, P., van den Bos, M., Shibuya, K., Kuwabara, S., Kiernan, M.C., Koinuma, M., Vucic, S., 2024. Reduction in short interval intracortical inhibition from the early stage reflects the pathophysiology in amyotrophic lateral sclerosis: A meta-analysis study. Eur J Neurol 31, 16281.

Hodge, R.D., Bakken, T.E., Miller, J.A., Smith, K.A., Barkan, E.R., Graybuck, L.T., Close, J.L., Long, B., Johansen, N., Penn, O., Yao, Z., Eggermont, J., Höllt, T., Levi, B.P., Shehata, S.I., Aevermann, B., Beller, A., Bertagnolli, D., Brouner, K., Casper, T., Cobbs, C., Dalley, R., Dee, N., Ding, S.-L., Ellenbogen, R.G., Fong, O., Garren, E., Goldy, J., Gwinn, R.P., Hirschstein, D., Keene, C.D., Keshk, M., Ko, A.L., Lathia, K., Mahfouz, A., Maltzer, Z., McGraw, M.,

Nguyen, T.N., Nyhus, J., Ojemann, J.G., Oldre, A., Parry, S., Reynolds, S., Rimorin, C., Shapovalova, N.V., Somasundaram, S., Szafer, A., Thomsen, E.R., Tieu, M., Quon, G., Scheuermann, R.H., Yuste, R., Sunkin, S.M., Lelieveldt, B., Feng, D., Ng, L., Bernard, A., Hawrylycz, M., Phillips, J.W., Tasic, B., Zeng, H., Jones, A.R., Koch, C., Lein, E.S., 2019. Conserved cell types with divergent features in human versus mouse cortex. Nature 573, 61–68.

Hoell, J.I., Larsson, E., Runge, S., Nusbaum, J.D., Duggimpudi, S., Farazi, T.A., Hafner, M., Borkhardt, A., Sander, C., Tuschl, T., 2011. RNA targets of wild-type and mutant FET family proteins. Nat Struct Mol Biol 18, 1428–1431.

Hofweber, M., Hutten, S., Bourgeois, B., Spreitzer, E., Niedner-Boblenz, A., Schifferer, M., Ruepp, M.-D., Simons, M., Niessing, D., Madl, T., Dormann, D., 2018. Phase Separation of FUS Is Suppressed by Its Nuclear Import Receptor and Arginine Methylation. Cell 173, 706-719.

Howells, J., Sangari, S., Matamala, J.M., Kiernan, M.C., Marchand-Pauvert, V., Burke, D., 2020. Interrogating interneurone function using threshold tracking of the H reflex in healthy subjects and patients with motor neurone disease. Clin Neurophysiol 131, 1986–1996.

Hu, H., Gan, J., Jonas, P., 2014. Interneurons. Fast-spiking, parvalbumin^{+} GABAergic interneurons: from cellular design to microcircuit function. Science 345, 1255263.

Hu, R.K., Zuo, Y., Ly, T., Wang, J., Meera, P., Wu, Y.E., Hong, W., 2021. An amygdala-to-hypothalamus circuit for social reward. Nat Neurosci 24, 831–842.

Huber, N., Korhonen, S., Hoffmann, D., Leskelä, S., Rostalski, H., Remes, A.M., Honkakoski, P., Solje, E., Haapasalo, A., 2022. Deficient neurotransmitter systems and synaptic function in frontotemporal lobar degeneration-Insights into disease mechanisms and current therapeutic approaches. Mol Psychiatry 27, 1300–1309.

Hübers, A., Just, W., Rosenbohm, A., Müller, K., Marroquin, N., Goebel, I., Högel, J., Thiele, H., Altmüller, J., Nürnberg, P., Weishaupt, J.H., Kubisch, C., Ludolph, A.C., Volk, A.E., 2015. De novo FUS mutations are the most frequent genetic cause in early-onset German ALS patients. Neurobiol Aging 36, 3117.

Hughes, L.E., Rittman, T., Robbins, T.W., Rowe, J.B., 2018. Reorganization of cortical oscillatory dynamics underlying disinhibition in frontotemporal dementia. Brain 141, 2486–2499.

Humphrey, J., Birsa, N., Milioto, C., McLaughlin, M., Ule, A.M., Robaldo, D., Eberle, A.B., Kräuchi, R., Bentham, M., Brown, A.-L., Jarvis, S., Bodo, C., Garone, M.G., Devoy, A., Soraru, G., Rosa, A., Bozzoni, I., Fisher, E.M.C., Mühlemann, O., Schiavo, G., Ruepp, M.-D., Isaacs, A.M., Plagnol, V., Fratta, P., 2020. FUS ALS-causative mutations impair FUS autoregulation and splicing factor networks through intron retention. Nucleic Acids Res 48, 6889–6905.

Husi, H., Ward, M.A., Choudhary, J.S., Blackstock, W.P., Grant, S.G., 2000. Proteomic analysis of NMDA receptor-adhesion protein signaling complexes. Nat Neurosci 3, 661–669.

- I -

Ikenaka, K., Ishigaki, S., Iguchi, Y., Kawai, K., Fujioka, Y., Yokoi, S., Abdelhamid, R.F., Nagano, S., Mochizuki, H., Katsuno, M., Sobue, G., 2020. Characteristic Features of FUS Inclusions in Spinal Motor Neurons of Sporadic Amyotrophic Lateral Sclerosis. J Neuropathol Exp Neurol 79, 370–377.

Ilieva, H., Vullaganti, M., Kwan, J., 2023. Advances in molecular pathology, diagnosis, and treatment of amyotrophic lateral sclerosis. BMJ 383, 075037.

Ince, P., Stout, N., Shaw, P., Slade, J., Hunziker, W., Heizmann, C.W., Baimbridge, K.G., 1993. Parvalbumin and calbindin D-28k in the human motor system and in motor neuron disease. Neuropathol Appl Neurobiol 19, 291–299.

Iñiguez, S.D., Riggs, L.M., Nieto, S.J., Dayrit, G., Zamora, N.N., Shawhan, K.L., Cruz, B., Warren, B.L., 2014. Social defeat stress induces a depression-like phenotype in adolescent male c57BL/6 mice. Stress 17, 247–255.

Ishigaki, S., Fujioka, Y., Okada, Y., Riku, Y., Udagawa, T., Honda, D., Yokoi, S., Endo, K., Ikenaka, K., Takagi, S., Iguchi, Y., Sahara, N., Takashima, A., Okano, H., Yoshida, M., Warita, H., Aoki, M., Watanabe, H., Okado, H., Katsuno, M., Sobue, G., 2017. Altered Tau Isoform Ratio Caused by Loss of FUS and SFPQ Function Leads to FTLD-like Phenotypes. Cell Rep 18, 1118–1131.

Ishigaki, S., Masuda, A., Fujioka, Y., Iguchi, Y., Katsuno, M., Shibata, A., Urano, F., Sobue, G., Ohno, K., 2012. Position-dependent FUS-RNA interactions regulate alternative splicing events and transcriptions. Sci Rep 2, 529.

Ishigaki, S., Sobue, G., 2018. Importance of Functional Loss of FUS in FTLD/ALS. Front. Mol. Biosci. 5, 44.

Iyer, P.M., Egan, C., Pinto-Grau, M., Burke, T., Elamin, M., Nasseroleslami, B., Pender, N., Lalor, E.C., Hardiman, O., 2015. Functional Connectivity Changes in Resting-State EEG as Potential Biomarker for Amyotrophic Lateral Sclerosis. PLoS One 10, 0128682.

- J -

Jabarin, R., Netser, S., Wagner, S., 2022. Beyond the three-chamber test: toward a multimodal and objective assessment of social behavior in rodents. Mol Autism 13, 41.

Jackson, M.G., Lightman, S.L., Gilmour, G., Marston, H., Robinson, E.S.J., 2021. Evidence for deficits in behavioural and physiological responses in aged mice relevant to the psychiatric symptom of apathy. Brain Neurosci Adv 5.

Jahn, K., Schlesinger, F., Jin, L.J., Dengler, R., Bufler, J., Krampfl, K., 2008. Molecular mechanisms of interaction between the neuroprotective substance riluzole and GABA(A)-receptors. Naunyn Schmiedebergs Arch Pharmacol 378, 53–63.

Janse van Mantgem, M.R., van Eijk, R.P.A., van der Burgh, H.K., Tan, H.H.G., Westeneng, H.-J., van Es, M.A., Veldink, J.H., van den Berg, L.H., 2020. Prognostic value of weight loss in patients with amyotrophic lateral sclerosis: a population-based study. J Neurol Neurosurg Psychiatry 91, 867–875.

Janssen, P., Houben, M., Hoff, E., 2016. Photosensitivity in a patient with C9orf72 repeat expansion. Amyotroph Lateral Scler Frontotemporal Degener 17, 266–269.

Jego, S., Glasgow, S.D., Herrera, C.G., Ekstrand, M., Reed, S.J., Boyce, R., Friedman, J., Burdakov, D., Adamantidis, A.R., 2013. Optogenetic identification of a rapid eye movement sleep modulatory circuit in the hypothalamus. Nat Neurosci 16, 1637–1643.

Jennings, J.H., Ung, R.L., Resendez, S.L., Stamatakis, A.M., Taylor, J.G., Huang, J., Veleta, K., Kantak, P.A., Aita, M., Shilling-Scrivo, K., Ramakrishnan, C., Deisseroth, K., Otte, S., Stuber, G.D., 2015. Visualizing hypothalamic network dynamics for appetitive and consummatory behaviors. Cell 160, 516–527.

Jiang, S., Wen, N., Li, Z., Dube, U., Del Aguila, J., Budde, J., Martinez, R., Hsu, S., Fernandez, M.V., Cairns, N.J., Dominantly Inherited Alzheimer Network (DIAN), International FTD-Genomics Consortium (IFGC), Harari, O., Cruchaga, C., Karch, C.M., 2018. Integrative system biology analyses of CRISPR-edited iPSC-derived neurons and human brains reveal deficiencies of presynaptic signaling in FTLD and PSP. Transl Psychiatry 8, 265.

Jinno, S., Kosaka, T., 2004. Parvalbumin is expressed in glutamatergic and GABAergic corticostriatal pathway in mice. J Comp Neurol 477, 188–201.

Jonsson, P.A., Graffmo, K.S., Andersen, P.M., Marklund, S.L., Brännström, T., 2009. Superoxide dismutase in amyotrophic lateral sclerosis patients homozygous for the D90A mutation. Neurobiol Dis 36, 421–424.

Ju, P., Chen, Jianhua, Ma, L., Cheng, Y., Liu, J., Sun, Y., Zhu, C., Shen, Z., Wang, W., Peng, Y., Ali, U., Xu, N., Chen, Jinghong, 2023. Histone deacetylase 4 inhibition ameliorates the social deficits induced by Ephrin-B2 mutation. Prog Neuropsychopharmacol Biol Psychiatry 120, 110622.

Julian, T.H., Glascow, N., Barry, A.D.F., Moll, T., Harvey, C., Klimentidis, Y.C., Newell, M., Zhang, S., Snyder, M.P., Cooper-Knock, J., Shaw, P.J., 2021. Physical exercise is a risk factor for amyotrophic lateral sclerosis: Convergent evidence from Mendelian randomisation, transcriptomics and risk genotypes. EBioMedicine 68, 103397.

Jyotika, J., McCutcheon, J., Laroche, J., Blaustein, J.D., Forger, N.G., 2007. Deletion of the Bax gene disrupts sexual behavior and modestly impairs motor function in mice. Dev Neurobiol 67, 1511–1519.

- K -

Kabashi, E., Bercier, V., Lissouba, A., Liao, M., Brustein, E., Rouleau, G.A., Drapeau, P., 2011. FUS and TARDBP but Not SOD1 Interact in Genetic Models of Amyotrophic Lateral Sclerosis. PLoS Genet 7, 1002214.

Kabashi, E., Valdmanis, P.N., Dion, P., Spiegelman, D., McConkey, B.J., Velde, C.V., Bouchard, J.-P., Lacomblez, L., Pochigaeva, K., Salachas, F., Pradat, P.-F., Camu, W., Meininger, V., Dupre, N., Rouleau, G.A., 2008. TARDBP mutations in individuals with sporadic and familial amyotrophic lateral sclerosis. Nature Genetics 40, 572–574.

Kaila, K., Price, T.J., Payne, J.A., Puskarjov, M., Voipio, J., 2014. Cation-chloride cotransporters in neuronal development, plasticity and disease. Nat Rev Neurosci 15, 637–654.

Kang, S.H., Li, Y., Fukaya, M., Lorenzini, I., Cleveland, D.W., Ostrow, L.W., Rothstein, J.D., Bergles, D.E., 2013. Degeneration and impaired regeneration of gray matter oligodendrocytes in amyotrophic lateral sclerosis. Nat Neurosci 16, 571–579.

Kansal, K., Mareddy, M., Sloane, K.L., Minc, A.A., Rabins, P.V., McGready, J.B., Onyike, C.U., 2016. Survival in Frontotemporal Dementia Phenotypes: A Meta-Analysis. Dement Geriatr Cogn Disord 41, 109–122.

Kapfer, C., Glickfeld, L.L., Atallah, B.V., Scanziani, M., 2007. Supralinear increase of recurrent inhibition during sparse activity in the somatosensory cortex. Nat Neurosci 10, 743–753.

Kavalali, E.T., 2015. The mechanisms and functions of spontaneous neurotransmitter release. Nat Rev Neurosci 16, 5–16.

Kepecs, A., Fishell, G., 2014. Interneuron cell types are fit to function. Nature 505, 318–326.

Kerlin, A.M., Andermann, M.L., Berezovskii, V.K., Reid, R.C., 2010. Broadly tuned response properties of diverse inhibitory neuron subtypes in mouse visual cortex. Neuron 67, 858–871.

Khademullah, C.S., Aqrabawi, A.J., Place, K.M., Dargaei, Z., Liang, X., Pressey, J.C., Bedard, S., Yang, J.W., Garand, D., Keramidis, I., Gasecka, A., Côté, D., De Koninck, Y., Keith, J., Zinman, L., Robertson, J., Kim, J.C., Woodin, M.A., 2020. Cortical interneuron-mediated inhibition delays the onset of amyotrophic lateral sclerosis. Brain 143, 800–810.

Khademullah, C.S., Bourbonnais, J., Chaineau, M.M., Castellanos-Montiel, M.J., Keramidis, I., Legault, A., Paquet, M.-È., Abrahao, A., Zinman, L., Robertson, J., Durcan, T.M., Woodin, M.A., Godin, A.G., Koninck, Y.D., 2023. KCC2 as a novel biomarker and therapeutic target for motoneuron degenerative disease.

Kikuma, K., Li, X., Kim, D., Sutter, D., Dickman, D.K., 2017. Extended Synaptotagmin Localizes to Presynaptic ER and Promotes Neurotransmission and Synaptic Growth in Drosophila. Genetics 207, 993–1006.

Kim, E., White, M.A., Phillips, B.U., Lopez-Cruz, L., Kim, H., Heath, C.J., Lee, J.E., Saksida, L.M., Sreedharan, J., Bussey, T.J., 2020. Coexistence of perseveration and apathy in the TDP-43Q331K knock-in mouse model of ALS-FTD. Transl Psychiatry 10, 377.

Kim, H., Ährlund-Richter, S., Wang, X., Deisseroth, K., Carlén, M., 2016. Prefrontal Parvalbumin Neurons in Control of Attention. Cell 164, 208–218.

Kim, J., Hughes, E.G., Shetty, A.S., Arlotta, P., Goff, L.A., Bergles, D.E., Brown, S.P., 2017. Changes in the Excitability of Neocortical Neurons in a Mouse Model of Amyotrophic Lateral Sclerosis Are Not Specific to Corticospinal Neurons and Are Modulated by Advancing Disease. J Neurosci 37, 9037–9053.

Kim, J.-I., Ganesan, S., Luo, S.X., Wu, Y.-W., Park, E., Huang, E.J., Chen, L., Ding, J.B., 2015. Aldehyde dehydrogenase 1a1 mediates a GABA synthesis pathway in midbrain dopaminergic neurons. Science 350, 102–106.

Kinney, G.A., 2005. GAT-3 transporters regulate inhibition in the neocortex. J Neurophysiol 94, 4533–4537.

Kino, Y., Washizu, C., Aquilanti, E., Okuno, M., Kurosawa, M., Yamada, M., Doi, H., Nukina, N., 2011. Intracellular localization and splicing regulation of FUS/TLS are variably affected by amyotrophic lateral sclerosis-linked mutations. Nucleic Acids Res 39, 2781–2798.

Kino, Y., Washizu, C., Kurosawa, M., Yamada, M., Miyazaki, H., Akagi, T., Hashikawa, T., Doi, H., Takumi, T., Hicks, G.G., Hattori, N., Shimogori, T., Nukina, N., 2015. FUS/TLS deficiency causes behavioral and pathological abnormalities distinct from amyotrophic lateral sclerosis. acta neuropathol commun 3, 24.

Kirkby, L.A., Sack, G.S., Firl, A., Feller, M.B., 2013. A role for correlated spontaneous activity in the assembly of neural circuits. Neuron 80, 1129–1144.

Kirmse, K., Kummer, M., Kovalchuk, Y., Witte, O.W., Garaschuk, O., Holthoff, K., 2015. GABA depolarizes immature neurons and inhibits network activity in the neonatal neocortex in vivo. Nat Commun 6, 7750.

Klavžar, P., Koritnik, B., Leonardis, L., Dolenc Grošelj, L., Kirbiš, M., Ristić Kovačič, S., Klinar, P., Pohar Perme, M., Zidar, J., 2020. Improvements in the multidisciplinary care are beneficial for survival in amyotrophic lateral sclerosis (ALS): experience from a tertiary ALS center. Amyotroph Lateral Scler Frontotemporal Degener 21, 203–208.

Knikou, M., 2008. The H-reflex as a probe: pathways and pitfalls. J Neurosci Methods 171, 1–12.

Kocar, T.D., Müller, H.-P., Ludolph, A.C., Kassubek, J., 2021. Feature selection from magnetic resonance imaging data in ALS: a systematic review. Ther Adv Chronic Dis 12.

Korobeynikov, V.A., Lyashchenko, A.K., Blanco-Redondo, B., Jafar-Nejad, P., Shneider, N.A., 2022. Antisense oligonucleotide silencing of FUS expression as a therapeutic approach in amyotrophic lateral sclerosis. Nat Med 28, 104–116.

Kosaka, Y., Kin, H., Tatetsu, M., Uema, I., Takayama, C., 2012. Distinct development of GABA system in the ventral and dorsal horns in the embryonic mouse spinal cord. Brain Res 1486, 39–52.

Kosse, C., Schöne, C., Bracey, E., Burdakov, D., 2017. Orexin-driven GAD65 network of the lateral hypothalamus sets physical activity in mice. Proc Natl Acad Sci U S A 114, 4525–4530.

Kovalchuk, M.O., Heuberger, J.A.A.C., Sleutjes, B.T.H.M., Ziagkos, D., van den Berg, L.H., Ferguson, T.A., Franssen, H., Groeneveld, G.J., 2018. Acute Effects of Riluzole and Retigabine on Axonal Excitability in Patients With Amyotrophic Lateral Sclerosis: A Randomized, Double-Blind, Placebo-Controlled, Crossover Trial. Clin Pharmacol Ther 104, 1136–1145.

Kraeuter, A.-K., Guest, P.C., Sarnyai, Z., 2019. The Open Field Test for Measuring Locomotor Activity and Anxiety-Like Behavior. Methods Mol Biol 1916, 99–103.

Krahe, T.E., Medina, A.E., Lantz, C.L., Filgueiras, C.C., 2015. Hyperactivity and depression-like traits in Bax KO mice. Brain Res 1625, 246–254.

Krienen, F.M., Goldman, M., Zhang, Q., C H Del Rosario, R., Florio, M., Machold, R., Saunders, A., Levandowski, K., Zaniewski, H., Schuman, B., Wu, C., Lutservitz, A., Mullally, C.D., Reed, N., Bien, E., Bortolin, L., Fernandez-Otero, M., Lin, J.D., Wysoker, A., Nemesh, J., Kulp, D., Burns, M., Tkachev, V., Smith, R., Walsh, C.A., Dimidschstein, J., Rudy, B., S Kean, L., Berretta, S., Fishell, G., Feng, G., McCarroll, S.A., 2020. Innovations present in the primate interneuron repertoire. Nature 586, 262–269.

Kwak, H., Koh, W., Kim, Sangwoo, Song, K., Shin, J.-I., Lee, J.M., Lee, E.H., Bae, J.Y., Ha, G.E., Oh, J.-E., Park, Y.M., Kim, Sunpil, Feng, J., Lee, S.E., Choi, J.W., Kim, K.H., Kim, Y.S., Woo, J., Lee, D., Son, T., Kwon, S.W., Park, K.D., Yoon, B.-E., Lee, J., Li, Y., Lee, H., Bae, Y.C., Lee, C.J., Cheong, E., 2020. Astrocytes Control Sensory Acuity via Tonic Inhibition in the Thalamus. Neuron 108, 691-706.

Kwiatkowski, T.J., Bosco, D.A., LeClerc, A.L., Tamrazian, E., Vanderburg, C.R., Russ, C., Davis, A., Gilchrist, J., Kasarskis, E.J., Munsat, T., Valdmanis, P., Rouleau, G.A., Hosler, B.A., Cortelli, P., de Jong, P.J., Yoshinaga, Y., Haines, J.L., Pericak-Vance, M.A., Yan, J., Ticozzi, N., Siddique, T., McKenna-Yasek, D., Sapp, P.C., Horvitz, H.R., Landers, J.E., Brown, R.H., 2009. Mutations in the FUS/TLS Gene on Chromosome 16 Cause Familial Amyotrophic Lateral Sclerosis. Science 323, 1205–1208.

- L -

Lagier-Tourenne, C., Polymenidou, M., Hutt, K.R., Vu, A.Q., Baughn, M., Huelga, S.C., Clutario, K.M., Ling, S.-C., Liang, T.Y., Mazur, C., Wancewicz, E., Kim, A.S., Watt, A., Freier, S., Hicks, G.G., Donohue, J.P., Shiue, L., Bennett, C.F., Ravits, J., Cleveland, D.W., Yeo, G.W., 2012. Divergent roles of ALS-linked proteins FUS/TLS and TDP-43 intersect in processing long pre-mRNAs. Nat Neurosci 15, 1488–1497.

Lam, P., Newland, J., Faull, R.L.M., Kwakowsky, A., 2023. Cation-Chloride Cotransporters KCC2 and NKCC1 as Therapeutic Targets in Neurological and Neuropsychiatric Disorders. Molecules 28, 1344.

Lanuza, G.M., Gosgnach, S., Pierani, A., Jessell, T.M., Goulding, M., 2004. Genetic identification of spinal interneurons that coordinate left-right locomotor activity necessary for walking movements. Neuron 42, 375–386.

Laszlo, Z.I., Hindley, N., Sanchez Avila, A., Kline, R.A., Eaton, S.L., Lamont, D.J., Smith, C., Spires-Jones, T.L., Wishart, T.M., Henstridge, C.M., 2022. Synaptic proteomics reveal distinct molecular signatures of cognitive change and C9ORF72 repeat expansion in the human ALS cortex. Acta Neuropathol Commun 10, 156.

Latal, A.T., Kremer, T., Gomeza, J., Eulenburg, V., Hülsmann, S., 2010. Development of synaptic inhibition in glycine transporter 2 deficient mice. Mol Cell Neurosci 44, 342–352.

Le Ber, I., De Septenville, A., Millecamps, S., Camuzat, A., Caroppo, P., Couratier, P., Blanc, F., Lacomblez, L., Sellal, F., Fleury, M.-C., Meininger, V., Cazeneuve, C., Clot, F., Flabeau, O., LeGuern, E., Brice, A., French Clinical and Genetic Research Network on FTLD/FTLD-ALS, 2015. TBK1 mutation frequencies in French frontotemporal dementia and amyotrophic lateral sclerosis cohorts. Neurobiol Aging 36, 3116.

Lebœuf, M., Vargas-Abonce, S.E., Pezé-Hedsieck, E., Dupont, E., Jimenez-Alonso, L., Moya, K.L., Prochiantz, A., 2023. ENGRAILED-1 transcription factor has a paracrine neurotrophic activity on adult spinal α-motoneurons. EMBO Rep 24, 56525.

Lederer, C.W., Torrisi, A., Pantelidou, M., Santama, N., Cavallaro, S., 2007. Pathways and genes differentially expressed in the motor cortex of patients with sporadic amyotrophic lateral sclerosis. BMC Genomics 8, 26.

Lee, A.T., Vogt, D., Rubenstein, J.L., Sohal, V.S., 2014. A class of GABAergic neurons in the prefrontal cortex sends long-range projections to the nucleus accumbens and elicits acute avoidance behavior. J Neurosci 34, 11519–11525.

Lee, SooHyun, Hjerling-Leffler, J., Zagha, E., Fishell, G., Rudy, B., 2010. The largest group of superficial neocortical GABAergic interneurons expresses ionotropic serotonin receptors. J Neurosci 30, 16796–16808.

Lee, Soojung, Yoon, B.-E., Berglund, K., Oh, S.-J., Park, H., Shin, H.-S., Augustine, G.J., Lee, C.J., 2010. Channel-mediated tonic GABA release from glia. Science 330, 790–796.

Lemon, R.N., 2008. Descending pathways in motor control. Annu Rev Neurosci 31, 195–218.

Levenga, J., Krishnamurthy, P., Rajamohamedsait, H., Wong, H., Franke, T.F., Cain, P., Sigurdsson, E.M., Hoeffer, C.A., 2013. Tau pathology induces loss of GABAergic interneurons leading to altered synaptic plasticity and behavioral impairments. Acta Neuropathol Commun 1, 34.

Levone, B.R., Lenzken, S.C., Antonaci, M., Maiser, A., Rapp, A., Conte, F., Reber, S., Mechtersheimer, J., Ronchi, A.E., Mühlemann, O., Leonhardt, H., Cardoso, M.C., Ruepp, M.-D., Barabino, S.M.L., 2021. FUS-dependent liquid-liquid phase separation is important for DNA repair initiation. J Cell Biol 220.

Liebscher, S., Keller, G.B., Goltstein, P.M., Bonhoeffer, T., Hübener, M., 2016. Selective Persistence of Sensorimotor Mismatch Signals in Visual Cortex of Behaving Alzheimer's Disease Mice. Curr Biol 26, 956–964.

Lin, Z., Kim, E., Ahmed, M., Han, G., Simmons, C., Redhead, Y., Bartlett, J., Pena Altamira, L.E., Callaghan, I., White, M.A., Singh, N., Sawiak, S., Spires-Jones, T., Vernon, A.C., Coleman, M.P., Green, J., Henstridge, C., Davies, J.S., Cash, D., Sreedharan, J., 2021. MRI-guided histology of TDP-43 knock-in mice implicates parvalbumin interneuron loss, impaired neurogenesis and aberrant neurodevelopment in amyotrophic lateral sclerosis-frontotemporal dementia. Brain Commun 3.

Lindau, M., Jelic, V., Johansson, S.-E., Andersen, C., Wahlund, L.-O., Almkvist, O., 2003. Quantitative EEG abnormalities and cognitive dysfunctions in frontotemporal dementia and Alzheimer's disease. Dement Geriatr Cogn Disord 15, 106–114.

Ling, S.-C., Dastidar, S.G., Tokunaga, S., Ho, W.Y., Lim, K., Ilieva, H., Parone, P.A., Tyan, S.-H., Tse, T.M., Chang, J.-C., Platoshyn, O., Bui, N.B., Bui, A., Vetto, A., Sun, S., McAlonis-Downes, M., Han, J.S., Swing, D., Kapeli, K., Yeo, G.W., Tessarollo, L., Marsala, M., Shaw, C.E., Tucker-Kellogg, G., La Spada, A.R., Lagier-Tourenne, C., Da Cruz, S., Cleveland, D.W., 2019. Overriding FUS autoregulation in mice triggers gain-of-toxic dysfunctions in RNA metabolism and autophagy-lysosome axis. Elife 8, 40811. 1

Ling, S.-C., Polymenidou, M., Cleveland, D.W., 2013. Converging Mechanisms in ALS and FTD: Disrupted RNA and Protein Homeostasis. Neuron 79, 416–438.

Liu, Y., Ouyang, P., Zheng, Y., Mi, L., Zhao, J., Ning, Y., Guo, W., 2021. A Selective Review of the Excitatory-Inhibitory Imbalance in Schizophrenia: Underlying Biology, Genetics, Microcircuits, and Symptoms. Front Cell Dev Biol 9, 664535.

Ljubenkov, P.A., Staffaroni, A.M., Rojas, J.C., Allen, I.E., Wang, P., Heuer, H., Karydas, A., Kornak, J., Cobigo, Y., Seeley, W.W., Grinberg, L.T., Spina, S., Fagan, A.M., Jerome, G., Knopman, D., Boeve, B.F., Dickerson, B.C., Kramer, J., Miller, B., Boxer, A.L., Rosen, H.J., 2018. Cerebrospinal fluid biomarkers predict frontotemporal dementia trajectory. Ann Clin Transl Neurol 5, 1250–1263.

Llorca, A., Deogracias, R., 2022. Origin, Development, and Synaptogenesis of Cortical Interneurons. Front Neurosci 16, 929469.

Lloyd, C.M., Richardson, M.P., Brooks, D.J., Al-Chalabi, A., Leigh, P.N., 2000. Extramotor involvement in ALS: PET studies with the GABA(A) ligand [(11)C]flumazenil. Brain 123, 2289–2296.

Lo Coco, D., Mattaliano, P., Spataro, R., Mattaliano, A., La Bella, V., 2011. Sleep-wake disturbances in patients with amyotrophic lateral sclerosis. J Neurol Neurosurg Psychiatry 82, 839–842.

Loeffler, T., Schilcher, I., Flunkert, S., Hutter-Paier, B., 2020. Neurofilament-Light Chain as Biomarker of Neurodegenerative and Rare Diseases With High Translational Value. Front Neurosci 14, 579.

Loerch, P.M., Lu, T., Dakin, K.A., Vann, J.M., Isaacs, A., Geula, C., Wang, J., Pan, Y., Gabuzda, D.H., Li, C., Prolla, T.A., Yankner, B.A., 2008. Evolution of the aging brain transcriptome and synaptic regulation. PLoS One 3, 3329.

Logroscino, G., Piccininni, M., Graff, C., Hardiman, O., Ludolph, A.C., Moreno, F., Otto, M., Remes, A.M., Rowe, J.B., Seelaar, H., Solje, E., Stefanova, E., Traykov, L., Jelic, V., Rydell, M.T., Pender, N., Anderl-Straub, S., Barandiaran, M., Gabilondo, A., Krüger, J., Murley, A.G., Rittman, T., van der Ende, E.L., van Swieten, J.C., Hartikainen, P., Stojmenovic, G.M., Mehrabian, S., Benussi, L., Alberici, A., Dell'Abate, M.T., Zecca, C., Borroni, B., FRONTIERS group, 2023. Incidence of Syndromes Associated With Frontotemporal Lobar Degeneration in 9 European Countries. JAMA Neurol 80, 279–286.

Longinetti, E., Fang, F., 2019. Epidemiology of amyotrophic lateral sclerosis: an update of recent literature. Curr Opin Neurol 32, 771–776.

López-Erauskin, J., Tadokoro, T., Baughn, M.W., Myers, B., McAlonis-Downes, M., Chillon-Marinas, C., Asiaban, J.N., Artates, J., Bui, A.T., Vetto, A.P., Lee, S.K., Le, A.V., Sun, Y., Jambeau, M., Boubaker, J., Swing, D., Qiu, J., Hicks, G.G., Ouyang, Z., Fu, X.-D., Tessarollo, L., Ling, S.-C., Parone, P.A., Shaw, C.E., Marsala, M., Lagier-Tourenne, C., Cleveland, D.W., Da Cruz, S., 2018. ALS/FTD-Linked Mutation in FUS Suppresses Intra-axonal Protein Synthesis and Drives Disease Without Nuclear Loss-of-Function of FUS. Neuron 100, 816-830.

López-Gómez, J.J., Ballesteros-Pomar, M.D., Torres-Torres, B., Pintor-De la Maza, B., Penacho-Lázaro, M.A., Palacio-Mures, J.M., Abreu-Padín, C., Sanz-Gallego, I., De Luis-Román, D.A., 2021. Impact of Percutaneous Endoscopic Gastrostomy (PEG) on the Evolution of Disease in Patients with Amyotrophic Lateral Sclerosis (ALS). Nutrients 13, 2765.

Lorenzo, L.-E., Barbe, A., Portalier, P., Fritschy, J.-M., Bras, H., 2006. Differential expression of GABAA and glycine receptors in ALS-resistant vs. ALS-vulnerable motoneurons: possible implications for selective vulnerability of motoneurons. Eur J Neurosci 23, 3161–3170.

Lu, C.-H., Macdonald-Wallis, C., Gray, E., Pearce, N., Petzold, A., Norgren, N., Giovannoni, G., Fratta, P., Sidle, K., Fish, M., Orrell, R., Howard, R., Talbot, K., Greensmith, L., Kuhle, J., Turner, M.R., Malaspina, A., 2015. Neurofilament light chain: A prognostic biomarker in amyotrophic lateral sclerosis. Neurology 84, 2247–2257.

Ludolph, A., Dupuis, L., Kasarskis, E., Steyn, F., Ngo, S., McDermott, C., 2023. Nutritional and metabolic factors in amyotrophic lateral sclerosis. Nat Rev Neurol 19, 511–524.

Ludolph, A.C., Dorst, J., Dreyhaupt, J., Weishaupt, J.H., Kassubek, J., Weiland, U., Meyer, T., Petri, S., Hermann, A., Emmer, A., Grosskreutz, J., Grehl, T., Zeller, D., Boentert, M., Schrank, B., Prudlo, J., Winkler, A.S., Gorbulev, S., Roselli, F., Schuster, J., Dupuis, L., LIPCAL-ALS Study Group, 2020. Effect of High-Caloric Nutrition on Survival in Amyotrophic Lateral Sclerosis. Ann Neurol 87, 206–216.

Lui, H., Zhang, J., Makinson, S.R., Cahill, M.K., Kelley, K.W., Huang, H.-Y., Shang, Y., Oldham, M.C., Martens, L.H., Gao, F., Coppola, G., Sloan, S.A., Hsieh, C.L., Kim, C.C., Bigio, E.H., Weintraub, S., Mesulam, M.-M., Rademakers, R., Mackenzie, I.R., Seeley, W.W., Karydas, A., Miller, B.L., Borroni, B., Ghidoni, R., Farese, R.V., Paz, J.T., Barres, B.A., Huang, E.J., 2016. Progranulin Deficiency Promotes Circuit-Specific Synaptic Pruning by Microglia via Complement Activation. Cell 165, 921–935.

Ly, J.Q.M., Gaggioni, G., Chellappa, S.L., Papachilleos, S., Brzozowski, A., Borsu, C., Rosanova, M., Sarasso, S., Middleton, B., Luxen, A., Archer, S.N., Phillips, C., Dijk, D.-J., Maquet, P., Massimini, M., Vandewalle, G., 2016. Circadian regulation of human cortical excitability. Nat Commun 7, 11828.

Lynch, T., Sano, M., Marder, K.S., Bell, K.L., Foster, N.L., Defendini, R.F., Sima, A.A., Keohane, C., Nygaard, T.G., Fahn, S., 1994. Clinical characteristics of a family with chromosome 17-linked disinhibition-dementia-parkinsonism-amyotrophy complex. Neurology 44, 1878–1884.

- M -

Mackenzie, I.R.A., Ansorge, O., Strong, M., Bilbao, J., Zinman, L., Ang, L.-C., Baker, M., Stewart, H., Eisen, A., Rademakers, R., Neumann, M., 2011a. Pathological heterogeneity in amyotrophic lateral sclerosis with FUS mutations: two distinct patterns correlating with disease severity and mutation. Acta Neuropathol 122, 87–98.

Mackenzie, I.R.A., Munoz, D.G., Kusaka, H., Yokota, O., Ishihara, K., Roeber, S., Kretzschmar, H.A., Cairns, N.J., Neumann, M., 2011b. Distinct pathological subtypes of FTLD-FUS. Acta Neuropathol 121, 207–218.

Madisen, L., Zwingman, T.A., Sunkin, S.M., Oh, S.W., Zariwala, H.A., Gu, H., Ng, L.L., Palmiter, R.D., Hawrylycz, M.J., Jones, A.R., Lein, E.S., Zeng, H., 2010. A robust and high-throughput Cre reporting and characterization system for the whole mouse brain. Nat Neurosci 13, 133–140.

Maeda, S., Djukic, B., Taneja, P., Yu, G.-Q., Lo, I., Davis, A., Craft, R., Guo, W., Wang, X., Kim, D., Ponnusamy, R., Gill, T.M., Masliah, E., Mucke, L., 2016. Expression of A152T human tau causes age-dependent neuronal dysfunction and loss in transgenic mice. EMBO Rep 17, 530–551.

Maekawa, S., Al-Sarraj, S., Kibble, M., Landau, S., Parnavelas, J., Cotter, D., Everall, I., Leigh, P.N., 2004. Cortical selective vulnerability in motor neuron disease: a morphometric study. Brain 127, 1237–1251.

Maharana, S., Wang, J., Papadopoulos, D.K., Richter, D., Pozniakovsky, A., Poser, I., Bickle, M., Rizk, S., Guillén-Boixet, J., Franzmann, T.M., Jahnel, M., Marrone, L., Chang, Y.-T., Sterneckert, J., Tomancak, P., Hyman, A.A., Alberti, S., 2018. RNA buffers the phase separation behavior of prion-like RNA binding proteins. Science 360, 918–921.

Mantz, J., Laudenbach, V., Lecharny, J.B., Henzel, D., Desmonts, J.M., 1994. Riluzole, a novel antiglutamate, blocks GABA uptake by striatal synaptosomes. Eur J Pharmacol 257, 7-8.

Maramai, S., Benchekroun, M., Ward, S.E., Atack, J.R., 2020. Subtype Selective γ-Aminobutyric Acid Type A Receptor (GABAAR) Modulators Acting at the Benzodiazepine Binding Site: An Update. J Med Chem 63, 3425–3446.

Marin, B., Arcuti, S., Jesus, P., Logroscino, G., Copetti, M., Fontana, A., Nicol, M., Raymondeau, M., Desport, J.C., Preux, P.M., Couratier, P., French register of ALS in Limousin (FRALim), 2016. Population-Based Evidence that Survival in Amyotrophic Lateral Sclerosis is Related to Weight Loss at Diagnosis. Neurodegener Dis 16, 225–234.

Marin, B., Fontana, A., Arcuti, S., Copetti, M., Boumédiene, F., Couratier, P., Beghi, E., Preux, P.M., Logroscino, G., 2018. Age-specific ALS incidence: a dose-response meta-analysis. Eur J Epidemiol 33, 621–634.

Marín, O., 2016. Developmental timing and critical windows for the treatment of psychiatric disorders. Nat Med 22, 1229–1238.

Marín, O., 2013. Cellular and molecular mechanisms controlling the migration of neocortical interneurons. Eur J Neurosci 38, 2019–2029.

Marshall, C.R., Hardy, C.J.D., Volkmer, A., Russell, L.L., Bond, R.L., Fletcher, P.D., Clark, C.N., Mummery, C.J., Schott, J.M., Rossor, M.N., Fox, N.C., Crutch, S.J., Rohrer, J.D., Warren, J.D., 2018. Primary progressive aphasia: a clinical approach. J Neurol 265, 1474–1490.

Martin, S., Trevor-Jones, E., Khan, S., Shaw, K., Marchment, D., Kulka, A., Ellis, C.E., Burman, R., Turner, M.R., Carroll, L., Mursaleen, L., Leigh, P.N., Shaw, C.E., Pearce, N., Stahl, D., Al-Chalabi, A., 2017. The benefit of evolving multidisciplinary care in ALS: a diagnostic cohort survival comparison. Amyotroph Lateral Scler Frontotemporal Degener 18, 569–575.

McDonnell, M.N., Orekhov, Y., Ziemann, U., 2006. The role of GABA(B) receptors in intracortical inhibition in the human motor cortex. Exp Brain Res 173, 86–93.

McGown, A., McDearmid, J.R., Panagiotaki, N., Tong, H., Al Mashhadi, S., Redhead, N., Lyon, A.N., Beattie, C.E., Shaw, P.J., Ramesh, T.M., 2013. Early interneuron dysfunction in ALS: insights from a mutant sod1 zebrafish model. Ann Neurol 73, 246–258.

McIntire, S.L., Reimer, R.J., Schuske, K., Edwards, R.H., Jorgensen, E.M., 1997. Identification and characterization of the vesicular GABA transporter. Nature 389, 870–876.

McKay, K.A., Smith, K.A., Smertinaite, L., Fang, F., Ingre, C., Taube, F., 2021. Military service and related risk factors for amyotrophic lateral sclerosis. Acta Neurol Scand 143, 39–50.

Mehta, P., Kreeger, L., Wylie, D.C., Pattadkal, J.J., Lusignan, T., Davis, M.J., Turi, G.F., Li, W.-K., Whitmire, M.P., Chen, Y., Kajs, B.L., Seidemann, E., Priebe, N.J., Losonczy, A., Zemelman, B.V., 2019. Functional Access to Neuron Subclasses in Rodent and Primate Forebrain. Cell Rep 26, 2818-2832.

Melis, M., Defazio, G., Casaglia, E., Melas, V., Floris, G., 2022. Early juvenile reading epilepsy and later frontotemporal dementia (FTD): expanding the clinical phenotype of C9ORF72 mutation? Amyotroph Lateral Scler Frontotemporal Degener 23, 139–142.

Meloni, E.G., Carlezon, W.A., Bolshakov, V.Y., 2024. Association between social dominance hierarchy and PACAP expression in the extended amygdala, corticosterone, and behavior in C57BL/6 male mice. Sci Rep 14, 8919.

Menon, P., Higashihara, M., van den Bos, M., Geevasinga, N., Kiernan, M.C., Vucic, S., 2020. Cortical hyperexcitability evolves with disease progression in ALS. Ann Clin Transl Neurol 7, 733–741.

Menon, P., Kiernan, M.C., Vucic, S., 2015. Cortical hyperexcitability precedes lower motor neuron dysfunction in ALS. Clin Neurophysiol 126, 803–809.

Menon, P., Kiernan, M.C., Vucic, S., 2014. Cortical dysfunction underlies the development of the split-hand in amyotrophic lateral sclerosis. PLoS One 9, 87124.

Merner, N.D., Girard, S.L., Catoire, H., Bourassa, C.V., Belzil, V.V., Rivière, J.-B., Hince, P., Levert, A., Dionne-Laporte, A., Spiegelman, D., Noreau, A., Diab, S., Szuto, A., Fournier, H., Raelson, J., Belouchi, M., Panisset, M., Cossette, P., Dupré, N., Bernard, G., Chouinard, S., Dion, P.A., Rouleau, G.A., 2012. Exome sequencing identifies FUS mutations as a cause of essential tremor. Am J Hum Genet 91, 313–319.

Mesulam, M.-M., Wieneke, C., Thompson, C., Rogalski, E., Weintraub, S., 2012. Quantitative classification of primary progressive aphasia at early and mild impairment stages. Brain 135, 1537–1553.

Meyer, H.S., Schwarz, D., Wimmer, V.C., Schmitt, A.C., Kerr, J.N.D., Sakmann, B., Helmstaedter, M., 2011. Inhibitory interneurons in a cortical column form hot zones of inhibition in layers 2 and 5A. Proc Natl Acad Sci U S A 108, 16807–16812.

Mickelsen, L.E., Kolling, F.W., Chimileski, B.R., Fujita, A., Norris, C., Chen, K., Nelson, C.E., Jackson, A.C., 2017. Neurochemical Heterogeneity Among Lateral Hypothalamic Hypocretin/Orexin and Melanin-Concentrating Hormone Neurons Identified Through Single-Cell Gene Expression Analysis. eNeuro 4, 13-17.

Miller, T., Cudkowicz, M., Shaw, P.J., Andersen, P.M., Atassi, N., Bucelli, R.C., Genge, A., Glass, J., Ladha, S., Ludolph, A.L., Maragakis, N.J., McDermott, C.J., Pestronk, A., Ravits, J., Salachas, F., Trudell, R., Van Damme, P., Zinman, L., Bennett, C.F., Lane, R., Sandrock, A., Runz, H., Graham, D., Houshyar, H., McCampbell, A., Nestorov, I., Chang, I., McNeill, M., Fanning, L., Fradette, S., Ferguson, T.A., 2020. Phase 1-2 Trial of Antisense Oligonucleotide Tofersen for SOD1 ALS. N Engl J Med 383, 109–119.

Mina, A.I., LeClair, R.A., LeClair, K.B., Cohen, D.E., Lantier, L., Banks, A.S., 2018. CalR: A Web-Based Analysis Tool for Indirect Calorimetry Experiments. Cell Metab 28, 656-666.

Minciacchi, D., Kassa, R.M., Del Tongo, C., Mariotti, R., Bentivoglio, M., 2009. Voronoi-based spatial analysis reveals selective interneuron changes in the cortex of FALS mice. Exp Neurol 215, 77–86.

Mitchell, J.C., McGoldrick, P., Vance, C., Hortobagyi, T., Sreedharan, J., Rogelj, B., Tudor, E.L., Smith, B.N., Klasen, C., Miller, C.C.J., Cooper, J.D., Greensmith, L., Shaw, C.E., 2013. Overexpression of human wild-type FUS causes progressive motor neuron degeneration in an age- and dose-dependent fashion. Acta Neuropathol 125, 273–288.

Miyamae, T., Chen, K., Lewis, D.A., Gonzalez-Burgos, G., 2017. Distinct Physiological Maturation of Parvalbumin-Positive Neuron Subtypes in Mouse Prefrontal Cortex. J Neurosci 37, 4883–4902.

Mòdol, L., Moissidis, M., Selten, M., Oozeer, F., Marín, O., 2024. Somatostatin interneurons control the timing of developmental desynchronization in cortical networks. Neuron 112, 2015-2030.

Moheb, N., Charuworn, K., Ashla, M.M., Desarzant, R., Chavez, D., Mendez, M.F., 2019. Repetitive Behaviors in Frontotemporal Dementia: Compulsions or Impulsions? J Neuropsychiatry Clin Neurosci 31, 132–136.

Montañana-Rosell, R., Selvan, R., Hernández-Varas, P., Kaminski, J.M., Sidhu, S.K., Ahlmark, D.B., Kiehn, O., Allodi, I., 2024. Spinal inhibitory neurons degenerate before motor neurons and excitatory neurons in a mouse model of ALS. Sci Adv 10, 3229.

Moore, J.D., Kleinfeld, D., Wang, F., 2014. How the brainstem controls orofacial behaviors comprised of rhythmic actions. Trends Neurosci 37, 370–380.

Moore, K.M., Nicholas, J., Grossman, M., McMillan, C.T., Irwin, D.J., Massimo, L., Van Deerlin, V.M., Warren, J.D., Fox, N.C., Rossor, M.N., Mead, S., Bocchetta, M., Boeve, B.F., Knopman, D.S., Graff-Radford, N.R., Forsberg, L.K., Rademakers, R., Wszolek, Z.K., van Swieten, J.C., Jiskoot, L.C., Meeter, L.H., Dopper, E.G., Papma, J.M., Snowden, J.S., Saxon, J., Jones, M., Pickering-Brown, S., Le Ber, I., Camuzat, A., Brice, A., Caroppo, P., Ghidoni, R., Pievani, M., Benussi, L., Binetti, G., Dickerson, B.C., Lucente, D., Krivensky, S., Graff, C., Öijerstedt, L., Fallström, M., Thonberg, H., Ghoshal, N., Morris, J.C., Borroni, B., Benussi, A., Padovani, A., Galimberti, D., Scarpini, E., Fumagalli, G.G., Mackenzie, I.R., Hsiung, G.-Y.R., Sengdy, P., Boxer, A.L., Rosen, H., Taylor, J.B., Synofzik, M., Wilke, C., Sulzer, P., Hodges, J.R., Halliday, G., Kwok, J., Sanchez-Valle, R., Lladó, A., Borrego-Ecija, S., Santana, I., Almeida, M.R., Tábuas-Pereira, M., Moreno, F., Barandiaran, M., Indakoetxea, B., Levin, J., Danek, A., Rowe, J.B., Cope, T.E., Otto, M., Anderl-Straub, S., de Mendonça, A., Maruta, C., Masellis, M., Black, S.E., Couratier, P., Lautrette, G., Huey, E.D., Sorbi, S., Nacmias, B., Laforce, R., Tremblay, M.-P.L., Vandenberghe, R., Damme, P.V., Rogalski, E.J., Weintraub, S., Gerhard, A., Onyike, C.U., Ducharme, S., Papageorgiou, S.G., Ng, A.S.L., Brodtmann, A., Finger, E., Guerreiro, R., Bras, J., Rohrer, J.D., FTD Prevention Initiative, 2020. Age at symptom onset and death and disease duration in genetic frontotemporal dementia: an international retrospective cohort study. Lancet Neurol 19, 145–156.

Mora, S., Allodi, I., 2023. Neural circuit and synaptic dysfunctions in ALS-FTD pathology. Front Neural Circuits 17, 1208876.

Mora, S., Stuckert, A., von Huth Friis, R., Pietersz, K., Noes-Holt, G., Montañana-Rosell, R., Wang, H., Sørensen, A.T., Selvan, R., Verhaagen, J., Allodi, I., 2024. Stabilization of V1 interneuron-motor neuron connectivity ameliorates motor phenotype in a mouse model of ALS. Nat Commun 15, 4867.

Mori, S., Honda, H., Ishii, T., Yoshimura, M., Sasagasako, N., Suzuki, S.O., Taniwaki, T., Iwaki, T., 2019. Expanded polyglutamine impairs normal nuclear distribution of fused in sarcoma and poly (rC)-binding protein 1 in Huntington's disease. Neuropathology 39, 358–367.

Morlando, M., Dini Modigliani, S., Torrelli, G., Rosa, A., Di Carlo, V., Caffarelli, E., Bozzoni, I., 2012. FUS stimulates microRNA biogenesis by facilitating co-transcriptional Drosha recruitment: FUS participates in microRNA biogenesis. The EMBO Journal 31, 4502–4510.

Morrison, J.H., Baxter, M.G., 2012. The ageing cortical synapse: hallmarks and implications for cognitive decline. Nat Rev Neurosci 13, 240–250.

Munoz, D.G., Neumann, M., Kusaka, H., Yokota, O., Ishihara, K., Terada, S., Kuroda, S., Mackenzie, I.R., 2009. FUS pathology in basophilic inclusion body disease. Acta Neuropathol 118, 617–627.

Murakami, T., Qamar, S., Lin, J.Q., Schierle, G.S.K., Rees, E., Miyashita, A., Costa, A.R., Dodd, R.B., Chan, F.T.S., Michel, C.H., Kronenberg-Versteeg, D., Li, Y., Yang, S.-P., Wakutani, Y., Meadows, W., Ferry, R.R., Dong, L., Tartaglia, G.G., Favrin, G., Lin, W.-L., Dickson, D.W., Zhen, M., Ron, D., Schmitt-Ulms, G., Fraser, P.E., Shneider, N.A., Holt, C., Vendruscolo, M., Kaminski, C.F., St George-Hyslop, P., 2015. ALS/FTD Mutation-Induced Phase Transition of FUS Liquid Droplets and Reversible Hydrogels into Irreversible Hydrogels Impairs RNP Granule Function. Neuron 88, 678–690.

Murata, Y., Colonnese, M.T., 2020. GABAergic interneurons excite neonatal hippocampus in vivo. Sci Adv 6, eaba1430.

Murley, A.G., Rouse, M.A., Jones, P.S., Ye, R., Hezemans, F.H., O'Callaghan, C., Frangou, P., Kourtzi, Z., Rua, C., Carpenter, T.A., Rodgers, C.T., Rowe, J.B., 2020. GABA and glutamate deficits from frontotemporal lobar degeneration are associated with disinhibition. Brain 143, 3449–3462.

Muroni, A., Floris, G., Polizzi, L., Fadda, L., Piga, G., Primicerio, G., Rocchi, L., Defazio, G., 2022. Does epilepsy contribute to the clinical phenotype of C9orf72 mutation in fronto-temporal dementia? Epilepsy Behav 133, 108783.

Murphy, J., Factor-Litvak, P., Goetz, R., Lomen-Hoerth, C., Nagy, P.L., Hupf, J., Singleton, J., Woolley, S., Andrews, H., Heitzman, D., Bedlack, R.S., Katz, J.S., Barohn, R.J., Sorenson, E.J., Oskarsson, B., Fernandes Filho, J.A.M., Kasarskis, E.J., Mozaffar, T., Rollins, Y.D., Nations, S.P., Swenson, A.J., Koczon-Jaremko, B.A., Mitsumoto, H., ALS COSMOS, 2016. Cognitive-behavioral screening reveals prevalent impairment in a large multicenter ALS cohort. Neurology 86, 813–820.

Murray, D.T., Kato, M., Lin, Y., Thurber, K.R., Hung, I., McKnight, S.L., Tycko, R., 2017. Structure of FUS Protein Fibrils and Its Relevance to Self-Assembly and Phase Separation of Low-Complexity Domains. Cell 171, 615-627.

Muthukumaraswamy, S.D., Myers, J.F.M., Wilson, S.J., Nutt, D.J., Lingford-Hughes, A., Singh, K.D., Hamandi, K., 2013. The effects of elevated endogenous GABA levels on movement-related network oscillations. Neuroimage 66, 36–41.

- N -

Nakaya, T., Alexiou, P., Maragkakis, M., Chang, A., Mourelatos, Z., 2013. FUS regulates genes coding for RNA-binding proteins in neurons by binding to their highly conserved introns. RNA 19, 498–509.

Nakazono, T., Jun, H., Blurton-Jones, M., Green, K.N., Igarashi, K.M., 2018. Gamma oscillations in the entorhinal-hippocampal circuit underlying memory and dementia. Neurosci Res 129, 40–46.

Nathanson, J.L., Yanagawa, Y., Obata, K., Callaway, E.M., 2009. Preferential labeling of inhibitory and excitatory cortical neurons by endogenous tropism of adeno-associated virus and lentivirus vectors. Neuroscience 161, 441–450.

Neumann, M., Bentmann, E., Dormann, D., Jawaid, A., DeJesus-Hernandez, M., Ansorge, O., Roeber, S., Kretzschmar, H.A., Munoz, D.G., Kusaka, H., Yokota, O., Ang, L.-C., Bilbao, J., Rademakers, R., Haass, C.,

Mackenzie, I.R.A., 2011. FET proteins TAF15 and EWS are selective markers that distinguish FTLD with FUS pathology from amyotrophic lateral sclerosis with FUS mutations. Brain 134, 2595–2609.

Neumann, M., Rademakers, R., Roeber, S., Baker, M., Kretzschmar, H.A., Mackenzie, I.R.A., 2009a. A new subtype of frontotemporal lobar degeneration with FUS pathology. Brain 132, 2922–2931.

Neumann, M., Roeber, S., Kretzschmar, H.A., Rademakers, R., Baker, M., Mackenzie, I.R.A., 2009b. Abundant FUS-immunoreactive pathology in neuronal intermediate filament inclusion disease. Acta Neuropathol 118, 605–616.

Neumann, M., Sampathu, D.M., Kwong, L.K., Truax, A.C., Micsenyi, M.C., Chou, T.T., Bruce, J., Schuck, T., Grossman, M., Clark, C.M., McCluskey, L.F., Miller, B.L., Masliah, E., Mackenzie, I.R., Feldman, H., Feiden, W., Kretzschmar, H.A., Trojanowski, J.Q., Lee, V.M.-Y., 2006. Ubiquitinated TDP-43 in Frontotemporal Lobar Degeneration and Amyotrophic Lateral Sclerosis. Science 314, 130–133.

Nigro, M.J., Hashikawa-Yamasaki, Y., Rudy, B., 2018. Diversity and Connectivity of Layer 5 Somatostatin-Expressing Interneurons in the Mouse Barrel Cortex. J Neurosci 38, 1622–1633.

Niu, C., Zhang, J., Gao, F., Yang, L., Jia, M., Zhu, H., Gong, W., 2012. FUS-NLS/Transportin 1 complex structure provides insights into the nuclear targeting mechanism of FUS and the implications in ALS. PLoS One 7, 47056.

Noda, S., Sato, S., Fukuda, T., Tada, N., Hattori, N., 2020. Aging-related motor function and dopaminergic neuronal loss in C57BL/6 mice. Mol Brain 13, 46.

Nolan, M., Scott, C., Gamarallage, M.P., Lunn, D., Carpenter, K., McDonough, E., Meyer, D., Kaanumalle, S., Santamaria-Pang, A., Turner, M.R., Talbot, K., Ansorge, O., 2020. Quantitative patterns of motor cortex proteinopathy across ALS genotypes. Acta Neuropathol Commun 8, 98.

- O -

Obermayer, J., Luchicchi, A., Heistek, T.S., de Kloet, S.F., Terra, H., Bruinsma, B., Mnie-Filali, O., Kortleven, C., Galakhova, A.A., Khalil, A.J., Kroon, T., Jonker, A.J., de Haan, R., van de Berg, W.D.J., Goriounova, N.A., de Kock, C.P.J., Pattij, T., Mansvelder, H.D., 2019. Prefrontal cortical ChAT-VIP interneurons provide local excitation by cholinergic synaptic transmission and control attention. Nat Commun 10, 5280.

O'Brien, M., Burke, T., Heverin, M., Vajda, A., McLaughlin, R., Gibbons, J., Byrne, S., Pinto-Grau, M., Elamin, M., Pender, N., Hardiman, O., 2017. Clustering of Neuropsychiatric Disease in First-Degree and Second-Degree Relatives of Patients With Amyotrophic Lateral Sclerosis. JAMA Neurol 74, 1425–1430.

Ojeda, J., Ávila, A., 2019. Early Actions of Neurotransmitters During Cortex Development and Maturation of Reprogrammed Neurons. Front Synaptic Neurosci 11, 33.

Okaty, B.W., Miller, M.N., Sugino, K., Hempel, C.M., Nelson, S.B., 2009. Transcriptional and electrophysiological maturation of neocortical fast-spiking GABAergic interneurons. J Neurosci 29, 7040–7052.

Orozco, D., Tahirovic, S., Rentzsch, K., Schwenk, B.M., Haass, C., Edbauer, D., 2012. Loss of fused in sarcoma (FUS) promotes pathological Tau splicing. EMBO Rep 13, 759–764.

Osman, K.L., Kohlberg, S., Mok, A., Brooks, R., Lind, L.A., McCormack, K., Ferreira, A., Kadosh, M., Fagan, M.K., Bearce, E., Nichols, N.L., Coates, J.R., Lever, T.E., 2020. Optimizing the Translational Value of Mouse Models of ALS for Dysphagia Therapeutic Discovery. Dysphagia 35, 343–359.

Owens, D.F., Kriegstein, A.R., 2002. Is there more to GABA than synaptic inhibition? Nat Rev Neurosci 3, 715–727.

Ozdinler, P.H., Benn, S., Yamamoto, T.H., Güzel, M., Brown, R.H., Macklis, J.D., 2011. Corticospinal motor neurons and related subcerebral projection neurons undergo early and specific neurodegeneration in hSOD1G^{93}A transgenic ALS mice. J Neurosci 31, 4166–4177.

Özyurt, M.G., Topkara, B., İşak, B., Türker, K.S., 2020. Amyotrophic lateral sclerosis weakens spinal recurrent inhibition and post-activation depression. Clin Neurophysiol 131, 2875–2886.

- P -

Palicz, R., Pater, B., Truschow, P., Witte, M., Staiger, J.F., 2024. Intersectional strategy to study cortical inhibitory parvalbumin-expressing interneurons. Sci Rep 14, 2829.

Pamphlett, R., Luquin, N., McLean, C., Jew, S.K., Adams, L., 2009. TDP-43 neuropathology is similar in sporadic amyotrophic lateral sclerosis with or without TDP-43 mutations. Neuropathol Appl Neurobiol 35, 222–225.

Pang, W., Hu, F., 2021. Cellular and physiological functions of C9ORF72 and implications for ALS/FTD. J Neurochem 157, 334–350.

Parrella, N.-F., Hill, A.T., Dipnall, L.M., Loke, Y.J., Enticott, P.G., Ford, T.C., 2024. Inhibitory dysfunction and social processing difficulties in autism: A comprehensive narrative review. J Psychiatr Res 169, 113–125.

Patel, A., Lee, H.O., Jawerth, L., Maharana, S., Jahnel, M., Hein, M.Y., Stoynov, S., Mahamid, J., Saha, S., Franzmann, T.M., Pozniakovski, A., Poser, I., Maghelli, N., Royer, L.A., Weigert, M., Myers, E.W., Grill, S., Drechsel, D., Hyman, A.A., Alberti, S., 2015. A Liquid-to-Solid Phase Transition of the ALS Protein FUS Accelerated by Disease Mutation. Cell 162, 1066–1077.

Paul, J., Zeilhofer, H.U., Fritschy, J.-M., 2012. Selective distribution of GABA(A) receptor subtypes in mouse spinal dorsal horn neurons and primary afferents. J Comp Neurol 520, 3895–3911.

Paushter, D.H., Du, H., Feng, T., Hu, F., 2018. The lysosomal function of progranulin, a guardian against neurodegeneration. Acta Neuropathol 136, 1–17.

Pavey, N., Hannaford, A., van den Bos, M., Kiernan, M.C., Menon, P., Vucic, S., 2024. Distinct neuronal circuits mediate cortical hyperexcitability in amyotrophic lateral sclerosis. Brain 147, 2344–2356.

Peerboom, C., Wierenga, C.J., 2021. The postnatal GABA shift: A developmental perspective. Neurosci Biobehav Rev 124, 179–192.

Pender, N., Pinto-Grau, M., Hardiman, O., 2020. Cognitive and behavioural impairment in amyotrophic lateral sclerosis. Curr Opin Neurol 33, 649–654.

Pengo, M., Alberici, A., Libri, I., Benussi, A., Gadola, Y., Ashton, N.J., Zetterberg, H., Blennow, K., Borroni, B., 2022. Sex influences clinical phenotype in frontotemporal dementia. Neurol Sci 43, 5281–5287.

Perry, D.C., Sturm, V.E., Wood, K.A., Miller, B.L., Kramer, J.H., 2015. Divergent processing of monetary and social reward in behavioral variant frontotemporal dementia and Alzheimer disease. Alzheimer Dis Assoc Disord 29, 161–164.

Peter, R.S., Rosenbohm, A., Dupuis, L., Brehme, T., Kassubek, J., Rothenbacher, D., Nagel, G., Ludolph, A.C., 2017. Life course body mass index and risk and prognosis of amyotrophic lateral sclerosis: results from the ALS registry Swabia. Eur J Epidemiol 32, 901–908.

Peters, S., Broberg, K., Gallo, V., Levi, M., Kippler, M., Vineis, P., Veldink, J., van den Berg, L., Middleton, L., Travis, R.C., Bergmann, M.M., Palli, D., Grioni, S., Tumino, R., Elbaz, A., Vlaar, T., Mancini, F., Kühn, T., Katzke, V., Agudo, A., Goñi, F., Gómez, J.-H., Rodríguez-Barranco, M., Merino, S., Barricarte, A., Trichopoulou, A., Jenab,

M., Weiderpass, E., Vermeulen, R., 2021. Blood Metal Levels and Amyotrophic Lateral Sclerosis Risk: A Prospective Cohort. Ann Neurol 89, 125–133.

Petri, S., Kollewe, K., Grothe, C., Hori, A., Dengler, R., Bufler, J., Krampfl, K., 2006. GABAA-receptor mRNA expression in the prefrontal and temporal cortex of ALS patients. Journal of the Neurological Sciences 250, 124–132.

Petri, S., Krampfl, K., Hashemi, F., Grothe, C., Hori, A., Dengler, R., Bufler, J., 2003. Distribution of GABAA Receptor mRNA in the Motor Cortex of ALS Patients. Journal of Neuropathology & Experimental Neurology 62, 1041–1051.

Picchiarelli, G., Demestre, M., Zuko, A., Been, M., Higelin, J., Dieterlé, S., Goy, M.-A., Mallik, M., Sellier, C., Scekic-Zahirovic, J., Zhang, L., Rosenbohm, A., Sijlmans, C., Aly, A., Mersmann, S., Sanjuan-Ruiz, I., Hübers, A., Messaddeq, N., Wagner, M., van Bakel, N., Boutillier, A.-L., Ludolph, A., Lagier-Tourenne, C., Boeckers, T.M., Dupuis, L., Storkebaum, E., 2019. FUS-mediated regulation of acetylcholine receptor transcription at neuromuscular junctions is compromised in amyotrophic lateral sclerosis. Nat Neurosci 22, 1793–1805.

Picher-Martel, V., Brunet, F., Dupré, N., Chrestian, N., 2020. The Occurrence of FUS Mutations in Pediatric Amyotrophic Lateral Sclerosis: A Case Report and Review of the Literature. J Child Neurol 35, 556–562.

Piguet, O., Kumfor, F., 2020. Frontotemporal dementias: main syndromes and underlying brain changes. Curr Opin Neurol 33, 215–221.

Pisella, L.I., Gaiarsa, J.-L., Diabira, D., Zhang, J., Khalilov, I., Duan, J., Kahle, K.T., Medina, I., 2019. Impaired regulation of KCC2 phosphorylation leads to neuronal network dysfunction and neurodevelopmental pathology. Sci Signal 12.

Polymenidou, M., Lagier-Tourenne, C., Hutt, K.R., Huelga, S.C., Moran, J., Liang, T.Y., Ling, S.-C., Sun, E., Wancewicz, E., Mazur, C., Kordasiewicz, H., Sedaghat, Y., Donohue, J.P., Shiue, L., Bennett, C.F., Yeo, G.W., Cleveland, D.W., 2011. Long pre-mRNA depletion and RNA missplicing contribute to neuronal vulnerability from loss of TDP-43. Nat Neurosci 14, 459–468.

Pottier, C., Bieniek, K.F., Finch, N., van de Vorst, M., Baker, M., Perkersen, R., Brown, P., Ravenscroft, T., van Blitterswijk, M., Nicholson, A.M., DeTure, M., Knopman, D.S., Josephs, K.A., Parisi, J.E., Petersen, R.C., Boylan, K.B., Boeve, B.F., Graff-Radford, N.R., Veltman, J.A., Gilissen, C., Murray, M.E., Dickson, D.W., Rademakers, R., 2015. Whole-genome sequencing reveals important role for TBK1 and OPTN mutations in frontotemporal lobar degeneration without motor neuron disease. Acta Neuropathol 130, 77–92.

Pottier, C., Mateiu, L., Baker, M.C., DeJesus-Hernandez, M., Teixeira Vicente, C., Finch, N.A., Tian, S., van Blitterswijk, M., Murray, M.E., Ren, Y., Petrucelli, L., Oskarsson, B., Biernacka, J.M., Graff-Radford, N.R., Boeve, B.F., Petersen, R.C., Josephs, K.A., Asmann, Y.W., Dickson, D.W., Rademakers, R., 2022. Shared brain transcriptomic signature in TDP-43 type A FTLD patients with or without GRN mutations. Brain 145, 2472–2485.

Priya, R., Paredes, M.F., Karayannis, T., Yusuf, N., Liu, X., Jaglin, X., Graef, I., Alvarez-Buylla, A., Fishell, G., 2018. Activity Regulates Cell Death within Cortical Interneurons through a Calcineurin-Dependent Mechanism. Cell Reports 22, 1695–1709.

Proudfoot, M., Colclough, G.L., Quinn, A., Wuu, J., Talbot, K., Benatar, M., Nobre, A.C., Woolrich, M.W., Turner, M.R., 2018. Increased cerebral functional connectivity in ALS: A resting-state magnetoencephalography study. Neurology 90, 1418–1424.

Proudfoot, M., Rohenkohl, G., Quinn, A., Colclough, G.L., Wuu, J., Talbot, K., Woolrich, M.W., Benatar, M., Nobre, A.C., Turner, M.R., 2017. Altered cortical beta-band oscillations reflect motor system degeneration in amyotrophic lateral sclerosis. Hum Brain Mapp 38, 237–254.

- Q -

Qamar, S., Wang, G., Randle, S.J., Ruggeri, F.S., Varela, J.A., Lin, J.Q., Phillips, E.C., Miyashita, A., Williams, D., Ströhl, F., Meadows, W., Ferry, R., Dardov, V.J., Tartaglia, G.G., Farrer, L.A., Kaminski Schierle, G.S., Kaminski, C.F., Holt, C.E., Fraser, P.E., Schmitt-Ulms, G., Klenerman, D., Knowles, T., Vendruscolo, M., St George-Hyslop, P., 2018. FUS Phase Separation Is Modulated by a Molecular Chaperone and Methylation of Arginine Cation-π Interactions. Cell 173, 720-734.

Qiu, H., Lee, S., Shang, Y., Wang, W.-Y., Au, K.F., Kamiya, S., Barmada, S.J., Finkbeiner, S., Lui, H., Carlton, C.E., Tang, A.A., Oldham, M.C., Wang, H., Shorter, J., Filiano, A.J., Roberson, E.D., Tourtellotte, W.G., Chen, B., Tsai, L.-H., Huang, E.J., 2014. ALS-associated mutation FUS-R521C causes DNA damage and RNA splicing defects. J Clin Invest 124, 981–999.

Quarta, E., Bravi, R., Scambi, I., Mariotti, R., Minciacchi, D., 2015. Increased anxiety-like behavior and selective learning impairments are concomitant to loss of hippocampal interneurons in the presymptomatic SOD1(G93A) ALS mouse model. Journal of Comparative Neurology 523, 1622–1638.

- R -

Radunovic, A., Annane, D., Rafiq, M.K., Brassington, R., Mustfa, N., 2017. Mechanical ventilation for amyotrophic lateral sclerosis/motor neuron disease. Cochrane Database Syst Rev 10, 4427.

Ramos-Miguel, A., Sawada, K., Jones, A.A., Thornton, A.E., Barr, A.M., Leurgans, S.E., Schneider, J.A., Bennett, D.A., Honer, W.G., 2017. Presynaptic proteins complexin-I and complexin-II differentially influence cognitive function in early and late stages of Alzheimer's disease. Acta Neuropathol 133, 395–407.

Ranganathan, R., Haque, S., Coley, K., Shepheard, S., Cooper-Knock, J., Kirby, J., 2020. Multifaceted Genes in Amyotrophic Lateral Sclerosis-Frontotemporal Dementia. Front Neurosci 14, 684.

Rao, Y., Lu, M., Ge, F., Marsh, D.J., Qian, S., Wang, A.H., Picciotto, M.R., Gao, X.-B., 2008. Regulation of Synaptic Efficacy in Hypocretin/Orexin-Containing Neurons by Melanin Concentrating Hormone in the Lateral Hypothalamus. J Neurosci 28, 9101–9110.

Rascovsky, K., Hodges, J.R., Knopman, D., Mendez, M.F., Kramer, J.H., Neuhaus, J., van Swieten, J.C., Seelaar, H., Dopper, E.G.P., Onyike, C.U., Hillis, A.E., Josephs, K.A., Boeve, B.F., Kertesz, A., Seeley, W.W., Rankin, K.P., Johnson, J.K., Gorno-Tempini, M.-L., Rosen, H., Prioleau-Latham, C.E., Lee, A., Kipps, C.M., Lillo, P., Piguet, O., Rohrer, J.D., Rossor, M.N., Warren, J.D., Fox, N.C., Galasko, D., Salmon, D.P., Black, S.E., Mesulam, M., Weintraub, S., Dickerson, B.C., Diehl-Schmid, J., Pasquier, F., Deramecourt, V., Lebert, F., Pijnenburg, Y., Chow, T.W., Manes, F., Grafman, J., Cappa, S.F., Freedman, M., Grossman, M., Miller, B.L., 2011. Sensitivity of revised diagnostic criteria for the behavioural variant of frontotemporal dementia. Brain 134, 2456–2477.

Rasmussen, H., Stordal, E., Rosness, T.A., 2018. Risk factors for frontotemporal dementia. Tidsskr Nor Laegeforen 138.

Reale, L.A., Dyer, M.S., Perry, S.E., Young, K.M., Dickson, T.C., Woodhouse, A., Blizzard, C.A., 2023. Pathologically mislocalised TDP-43 in upper motor neurons causes a die-forward spread of ALS-like pathogenic changes throughout the mouse corticomotor system. Prog Neurobiol 226, 102449.

Reber, S., Stettler, J., Filosa, G., Colombo, M., Jutzi, D., Lenzken, S.C., Schweingruber, C., Bruggmann, R., Bachi, A., Barabino, S.M., Mühlemann, O., Ruepp, M.-D., 2016. Minor intron splicing is regulated by FUS and affected by ALS-associated FUS mutants. EMBO J 35, 1504–1521.

Renton, A.E., Majounie, E., Waite, A., Simón-Sánchez, J., Rollinson, S., Gibbs, J.R., Schymick, J.C., Laaksovirta, H., van Swieten, J.C., Myllykangas, L., Kalimo, H., Paetau, A., Abramzon, Y., Remes, A.M., Kaganovich, A., Scholz, S.W., Duckworth, J., Ding, J., Harmer, D.W., Hernandez, D.G., Johnson, J.O., Mok, K., Ryten, M., Trabzuni, D.,

Guerreiro, R.J., Orrell, R.W., Neal, J., Murray, A., Pearson, J., Jansen, I.E., Sondervan, D., Seelaar, H., Blake, D., Young, K., Halliwell, N., Callister, J.B., Toulson, G., Richardson, A., Gerhard, A., Snowden, J., Mann, D., Neary, D., Nalls, M.A., Peuralinna, T., Jansson, L., Isoviita, V.-M., Kaivorinne, A.-L., Hölttä-Vuori, M., Ikonen, E., Sulkava, R., Benatar, M., Wuu, J., Chiò, A., Restagno, G., Borghero, G., Sabatelli, M., ITALSGEN Consortium, Heckerman, D., Rogaeva, E., Zinman, L., Rothstein, J.D., Sendtner, M., Drepper, C., Eichler, E.E., Alkan, C., Abdullaev, Z., Pack, S.D., Dutra, A., Pak, E., Hardy, J., Singleton, A., Williams, N.M., Heutink, P., Pickering-Brown, S., Morris, H.R., Tienari, P.J., Traynor, B.J., 2011. A hexanucleotide repeat expansion in C9ORF72 is the cause of chromosome 9p21-linked ALS-FTD. Neuron 72, 257–268.

Riva, N., Falini, A., Inuggi, A., Gonzalez-Rosa, J.J., Amadio, S., Cerri, F., Fazio, R., Del Carro, U., Comola, M., Comi, G., Leocani, L., 2012. Cortical activation to voluntary movement in amyotrophic lateral sclerosis is related to corticospinal damage: electrophysiological evidence. Clin Neurophysiol 123, 1586–1592.

Roche, J.C., Rojas-Garcia, R., Scott, K.M., Scotton, W., Ellis, C.E., Burman, R., Wijesekera, L., Turner, M.R., Leigh, P.N., Shaw, C.E., Al-Chalabi, A., 2012. A proposed staging system for amyotrophic lateral sclerosis. Brain 135, 847–852.

Rohrer, J.D., Guerreiro, R., Vandrovcova, J., Uphill, J., Reiman, D., Beck, J., Isaacs, A.M., Authier, A., Ferrari, R., Fox, N.C., Mackenzie, I.R.A., Warren, J.D., de Silva, R., Holton, J., Revesz, T., Hardy, J., Mead, S., Rossor, M.N., 2009. The heritability and genetics of frontotemporal lobar degeneration. Neurology 73, 1451–1456.

Rohrer, J.D., Woollacott, I.O.C., Dick, K.M., Brotherhood, E., Gordon, E., Fellows, A., Toombs, J., Druyeh, R., Cardoso, M.J., Ourselin, S., Nicholas, J.M., Norgren, N., Mead, S., Andreasson, U., Blennow, K., Schott, J.M., Fox, N.C., Warren, J.D., Zetterberg, H., 2016. Serum neurofilament light chain protein is a measure of disease intensity in frontotemporal dementia. Neurology 87, 1329–1336.

Rojas, J.C., Wang, P., Staffaroni, A.M., Heller, C., Cobigo, Y., Wolf, A., Goh, S.-Y.M., Ljubenkov, P.A., Heuer, H.W., Fong, J.C., Taylor, J.B., Veras, E., Song, L., Jeromin, A., Hanlon, D., Yu, L., Khinikar, A., Sivasankaran, R., Kieloch, A., Valentin, M.-A., Karydas, A.M., Mitic, L.L., Pearlman, R., Kornak, J., Kramer, J.H., Miller, B.L., Kantarci, K., Knopman, D.S., Graff-Radford, N., Petrucelli, L., Rademakers, R., Irwin, D.J., Grossman, M., Ramos, E.M., Coppola, G., Mendez, M.F., Bordelon, Y., Dickerson, B.C., Ghoshal, N., Huey, E.D., Mackenzie, I.R., Appleby, B.S., Domoto-Reilly, K., Hsiung, G.-Y.R., Toga, A.W., Weintraub, S., Kaufer, D.I., Kerwin, D., Litvan, I., Onyike, C.U., Pantelyat, A., Roberson, E.D., Tartaglia, M.C., Foroud, T., Chen, W., Czerkowicz, J., Graham, D.L., van Swieten, J.C., Borroni, B., Sanchez-Valle, R., Moreno, F., Laforce, R., Graff, C., Synofzik, M., Galimberti, D., Rowe, J.B., Masellis, M., Finger, E., Vandenberghe, R., de Mendonça, A., Tagliavini, F., Santana, I., Ducharme, S., Butler, C.R., Gerhard, A., Levin, J., Danek, A., Otto, M., Sorbi, S., Cash, D.M., Convery, R.S., Bocchetta, M., Foiani, M., Greaves, C.V., Peakman, G., Russell, L., Swift, I., Todd, E., Rohrer, J.D., Boeve, B.F., Rosen, H.J., Boxer, A.L., ALLFTD and GENFI consortia, 2021. Plasma Neurofilament Light for Prediction of Disease Progression in Familial Frontotemporal Lobar Degeneration. Neurology 96, 2296–2312.

Root, D.H., Zhang, S., Barker, D.J., Miranda-Barrientos, J., Liu, B., Wang, H.-L., Morales, M., 2018. Selective Brain Distribution and Distinctive Synaptic Architecture of Dual Glutamatergic-GABAergic Neurons. Cell Rep 23, 3465–3479.

Rosen, D.R., Siddique, T., Patterson, D., Figlewicz, D.A., Sapp, P., Hentati, A., Donaldson, D., Goto, J., O'Regan, J.P., Deng, H.X., 1993. Mutations in Cu/Zn superoxide dismutase gene are associated with familial amyotrophic lateral sclerosis. Nature 362, 59–62.

Rozycka, A., Liguz-Lecznar, M., 2017. The space where aging acts: focus on the GABAergic synapse. Aging Cell 16, 634–643.

Ryan, M., Heverin, M., McLaughlin, R.L., Hardiman, O., 2019. Lifetime Risk and Heritability of Amyotrophic Lateral Sclerosis. JAMA Neurol 76, 1367–1374.

- S -

Sagné, C., El Mestikawy, S., Isambert, M.F., Hamon, M., Henry, J.P., Giros, B., Gasnier, B., 1997. Cloning of a functional vesicular GABA and glycine transporter by screening of genome databases. FEBS Lett 417, 177–183.

Sagner, A., Briscoe, J., 2019. Establishing neuronal diversity in the spinal cord: a time and a place. Development 146, 182154.

Sahadevan, S., Hembach, K.M., Tantardini, E., Pérez-Berlanga, M., Hruska-Plochan, M., Megat, S., Weber, J., Schwarz, P., Dupuis, L., Robinson, M.D., De Rossi, P., Polymenidou, M., 2021. Synaptic FUS accumulation triggers early misregulation of synaptic RNAs in a mouse model of ALS. Nat Commun 12, 3027.

Saint, M., Alakbarzade, V., McLean, B., 2021. Frontotemporal Dementia with Parkinsonism and Epilepsy Associated with VGKC Antibodies: Case Report and Literature Review. Case Rep Neurol 13, 205–210.

Saito, K., Kakizaki, T., Hayashi, R., Nishimaru, H., Furukawa, T., Nakazato, Y., Takamori, S., Ebihara, S., Uematsu, M., Mishina, M., Miyazaki, J., Yokoyama, M., Konishi, S., Inoue, K., Fukuda, A., Fukumoto, M., Nakamura, K., Obata, K., Yanagawa, Y., 2010. The physiological roles of vesicular GABA transporter during embryonic development: a study using knockout mice. Mol Brain 3, 40.

Sakakibara, H., Suzuki, A., Kobayashi, A., Motoyama, K., Matsui, A., Sayama, K., Kato, A., Ohashi, N., Akimoto, M., Nakayama, T., Shimoi, K., 2012. Social isolation stress induces hepatic hypertrophy in C57BL/6J mice. J Toxicol Sci 37, 1071–1076.

Salamatina, A., Yang, J.H., Brenner-Morton, S., Bikoff, J.B., Fang, L., Kintner, C.R., Jessell, T.M., Sweeney, L.B., 2020. Differential Loss of Spinal Interneurons in a Mouse Model of ALS. Neuroscience, A commemoration of Thomas M. Jessell's Contributions to Neuroscience 450, 81–95.

Sanches, C., Stengel, C., Godard, J., Mertz, J., Teichmann, M., Migliaccio, R., Valero-Cabré, A., 2020. Past, Present, and Future of Non-invasive Brain Stimulation Approaches to Treat Cognitive Impairment in Neurodegenerative Diseases: Time for a Comprehensive Critical Review. Front Aging Neurosci 12, 578339.

Sangari, S., Peyre, I., Lackmy-Vallée, A., Bayen, E., Pradat, P.-F., Marchand-Pauvert, V., 2022. Transient increase in recurrent inhibition in amyotrophic lateral sclerosis as a putative protection from neurodegeneration. Acta Physiol 234, 13758.

Sanjuan-Ruiz, I., Govea-Perez, N., McAlonis-Downes, M., Dieterle, S., Megat, S., Dirrig-Grosch, S., Picchiarelli, G., Piol, D., Zhu, Q., Myers, B., Lee, C.-Z., Cleveland, D.W., Lagier-Tourenne, C., Da Cruz, S., Dupuis, L., 2021. Wild-type FUS corrects ALS-like disease induced by cytoplasmic mutant FUS through autoregulation. Mol Neurodegener 16, 61.

Sasayama, H., Shimamura, M., Tokuda, T., Azuma, Y., Yoshida, T., Mizuno, T., Nakagawa, M., Fujikake, N., Nagai, Y., Yamaguchi, M., 2012. Knockdown of the Drosophila fused in sarcoma (FUS) homologue causes deficient locomotive behavior and shortening of motoneuron terminal branches. PLoS One 7, 39483.

Scarioni, M., Gami-Patel, P., Timar, Y., Seelaar, H., van Swieten, J.C., Rozemuller, A.J.M., Dols, A., Scarpini, E., Galimberti, D., Netherlands Brain Bank, Hoozemans, J.J.M., Pijnenburg, Y.A.L., Dijkstra, A.A., 2020. Frontotemporal Dementia: Correlations Between Psychiatric Symptoms and Pathology. Ann Neurol 87, 950–961.

Scattoni, M.L., Crawley, J., Ricceri, L., 2009. Ultrasonic vocalizations: a tool for behavioural phenotyping of mouse models of neurodevelopmental disorders. Neurosci Biobehav Rev 33, 508–515.

Scekic-Zahirovic, J., Oussini, H.E., Mersmann, S., Drenner, K., Wagner, M., Sun, Y., Allmeroth, K., Dieterlé, S., Sinniger, J., Dirrig-Grosch, S., René, F., Dormann, D., Haass, C., Ludolph, A.C., Lagier-Tourenne, C., Storkebaum, E., Dupuis, L., 2017. Motor neuron intrinsic and extrinsic mechanisms contribute to the pathogenesis of FUS-associated amyotrophic lateral sclerosis. Acta Neuropathol 133, 887–906.

Scekic-Zahirovic, J., Sanjuan-Ruiz, I., Kan, V., Megat, S., De Rossi, P., Dieterlé, S., Cassel, R., Jamet, M., Kessler, P., Wiesner, D., Tzeplaeff, L., Demais, V., Sahadevan, S., Hembach, K.M., Muller, H.-P., Picchiarelli, G., Mishra, N., Antonucci, S., Dirrig-Grosch, S., Kassubek, J., Rasche, V., Ludolph, A., Boutillier, A.-L., Roselli, F., Polymenidou, M., Lagier-Tourenne, C., Liebscher, S., Dupuis, L., 2021. Cytoplasmic FUS triggers early behavioral alterations linked to cortical neuronal hyperactivity and inhibitory synaptic defects. Nat Commun 12, 3028.

Scekic-Zahirovic, J., Sendscheid, O., El Oussini, H., Jambeau, M., Sun, Y., Mersmann, S., Wagner, M., Dieterlé, S., Sinniger, J., Dirrig-Grosch, S., Drenner, K., Birling, M.-C., Qiu, J., Zhou, Y., Li, H., Fu, X.-D., Rouaux, C., Shelkovnikova, T., Witting, A., Ludolph, A.C., Kiefer, F., Storkebaum, E., Lagier-Tourenne, C., Dupuis, L., 2016. Toxic gain of function from mutant FUS protein is crucial to trigger cell autonomous motor neuron loss. EMBO J 35, 1077–1097.

Schaal, B., Al Aïn, S., Patris, B., 2013. Testing smell when it is really vital: behavioral assays of social odors in the neonatal mouse. Methods Mol Biol 1068, 349–371.

Schijven, D., Stevelink, R., McCormack, M., van Rheenen, W., Luykx, J.J., Koeleman, B.P.C., Veldink, J.H., Project MinE ALS GWAS Consortium, International League Against Epilepsy Consortium on Complex Epilepsies, 2020. Analysis of shared common genetic risk between amyotrophic lateral sclerosis and epilepsy. Neurobiol Aging 92, 153.

Schoen, M., Reichel, J.M., Demestre, M., Putz, S., Deshpande, D., Proepper, C., Liebau, S., Schmeisser, M.J., Ludolph, A.C., Michaelis, J., Boeckers, T.M., 2015. Super-Resolution Microscopy Reveals Presynaptic Localization of the ALS/FTD Related Protein FUS in Hippocampal Neurons. Front Cell Neurosci 9, 496.

Seelaar, H., Klijnsma, K.Y., de Koning, I., van der Lugt, A., Chiu, W.Z., Azmani, A., Rozemuller, A.J.M., van Swieten, J.C., 2010. Frequency of ubiquitin and FUS-positive, TDP-43-negative frontotemporal lobar degeneration. J Neurol 257, 747–753.

Seeley, W.W., Merkle, F.T., Gaus, S.E., Craig, A.D.B., Allman, J.M., Hof, P.R., 2012. Distinctive neurons of the anterior cingulate and frontoinsular cortex: a historical perspective. Cereb Cortex 22, 245–250.

Sellier, C., Corcia, P., Vourc'h, P., Dupuis, L., 2024. C9ORF72 hexanucleotide repeat expansion: From ALS and FTD to a broader pathogenic role? Rev Neurol 180, 417–428.

Sephton, C.F., Tang, A.A., Kulkarni, A., West, J., Brooks, M., Stubblefield, J.J., Liu, Y., Zhang, M.Q., Green, C.B., Huber, K.M., Huang, E.J., Herz, J., Yu, G., 2014. Activity-dependent FUS dysregulation disrupts synaptic homeostasis. Proceedings of the National Academy of Sciences 111, 4769–4778.

Sévigny, M., Bourdeau Julien, I., Venkatasubramani, J.P., Hui, J.B., Dutchak, P.A., Sephton, C.F., 2020. FUS contributes to mTOR-dependent inhibition of translation. J Biol Chem 295, 18459–18473.

Sgobio, C., Trabalza, A., Spalloni, A., Zona, C., Carunchio, I., Longone, P., Ammassari-Teule, M., 2008. Abnormal medial prefrontal cortex connectivity and defective fear extinction in the presymptomatic G93A SOD1 mouse model of ALS. Genes Brain Behav 7, 427–434.

Shahim, P., Norato, G., Sinaii, N., Zetterberg, H., Blennow, K., Chan, L., Grunseich, C., 2024. Neurofilaments in Sporadic and Familial Amyotrophic Lateral Sclerosis: A Systematic Review and Meta-Analysis. Genes 15, 496.

Shibuya, K., Park, S.B., Geevasinga, N., Menon, P., Howells, J., Simon, N.G., Huynh, W., Noto, Y.-I., Götz, J., Kril, J.J., Ittner, L.M., Hodges, J., Halliday, G., Vucic, S., Kiernan, M.C., 2016. Motor cortical function determines prognosis in sporadic ALS. Neurology 87, 513–520.

Shibuya, K., Simon, N.G., Geevasinga, N., Menon, P., Howells, J., Park, S.B., Huynh, W., Noto, Y.-I., Vucic, S., Kiernan, M.C., 2017. The evolution of motor cortical dysfunction in amyotrophic lateral sclerosis. Clin Neurophysiol 128, 1075–1082.

Shimizu, T., Nakayama, Y., Matsuda, C., Haraguchi, M., Bokuda, K., Ishikawa-Takata, K., Kawata, A., Isozaki, E., 2019. Prognostic significance of body weight variation after diagnosis in ALS: a single-centre prospective cohort study. J Neurol 266, 1412–1420.

Shimizu-Okabe, C., Kobayashi, S., Kim, J., Kosaka, Y., Sunagawa, M., Okabe, A., Takayama, C., 2022. Developmental Formation of the GABAergic and Glycinergic Networks in the Mouse Spinal Cord. Int J Mol Sci 23, 834.

Shimojo, M., Takuwa, H., Takado, Y., Tokunaga, M., Tsukamoto, S., Minatohara, K., Ono, M., Seki, C., Maeda, J., Urushihata, T., Minamihisamatsu, T., Aoki, I., Kawamura, K., Zhang, M.-R., Suhara, T., Sahara, N., Higuchi, M., 2020. Selective Disruption of Inhibitory Synapses Leading to Neuronal Hyperexcitability at an Early Stage of Tau Pathogenesis in a Mouse Model. J Neurosci 40, 3491–3501.

Shoji, H., Miyakawa, T., 2019. Age-related behavioral changes from young to old age in male mice of a C57BL/6J strain maintained under a genetic stability program. Neuropsychopharmacol Rep 39, 100–118.

Sieghart, W., Sperk, G., 2002. Subunit composition, distribution and function of GABA(A) receptor subtypes. Curr Top Med Chem 2, 795–816.

Silberberg, G., Markram, H., 2007. Disynaptic inhibition between neocortical pyramidal cells mediated by Martinotti cells. Neuron 53, 735–746.

Silbereis, J.C., Pochareddy, S., Zhu, Y., Li, M., Sestan, N., 2016. The Cellular and Molecular Landscapes of the Developing Human Central Nervous System. Neuron 89, 248–268.

Silva, J.C., Vivash, L., Malpas, C.B., Hao, Y., McLean, C., Chen, Z., O'Brien, T.J., Jones, N.C., Kwan, P., 2021. Low prevalence of amyloid and tau pathology in drug-resistant temporal lobe epilepsy. Epilepsia 62, 3058–3067.

Silverman, J.L., Yang, M., Lord, C., Crawley, J.N., 2010. Behavioural phenotyping assays for mouse models of autism. Nat Rev Neurosci 11, 490–502.

Simmons, D.H., Titley, H.K., Hansel, C., Mason, P., 2021. Behavioral Tests for Mouse Models of Autism: An Argument for the Inclusion of Cerebellum-Controlled Motor Behaviors. Neuroscience 462, 303–319.

Simon, H.H., Saueressig, H., Wurst, W., Goulding, M.D., O'Leary, D.D., 2001. Fate of midbrain dopaminergic neurons controlled by the engrailed genes. J Neurosci 21, 3126–3134.

Simon, M.M., Greenaway, S., White, J.K., Fuchs, H., Gailus-Durner, V., Wells, S., Sorg, T., Wong, K., Bedu, E., Cartwright, E.J., Dacquin, R., Djebali, S., Estabel, J., Graw, J., Ingham, N.J., Jackson, I.J., Lengeling, A., Mandillo, S., Marvel, J., Meziane, H., Preitner, F., Puk, O., Roux, M., Adams, D.J., Atkins, S., Ayadi, A., Becker, L., Blake, A., Brooker, D., Cater, H., Champy, M.-F., Combe, R., Danecek, P., di Fenza, A., Gates, H., Gerdin, A.-K., Golini, E., Hancock, J.M., Hans, W., Hölter, S.M., Hough, T., Jurdic, P., Keane, T.M., Morgan, H., Müller, W., Neff, F., Nicholson, G., Pasche, B., Roberson, L.-A., Rozman, J., Sanderson, M., Santos, L., Selloum, M., Shannon, C., Southwell, A., Tocchini-Valentini, G.P., Vancollie, V.E., Westerberg, H., Wurst, W., Zi, M., Yalcin, B., Ramirez-Solis, R., Steel, K.P., Mallon, A.-M., de Angelis, M.H., Herault, Y., Brown, S.D.M., 2013. A comparative phenotypic and genomic analysis of C57BL/6J and C57BL/6N mouse strains. Genome Biol 14, 82.

Škarabot, J., Mesquita, R.N.O., Brownstein, C.G., Ansdell, P., 2019. Myths and Methodologies: How loud is the story told by the transcranial magnetic stimulation-evoked silent period? Exp Physiol 104, 635–642.

Skillbäck, T., Mattsson, N., Blennow, K., Zetterberg, H., 2017. Cerebrospinal fluid neurofilament light concentration in motor neuron disease and frontotemporal dementia predicts survival. Amyotroph Lateral Scler Frontotemporal Degener 18, 397–403.

Small, L., Gong, H., Yassmin, C., Cooney, G.J., Brandon, A.E., 2018. Thermoneutral housing does not influence fat mass or glucose homeostasis in C57BL/6 mice. J Endocrinol 239, 313–324.

Smittkamp, S.E., Brown, J.W., Stanford, J.A., 2008. Time-course and characterization of orolingual motor deficits in B6SJL-Tg(SOD1-G93A)1Gur/J mice. Neuroscience 151, 613–621.

Snowden, J.S., Adams, J., Harris, J., Thompson, J.C., Rollinson, S., Richardson, A., Jones, M., Neary, D., Mann, D.M., Pickering-Brown, S., 2015. Distinct clinical and pathological phenotypes in frontotemporal dementia associated with MAPT, PGRN and C9orf72 mutations. Amyotroph Lateral Scler Frontotemporal Degener 16, 497–505.

Snowden, J.S., Hu, Q., Rollinson, S., Halliwell, N., Robinson, A., Davidson, Y.S., Momeni, P., Baborie, A., Griffiths, T.D., Jaros, E., Perry, R.H., Richardson, A., Pickering-Brown, S.M., Neary, D., Mann, D.M.A., 2011. The most common type of FTLD-FUS (aFTLD-U) is associated with a distinct clinical form of frontotemporal dementia but is not related to mutations in the FUS gene. Acta Neuropathol 122, 99–110.

Sohal, V.S., Zhang, F., Yizhar, O., Deisseroth, K., 2009. Parvalbumin neurons and gamma rhythms enhance cortical circuit performance. Nature 459, 698–702.

Soler, H., Dorca-Arévalo, J., González, M., Rubio, S.E., Ávila, J., Soriano, E., Pascual, M., 2017. The GABAergic septohippocampal connection is impaired in a mouse model of tauopathy. Neurobiol Aging 49, 40–51.

Southwell, D.G., Paredes, M.F., Galvao, R.P., Jones, D.L., Froemke, R.C., Sebe, J.Y., Alfaro-Cervello, C., Tang, Y., Garcia-Verdugo, J.M., Rubenstein, J.L., Baraban, S.C., Alvarez-Buylla, A., 2012. Intrinsically determined cell death of developing cortical interneurons. Nature 491, 109–113.

Specht, C.G., Izeddin, I., Rodriguez, P.C., El Beheiry, M., Rostaing, P., Darzacq, X., Dahan, M., Triller, A., 2013. Quantitative nanoscopy of inhibitory synapses: counting gephyrin molecules and receptor binding sites. Neuron 79, 308–321.

Sperfeld, A.D., Collatz, M.B., Baier, H., Palmbach, M., Storch, A., Schwarz, J., Tatsch, K., Reske, S., Joosse, M., Heutink, P., Ludolph, A.C., 1999. FTDP-17: an early-onset phenotype with parkinsonism and epileptic seizures caused by a novel mutation. Ann Neurol 46, 708–715.

Sreedharan, J., Blair, I.P., Tripathi, V.B., Hu, X., Vance, C., Rogelj, B., Ackerley, S., Durnall, J.C., Williams, K.L., Buratti, E., Baralle, F., de Belleroche, J., Mitchell, J.D., Leigh, P.N., Al-Chalabi, A., Miller, C.C., Nicholson, G., Shaw, C.E., 2008. TDP-43 mutations in familial and sporadic amyotrophic lateral sclerosis. Science 319, 1668–1672.

Stark, E., Eichler, R., Roux, L., Fujisawa, S., Rotstein, H.G., Buzsáki, G., 2013. Inhibition-induced theta resonance in cortical circuits. Neuron 80, 1263–1276.

Stein, V., Hermans-Borgmeyer, I., Jentsch, T.J., Hübner, C.A., 2004. Expression of the KCl cotransporter KCC2 parallels neuronal maturation and the emergence of low intracellular chloride. J Comp Neurol 468, 57–64.

Stephens, B., Guiloff, R.J., Navarrete, R., Newman, P., Nikhar, N., Lewis, P., 2006. Widespread loss of neuronal populations in the spinal ventral horn in sporadic motor neuron disease. A morphometric study. J Neurol Sci 244, 41–58.

Stessman, H.A.F., Willemsen, M.H., Fenckova, M., Penn, O., Hoischen, A., Xiong, B., Wang, T., Hoekzema, K., Vives, L., Vogel, I., Brunner, H.G., van der Burgt, I., Ockeloen, C.W., Schuurs-Hoeijmakers, J.H., Klein Wassink-Ruiter, J.S., Stumpel, C., Stevens, S.J.C., Vles, H.S., Marcelis, C.M., van Bokhoven, H., Cantagrel, V., Colleaux, L., Nicouleau, M., Lyonnet, S., Bernier, R.A., Gerdts, J., Coe, B.P., Romano, C., Alberti, A., Grillo, L., Scuderi, C., Nordenskjöld, M., Kvarnung, M., Guo, H., Xia, K., Piton, A., Gerard, B., Genevieve, D., Delobel, B., Lehalle, D., Perrin, L., Prieur, F., Thevenon, J., Gecz, J., Shaw, M., Pfundt, R., Keren, B., Jacquette, A., Schenck, A., Eichler, E.E., Kleefstra, T., 2016. Disruption of POGZ Is Associated with Intellectual Disability and Autism Spectrum Disorders. Am J Hum Genet 98, 541–552.

Straub, J., Gawda, A., Ravichandran, P., McGrew, B., Nylund, E., Kang, J., Burke, C., Vitko, I., Scott, M., Williamson, J., Joshi, S., Kapur, J., Perez-Reyes, E., 2020. Characterization of kindled VGAT-Cre mice as a new animal model of temporal lobe epilepsy. Epilepsia 61, 2277–2288.

Su, F.-C., Goutman, S.A., Chernyak, S., Mukherjee, B., Callaghan, B.C., Batterman, S., Feldman, E.L., 2016. Association of Environmental Toxins With Amyotrophic Lateral Sclerosis. JAMA Neurol 73, 803–811.

Suárez-Calvet, M., Neumann, M., Arzberger, T., Abou-Ajram, C., Funk, E., Hartmann, H., Edbauer, D., Kremmer, E., Göbl, C., Resch, M., Bourgeois, B., Madl, T., Reber, S., Jutzi, D., Ruepp, M.-D., Mackenzie, I.R.A., Ansorge, O., Dormann, D., Haass, C., 2016. Monomethylated and unmethylated FUS exhibit increased binding to Transportin and distinguish FTLD-FUS from ALS-FUS. Acta Neuropathol 131, 587–604.

Sukhanova, M.V., Singatulina, A.S., Pastré, D., Lavrik, O.I., 2020. Fused in Sarcoma (FUS) in DNA Repair: Tango with Poly(ADP-ribose) Polymerase 1 and Compartmentalisation of Damaged DNA. Int J Mol Sci 21, 7020.

Suliman-Lavie, R., Title, B., Cohen, Y., Hamada, N., Tal, M., Tal, N., Monderer-Rothkoff, G., Gudmundsdottir, B., Gudmundsson, K.O., Keller, J.R., Huang, G.-J., Nagata, K.-I., Yarom, Y., Shifman, S., 2020. Pogz deficiency leads to transcription dysregulation and impaired cerebellar activity underlying autism-like behavior in mice. Nat Commun 11, 5836.

Sun, M., Choi, E.Y., Magee, D.J., Stets, C.W., During, M.J., Lin, E.-J.D., 2014. Metabolic Effects of Social Isolation in Adult C57BL/6 Mice. Int Sch Res Notices 2014, 690950.

Sun, S., Ling, S.-C., Qiu, J., Albuquerque, C.P., Zhou, Y., Tokunaga, S., Li, H., Qiu, H., Bui, A., Yeo, G.W., Huang, E.J., Eggan, K., Zhou, H., Fu, X.-D., Lagier-Tourenne, C., Cleveland, D.W., 2015. ALS-causative mutations in FUS/TLS confer gain and loss of function by altered association with SMN and U1-snRNP. Nat Commun 6, 6171.

Sun, X., Zhao, X., Liu, Q., Liu, S., Zhang, K., Wang, Z.-L., Yang, X., Shang, L., Huang, Y., Cui, L., Zhang, X., 2020. Study on sleep-wake disorders in patients with genetic and non-genetic amyotrophic lateral sclerosis. J Neurol Neurosurg Psychiatry jnnp-2020-324544.

Sunagawa, M., Shimizu-Okabe, C., Kim, J., Kobayashi, S., Kosaka, Y., Yanagawa, Y., Matsushita, M., Okabe, A., Takayama, C., 2017. Distinct development of the glycinergic terminals in the ventral and dorsal horns of the mouse cervical spinal cord. Neuroscience 343, 459–471.

Sweeney, L.B., Bikoff, J.B., Gabitto, M.I., Brenner-Morton, S., Baek, M., Yang, J.H., Tabak, E.G., Dasen, J.S., Kintner, C.R., Jessell, T.M., 2018. Origin and Segmental Diversity of Spinal Inhibitory Interneurons. Neuron 97, 341-355.

- T -

Tai, X.Y., Koepp, M., Duncan, J.S., Fox, N., Thompson, P., Baxendale, S., Liu, J.Y.W., Reeves, C., Michalak, Z., Thom, M., 2016. Hyperphosphorylated tau in patients with refractory epilepsy correlates with cognitive decline: a study of temporal lobe resections. Brain 139, 2441–2455.

Takeshita, H., Yamamoto, K., Nozato, S., Inagaki, T., Tsuchimochi, H., Shirai, M., Yamamoto, R., Imaizumi, Y., Hongyo, K., Yokoyama, S., Takeda, M., Oguro, R., Takami, Y., Itoh, N., Takeya, Y., Sugimoto, K., Fukada, S.-I., Rakugi, H., 2017. Modified forelimb grip strength test detects aging-associated physiological decline in skeletal muscle function in male mice. Sci Rep 7, 42323.

Tamamaki, N., Tomioka, R., 2010. Long-Range GABAergic Connections Distributed throughout the Neocortex and their Possible Function. Front Neurosci 4, 202.

Tang, B.L., 2019. Amyloid Precursor Protein (APP) and GABAergic Neurotransmission. Cells 8, 550.

Taniguchi, H., He, M., Wu, P., Kim, S., Paik, R., Sugino, K., Kvitsani, D., Fu, Y., Lu, J., Lin, Y., Miyoshi, G., Shima, Y., Fishell, G., Nelson, S.B., Huang, Z.J., 2011. A Resource of Cre Driver Lines for Genetic Targeting of GABAergic Neurons in Cerebral Cortex. Neuron 71, 995–1013.

Tasic, B., Menon, V., Nguyen, T.N., Kim, T.K., Jarsky, T., Yao, Z., Levi, B., Gray, L.T., Sorensen, S.A., Dolbeare, T., Bertagnolli, D., Goldy, J., Shapovalova, N., Parry, S., Lee, C., Smith, K., Bernard, A., Madisen, L., Sunkin, S.M.,

Hawrylycz, M., Koch, C., Zeng, H., 2016a. Adult mouse cortical cell taxonomy revealed by single cell transcriptomics. Nat Neurosci 19, 335–346.

Theunissen, F., Flynn, L.L., Anderton, R.S., Mastaglia, F., Pytte, J., Jiang, L., Hodgetts, S., Burns, D.K., Saunders, A., Fletcher, S., Wilton, S.D., Akkari, P.A., 2020. Structural Variants May Be a Source of Missing Heritability in sALS. Front Neurosci 14, 47.

Thomas, A., Burant, A., Bui, N., Graham, D., Yuva-Paylor, L.A., Paylor, R., 2009. Marble burying reflects a repetitive and perseverative behavior more than novelty-induced anxiety. Psychopharmacology 204, 361–373.

Tibshirani, M., Tradewell, M.L., Mattina, K.R., Minotti, S., Yang, W., Zhou, H., Strong, M.J., Hayward, L.J., Durham, H.D., 2015. Cytoplasmic sequestration of FUS/TLS associated with ALS alters histone marks through loss of nuclear protein arginine methyltransferase 1. Human Molecular Genetics 24, 773–786.

Tomioka, R., Sakimura, K., Yanagawa, Y., 2015. Corticofugal GABAergic projection neurons in the mouse frontal cortex. Front Neuroanat 9, 133.

Tradewell, M.L., Yu, Z., Tibshirani, M., Boulanger, M.-C., Durham, H.D., Richard, S., 2012. Arginine methylation by PRMT1 regulates nuclear-cytoplasmic localization and toxicity of FUS/TLS harbouring ALS-linked mutations. Hum Mol Genet 21, 136–149.

Tremblay, R., Lee, S., Rudy, B., 2016. GABAergic Interneurons in the Neocortex: From Cellular Properties to Circuits. Neuron 91, 260–292.

Tritsch, N.X., Ding, J.B., Sabatini, B.L., 2012. Dopaminergic neurons inhibit striatal output through non-canonical release of GABA. Nature 490, 262–266.

Trubshaw, M., Gohil, C., Yoganathan, K., Kohl, O., Edmond, E., Proudfoot, M., Thompson, A.G., Talbot, K., Stagg, C.J., Nobre, A.C., Woolrich, M., Turner, M.R., 2024. The cortical neurophysiological signature of amyotrophic lateral sclerosis. Brain Commun 6, 64.

Trucco, A.P., Backhouse, T., Mioshi, E., 2024. Describing and assessing behavioural symptoms in amyotrophic lateral sclerosis with and without frontotemporal dementia: a scoping review. Curr Opin Neurol.

Tsai, R.M., Boxer, A.L., 2016. Therapy and clinical trials in frontotemporal dementia: past, present, and future. J Neurochem 138 Suppl 1, 211–221.

Tsuiji, H., Iguchi, Y., Furuya, A., Kataoka, A., Hatsuta, H., Atsuta, N., Tanaka, F., Hashizume, Y., Akatsu, H., Murayama, S., Sobue, G., Yamanaka, K., 2013. Spliceosome integrity is defective in the motor neuron diseases ALS and SMA. EMBO Mol Med 5, 221–234.

Tsuiji, H., Inoue, I., Takeuchi, M., Furuya, A., Yamakage, Y., Watanabe, S., Koike, M., Hattori, M., Yamanaka, K., 2017. TDP-43 accelerates age-dependent degeneration of interneurons. Sci Rep 7, 14972.

Tuncdemir, S.N., Wamsley, B., Stam, F.J., Osakada, F., Goulding, M., Callaway, E.M., Rudy, B., Fishell, G., 2016. Early Somatostatin Interneuron Connectivity Mediates the Maturation of Deep Layer Cortical Circuits. Neuron 89, 521–535.

Turner, M., Hammers, A., Al-Chalabi, A., Shaw, C.E., Andersen, P.M., Brooks, D.J., Leigh, P.N., 2005a. Distinct cerebral lesions in sporadic and “D90A” SOD1 ALS: studies with [11C]flumazenil PET. Brain 128, 1323–1329.

Turner, M., Osei-Lah, A., Hammers, A., Al-Chalabi, A., Shaw, C., Andersen, P., Brooks, D., Leigh, P., Mills, K., 2005b. Abnormal cortical excitability in sporadic but not homozygous D90A SOD1 ALS. J Neurol Neurosurg Psychiatry 76, 1279–1285.

Tyzack, G.E., Luisier, R., Taha, D.M., Neeves, J., Modic, M., Mitchell, J.S., Meyer, I., Greensmith, L., Newcombe, J., Ule, J., Luscombe, N.M., Patani, R., 2019. Widespread FUS mislocalization is a molecular hallmark of amyotrophic lateral sclerosis. Brain 142, 2572–2580.

Tzeplaeff, L., Wilfling, S., Requardt, M.V., Herdick, M., 2023. Current State and Future Directions in the Therapy of ALS. Cells 12, 1523.

- U -

Udagawa, T., Fujioka, Y., Tanaka, M., Honda, D., Yokoi, S., Riku, Y., Ibi, D., Nagai, T., Yamada, K., Watanabe, H., Katsuno, M., Inada, T., Ohno, K., Sokabe, M., Okado, H., Ishigaki, S., Sobue, G., 2015. FUS regulates AMPA receptor function and FTLD/ALS-associated behaviour via GluA1 mRNA stabilization. Nat Commun 6, 7098.

Uhlhaas, P.J., Roux, F., Rodriguez, E., Rotarska-Jagiela, A., Singer, W., 2010. Neural synchrony and the development of cortical networks. Trends Cogn Sci 14, 72–80.

Urwin, H., Josephs, K.A., Rohrer, J.D., Mackenzie, I.R., Neumann, M., Authier, A., Seelaar, H., Van Swieten, J.C., Brown, J.M., Johannsen, P., Nielsen, J.E., Holm, I.E., FReJA Consortium, Dickson, D.W., Rademakers, R., Graff-Radford, N.R., Parisi, J.E., Petersen, R.C., Hatanpaa, K.J., White, C.L., Weiner, M.F., Geser, F., Van Deerlin, V.M., Trojanowski, J.Q., Miller, B.L., Seeley, W.W., van der Zee, J., Kumar-Singh, S., Engelborghs, S., De Deyn, P.P., Van Broeckhoven, C., Bigio, E.H., Deng, H.-X., Halliday, G.M., Kril, J.J., Munoz, D.G., Mann, D.M., Pickering-Brown, S.M., Doodeman, V., Adamson, G., Ghazi-Noori, S., Fisher, E.M.C., Holton, J.L., Revesz, T., Rossor, M.N., Collinge, J., Mead, S., Isaacs, A.M., 2010. FUS pathology defines the majority of tau- and TDP-43-negative frontotemporal lobar degeneration. Acta Neuropathol 120, 33–41.

- V -

Valls-Carbó, A., Gajate, V., Romeral, M., Gutiérrez-Viedma, Á., Parejo-Carbonell, B., Cabrera-Martín, M.N., Matías-Guiu, J., Matías-Guiu, J.A., García-Morales, I., 2020. Non-Convulsive Status Epilepticus in Behavioral Variant Frontotemporal Dementia. J Alzheimers Dis 77, 985–991.

van den Ameele, J., Jedlickova, I., Pristoupilova, A., Sieben, A., Van Mossevelde, S., Ceuterick-de Groote, C., Hůlková, H., Matej, R., Meurs, A., Van Broeckhoven, C., Berkovic, S.F., Santens, P., Kmoch, S., Dermaut, B., 2018. Teenage-onset progressive myoclonic epilepsy due to a familial C9orf72 repeat expansion. Neurology 90, 658–663.

Van den Bos, M.A.J., Higashihara, M., Geevasinga, N., Menon, P., Kiernan, M.C., Vucic, S., 2018. Imbalance of cortical facilitatory and inhibitory circuits underlies hyperexcitability in ALS. Neurology 91, 1669–1676.

Vance, C., Rogelj, B., Hortobagyi, T., De Vos, K.J., Nishimura, A.L., Sreedharan, J., Hu, X., Smith, B., Ruddy, D., Wright, P., Ganesalingam, J., Williams, K.L., Tripathi, V., Al-Saraj, S., Al-Chalabi, A., Leigh, P.N., Blair, I.P., Nicholson, G., de Belleroche, J., Gallo, J.-M., Miller, C.C., Shaw, C.E., 2009. Mutations in FUS, an RNA Processing Protein, Cause Familial Amyotrophic Lateral Sclerosis Type 6. Science 323, 1208–1211.

Venkatesan, K., Alix, P., Marquet, A., Doupagne, M., Niespodziany, I., Rogister, B., Seutin, V., 2012. Altered balance between excitatory and inhibitory inputs onto CA1 pyramidal neurons from SV2A-deficient but not SV2B-deficient mice. J Neurosci Res 90, 2317–2327.

Venner, A., Anaclet, C., Broadhurst, R.Y., Saper, C.B., Fuller, P.M., 2016. A Novel Population of Wake-Promoting GABAergic Neurons in the Ventral Lateral Hypothalamus. Curr Biol 26, 2137–2143.

Venugopal, S., Ghulam-Jelani, Z., Ahn, I.S., Yang, X., Wiedau, M., Simmons, D., Chandler, S.H., 2023. Early deficits in GABA inhibition parallels an increase in L-type Ca2+ currents in the jaw motor neurons of SOD1G93A mouse model for ALS. Neurobiology of Disease 177, 105992.

Vernay, A., Sellal, F., René, F., 2016. Evaluating Behavior in Mouse Models of the Behavioral Variant of Frontotemporal Dementia: Which Test for Which Symptom? Neurodegener Dis 16, 127–139.

Vignaud, P., Mondino, M., Poulet, E., Palm, U., Brunelin, J., 2018. Duration but not intensity influences transcranial direct current stimulation (tDCS) after-effects on cortical excitability. Neurophysiol Clin 48, 89–92.

Vöglein, J., Kostova, I., Arzberger, T., Noachtar, S., Dieterich, M., Herms, J., Schmitz, P., Ruf, V., Windl, O., Roeber, S., Simons, M., Höglinger, G.U., Danek, A., Giese, A., Levin, J., 2022. Seizure prevalence in neurodegenerative diseases-a study of autopsy proven cases. Eur J Neurol 29, 12–18.

Vong, L., Ye, C., Yang, Z., Choi, B., Chua, S., Lowell, B.B., 2011. Leptin action on GABAergic neurons prevents obesity and reduces inhibitory tone to POMC neurons. Neuron 71, 142–154.

Vucic, S., Kiernan, M.C., 2017. Transcranial Magnetic Stimulation for the Assessment of Neurodegenerative Disease. Neurotherapeutics 14, 91–106.

Vucic, S., Kiernan, M.C., 2006. Novel threshold tracking techniques suggest that cortical hyperexcitability is an early feature of motor neuron disease. Brain 129, 2436–2446.

Vucic, S., Lin, C.S.-Y., Cheah, B.C., Murray, J., Menon, P., Krishnan, A.V., Kiernan, M.C., 2013. Riluzole exerts central and peripheral modulating effects in amyotrophic lateral sclerosis. Brain 136, 1361–1370.

Vucic, S., Nicholson, G.A., Kiernan, M.C., 2008. Cortical hyperexcitability may precede the onset of familial amyotrophic lateral sclerosis. Brain 131, 1540–1550.

Vucic, S., Stanley Chen, K.-H., Kiernan, M.C., Hallett, M., Benninger, D.H., Di Lazzaro, V., Rossini, P.M., Benussi, A., Berardelli, A., Currà, A., Krieg, S.M., Lefaucheur, J.-P., Long Lo, Y., Macdonell, R.A., Massimini, M., Rosanova, M., Picht, T., Stinear, C.M., Paulus, W., Ugawa, Y., Ziemann, U., Chen, R., 2023. Clinical diagnostic utility of transcranial magnetic stimulation in neurological disorders. Updated report of an IFCN committee. Clin Neurophysiol 150, 131–175.

- W -

Waibel, S., Neumann, M., Rabe, M., Meyer, T., Ludolph, A.C., 2010. Novel missense and truncating mutations in FUS/TLS in familial ALS. Neurology 75, 815–817.

Waibel, S., Neumann, M., Rosenbohm, A., Birve, A., Volk, A.E., Weishaupt, J.H., Meyer, T., Müller, U., Andersen, P.M., Ludolph, A.C., 2013. Truncating mutations in FUS/TLS give rise to a more aggressive ALS-phenotype than missense mutations: a clinico-genetic study in Germany. European Journal of Neurology 20, 540–546.

Wainger, B.J., Kiskinis, E., Mellin, C., Wiskow, O., Han, S.S.W., Sandoe, J., Perez, N.P., Williams, L.A., Lee, S., Boulting, G., Berry, J.D., Brown, R.H., Cudkowicz, M.E., Bean, B.P., Eggan, K., Woolf, C.J., 2014. Intrinsic membrane hyperexcitability of amyotrophic lateral sclerosis patient-derived motor neurons. Cell Rep 7, 1–11.

Wainger, B.J., Macklin, E.A., Vucic, S., McIlduff, C.E., Paganoni, S., Maragakis, N.J., Bedlack, R., Goyal, N.A., Rutkove, S.B., Lange, D.J., Rivner, M.H., Goutman, S.A., Ladha, S.S., Mauricio, E.A., Baloh, R.H., Simmons, Z., Pothier, L., Kassis, S.B., La, T., Hall, M., Evora, A., Klements, D., Hurtado, A., Pereira, J.D., Koh, J., Celnik, P.A., Chaudhry, V., Gable, K., Juel, V.C., Phielipp, N., Marei, A., Rosenquist, P., Meehan, S., Oskarsson, B., Lewis, R.A., Kaur, D., Kiskinis, E., Woolf, C.J., Eggan, K., Weiss, M.D., Berry, J.D., David, W.S., Davila-Perez, P., Camprodon, J.A., Pascual-Leone, A., Kiernan, M.C., Shefner, J.M., Atassi, N., Cudkowicz, M.E., 2021. Effect of Ezogabine on Cortical and Spinal Motor Neuron Excitability in Amyotrophic Lateral Sclerosis: A Randomized Clinical Trial. JAMA Neurol 78, 186–196.

Walhout, R., Verstraete, E., van den Heuvel, M.P., Veldink, J.H., van den Berg, L.H., 2018. Patterns of symptom development in patients with motor neuron disease. Amyotroph Lateral Scler Frontotemporal Degener 19, 21–28.

Wallace, M.L., Sabatini, B.L., 2023. Synaptic and circuit functions of multitransmitter neurons in the mammalian brain. Neuron 111, 2969–2983.

Wang, J., Li, J., Yang, Q., Xie, Y.-K., Wen, Y.-L., Xu, Z.-Z., Li, Y., Xu, T., Wu, Z.-Y., Duan, S., Xu, H., 2021. Basal forebrain mediates prosocial behavior via disinhibition of midbrain dopamine neurons. Proc Natl Acad Sci U S A 118.

Wang, W.-Y., Pan, L., Su, S.C., Quinn, E.J., Sasaki, M., Jimenez, J.C., Mackenzie, I.R.A., Huang, E.J., Tsai, L.-H., 2013. Interaction of FUS and HDAC1 regulates DNA damage response and repair in neurons. Nat Neurosci 16, 1383–1391.

Wang, X., Loi, S.M., Foster, E., Chen, Z., Velakoulis, D., Kwan, P., 2021. Predictors of New-Onset Epilepsy in People With Younger-Onset Neurocognitive Disorders. Front Aging Neurosci 13, 637260.

Wang, X., Schwartz, J.C., Cech, T.R., 2015. Nucleic acid-binding specificity of human FUS protein. Nucleic Acids Res 43, 7535–7543.

Wang, Y., Mandelkow, E., 2016. Tau in physiology and pathology. Nat Rev Neurosci 17, 5–21.

Wang, Y.-F., Sun, M.-Y., Hou, Q., Hamilton, K.A., 2013. GABAergic inhibition through synergistic astrocytic neuronal interaction transiently decreases vasopressin neuronal activity during hypoosmotic challenge. Eur J Neurosci 37, 1260–1269.

Weber, M., Eisen, A., Stewart, H.G., Andersen, P.M., 2000. Preserved slow conducting corticomotoneuronal projections in amyotrophic lateral sclerosis with autosomal recessive D90A CuZn-superoxide dismutase mutation. Brain 123, 1505–1515.

Weerasekera, A., Peeters, R., Sima, D., Dresselaers, T., Sunaert, S., De Vocht, J., Claeys, K., Van Huffel, S., Van Damme, P., Himmelreich, U., 2019. Motor cortex metabolite alterations in amyotrophic lateral sclerosis assessed in vivo using edited and non-edited magnetic resonance spectroscopy. Brain Res 1718, 22–31.

Wei, Q., Ou, R., Chen, Y., Chen, X., Cao, B., Hou, Y., Zhang, L., Shang, H., 2019. RNM-01 Weight stability is associated with longer survival in amyotrophic lateral sclerosis. Amyotroph Lateral Scler Frontotemporal Degener 20, 309–326.

Wei, Q.-Q., Ou, R., Cao, B., Chen, Y., Hou, Y., Zhang, L., Wu, F., Shang, H., 2021. Early weight instability is associated with cognitive decline and poor survival in amyotrophic lateral sclerosis. Brain Res Bull 171, 10–15.

Weir, J.B.D.B., 1949. New methods for calculating metabolic rate with special reference to protein metabolism. J Physiol 109, 1–9.

Wengert, E.R., Wenker, I.C., Wagner, E.L., Wagley, P.K., Gaykema, R.P., Shin, J.-B., Patel, M.K., 2021. Adrenergic Mechanisms of Audiogenic Seizure-Induced Death in a Mouse Model of SCN8A Encephalopathy. Front Neurosci 15, 581048.

Weydt, P., Oeckl, P., Huss, A., Müller, K., Volk, A.E., Kuhle, J., Knehr, A., Andersen, P.M., Prudlo, J., Steinacker, P., Weishaupt, J.H., Ludolph, A.C., Otto, M., 2016. Neurofilament levels as biomarkers in asymptomatic and symptomatic familial amyotrophic lateral sclerosis. Ann Neurol 79, 152–158.

White, M.A., Kim, E., Duffy, A., Adalbert, R., Phillips, B.U., Peters, O.M., Stephenson, J., Yang, S., Massenzio, F., Lin, Z., Andrews, S., Segonds-Pichon, A., Metterville, J., Saksida, L.M., Mead, R., Ribchester, R.R., Barhomi, Y., Serre, T., Coleman, M.P., Fallon, J.R., Bussey, T.J., Brown, R.H., Sreedharan, J., 2018. TDP-43 gains function due to perturbed autoregulation in a Tardbp knock-in mouse model of ALS-FTD. Nat Neurosci 21, 552–563.

Wicks, P., Turner, M.R., Abrahams, S., Hammers, A., Brooks, D.J., Leigh, P.N., Goldstein, L.H., 2008. Neuronal loss associated with cognitive performance in amyotrophic lateral sclerosis: an (11C)-flumazenil PET study. Amyotroph Lateral Scler 9, 43–49.

Wiesenfarth, M., Dorst, J., Brenner, D., Elmas, Z., Parlak, Ö., Uzelac, Z., Kandler, K., Mayer, K., Weiland, U., Herrmann, C., Schuster, J., Freischmidt, A., Müller, K., Siebert, R., Bachhuber, F., Simak, T., Günther, K., Fröhlich, E., Knehr, A., Regensburger, M., German, A., Petri, S., Grosskreutz, J., Klopstock, T., Reilich, P., Schöberl, F., Hagenacker, T., Weyen, U., Günther, R., Vidovic, M., Jentsch, M., Haarmeier, T., Weydt, P., Valkadinov, I., Hesebeck-Brinckmann, J., Conrad, J., Weishaupt, J.H., Schumann, P., Körtvélyessy, P., Meyer, T., Ruf, W.P., Witzel, S., Senel, M., Tumani, H., Ludolph, A.C., 2024. Effects of tofersen treatment in patients with SOD1-ALS in a "real-world" setting - a 12-month multicenter cohort study from the German early access program. EClinicalMedicine 69, 102495.

Williams, K.L., Fifita, J.A., Vucic, S., Durnall, J.C., Kiernan, M.C., Blair, I.P., Nicholson, G.A., 2013. Pathophysiological insights into ALS with C9ORF72 expansions. J Neurol Neurosurg Psychiatry 84, 931–935.

Witzel, S., Maier, A., Steinbach, R., Grosskreutz, J., Koch, J.C., Sarikidi, A., Petri, S., Günther, R., Wolf, J., Hermann, A., Prudlo, J., Cordts, I., Lingor, P., Löscher, W.N., Kohl, Z., Hagenacker, T., Ruckes, C., Koch, B., Spittel, S., Günther, K., Michels, S., Dorst, J., Meyer, T., Ludolph, A.C., German Motor Neuron Disease Network (MND-NET), 2022. Safety and Effectiveness of Long-term Intravenous Administration of Edaravone for Treatment of Patients With Amyotrophic Lateral Sclerosis. JAMA Neurol 79, 121–130.

Wojcik, S.M., Katsurabayashi, S., Guillemin, I., Friauf, E., Rosenmund, C., Brose, N., Rhee, J.-S., 2006. A shared vesicular carrier allows synaptic corelease of GABA and glycine. Neuron 50, 575–587.

Wong, F.K., Bercsenyi, K., Sreenivasan, V., Portalés, A., Fernández-Otero, M., Marín, O., 2018. Pyramidal cell regulation of interneuron survival sculpts cortical networks. Nature 557, 668–673.

Wong, S., Wei, G., Husain, M., Hodges, J.R., Piguet, O., Irish, M., Kumfor, F., 2023. Altered reward processing underpins emotional apathy in dementia. Cogn Affect Behav Neurosci 23, 354–370.

Woolley, S.C., York, M.K., Moore, D.H., Strutt, A.M., Murphy, J., Schulz, P.E., Katz, J.S., 2010. Detecting frontotemporal dysfunction in ALS: utility of the ALS Cognitive Behavioral Screen (ALS-CBS). Amyotroph Lateral Scler 11, 303–311.

Wootz, H., Fitzsimons-Kantamneni, E., Larhammar, M., Rotterman, T.M., Enjin, A., Patra, K., André, E., Van Zundert, B., Kullander, K., Alvarez, F.J., 2013. Alterations in the motor neuron-renshaw cell circuit in the Sod1(G93A) mouse model. J Comp Neurol 521, 1449–1469.

- X -

Xie, M., Pallegar, P.N., Parusel, S., Nguyen, A.T., Wu, L.-J., 2023. Regulation of cortical hyperexcitability in amyotrophic lateral sclerosis: focusing on glial mechanisms. Mol Neurodegener 18, 75.

Xu, H., Jeong, H.-Y., Tremblay, R., Rudy, B., 2013. Neocortical somatostatin-expressing GABAergic interneurons disinhibit the thalamorecipient layer 4. Neuron 77, 155–167.

Xu, J., Jo, A., DeVries, R.P., Deniz, S., Cherian, S., Sunmola, I., Song, X., Marshall, J.J., Gruner, K.A., Daigle, T.L., Contractor, A., Lerner, T.N., Zeng, H., Zhu, Y., 2022. Intersectional mapping of multi-transmitter neurons and other cell types in the brain. Cell Rep 40, 111036.

Xu, L., Liu, T., Liu, L., Yao, X., Chen, L., Fan, D., Zhan, S., Wang, S., 2020. Global variation in prevalence and incidence of amyotrophic lateral sclerosis: a systematic review and meta-analysis. J Neurol 267, 944–953.

- Y -

Yamada, C., Saegusa, Y., Nahata, M., Sadakane, C., Hattori, T., Takeda, H., 2015. Influence of Aging and Gender Differences on Feeding Behavior and Ghrelin-Related Factors during Social Isolation in Mice. PLoS One 10, 0140094.

Yamada, M.H., Nishikawa, K., Kubo, K., Yanagawa, Y., Saito, S., 2012. Impaired glycinergic synaptic transmission and enhanced inflammatory pain in mice with reduced expression of vesicular GABA transporter (VGAT). Mol Pharmacol 81, 610–619.

Yamanaka, K., Chun, S.J., Boillee, S., Fujimori-Tonou, N., Yamashita, H., Gutmann, D.H., Takahashi, R., Misawa, H., Cleveland, D.W., 2008. Astrocytes as determinants of disease progression in inherited amyotrophic lateral sclerosis. Nat Neurosci 11, 251–253.

Yamashita, S., Mori, A., Sakaguchi, H., Suga, T., Ishihara, D., Ueda, A., Yamashita, T., Maeda, Y., Uchino, M., Hirano, T., 2012. Sporadic juvenile amyotrophic lateral sclerosis caused by mutant FUS/TLS: possible association of mental retardation with this mutation. J Neurol 259, 1039–1044.

Yamazaki, T., Chen, S., Yu, Y., Yan, B., Haertlein, T.C., Carrasco, M.A., Tapia, J.C., Zhai, B., Das, R., Lalancette-Hebert, M., Sharma, A., Chandran, S., Sullivan, G., Nishimura, A.L., Shaw, C.E., Gygi, S.P., Shneider, N.A., Maniatis, T., Reed, R., 2012. FUS-SMN Protein Interactions Link the Motor Neuron Diseases ALS and SMA. Cell Reports 2, 799–806.

Yan, J., Deng, H.-X., Siddique, N., Fecto, F., Chen, W., Yang, Y., Liu, E., Donkervoort, S., Zheng, J.G., Shi, Y., Ahmeti, K.B., Brooks, B., Engel, W.K., Siddique, T., 2010. Frameshift and novel mutations in FUS in familial amyotrophic lateral sclerosis and ALS/dementia. Neurology 75, 807–814.

Yanai, S., Endo, S., 2021. Functional Aging in Male C57BL/6J Mice Across the Life-Span: A Systematic Behavioral Analysis of Motor, Emotional, and Memory Function to Define an Aging Phenotype. Front Aging Neurosci 13, 697621.

Yang, F., Chen, Liling, Yu, Y., Xu, T., Chen, Lu, Yang, W., Wu, Q., Han, Y., 2022. Alzheimer's disease and epilepsy: An increasingly recognized comorbidity. Front Aging Neurosci 14, 940515.

Yang, T., Hou, Y., Li, C., Cao, B., Cheng, Y., Wei, Q., Zhang, L., Shang, H., 2021. Risk factors for cognitive impairment in amyotrophic lateral sclerosis: a systematic review and meta-analysis. J Neurol Neurosurg Psychiatry 92, 688–693.

Yasuda, K., Clatterbuck-Soper, S.F., Jackrel, M.E., Shorter, J., Mili, S., 2017. FUS inclusions disrupt RNA localization by sequestering kinesin-1 and inhibiting microtubule detyrosination. J Cell Biol 216, 1015–1034.

Yasuda, K., Zhang, H., Loiselle, D., Haystead, T., Macara, I.G., Mili, S., 2013. The RNA-binding protein Fus directs translation of localized mRNAs in APC-RNP granules. J Cell Biol 203, 737–746.

Yokoi, S., Udagawa, T., Fujioka, Y., Honda, D., Okado, H., Watanabe, H., Katsuno, M., Ishigaki, S., Sobue, G., 2017. 3'UTR Length-Dependent Control of SynGAP Isoform α2 mRNA by FUS and ELAV-like Proteins Promotes Dendritic Spine Maturation and Cognitive Function. Cell Rep 20, 3071–3084.

Yoshizawa, T., Ali, R., Jiou, J., Fung, H.Y.J., Burke, K.A., Kim, S.J., Lin, Y., Peeples, W.B., Saltzberg, D., Soniat, M., Baumhardt, J.M., Oldenbourg, R., Sali, A., Fawzi, N.L., Rosen, M.K., Chook, Y.M., 2018. Nuclear Import Receptor Inhibits Phase Separation of FUS through Binding to Multiple Sites. Cell 173, 693-705.

Yu, X., Zhao, Z., Shen, H., Bing, Q., Li, N., Hu, J., 2018. Clinical and Genetic Features of Patients with Juvenile Amyotrophic Lateral Sclerosis with Fused in Sarcoma (FUS) Mutation. Med Sci Monit 24, 8750–8757.

- Z -

Zajicek, A.S., Ruan, H., Dai, H., Skolfield, M.C., Phillips, H.L., Burnette, W.J., Javidfar, B., Sun, S.-C., Akbarian, S., Yao, W.-D., 2022. Cylindromatosis drives synapse pruning and weakening by promoting macroautophagy through Akt-mTOR signaling. Mol Psychiatry 27, 2414–2424.

Zanette, G., Tamburin, S., Manganotti, P., Refatti, N., Forgione, A., Rizzuto, N., 2002. Changes in motor cortex inhibition over time in patients with amyotrophic lateral sclerosis. J Neurol 249, 1723–1728.

Zeisel, A., Muñoz-Manchado, A.B., Codeluppi, S., Lönnerberg, P., La Manno, G., Juréus, A., Marques, S., Munguba, H., He, L., Betsholtz, C., Rolny, C., Castelo-Branco, G., Hjerling-Leffler, J., Linnarsson, S., 2015. Brain structure. Cell types in the mouse cortex and hippocampus revealed by single-cell RNA-seq. Science 347, 1138–1142.

Zhang, J., Lanuza, G.M., Britz, O., Wang, Z., Siembab, V.C., Zhang, Y., Velasquez, T., Alvarez, F.J., Frank, E., Goulding, M., 2014. V1 and v2b interneurons secure the alternating flexor-extensor motor activity mice require for limbed locomotion. Neuron 82, 138–150.

Zhang, S., Cooper-Knock, J., Weimer, A.K., Shi, M., Moll, T., Marshall, J.N.G., Harvey, C., Nezhad, H.G., Franklin, J., Souza, C.D.S., Ning, K., Wang, C., Li, J., Dilliott, A.A., Farhan, S., Elhaik, E., Pasniceanu, I., Livesey, M.R., Eitan, C., Hornstein, E., Kenna, K.P., Project MinE ALS Sequencing Consortium, Veldink, J.H., Ferraiuolo, L., Shaw, P.J., Snyder, M.P., 2022. Genome-wide identification of the genetic basis of amyotrophic lateral sclerosis. Neuron 110, 992-1008.

Zhang, W., Zhang, L., Liang, B., Schroeder, D., Zhang, Z., Cox, G.A., Li, Y., Lin, D.-T., 2016. Hyperactive Somatostatin Interneurons Contribute to Excitotoxicity in Neurodegenerative Disorders. Nat Neurosci 19, 557–559.

Zhang, Z., Jiao, Y.-Y., Sun, Q.-Q., 2011. Developmental maturation of excitation and inhibition balance in principal neurons across four layers of somatosensory cortex. Neuroscience 174, 10–25.

Zhou, Y., Liu, S., Liu, G., Öztürk, A., Hicks, G.G., 2013. ALS-Associated FUS Mutations Result in Compromised FUS Alternative Splicing and Autoregulation. PLoS Genet 9, 1003895.

Zou, H., Wang, J.-Y., Ma, G.-M., Xu, M.-M., Luo, F., Zhang, L., Wang, W.-Y., 2022. The function of FUS in neurodevelopment revealed by the brain and spinal cord organoids. Mol Cell Neurosci 123, 103771.

Annexes

Publication 3: FUS-dependent gene expression links neuronal vulnerability to genetic risk in ALS/FTD

Dr Raphaelle Cassel created a novel mouse model in which she truncated the nuclear localisation signal domain of the *Fus* gene exclusively in projection neurons in adult mice. This was done to determine whether the cytoplasmic delocalisation of FUS in adult excitatory neurons is sufficient to induce ALS- and FTD-like symptoms.

I was delighted to contribute to this project by assisting with the preparation of sample materials, as well as with the analysis of the subcellular localisation of FUS, the four-limb inverted grid test, the three-chamber social task, the novel object recognition task and the nest building test.

Publication 3

FUS-mediated gene expression links genetic risk to selective neuronal degeneration and cognitive deficits in neurodegenerative diseases

Raphaelle Cassel, Félicie Lorenc, Aurélie Bombardier, Claudia De Tapia, Stéphane Dieterlé, Geoffrey Stuart-Lopez, Caroline Rouaux, Simon J. Guillot, Pascal Kessler, Marie-Christine Birling, Jenna Gregory, James Shorter, Luc Dupuis, Salim Megat

In preparation

FUS-mediated gene expression links genetic risk to selective neuronal degeneration and cognitive deficits in neurodegenerative diseases

Raphaelle Cassel[1], Félicie Lorenc[1], Aurélie Bombardier[1], Claudia De Tapia[1], Stéphane Dieterlé[1], Geoffrey Stuart-Lopez[1], Caroline Rouaux[1], Simon J. Guillot[1], Pascal Kessler[2], Marie-Christine Birling[3], Jenna Gregory[4], James Shorter[5], Luc Dupuis[# 1], Salim Megat[# 1]

[1] Université de Strasbourg, INSERM, UMR-S 1329, Strasbourg Translational Neuroscience and Psychiatry, CRBS, Strasbourg, France.
[2] Université de Strasbourg, INSERM, UMS 38, Imaging Core Facility PIC-STRA, CRBS, Strasbourg, France.
[3] Université de Strasbourg, INSERM, CNRS, PHENOMIN-Institut Clinique de la Souris, Strasbourg, France.
[4] Institute of Medical Sciences, University of Aberdeen, Aberdeen, United Kingdom.
[5] Department of Biochemistry and Biophysics, University of Pennsylvania, Philadelphia, United States of America.

# Contributed equally.

raphaelle.cassel@inserm.fr / https://orcid.org/0000-0002-3157-3798
ldupuis@unistra.fr / https://orcid.org/0000-0002-0902-5824
salim.megat@inserm.fr / https://orcid.org/0000-0003-2186-6770

Abstract

Pathological aggregates of RNA-binding proteins are widely found in brains of patients with neurodegenerative diseases, in particular amyotrophic lateral sclerosis (ALS). However, apart from TDP-43, the relationships between specific RNA binding proteins, genetic susceptibility and clinical phenotype are unclear in these diseases. Here we show that heritability of neurodegenerative diseases is enriched in targets of TDP-43, but also, more surprisingly of FUS. Using single cell transcriptomics in *Fus* knock-in mice and integration with snRNAseq datasets from sporadic ALS patients, we show that mislocalization of FUS is sufficient to recapitulate transcriptomic alterations in excitatory projection neurons in the motor cortex. Furthermore, inducing FUS mislocalization in adult mouse projection neurons leads to neuronal degeneration, compromised cognitive functions, social interactions, and social memory and disrupted cortical electrical activity. Systems biology approaches allowed us to identify a gene module that is downregulated in vulnerable neurons in ALS in a FUS and TDP-43 dependent manner, but also more broadly in vulnerable neuronal populations in other neurodegenerative diseases. Importantly, this FUS gene module is highly enriched in ALS heritability. We reasoned that this FUS dependent gene module could include additional currently unknown ALS genes, and rare variant burden analysis

highlighted enrichment of loss of function variants in CLPB in ALS patients. In all, we identify FUS dependent gene expression as a mechanism that links neuronal degeneration and subsequent cognitive impairment to genetic risk in multiple neurodegenerative diseases.

The following sections of the publication are not available
in the online version of this PhD manuscript.

Publication 4: ALS/FTD-linked TBK1 deficiency in microglia induces an aged-liked, primed microglial signature and drives social memory deficits in mice

Dr Isadora Lenoël and Dr Christian S. Lobsiger created a novel mouse model in which they deleted the *Tbk1* gene exclusively in microglia with the objective of determining whether the loss of microglial TBK1 is sufficient to induce ALS- and FTD-like symptoms. In this manuscript, they elegantly show that TBK1 in microglial cells plays a pivotal role in maintaining microglial homeostasis and social memory.

In particular, the comparison of *Tbk1* deletion in microglial cells and *Tbk1* deletion in motor neurons reveals that motor neurons are resistant to the loss of TBK1, whereas microglia are strongly affected. This was evidenced by an increase in microglial cell density in the spinal cord, but not in the brain, in the absence of neuroinflammatory signs. In addition, they demonstrate that microglial *Tbk1* deletion is not sufficient to induce motor impairments but is sufficient to cause social memory deficits. Finally, they show that the loss of TBK1 in microglia results in a transcriptomic shift towards an aged-like microglial signature, which is reminiscent of the microglial transcriptional changes associated with ageing and neurodegeneration. Collectively, they present compelling evidence that microglial TBK1 is essential for preventing an aged-like microglial activation (also referred to as priming) and ensuring social recognition in mice.

I was delighted to contribute to this project by assisting with the behavioural phenotyping of the mice. I provided guidance to Isadora in optimising the protocols and conducted the analysis of the three-chamber social task, as well as the novel object recognition task and object location task. The last two tests were not included in the manuscript, as the control mice did not exhibit a compelling capacity to discriminate between the two objects.

Publication 4

ALS/FTD-linked TBK1 deficiency in microglia induces an aged-liked, primed microglial signature and drives social memory deficits in mice

Isadora Lenoël, Matthieu Ribon, Félicie Lorenc, Aurelien Diebold, Clémentine Philibert, David Robaldo, Manel Badsi, Julianne Perronnet, Julie Lameth, Félix Berriat, Hidemi Misawa, Marie Coutelier, Raphaelle Cassel, Delphine Bohl, Stéphanie Millecamps, Michel Mallat, David Brenner, Jochen H. Weishaupt, Séverine Boillée, Christian S. Lobsiger

In revision for Nature Communications

ALS/FTD-linked TBK1 deficiency in microglia induces an aged-like, primed microglial signature and drives social memory deficits in mice

Isadora Lenoel[1], Matthieu Ribon[1], Félicie Lorenc[2], Aurélien Diebold[1], Clémentine Philibert[1,3], David Robaldo[1], Manel Badsi[1], Julianne Perronnet[4], Julie Lameth[1], Felix Berriat[1], Hidemi Misawa[5], Marie Coutelier[1], Raphaelle Cassel[2], Delphine Bohl[1], Stéphanie Millecamps[1], Michel Mallat[1], David Brenner[6], Jochen H. Weishaupt[7], Séverine Boillée[1], Christian S. Lobsiger[1]

[1] Sorbonne Université, Institut du Cerveau - Paris Brain Institute - ICM, Inserm, CNRS, APHP, Hôpital de la Pitié Salpêtrière, Paris, France
[2] Université de Strasbourg, INSERM, UMR-S 1329, STEP laboratory, CRBS, Strasbourg, France.
[3] *present address:* Department of Biochemistry & Cell Biology, Chobanian & Avedisian School of Medicine, Boston University, Boston, USA
[4] Phénotypage du petit animal, UMS 28, Sorbonne Université, Paris, France
[5] Division of Pharmacology, Faculty of Pharmacy, Keio University, Minato-ku, Tokyo, Japan
[6] Ulm University, Department of Neurology, Ulm, Germany
[7] Division of Neurodegeneration, Dep. of Neurology, Mannheim Center for Translational Neurosciences, Medical Faculty Mannheim, Heidelberg University, Mannheim, Germany

isadora.lenoel@icm-institute.org / https://orcid.org/0009-0008-1096-5902
christian.lobsiger@icm-institute.org / https://orcid.org/0000-0002-4313-010X

Abstract

The TANK-Binding Kinase 1 (*TBK1*) is a ubiquitously expressed kinase notably involved in autophagy and immune signaling. Dominant loss-of-function mutations in *TBK1* have been linked to Amyotrophic Lateral Sclerosis (ALS), Fronto-temporal dementia (FTD) and ALS/FTD. However, pathogenic mechanisms remain unclear, particularly the cell-type specific disease contributions of *TBK1* mutations. Here, we focus on motor neurons and microglial cells and show that deletion of *Tbk1* only in microglial cells is sufficient to induce social memory deficits and a primed microglial signature in mice. We find that deleting *Tbk1* from motor neurons does not induce a transcriptional stress response, despite lifelong and increasing accumulation of intra-cellular p62^{+} inclusions. Conversely, *Tbk1* deletion in microglial cells strongly alters microglial reactive responses. In the spinal cord, TBK1 defines homeostatic microglial density as microglial *Tbk1* deletion leads to increased microglial numbers, but is not sufficient to induce or modify ALS-like motor neuron damage. In contrast, in the brain, microglial *Tbk1* deletion causes early social memory deficits, consistent with *TBK1*-linked FTD. These deficits are linked to a shift towards an aged-like, pro-inflammatory microglial signature, indicating that TBK1 restricts aged-like microglial activation. Our

results reveal that part of *TBK1*-linked FTD disease originates from microglial dysfunction.

The following sections of the publication are not available
in the online version of this PhD manuscript.

Université de Strasbourg

Félicie LORENC

École Doctorale des Sciences de la Vie et de la Santé STRASBOURG

Contribution of inhibitory neurons to the amyotrophic lateral sclerosis and frontotemporal dementia continuum: Focus on the motor and social phenotypes associated with FUS protein

Abstract

Amyotrophic lateral sclerosis (ALS) and frontotemporal dementia (FTD) are progressive, invalidating and fatal neurodegenerative disorders forming a continuum. ALS is primarily characterised by the degeneration of motor neurons resulting in paralysis. FTD is defined by a degeneration of the frontal and temporal lobes, which causes behavioural and cognitive decline. The cytoplasmic accumulation of fused in sarcoma (FUS), a ubiquitous and multifunctional DNA/RNA-binding protein, is involved in the aetiology of ALS and FTD. Inhibitory neurons impairments appear to be an early feature of both diseases, and may contribute to the onset and progression of symptoms. However, the role of inhibitory neurons in FUS-related phenotypes remains to be elucidated. Here, we generated novel mouse models in which the subcellular localisation of FUS can be manipulated in cells expressing the vesicular GABA transporter (VGAT). Our findings demonstrate that the localisation of FUS in cerebral and spinal GABAergic and glycinergic neurons is a key regulator of motor and social phenotypes, as well as neuronal activity.

Keywords: amyotrophic lateral sclerosis, frontotemporal dementia, fused in sarcoma, GABAergic and glycinergic neurons, vesicular GABA transporter, motor and behavioural characterisation

Résumé

La sclérose latérale amyotrophique (SLA) et la démence frontotemporale (DFT) sont deux maladies neurodégénératives progressives, invalidantes et fatales formant un continuum. La SLA se caractérise principalement par la dégénérescence des neurones moteurs entrainant une paralysie. La DFT se définit par une dégénérescence des lobes frontaux et temporaux entrainant des déficits comportementaux et cognitifs. L'accumulation cytoplasmique de *fused in sarcoma* (FUS), une protéine ubiquitaire et multifonctionnelle se liant à l'ARN et l'ADN, est impliquée dans l'étiologie de la SLA et de la DFT. Les neurones inhibiteurs semblent être altérés précocement dans ces deux maladies, et pourraient contribuer à l'apparition et à la progression des symptômes. Cependant, la contribution des neurones inhibiteurs aux phénotypes liés à FUS reste à élucider. Dans cette étude, nous avons généré de nouveaux modèles murins dans lesquels la localisation subcellulaire de FUS peut être manipulée dans les cellules exprimant le transporteur vésiculaire du GABA (VGAT). Nos résultats montrent que la localisation de FUS dans les neurones GABAergiques et glycinergiques du cerveau et de la moelle épinière est un important régulateur des phénotypes moteurs et sociaux, ainsi que de l'activité neuronale.

Mots-clés : sclérose latérale amyotrophique, démence frontotemporale, FUS, neurones GABAergiques et glycinergiques, transporteur vésiculaire du GABA, caractérisation motrice et comportementale